

LA-UR- 98-2059

Tests of the Higher Order Turbulence Model  
for Atmospheric Circulations (HOTMAC) at  
Deseret Chemical Dep

RECEIVED  
NOV 24 1998  
OSTI

Keeley R. Costigan

*Atmospheric and Climate Sciences Group (EES-8)*  
*Earth and Environmental Sciences Division*  
*Los Alamos National Laboratory*  
*Los Alamos, New Mexico 87545*

YDT  
MASTER

DISTRIBUTION OF THIS DOCUMENT IS UNLIMITED

## **DISCLAIMER**

This report was prepared as an account of work sponsored by an agency of the United States Government. Neither the United States Government nor any agency thereof, nor any of their employees, make any warranty, express or implied, or assumes any legal liability or responsibility for the accuracy, completeness, or usefulness of any information, apparatus, product, or process disclosed, or represents that its use would not infringe privately owned rights. Reference herein to any specific commercial product, process, or service by trade name, trademark, manufacturer, or otherwise does not necessarily constitute or imply its endorsement, recommendation, or favoring by the United States Government or any agency thereof. The views and opinions of authors expressed herein do not necessarily state or reflect those of the United States Government or any agency thereof.

## **DISCLAIMER**

**Portions of this document may be illegible in electronic image products. Images are produced from the best available original document.**

## 1.0 Introduction

The Deseret Chemical Depot is located in the high, broad Rush Valley of North-Central Utah. The valley is approximately 1560 m above sea level and roughly 20 km across from East to West and 45 km long from North to South. It is surrounded on three sides by mountain ranges with the Oquirrh Mountains to the East, the Stansbury and Onaqui Mountains to the West, and the Sheep Rock and East Tintic Mountains to the South. These mountain ranges include peaks from about 2400 m to 3350 m MSL. A somewhat shorter barrier (2000 m South Mountain) exists on the North end of the valley and the lowest passes are on the north and east sides. Further to the North lies Tooele Valley and the Great Salt Lake. Another significant lake, Utah Lake, is in the adjacent valley to the east of Rush Valley and the small Rush Lake is at the North end of Rush Valley. The combination of the topography and the lakes leads to interesting local meteorology affected by slope and valley flows and lake breezes (Stone et al., 1989; Yamada et al., 1989).

Deseret Chemical Depot is one of the U.S. Army's storage facilities for its stockpile of chemical weapon agents. Congress has directed the Department of Defense to eliminate the aging stockpiles, which have existed since the end of World War II, and the U. S. Army is destroying these lethal chemical munitions. Although the danger is slight, accurate predictions of the wind fields in the valley are necessary for dispersion calculations in the event of an accident involving toxic chemicals at the depot. There are several small communities in Rush and Tooele valleys, including the town of Tooele, and Salt Lake City is located 65 km to the Northeast of Deseret Chemical Depot South Area, at 1300 m MSL and beyond the Oquirrh Mountains.

The purpose of this report is to carry out three-dimensional numerical simulations of the atmospheric circulations in the region around Deseret Chemical Depot with the Higher Order Turbulence Model for Atmospheric Circulations (HOTMAC) and to evaluate the performance of the model. The code had been modified to assimilate local meteorological observations through the use of Newtonian nudging. The nudging scheme takes advantage of the extensive network of local observations in the valley.

This evaluation is the an initial step in the validation and verification process for the use of HOTMAC and RAPTAD (RANDOM Particle Transport and Diffusion) codes for operational use at Deseret Chemical Depot. Because there are no routine measurements of tracers released from the depot, direct comparisons of model predicted dosages are not possible. As a first indication of how well the models might perform, we evaluate the ability of the HOTMAC model to characterize the wind fields in the region, compared to observed wind fields. In order to study the model's performance under a variety of meteorological conditions we had intended to run a series of simulations for a week out of each season, during the year from July 1996 to June 1997 when a doppler wind profiler was operational at the depot. The wind profiler was on loan to the depot in order to give vertical profiles of wind and temperature for input as initial conditions and data assimilation in the HOTMAC model. However, there were large gaps in both the profiler and the surface observations in the data archive and we were limited to a week during a single season, the winter of 1997, when there was sufficient data to carry out the evaluation reported here.

## 2.0 Test Setup

### 2.1 The meteorological conditions and input data

The choice of the seven day period to simulate a week in winter was based upon the availability of the surface and wind profiler observations and on a time period when the weather was repre-

sentative of that season. Several week-long time periods were identified by reviewing weather maps and then the archived data were examined for completeness. Thus the week of 13-19 February 1997 was chosen. Figure 1 presents the large-scale weather conditions depicted in the Daily Weather Maps (National Oceanographic and Atmospheric Association, 1997) at 1200 UTC each day. The precipitation and maximum and minimum temperature plots represent what was reported for the previous 24 hours, ending at 1200 UTC. From the 500 mb charts, it can be seen that an upper level ridge was dominant in the western U. S. during the first half of the period, with its axis just to the west of the study area. At the surface, relatively high pressure was also evident with the center of the high north just west of the study area. Cold air masses were moving southward through the central part of the U. S. with associated fronts along the Rocky Mountains, to the east of the study area. By the end of the period, the 500 mb flow had become zonal with short wave disturbances through the region. The surface conditions had also changed with a frontal system approaching from the west, associated with a low in the Northwestern U. S. Measurable amounts of precipitation did fall in the region during the last 3 days of the period.

Input data for HOTMAC was derived from the archived meteorological data from the eight surface stations and the 30 meter tower located on the depot and the 26 surface meteorological observing stations operated by Tooele County. These data are routinely stored at the depot and the 1997 data are stored in a data base which is accessed by software written by Applied Computing Systems. The software program SOUNDER retrieves the data, converts it to the units required by HOTMAC, and places it in files which can be read by HOTMAC. It is part of a software package which allows the users at the depot to retrieve the data and run HOTMAC and RAPTAD. For this study, the data were retrieved and brought to a Sun Ultra Sparc 2 workstation at Los Alamos. The data were then browsed visually for observations which were inconsistent with other observations at that station and close in time. Any obviously "out of character" observations were changed to missing data. That is, any sudden, short-duration changes in the u- or v-components of the winds in space and time were removed. The data from station 9 (the 30 meter tower) on the depot did not make sense and its data were set to missing for these runs. There may be a problem with the SOUNDER code for this station, because it is a tower with multiple levels of observations. Other than station 9, very little of the surface data that was available needed to be removed, just a couple of data points. However, a number of surface stations did not have data available during the study period. These included station 2 (which has been out of order for some time) and station 7 on the depot and stations 10, 11, 14, 19, 23, 26, 28, and 31 operated by Tooele county. In addition, station 6 on the depot has data missing after 0809 MST on 13 February 1997. Some of the other stations would also have data missing for portions of the study period.

Wind profiler data were also obtained using the same retrieval software. Obviously "bad" data were also removed from the files to be read by HOTMAC in the same manner as the surface data plus each level of a sounding was compared to adjacent levels. There were a number of soundings where the lowest level (usually 1840 m MSL) wind field was changed to missing data because the u or v component of the wind was reported to be excessively large. Some other data points at higher levels were also removed because they were single points that were significantly different from the surrounding levels and times. In addition, a number of the levels from individual soundings were removed because the sounding contained more than 50 levels and HOTMAC can only read 50 levels per sounding. The levels that were removed were either above the top of the model domain or contained only temperature information that was not being assimilated for these simulations.

## 2.2 The model setup

The model simulations were carried out for the period of 13-19 February 1997. Four runs were performed each day, beginning at 0500, 1100, 1700, and 2300 MST (1200, 1800, 0000, and 0600 UTC). Each of these runs utilized data assimilation for four hours, followed by 12 hours of the model running in a purely predictive mode, for a total of 16 hours. The initial run began at 0500 MST (1200 UTC) with an initialization which assumed that the wind and temperature vertical profiles were horizontally homogeneous throughout the domain. Each successive run began six hours later and would use the predictions from the previous run at that time to restart the model. Thus these subsequent runs do not assume the wind and temperature fields are horizontally homogeneous but use the three-dimensional fields from the previous simulation to initialize and their simulation period overlaps that of the previous run by 10 hours. One exception to this was at 500 MST (1200 UTC) on 16 February. This run was initialized with horizontally homogeneous temperature and wind profiles because the observed winds in the region had nearly reversed direction since the previous run had begun. This was too large of a change for the data assimilation alone to correct and the model had no other way of adjusting for what appeared to be a synoptic-scale influence in the area. The model results were output and saved each hour of simulation time, at the beginning of the hour.

Figure 2 presents the model domain used in these calculations. The contour lines denote the topography heights in increments of 200 m. The first grid uses 10 km grid spacing and extends from Nevada to eastern Utah in the east-west direction. This was chosen so that the model boundaries were placed at similar elevations in order to avoid problems with model depths being different on the upwind side of the domain, compared to the downwind side. If the model depth at the upwind and downwind boundaries are very different, the winds at the boundary over the higher terrain will need to be stronger to maintain a mass balance between inflow and outflow. This is an important consideration in HOTMAC which has a limited model depth and a vertical coordinate which is terrain following and a flat domain top. The sites labeled S1 and S2 give the approximate locations of the wind profiler at the depot and the Salt Lake City airport, respectively. Although they are not depicted in the figure, The Great Salt Lake, Utah Lake, and Rush Lake are included within the model domain.

The second grid used 5 km grid spacing and focused on the area within and immediately surrounding Rush Valley. The North-South running Stansbury and Oquirrh mountain ranges are evident on the west and east sides of Rush Valley.

The arrows in Figure 2 represent the winds after one timestep on 13 February 1997. The horizontally homogenous initialization of the winds is evident. There is a slight modification of the winds over Tooele Valley and Rush Valley due to the data assimilation that took place during the first timestep. The data assimilation was only performed on the u and v components of the winds. The temperature and humidity data were not included in the data assimilation because very small errors in the observed temperatures would cause significant unrealistic wind responses in the model. To obtain the potential temperature for the model input, the observed temperature was converted using observed pressures where available, but the pressure instruments had not been calibrated in several years. Also, to obtain the profiler potential temperatures above the surface, the pressure had to be assumed to follow the hydrostatic assumption above the measurement at the surface. With the uncertainties in the measured temperatures, the code to assimilate temperatures and humidities was turned off in HOTMAC, for these runs.

## 2.3 How the model's performance was evaluated

For this study, the model predicted winds were compared to the observed winds. The decision to only look at winds was made to limit the scope of these initial tests. The wind direction and speed are very important in determining where released agent will go and the accuracy of the winds that HOTMAC predicts will have a large influence on the accuracy of the RAPTAD predictions of dosage. Future studies should also evaluate the model's predictions of temperature (including stability and mixing height) and humidity.

To compare the model results with the observed data, the model predictions were interpolated to each observation point, using a bilinear interpolation. This is somewhat of a disadvantage to the model because it was not predicting for the exact location and the assumption was made that the predictions would vary linearly between points. In addition, to facilitate the comparisons to the model output, the surface observations were linearly interpolated in time (if needed) to the top of each hour. That is, if the observations did not occur exactly on the hour, a value of the  $u$  and  $v$  components of the wind at that site was obtained by using a linear interpolation between the observation just prior to that time and the observation just after the hour. In most cases, these observations were within 15 minutes of the desired time, because the observations were recorded every 15 minutes. The exceptions would be if there was missing data. The analysis did not interpolate from data that was more than 30 minutes from the hour for the surface data. Instead, the data were considered missing at that time.

The sounding data were reported hourly and did not need to be interpolated in time. The profiler sampled the data for 50 minutes out of each hour and reported the average winds over that hour. However, the profiler data were interpolated vertically to the heights above the ground that corresponded to the model vertical levels.

It should be pointed out that both the surface and profiler data were averaged over a period of time. The surface observations were reported four times per hour and represented an averaged wind over 15 minutes and the profiler data were averaged over 50 minutes and reported hourly. The model output represents instantaneous "snapshots" of the winds at the output time. Thus comparisons between the model and observations will reflect some error due to differences in comparing averaged to instantaneous data.

The root mean square error (rmse) of the model prediction was then calculated with the equation

$$rmse = \sqrt{\frac{\sum (observed - predicted)^2}{N}}, \text{ following Panofsky and Brier (1958) and Pielke}$$

(1984). The comparison to the surface data were carried out where  $N$  represented the total number of observation sites (possible maximum of 35 stations) with data available at that given time and the rmse was calculated for each hour of predictions. Because there was only one profiler observation each hour the model results were compared to the profiler results at the 1072 m AGL level and  $N$  represented the number of hours of available profiler data (maximum of 16) for each 16 hour run.

## 3.0 Results

Figures 3 through 27 summarize the results of the 25 runs that were carried out for the week-long study period. Each figure depicts a single simulation and contains 10 parts. For example,

Figure 3a gives a time series of the wind direction at 1072 m AGL, for the time period of the simulation that began at 1200 UTC (0500 MST) on 13 February 1997. The black line denoted by open squares indicates the observed winds from the wind profiler, interpolated to that level. The red line denoted by open circles represents the model predictions, interpolated to the same location as the wind profiler. The green line denoted by closed circles represents the assumption that the winds are constant for the duration of the simulation. Thus, the value of the green line equals the value of the black line at the initial time and remains constant through the time period. This is to illustrate the assumption that the winds do not change with time. Figure 3b is the same as Figure 3a, except that it is a time series of the wind speed at 1072 m AGL instead of wind direction.

### 3.1 Upper air winds

We begin by examining the wind direction at 1072 m AGL, plotted in Figures 3a - 27a. The model gives reasonable predictions of the wind direction at this level for the first several simulations, and even captures the observed wind shift at 2100 UTC on 13 February. Beginning with the simulation that starts at 0000 UTC on the 14th (Figure 5a), the model predicted wind direction tends to veer from the North-northwest to the North-northeast five or six hours into each simulation. Sometimes the wind directions continue to veer through the end of the simulation, for example Figures 5a, 10a, 12a, and 13a, while in other runs the wind direction returns to the North-northwest. After the model was initialized from a cold start at 1200 UTC on the 16th (Figure 15a), the wind does not veer, but a number of the runs that begin somewhat later also exhibit odd wind direction changes after five to six hours into the simulation, just after the data assimilation ends and the model continues in the prognostic mode.

The model predictions of wind speeds, Figures 3b - 27b, generally compare well to the observed wind speeds during the data assimilation period of the first four hours of each run and Figure 12b is an example of a run where the winds speeds are reproduced well. In both runs where the model was initialized from horizontally-homogeneous fields (cold start) the predicted wind speeds were consistently too low (Figures 3b and 15b). This is a reflection a limitation of the horizontally homogeneous initialization in HOTMAC, where initial winds are determined by a logarithmic profile that assumes low wind speeds. In the simulations where the winds veer through the run, the wind speed drops with the shift from North-northwesterly to North-northeasterly, and then increases as the winds continue to veer. When the winds veer and then shift back to the north-northwest, the wind speeds tend to drop to very low magnitudes (i. e. Figure 10b).

Both the upper level wind speeds and wind directions predicted by HOTMAC have displayed some sort of oscillations in a number of the simulations, which are not consistent with the observations. These occur after the data assimilation period and indicate that there may be a problem with nudging the model solution in these runs. The problem may be that the nudging factor is set too high in the model setup and the model solution during the assimilation period is nudged too strongly toward the observations. Alternatively, the problem may be due to the fact that the data used for the nudging is concentrated in Rush Valley and Tooele Valley, a relatively small portion of the entire domain.

### 3.2 Surface winds

Figures 3c-3f give the time series of wind direction, wind speed, u-component of the wind, and v-component of the wind (respectively) for the observations at surface station number 1 and for the model predictions at 10 m AGL. The black line with the open squares is the data observed at station 1. The red line with the open circles is the model predictions interpolated to the same location



as station 1. The green line with the closed circles represents the winds observed at surface station 8 at the initial time and held constant for the length of the simulation. This is to illustrate the assumption that a single wind observation, which does not change with time, represents the wind in the region for the length of the simulation. This is the assumption that is used by Gaussian Plume models like D2PC. (It should be noted that for the simulation that began at 0600 UTC on 18 February the station 8 data were missing and the initial winds from station 1 were used to illustrate the constant wind assumption.) Stations 1 and 8 are both located on Deseret Chemical Depot and are maintained by the Army. Station 8 is the surface station closest to the wind profiler and a station very likely to be used for input wind observations to D2PC. Station 1 was just chosen to illustrate the time series of the model predictions and the observations because it is on the depot but not co-located with station 8. It is roughly 2.5 km south of station 8. To include this time series for all the surface stations and each simulation would be too cumbersome and examination of root mean square errors as they varied from station to station did not indicate that the model predicted consistently better or worse at any particular stations.

The time series of wind directions at station 1 that are presented in Figures 3c - 27c indicate that the observations of surface wind directions can be highly variable. The model predictions sometimes follow the character of the observations but may miss the timing of the wind direction changes somewhat. Some examples include Figures 4c, 17c, and 25c. There are also instances when the model winds and the observed winds change, but the model direction changes are larger than observed. In a few of the runs, some of the veering that occurs at the 1072 m level can also be seen at the 10 m level at station 1 (Figures 21c and 22c)

The HOTMAC predicted wind speeds generally agreed with the observations at station 1 better than the wind directions (Figures 3d - 27d). Again the cold starts, Figures 3d and 15d, indicate a bias of underpredicting the wind speeds when the horizontally homogeneous initialization is used. There are a number of times where the observations indicate wind changes that the model does not predict. These instances seem to be related to synoptic-scale disturbances that HOTMAC cannot predict and not thermally-driven, mesoscale circulations, such as slope flows. Some examples occur from 2000 UTC on the 15th to 0100 UTC on the 16th, from 1700 UTC on the 16th to 0300 UTC on the 17th (when the remnants of a front approached from the east), and most notably from 0600 to 1200 UTC on the 18th (which is also a time period when the wind direction changes significantly). A series of synoptic disturbances is not unusual for this time of year, but the HOTMAC model is not capable of including synoptic-scale disturbances, unless they can be fully resolved, temporally and spatially, in the data used for assimilation. With the current observations concentrated in a small portion of the model domain, HOTMAC is not likely to know of synoptic systems, such as the short waves or the precipitation that occur later in the study period.

Examining Figures 3e- 27e and Figures 3f - 27f, it appears that the model predictions of the magnitudes of the u-component and the v-component of the wind are similar to the observations. The differences between the predicted and observed magnitudes of the individual components of the horizontal wind may be reasonable but, when the two components are combined to give the wind direction, their errors are combined. The effect of synoptic disturbances can also be seen in the individual u- and v-components.

### 3.3 Root mean square errors

Figures 3g-3j give the time series of the rmse in wind direction, wind speed, u-component of the wind, and v-component of the wind (respectively) from all the surface stations. The red line with the open circles represents the rmse between the model predictions interpolated to the obser-

vation location and the observation at that station, over all surface stations with data at that time. The green line with the solid circles represents the rmse between the assumption of a constant wind equal to the wind at surface station 8 (except Figure 22 where station 1 data are used) at the initial time and the observations at all stations with available data.

The time series of rmse in the surface wind directions given in Figures 3g - 27g indicate that the model predictions and the assumption of constant winds have similar errors. Almost all of the errors are greater than 30 m/s. The errors tend to be larger during the synoptic events, if the events occur later in the simulations, but the errors are not as high if the synoptic events occur during the data assimilation period. There is only a slight indication of a tendency for the errors to increase as the simulations progress.

The time series of rmse in the surface wind speeds found in Figures 3h -27h show that the errors for the model and the constant wind assumption both tend to be around a few meters per second. The bias in wind speeds with a horizontally homogeneous initialization are evident, especially in Figure 3h when the observed winds were relatively strong. The errors in Figure 15h begin smaller but increase as the observed winds increase, later in the simulation.

The rmse of the u- and v-components of the winds (Figures 3i - 27i and Figures 3j -27j) do not indicate any trends in the errors. Again, the errors in the individual components are small but their combination produces larger errors in the wind direction.

Table 1 summarizes the results of the rmse for the surface (10 m) level. The rmse is given for the HOTMAC predicted wind speed and direction, compared to the measured wind speed and direction at each of the surface stations that reported data and over the 16 hour simulation time. The rmse produced by assuming the wind speed and direction are constant are also given for each simulation. The model predictions and the constant wind assumption had similar magnitudes in their errors compared to the observations. In some cases the model gave better results and in other cases it did not. It should be pointed out that the rmse calculations only look at errors at each point in time and do not note any added value given by the model when the model predicts a wind shift that is observed but the timing or extent is off a little.

Table 2 summarizes the results of the rmse for the 1072 m level. Each line in Table 2 represents only 16 samples because there is only one sounding reported each hour. At this level the constant wind assumption gives better wind direction results because the winds typically change more slowly above the surface. It should be pointed out that the wind at 1072 m AGL would not likely be used for Gaussian Plume models like D2PC because the releases are near the surface and surface winds would first affect the plume. For both the model and the constant wind assumption, the errors in the wind speeds are higher than at the surface, but this is not too surprising because the wind speed tends to be higher above the surface.

## 4.0 Recommendations

In a paper by Cox et al. (1998), the results of a model intercomparison were reported and the criteria that was used to measure model forecast skill was established by the United States Air Force and the Defense Special Weapons Agency. These criteria included the rmse of wind direction of less than 30 degrees and the rmse of wind speed of less than 1 m/s when the winds were light (with magnitudes less than 10 m/s) and a rmse of less than 2.5 m/s when the winds were stronger (with magnitudes greater than 10 m/s). The results reported above show that HOTMAC meets these criteria only occasionally. While most models would fail to achieve these criteria the

majority of the time, the results reported here do indicate that there is a great deal of room for improvement in HOTMAC's predictions. Thus it is recommended that further work with the model continue in order to improve its performance. In particular, the source of the apparent oscillations in the winds should be investigated. This may simply be due to the nudging factor being set too high. The best value of the nudging factor is often determined by trying a range of values.

Another recommendation is to include regional meteorological observations in the data assimilation. One explanation for the apparent wind oscillations could also be that the data that is assimilated is physically located within a small portion of the entire model domain. The data assimilation technique that was added to HOTMAC for this application was based on the "obs nudging" described by Stauffer and Seaman (1990, 1991, and 1994). This is the nudging technique that incorporates point observations based on the distance between the observation and the individual model grid points. However, this is just one of the two nudging techniques employed by Stauffer and Seaman and they applied it to their smallest grid to make use of local observations that were collected at irregular intervals. They also used "analysis nudging" that used nudging toward gridded analyses based on synoptic observations and interpolated to the model's current time step. They applied the "analysis nudging" to their large grid to successfully include mesoalpha-scale forcings on that grid. For the work reported here, the "analysis nudging" technique was not possible because it was not possible to make the synoptic and regional scale observations available to the model. This data and other gridded analyses, such as ETA model forecasts, are available from the internet, but the computers where HOTMAC would be run did not have access to the internet. The use of "analysis nudging" on the large grid would help HOTMAC incorporate the larger scale forcings from the short-wave disturbances that pass through the region and may eliminate the model's tendency to have the wind veer with time.

This preliminary test of HOTMAC indicates that there are times when the model should be started without using the previous forecast. Currently, the "cold" initialization for HOTMAC is quite simple, assuming not only horizontally homogeneous initial fields but also assuming that there are only two layers in the thermal structure with height and a simple logarithmic wind profile with a friction velocity that does not vary from case to case. The data assimilation is not enough to overcome the severe limitations that such an initialization imposes on the model fields. Therefore it is recommended that the "cold" initialization be improved to at least accept an observed wind and temperature vertical structure.

There are also recommendations with regard to the meteorological observations that are collected by the Army on Deseret Chemical Depot and by Tooele County. First, there seems to be no Tooele County plan to maintain and calibrate the meteorological instruments at their stations. Proper maintenance of the equipment is crucial to providing data that is of value to the model. Poor quality data could do more harm to the model predictions than no data at all. Secondly, it is recommended that all the data undergo systematic quality control. To use the modeling system in an operational setting, some sort of automated error checking should be performed on the data and, ideally, the data should also be checked by an expert.

It is also recommended that a radar wind profiler be permanently installed at the depot to provide vertical wind and temperature information to the model and meteorologists at the depot. A sodar sounder would also be useful because the profiler routinely does not provide reliable information below several hundred meters above the surface. There can be dramatic changes in the vertical wind and temperature profiles between the surface and 300 m AGL that are important for the model initialization and data assimilation. It is also recommended that the data that was already collected between June 1996 and June 1997 be retrieved from where it is now stored and that qual-

ity control be applied to this data set. It should be placed in the data base that is accessible by the SOUNDER code so that it can be used for further tests for HOTMAC and used for analysis by the meteorologist at the depot to further understand the local meteorology.

With regard to the SOUNDER code, there are a number of improvements that are recommended. First, the 30 m tower on the depot (tower 9) is not handled properly by the SOUNDER code. There are several level where the observations are collect on this tower that could give more insight into the vertical structure of the atmosphere, but the code only reports one level and the data appears to have errors in its conversion to the units and a format needed for HOTMAC because the data does not make sense for that tower. Secondly, SOUNDER code also needs correct station elevations with respect to mean sea level for all the stations. Some of the elevations that Toole County provided were obtained with a GPS system and are inconsistent with topographic maps. Thirdly, if the temperature and humidity data are to be used in the future, the calculation of these quantities needs to be included at the Tooele County stations.

## **5.0 Acknowledgments**

This work is supported by the U. S. Army Nuclear and Chemical Agency under contract number USANCA93R01010, with James Walters as program manager. The author is grateful to Dr. James Bower and Mr. Michael Myirski for their suggestions and input on how to begin the validation of HOTMAC at Deseret Chemical Depot.

## 6.0 REFERENCES

- Cox, R., B. L. Bauer, and T. Smith, 1998: A mesoscale model intercomparison. *Bull. Amer. Meteor. Soc.*, **79**, 265-283.
- National Atmospheric and Oceanographic Administration, 1997: *Daily Weather Maps*, Climatic Analysis Center, Washington, D. C.
- Panofsky, H. A. and G. W. Breir, 1958: *Some Applications of Statistics to Meteorology*. 224 pp.
- Pielke, R. A., 1984: *Mesoscale Meteorological Modeling*. 612 pp.
- Stauffer, D. R., and N. L. Seaman, 1990: Use of four-dimensional data assimilation in a limited-area mesoscale model. Part I: Experiments with synoptic data. *Mon. Wea. Rev.*, **118**, 1250-1277.
- Stauffer, D. R., and N. L. Seaman, 1991: Use of four-dimensional data assimilation in a limited-area mesoscale model. Part II: Effects of data assimilation within the planetary boundary layer. *Mon. Wea. Rev.*, **119**, 734-754.
- Stauffer, D. R., and N. L. Seaman, 1994: Multiscale four-dimensional data assimilation. *J. Appl. Meteor.*, **33**, 416-434.
- Stone, G. L. D. E. Hoard, G. E. Start, J. F. Sagendorf, G. R. Ackermann, N. F. Hukari, K. L. Clawson, and C. R. Dickson, 1989: 1987 meteorological and tracer experiments at the Tooele Army Depot. Los Alamos National Laboratory document LA-UR-89-1157.
- Yamada, T., M. Williams, and G. Stone, 1989: Chemical downwind hazard modeling study. Los Alamos National Laboratory document LA-UR-89-1061.

TABLE 1. Root Mean Square Error of Surface Predictions

start date	start time	model speed rmse (m/s)	constant speed rmse (m/s)	model direction rmse (degrees)	constant direction rmse (degrees)
13 Feb 97	1200 UTC	3.1	1.9	88	71
13 Feb 97	1800 UTC	2.6	5.3	90	90
14 Feb 97	0000 UTC	2.0	3.6	91	110
14 Feb 97	0600 UTC	2.3	1.8	105	91
14 Feb 97	1200 UTC	2.7	3.2	119	130
14 Feb 97	1800 UTC	2.7	2.0	105	75
15 Feb 97	0000 UTC	2.3	1.8	96	81
15 Feb 97	0600 UTC	1.8	1.5	98	91
15 Feb 97	1200 UTC	1.8	1.3	100	96
15 Feb 97	1800 UTC	2.0	1.4	99	109
16 Feb 97	0000 UTC	2.0	2.5	94	83
16 Feb 97	0600 UTC	2.4	1.9	104	89
16 Feb 97	1200 UTC	3.2	3.1	86	81
16 Feb 97	1800 UTC	3.7	2.4	90	74
17 Feb 97	0000 UTC	4.2	2.9	83	68
17 Feb 97	0600 UTC	4.3	2.9	92	82
17 Feb 97	1200 UTC	3.4	3.3	88	97
17 Feb 97	1800 UTC	2.7	3.4	94	112
18 Feb 97	0000 UTC	2.0	2.2	101	79
18 Feb 97	0600 UTC	2.2	3.7	106	115
18 Feb 97	1200 UTC	1.9	2.3	113	82
18 Feb 97	1800 UTC	2.4	2.5	103	89
19 Feb 97	0000 UTC	2.4	3.9	92	118
19 Feb 97	0600 UTC	2.7	3.0	103	90
19 Feb 97	1200 UTC	3.0	3.3	105	69
average		2.6	2.7	98	91
13-19 Feb 97					

**TABLE 2. Root Mean Square Error of Predictions at 1072 m AGL.**

<b>start date</b>	<b>start time</b>	<b>model speed rmse (m/s)</b>	<b>constant speed rmse (m/s)</b>	<b>model direction rmse (degrees)</b>	<b>constant direction rmse (degrees)</b>
13 Feb 97	1200 UTC	4.1	7.3	31	20
13 Feb 97	1800 UTC	2.3	1.3	20	36
14 Feb 97	0000 UTC	4.6	2.2	72	5
14 Feb 97	0600 UTC	4.3	1.8	40	16
14 Feb 97	1200 UTC	3.0	1.7	39	16
14 Feb 97	1800 UTC	4.5	2.2	56	21
15 Feb 97	0000 UTC	5.5	3.5	36	16
15 Feb 97	0600 UTC	3.2	2.9	81	29
15 Feb 97	1200 UTC	2.3	5.4	32	15
15 Feb 97	1800 UTC	1.4	4.2	86	27
16 Feb 97	0000 UTC	7.9	2.5	103	86
16 Feb 97	0600 UTC	1.6	2.9	84	116
16 Feb 97	1200 UTC	4.7	6.4	71	148
16 Feb 97	1800 UTC	8.5	7.0	72	42
17 Feb 97	0000 UTC	8.9	3.2	92	6
17 Feb 97	0600 UTC	6.1	3.5	97	10
17 Feb 97	1200 UTC	5.0	8.4	51	26
17 Feb 97	1800 UTC	2.4	2.1	98	55
18 Feb 97	0000 UTC	2.5	2.7	124	102
18 Feb 97	0600 UTC	5.2	2.5	111	107
18 Feb 97	1200 UTC	2.6	4.0	120	24
18 Feb 97	1800 UTC	9.7	1.7	107	17
19 Feb 97	0000 UTC	8.6	2.3	125	39
19 Feb 97	0600 UTC	7.9	3.2	117	62
19 Feb 97	1200 UTC	5.4	2.8	100	37
average		4.9	3.5	79	44
13-19 Feb 97					

## 7.0 Figure Captions

FIGURE 1. Daily Weather Maps (National Oceanographic and Atmospheric Administration, 1997) for a) 13 February, b) 14 February, c) 15 February, d) 16 February, e) 17 February, f) 18 February, and g) 19 February 1997.

FIGURE 2. HOTMAC model domain and wind fields at 1206 UTC 13 February 1997 for validation tests on a) Grid 1 and b) Grid 2.

FIGURE 3. Time series of model predicted wind fields, observations, and an assumption of constant winds for the simulation started at 1200 UTC on 13 February 1997, including a) wind direction and b) wind speed at 1072 m AGL, c) wind direction, d) wind speed, e) u-component of the wind, and f) v-component of the wind at surface station 1 (10 m AGL), and root mean square error at station 1 for g) wind direction, h) wind speed, i) u-component of the wind, and j) v-component of the wind.

FIGURE 4. Same as Figure 3, except for the simulation started at 1800 UTC on 13 February.

FIGURE 5. Same as Figure 3, except for the simulation started at 0000 UTC on 14 February.

FIGURE 6. Same as Figure 3, except for the simulation started at 0600 UTC on 14 February.

FIGURE 7. Same as Figure 3, except for the simulation started at 1200 UTC on 14 February.

FIGURE 8. Same as Figure 3, except for the simulation started at 1800 UTC on 14 February.

FIGURE 9. Same as Figure 3, except for the simulation started at 0000 UTC on 15 February.

FIGURE 10. Same as Figure 3, except for the simulation started at 0600 UTC on 15 February.

FIGURE 11. Same as Figure 3, except for the simulation started at 1200 UTC on 15 February.

FIGURE 12. Same as Figure 3, except for the simulation started at 1800 UTC on 15 February.

FIGURE 13. Same as Figure 3, except for the simulation started at 0000 UTC on 16 February.

FIGURE 14. Same as Figure 3, except for the simulation started at 0600 UTC on 16 February.

FIGURE 15. Same as Figure 3, except for the simulation started at 1200 UTC on 16 February.

FIGURE 16. Same as Figure 3, except for the simulation started at 1800 UTC on 16 February.

FIGURE 17. Same as Figure 3, except for the simulation started at 0000 UTC on 17 February.

FIGURE 18. Same as Figure 3, except for the simulation started at 0600 UTC on 17 February.

FIGURE 19. Same as Figure 3, except for the simulation started at 1200 UTC on 17 February.

FIGURE 20. Same as Figure 3, except for the simulation started at 1800 UTC on 17 February.

FIGURE 21. Same as Figure 3, except for the simulation started at 0000 UTC on 18 February.

FIGURE 22. Same as Figure 3, except for the simulation started at 0600 UTC on 18 February.



FIGURE 23. Same as Figure 3, except for the simulation started at 1200 UTC on 18 February.

FIGURE 24. Same as Figure 3, except for the simulation started at 1800 UTC on 18 February.

FIGURE 25. Same as Figure 3, except for the simulation started at 0000 UTC on 19 February.

FIGURE 26. Same as Figure 3, except for the simulation started at 0600 UTC on 19 February.

FIGURE 27. Same as Figure 3, except for the simulation started at 1200 UTC on 19 February.

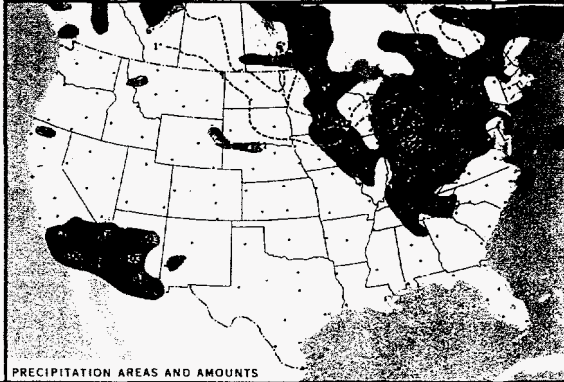
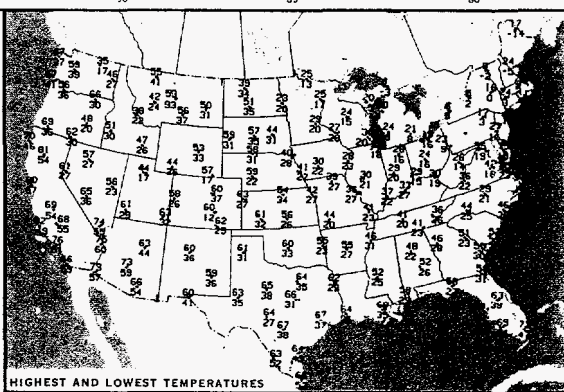
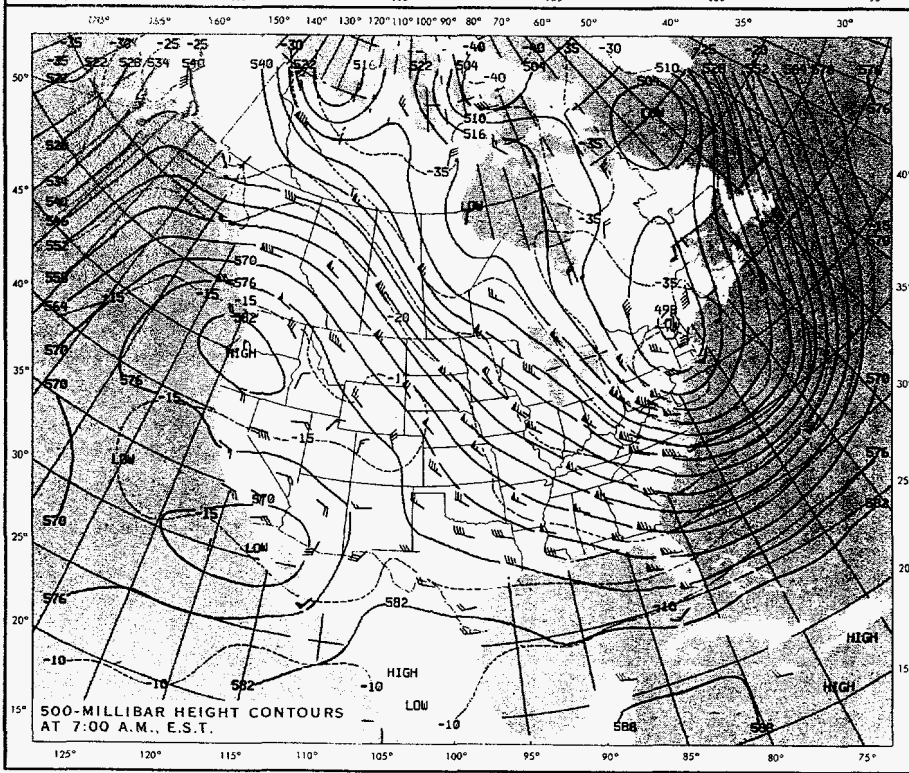
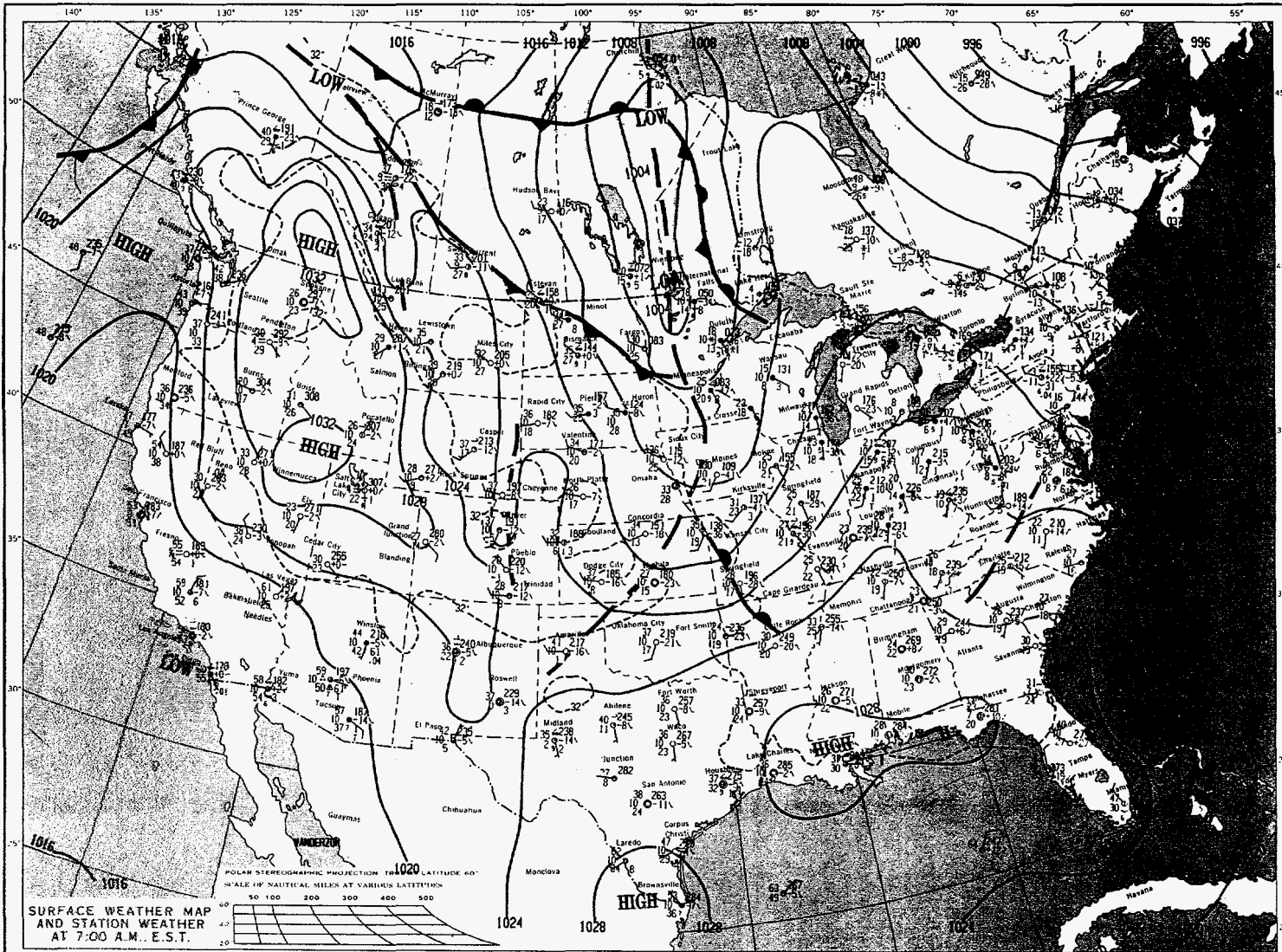


Figure 1a.

MEDNESDAY, FEBRUARY 14, 1996

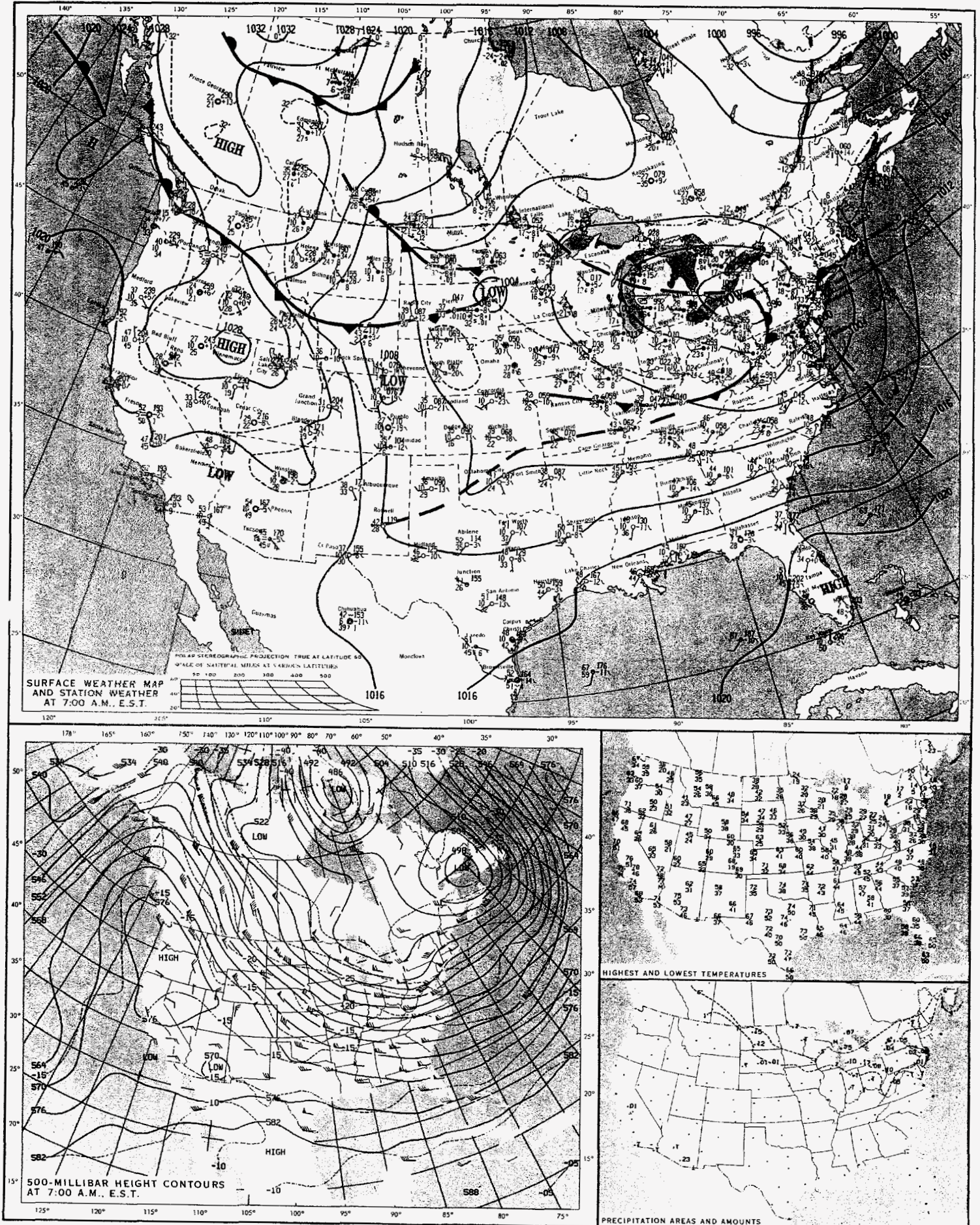


Figure 1b.

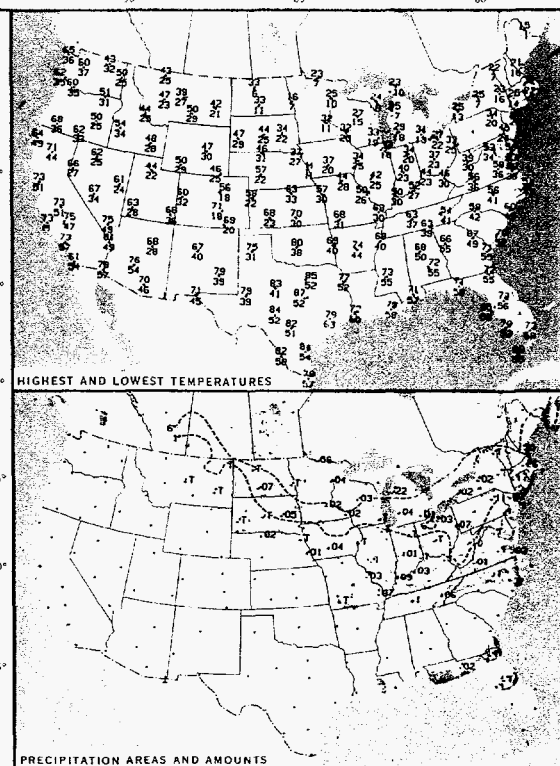
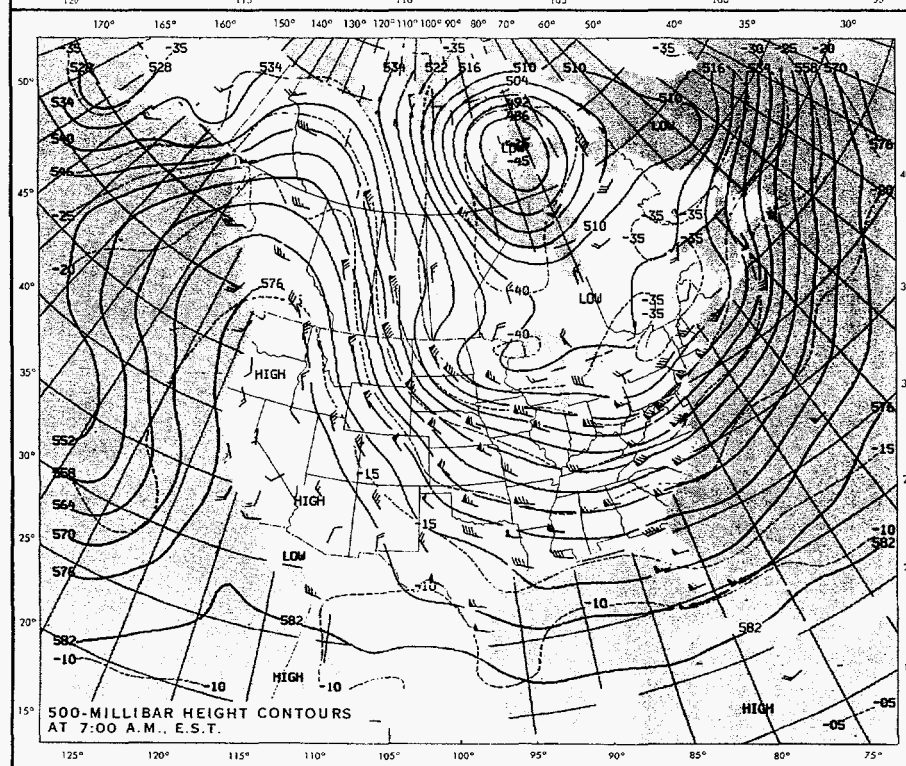
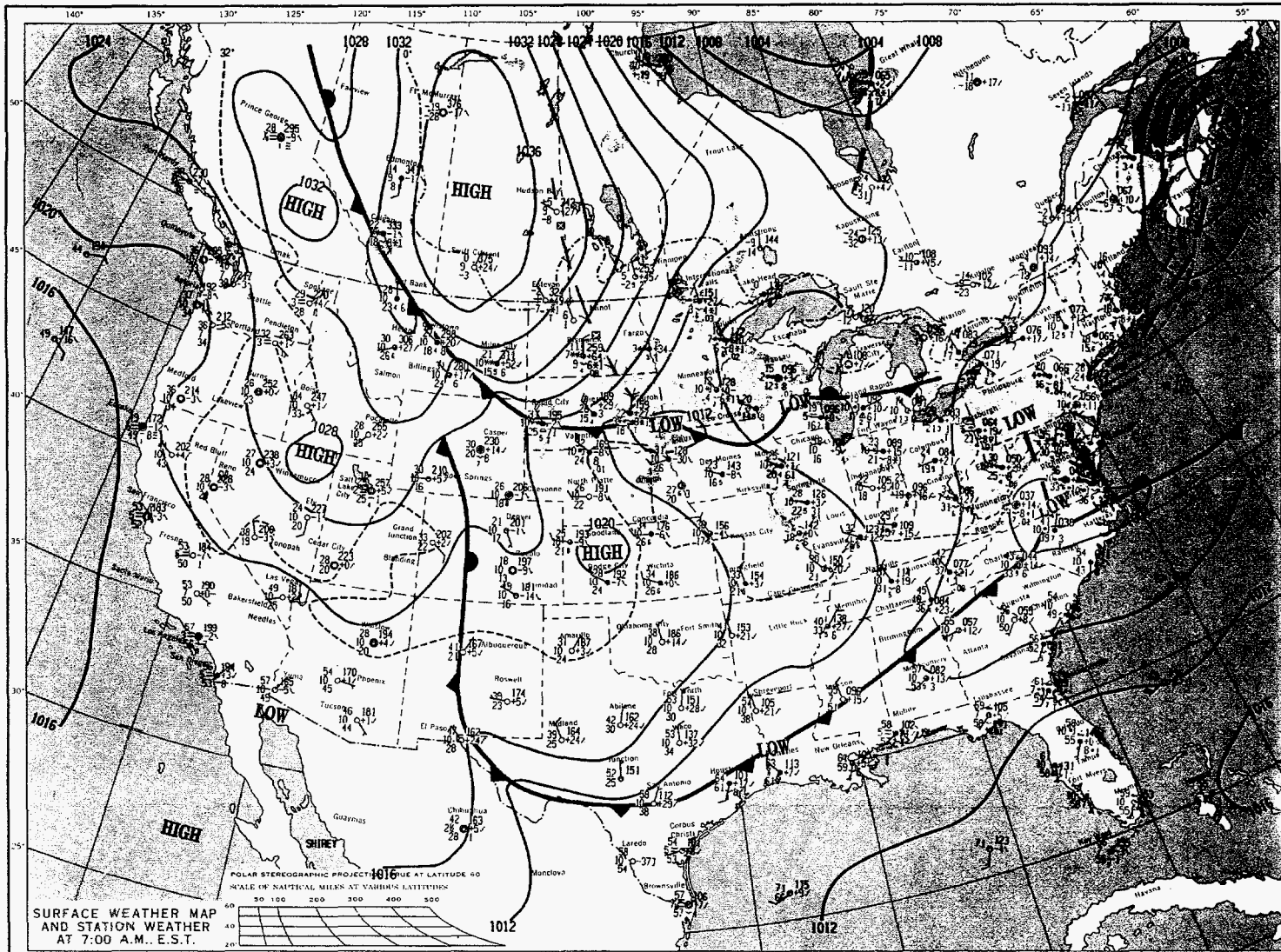


Figure 1c.

FRIDAY, FEBRUARY 16, 1996

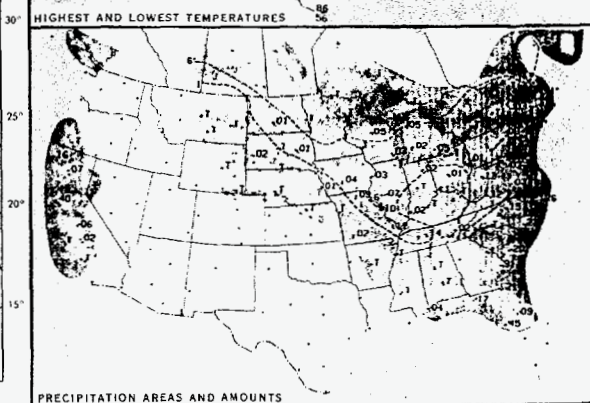
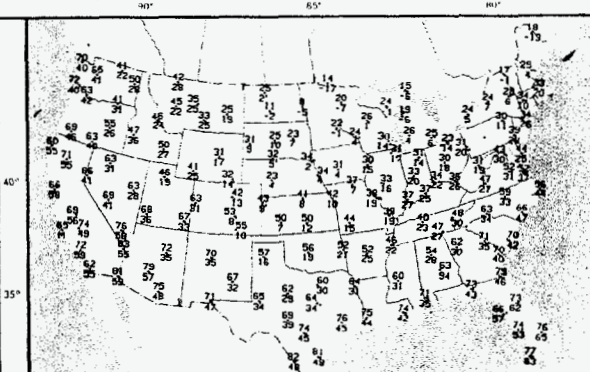
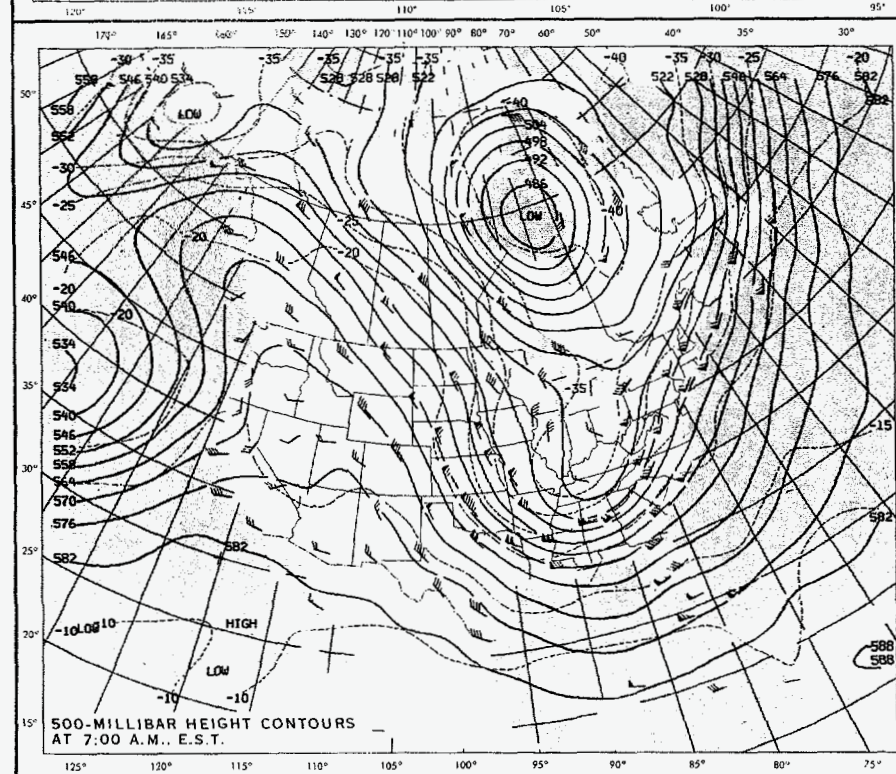
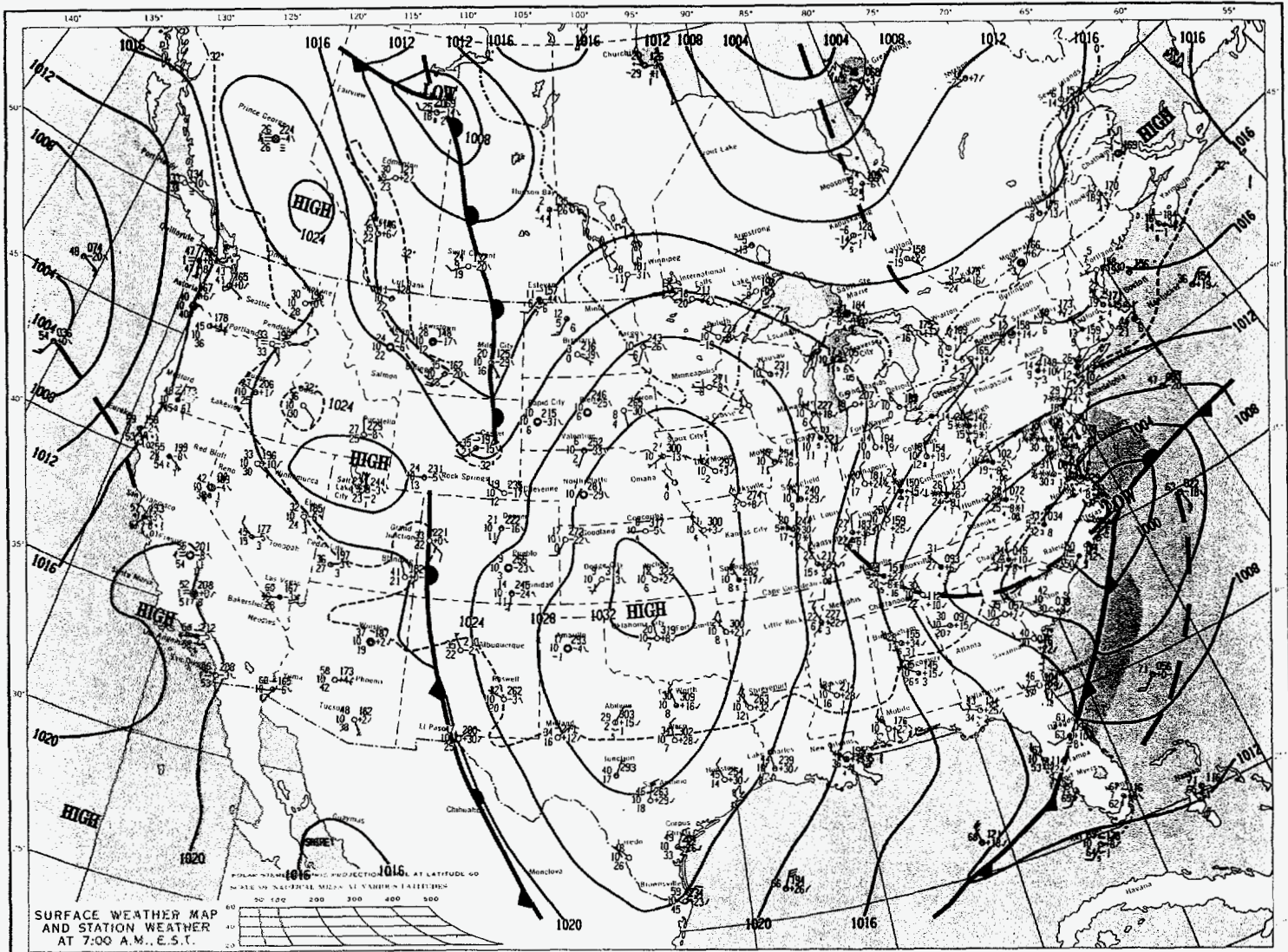


Figure 1d.

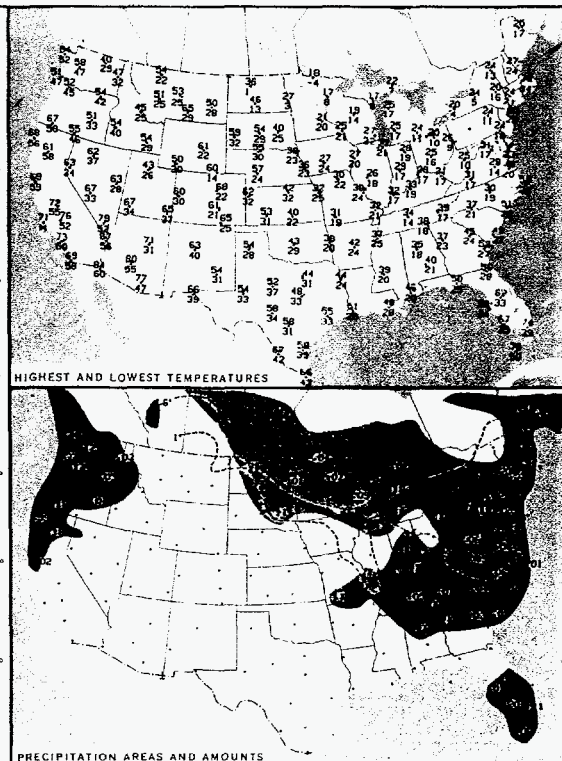
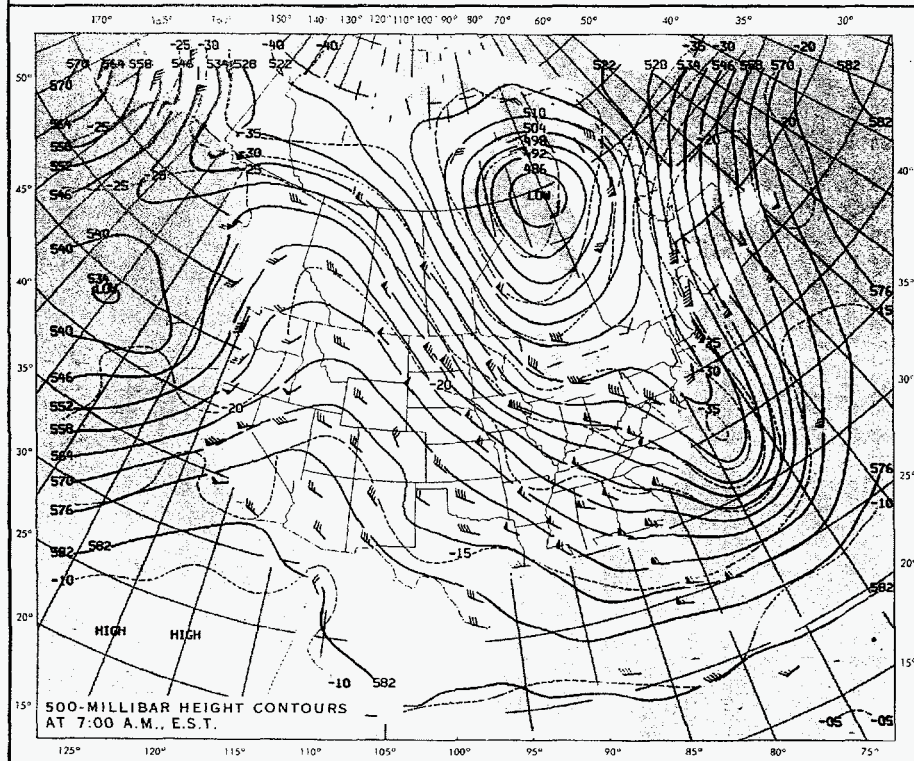
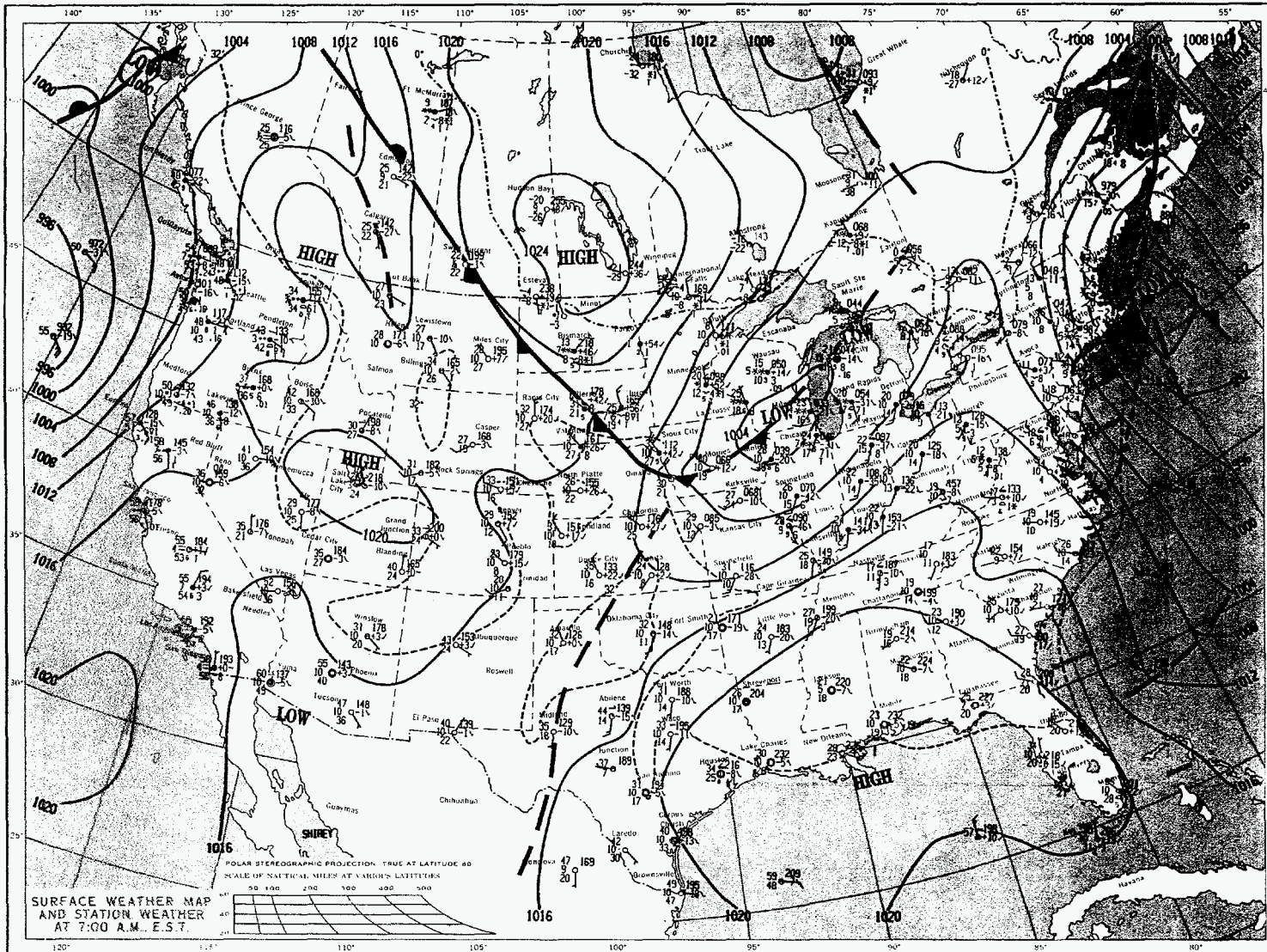


Figure 1e.

SUNDAY, FEBRUARY 18, 1996

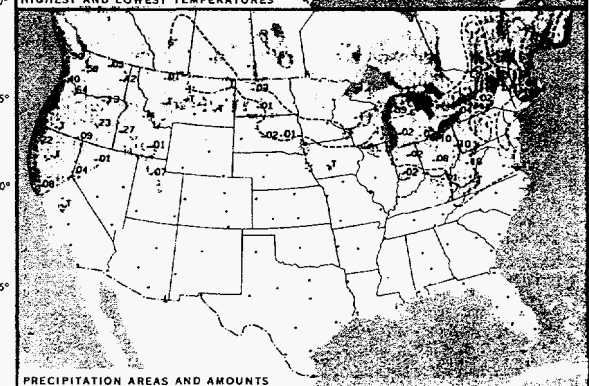
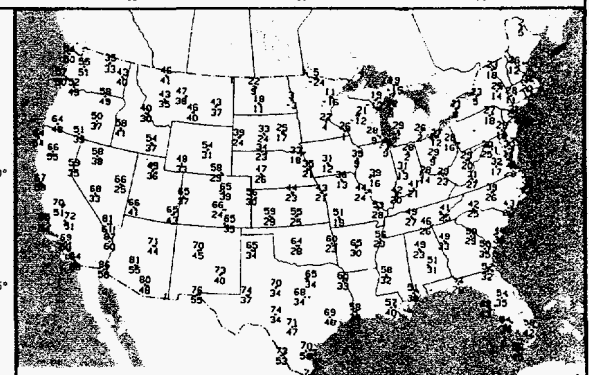
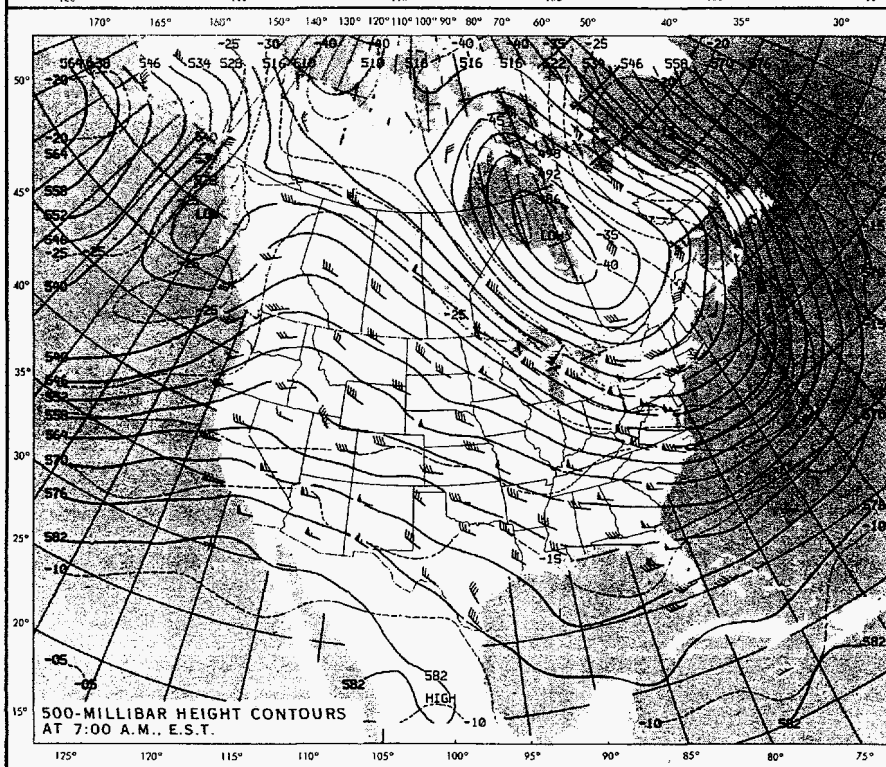
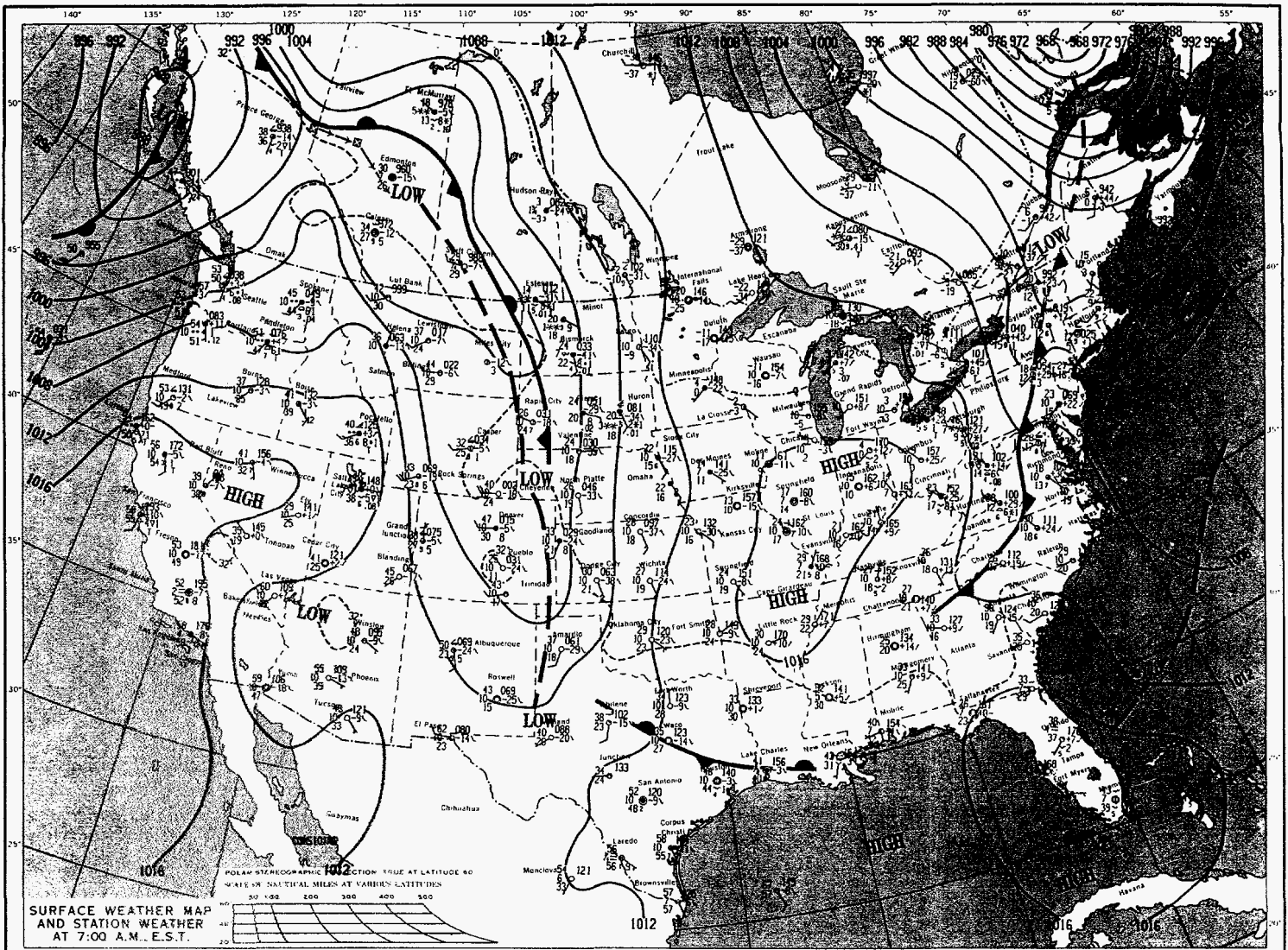


Figure 1f.

MONDAY, FEBRUARY 19, 1996

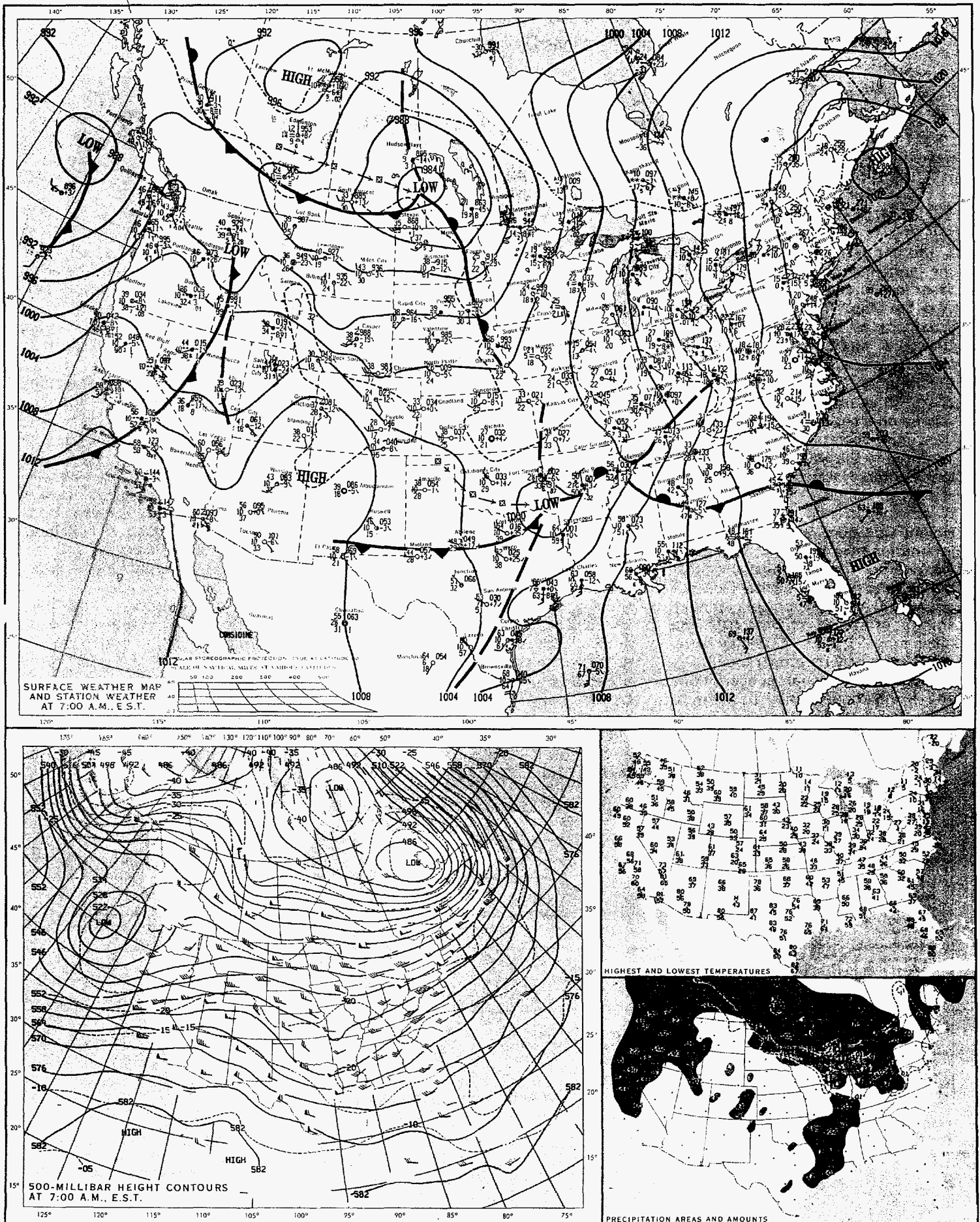


Figure 19.



height 10 m  
day 44 0506 1st

→ 5 m/s

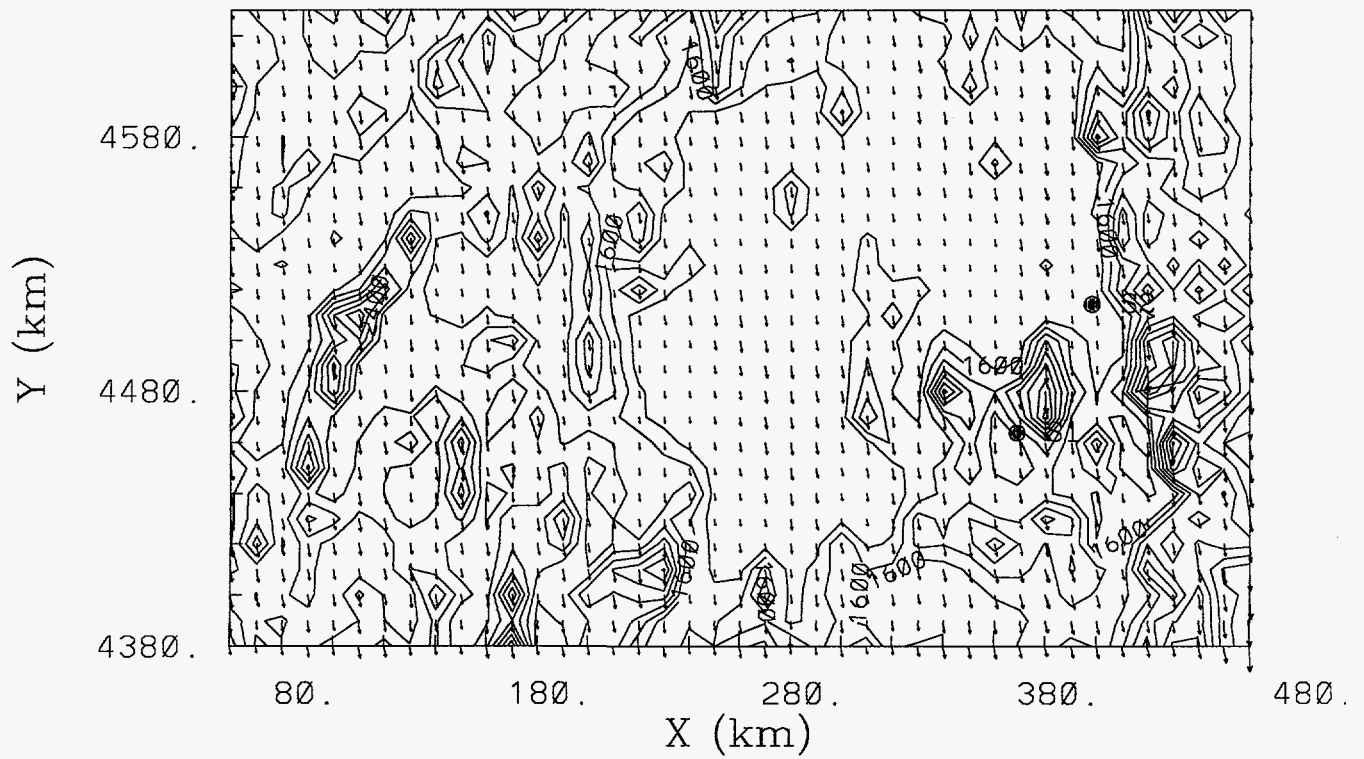


Figure 2a.

height 10 m  
day 44 0506 lst

● S2

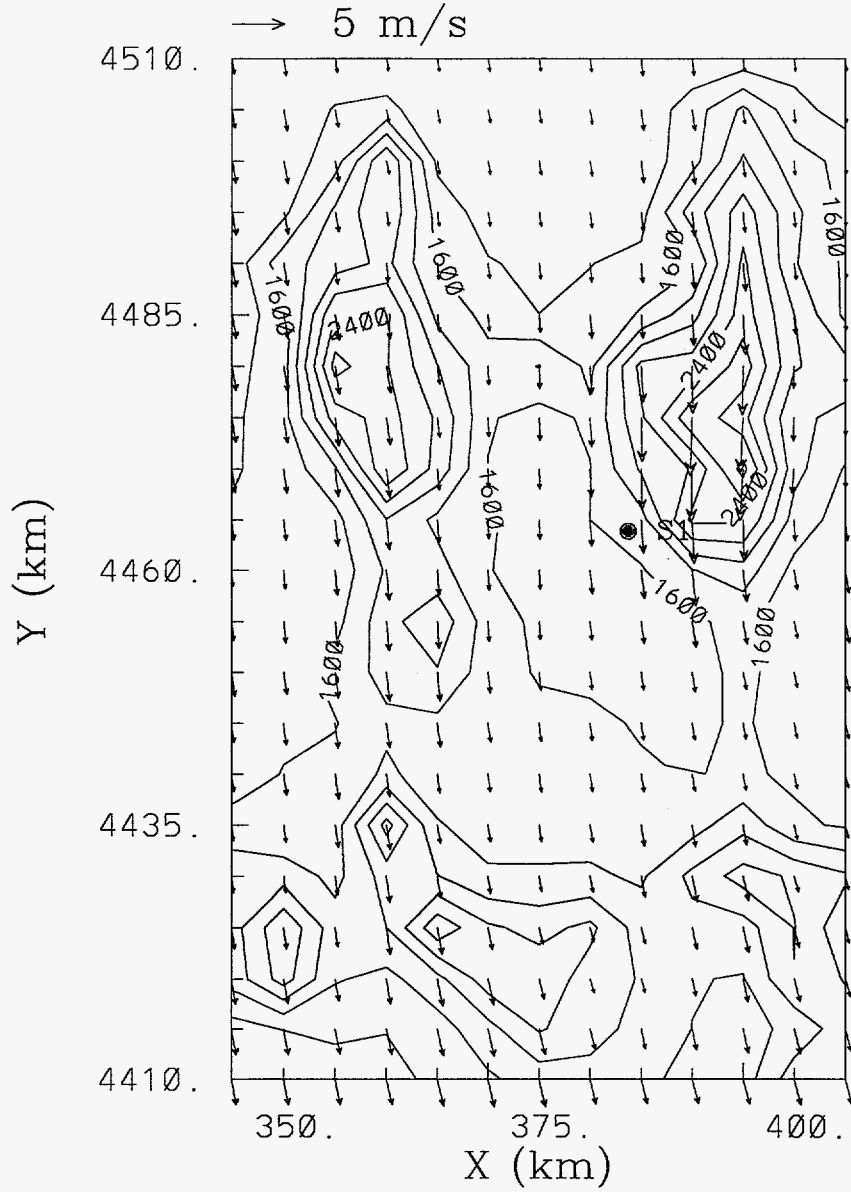


Figure 2b.

# wind direction sounding 1, 1072 m

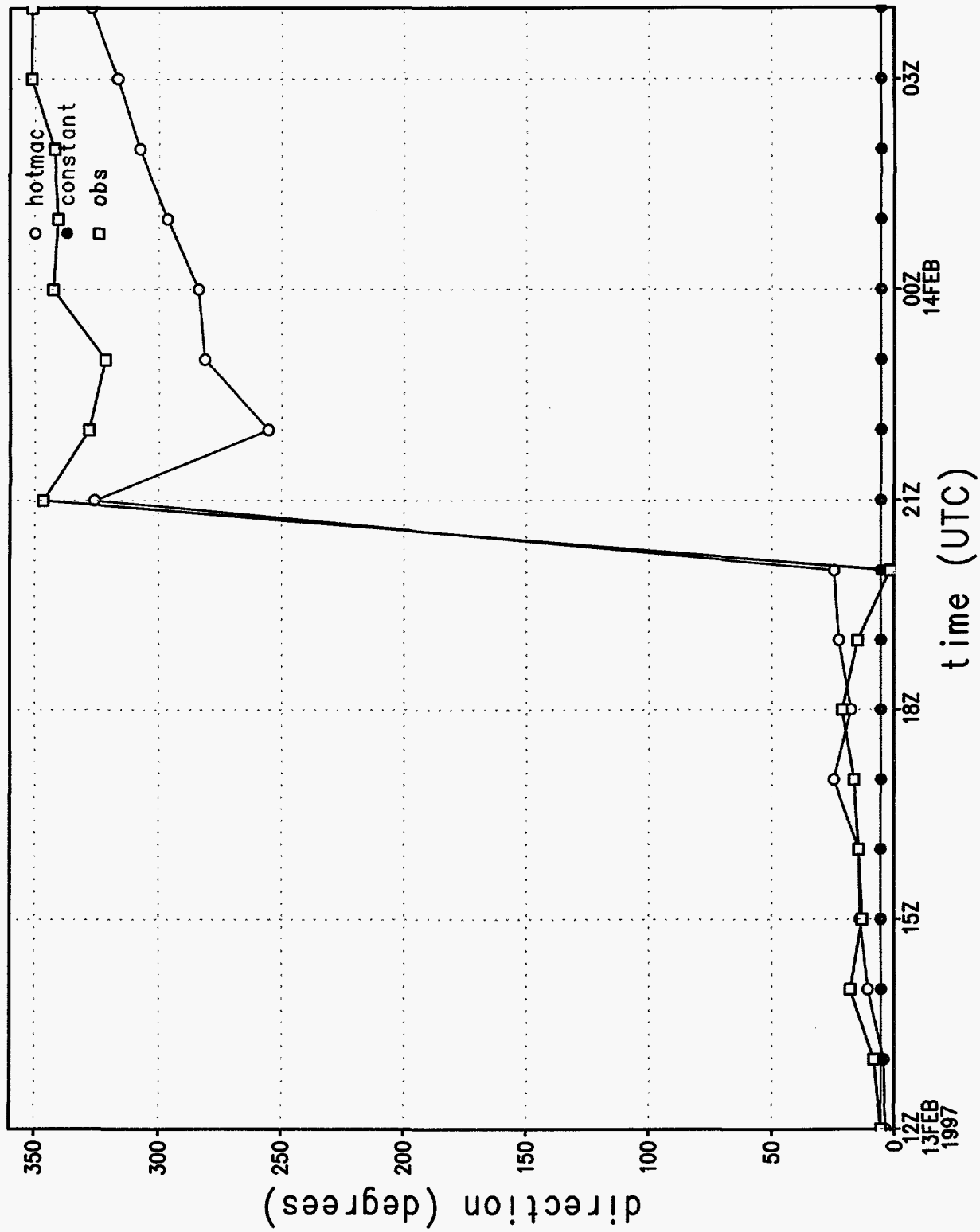


Figure 3a.

# wind speed sounding 1, 1072 m

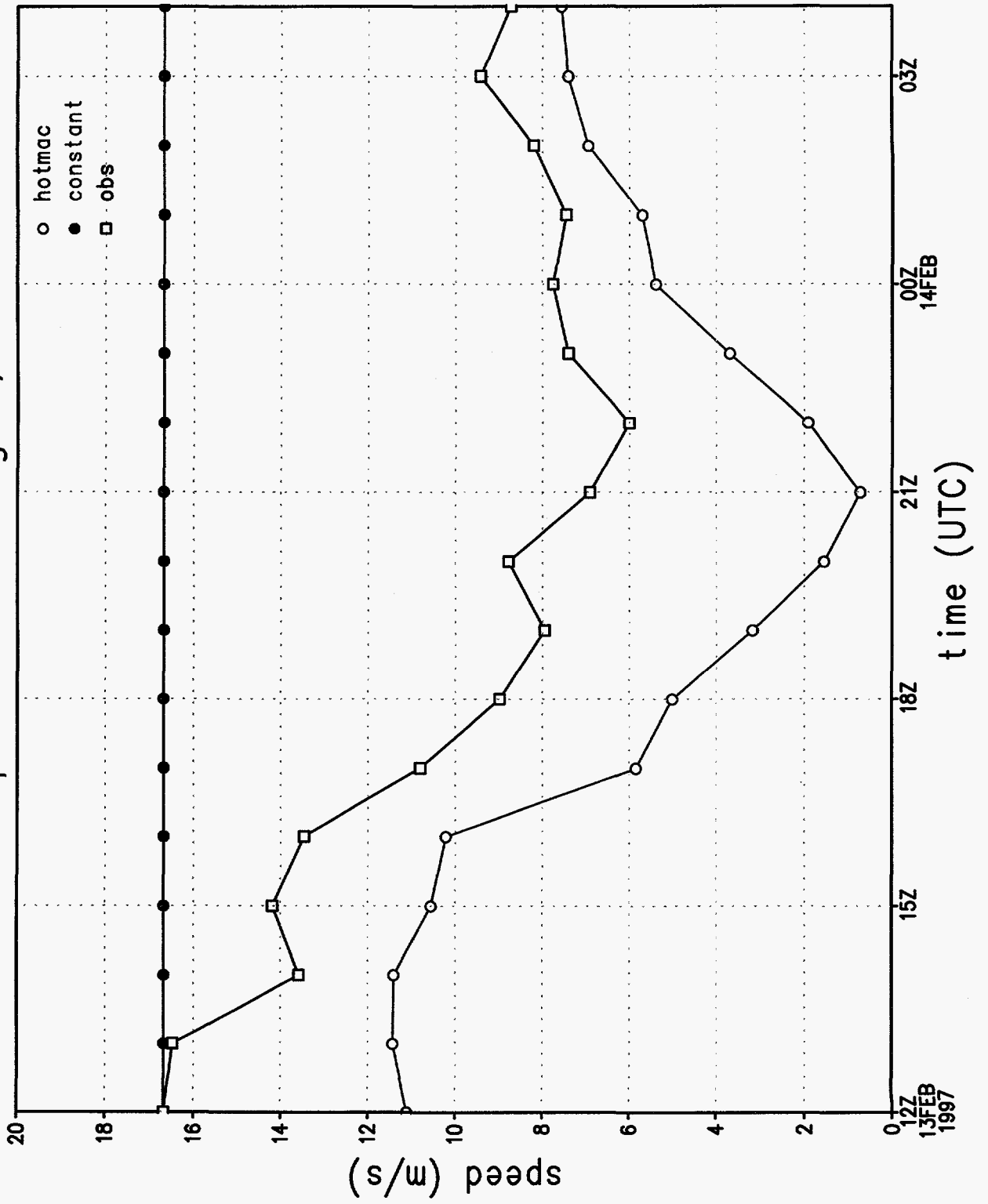


Figure 3b.

# wind direction at station 1

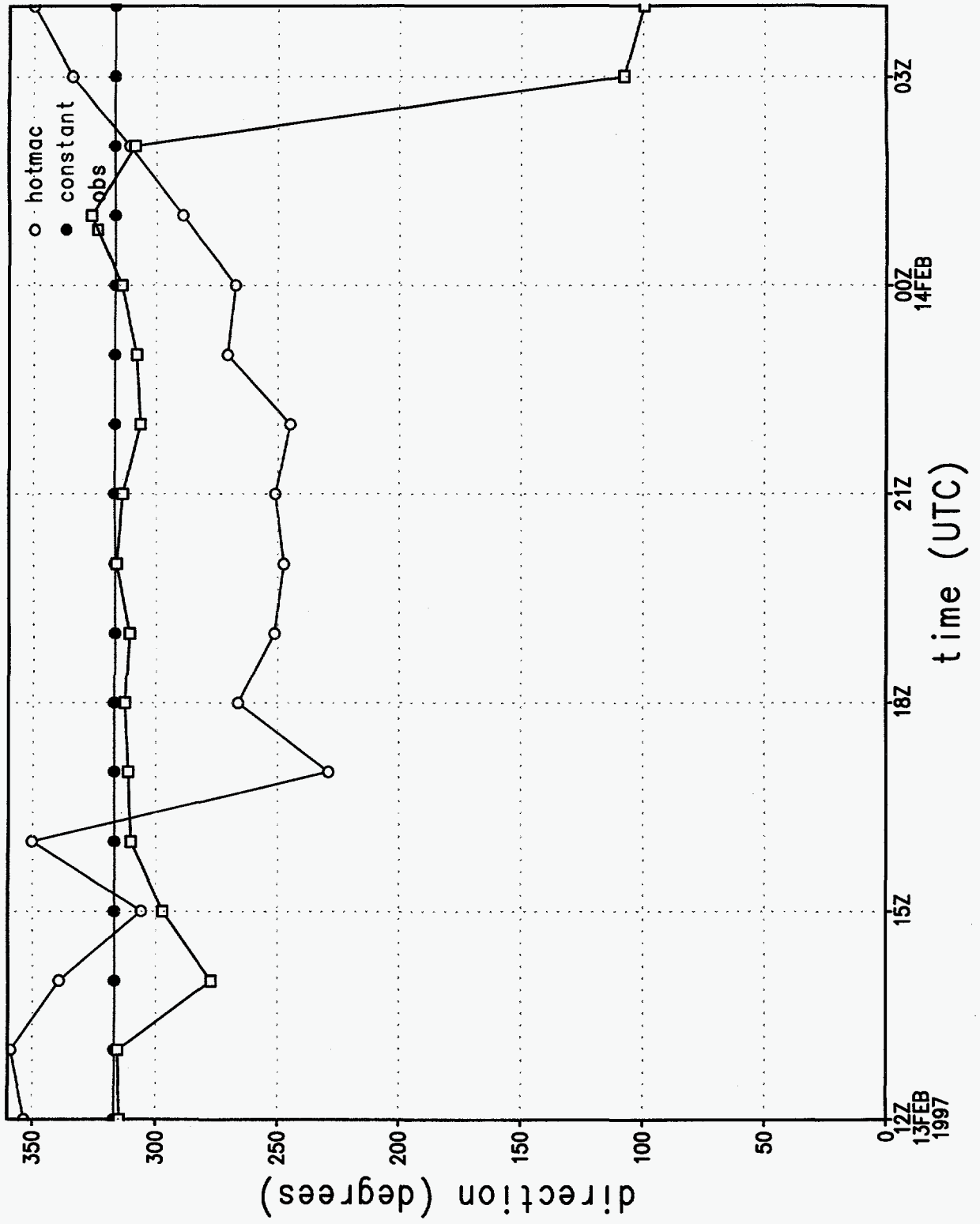


Figure 3c.

# wind speed at station 1

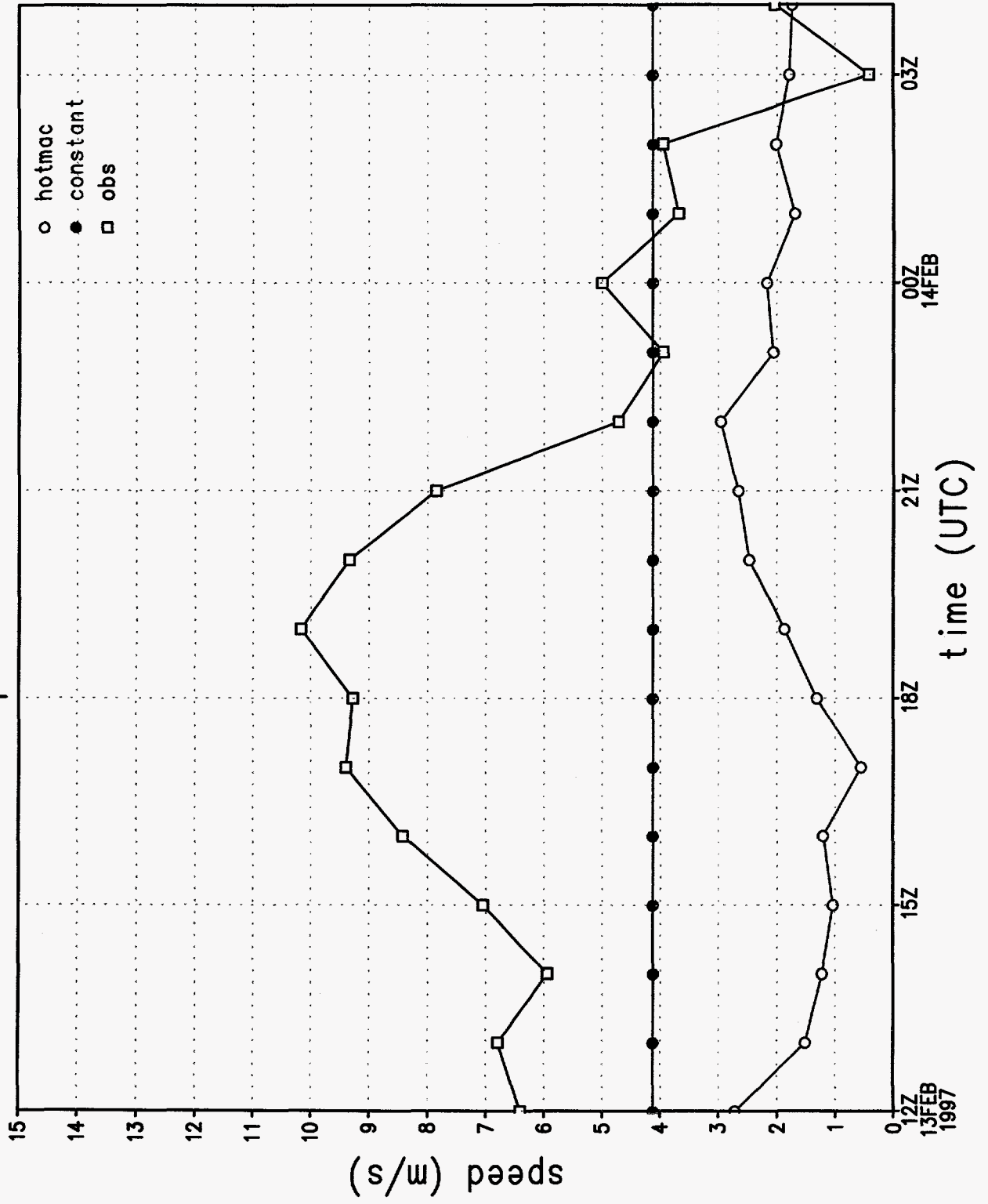


Figure 3d.

u wind component at station 1

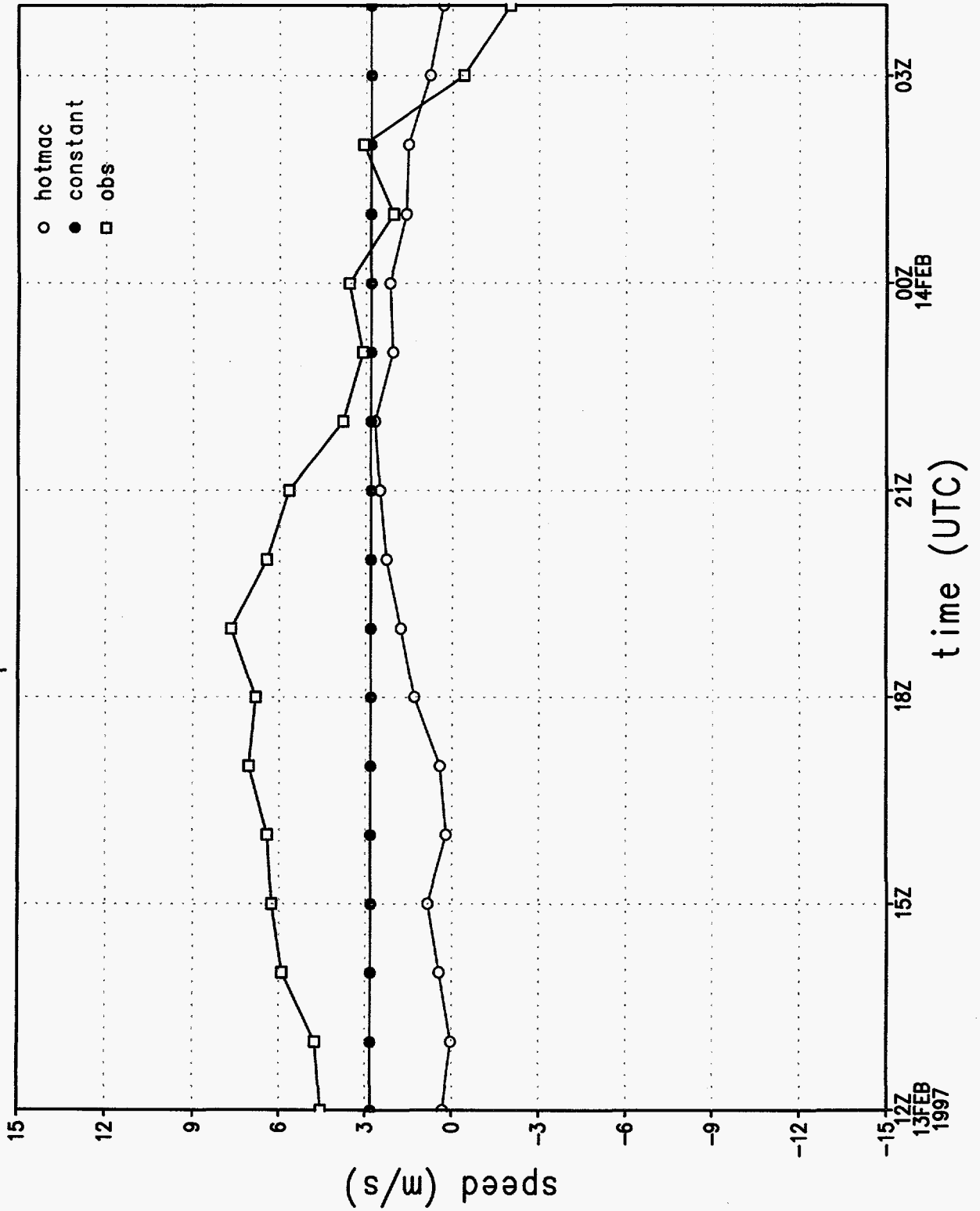


Figure 3e.

# v wind component at station 1

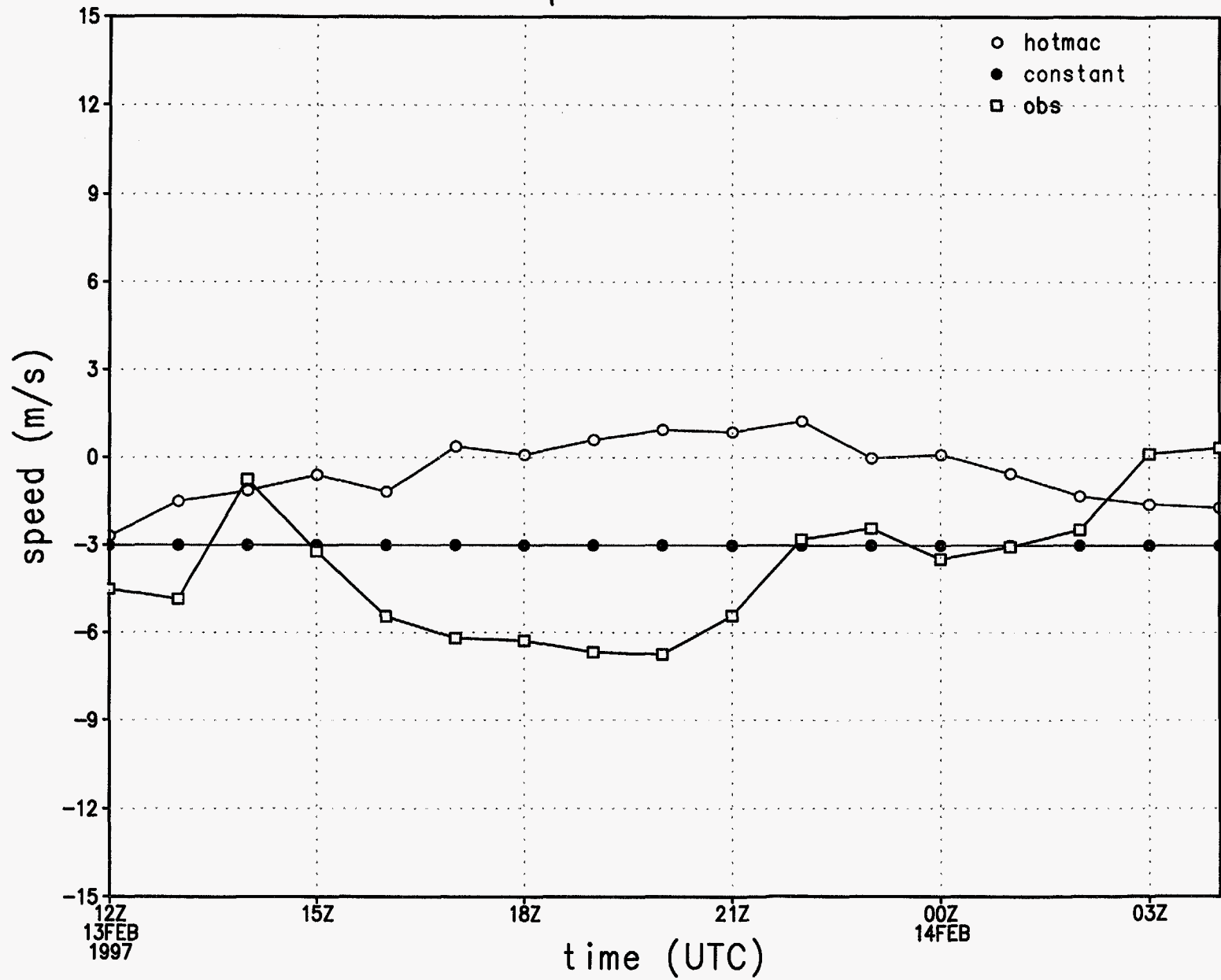


Figure 3f.



# rmse of wind direction by hour

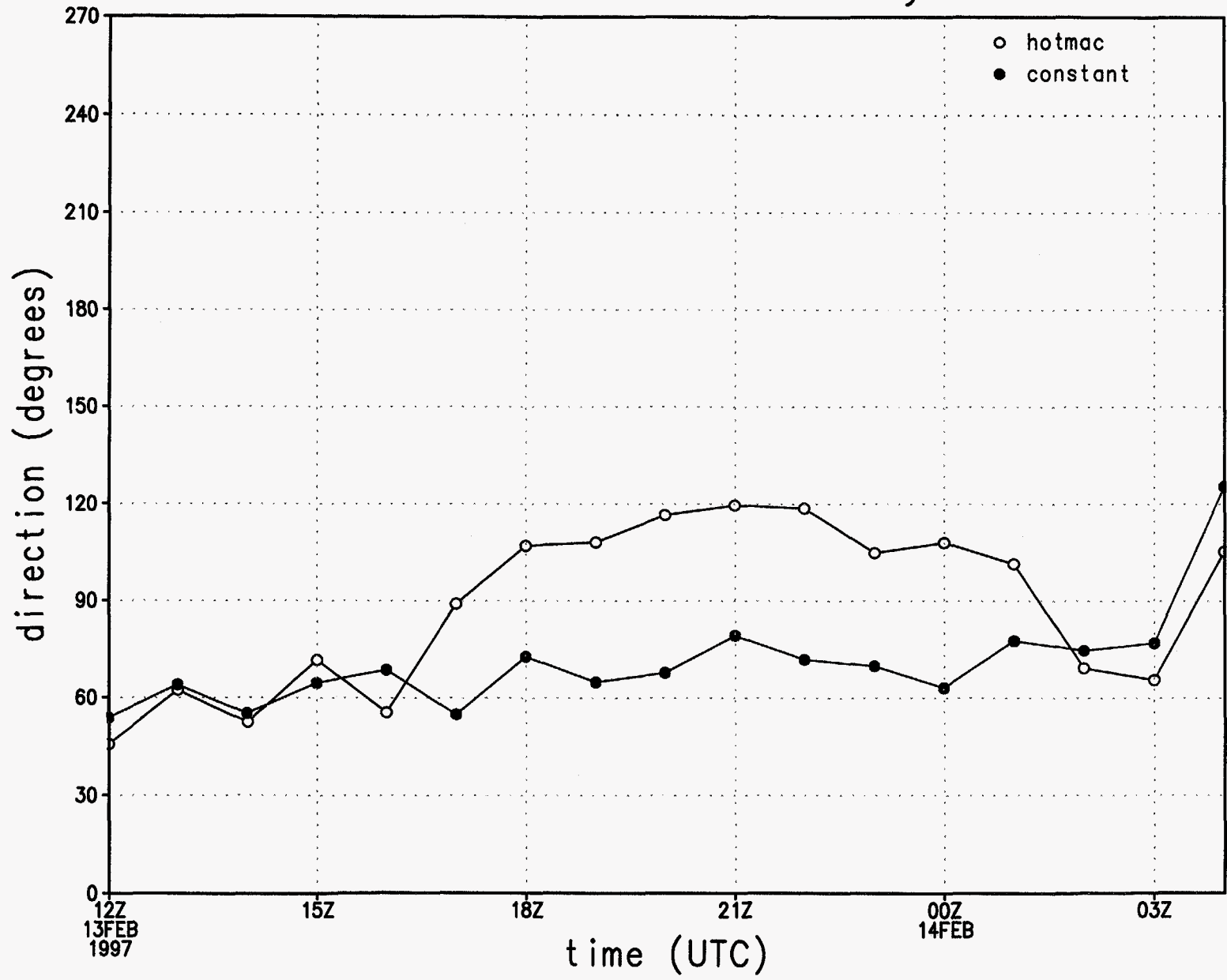


Figure 3g.

# rmse of wind speed by hour

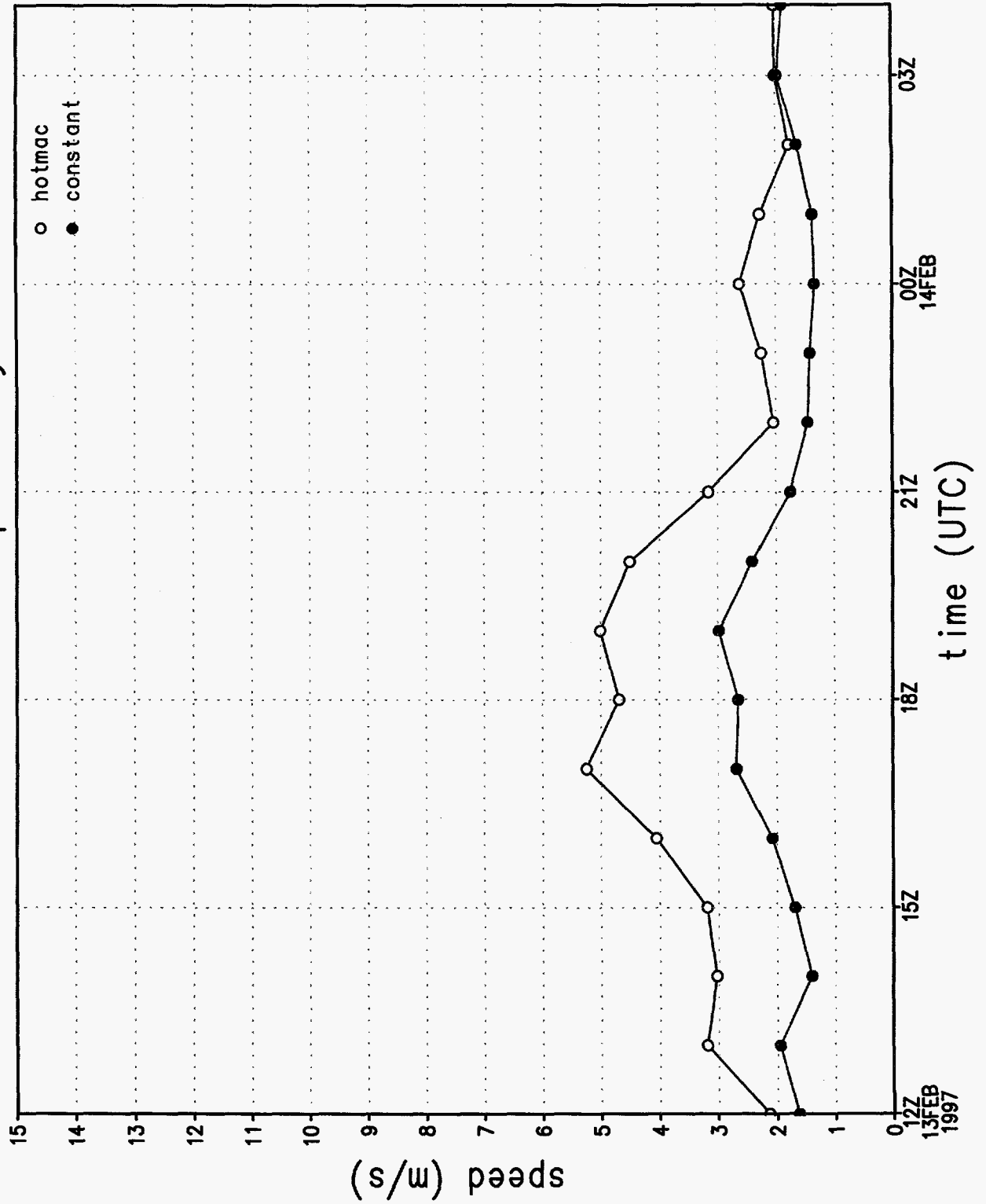


Figure 3h.

# rmse of u wind component by hour

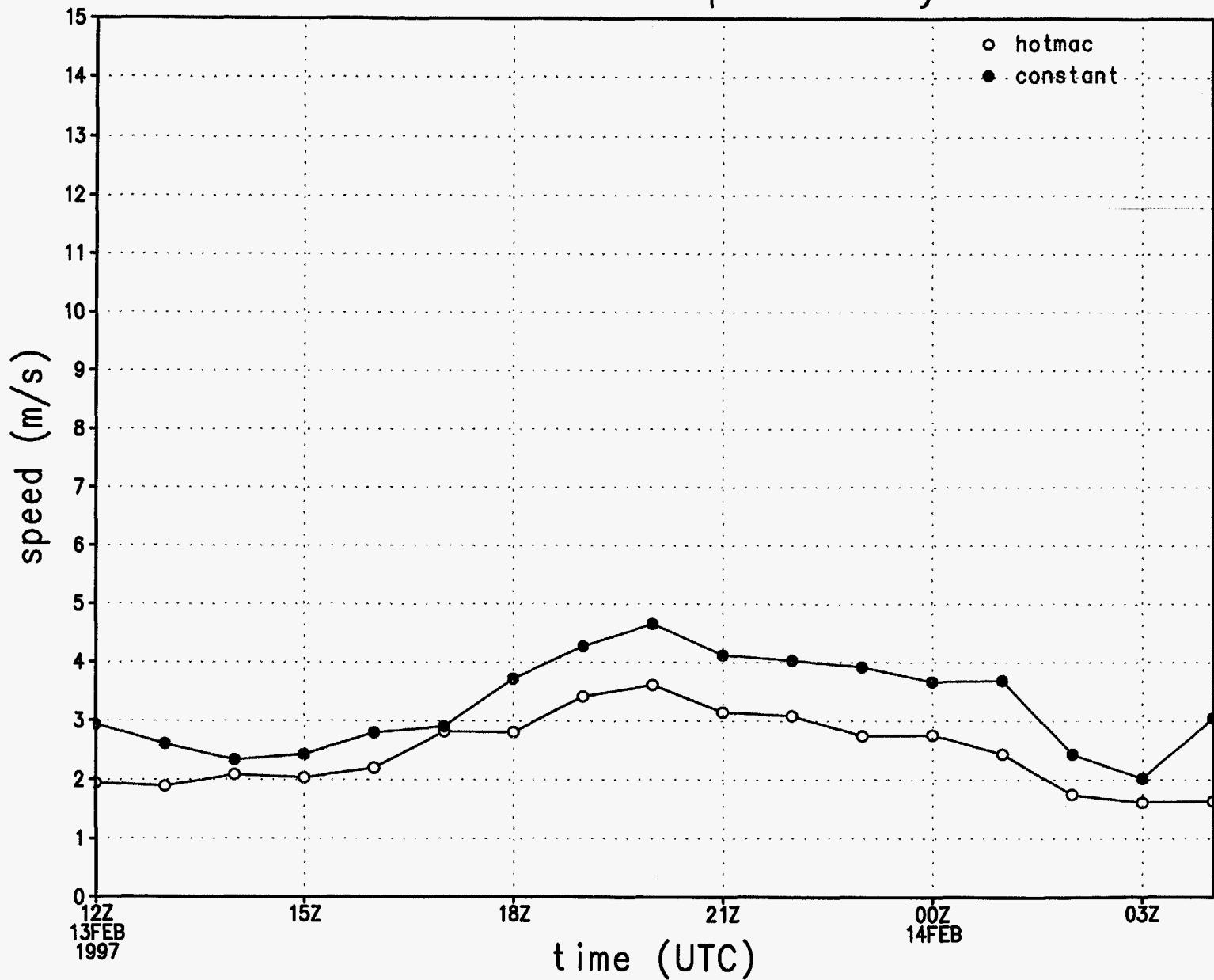


Figure 3i.

rmse of v wind component by hour

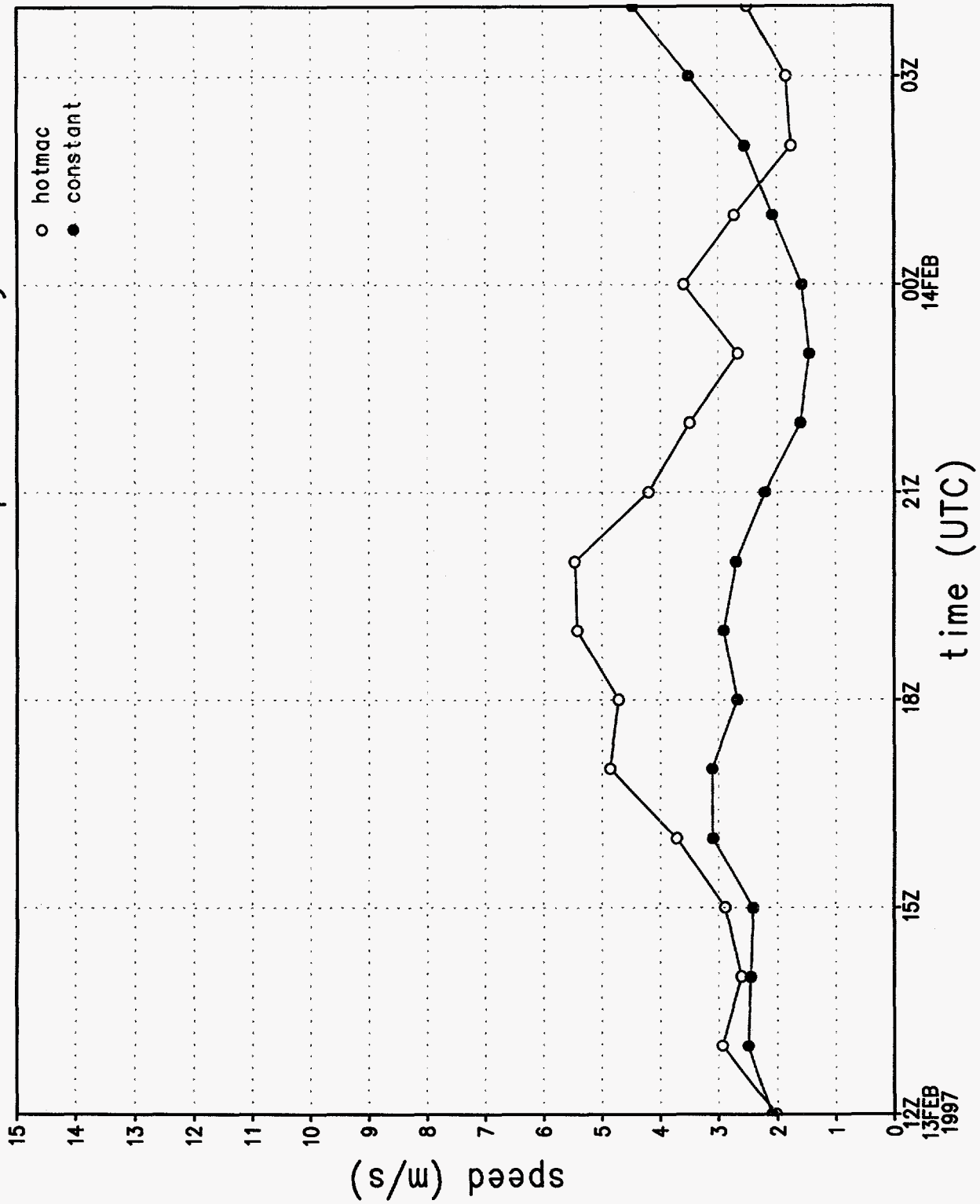


Figure 3j.

# wind direction sounding 1, 1072 m

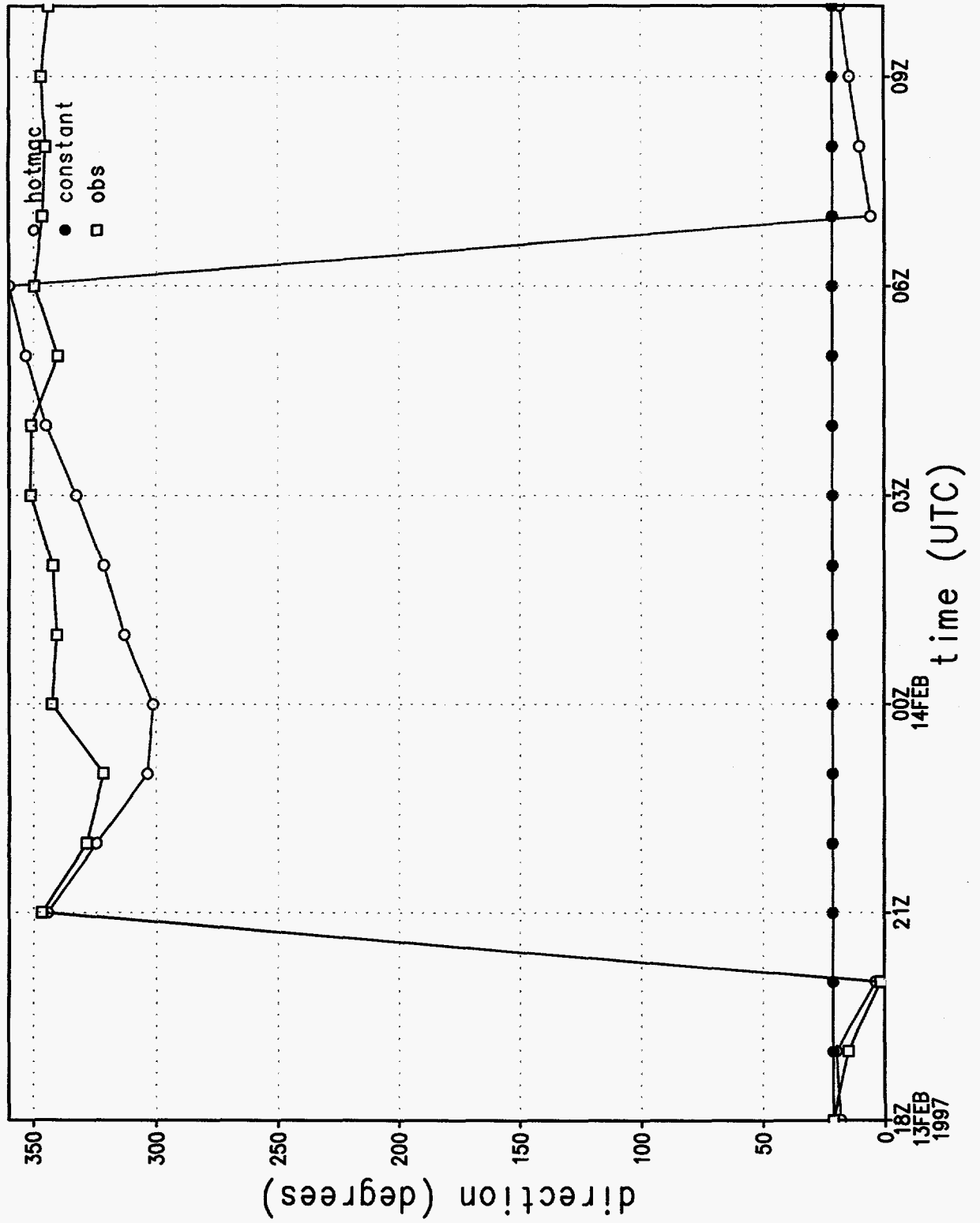


Figure 4a.

# wind speed sounding 1, 1072 m

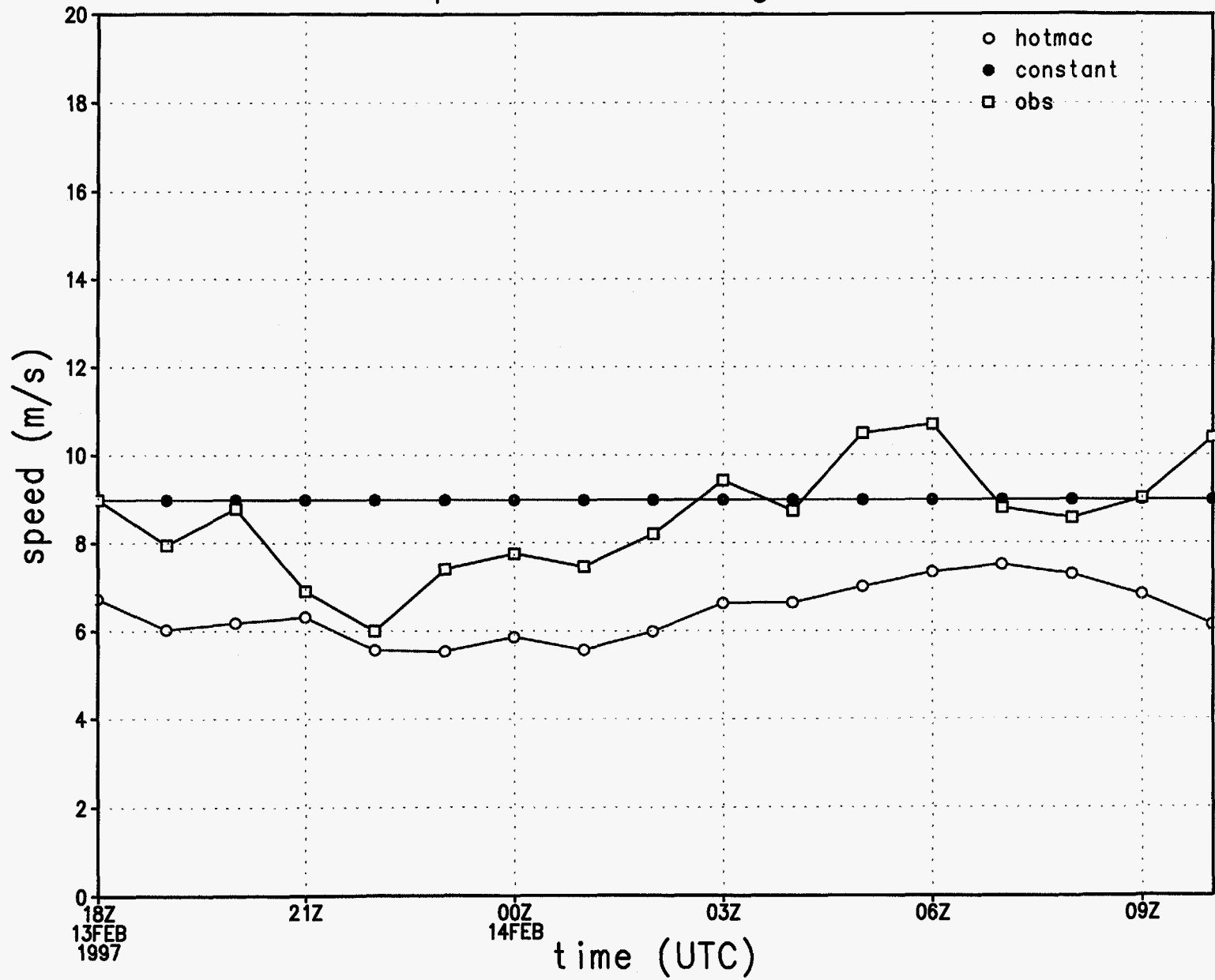


Figure 4b.

# wind direction at station 1

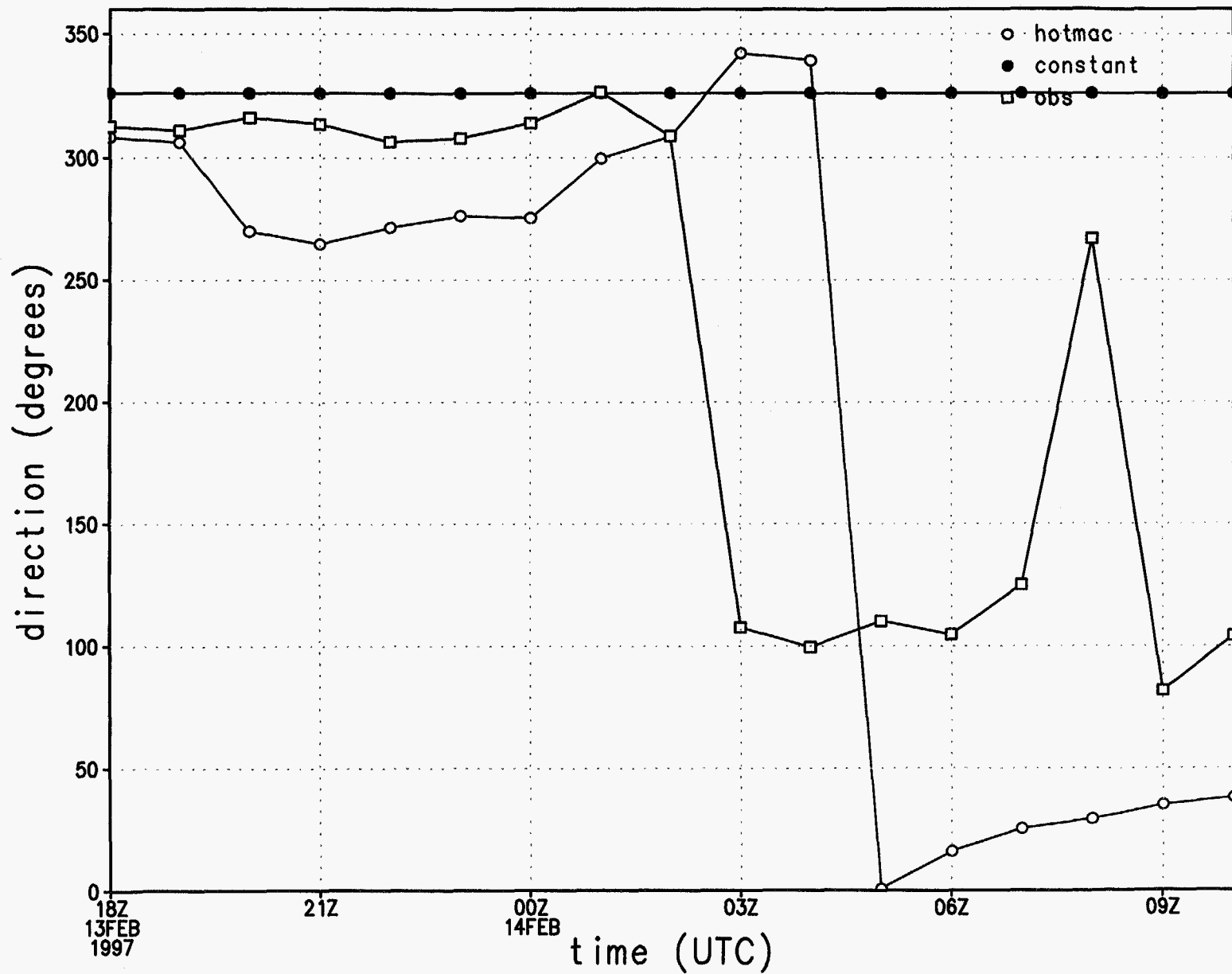


Figure 4c.

# wind speed at station 1

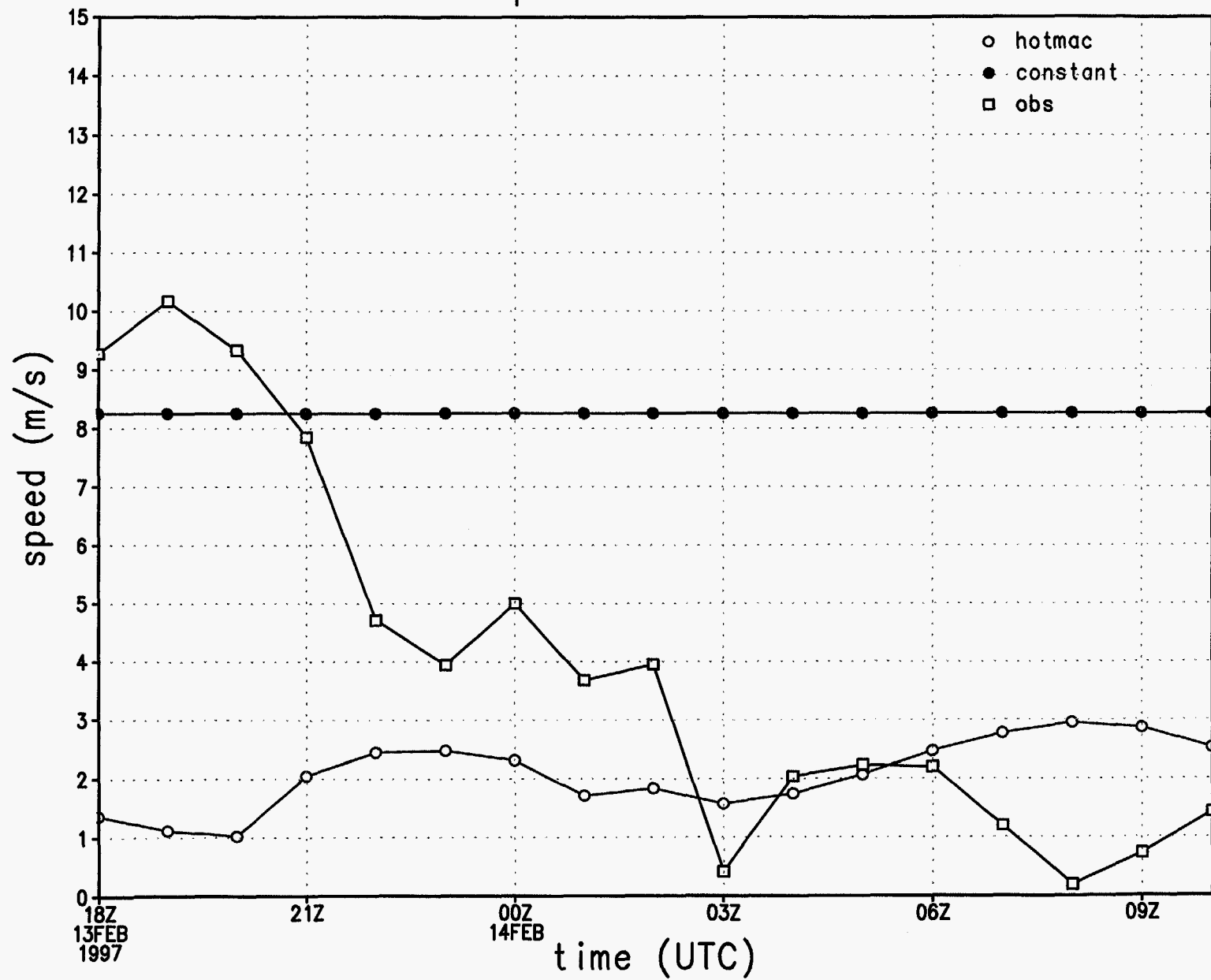


Figure 4d.



# u wind component at station 1

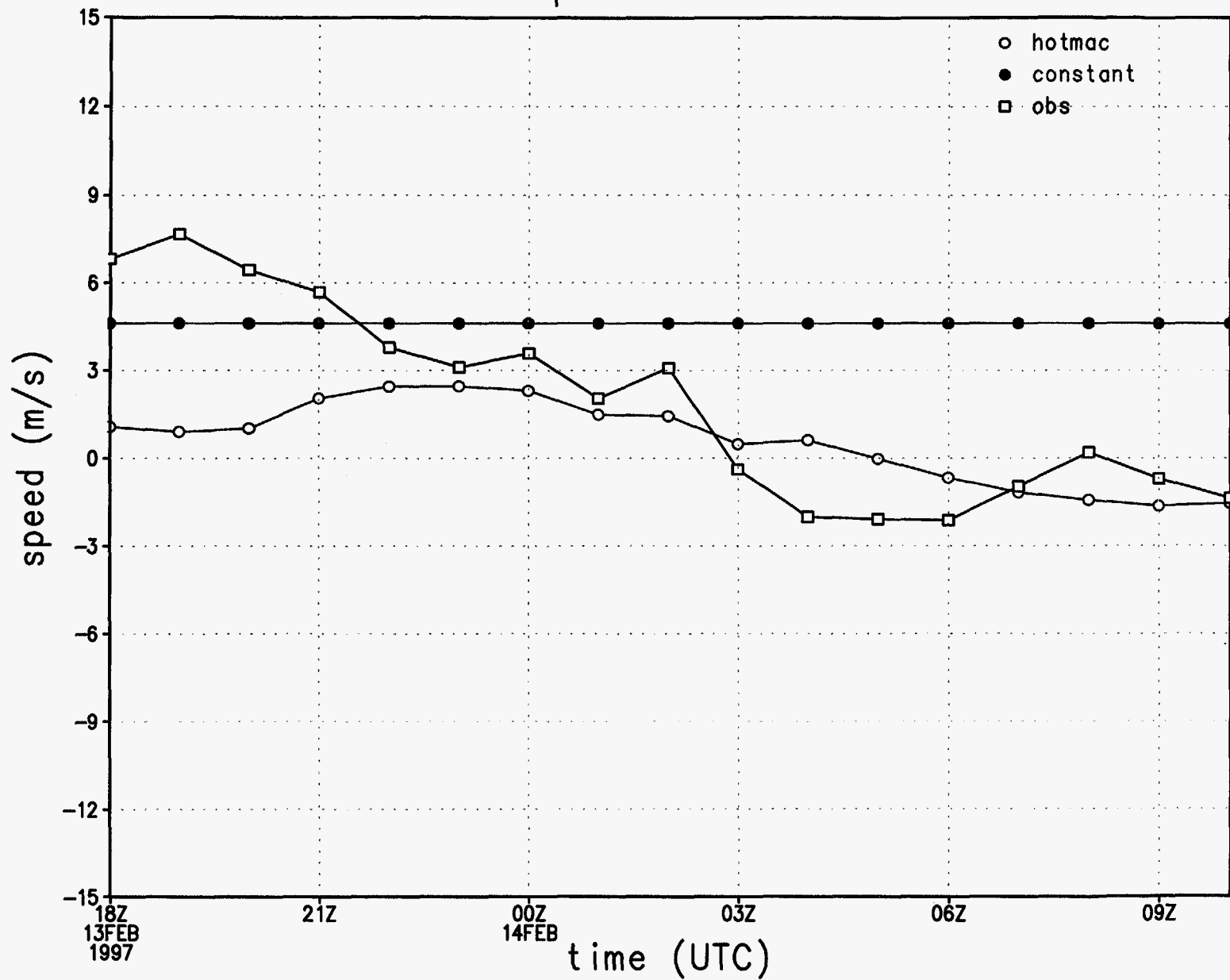


Figure 4e.

# v wind component at station 1

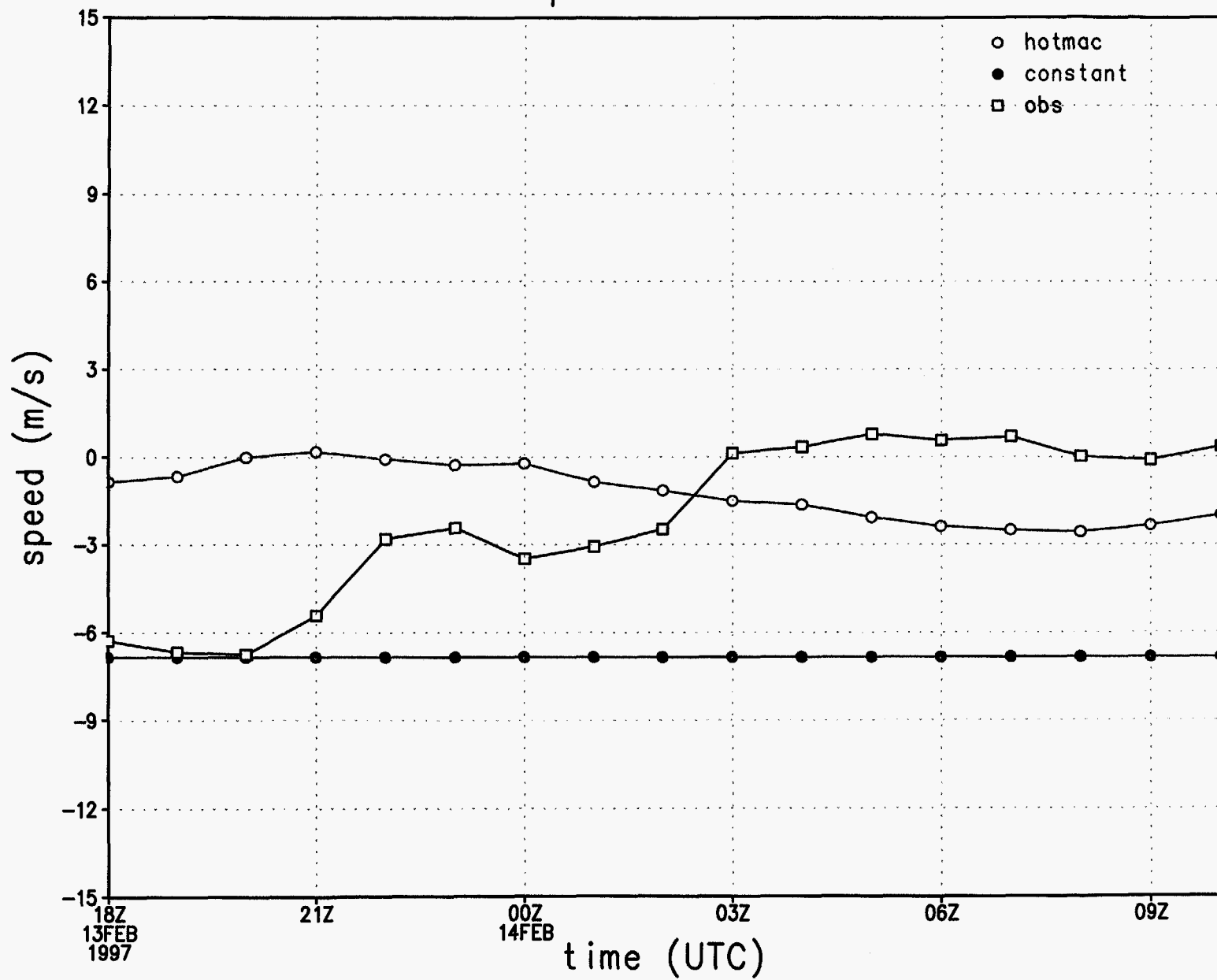


Figure 4f.

# rmse of wind direction by hour

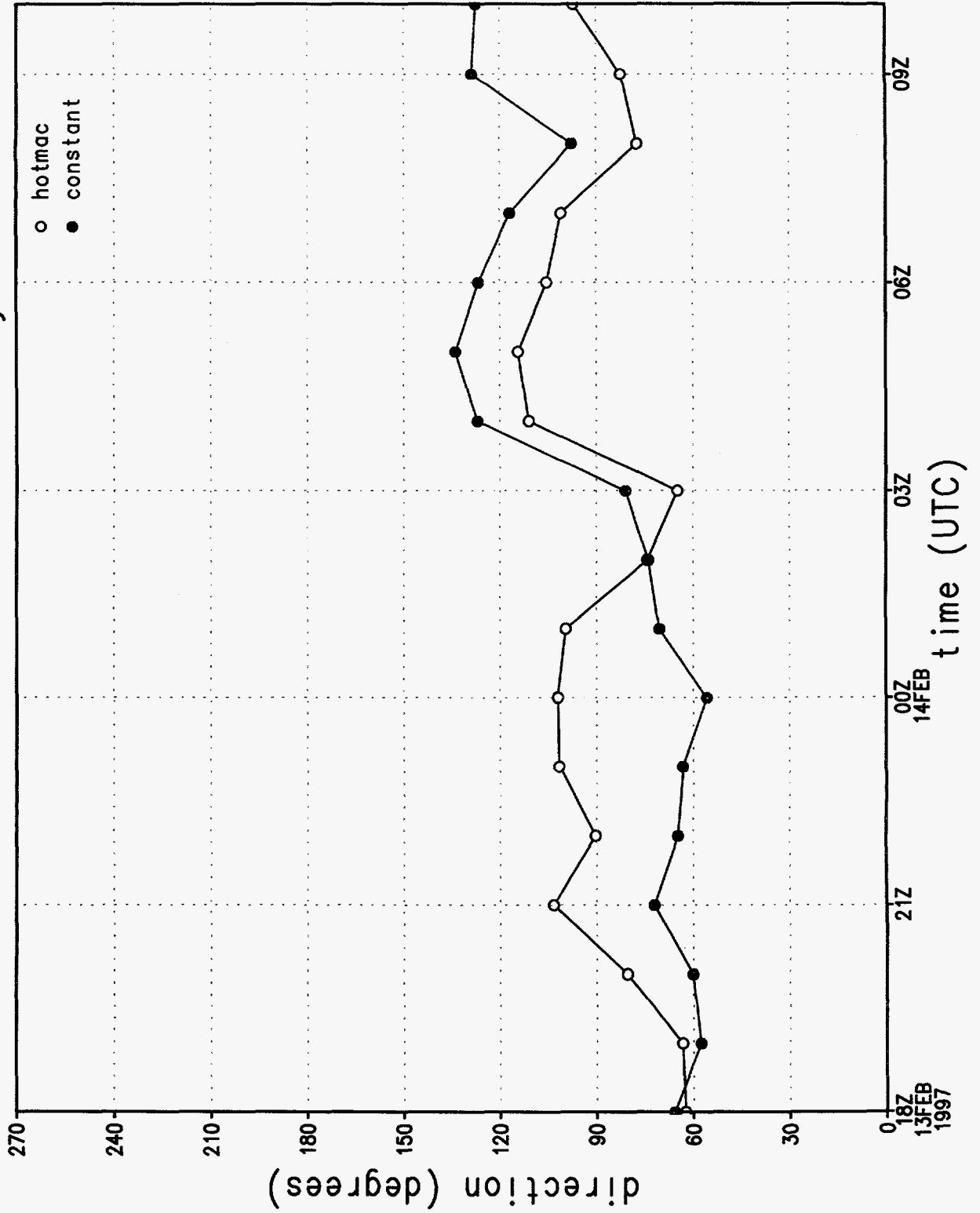


Figure 4g.

# rmse of wind speed by hour

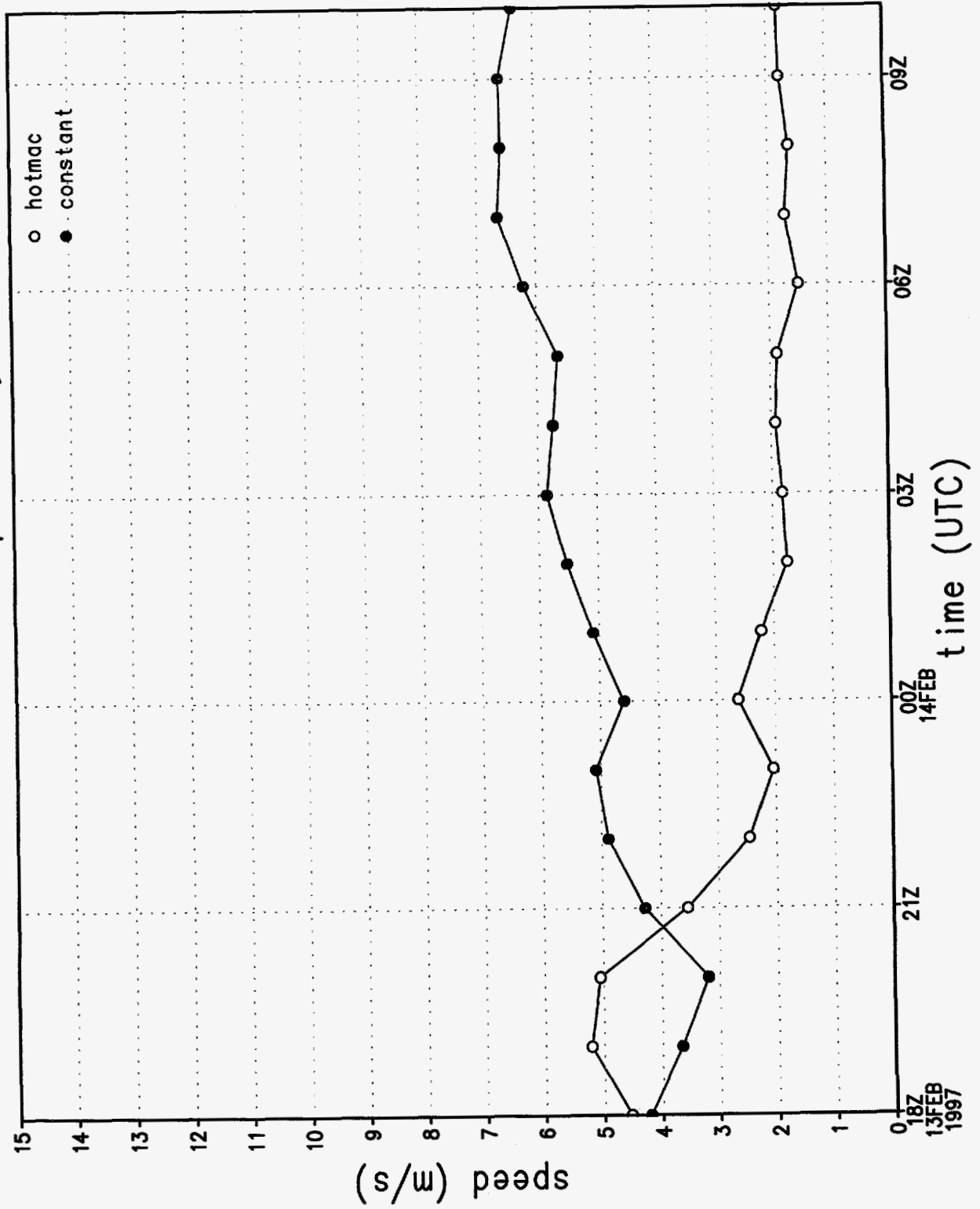


Figure 4h.

# rmse of v wind component by hour

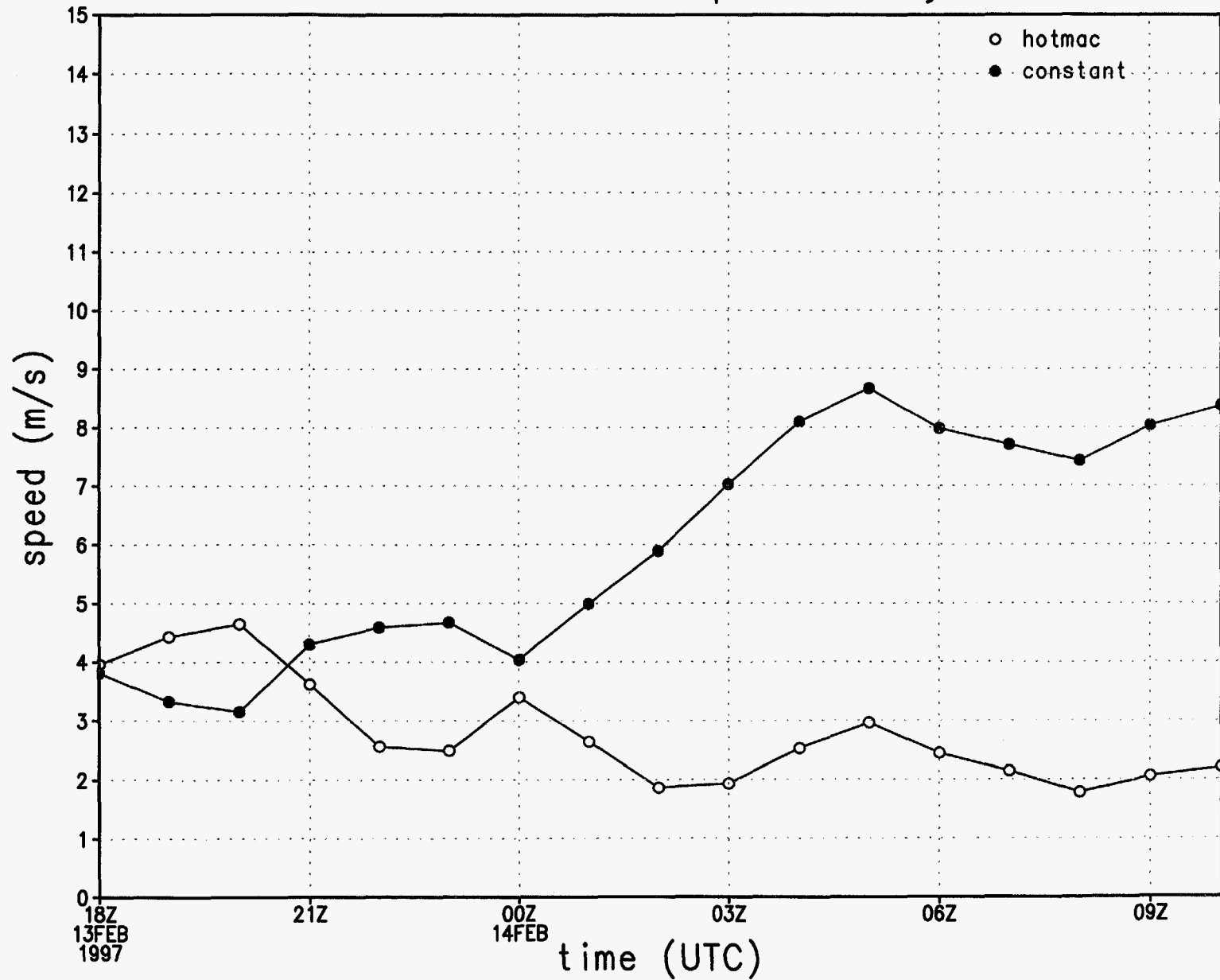


Figure 4i.

rmse of v wind component by hour

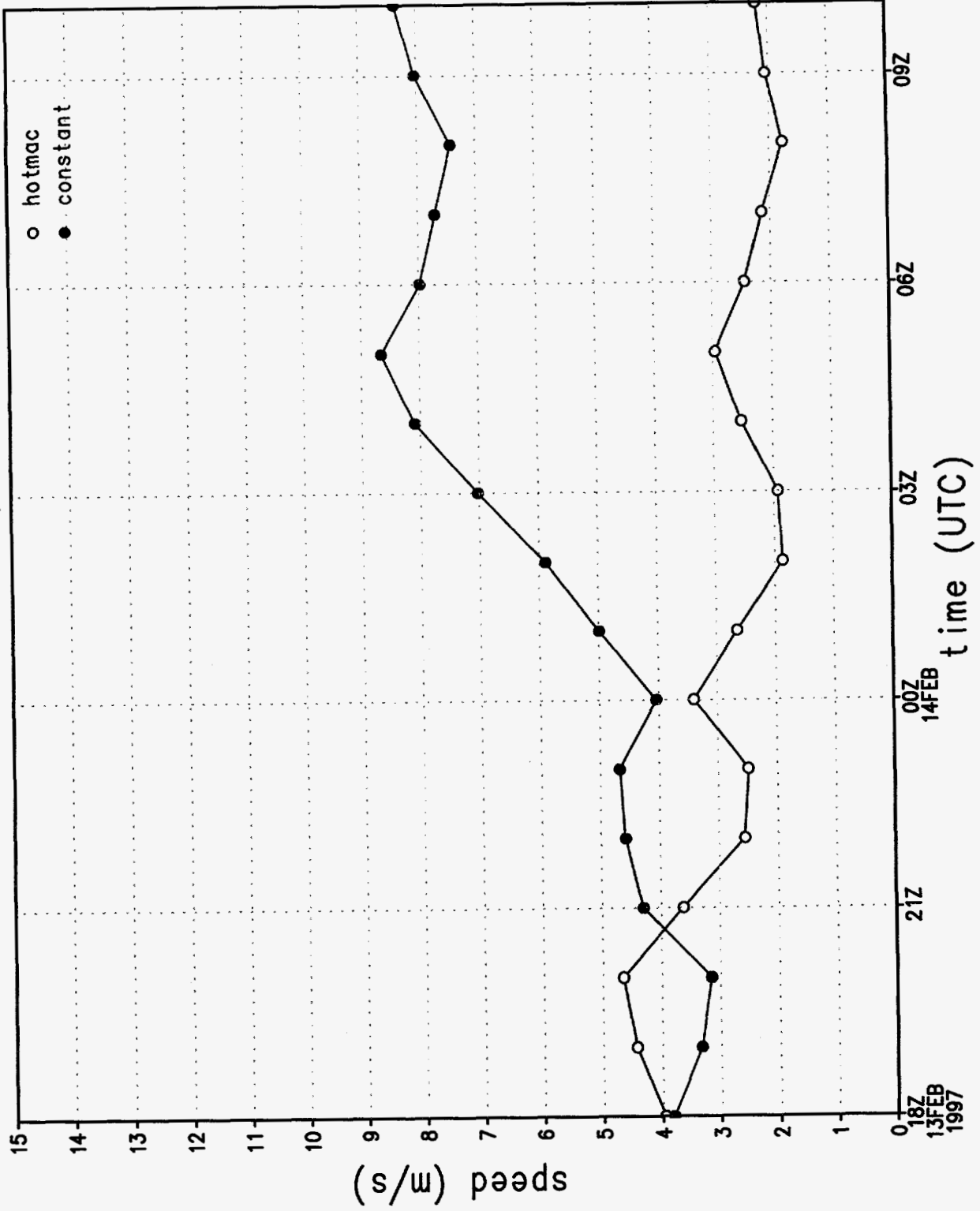


Figure 4j.

wind direction sounding 1, 1072 m

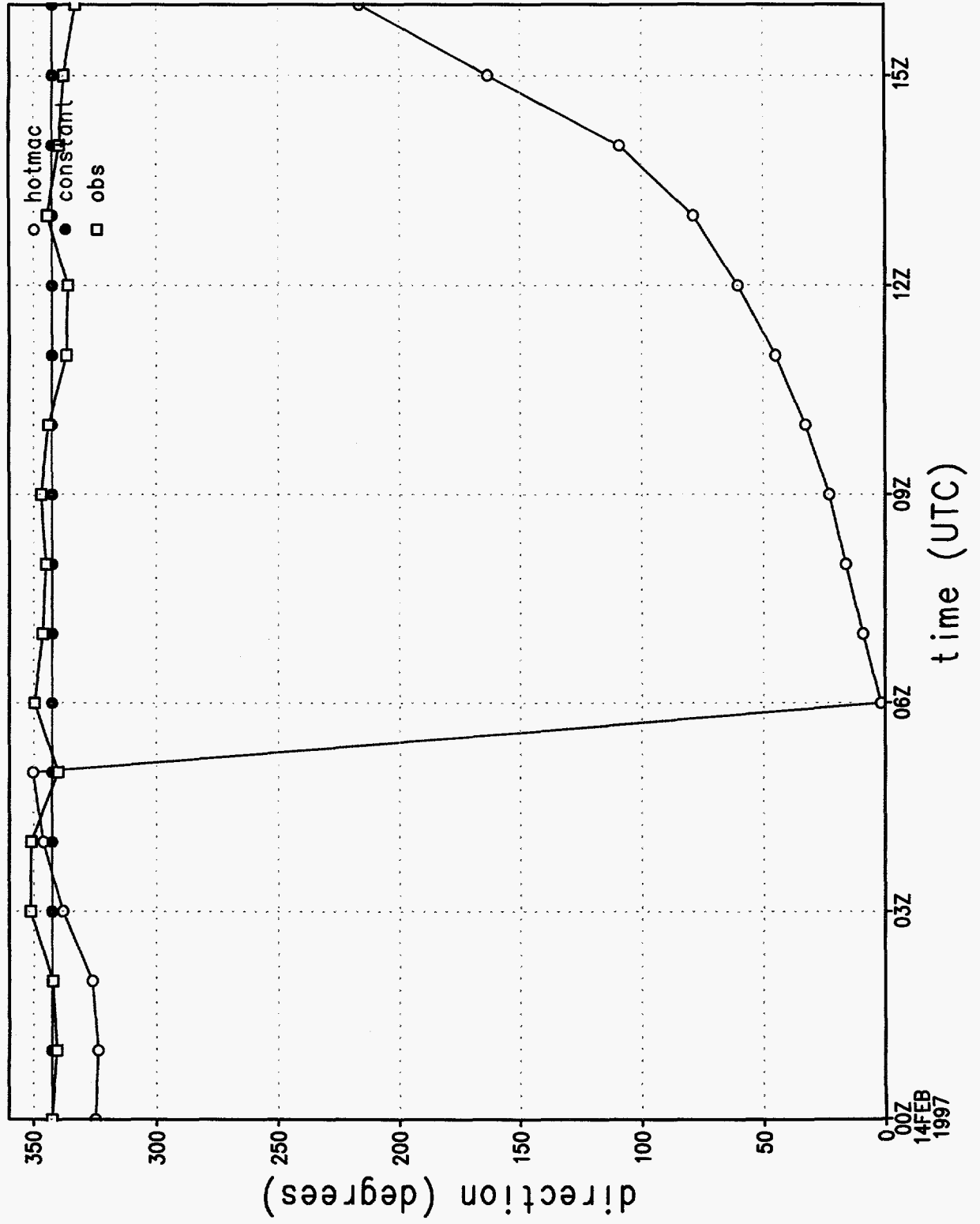


Figure 5a.

# wind speed sounding 1, 1072 m

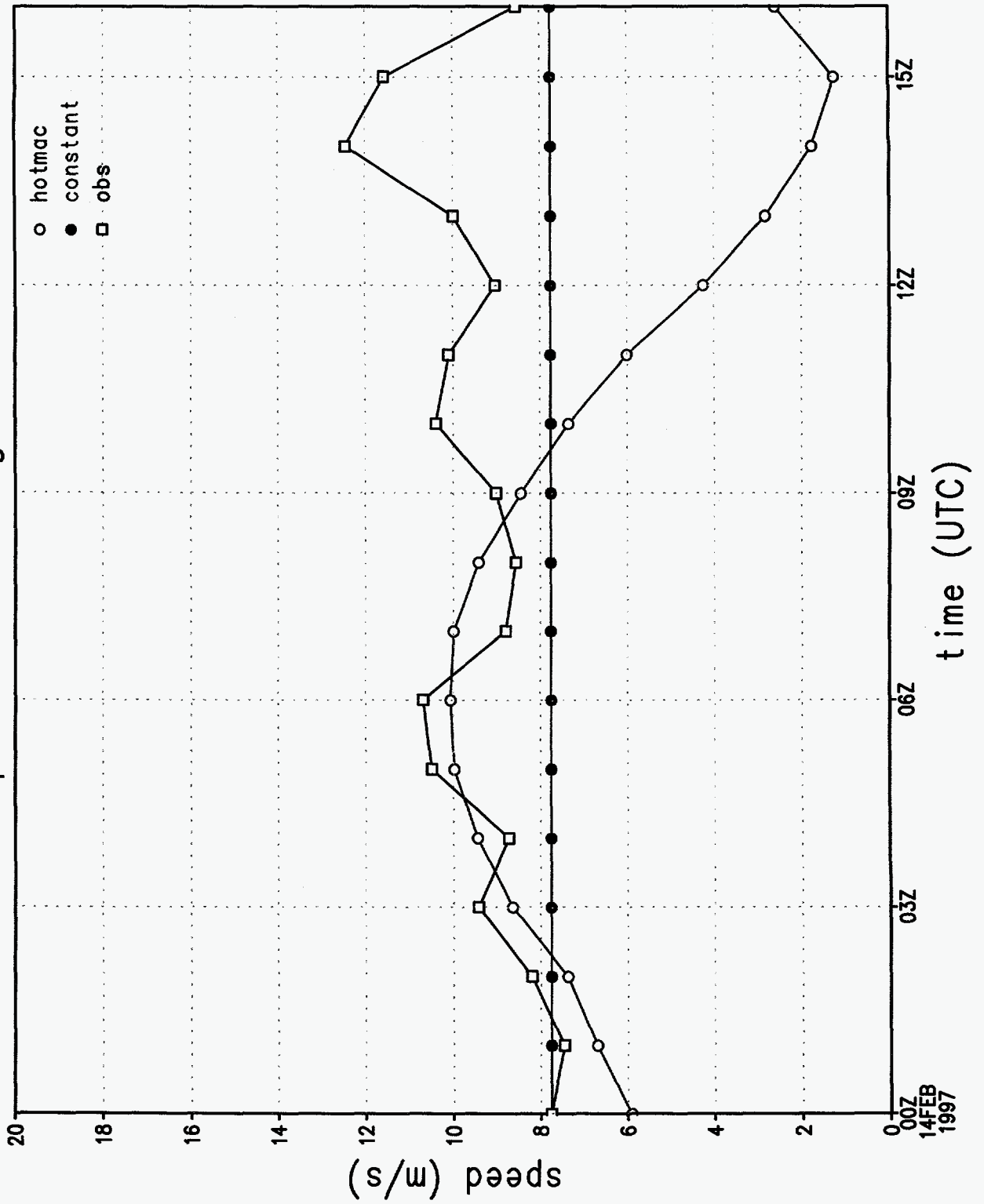


Figure 5b.



wind direction at station 1

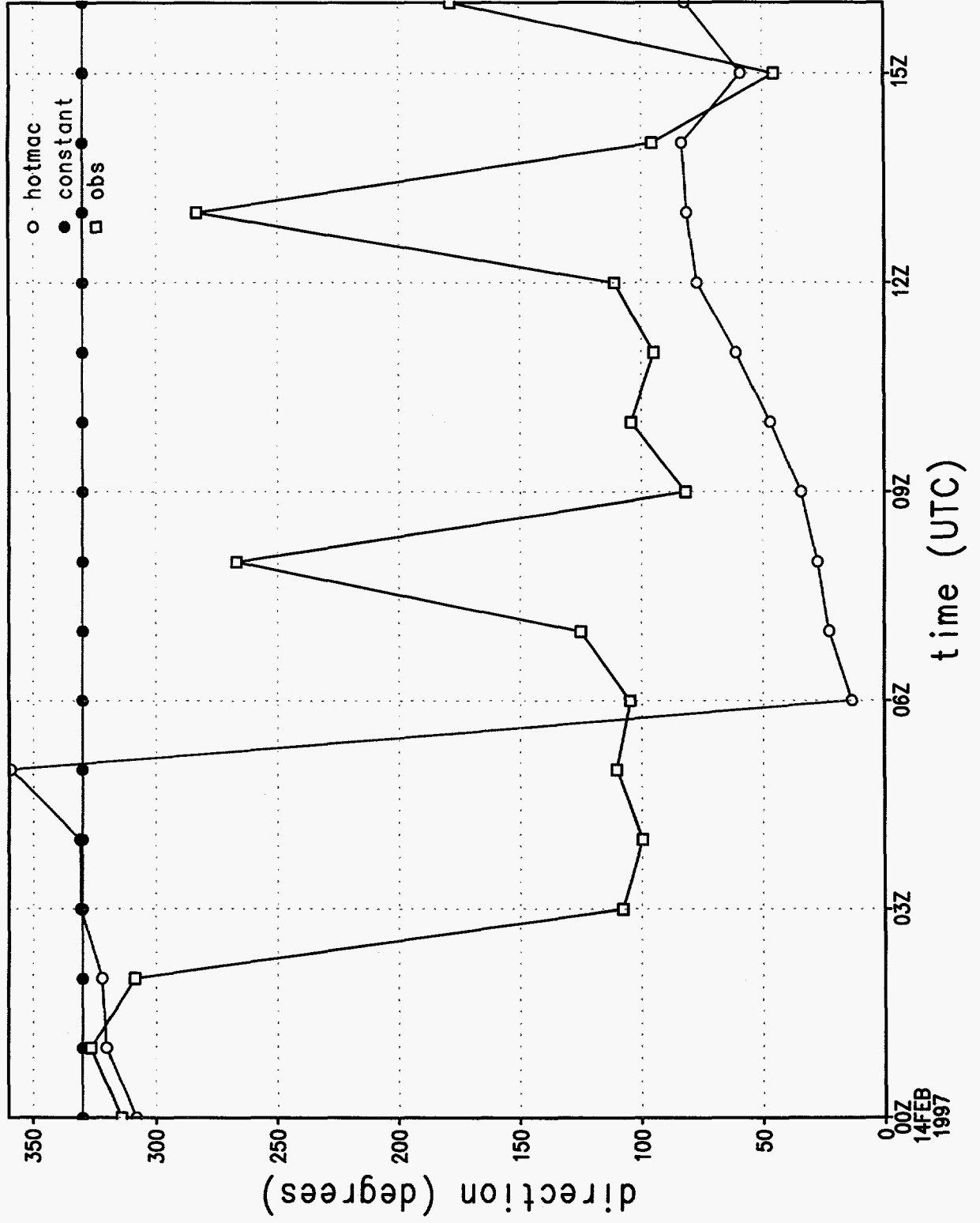


Figure 5c.

# wind speed at station 1

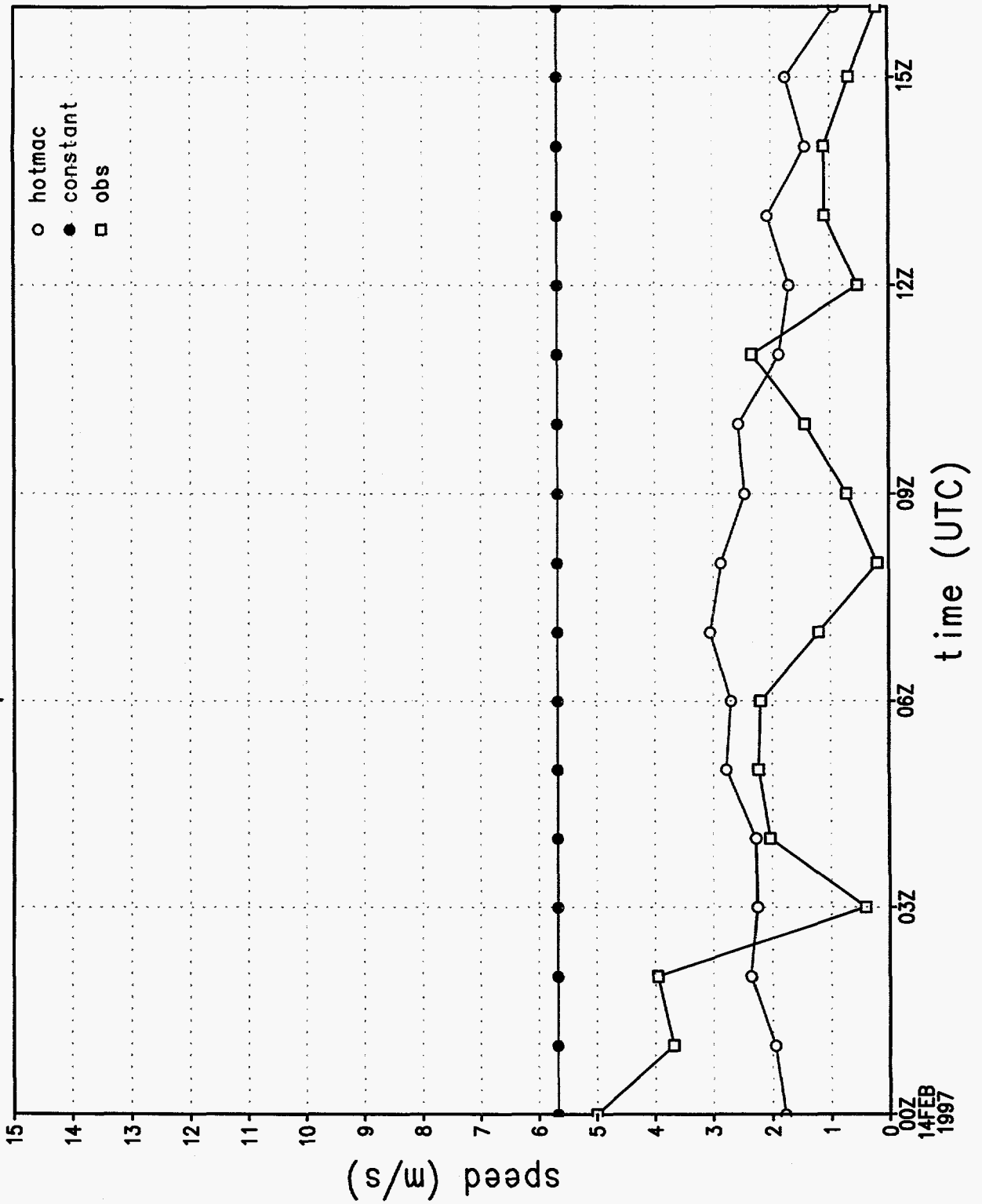


Figure 5d.

# u wind component at station 1

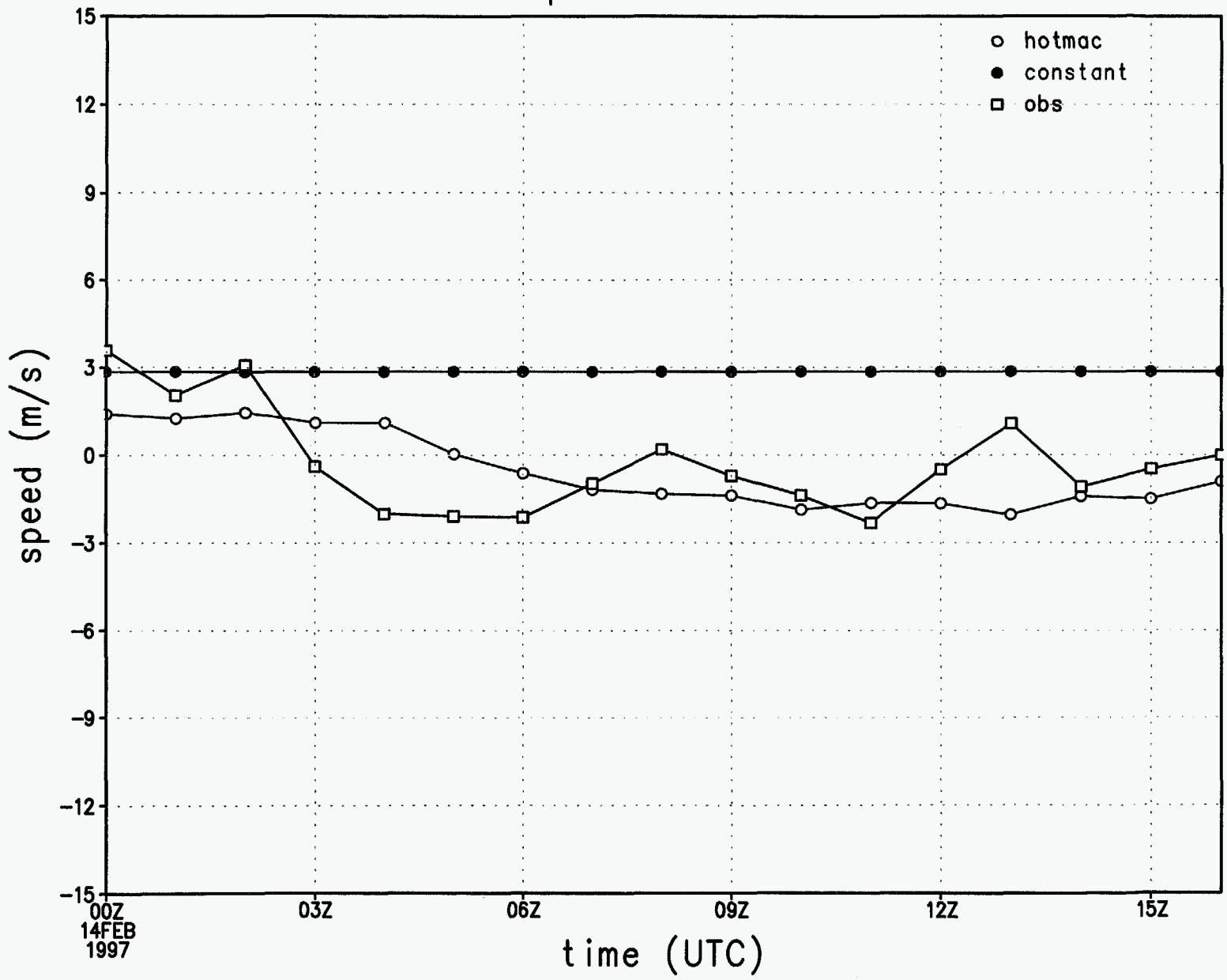


Figure 5e.

# v wind component at station 1

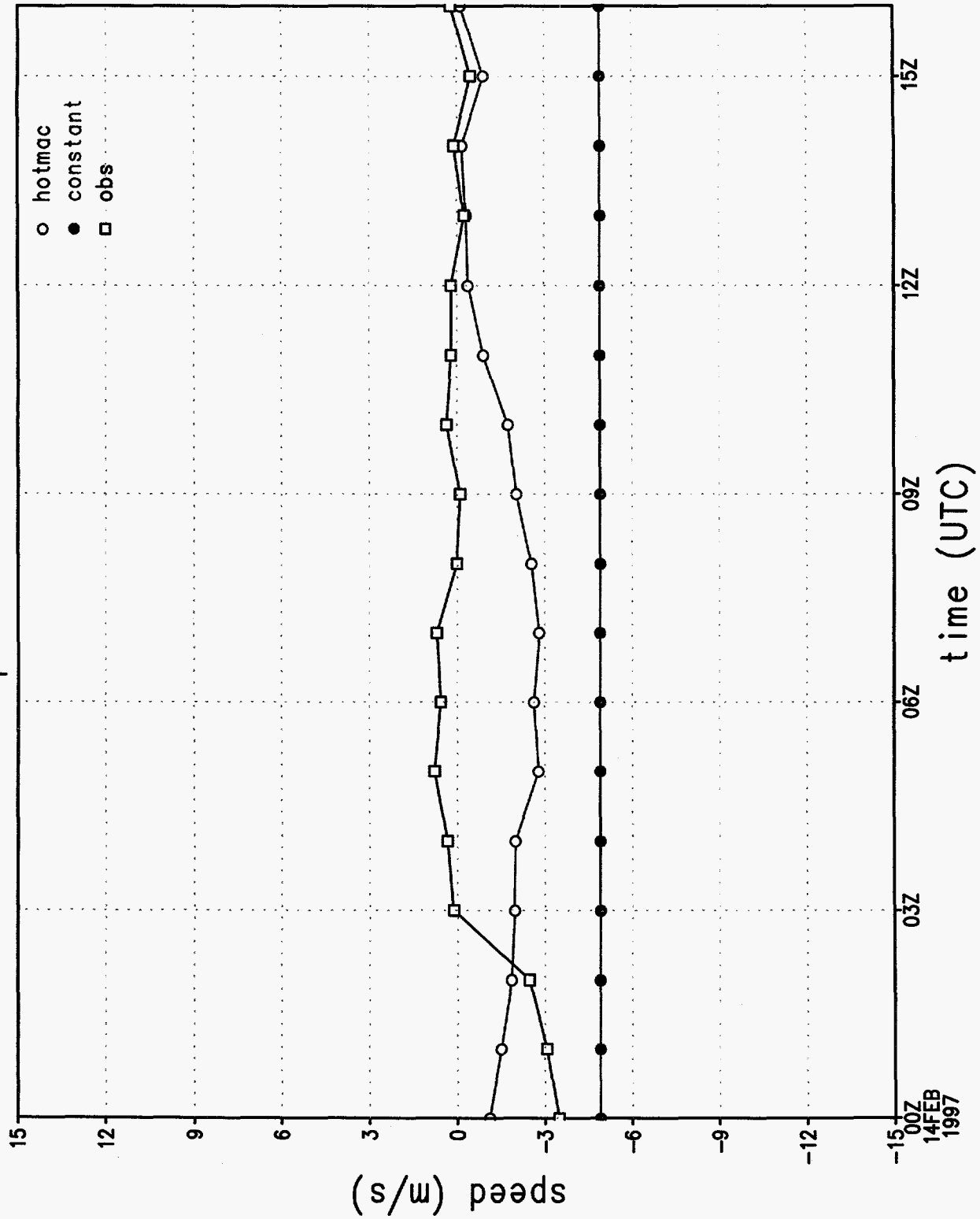


Figure 5f.

rmse of wind direction by hour

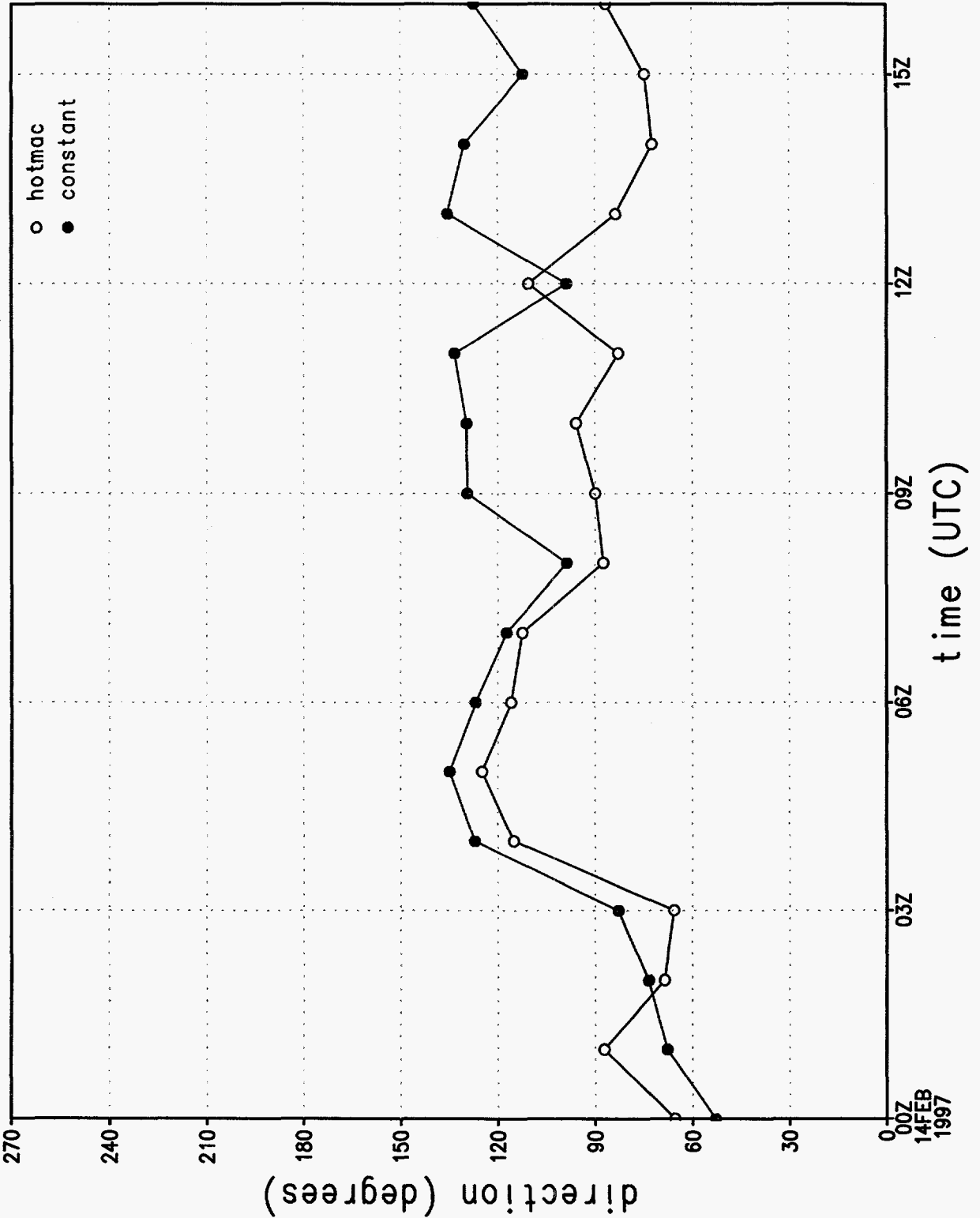


Figure 5g.

# rmse of wind speed by hour

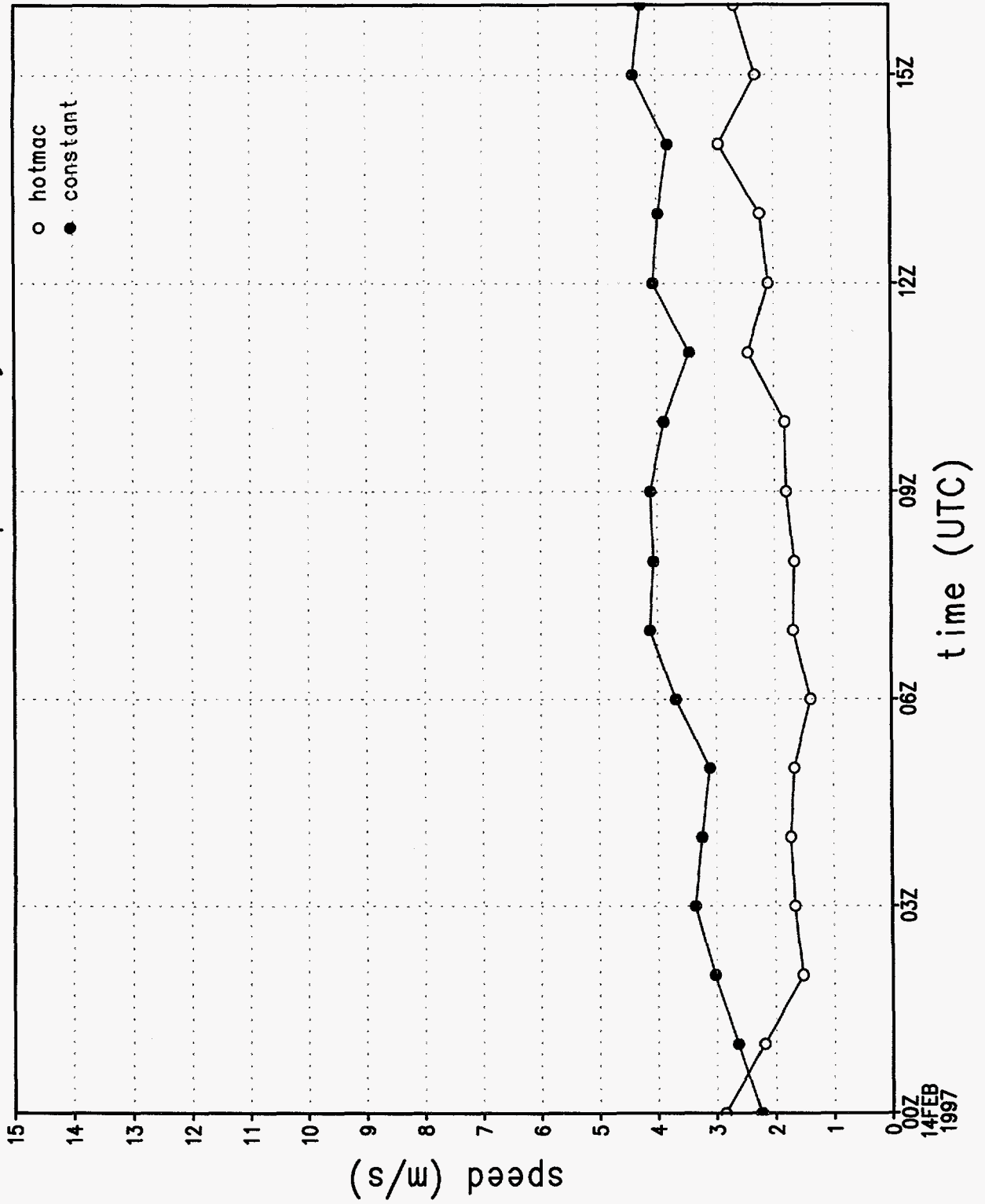


Figure 5h.

rmse of u wind component by hour

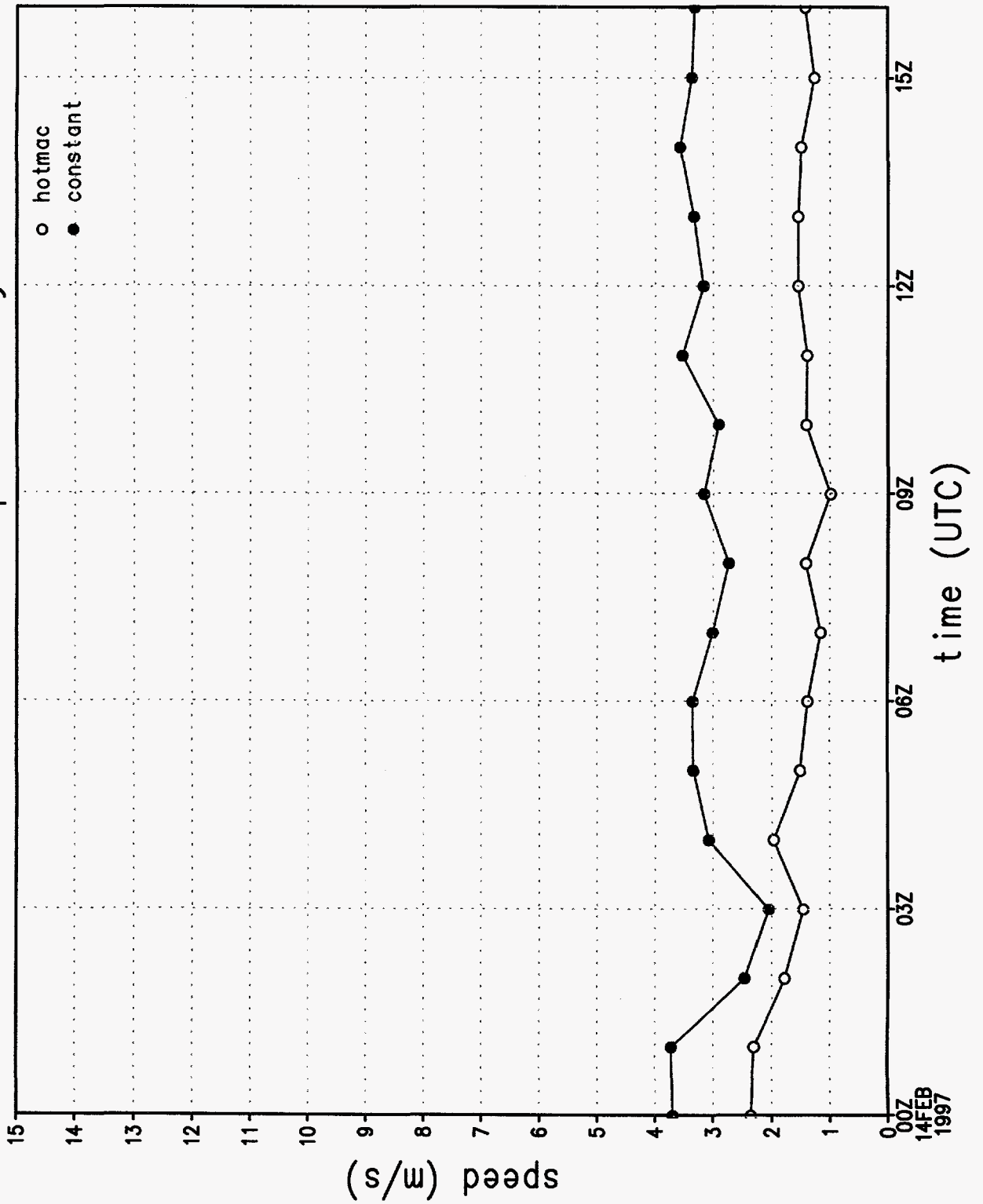


Figure 5i.

rmse of v wind component by hour

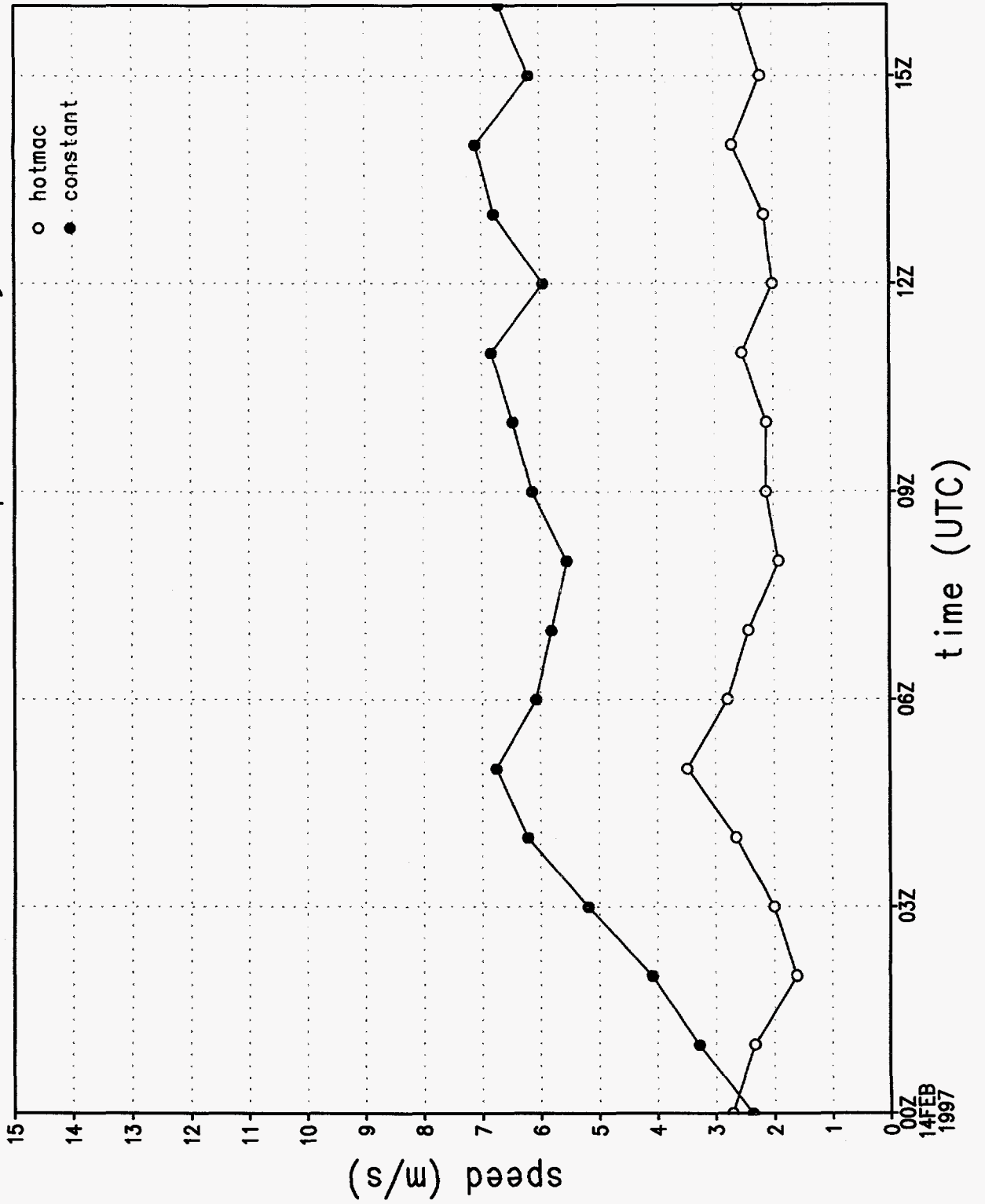


Figure 5j.



wind direction sounding 1, 1072 m

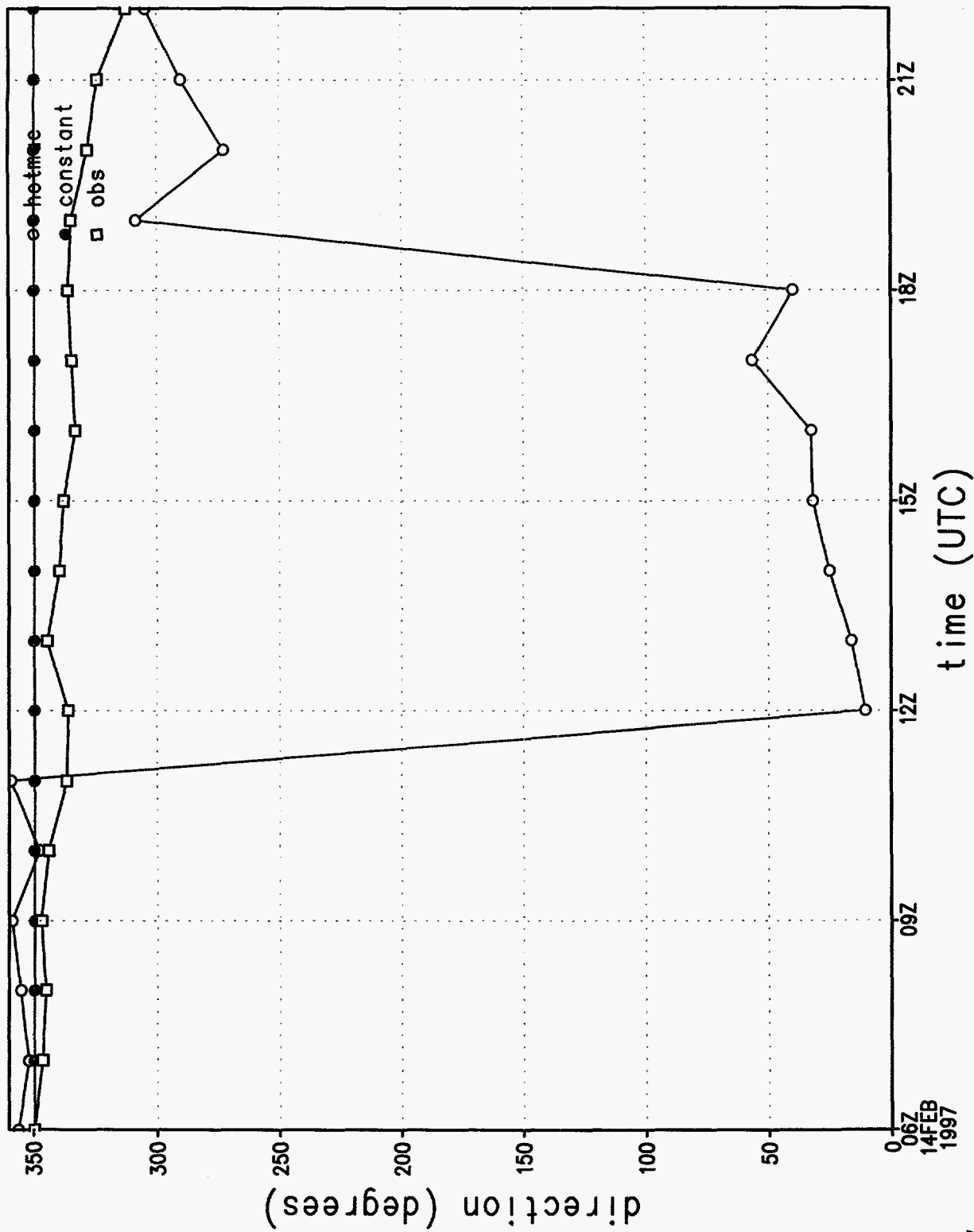


Figure 6a.

wind speed sounding 1, 1072 m

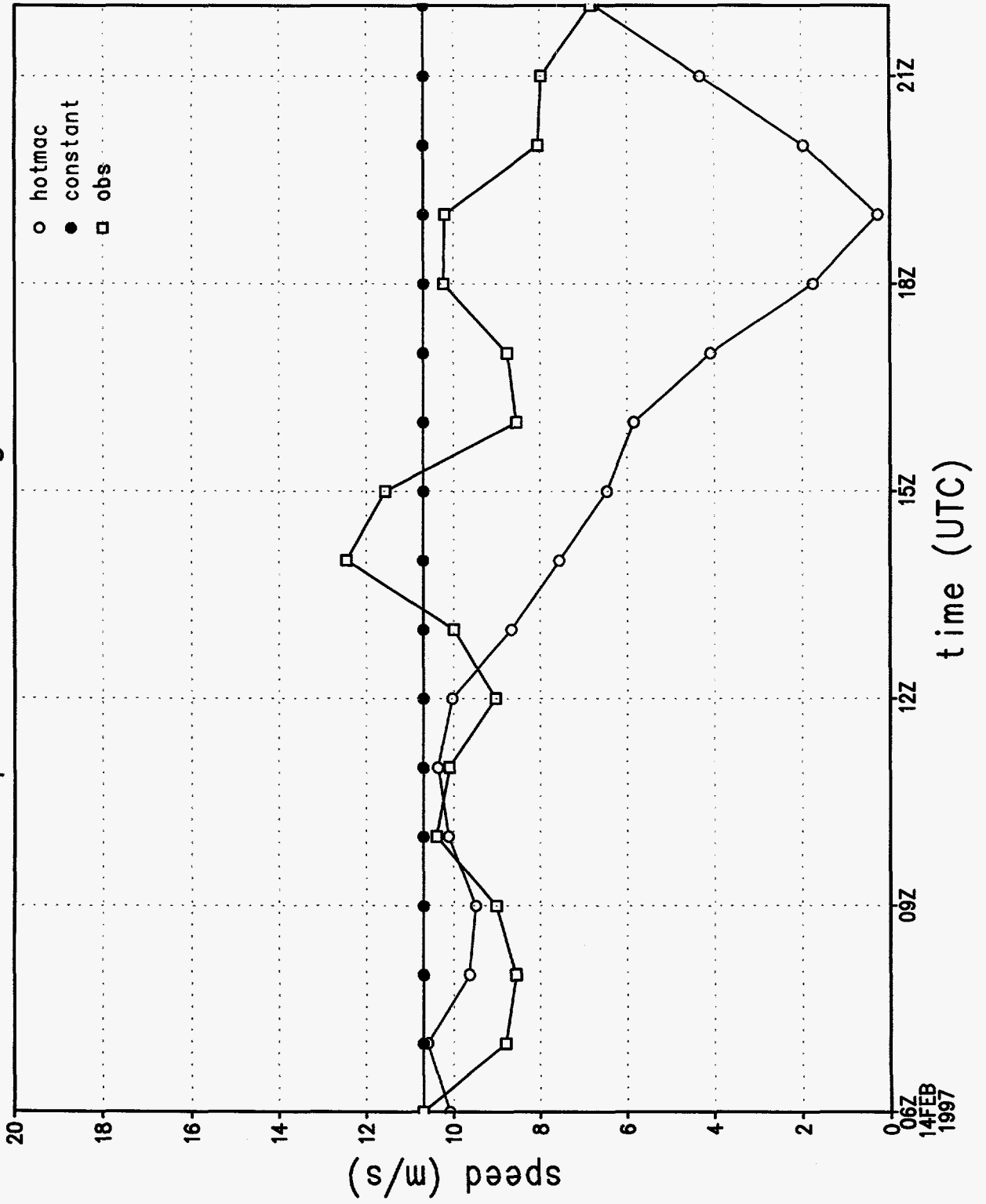


Figure 6b.

# wind direction at station 1

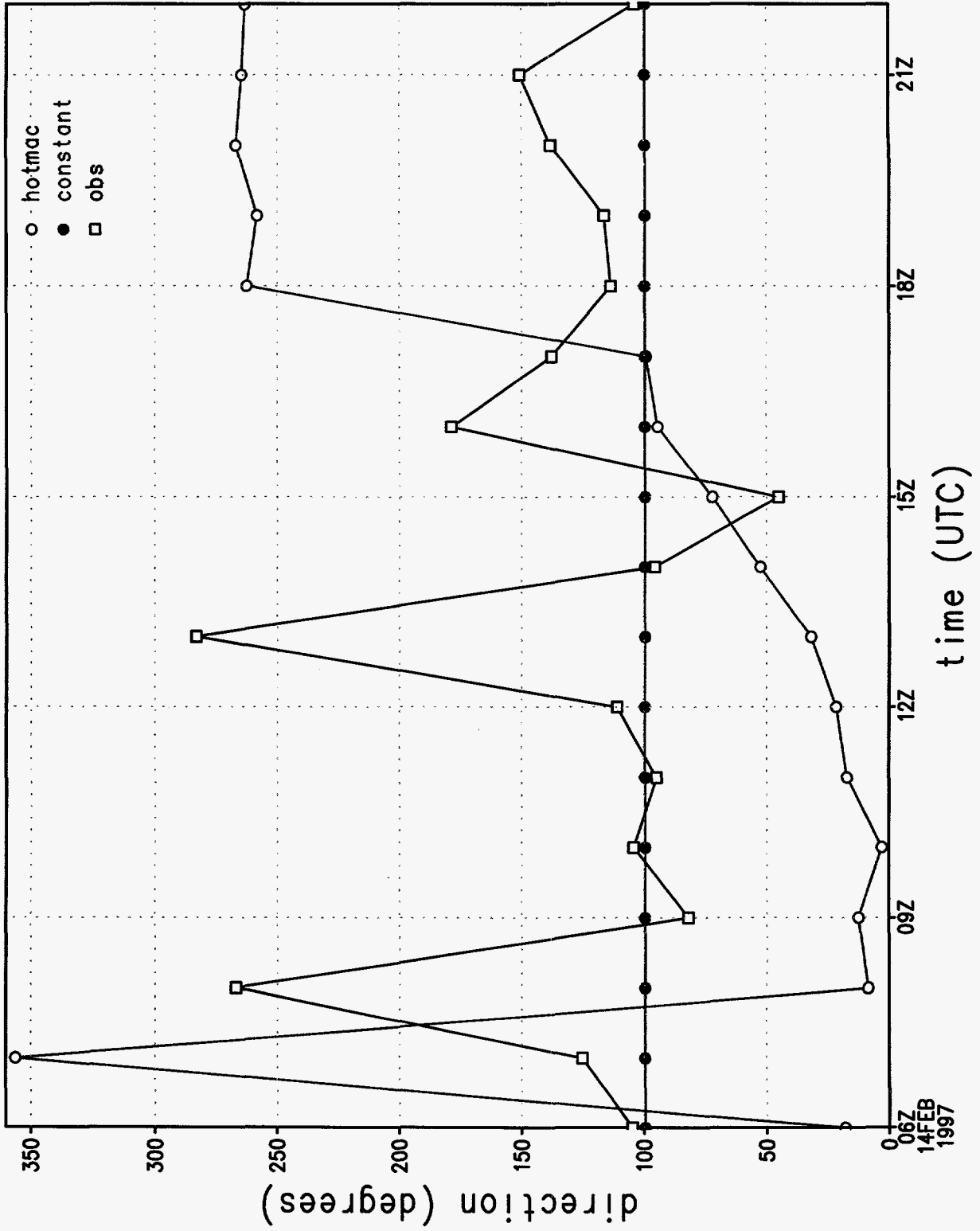


Figure 6c.

# wind speed at station 1

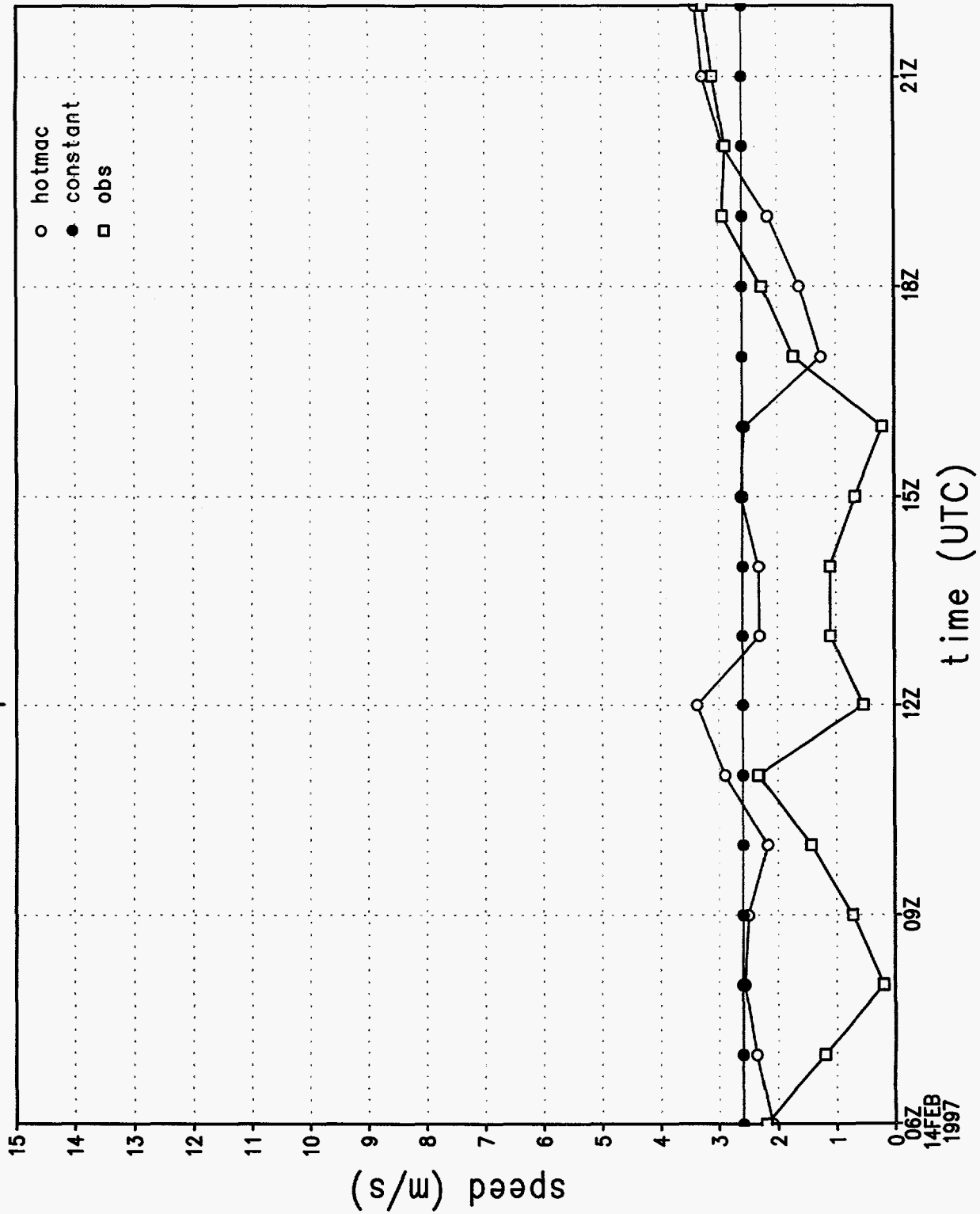


Figure 6d.

# u wind component at station 1

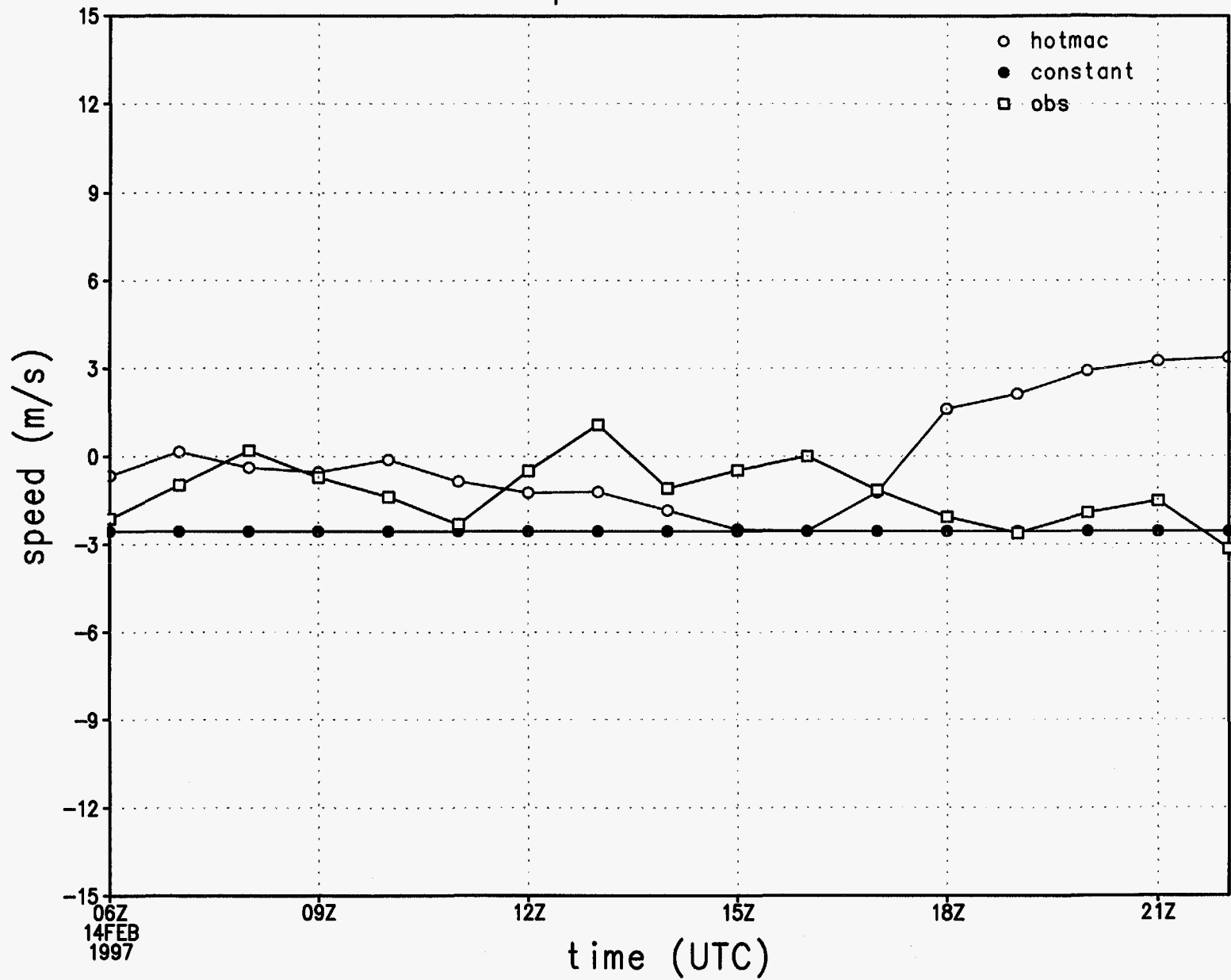


Figure 6e.

# v wind component at station 1

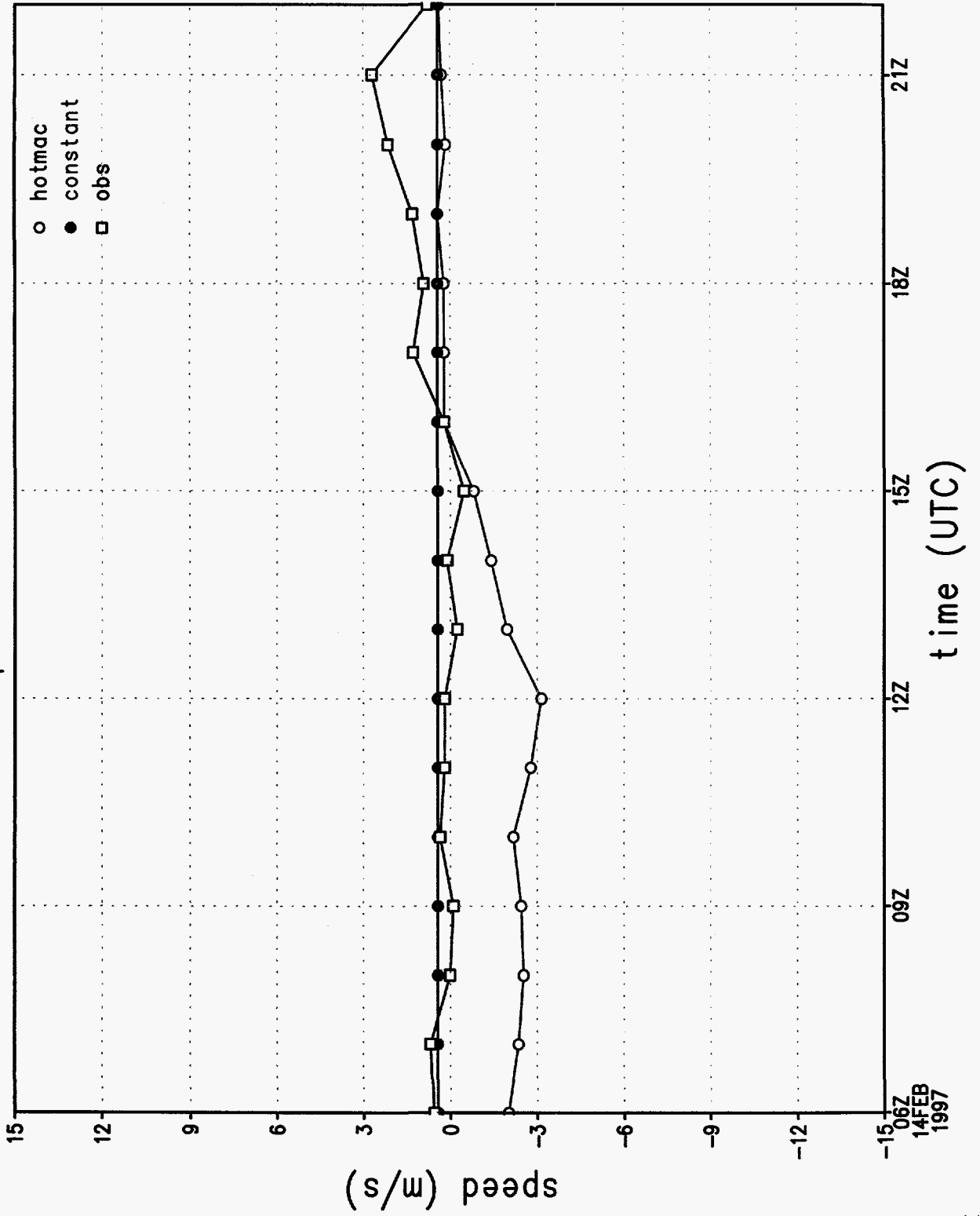


Figure 6f.

# rmse of wind direction by hour

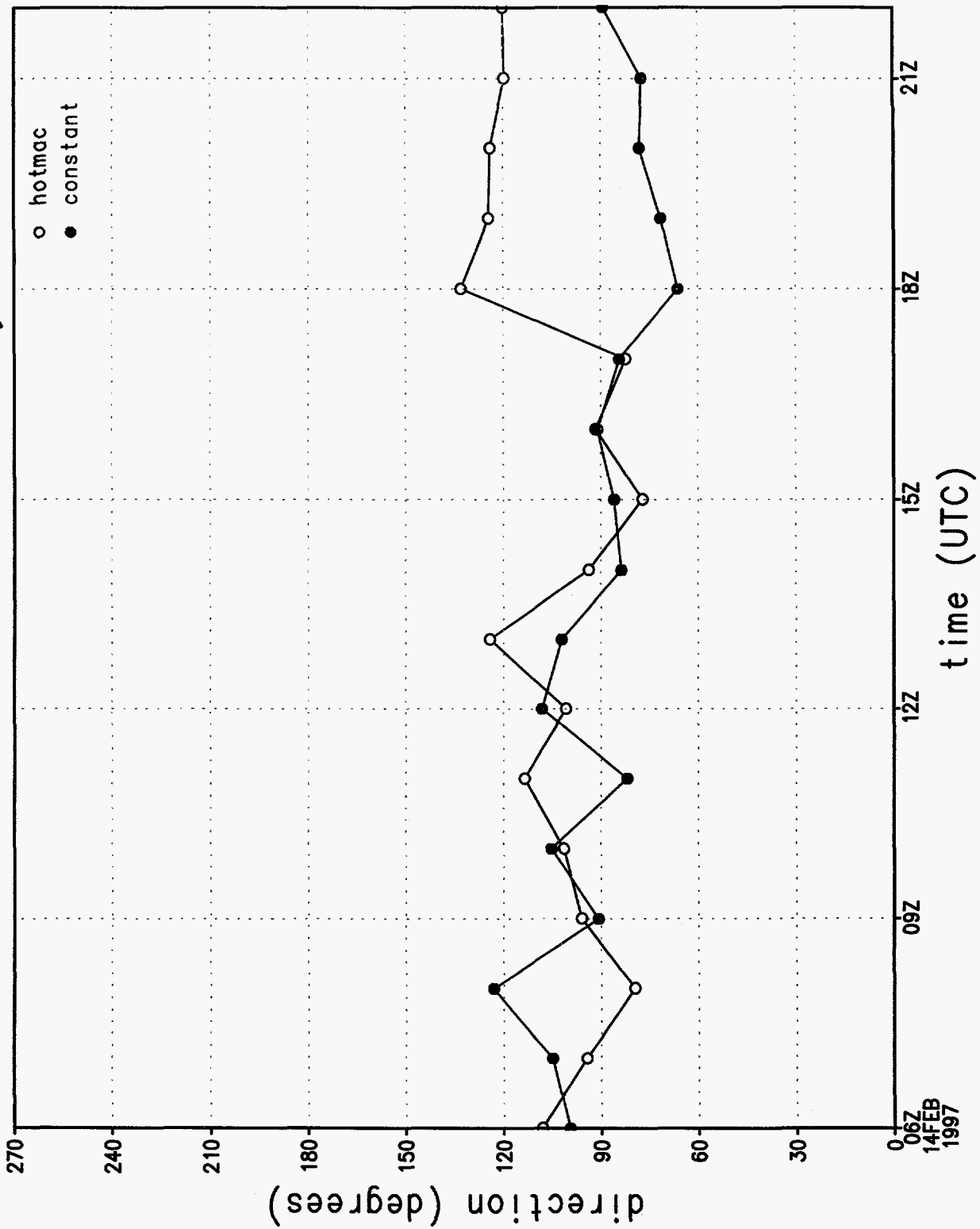


Figure 69.

# rmse of wind speed by hour

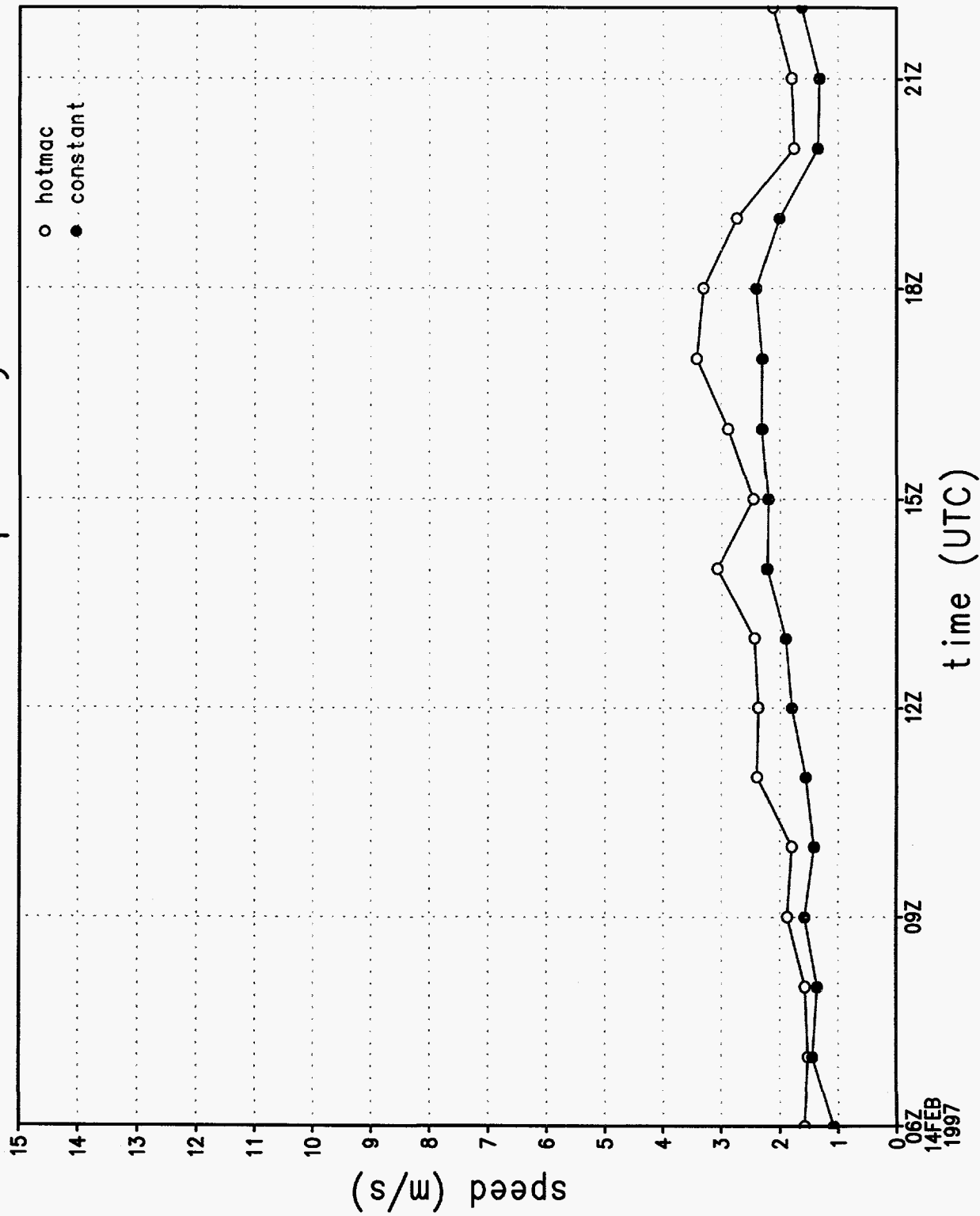


Figure 6h.



rmse of u wind component by hour

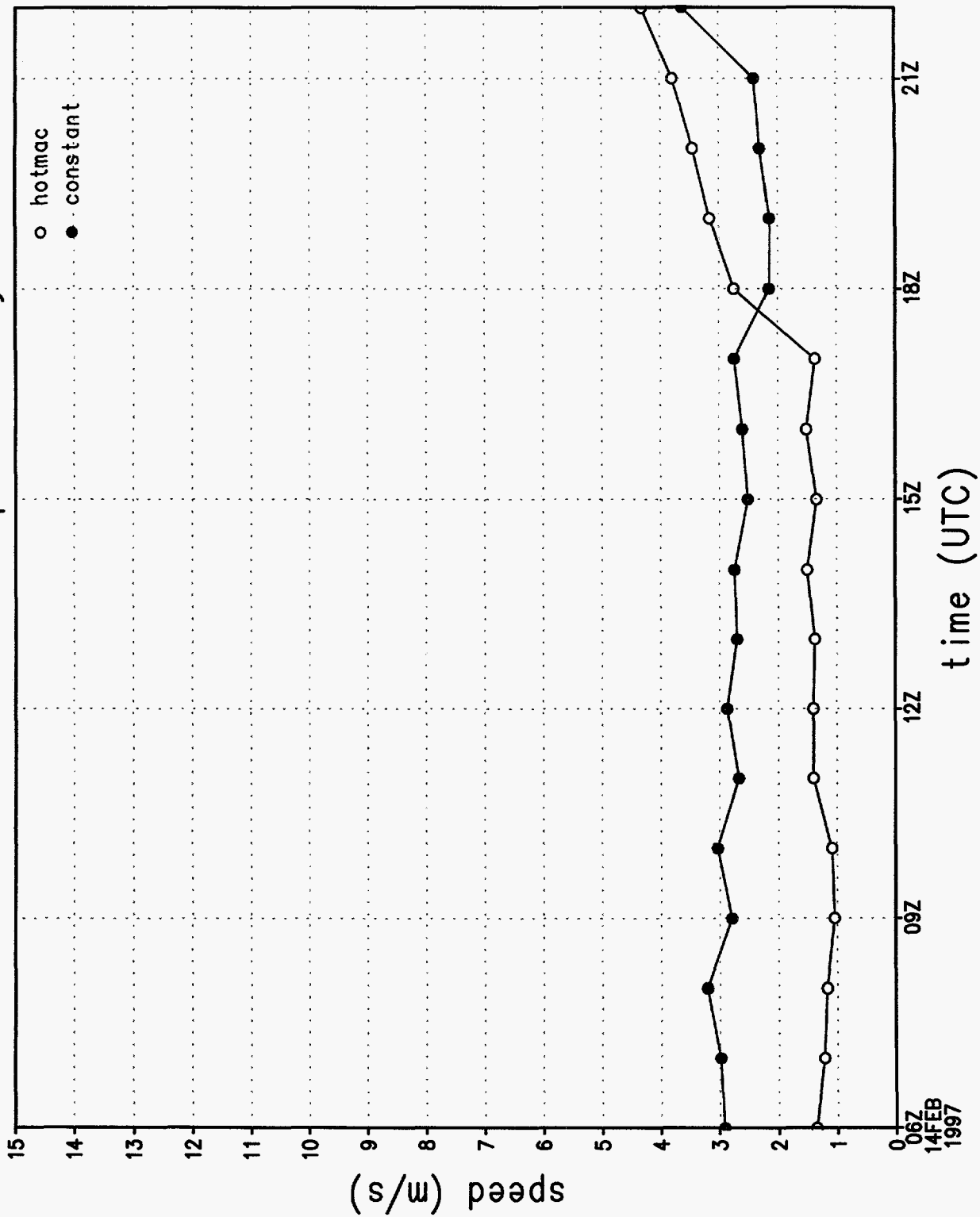


Figure 6i.

rmse of v wind component by hour

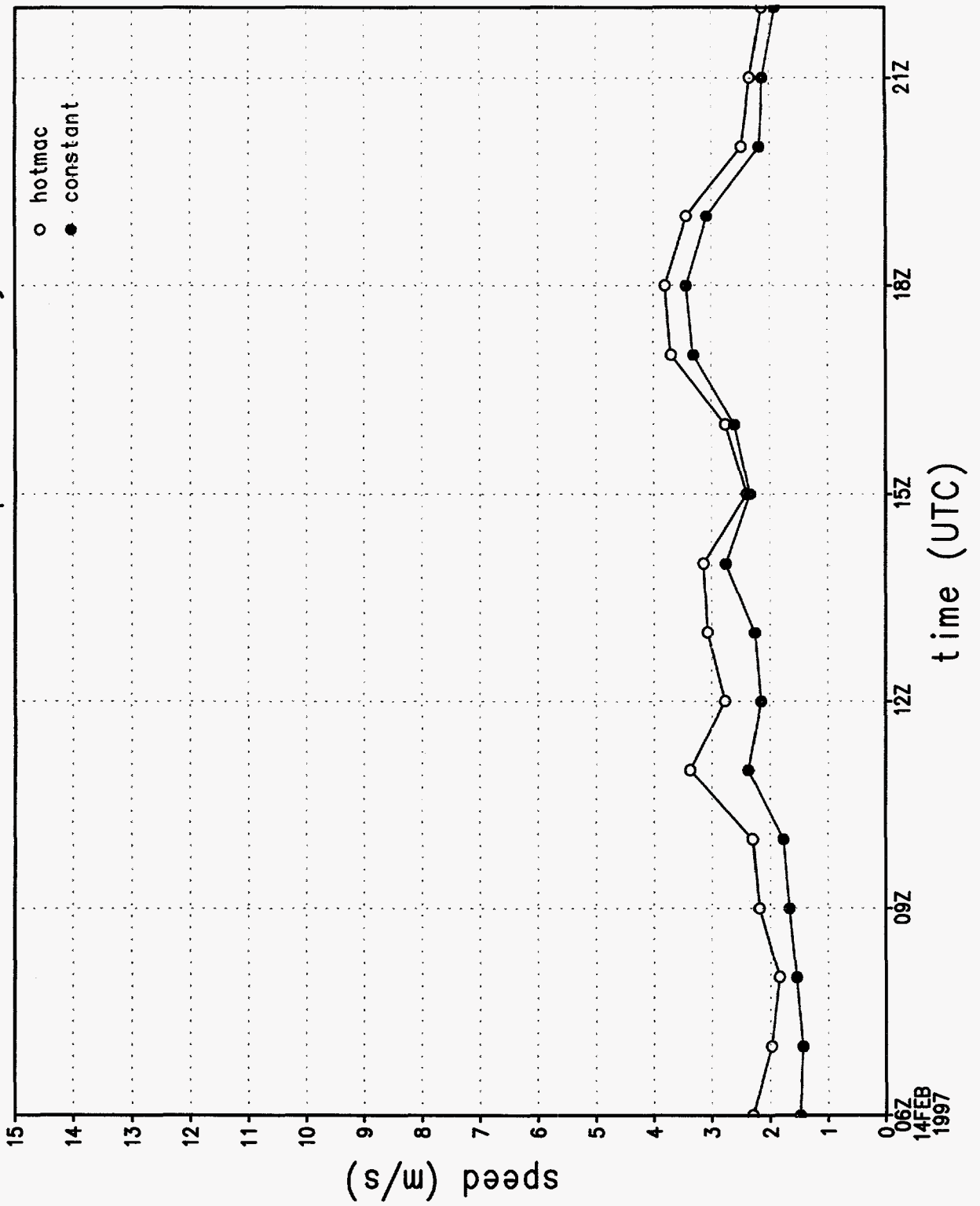


Figure 6j.

wind direction sounding 1, 1072 m

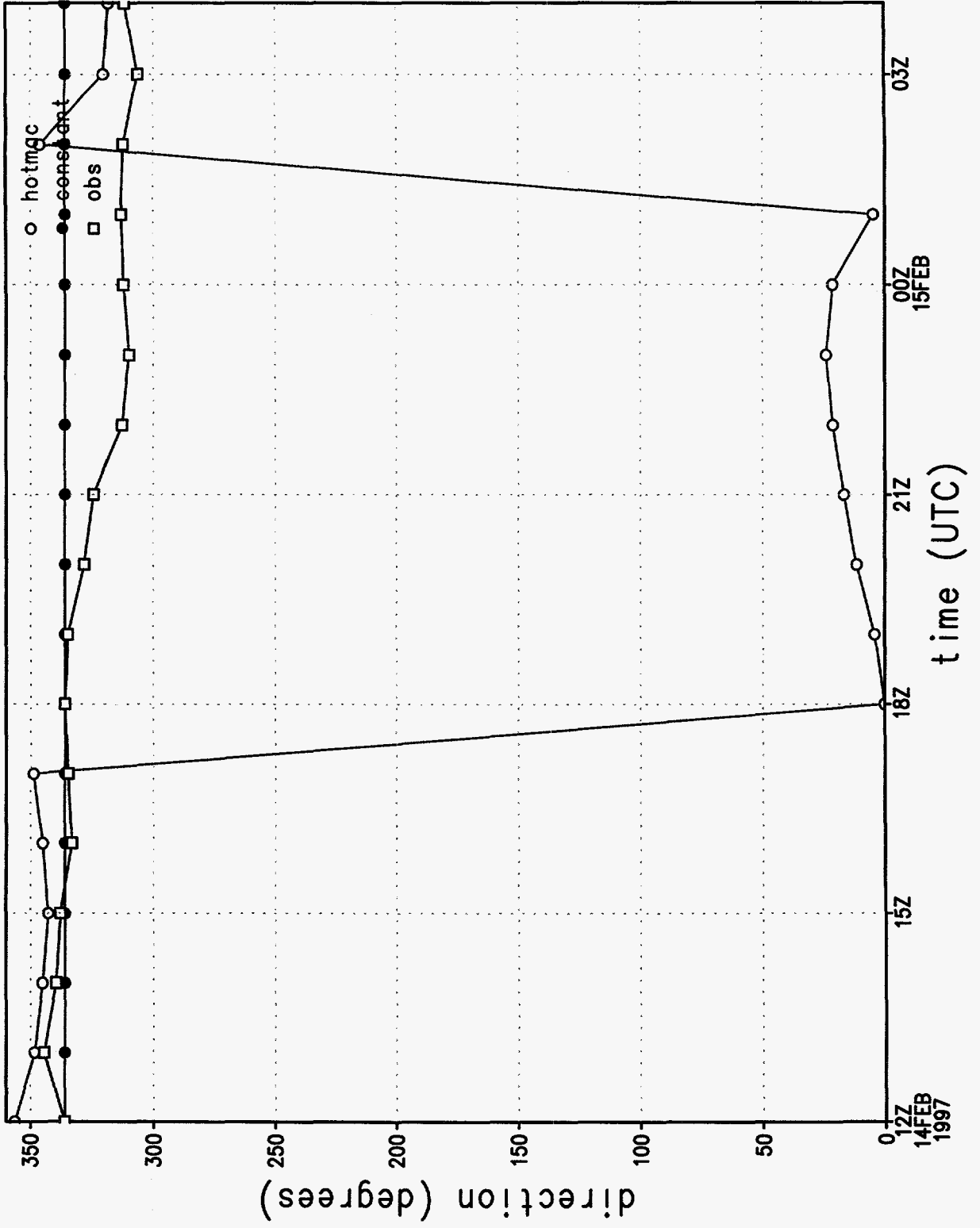


Figure 7a.

# wind speed sounding 1, 1072 m

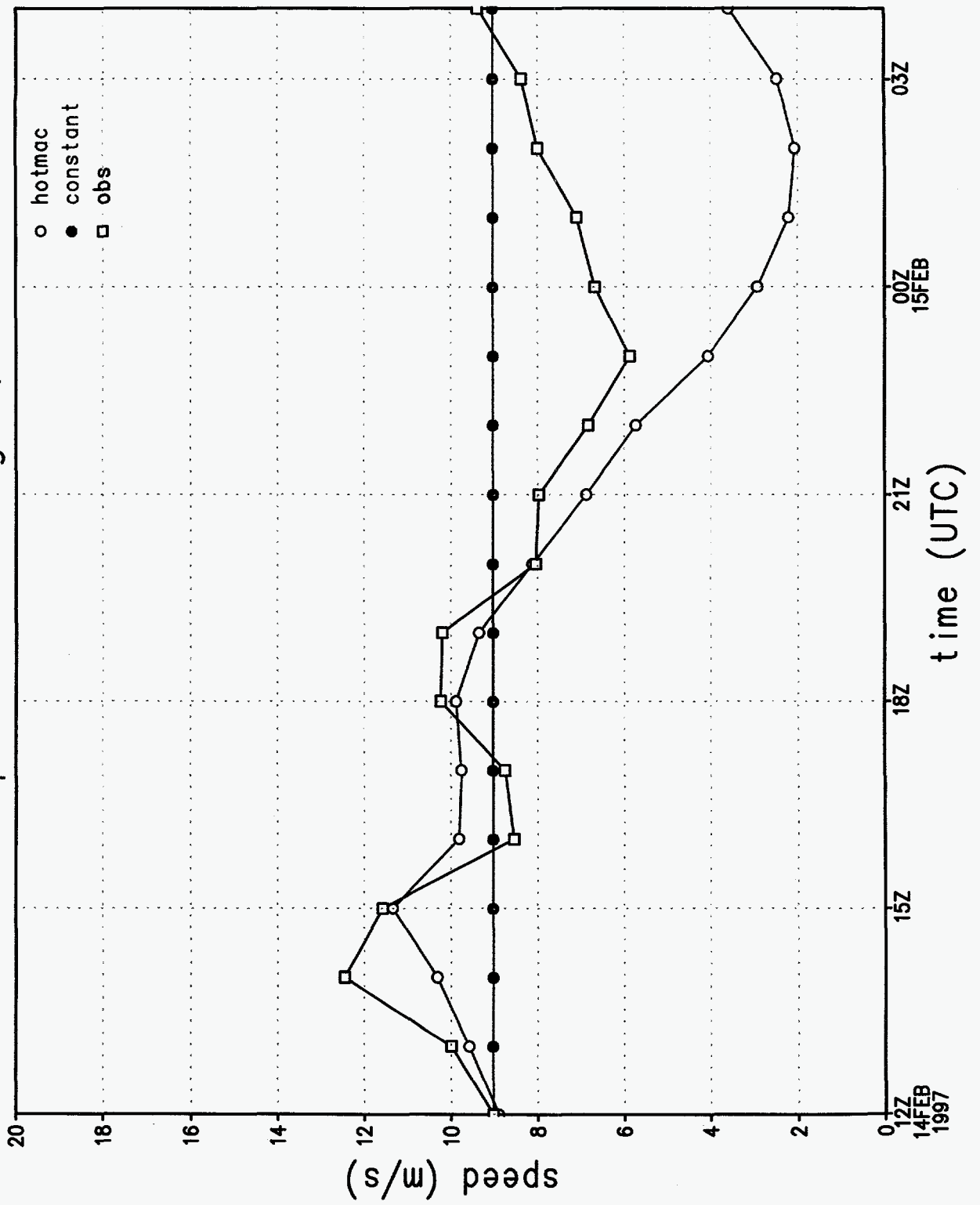


Figure 7b.

# wind direction at station 1

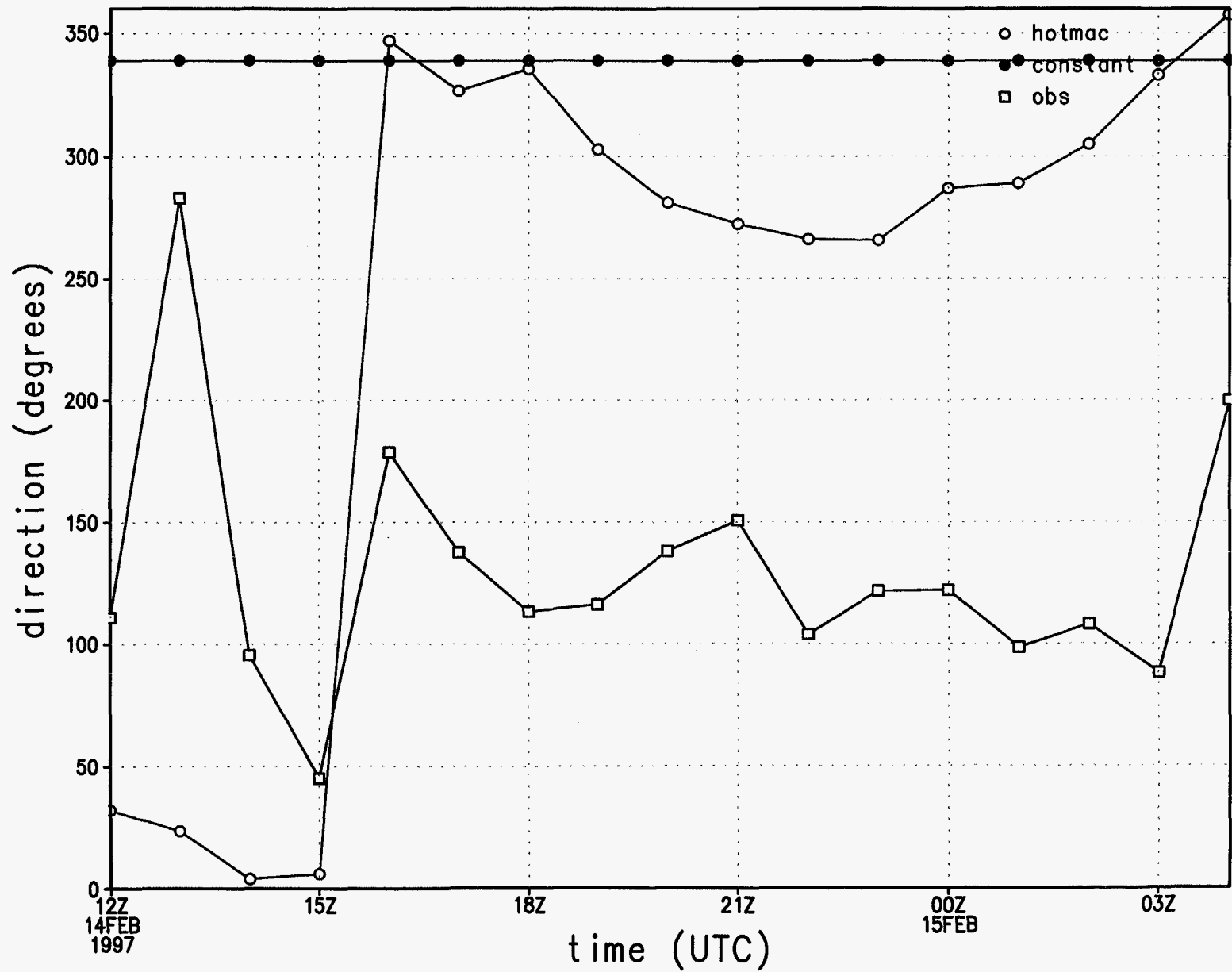


Figure 7c.

# wind speed at station 1

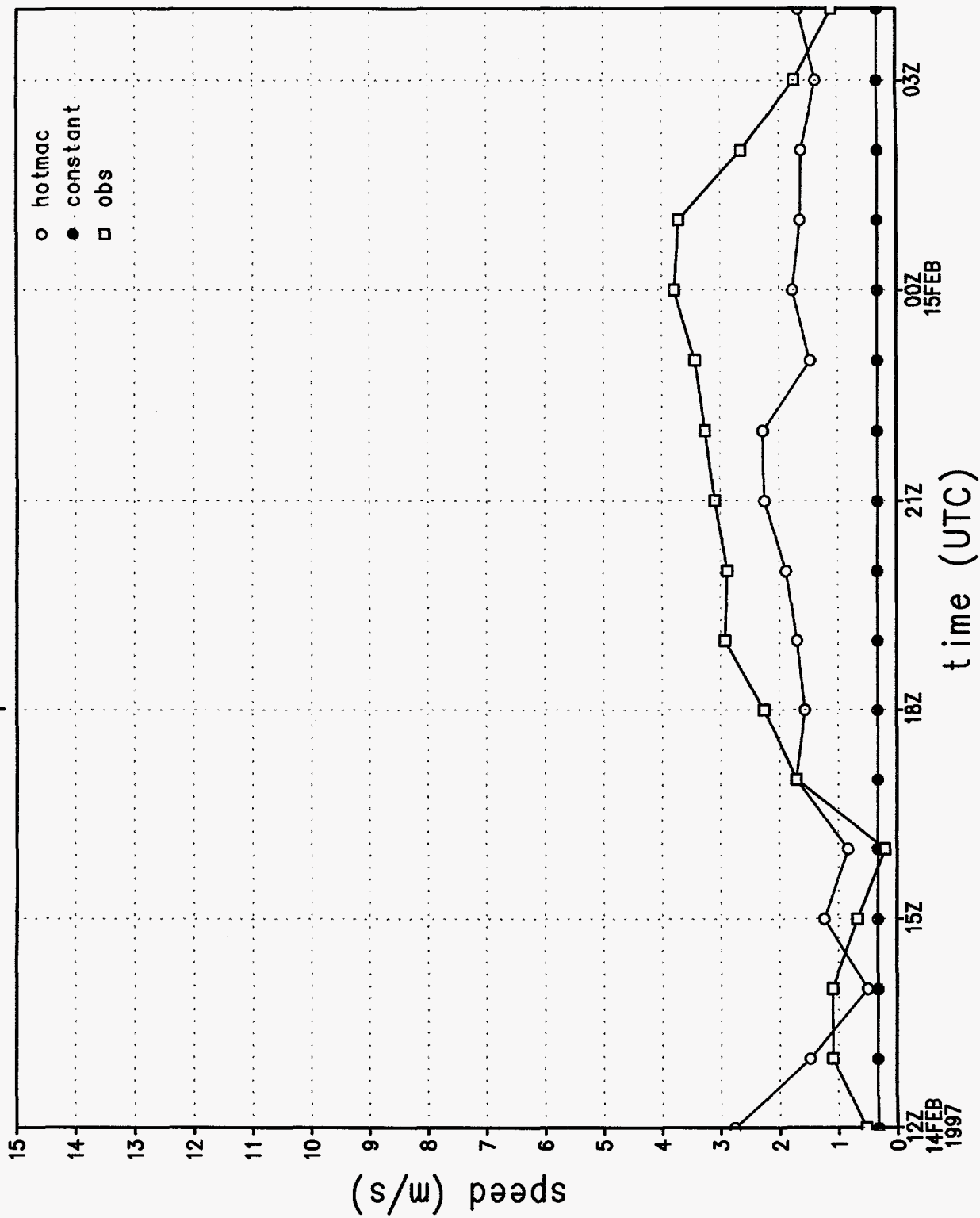


Figure 7d.

# u wind component at station 1

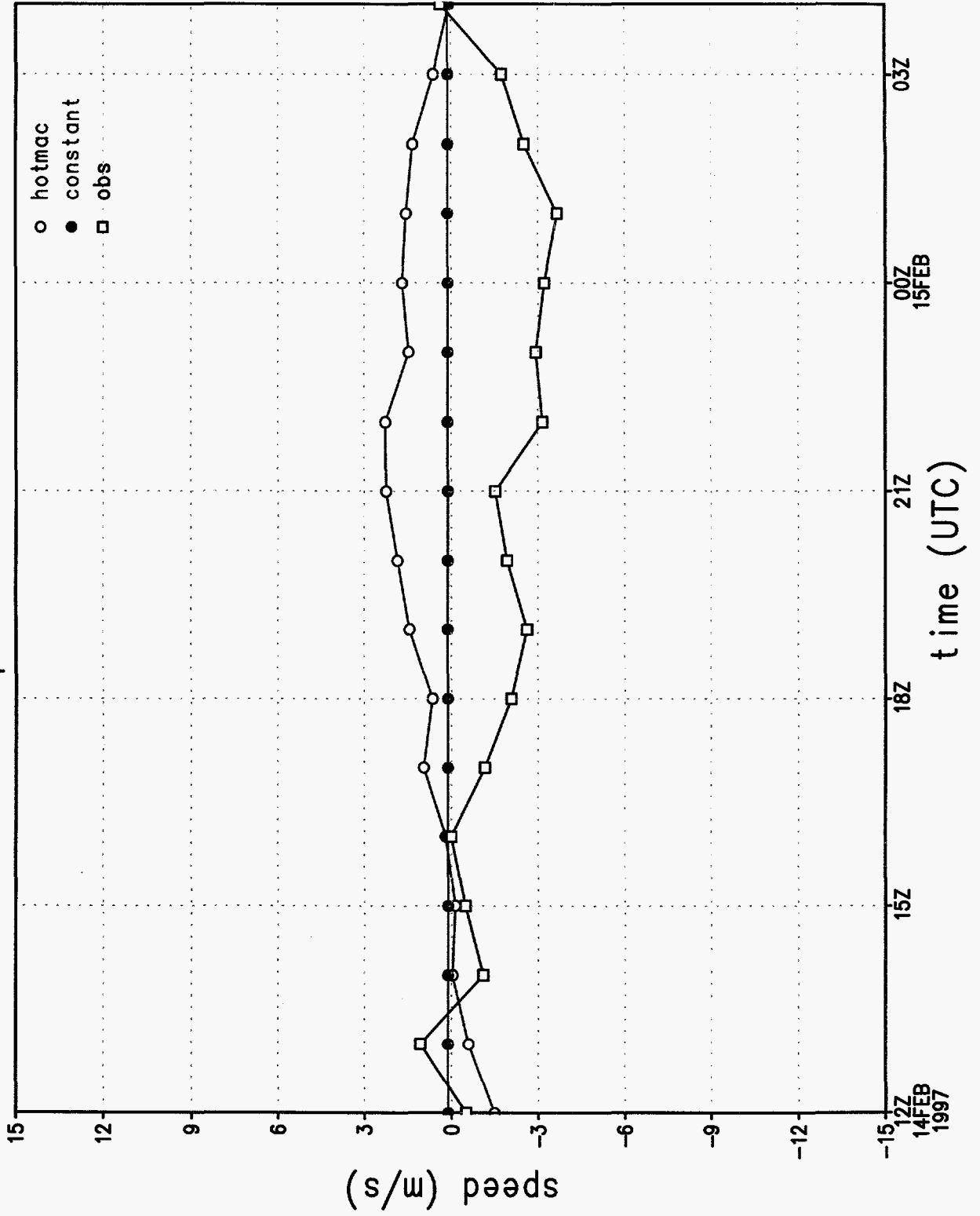


Figure 7e.

# v wind component at station 1

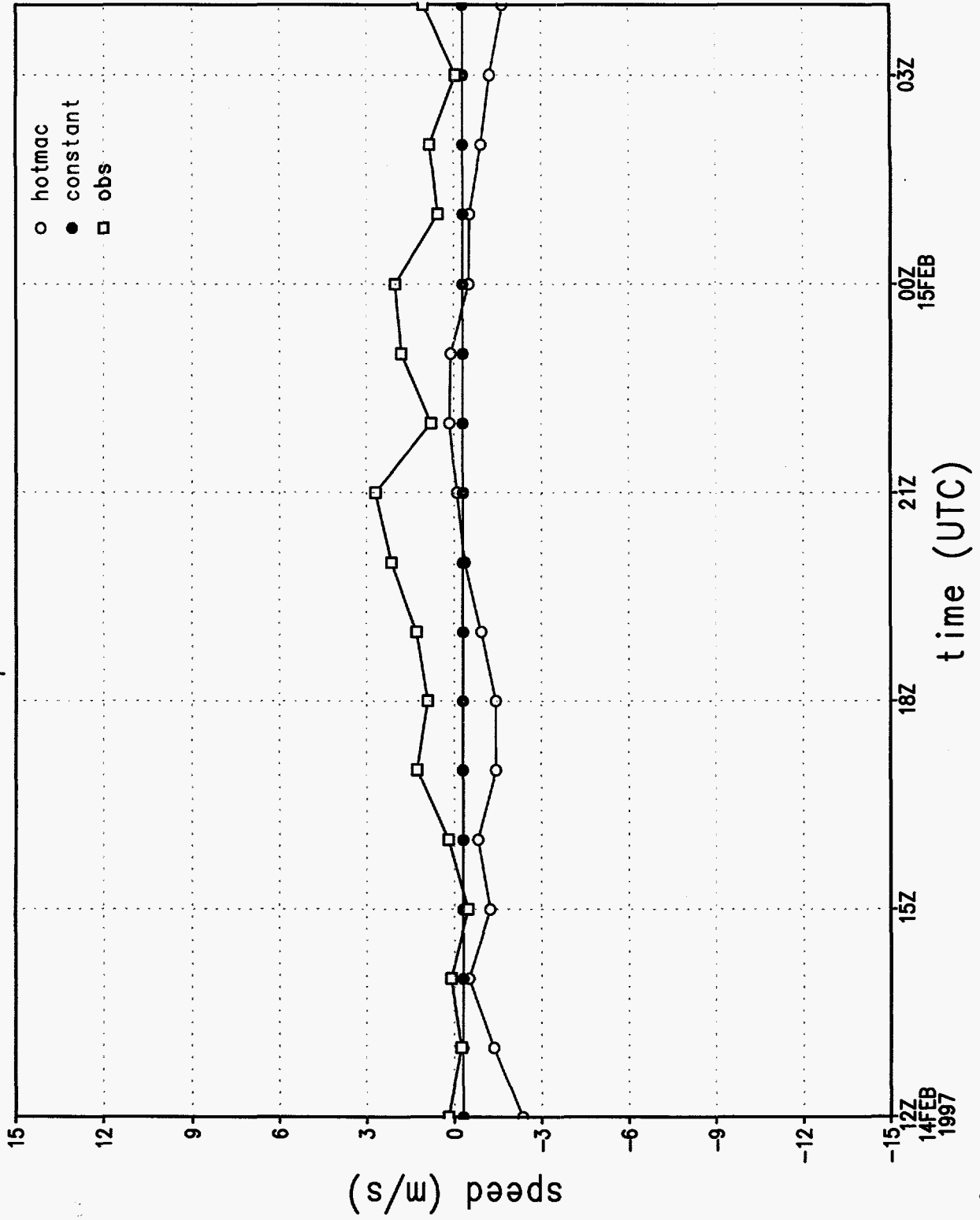


Figure 7f.



# rmse of wind direction by hour

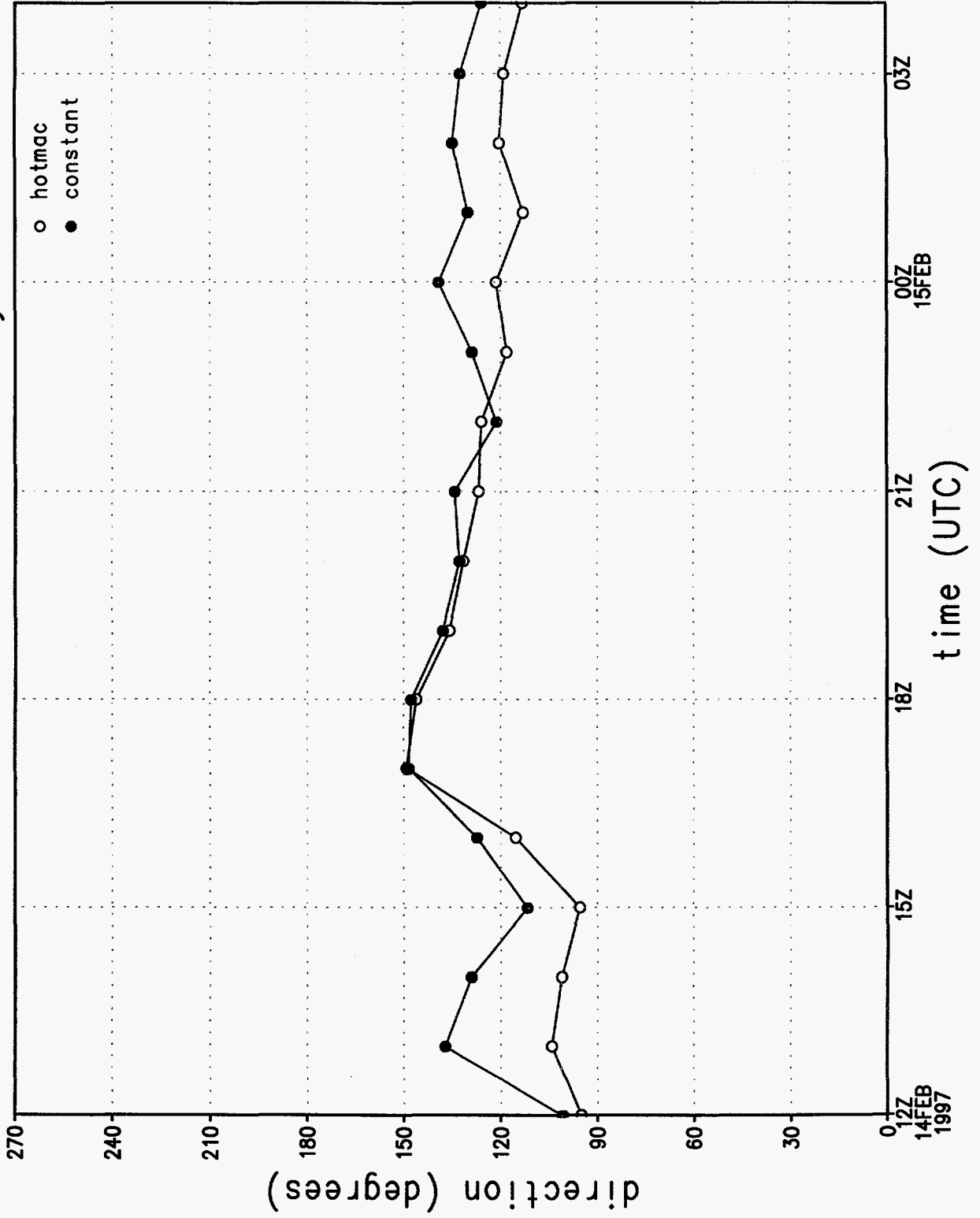


Figure 7g

# rmse of wind speed by hour

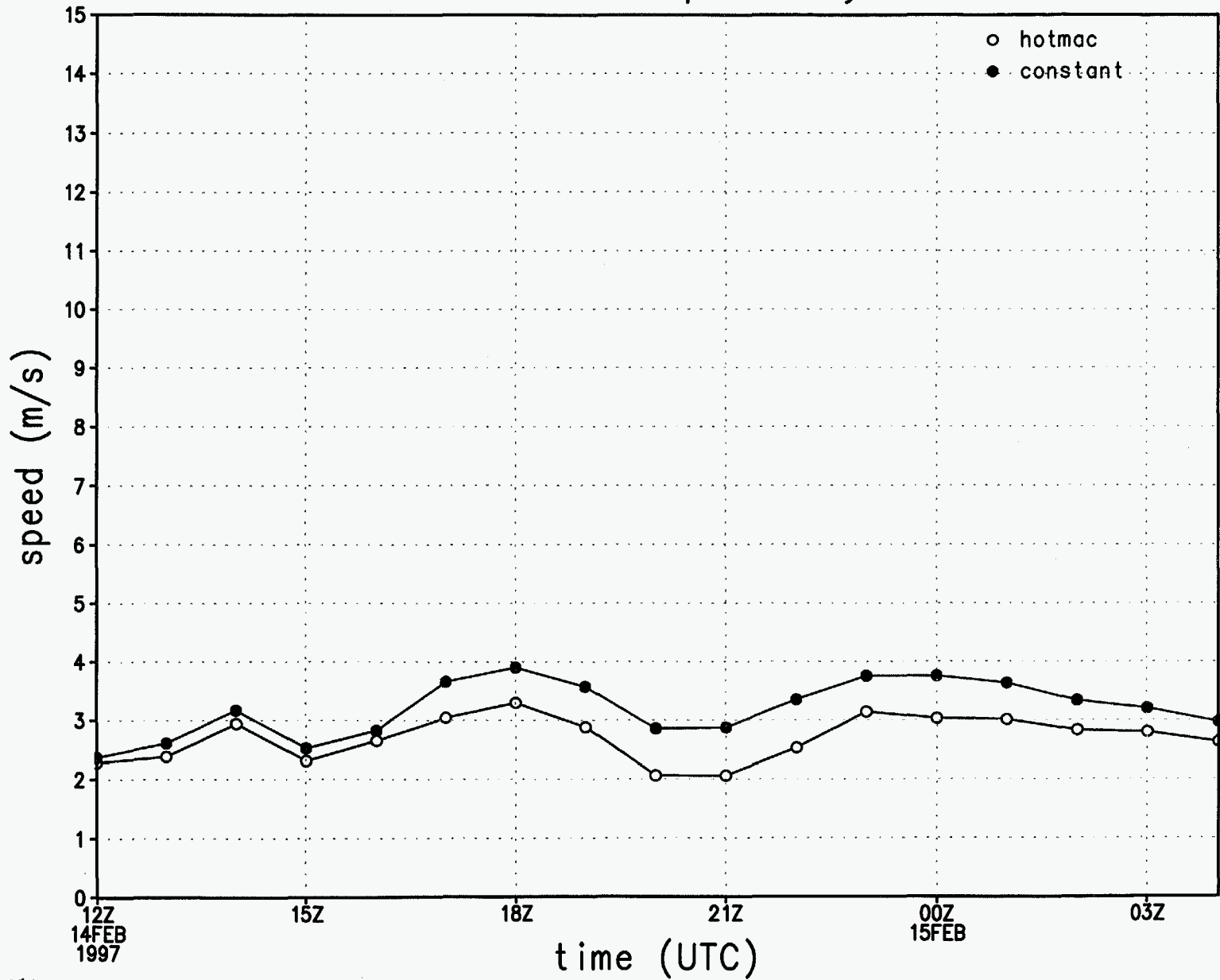


Figure 7h.

rmse of u wind component by hour

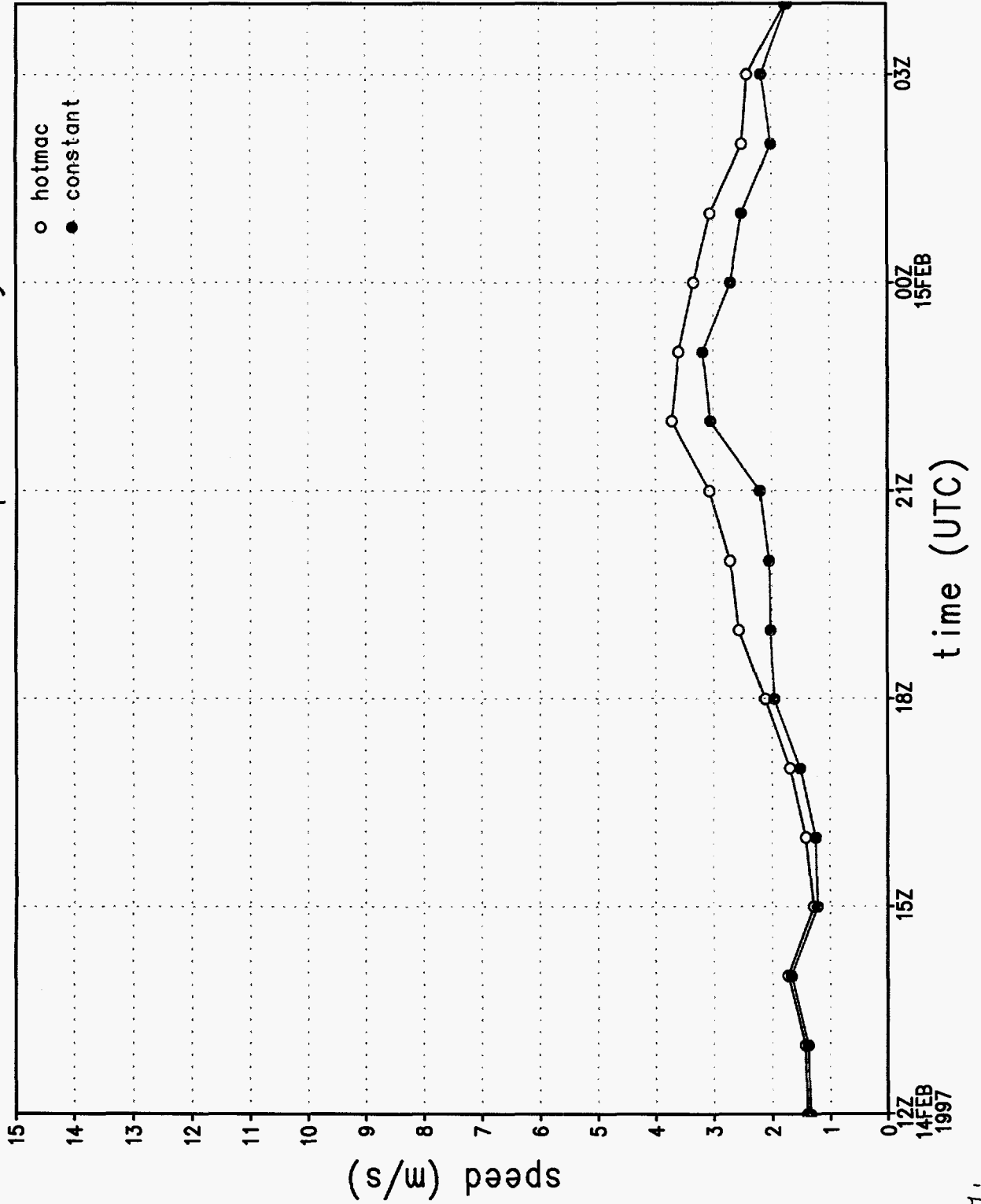


Figure 7i.

rmse of v wind component by hour

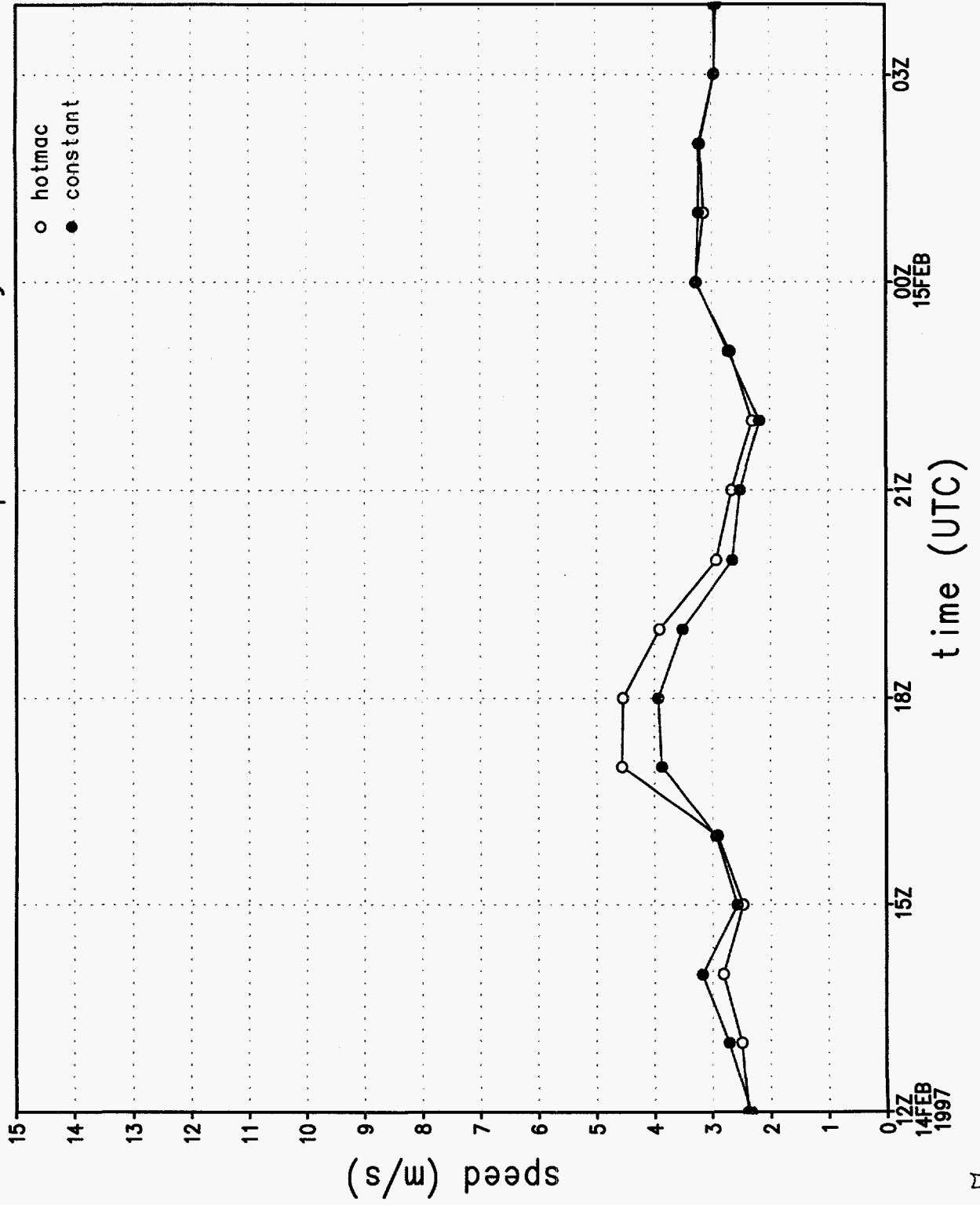


Figure 7j.

wind direction sounding 1, 1072 m

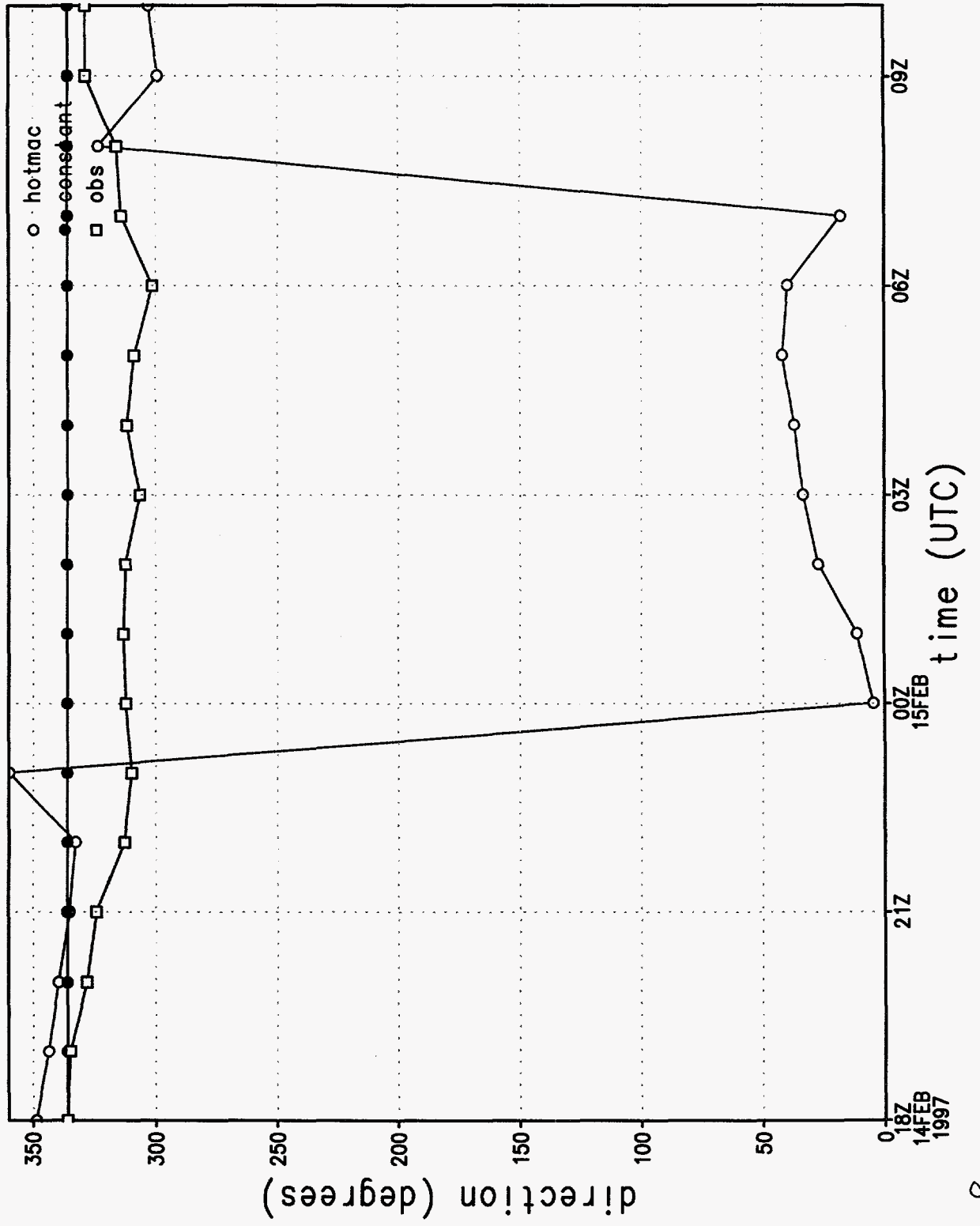


Figure 8a.

# wind speed sounding 1, 1072 m

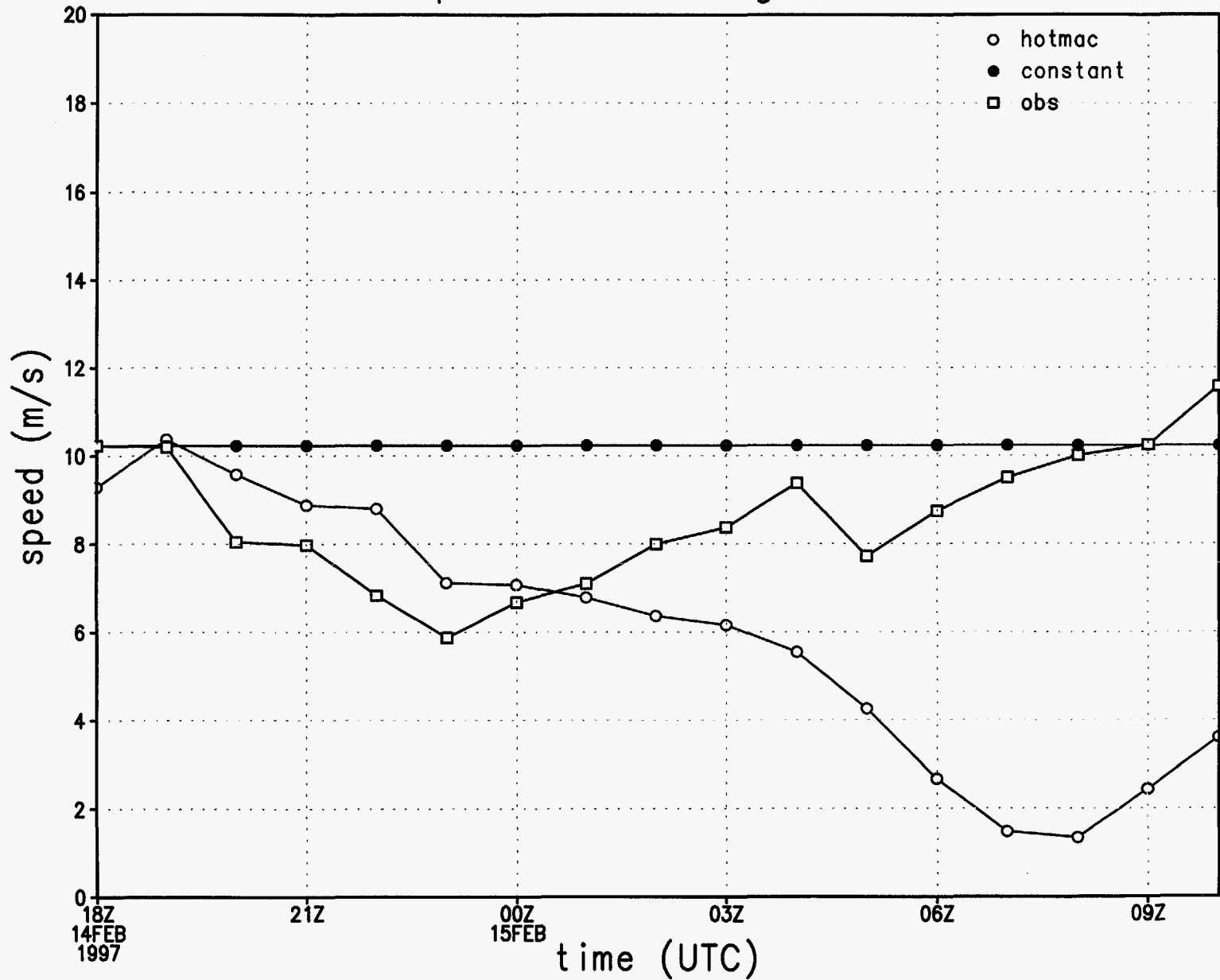


Figure 8b.

wind direction at station 1

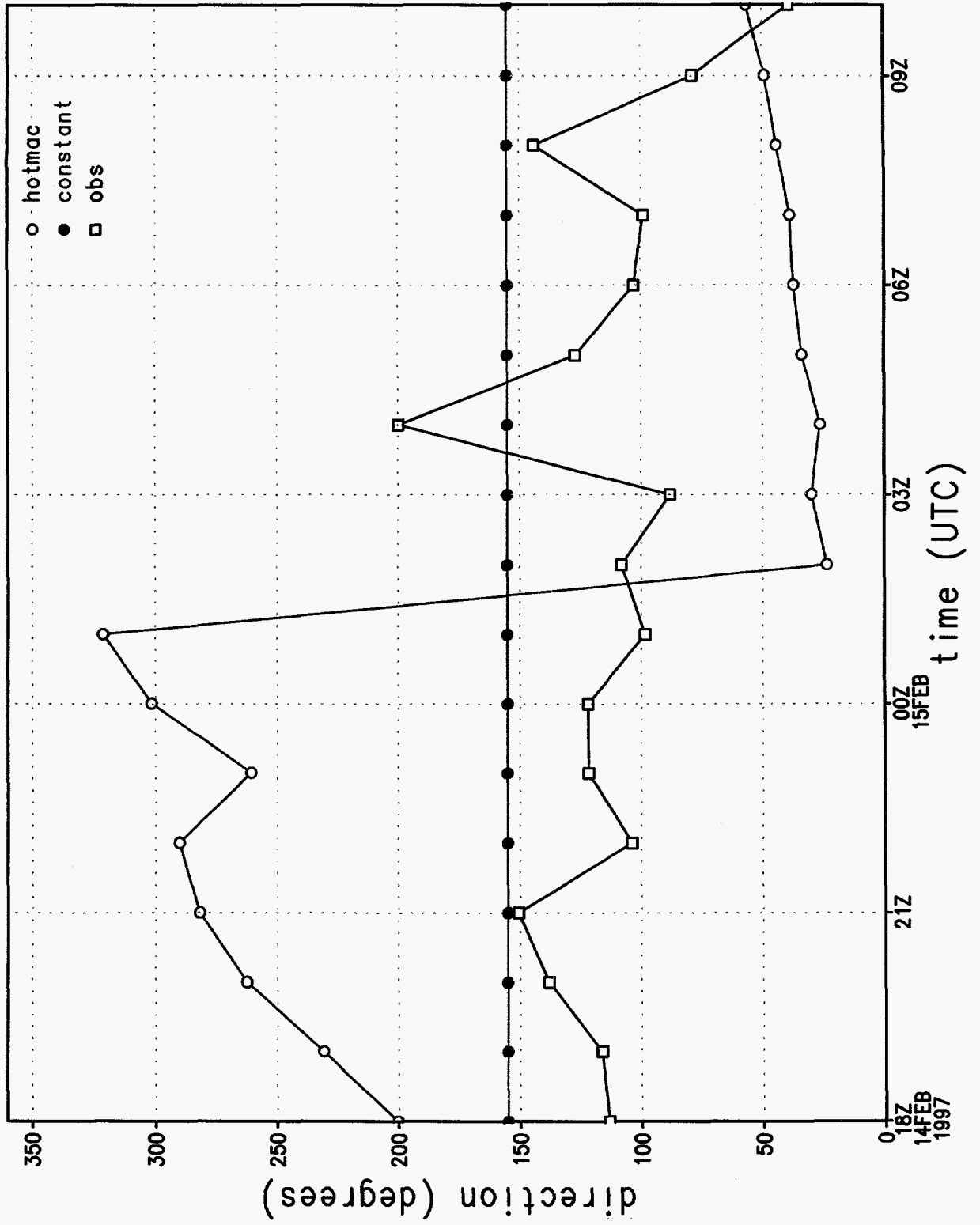


Figure 8c.

# wind speed at station 1

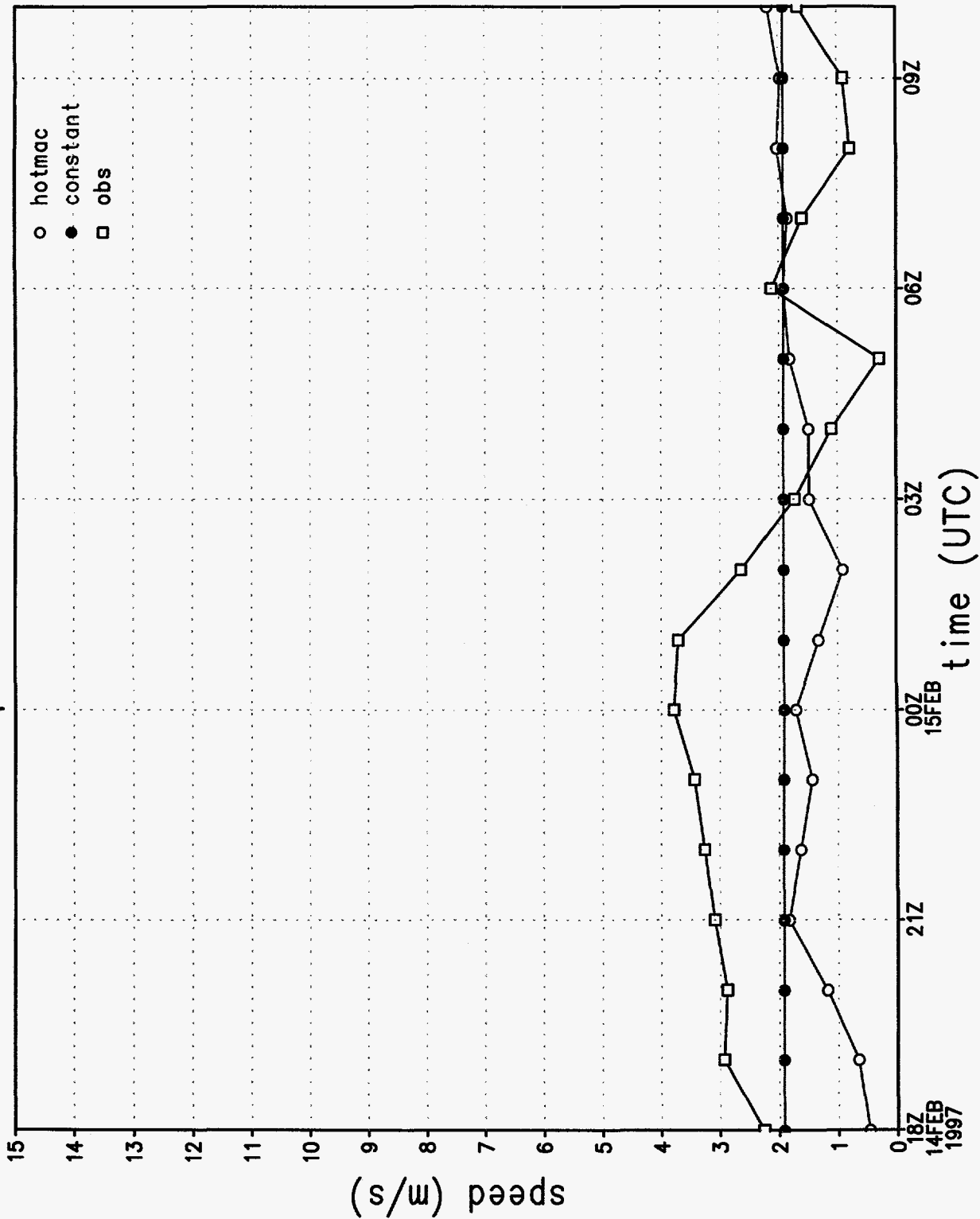


Figure 8d.



# u wind component at station 1

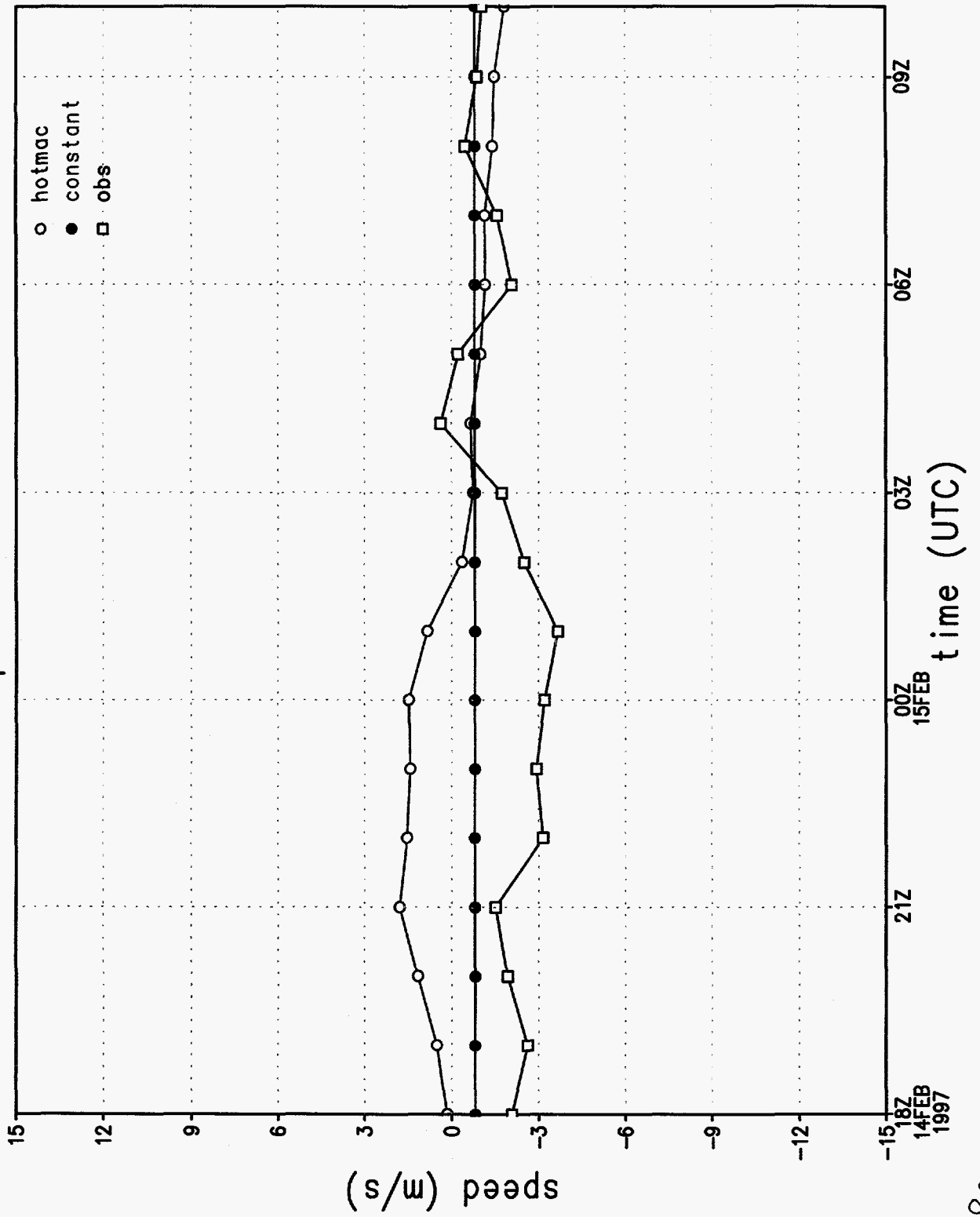


Figure 8e.

# v wind component at station 1

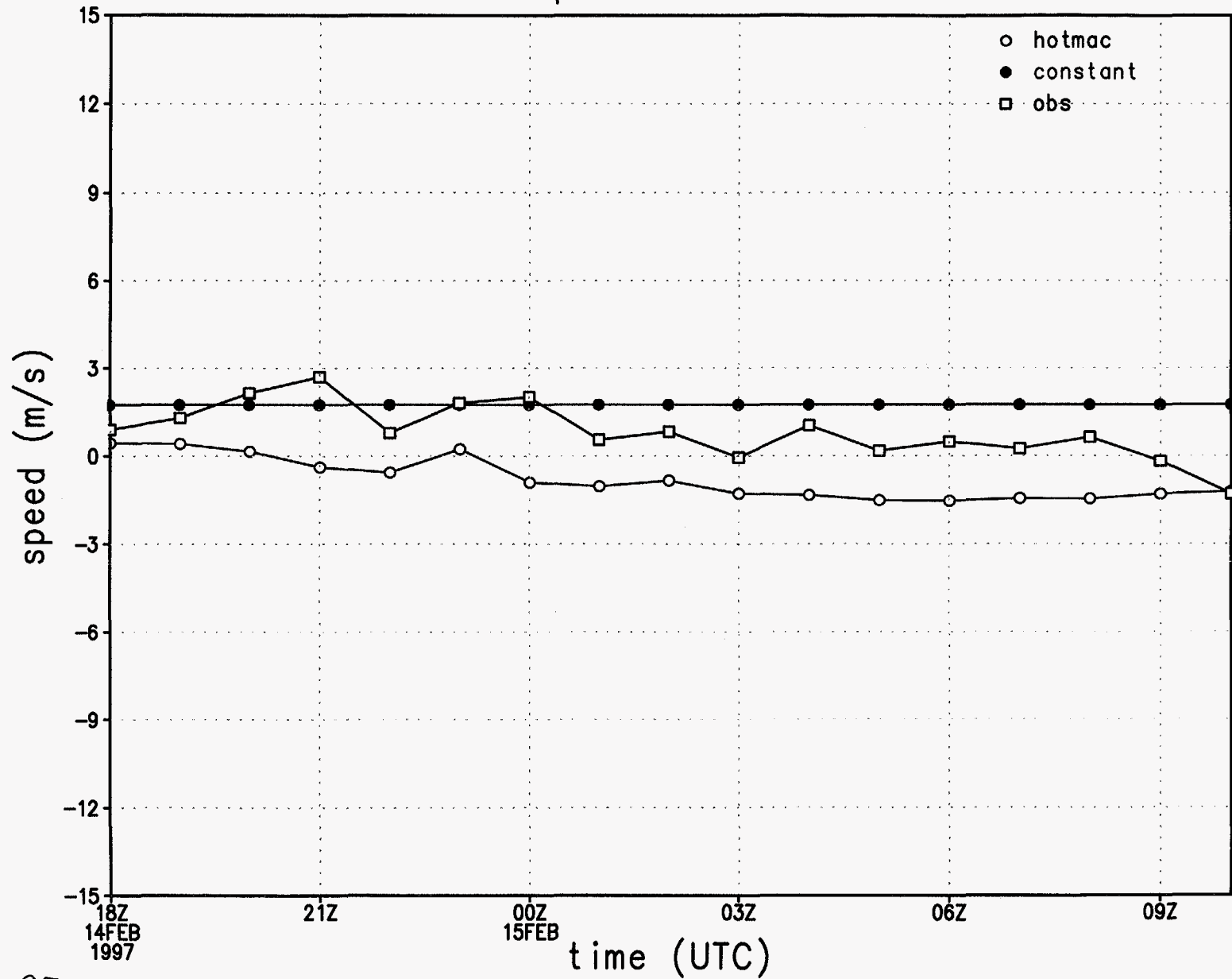


Figure 8f.

# rmse of wind direction by hour

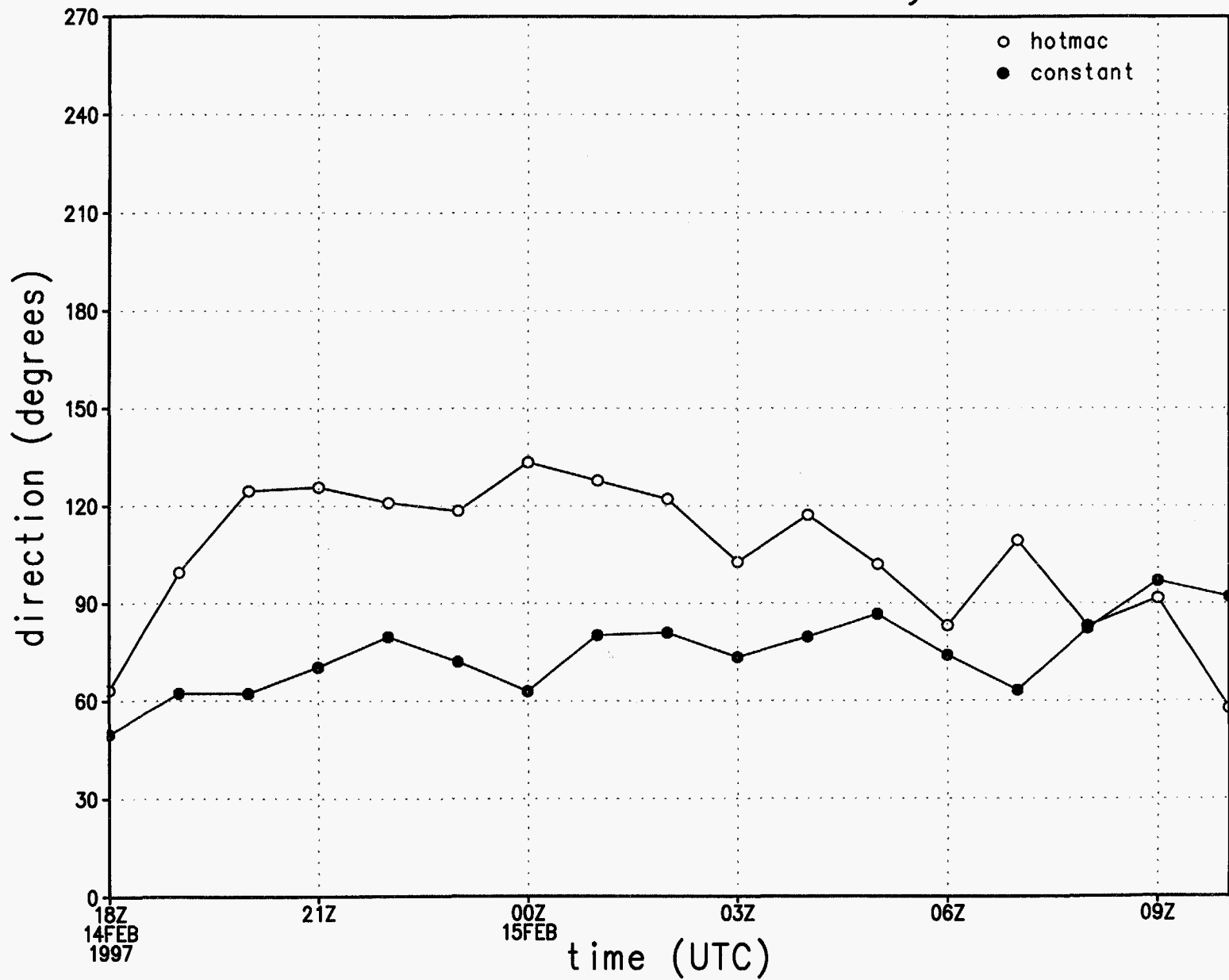


Figure 8g.

# rmse of wind speed by hour

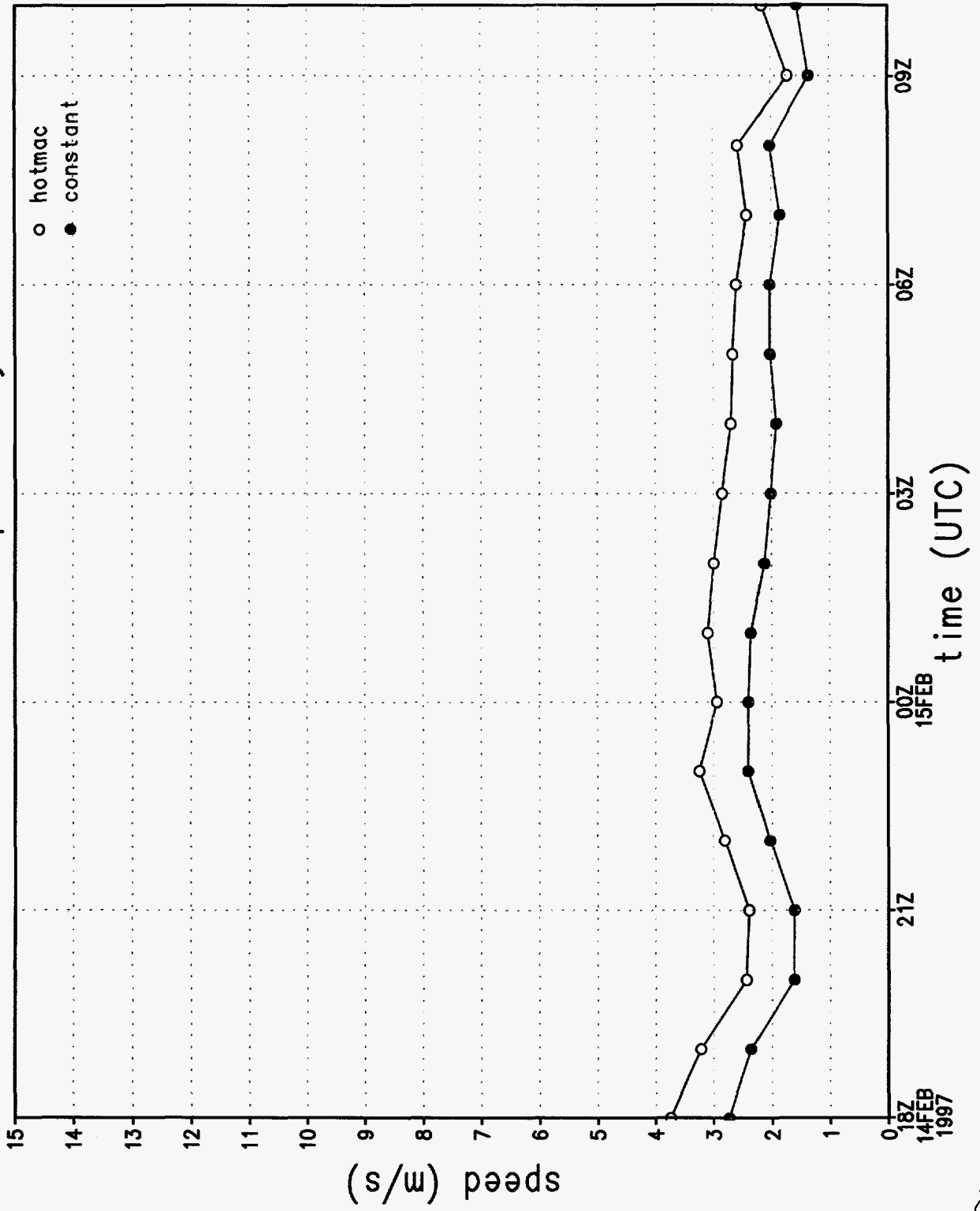


Figure 8h.

rmse of u wind component by hour

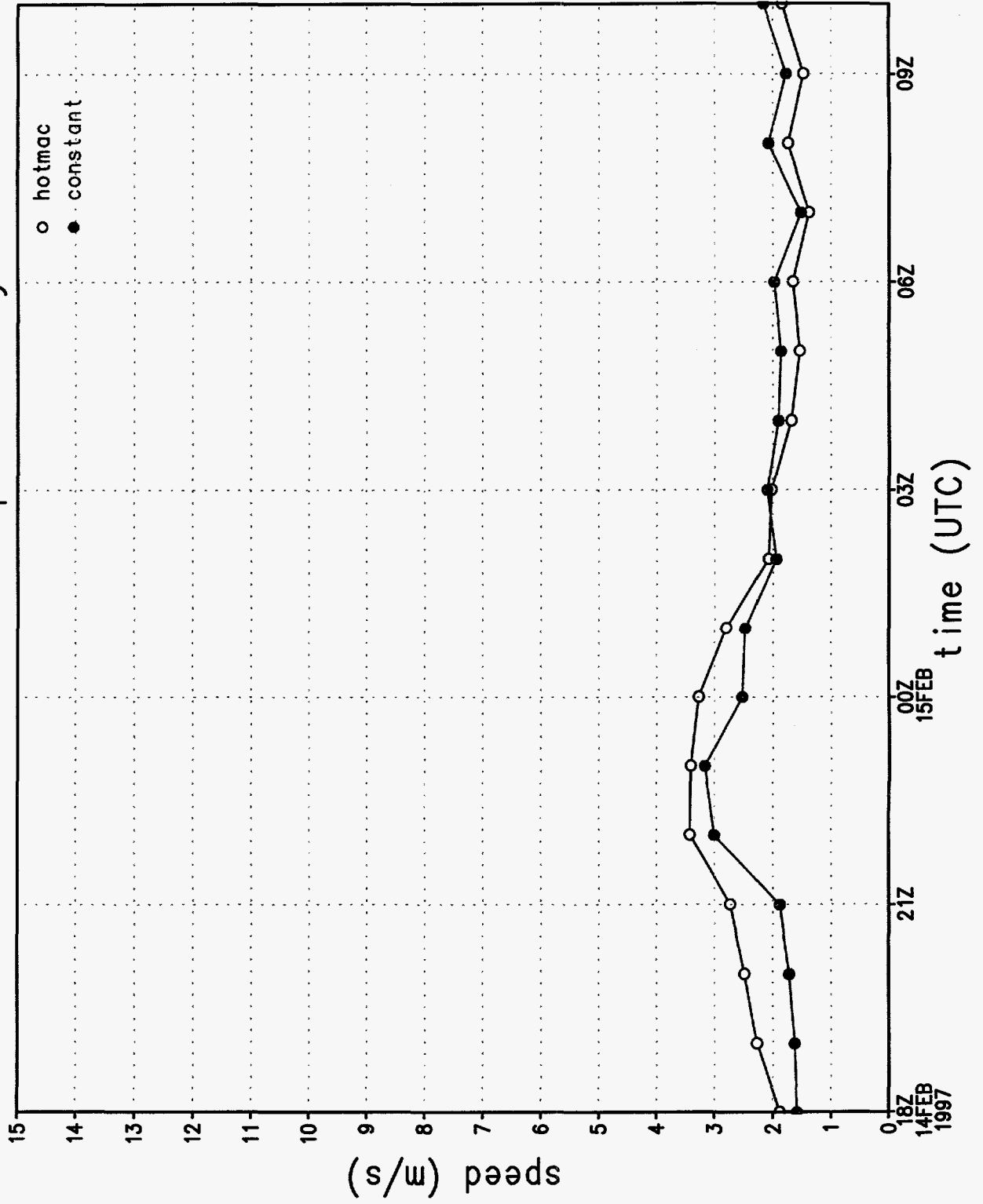


Figure 8i.

# rmse of v wind component by hour

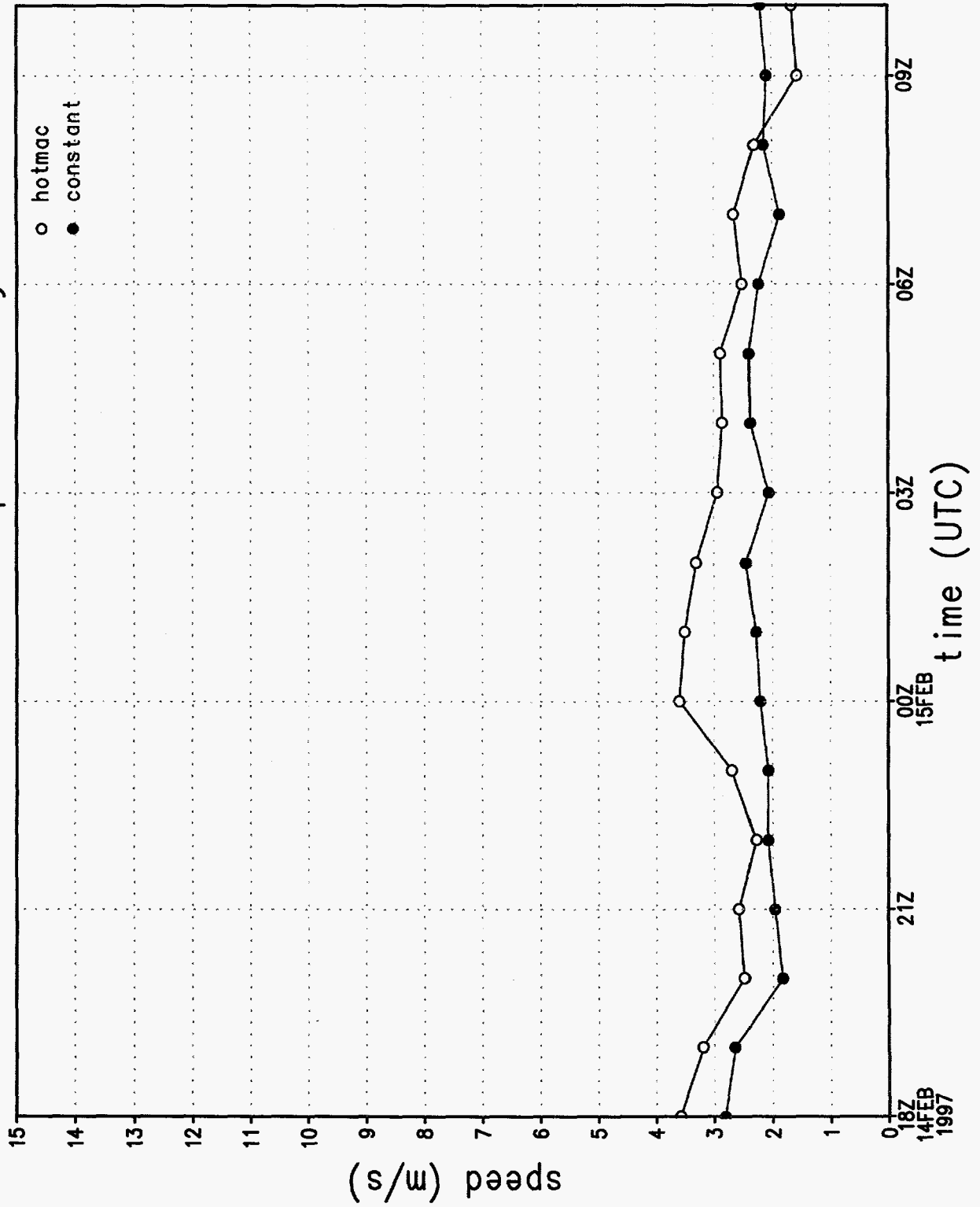


Figure 8j.

wind direction sounding 1, 1072 m

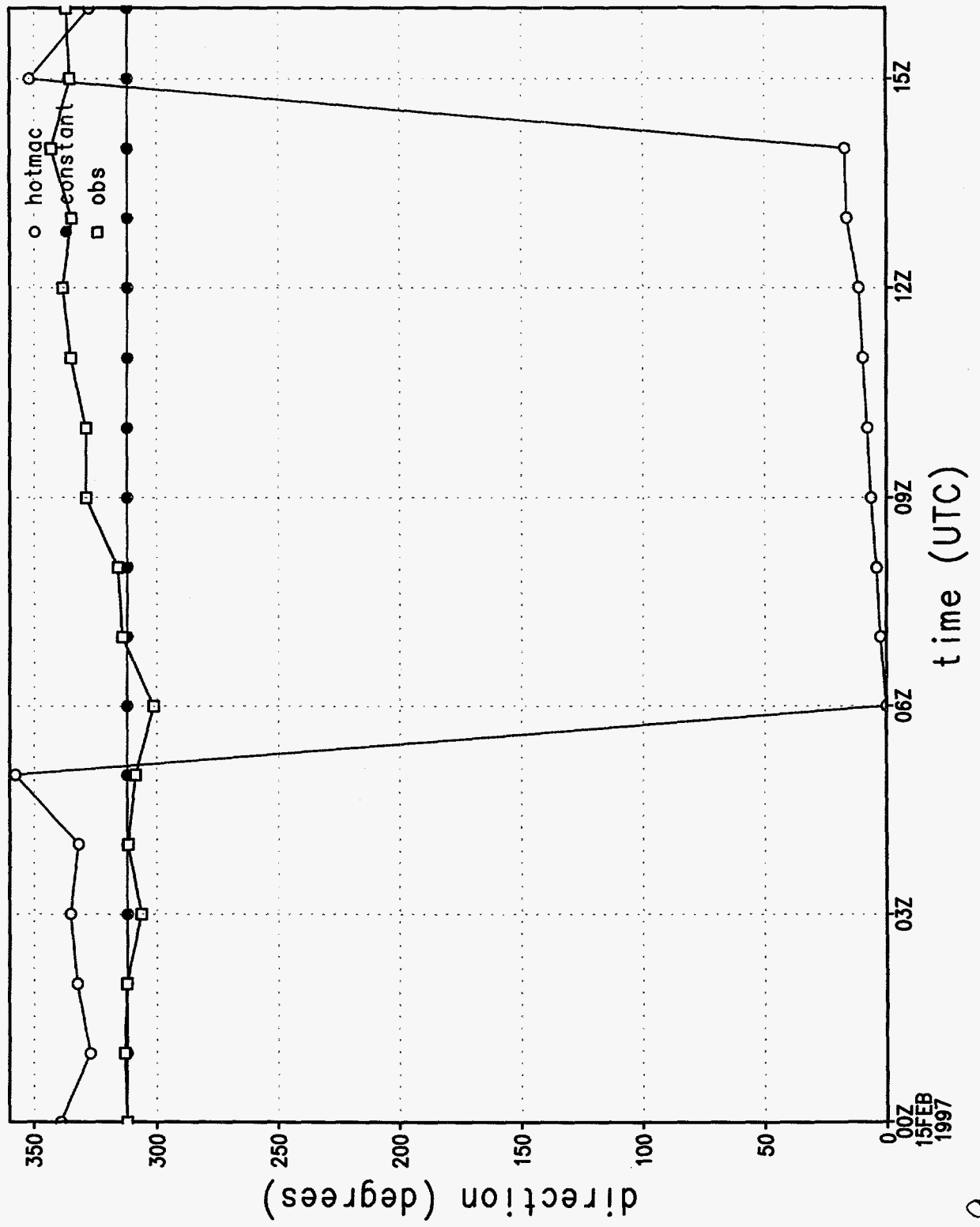


Figure 9a.

wind speed sounding 1, 1072 m

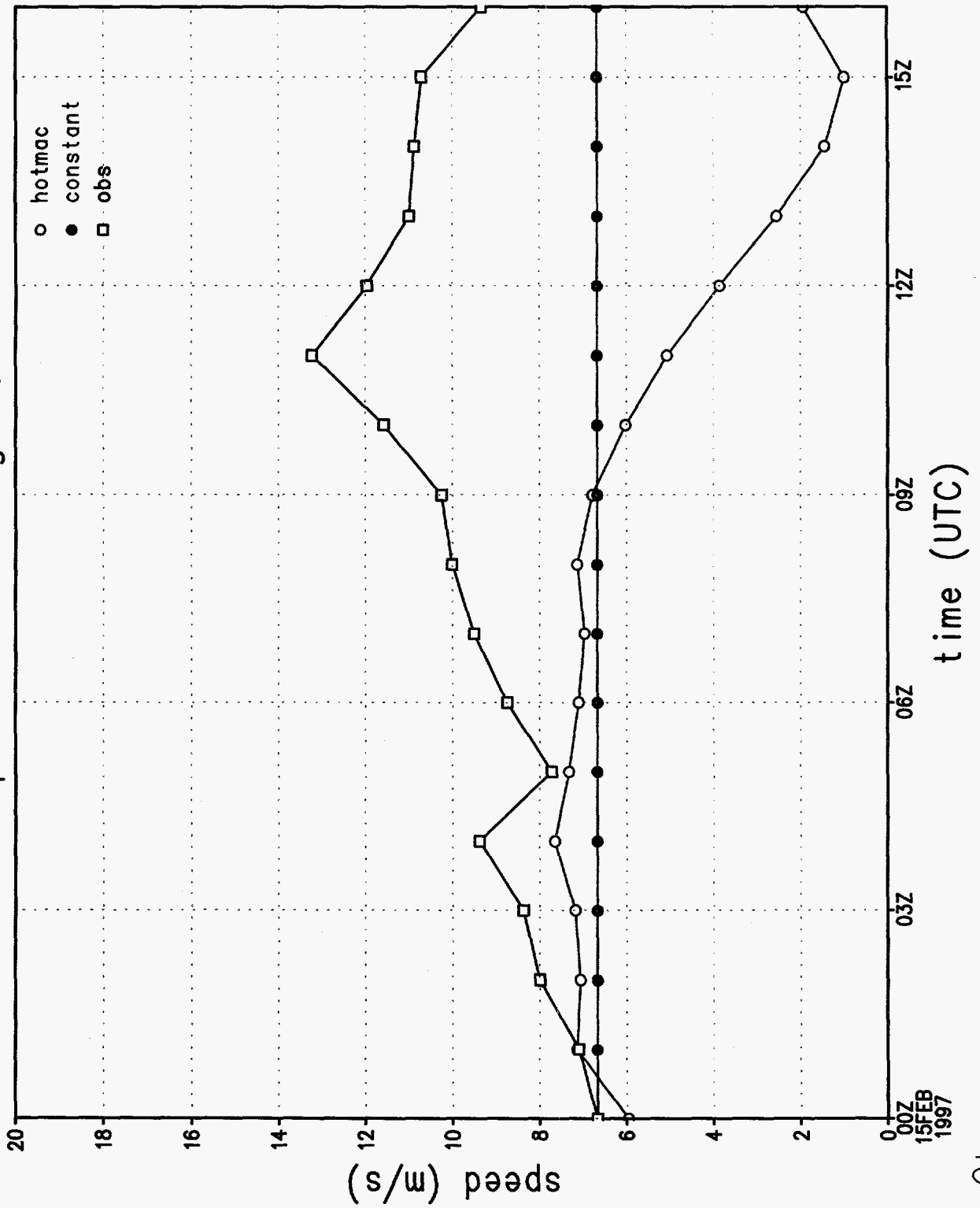


Figure 9b.



# wind direction at station 1

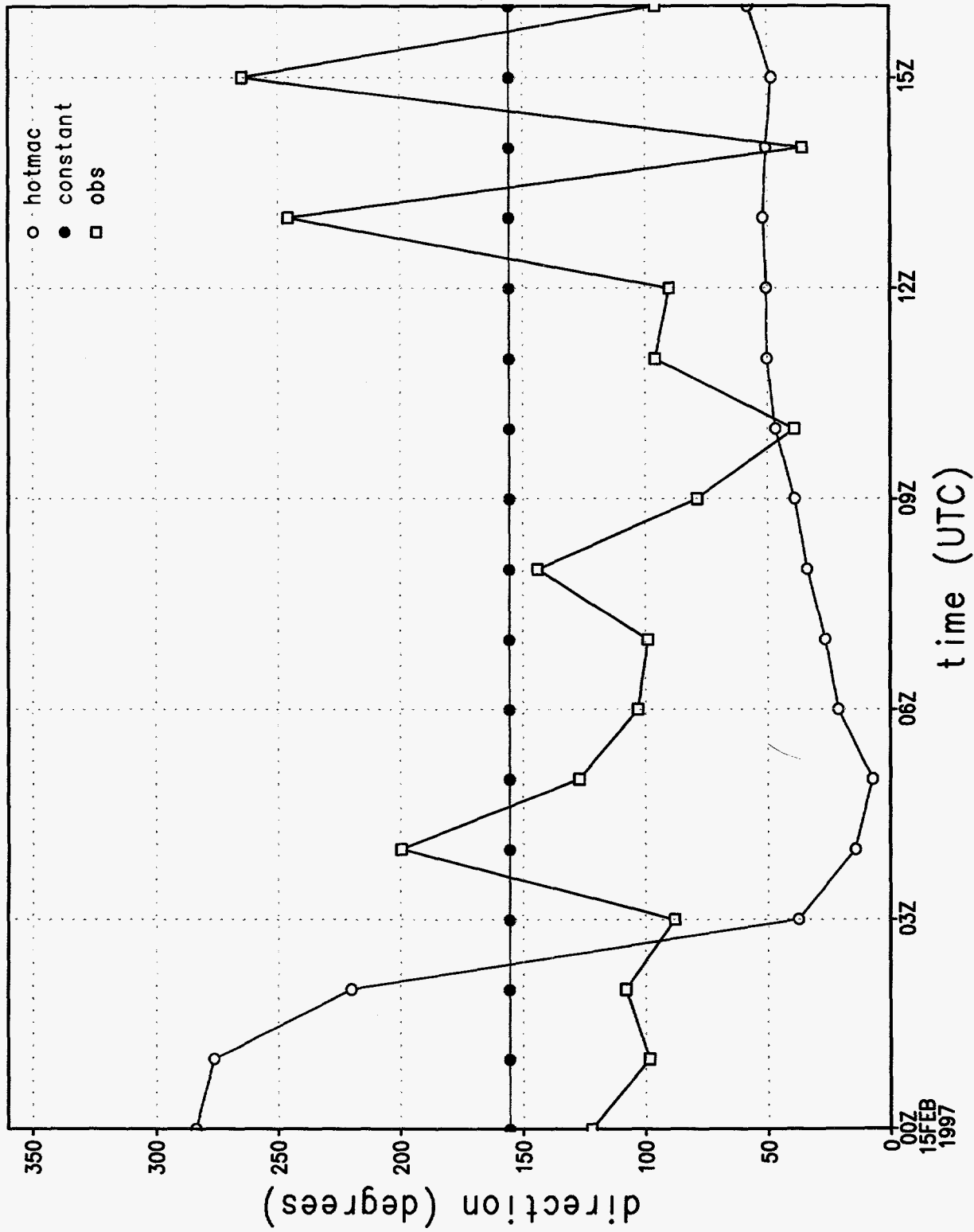


Figure 9c.

# wind speed at station 1

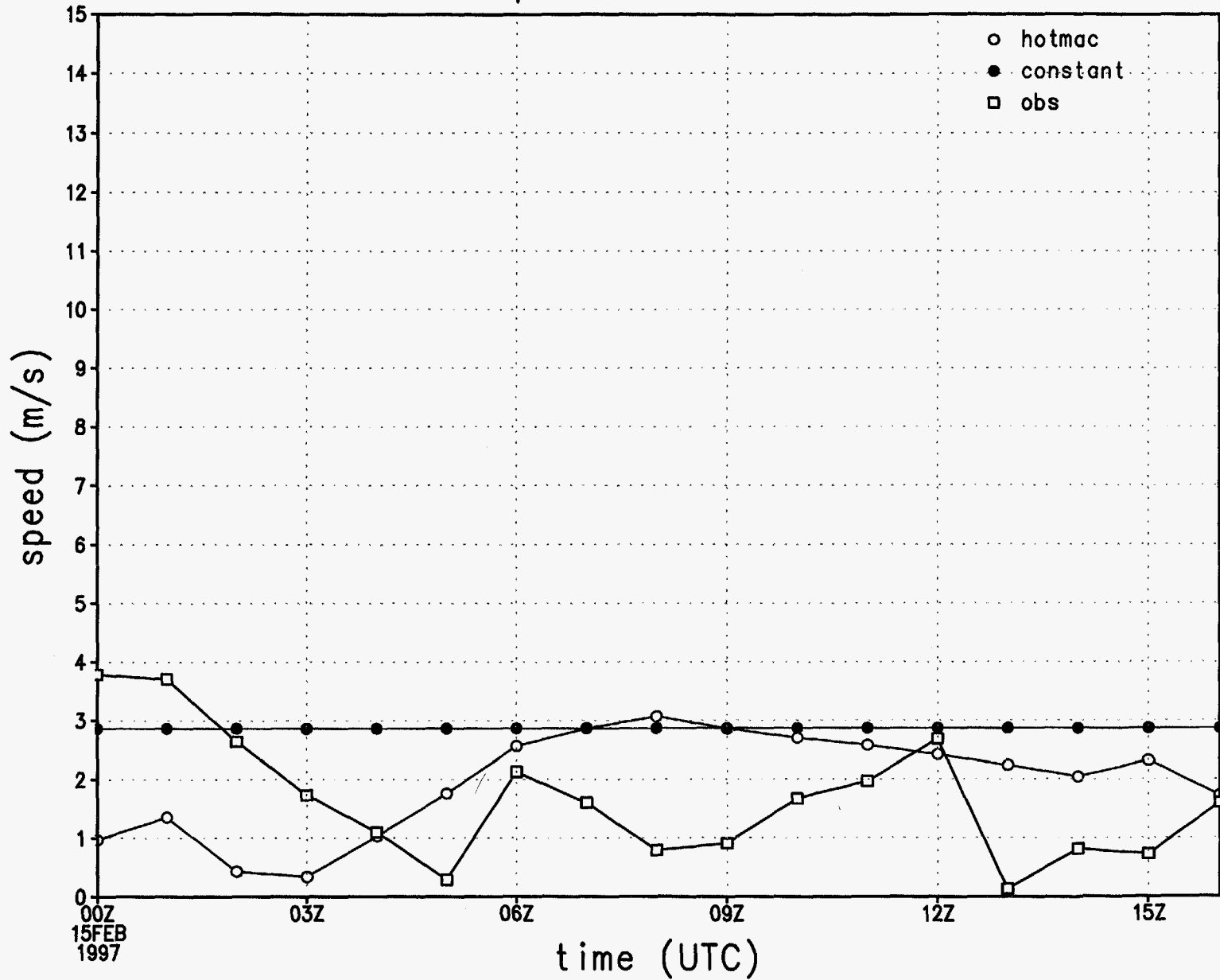


Figure 9d.

# u wind component at station 1

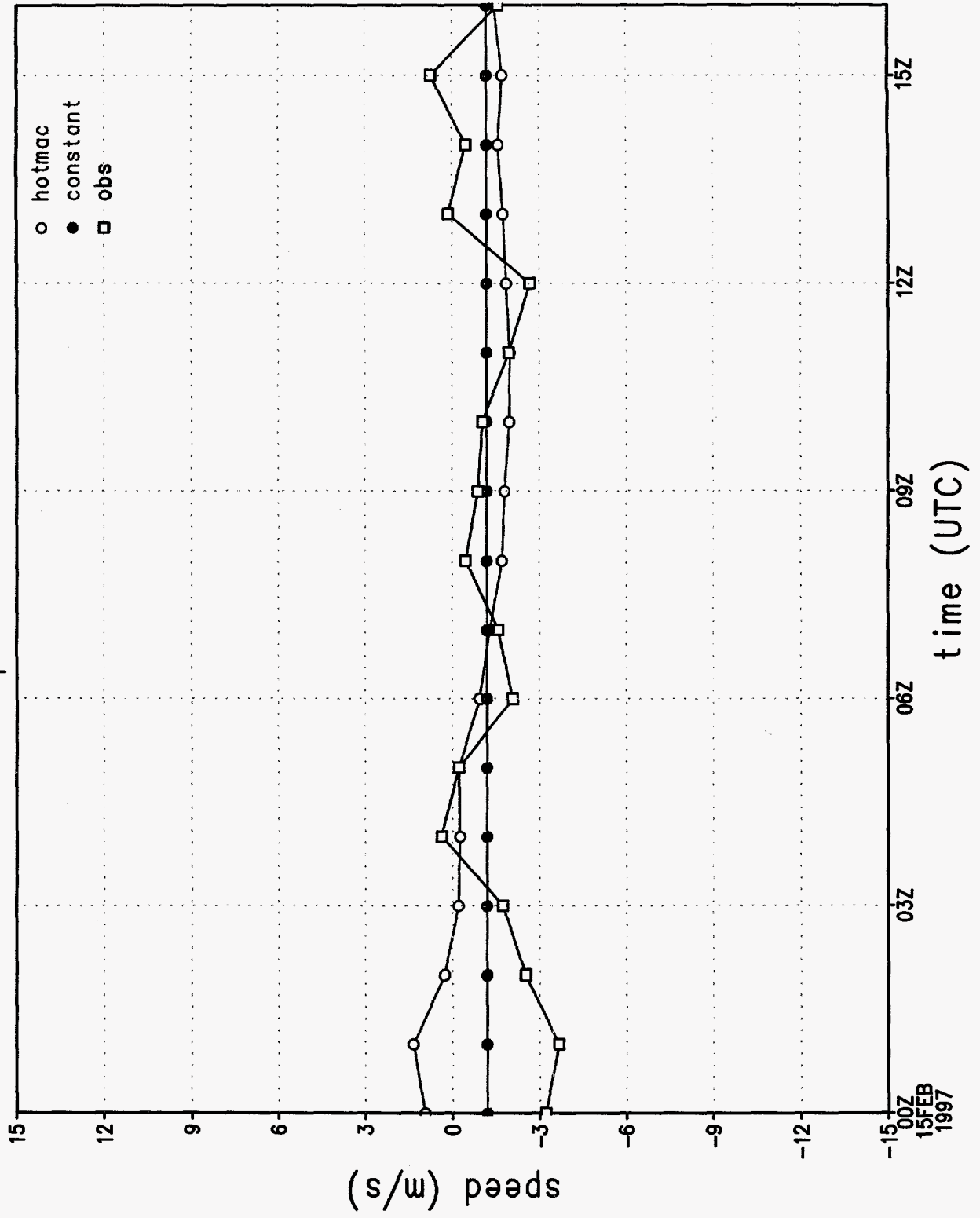


Figure 9e.

v wind component at station 1

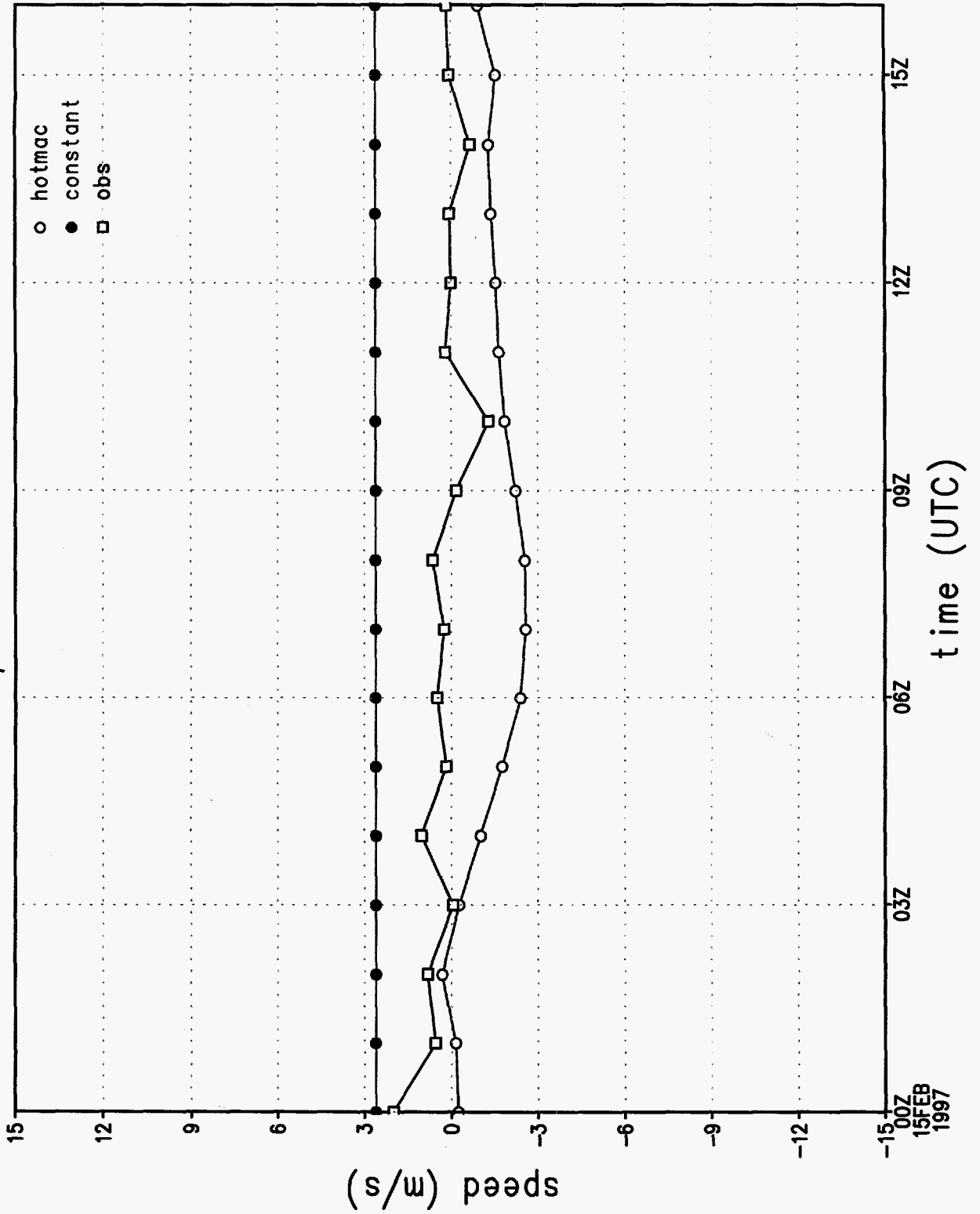


Figure 9 f.

# rmse of wind direction by hour

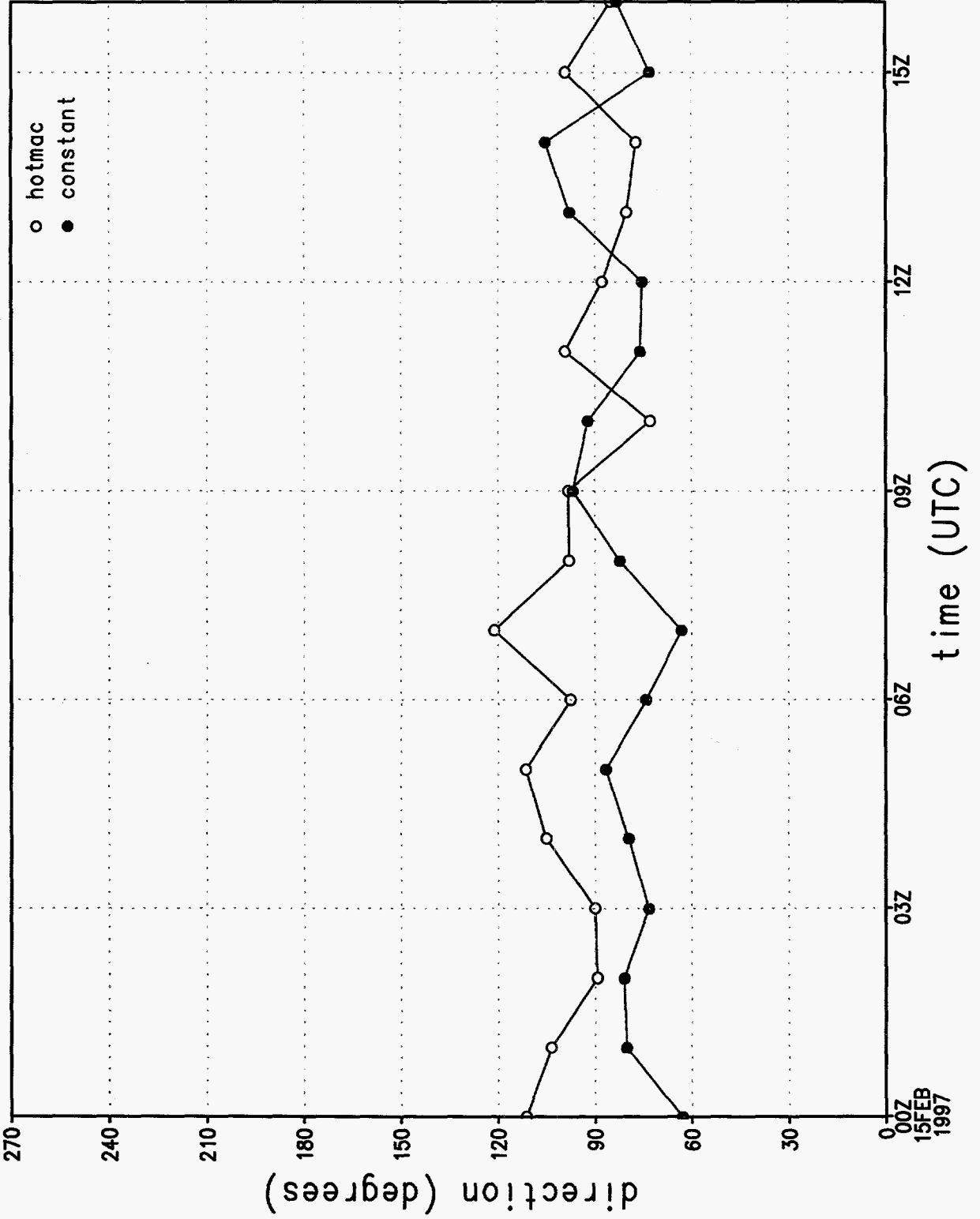


Figure 9g.

# rmse of wind speed by hour

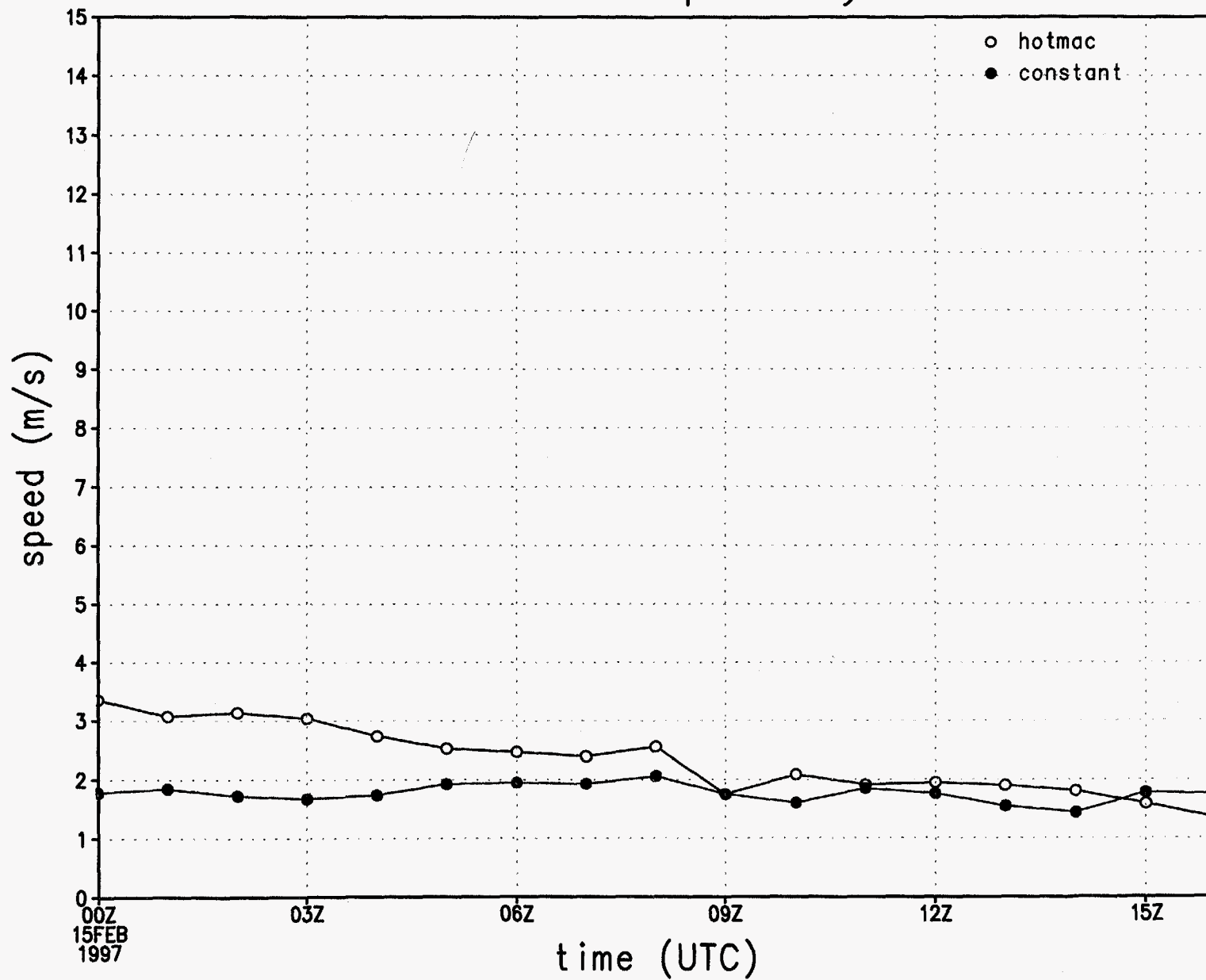


Figure 9h.

rmse of u wind component by hour

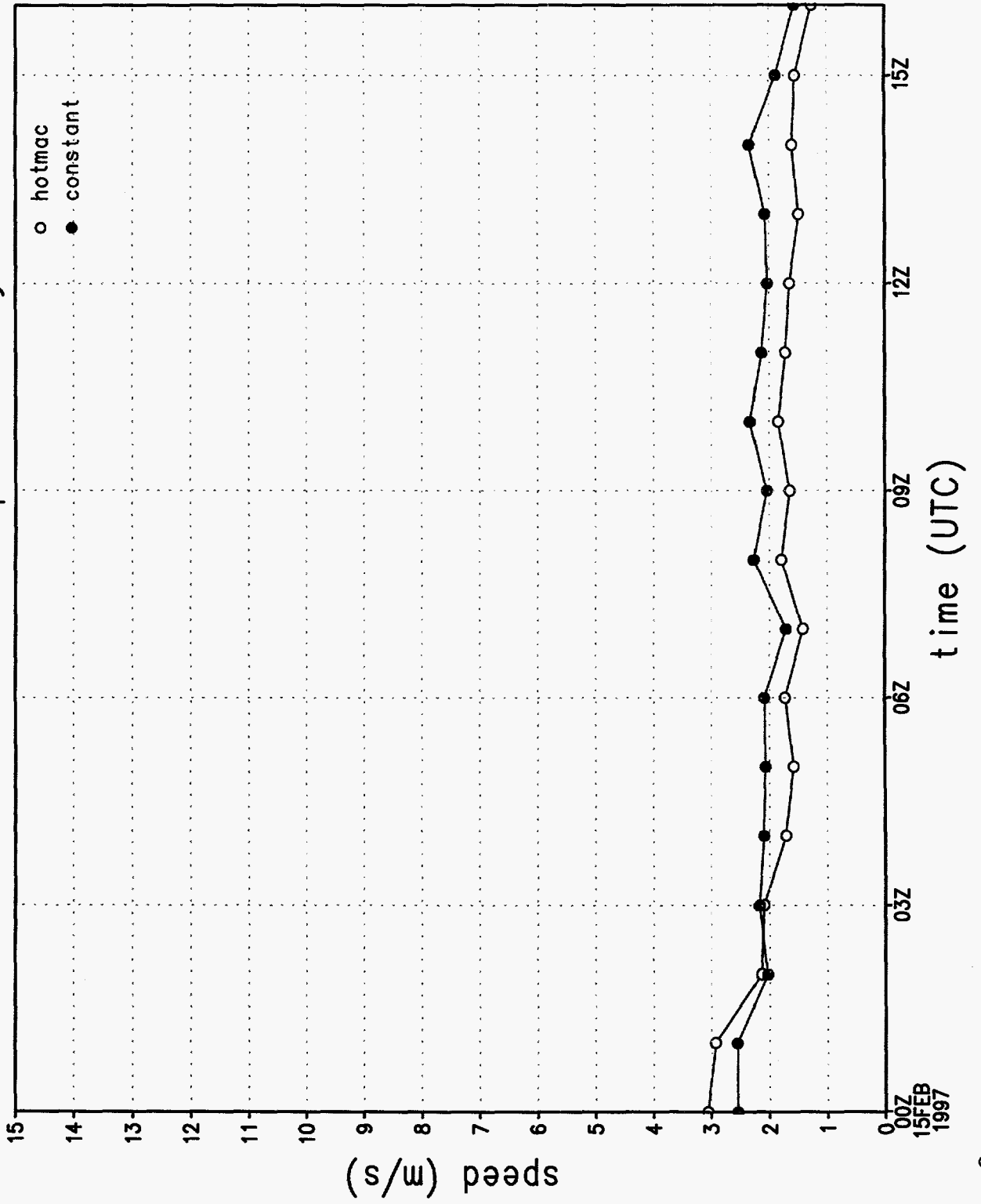


Figure 91.

rmse of v wind component by hour

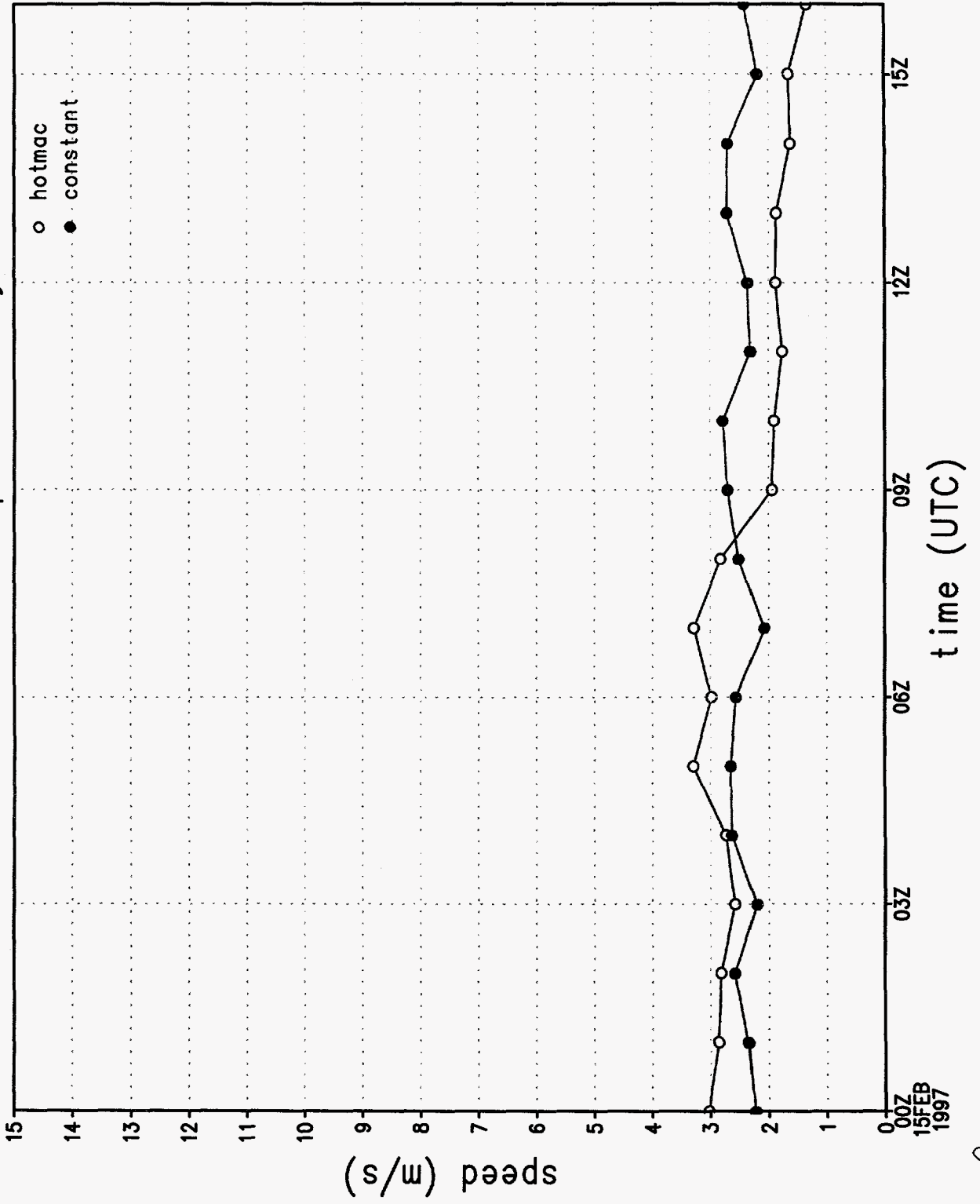


Figure 9j.



wind direction sounding 1, 1072 m

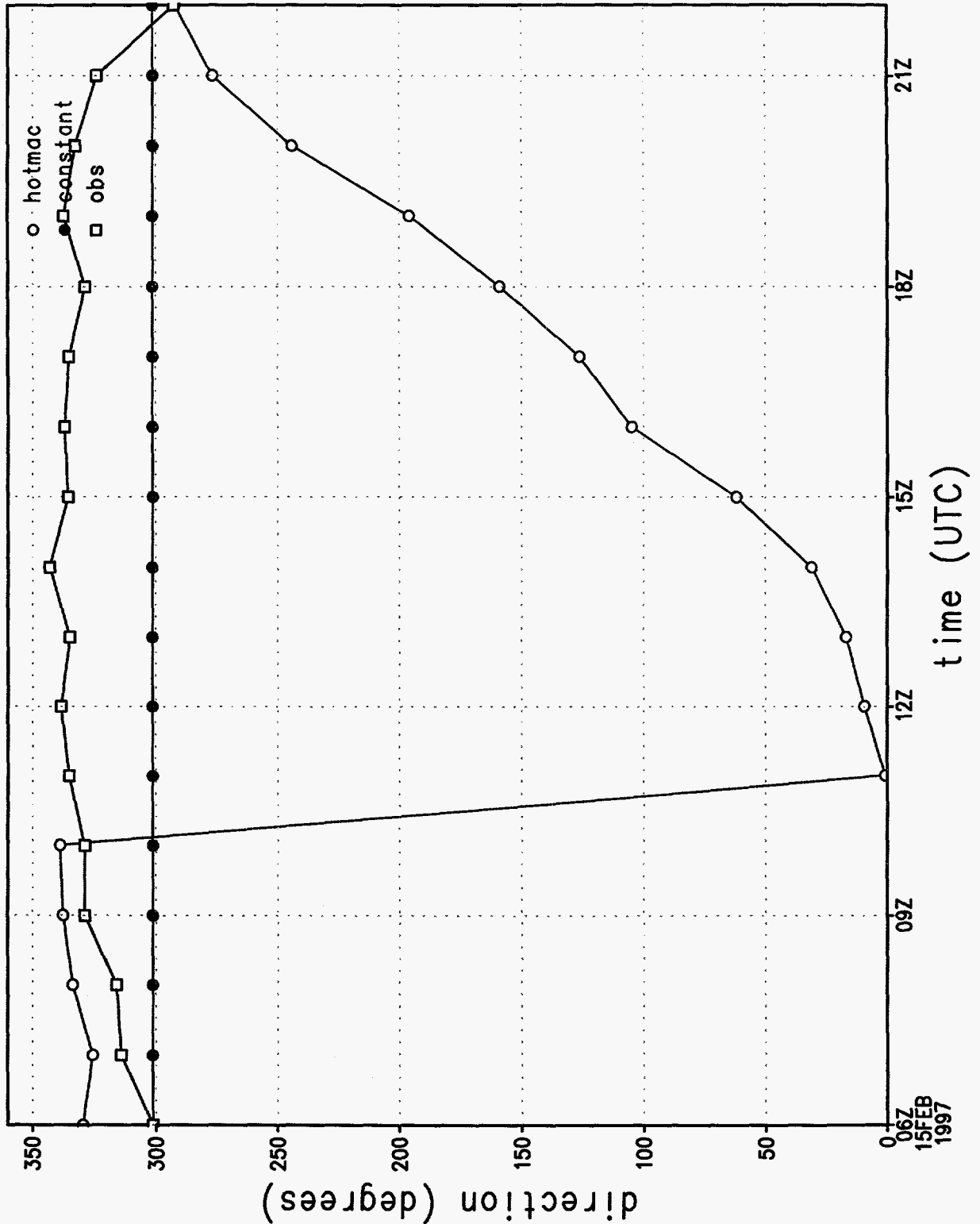


Figure 10a.

wind speed sounding 1, 1072 m

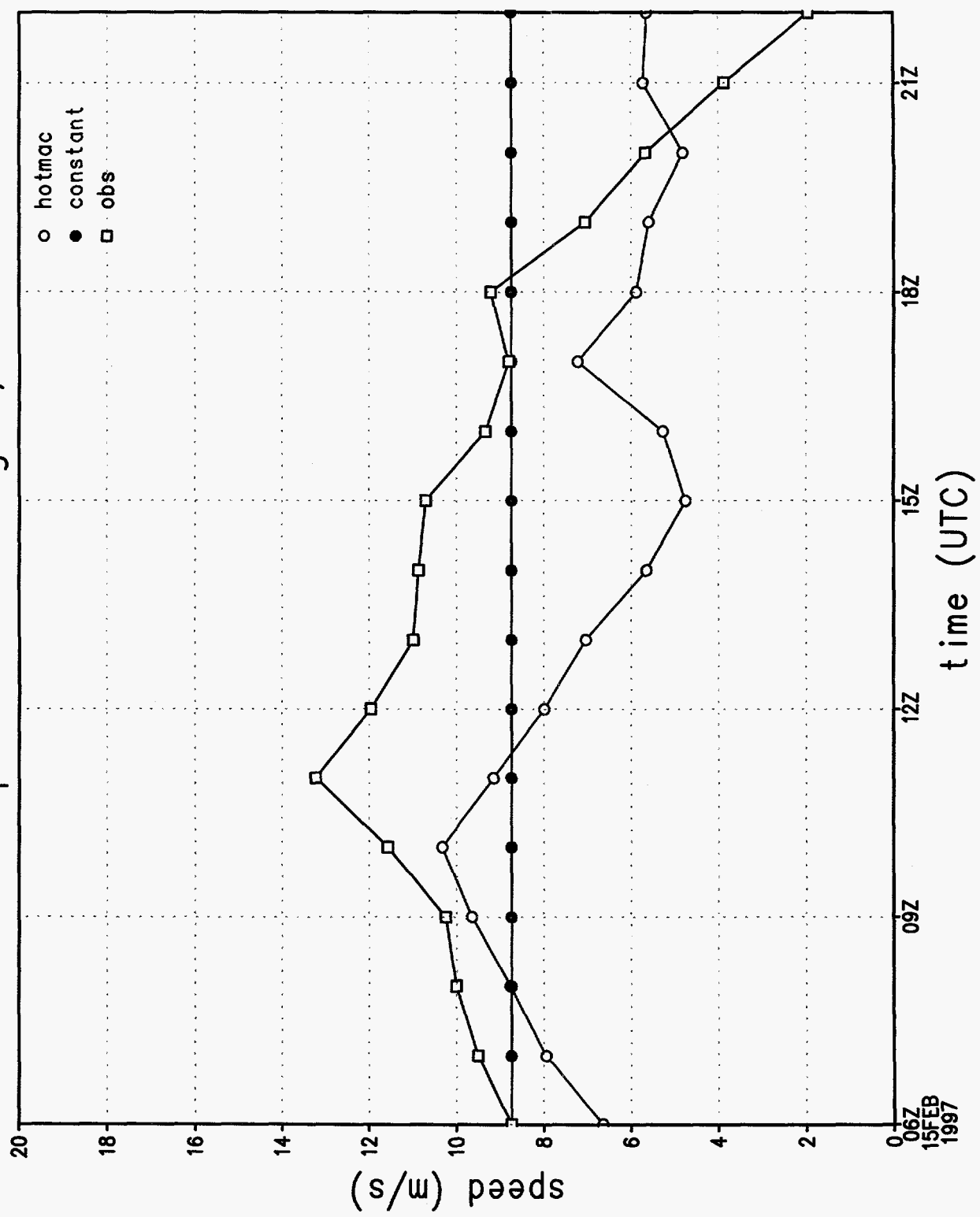


Figure 10b.

# wind direction at station 1

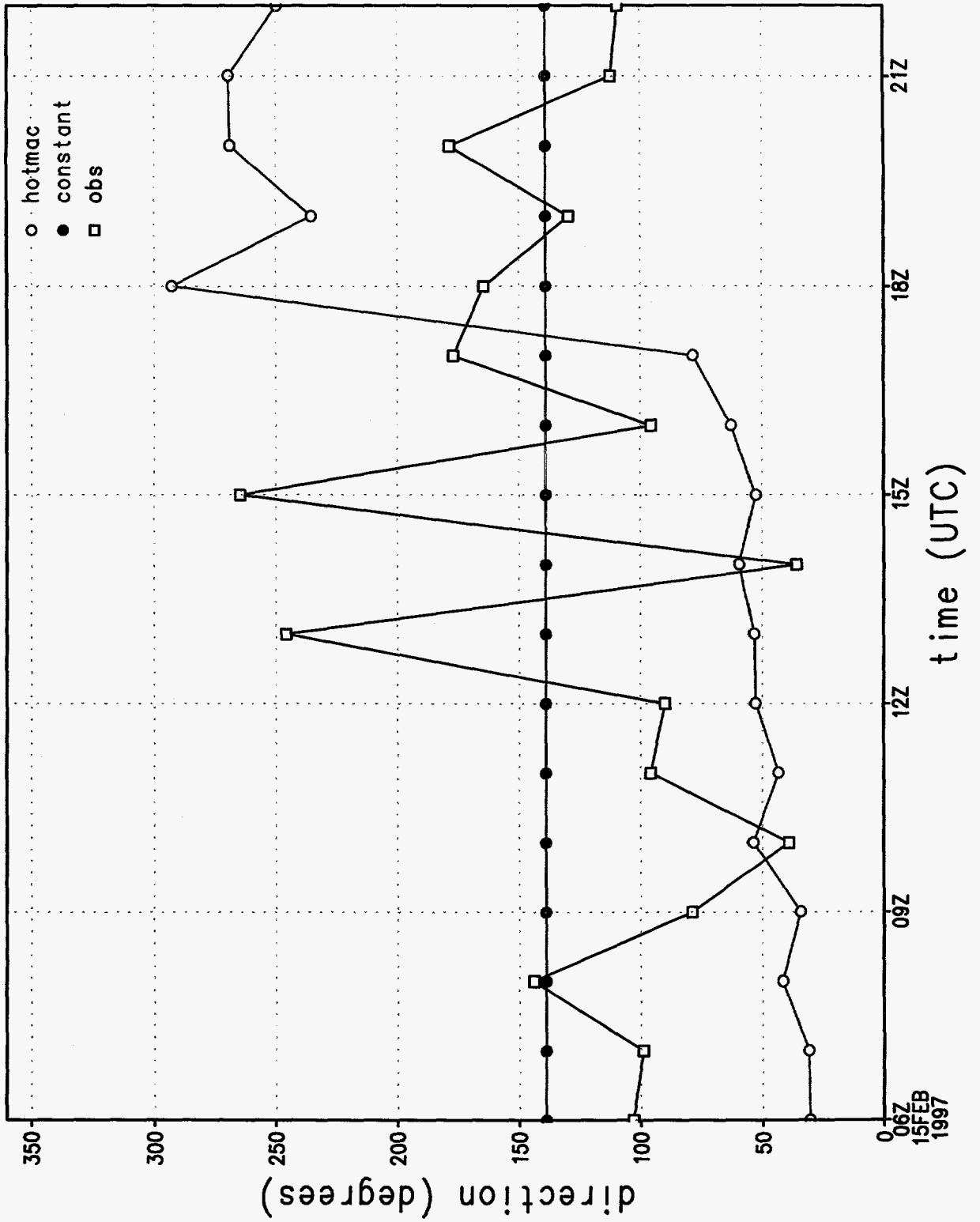


Figure 10c.

# wind speed at station 1

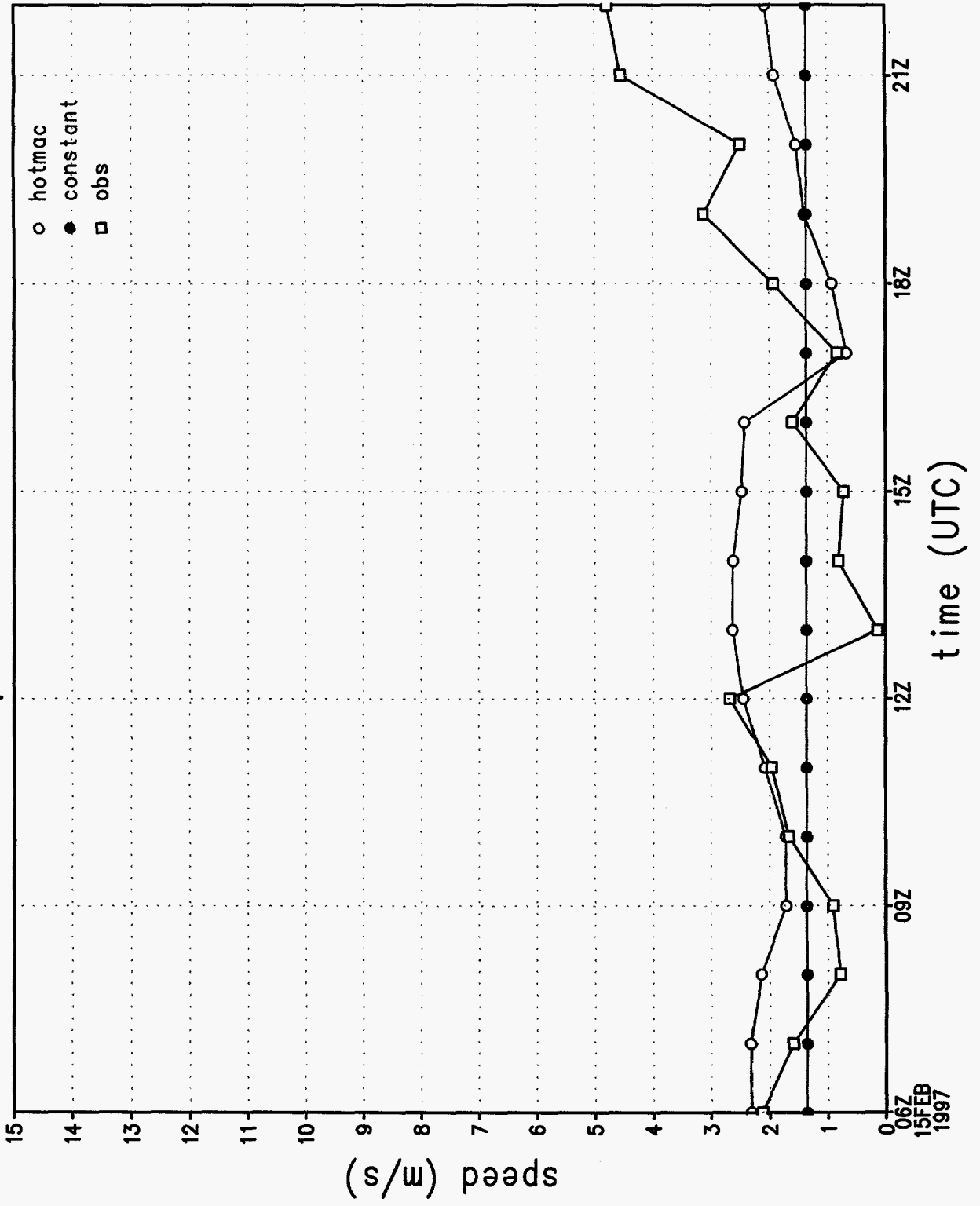


Figure 10d.

# u wind component at station 1

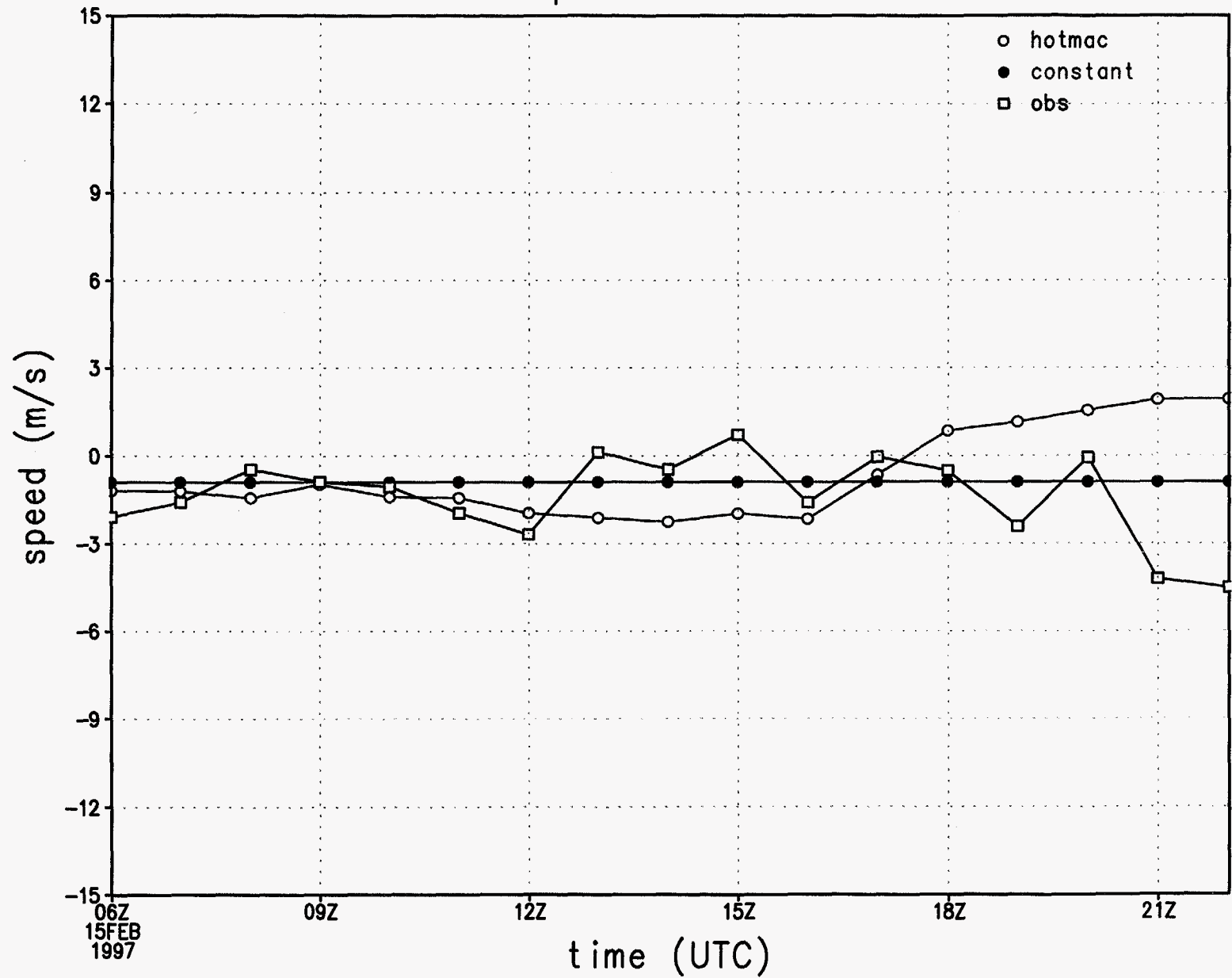


Figure 10e.

v wind component at station 1

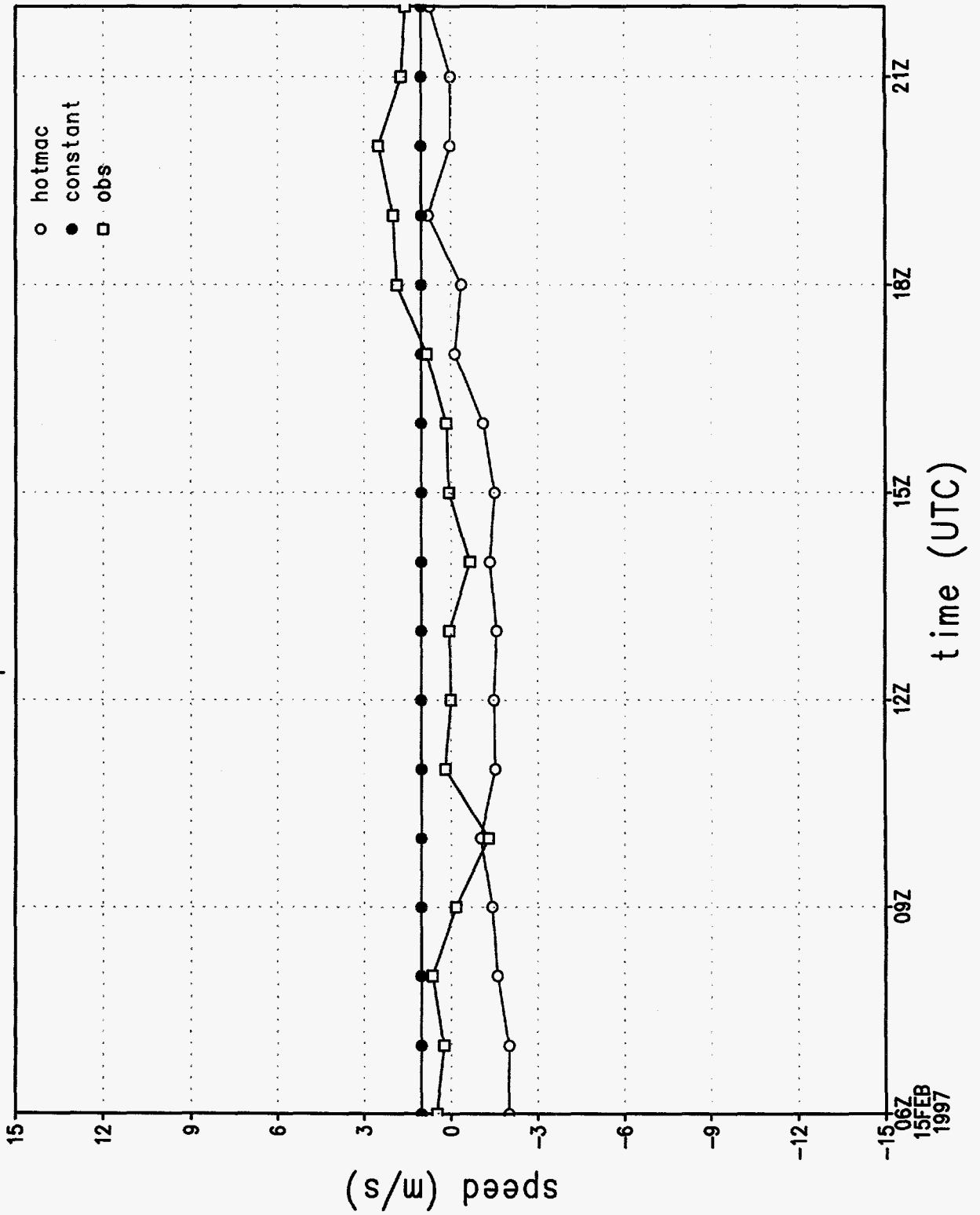


Figure 10f.

rmse of wind direction by hour

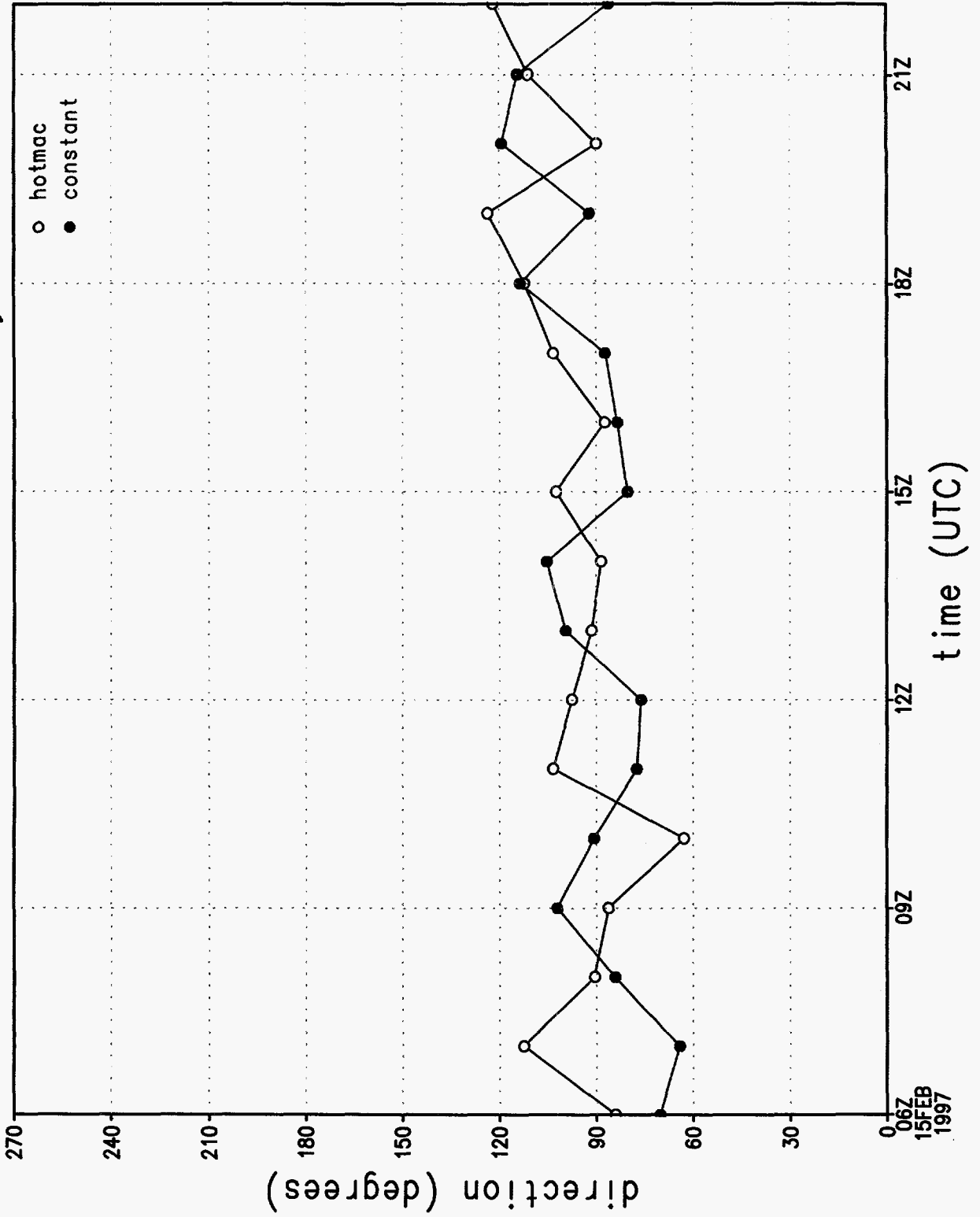


Figure 10g.

# rmse of wind speed by hour

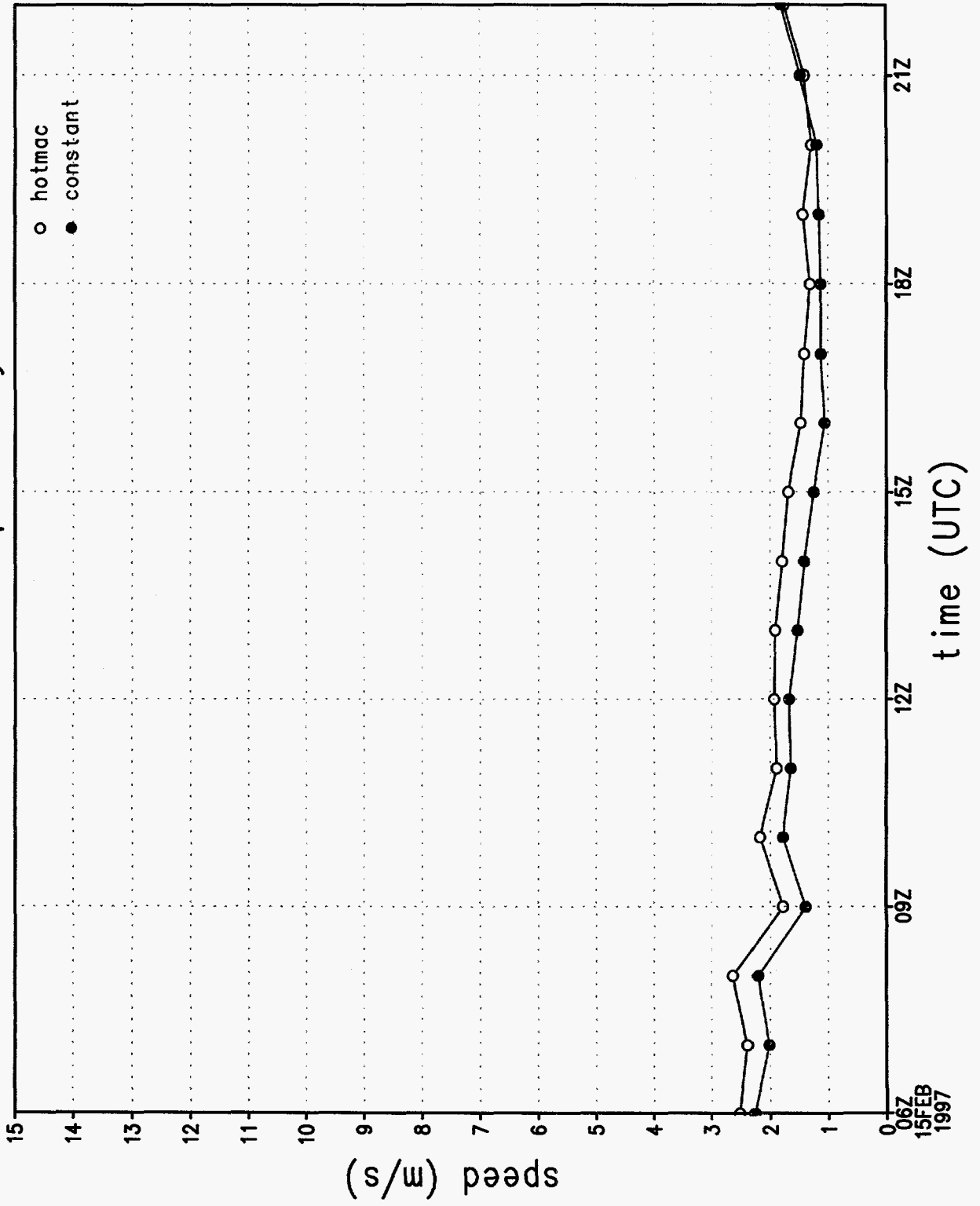


Figure 10h.



rmse of u wind component by hour

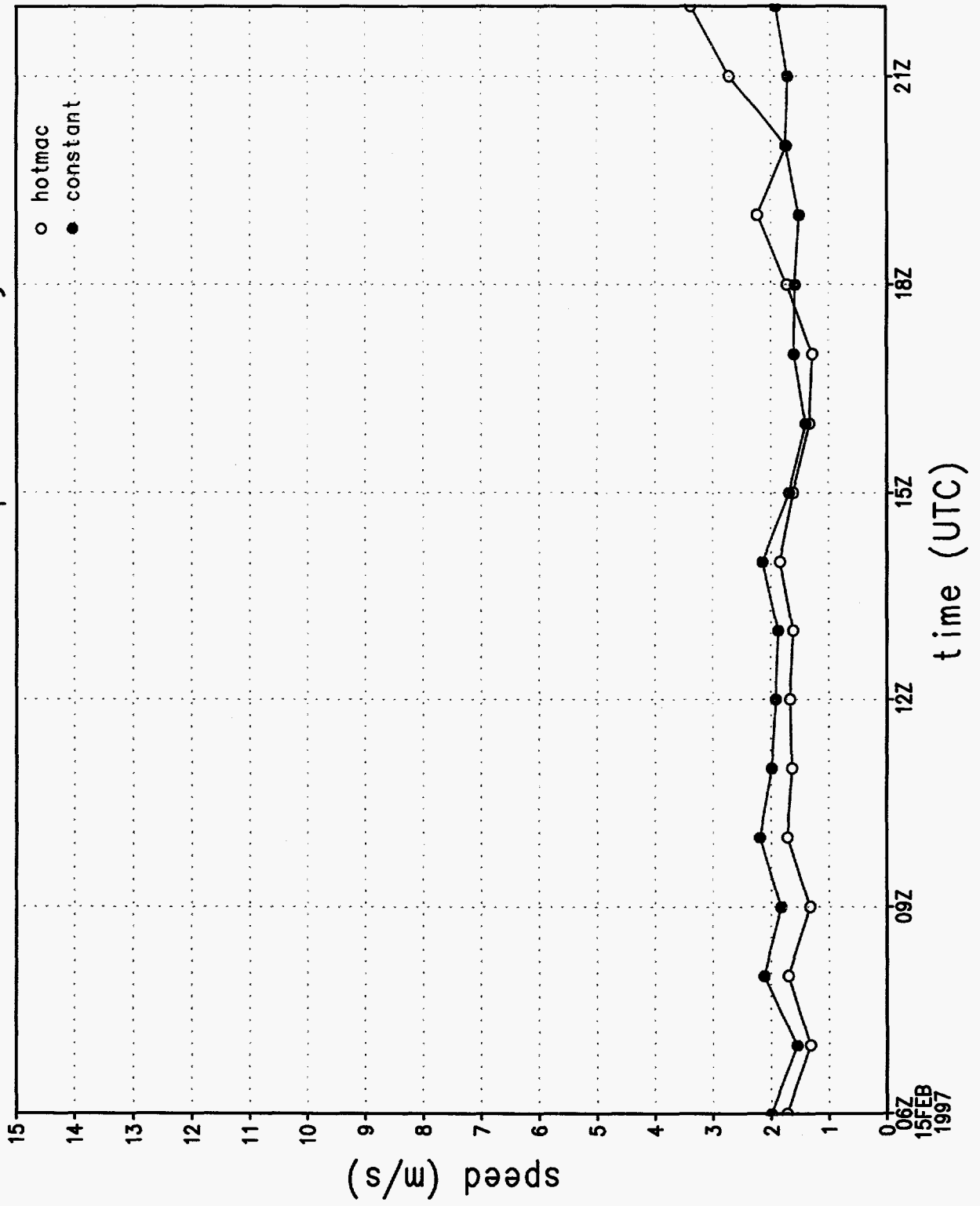


Figure 10i.

rmse of v wind component by hour

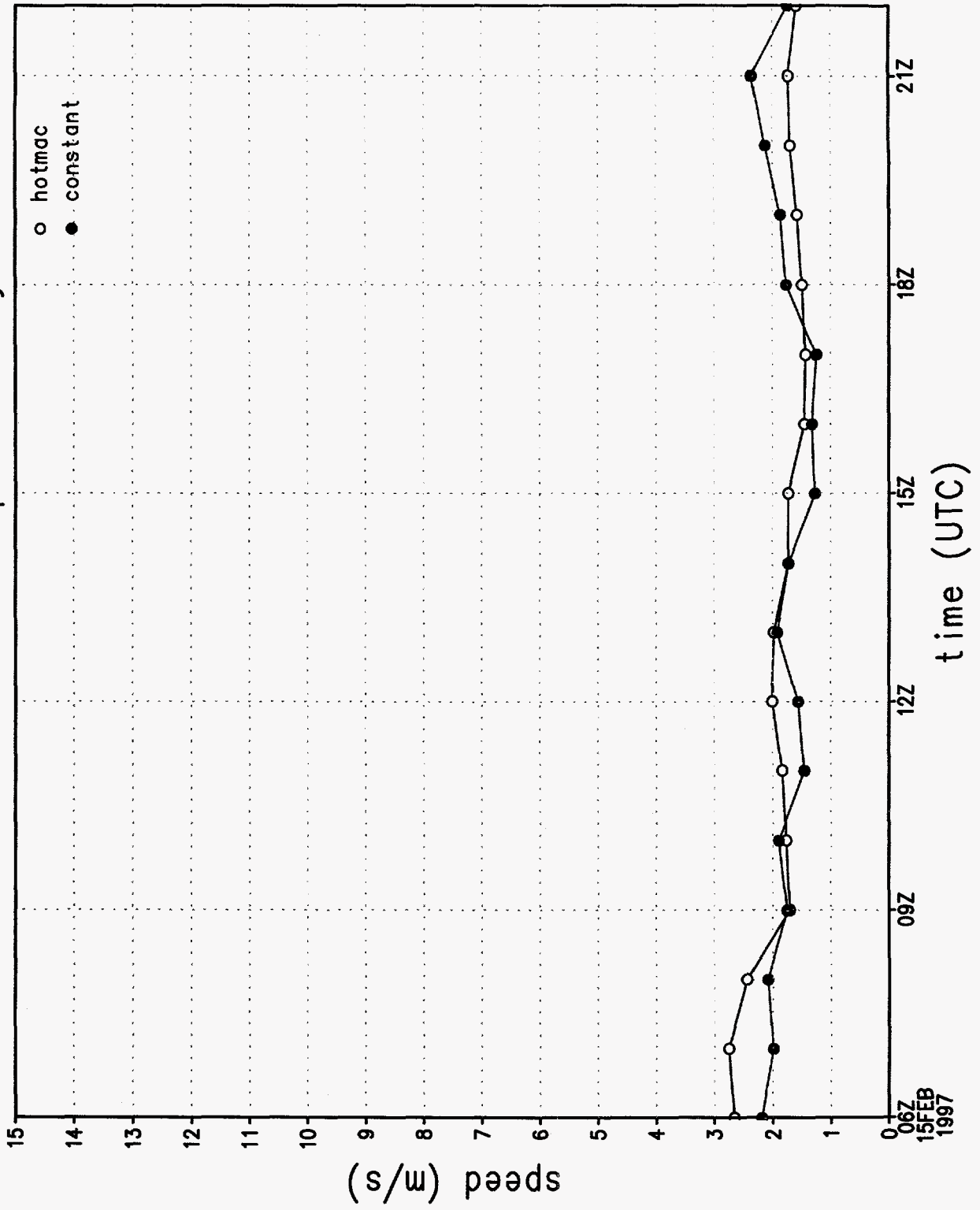


Figure 10j.

wind direction sounding 1, 1072 m

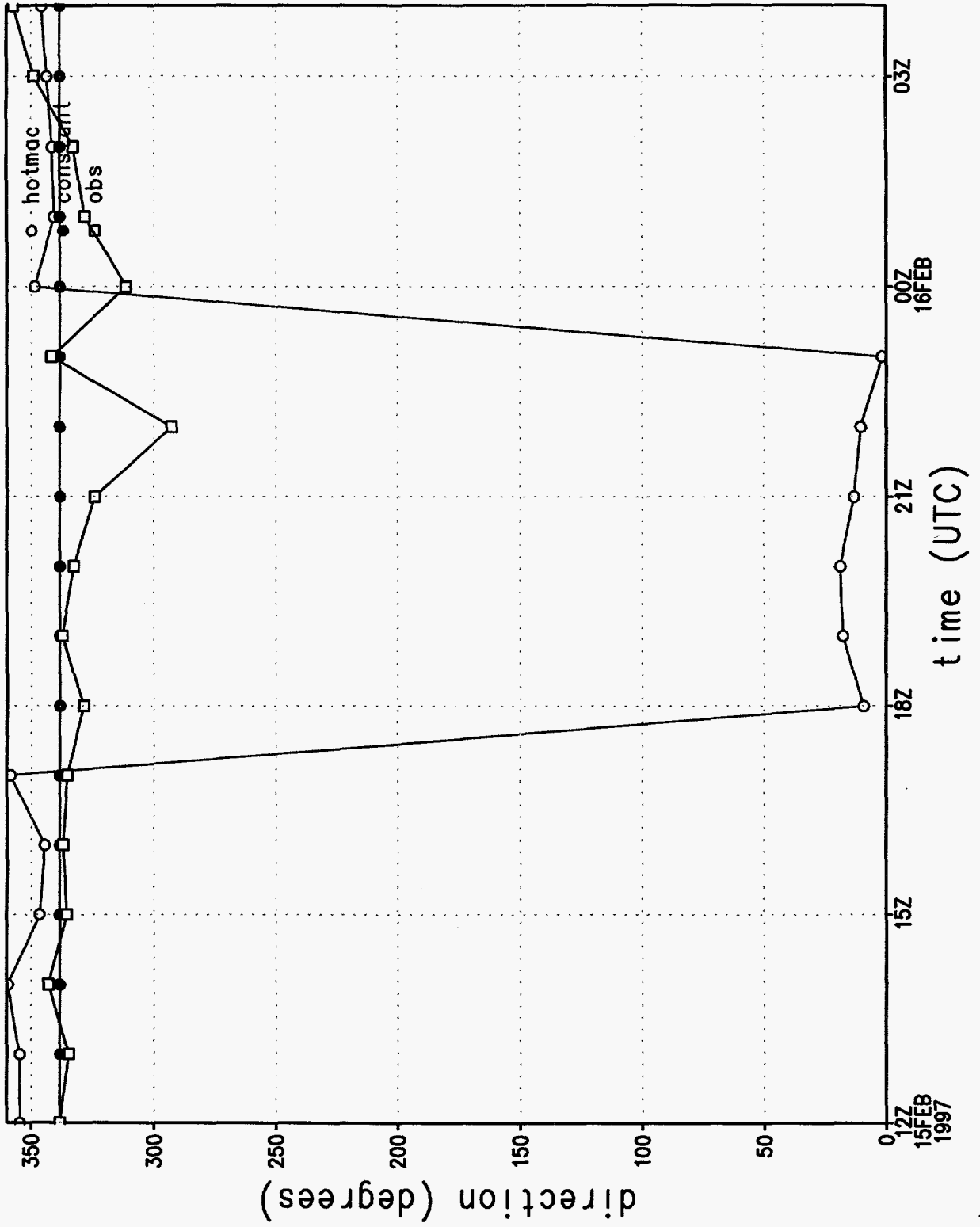


Figure 11a.

# wind speed sounding 1, 1072 m

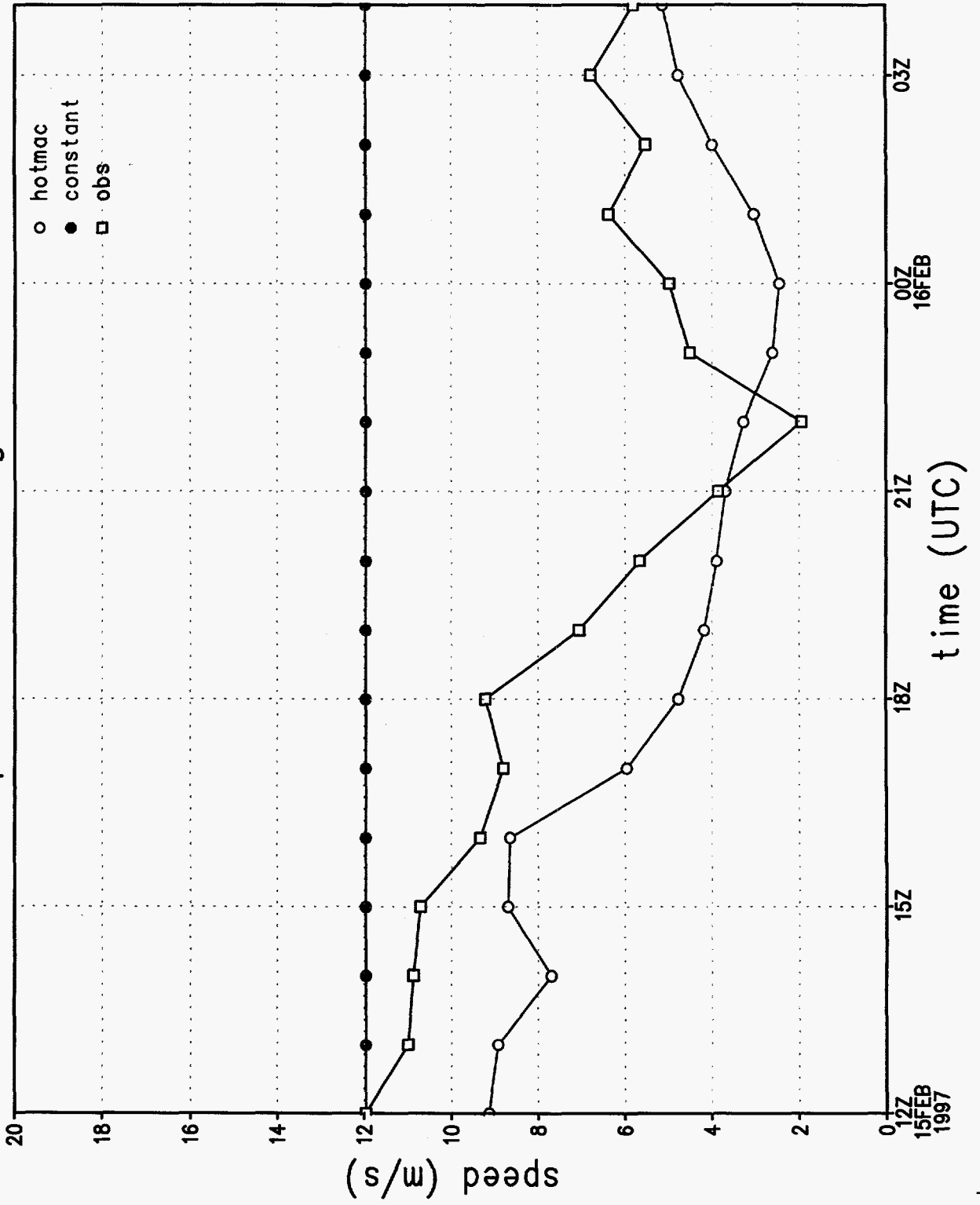


Figure 11b.

# wind direction at station 1

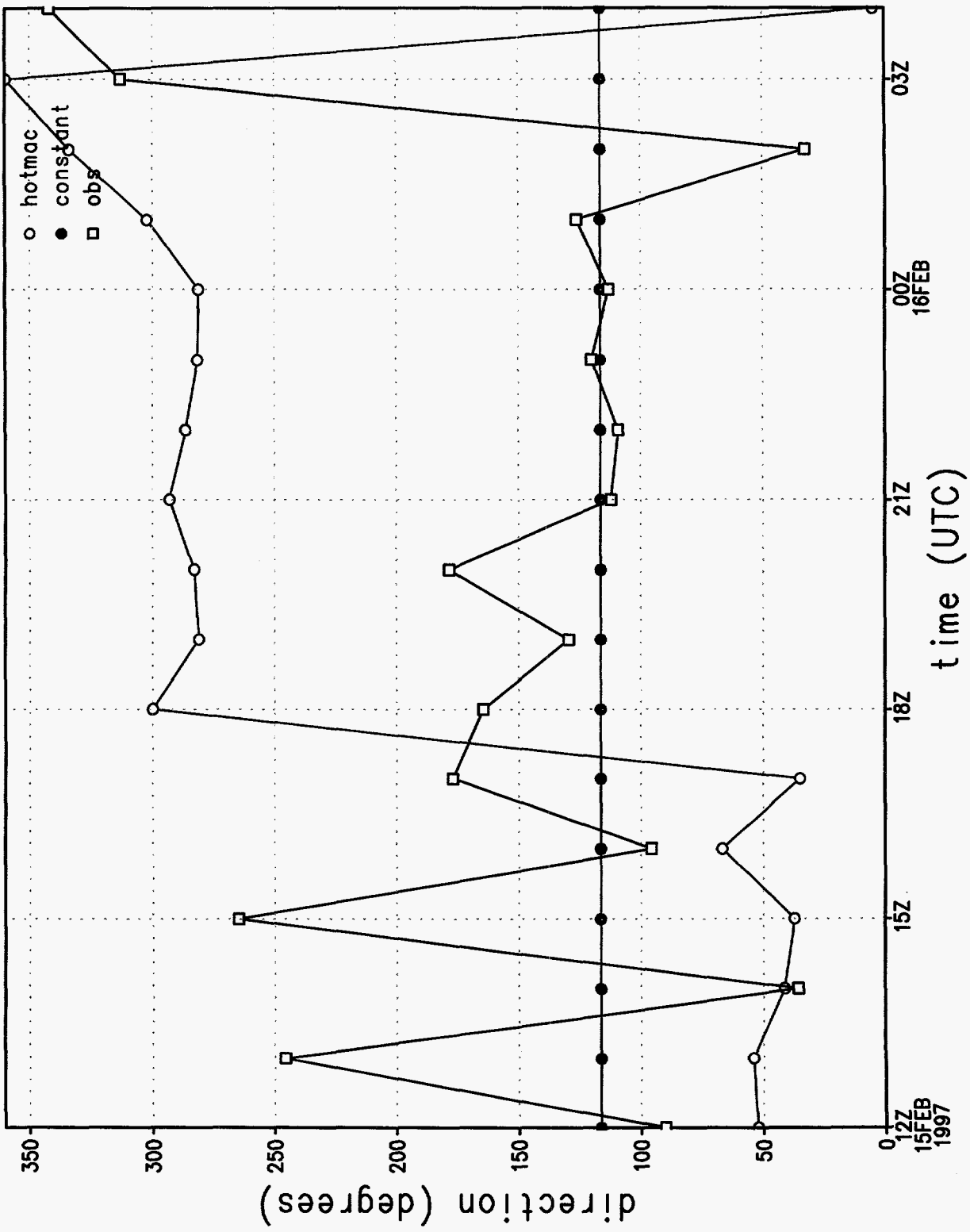


Figure 11c.

# wind speed at station 1

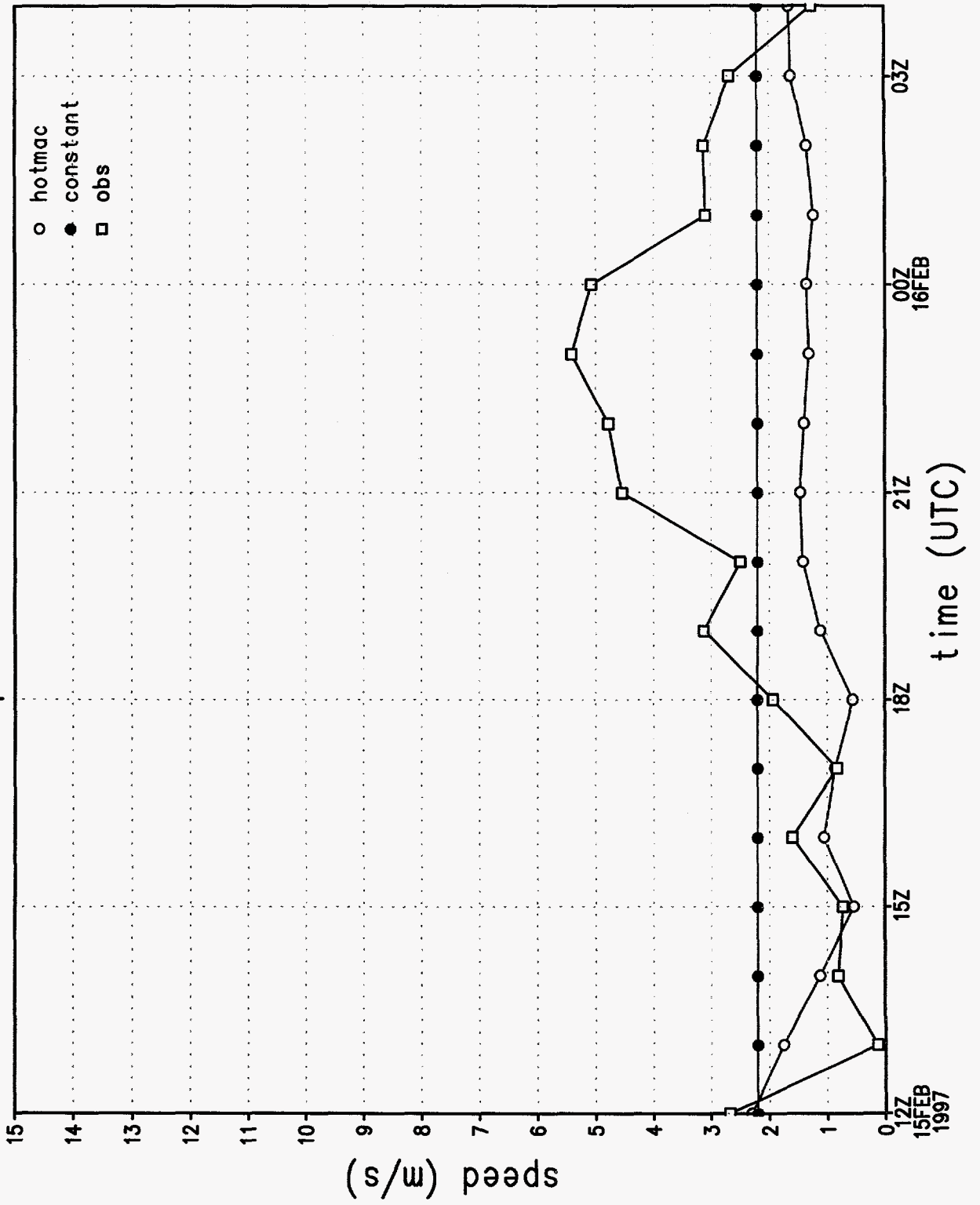


Figure 11d.

# u wind component at station 1

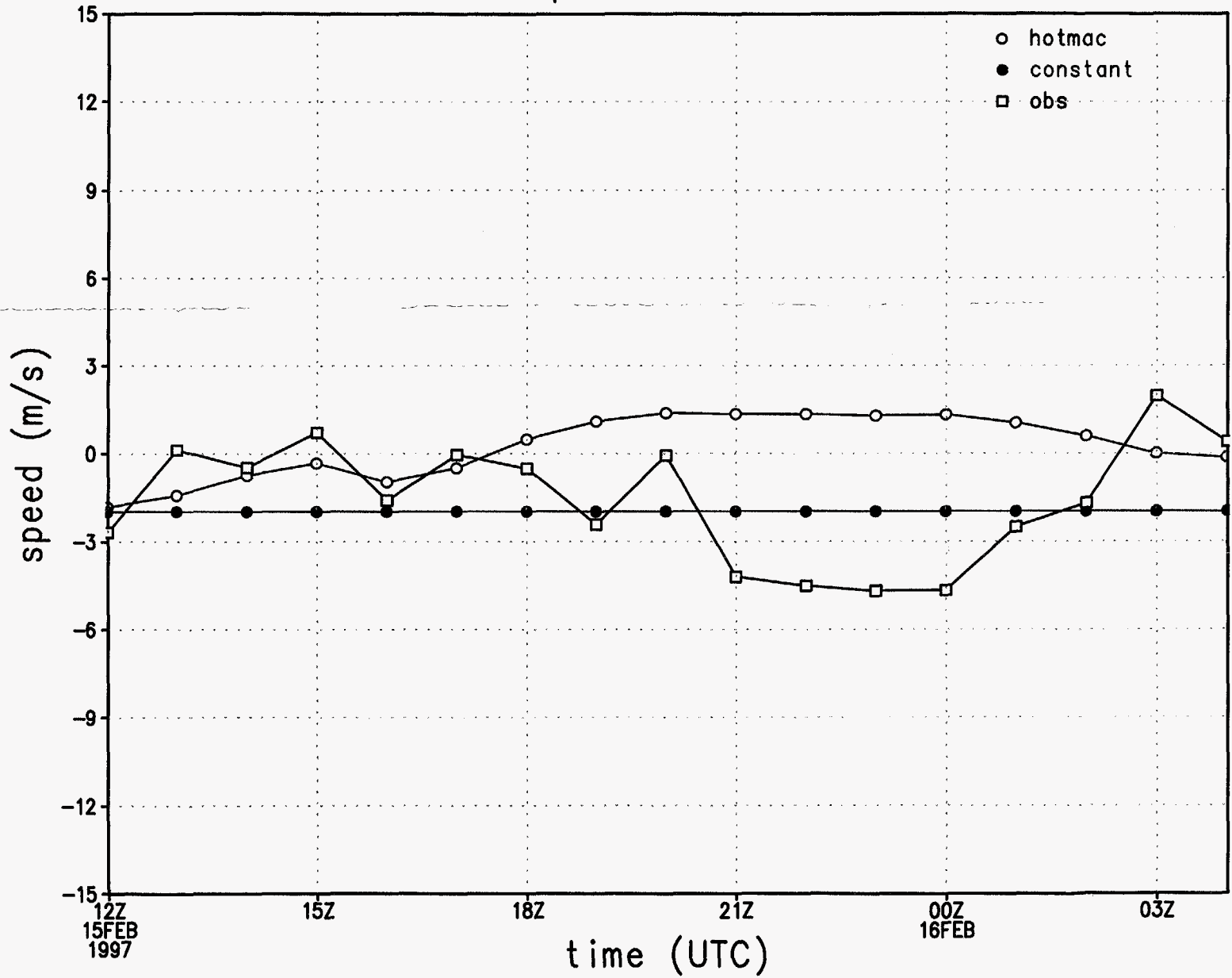


Figure 11e.

# v wind component at station 1

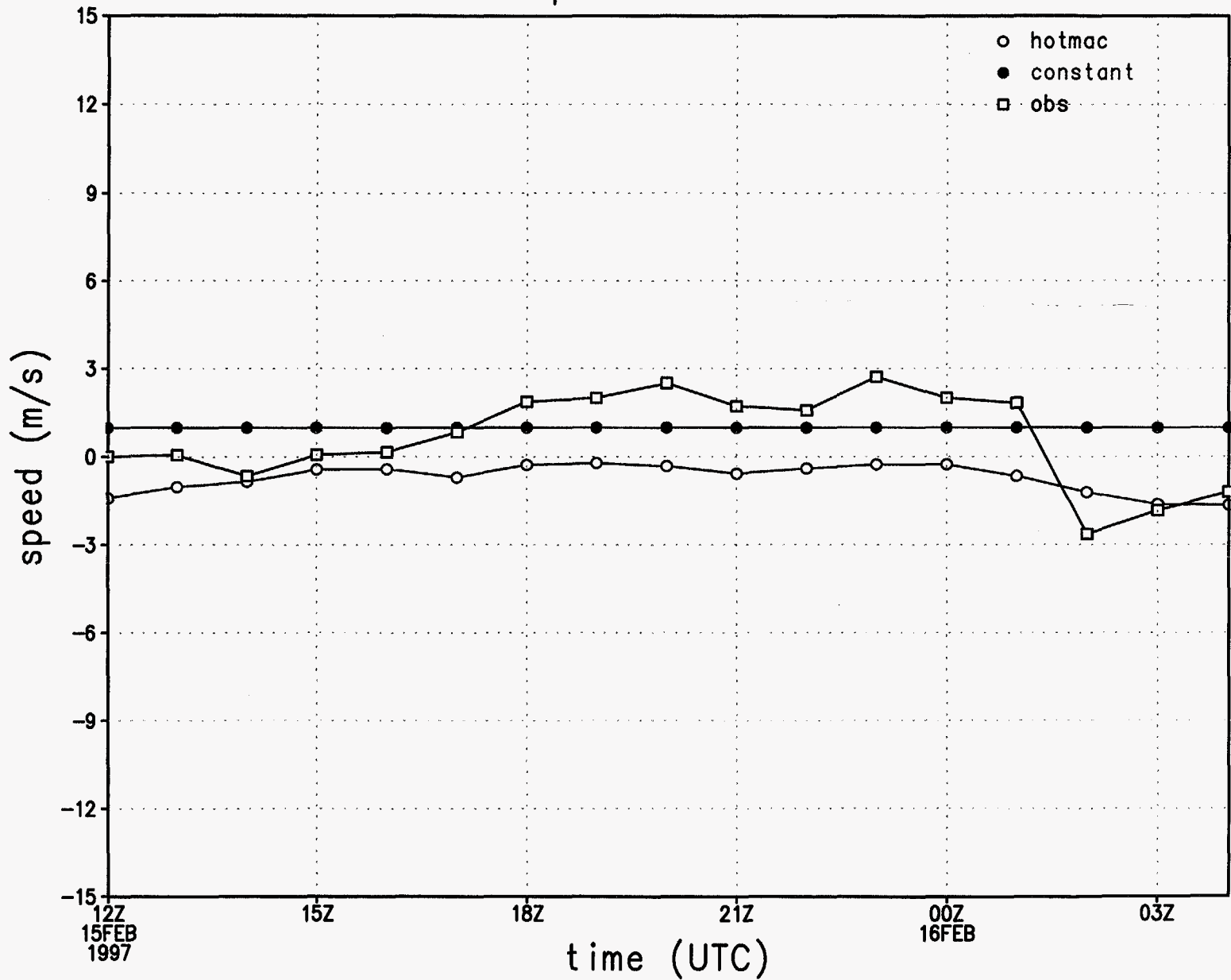


Figure 11f.



# rmse of wind direction by hour

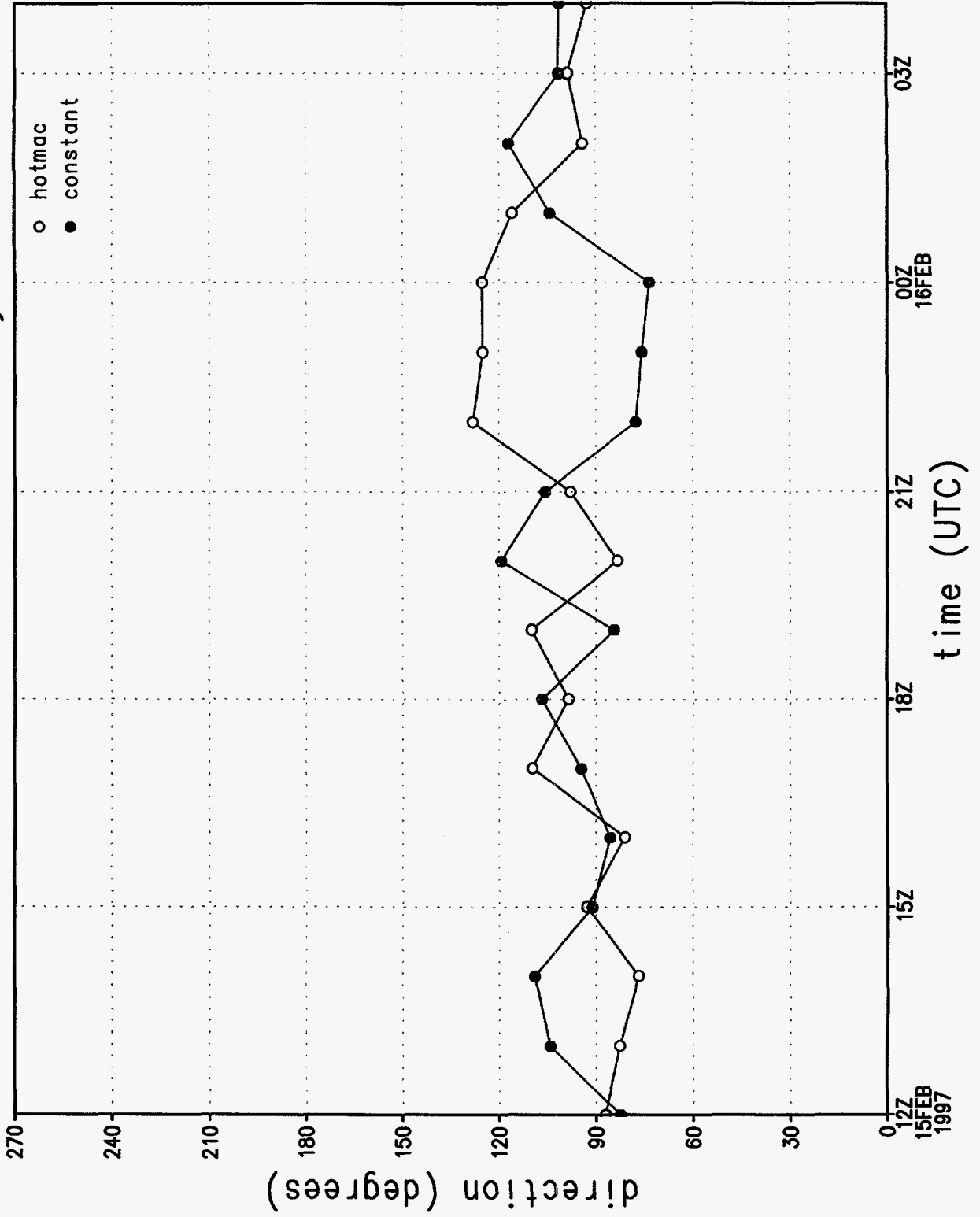


Figure 11g.

rmse of wind speed by hour

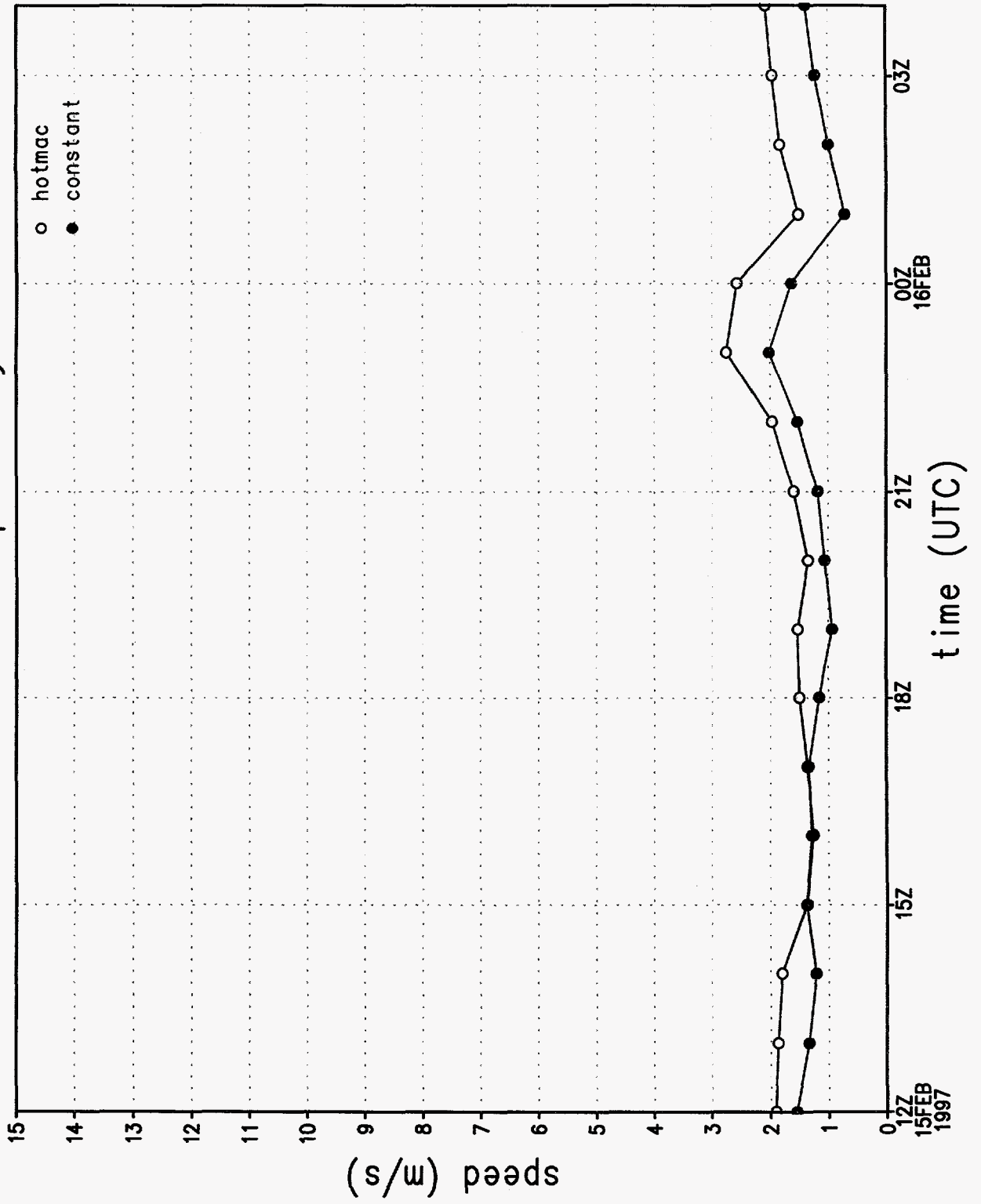


Figure 11h.

# rmse of u wind component by hour

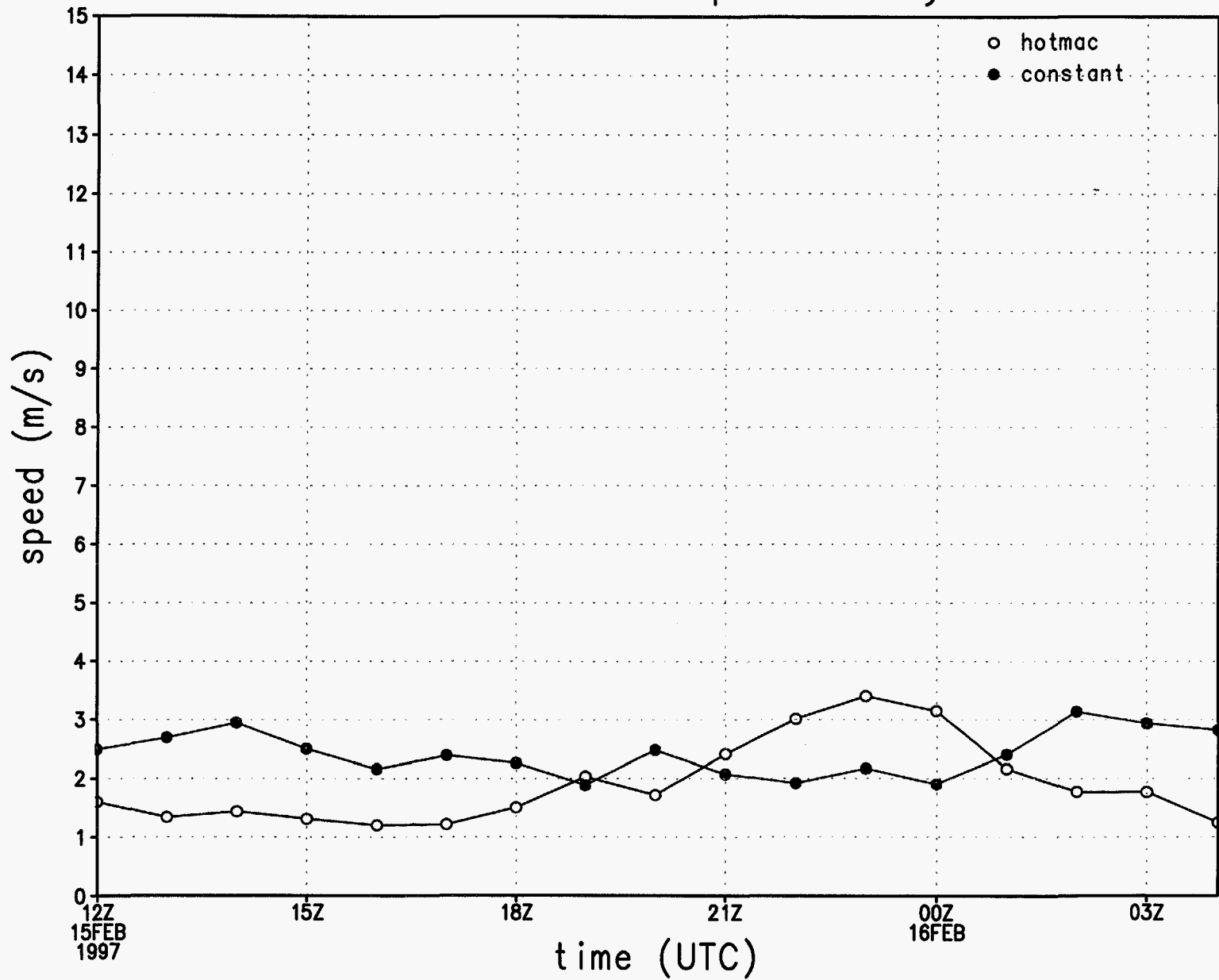


Figure 11i.

rmse of v wind component by hour

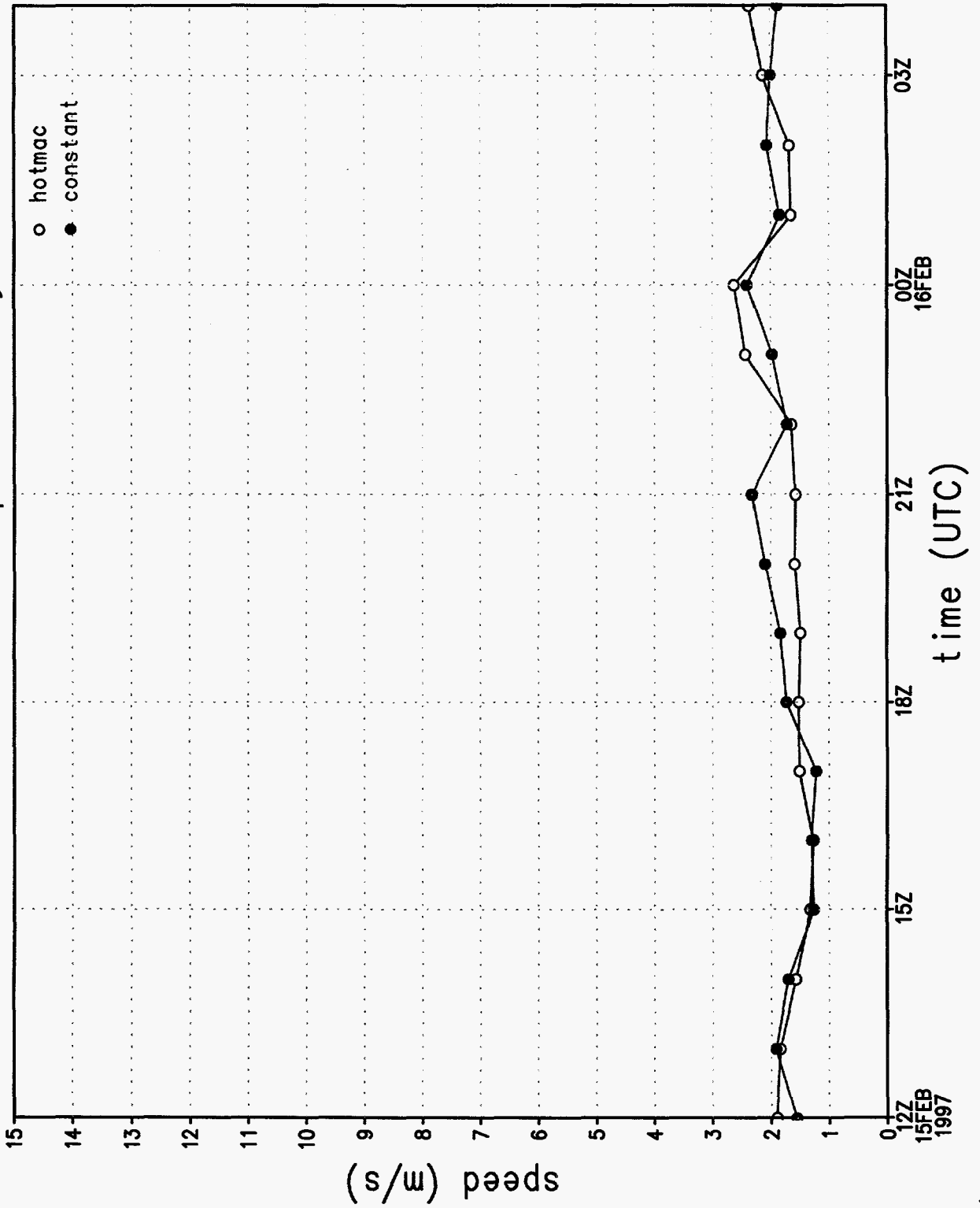


Figure 11j.

wind direction sounding 1, 1072 m

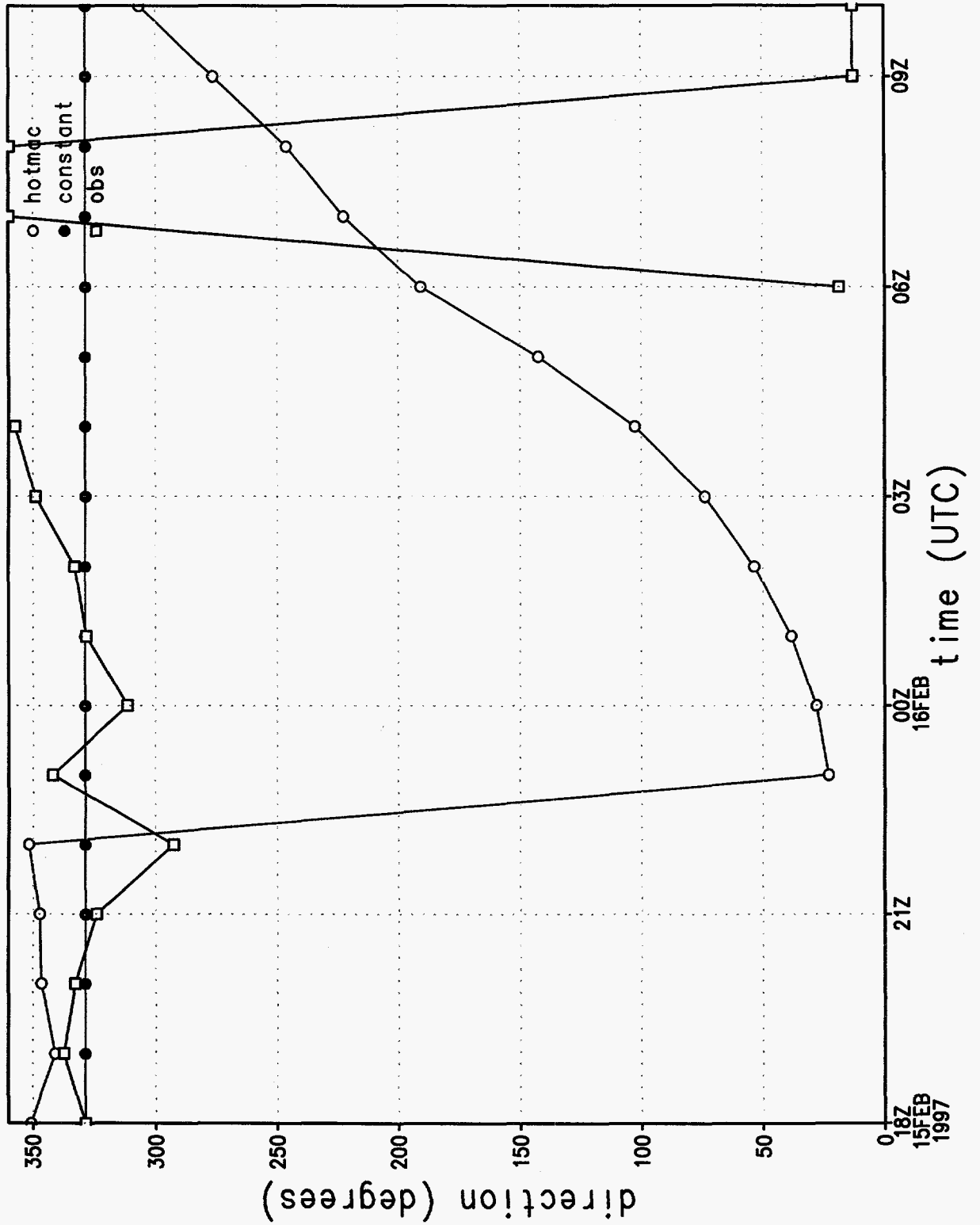


Figure 12a.

# wind speed sounding 1, 1072 m

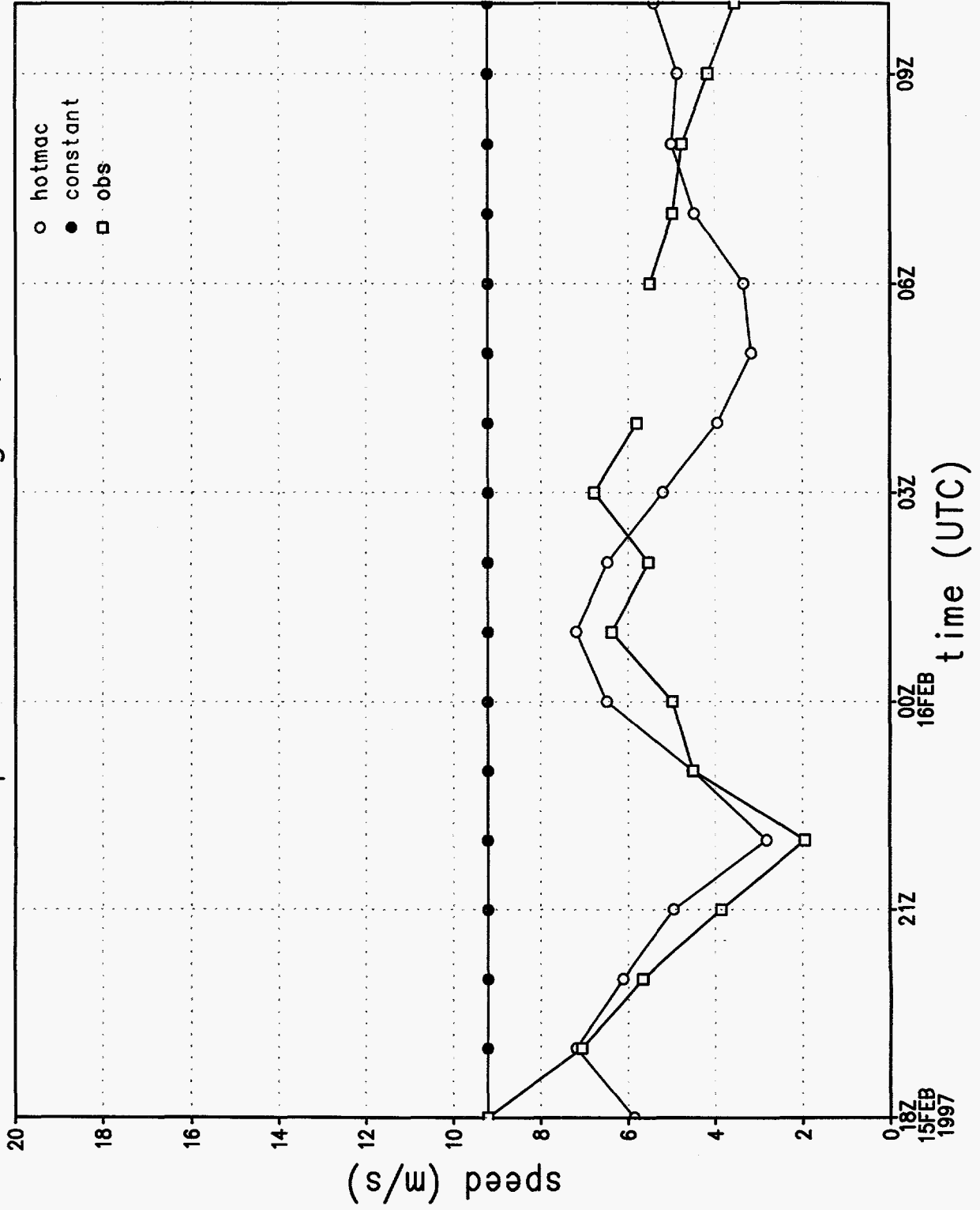


Figure 12b.

# wind direction at station 1

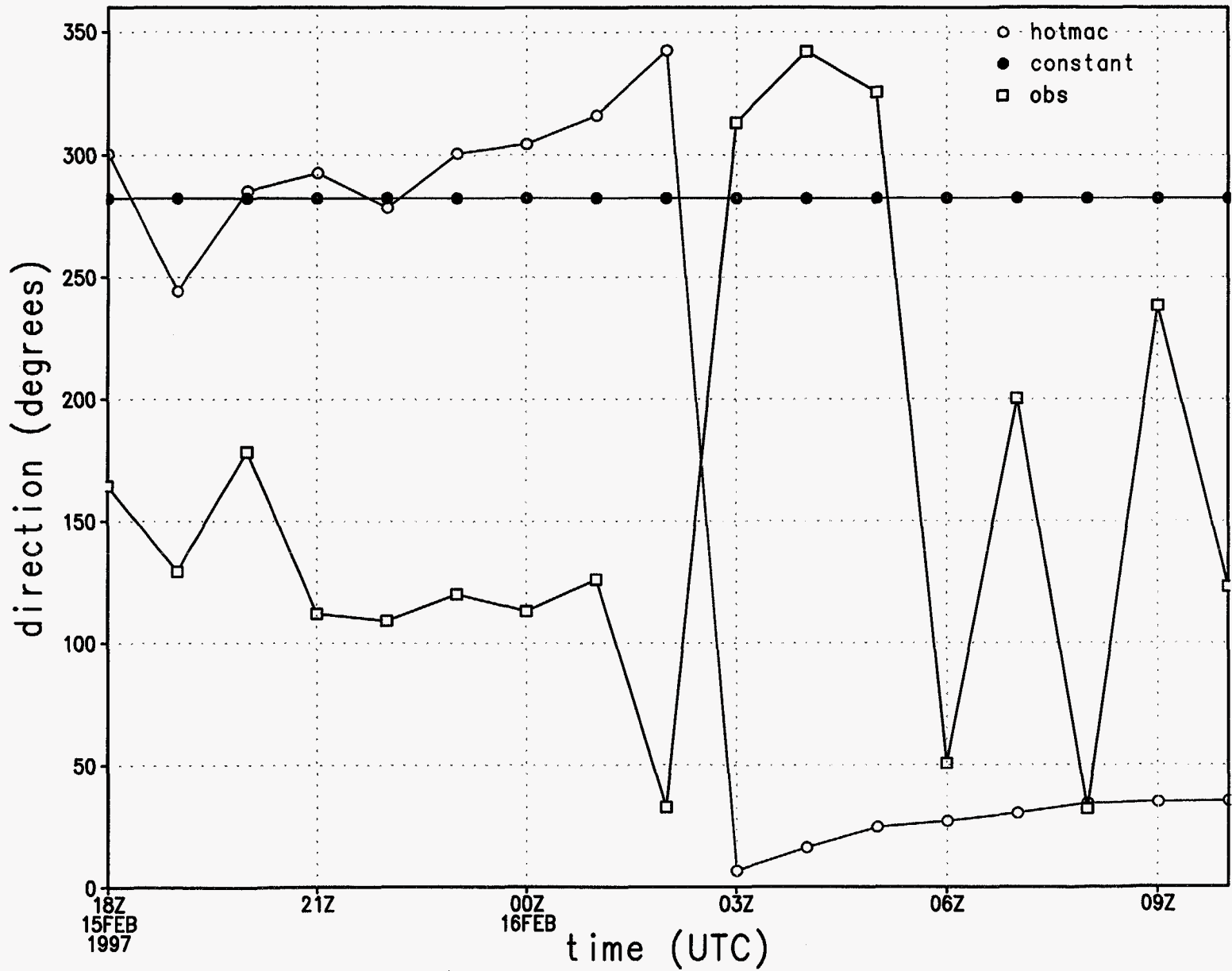


Figure 12c.

# wind speed at station 1

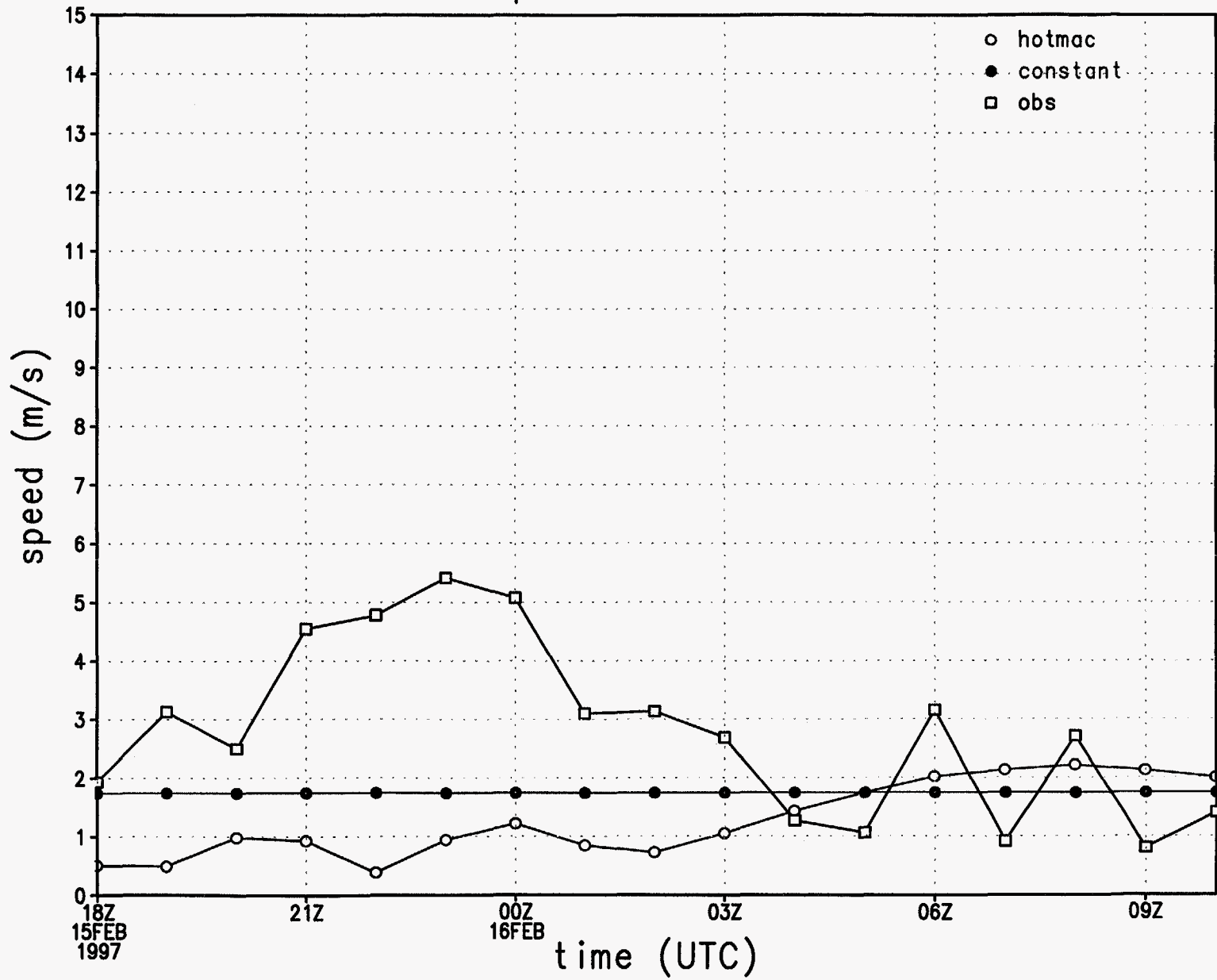


Figure 12d.



# u wind component at station 1

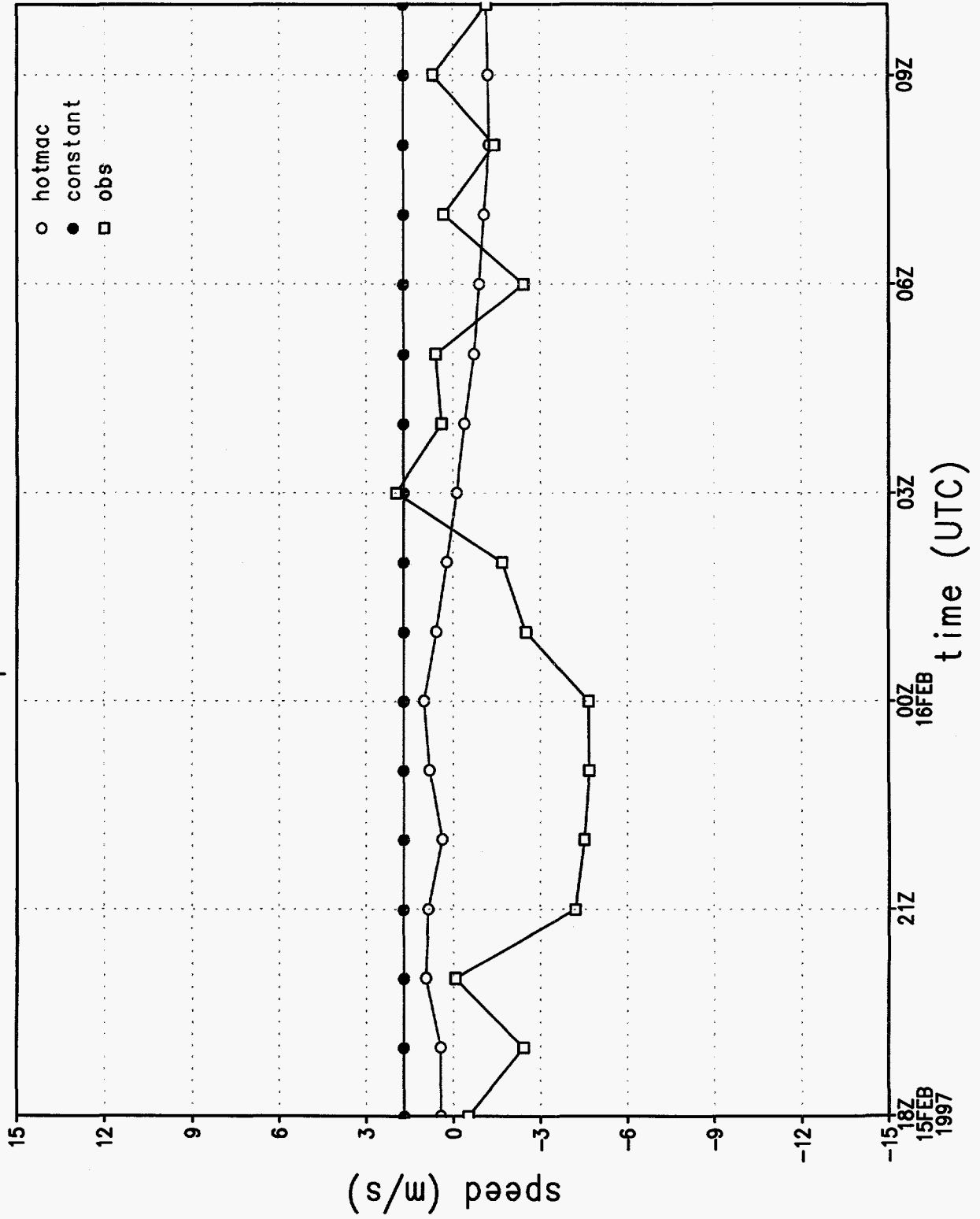


Figure 12e.

v wind component at station 1

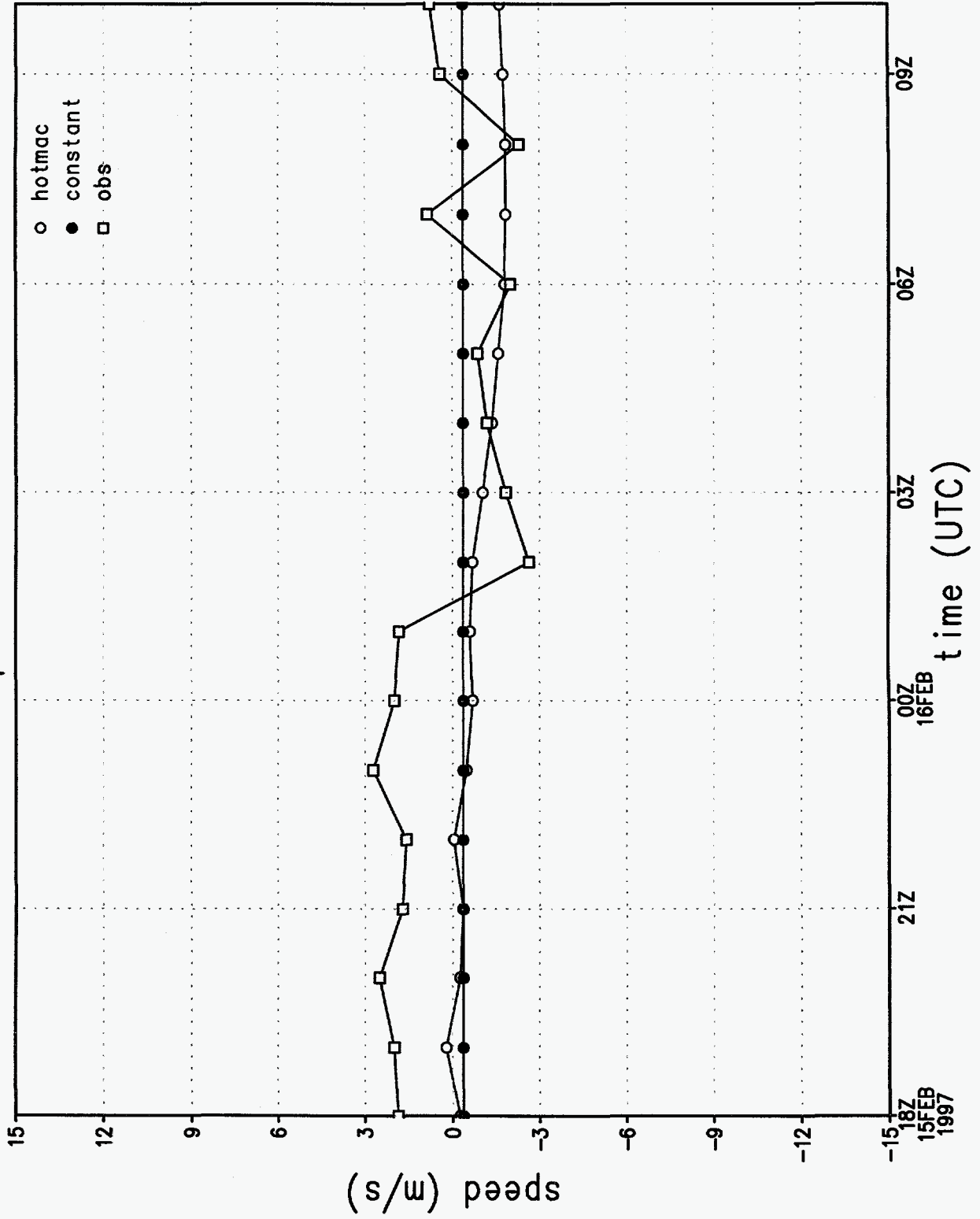


Figure 12f.

# rmse of wind direction by hour

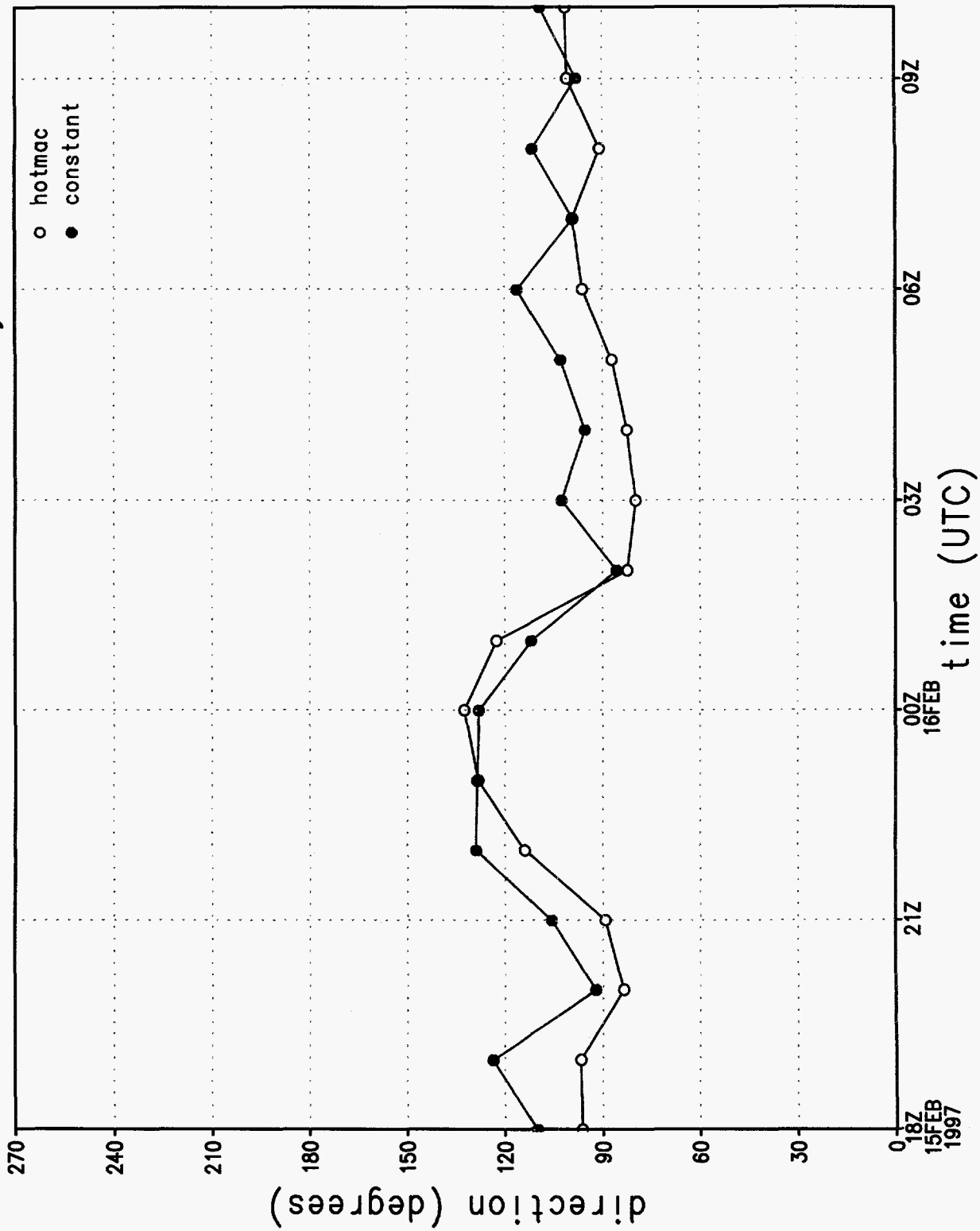


Figure 12g.

# rmse of wind speed by hour

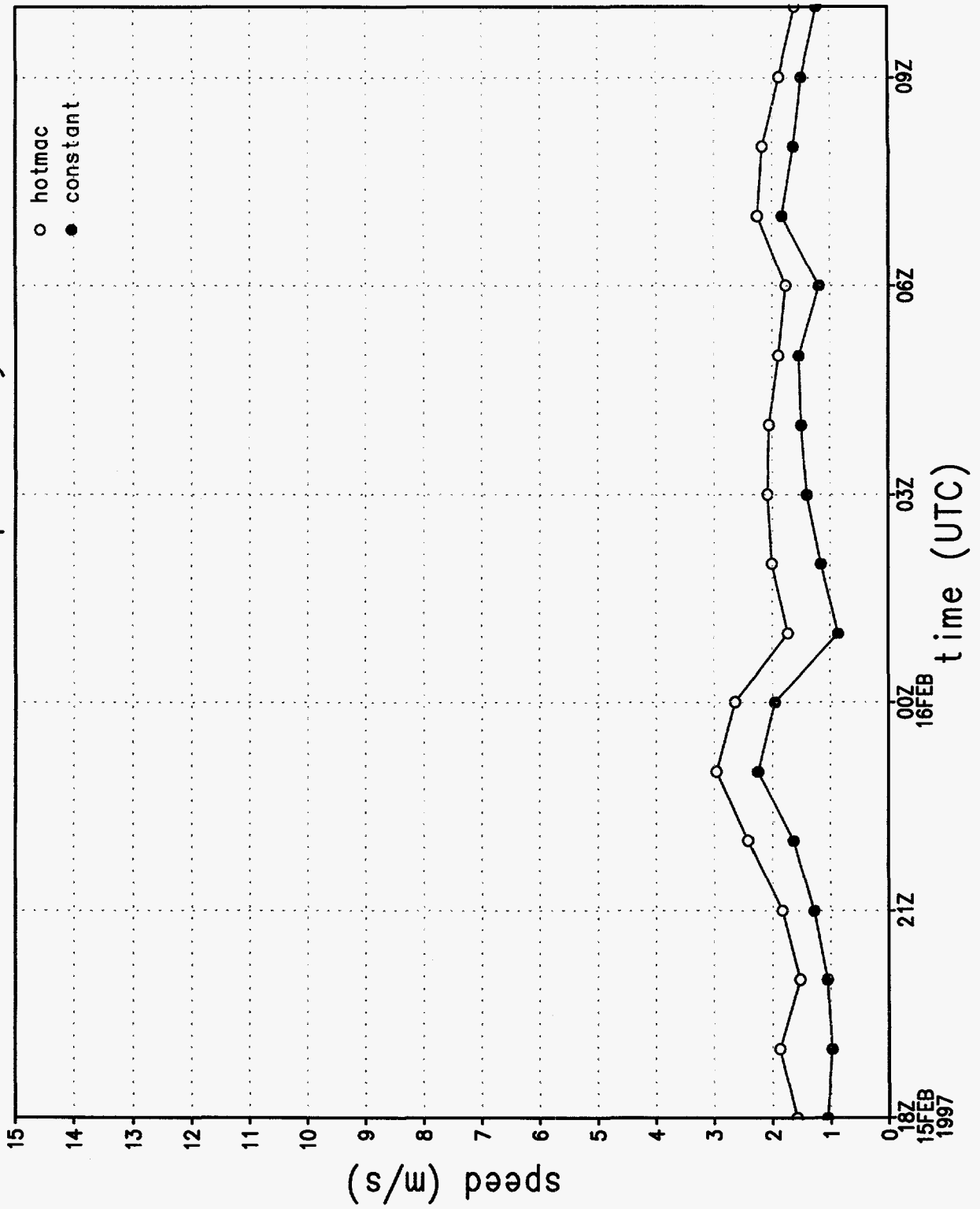


Figure 12h.

rmse of u wind component by hour

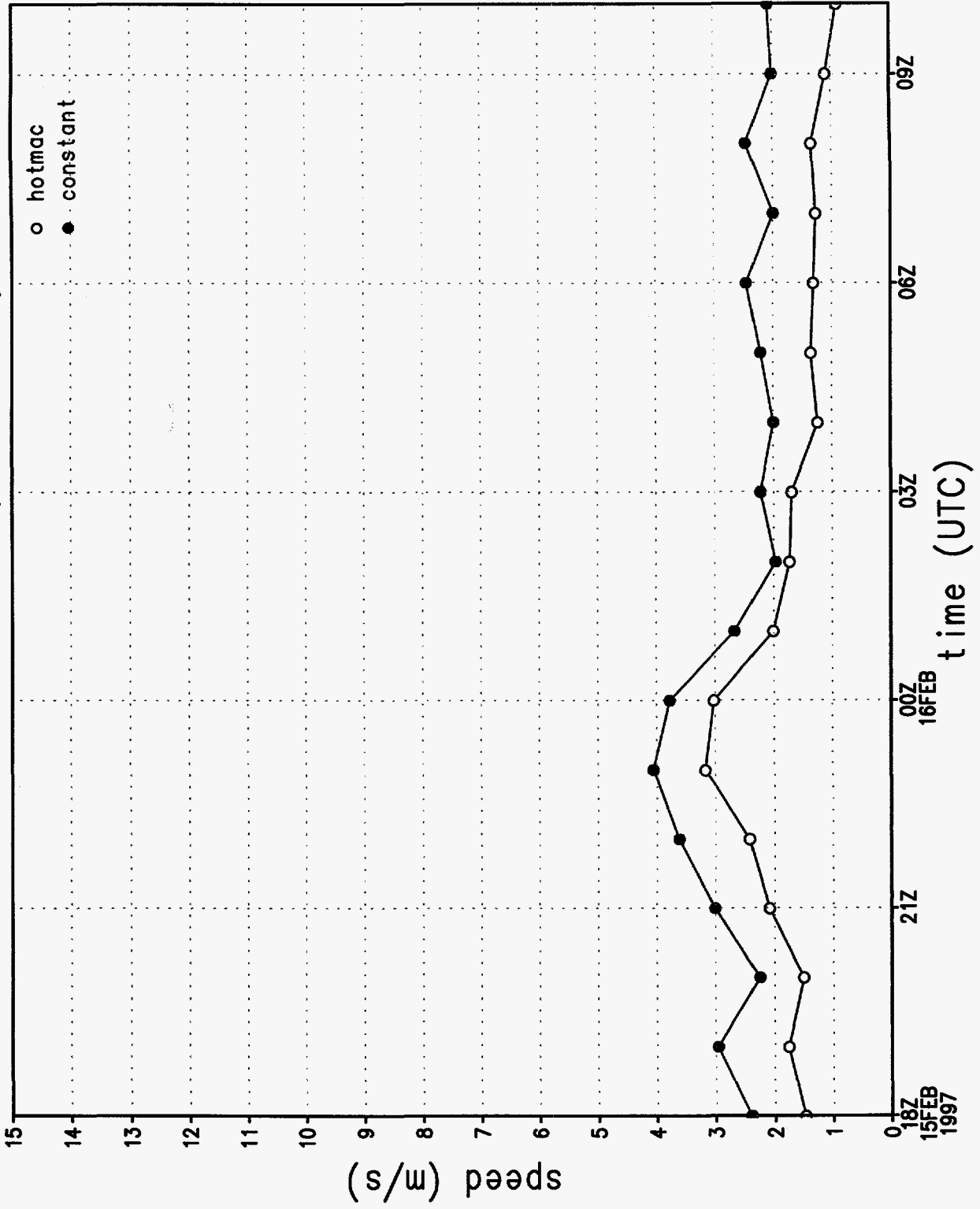


Figure 12.6.

rmse of v wind component by hour

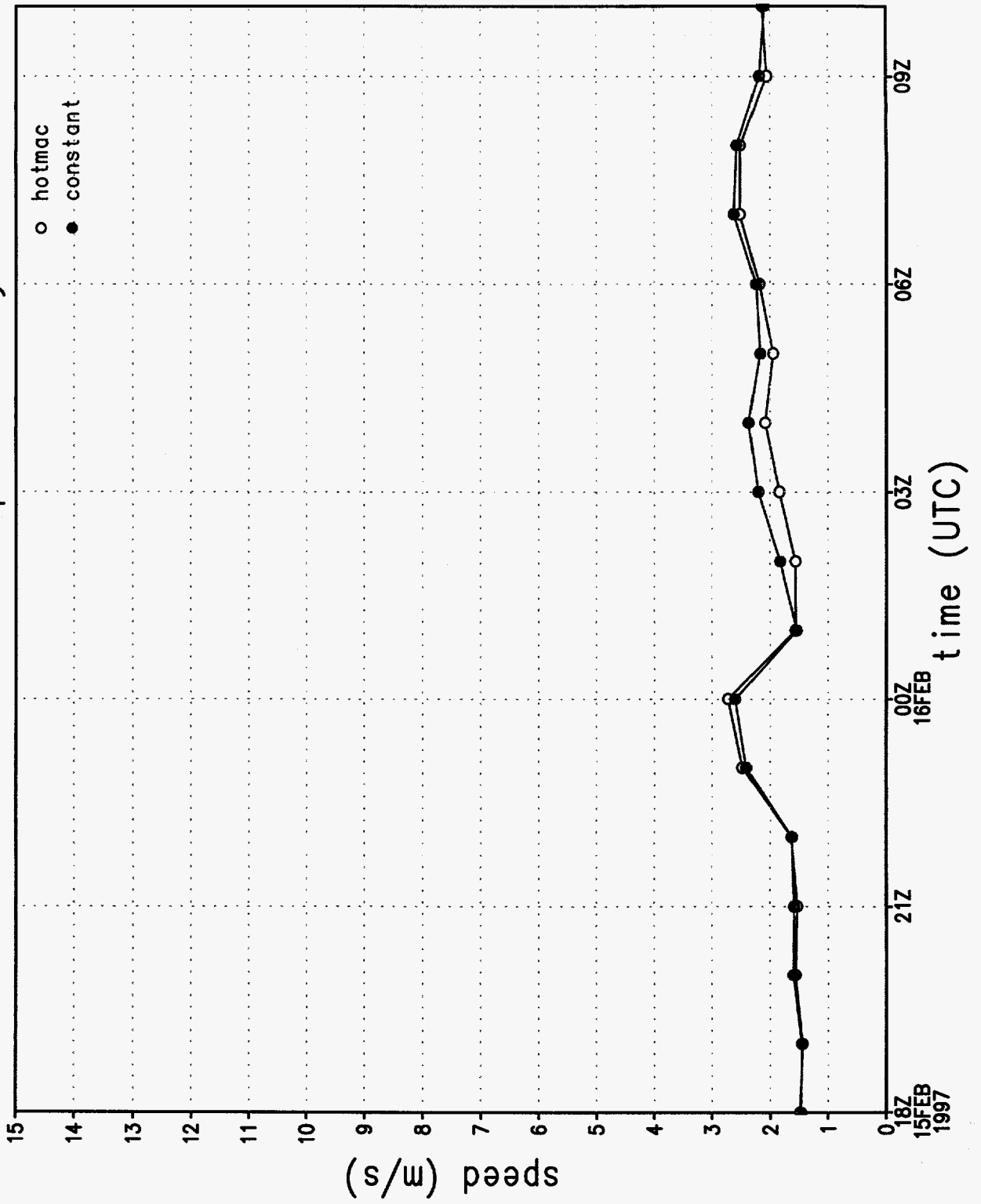


Figure 12j.

# wind direction sounding 1, 1072 m

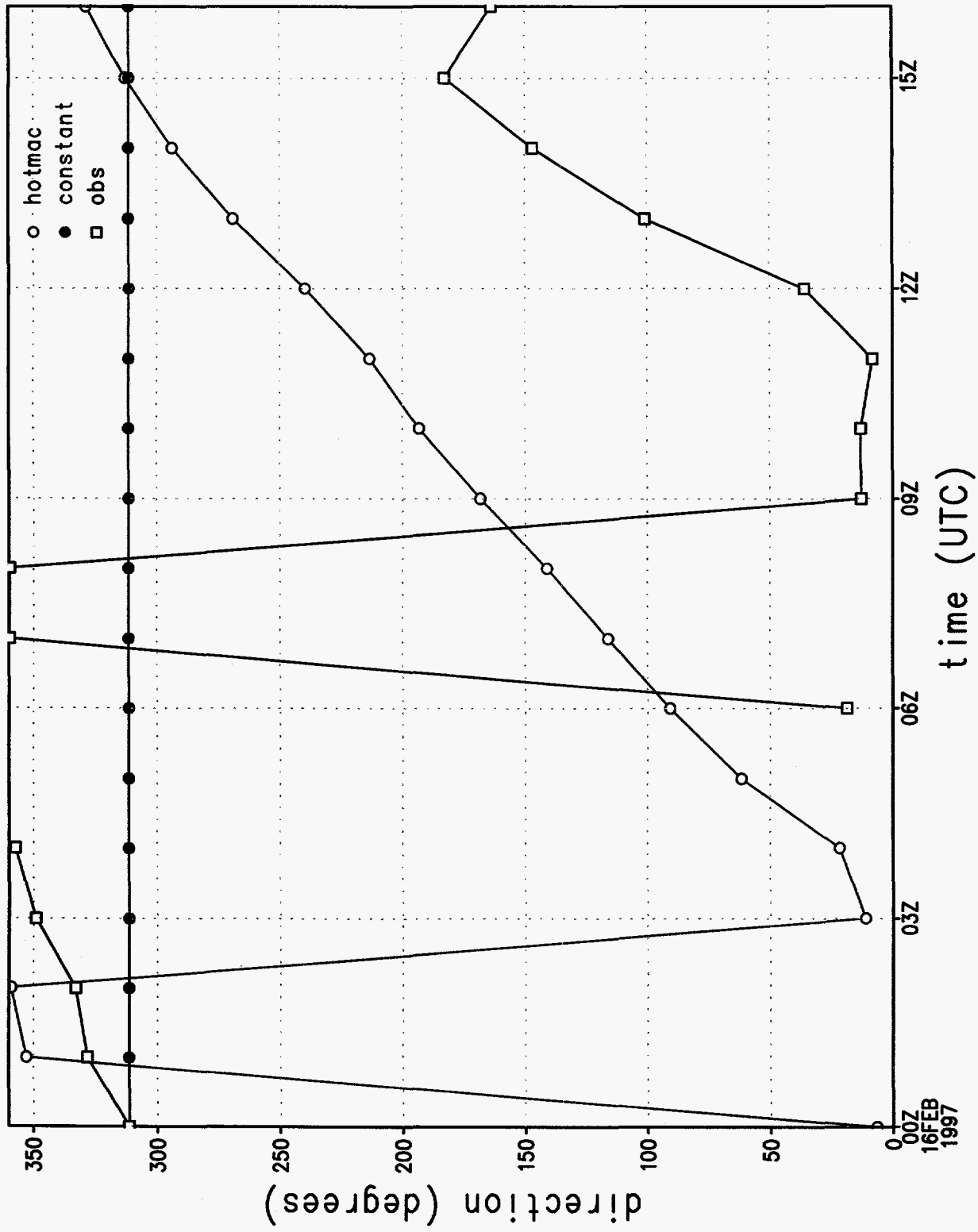


Figure 13a.

# wind speed sounding 1, 1072 m

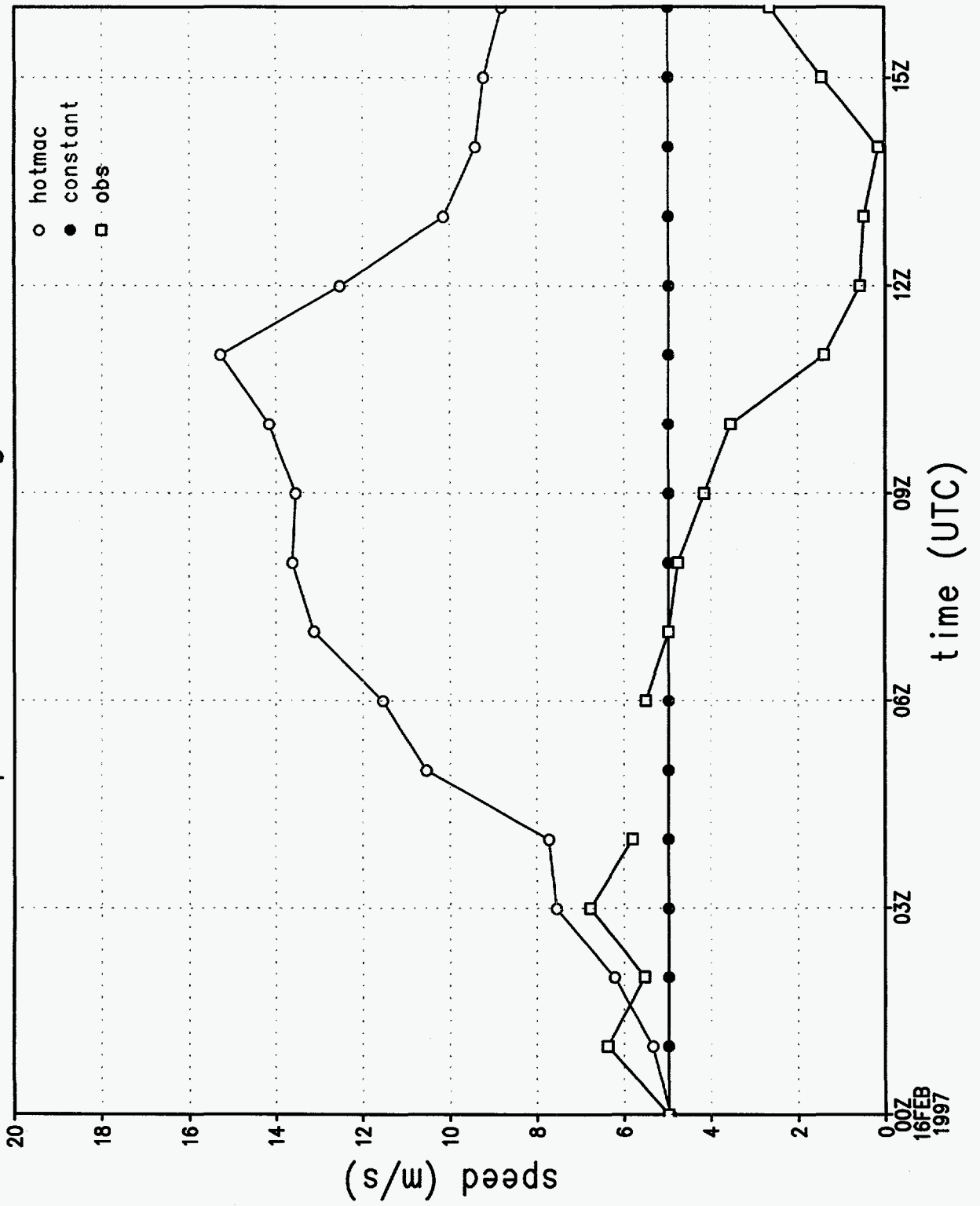


Figure 13b.



# wind direction at station 1

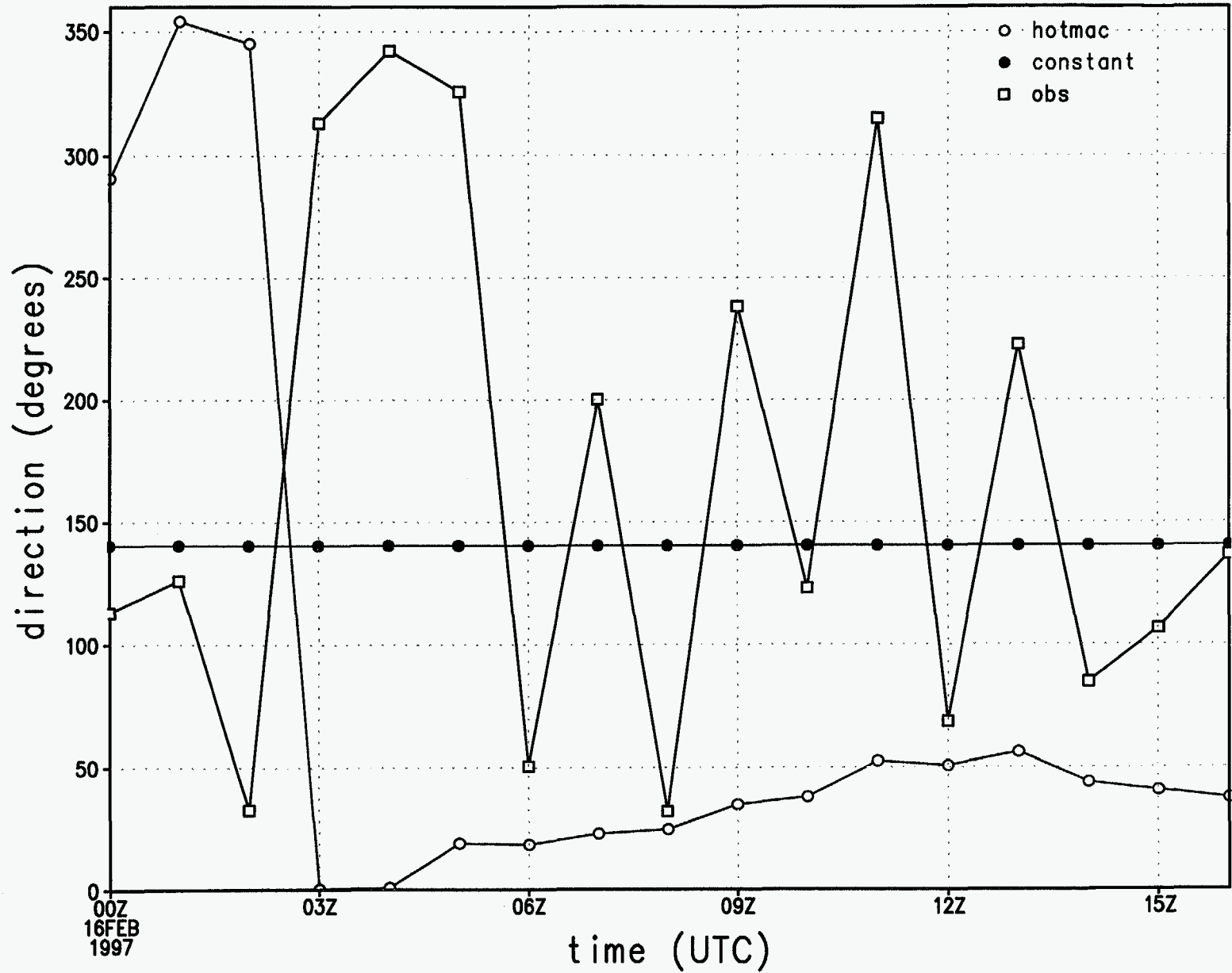


Figure 13c.

# wind speed at station 1

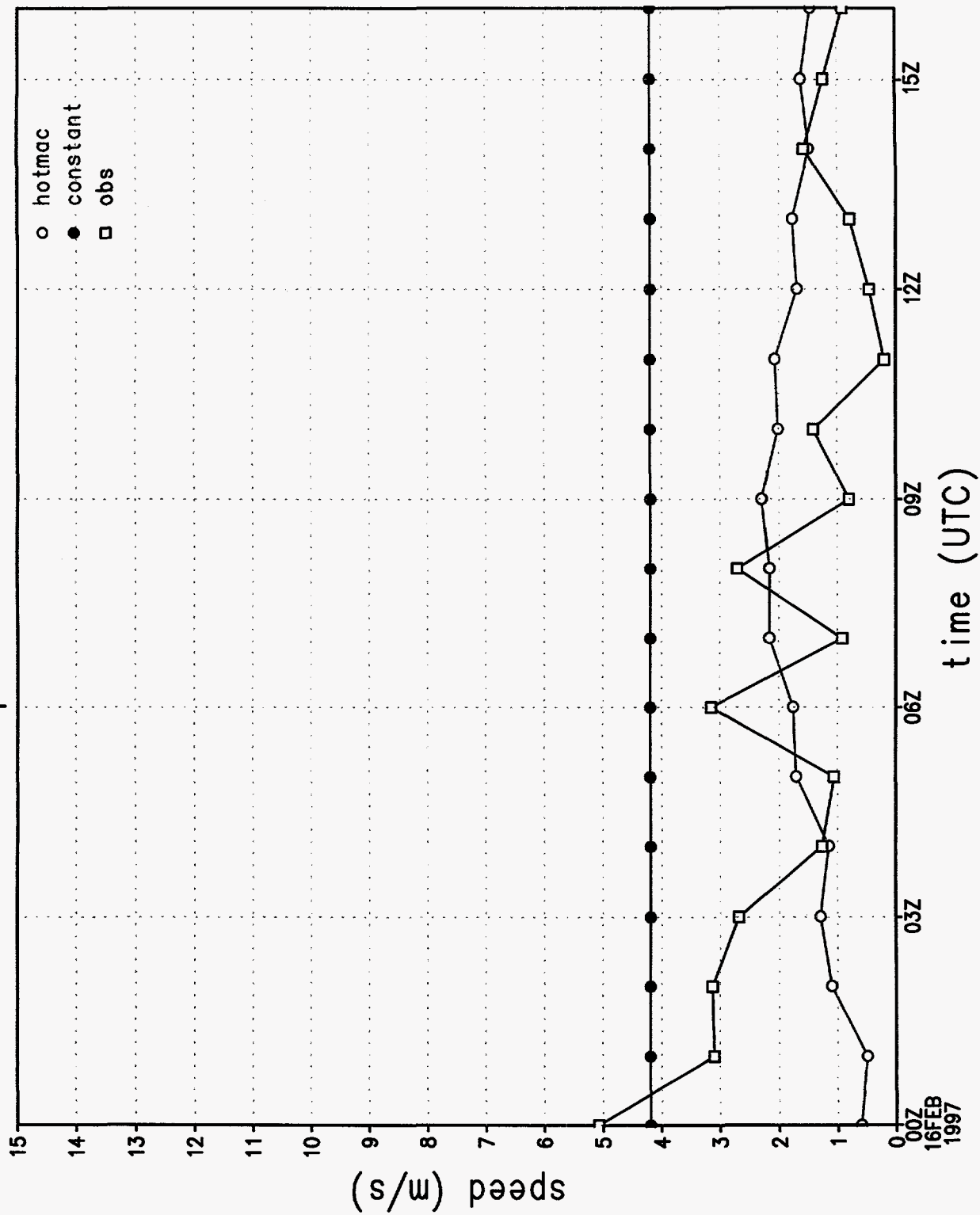


Figure 13d.

# u wind component at station 1

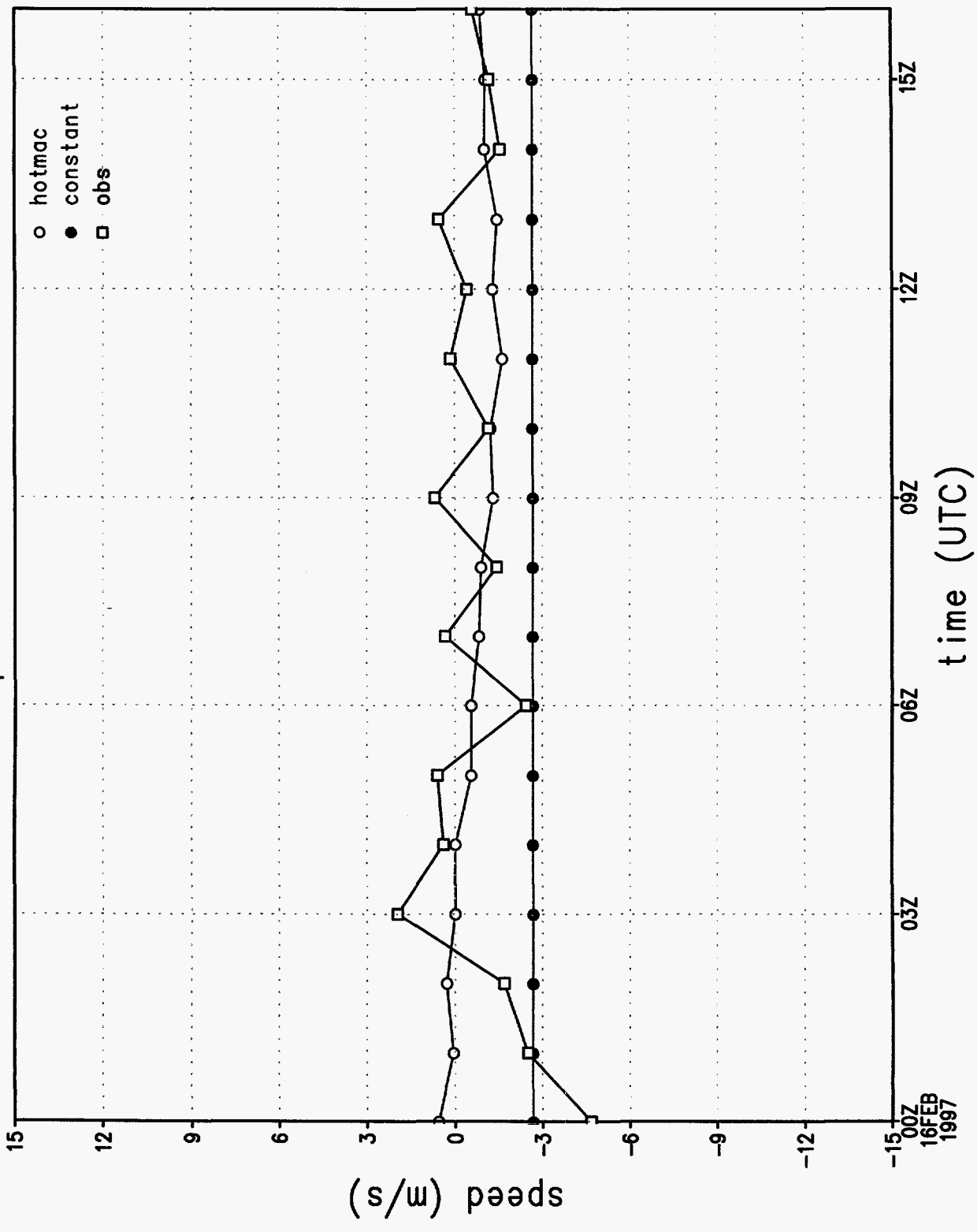


Figure 13e.

v wind component at station 1

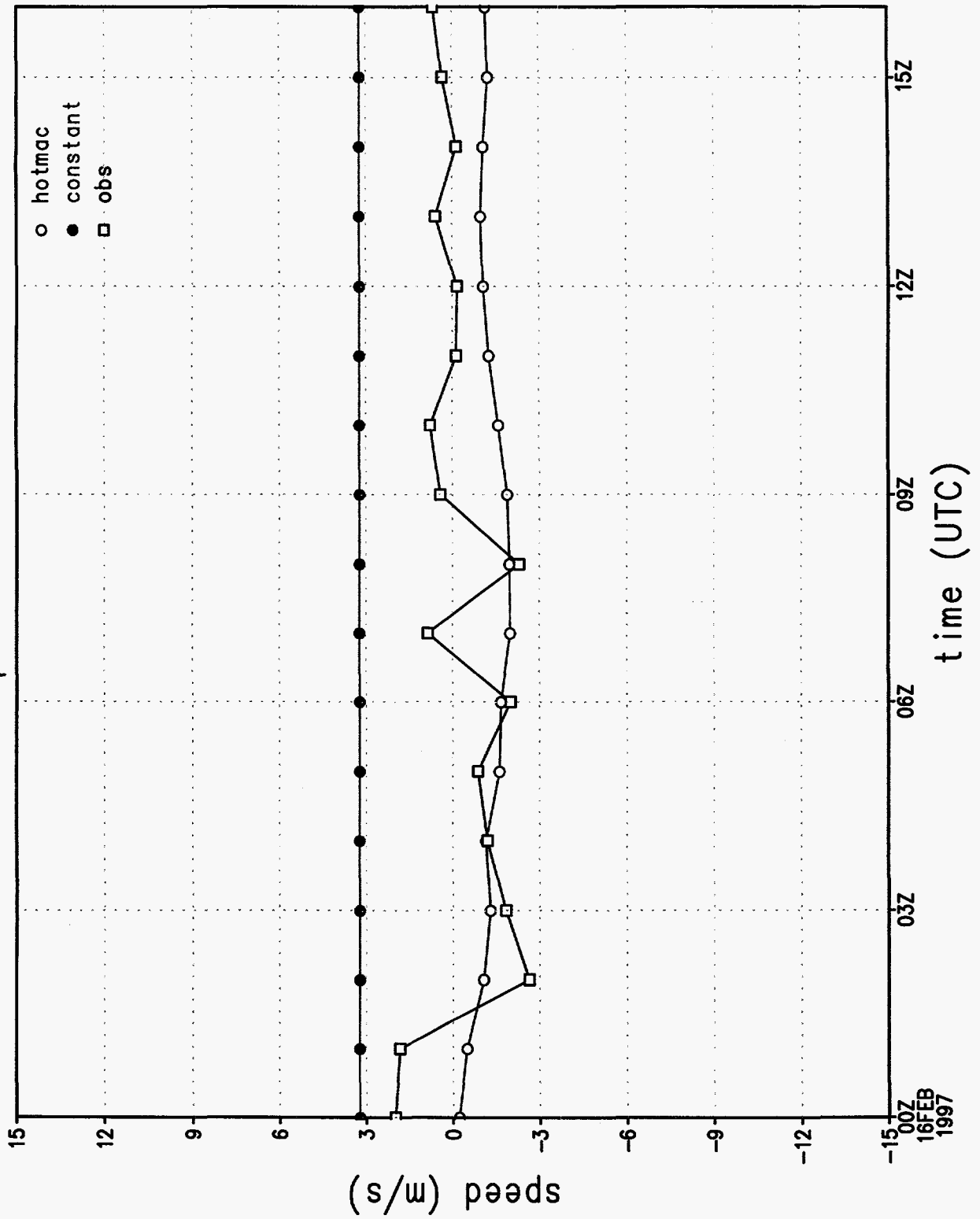


Figure 13f.

# rmse of wind direction by hour

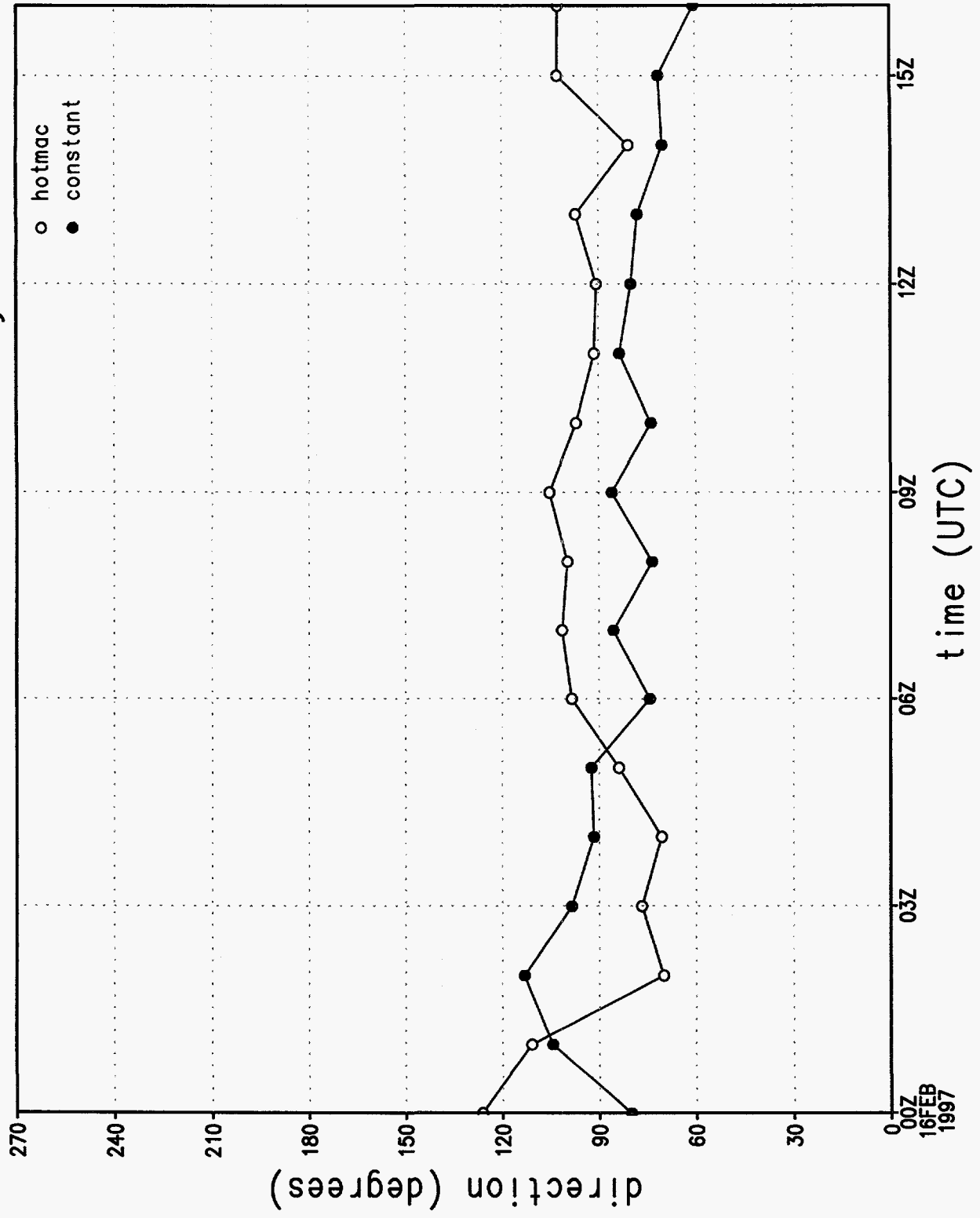


Figure 13g.

# rmse of wind speed by hour

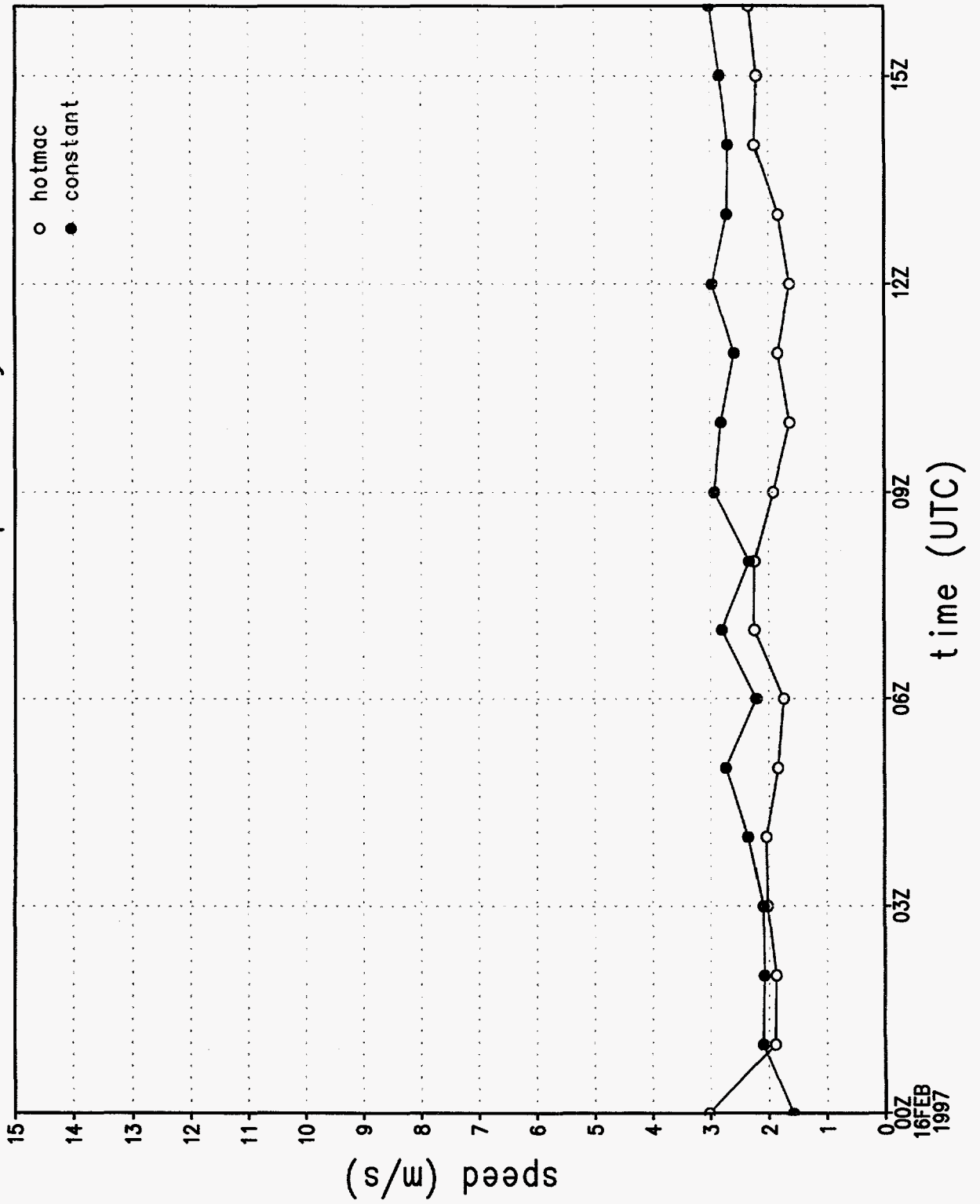


Figure 13h.

rmse of u wind component by hour

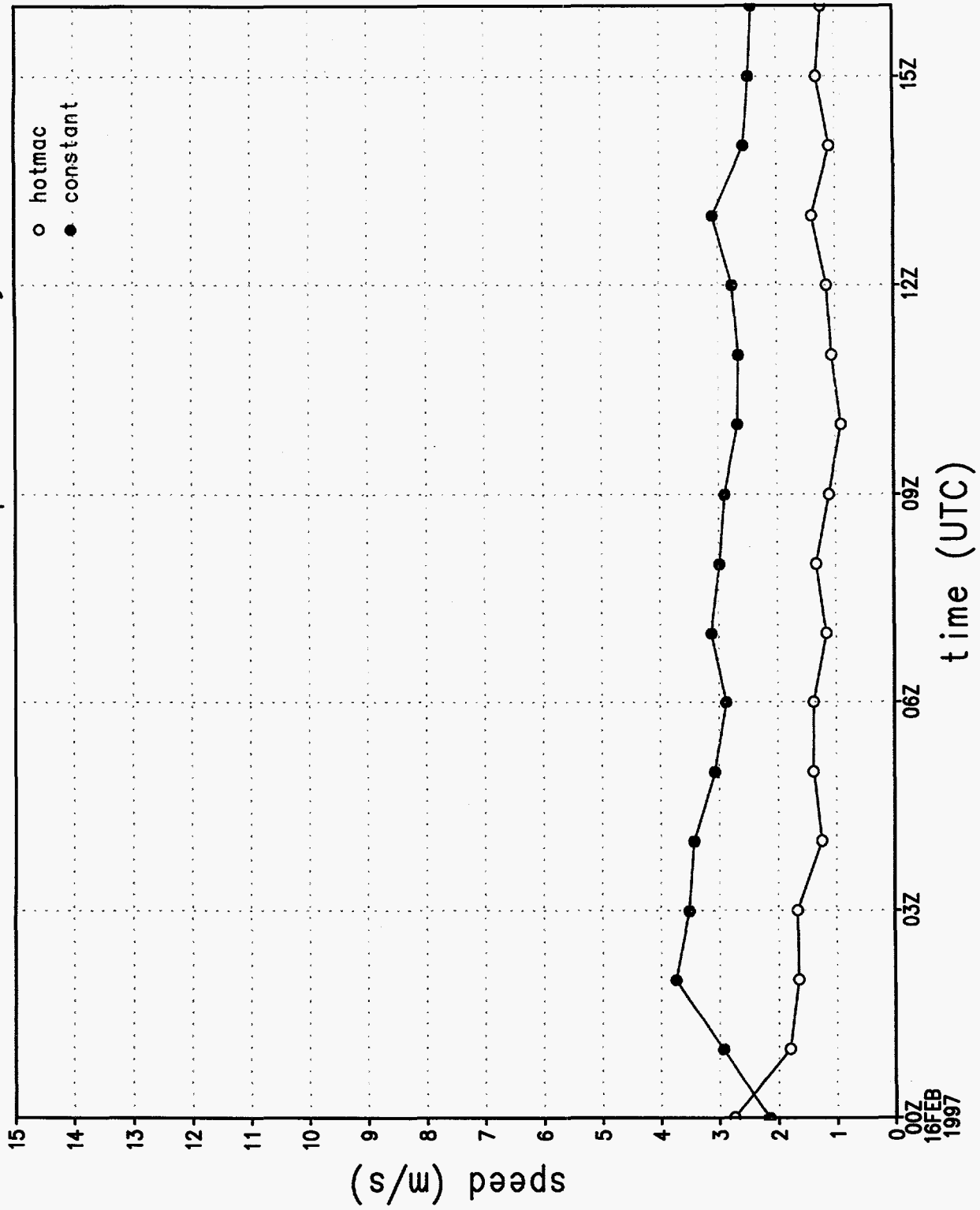


Figure 13i.

rmse of v wind component by hour

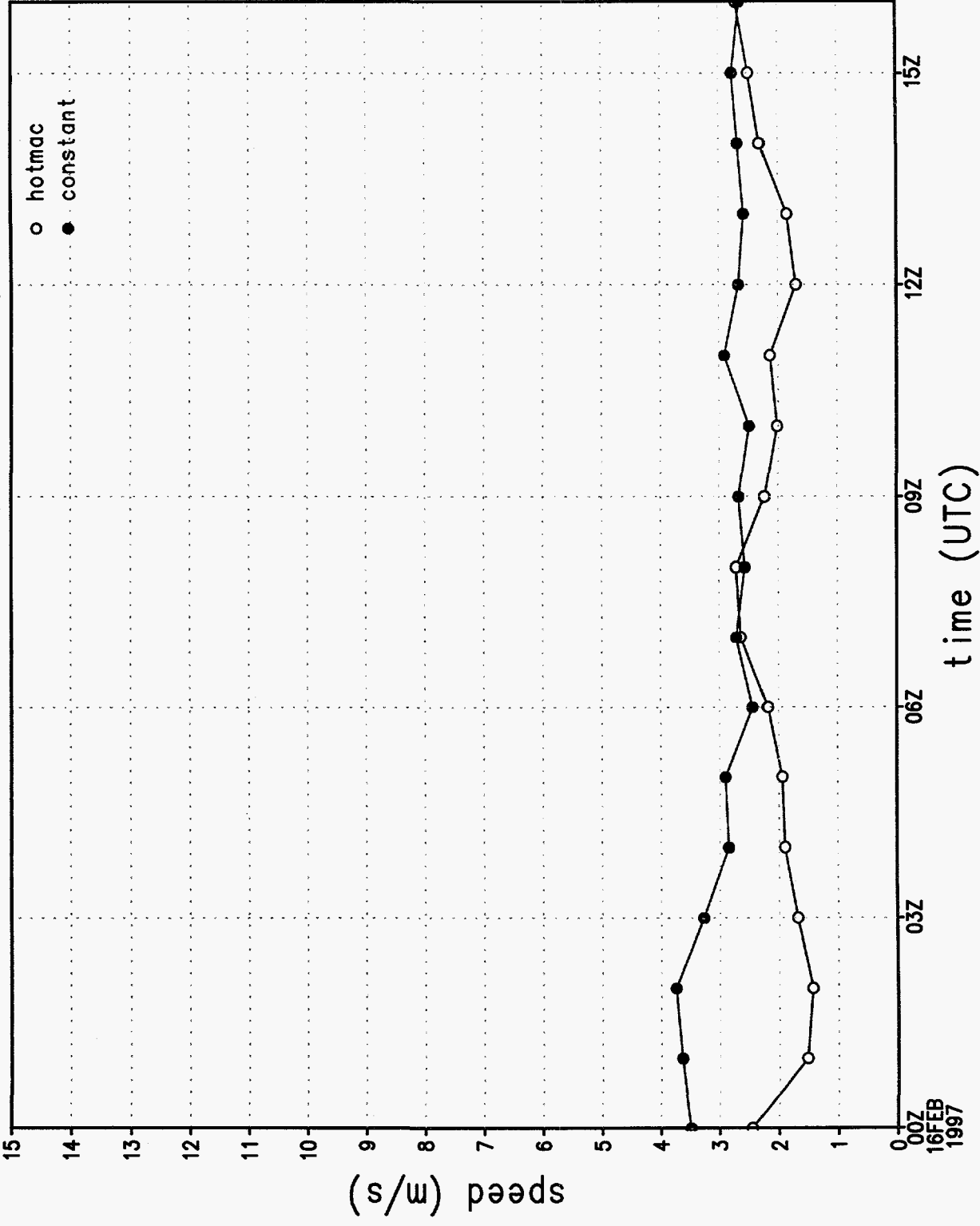


Figure 13j.



wind direction sounding 1, 1072 m

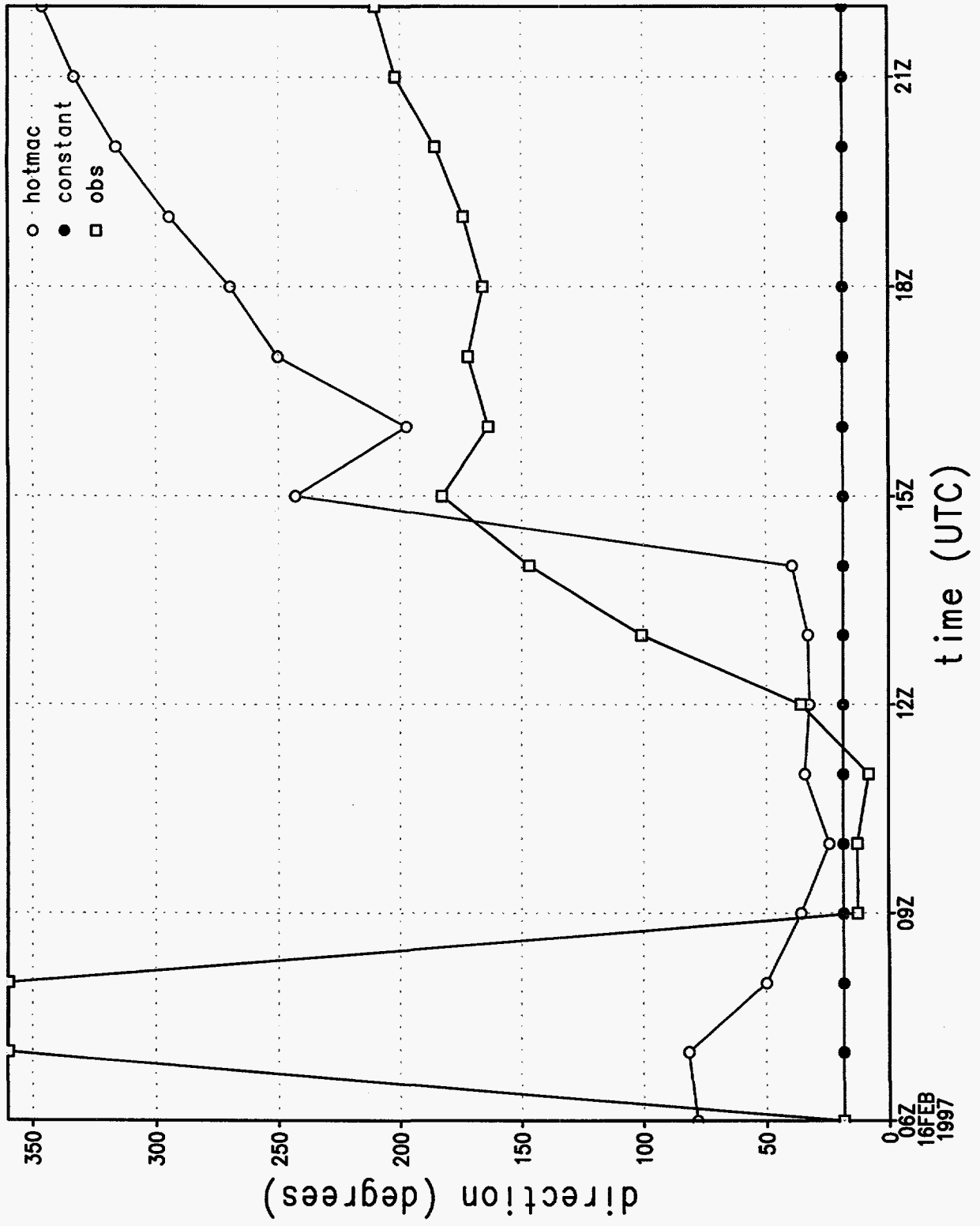


Figure 14a.

# wind speed sounding 1, 1072 m

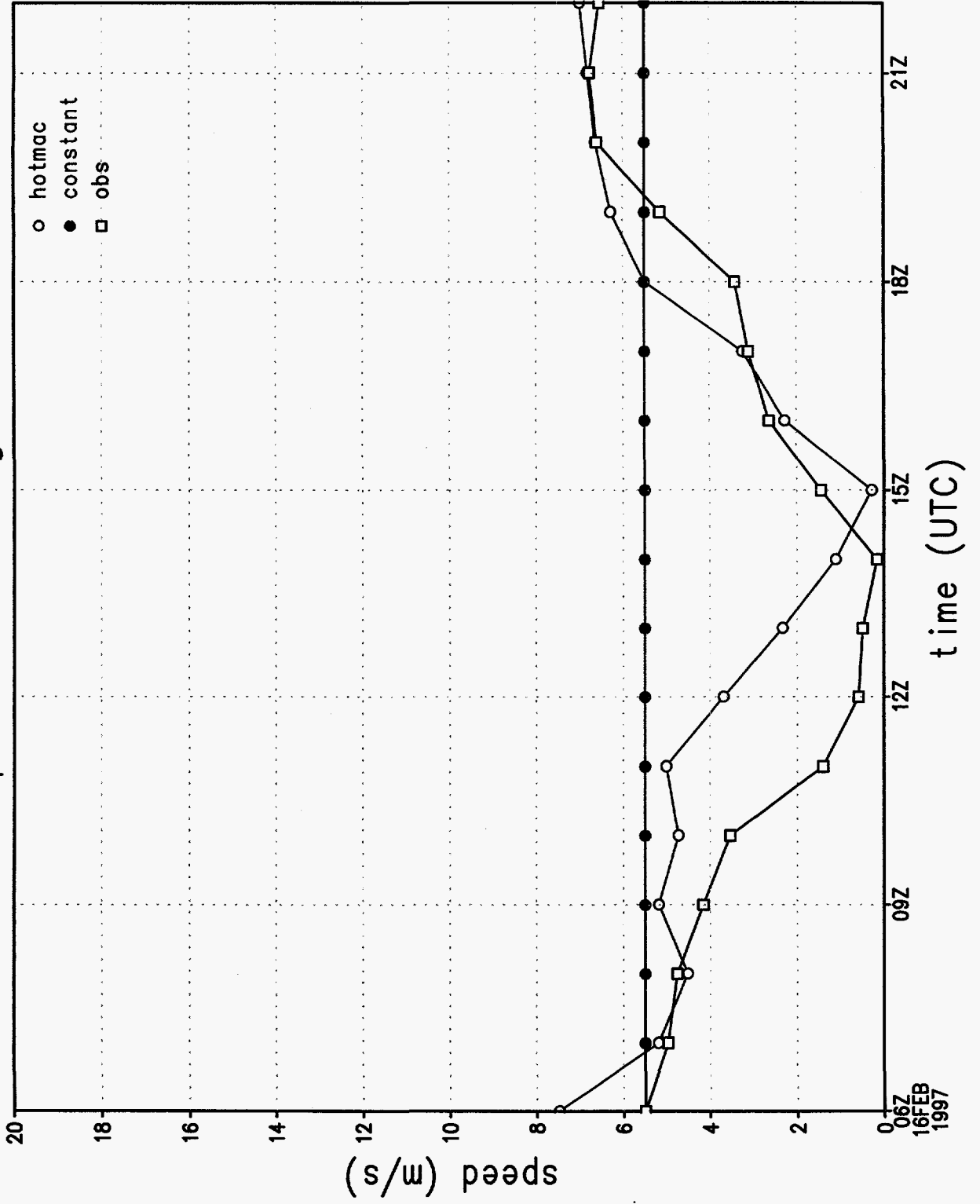


Figure 14b.

wind direction at station 1

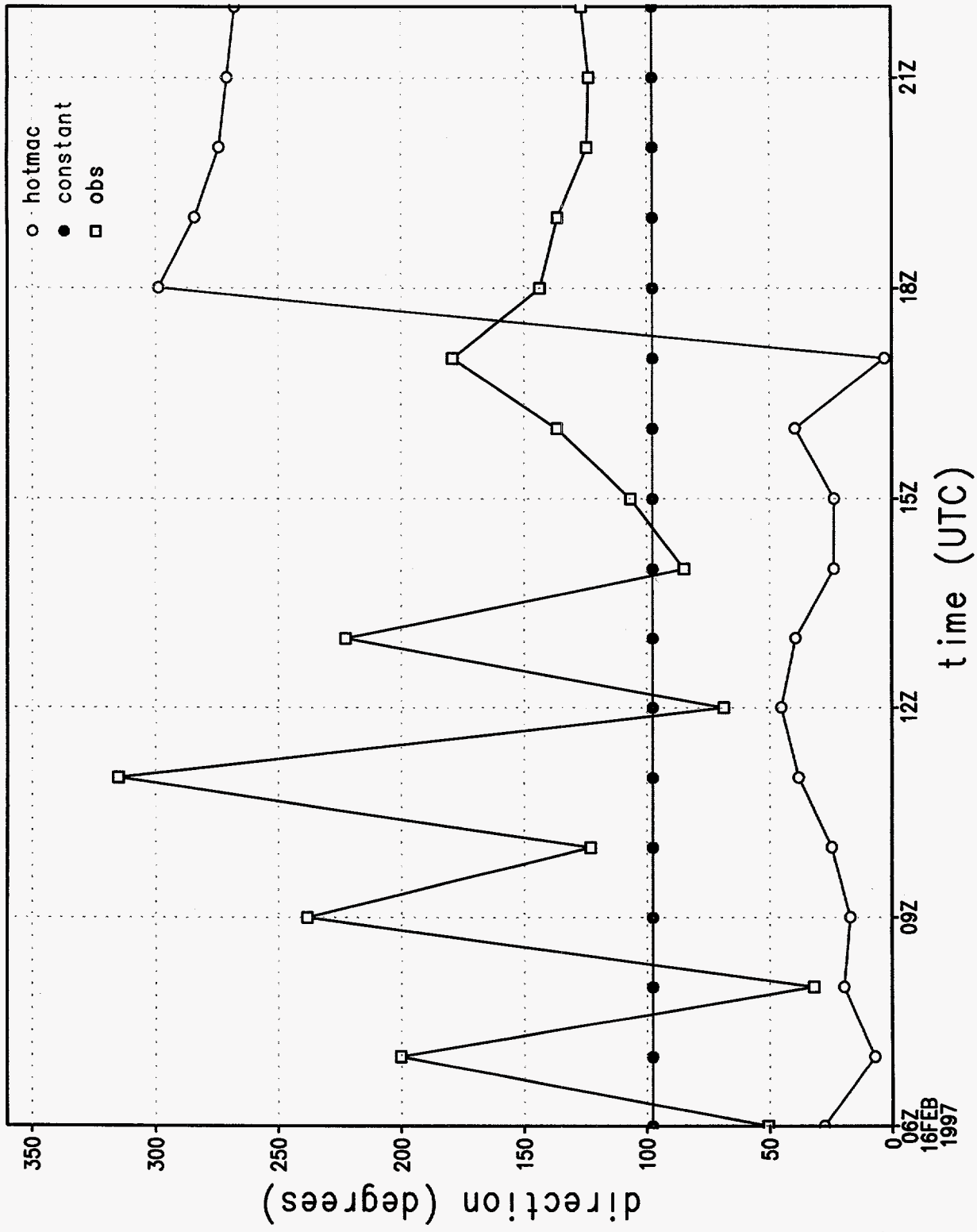


Figure 14c.

# wind speed at station 1

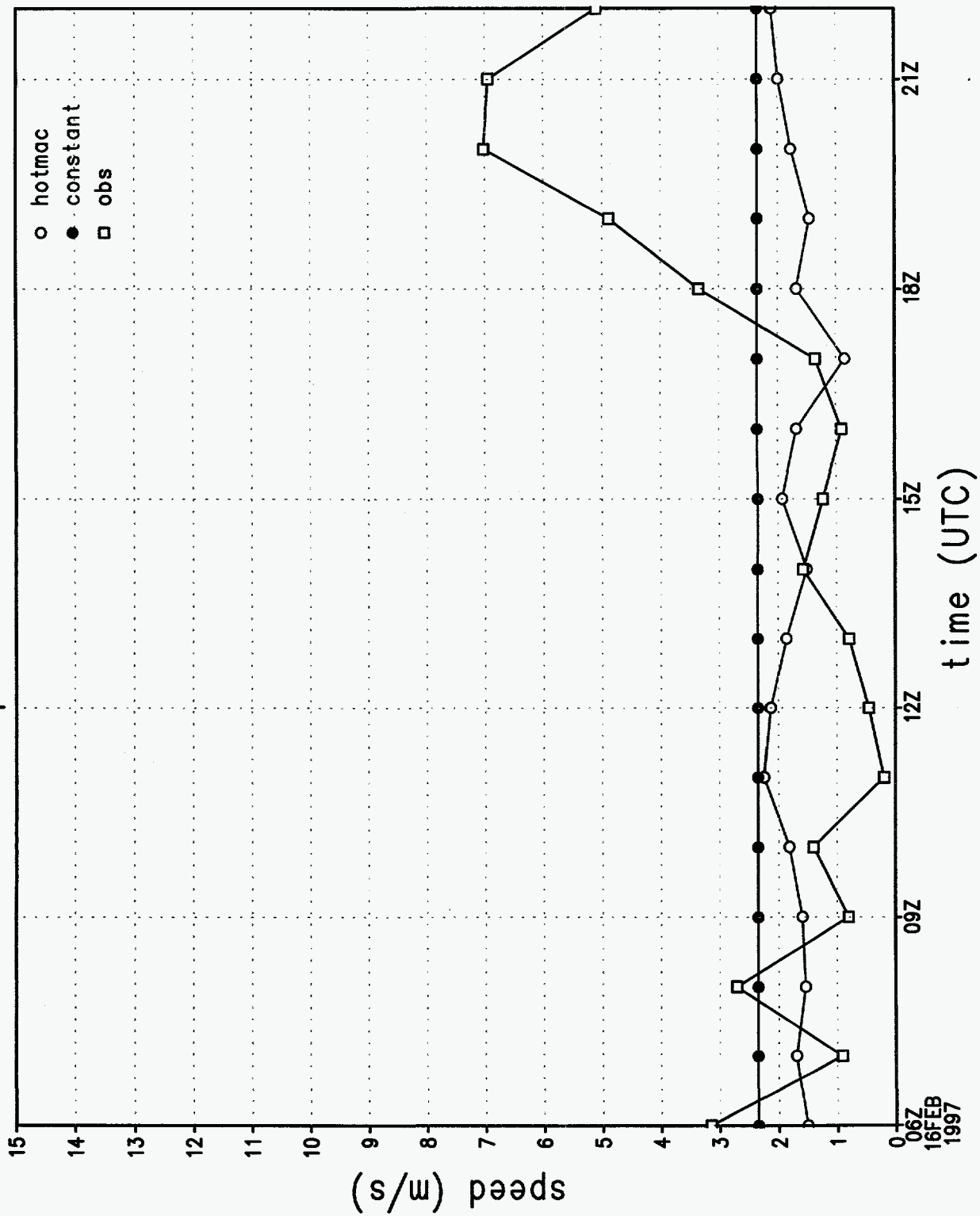


Figure 14d.

# u wind component at station 1

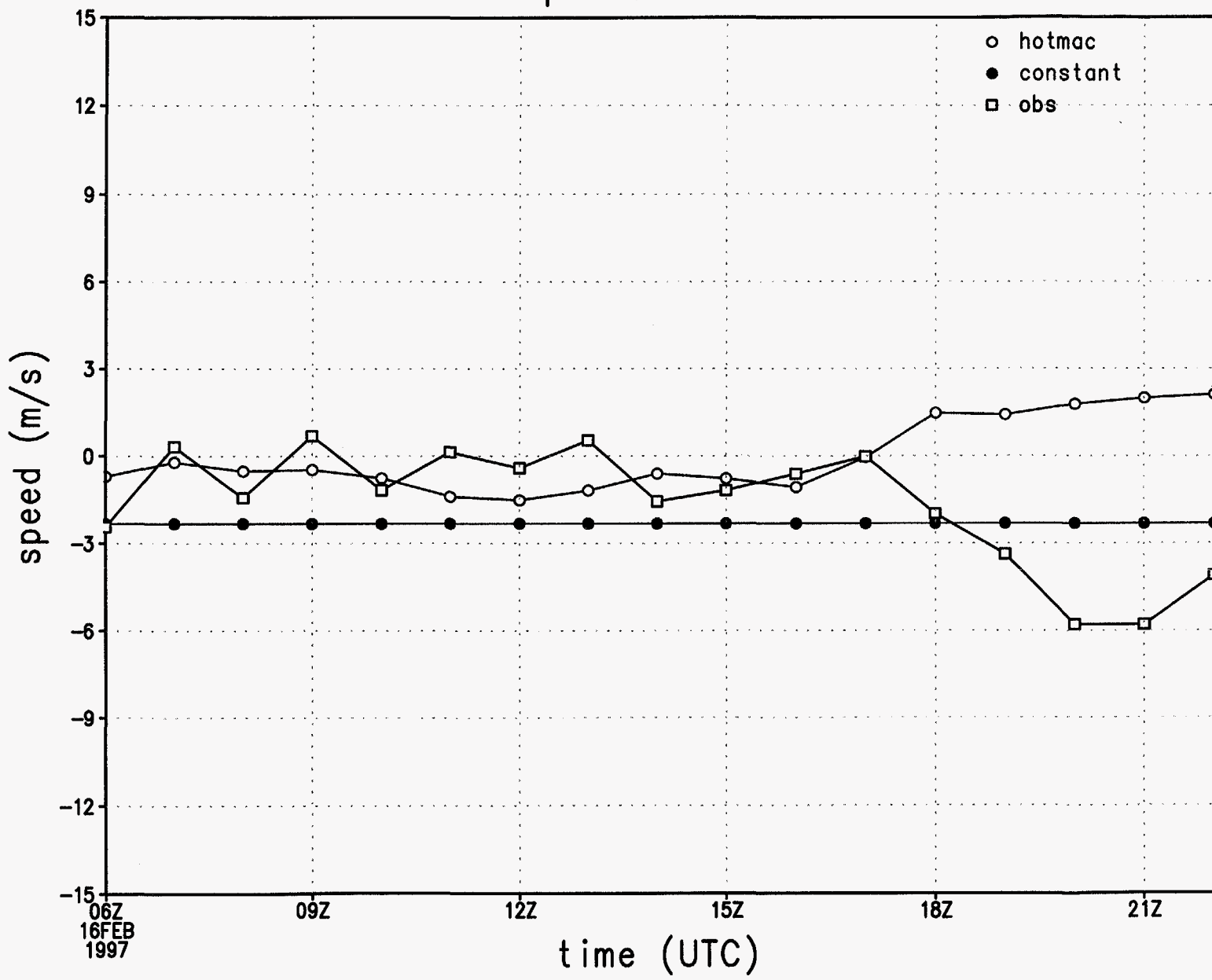


Figure 14e.

v wind component at station 1

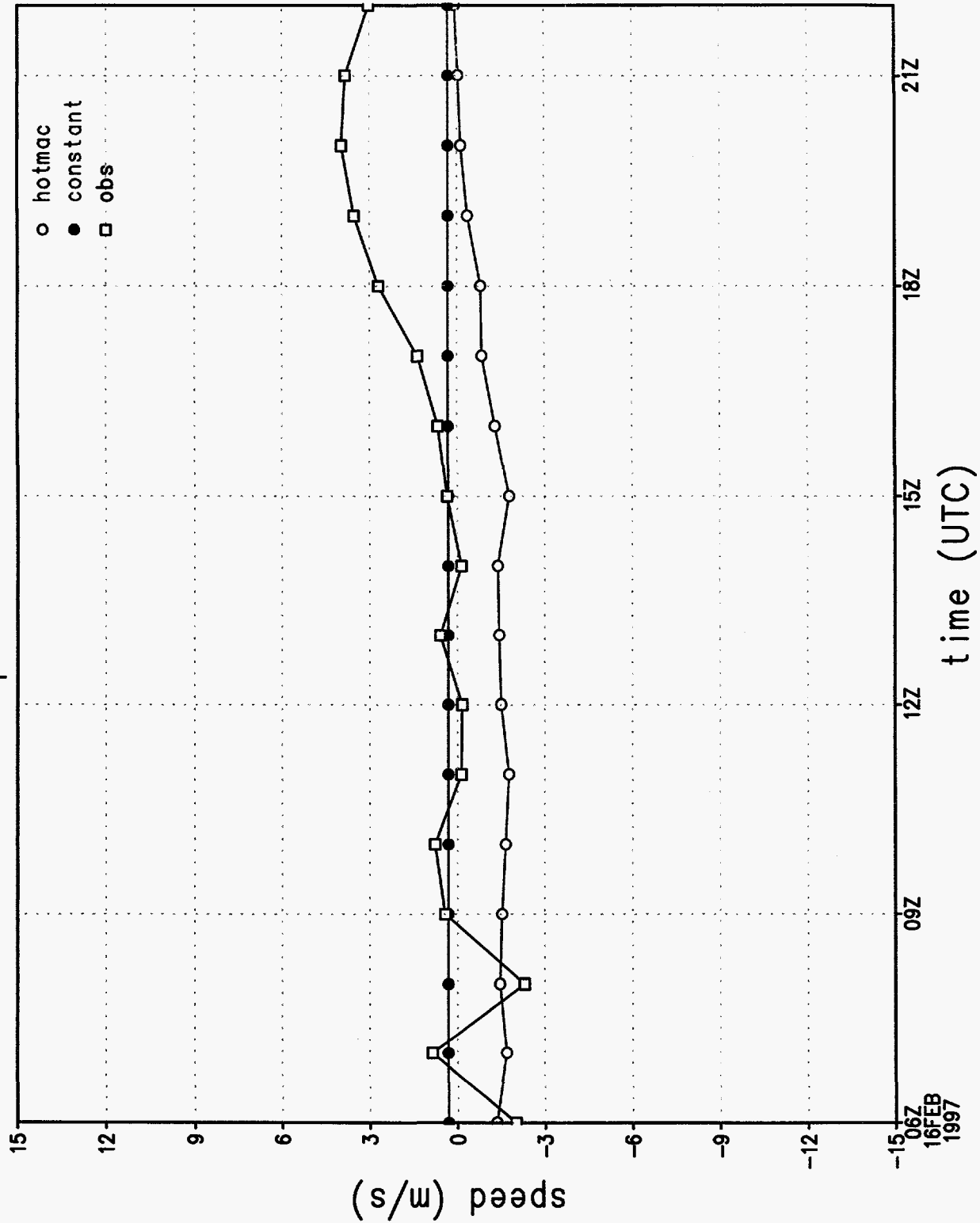


Figure 14f.

# rmse of wind direction by hour

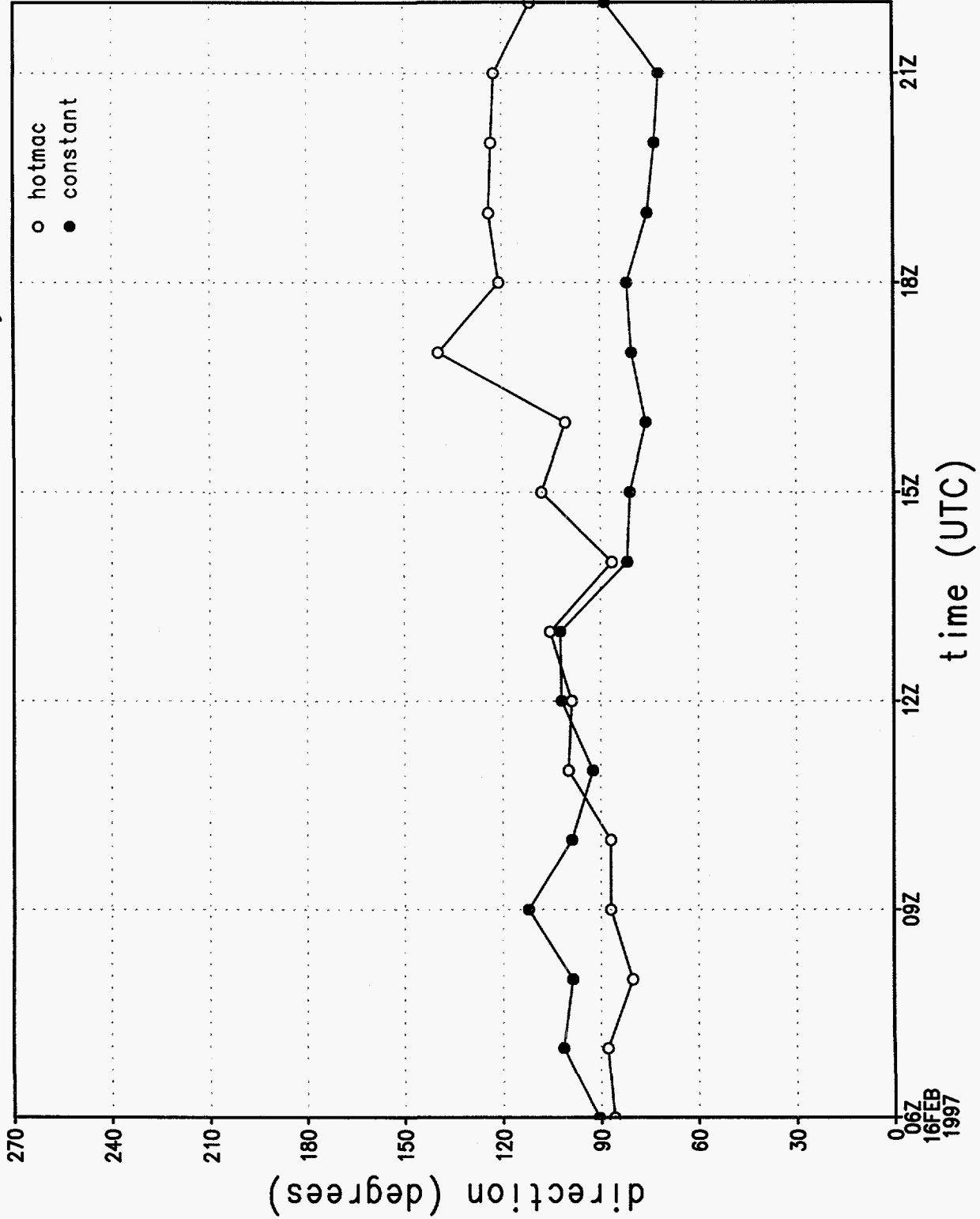


Figure 14g

# rmse of wind speed by hour

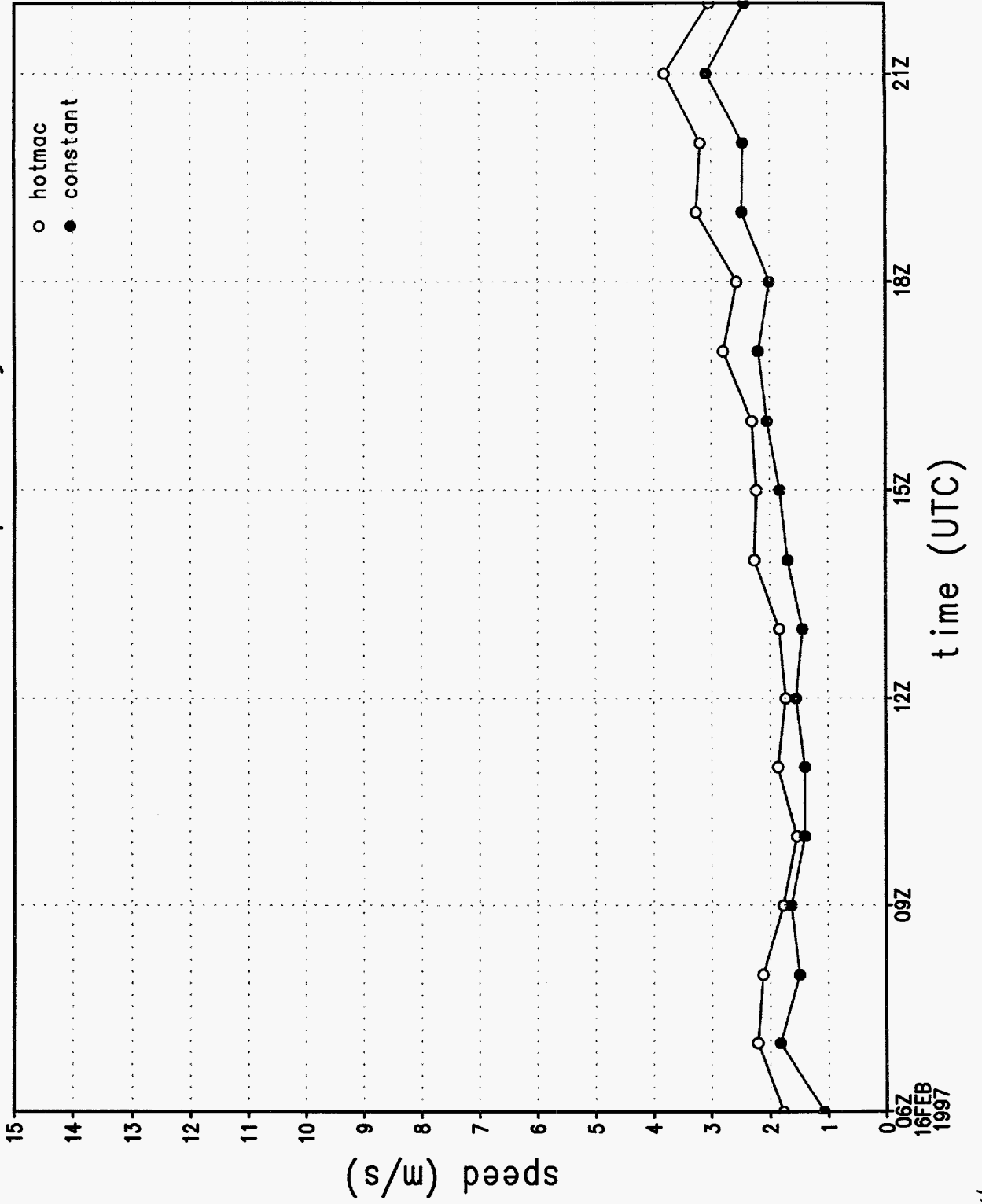


Figure 14h.



# rmse of u wind component by hour

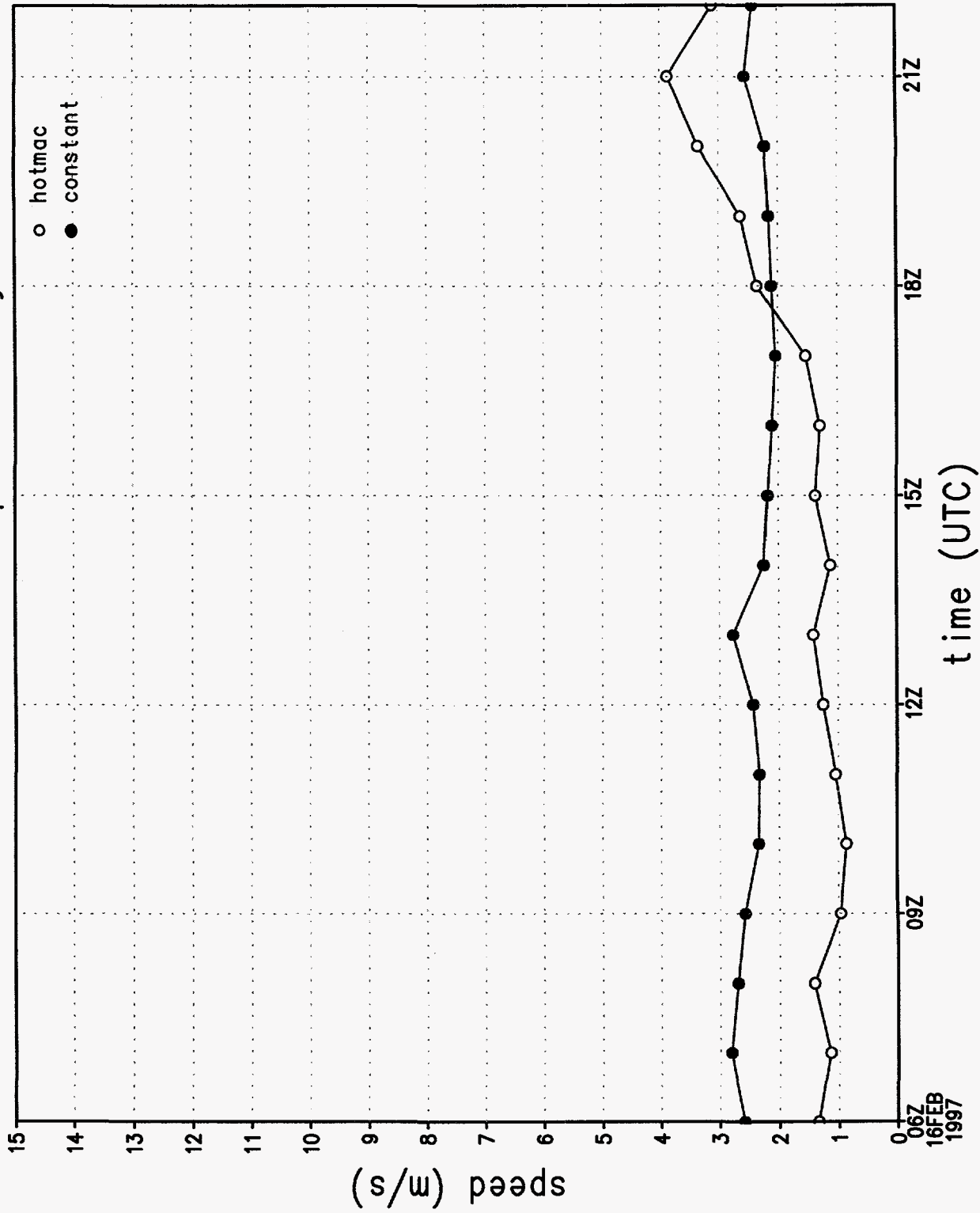


Figure 14i.

rmse of v wind component by hour

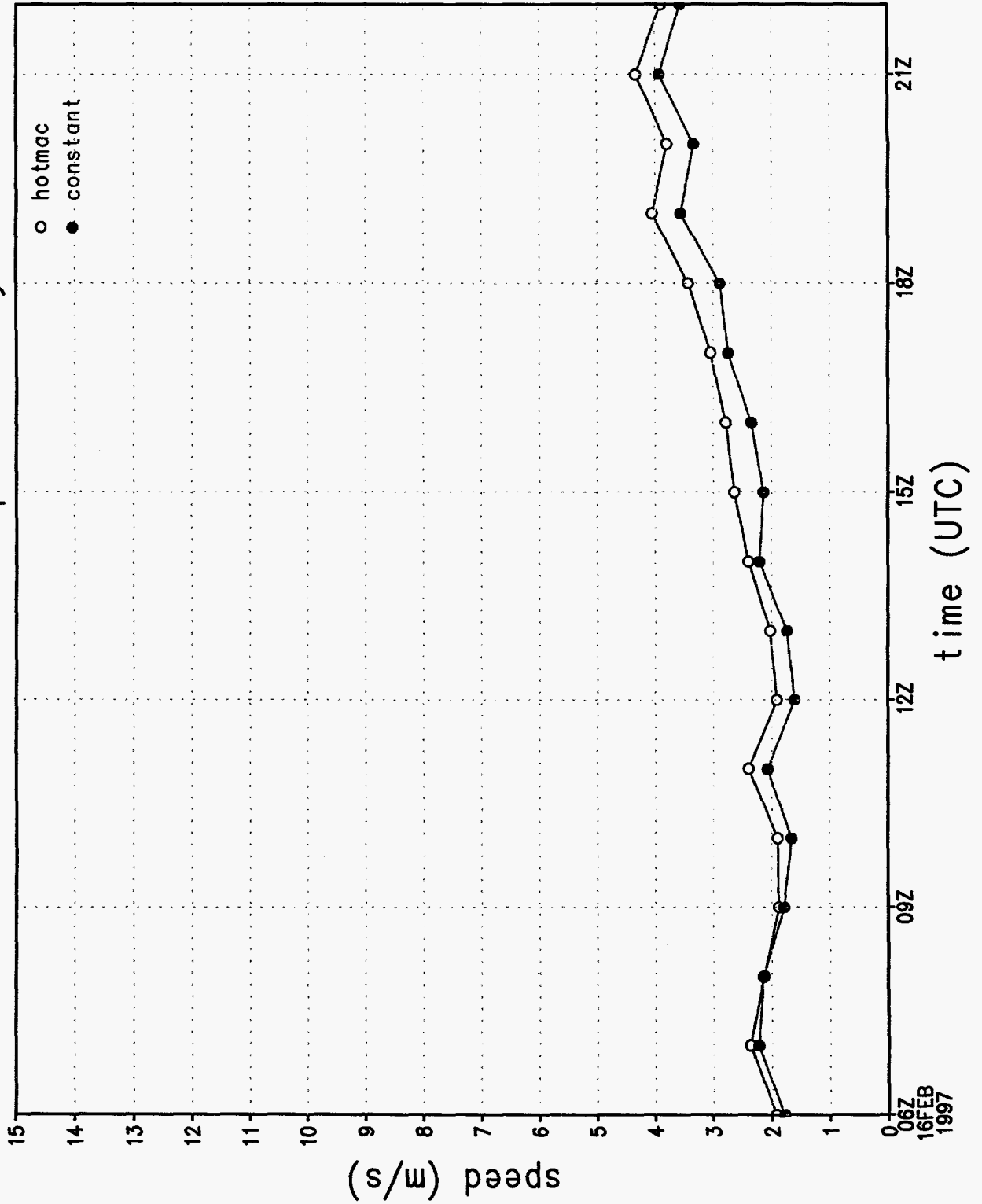


Figure 14j.

# wind direction sounding 1, 1072 m

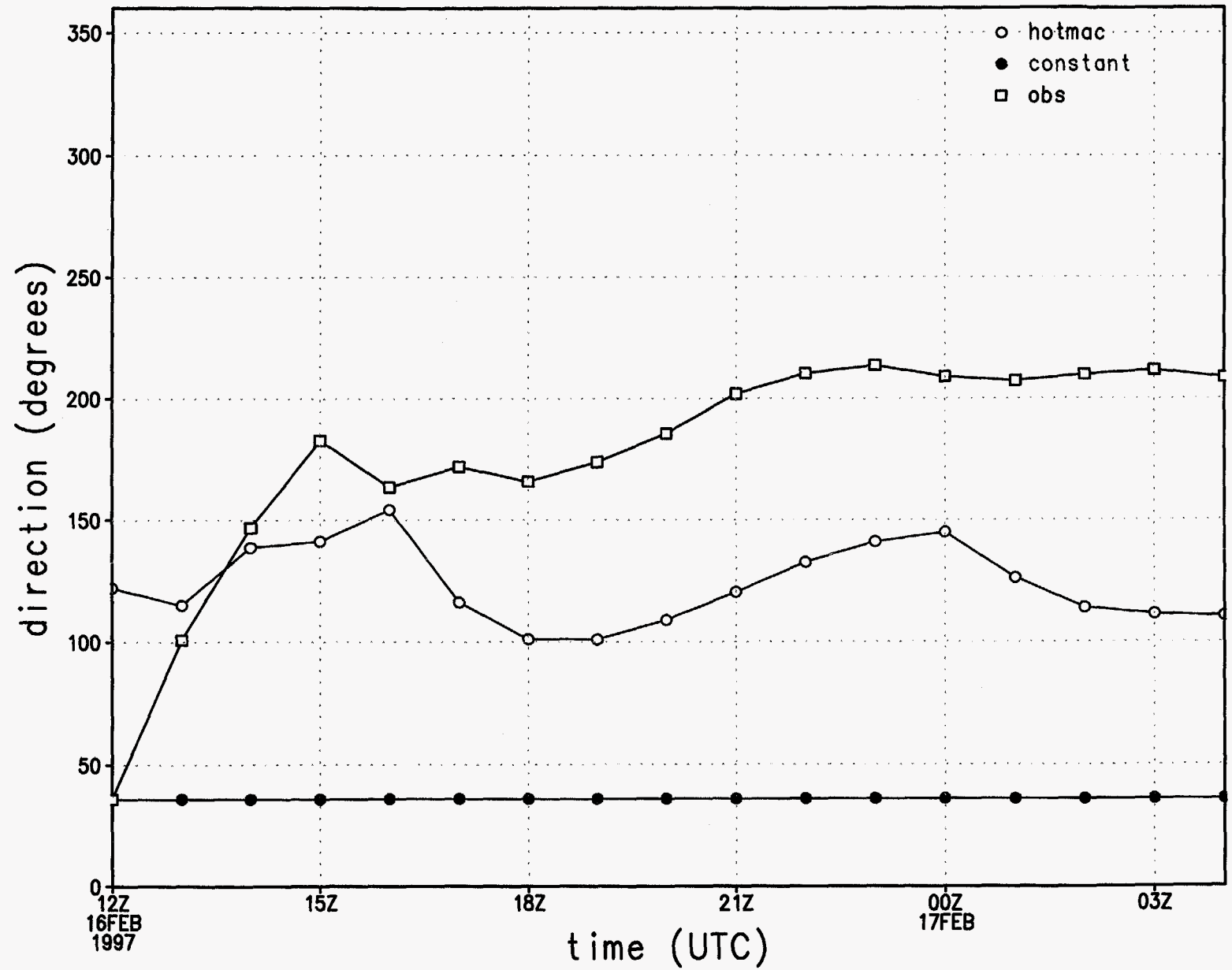


Figure 15a.

# wind speed sounding 1, 1072 m

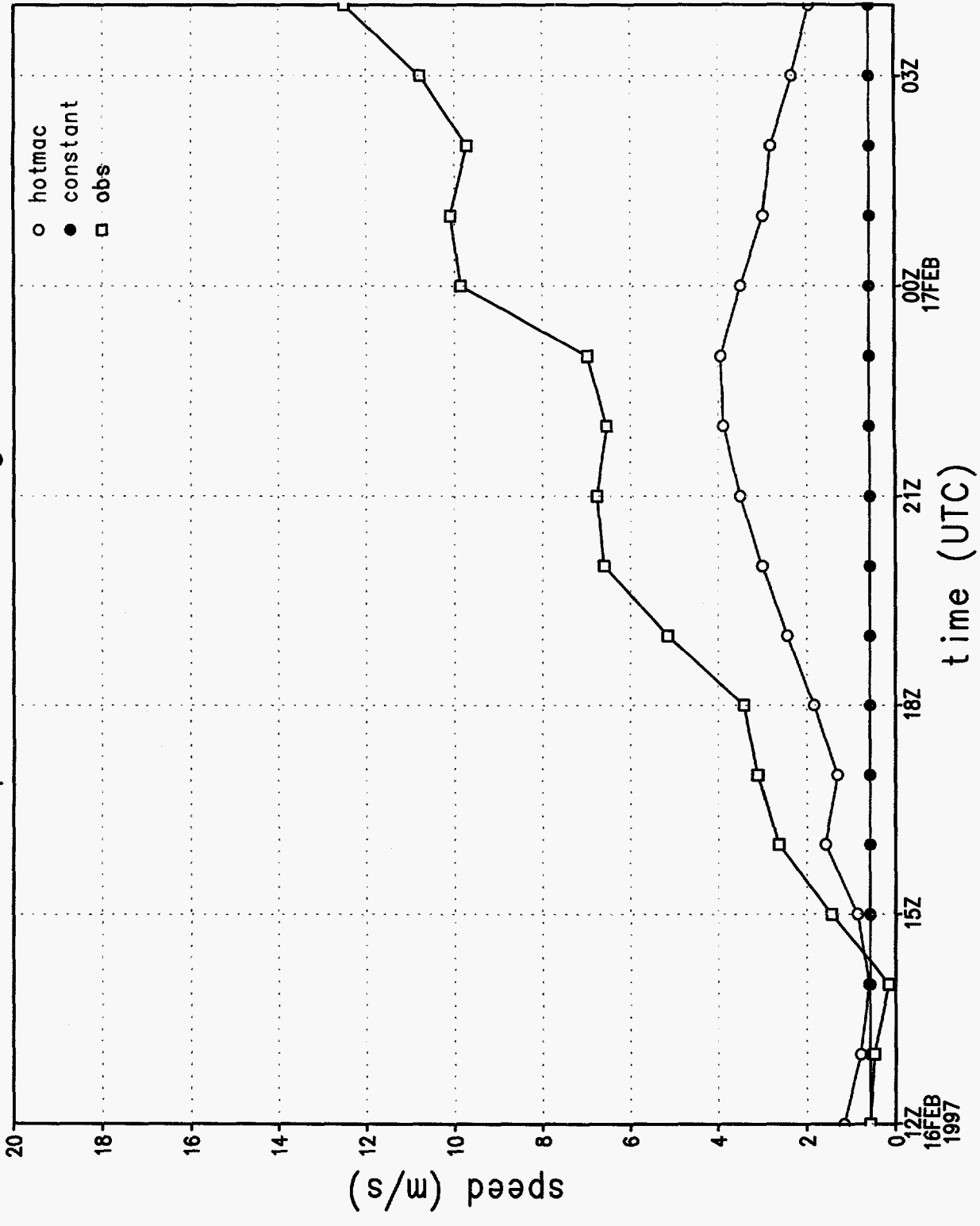


Figure 15b.

# wind direction at station 1

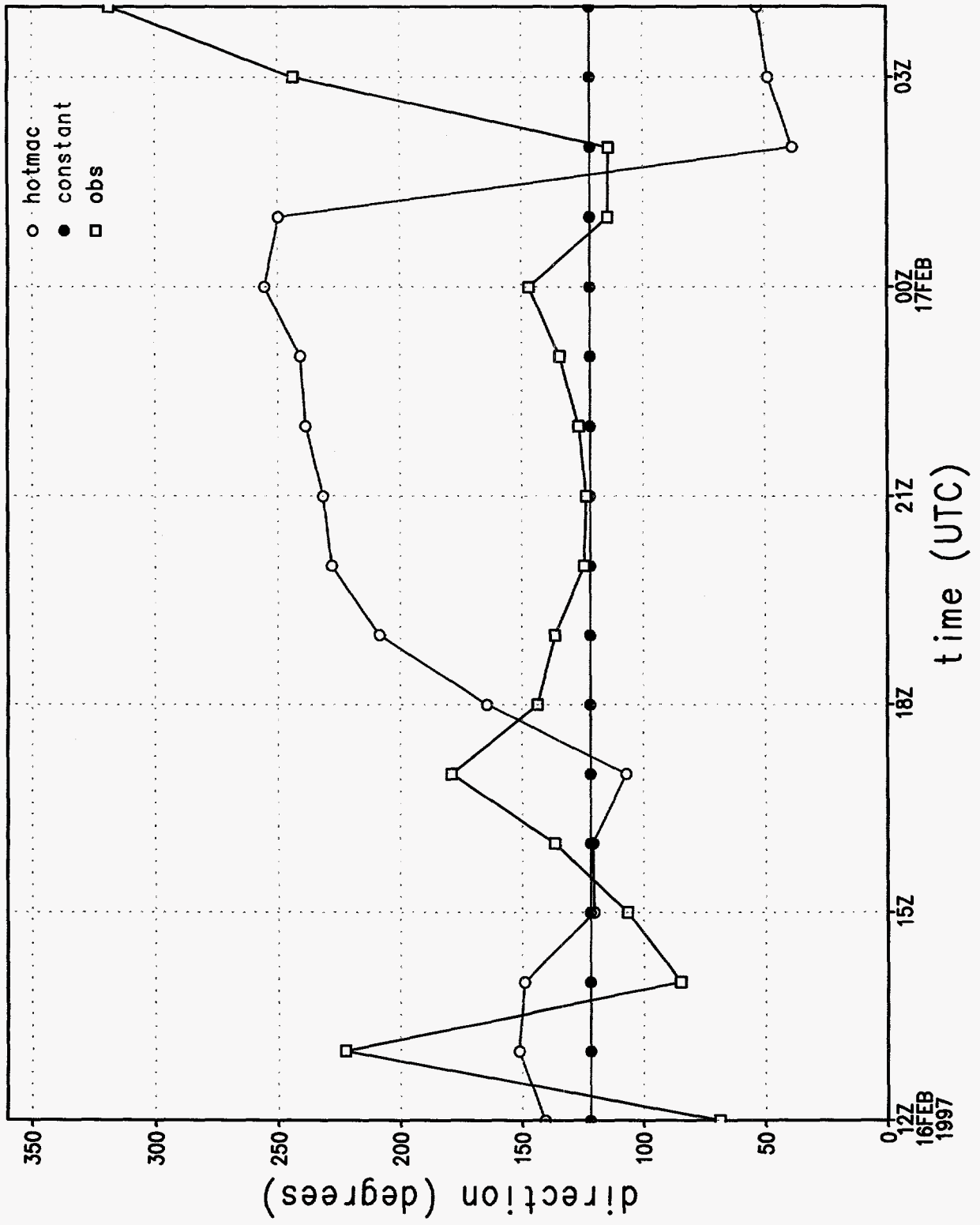


Figure 15c.

# wind speed at station 1

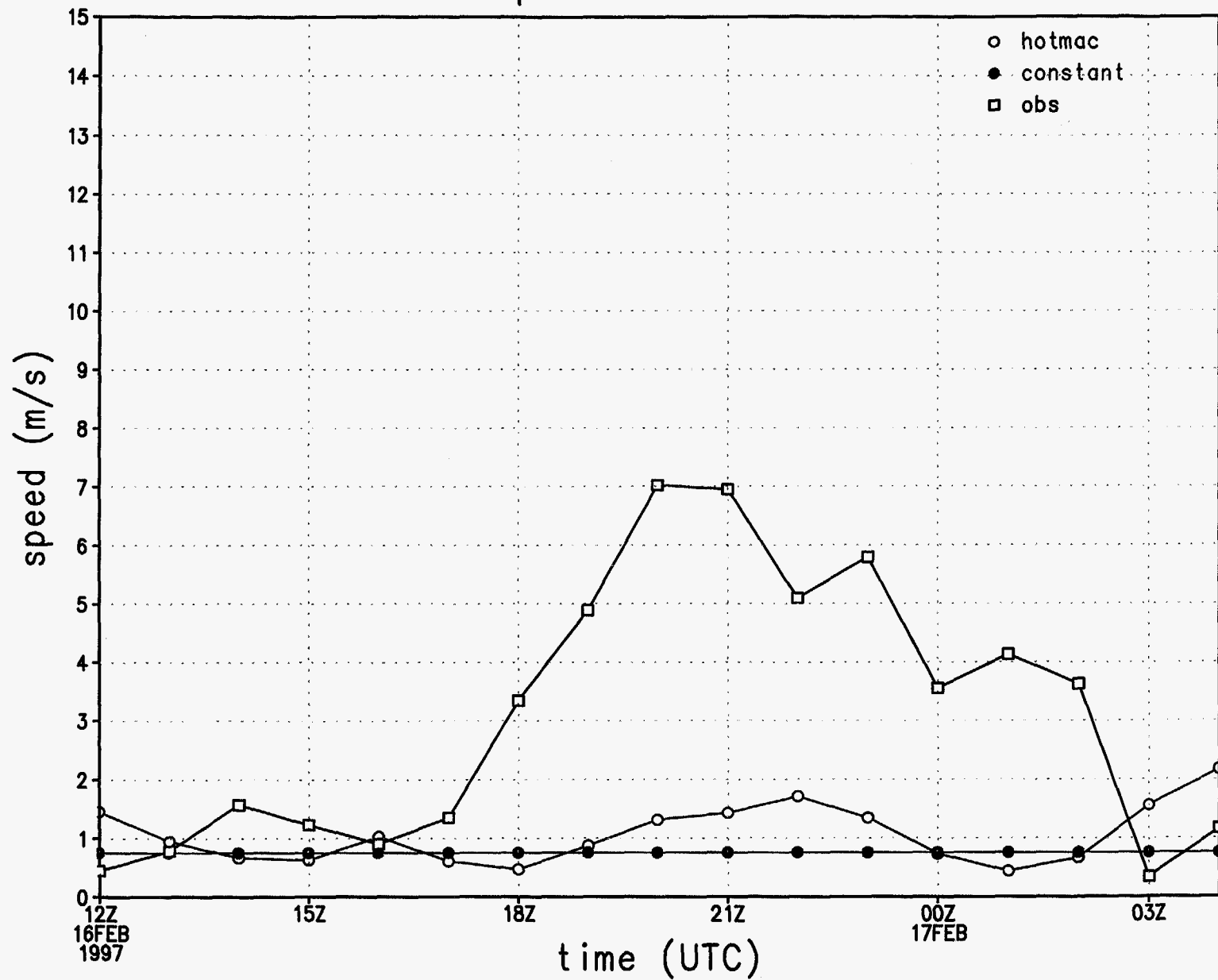


Figure 15d.

# u wind component at station 1

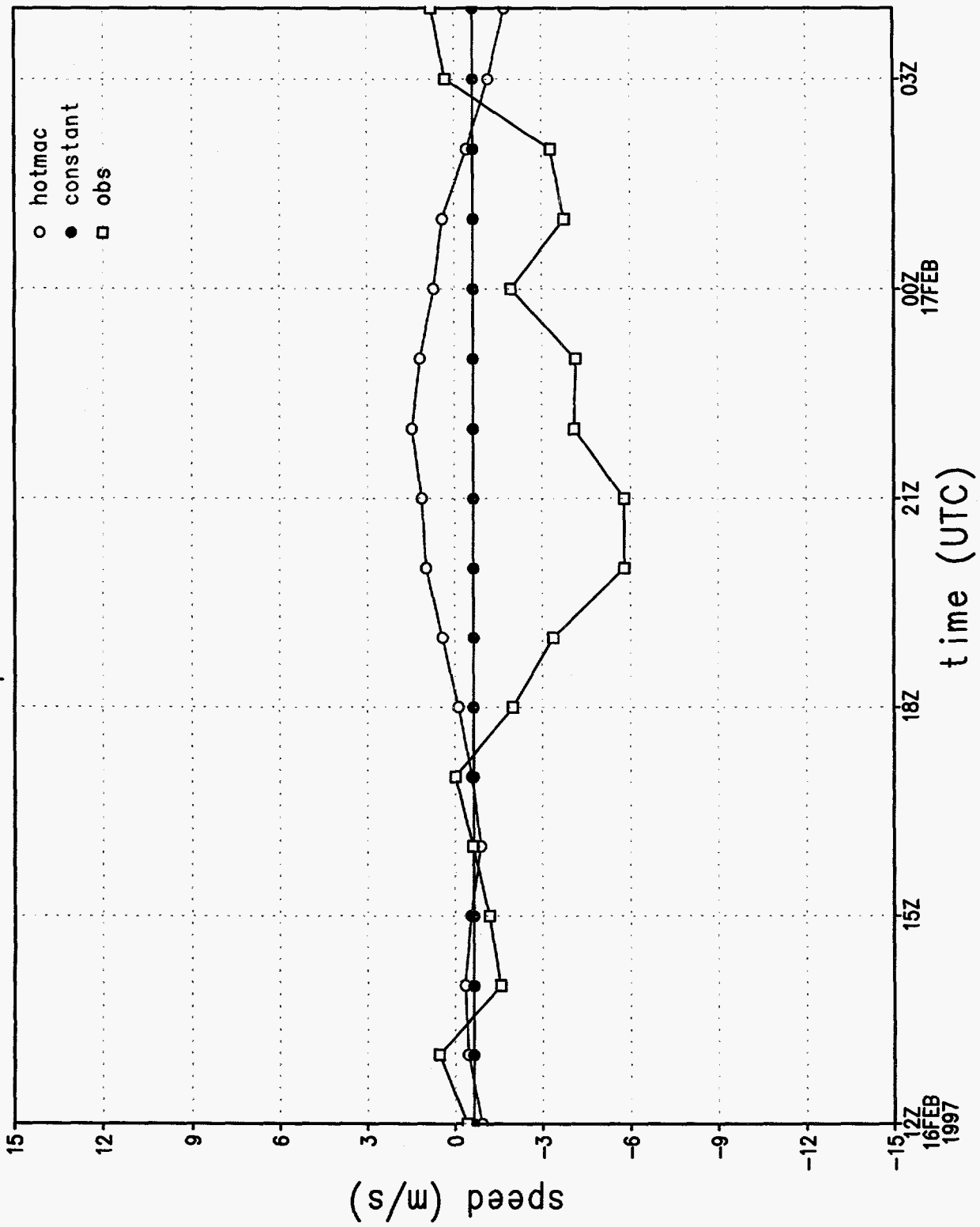


Figure 15e.

v wind component at station 1

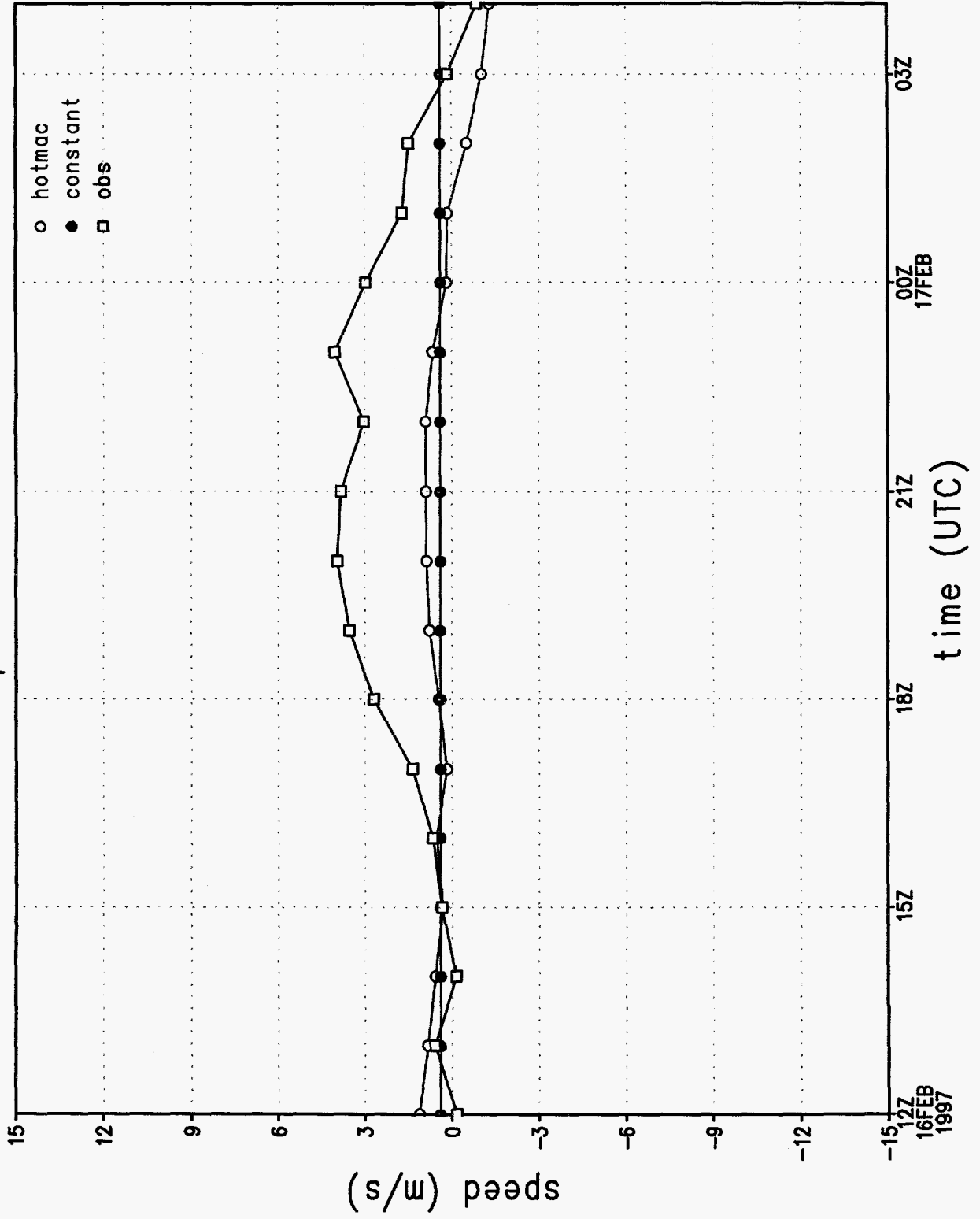


Figure 15f.



# rmse of wind direction by hour

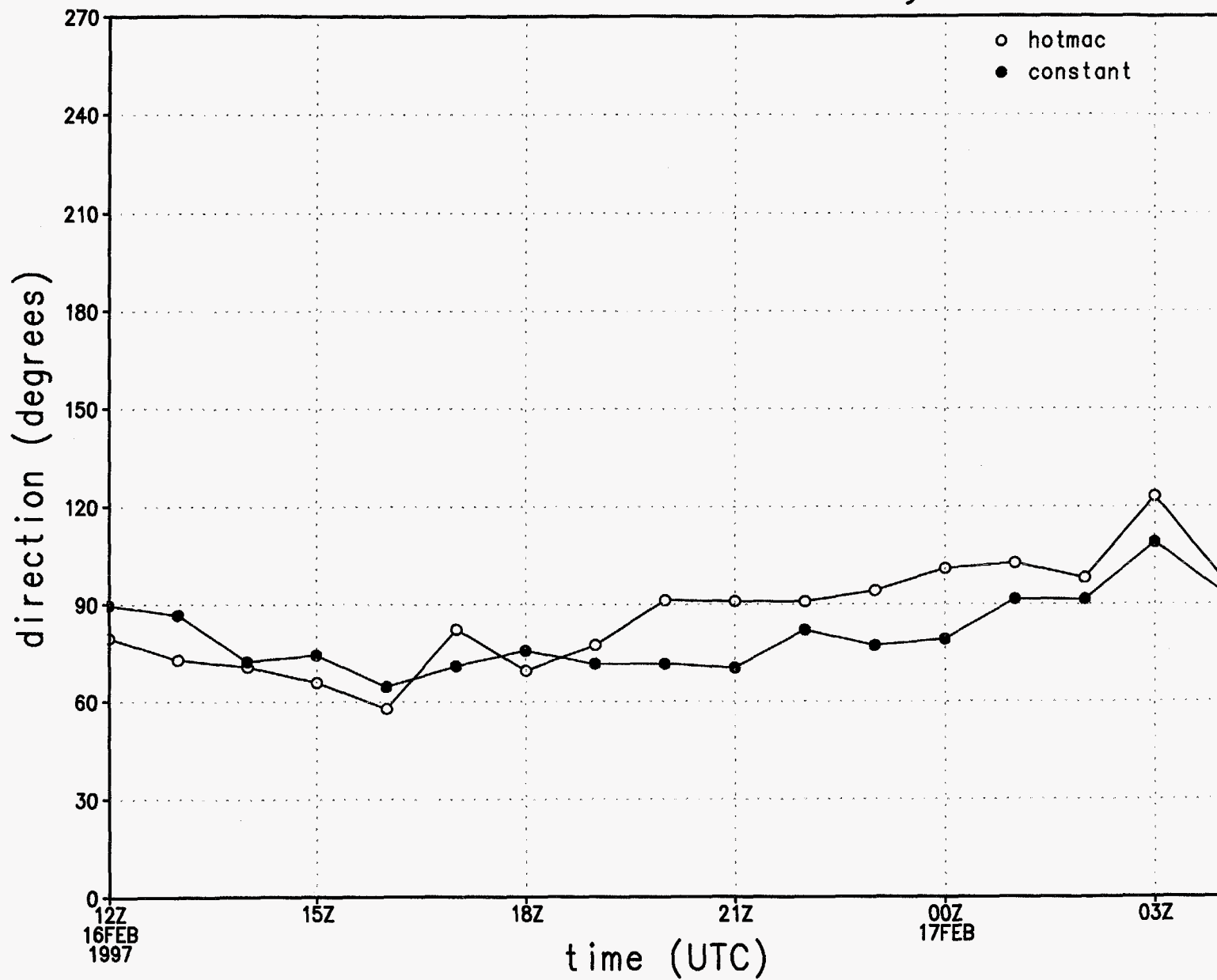


Figure 15g.

# rmse of wind speed by hour

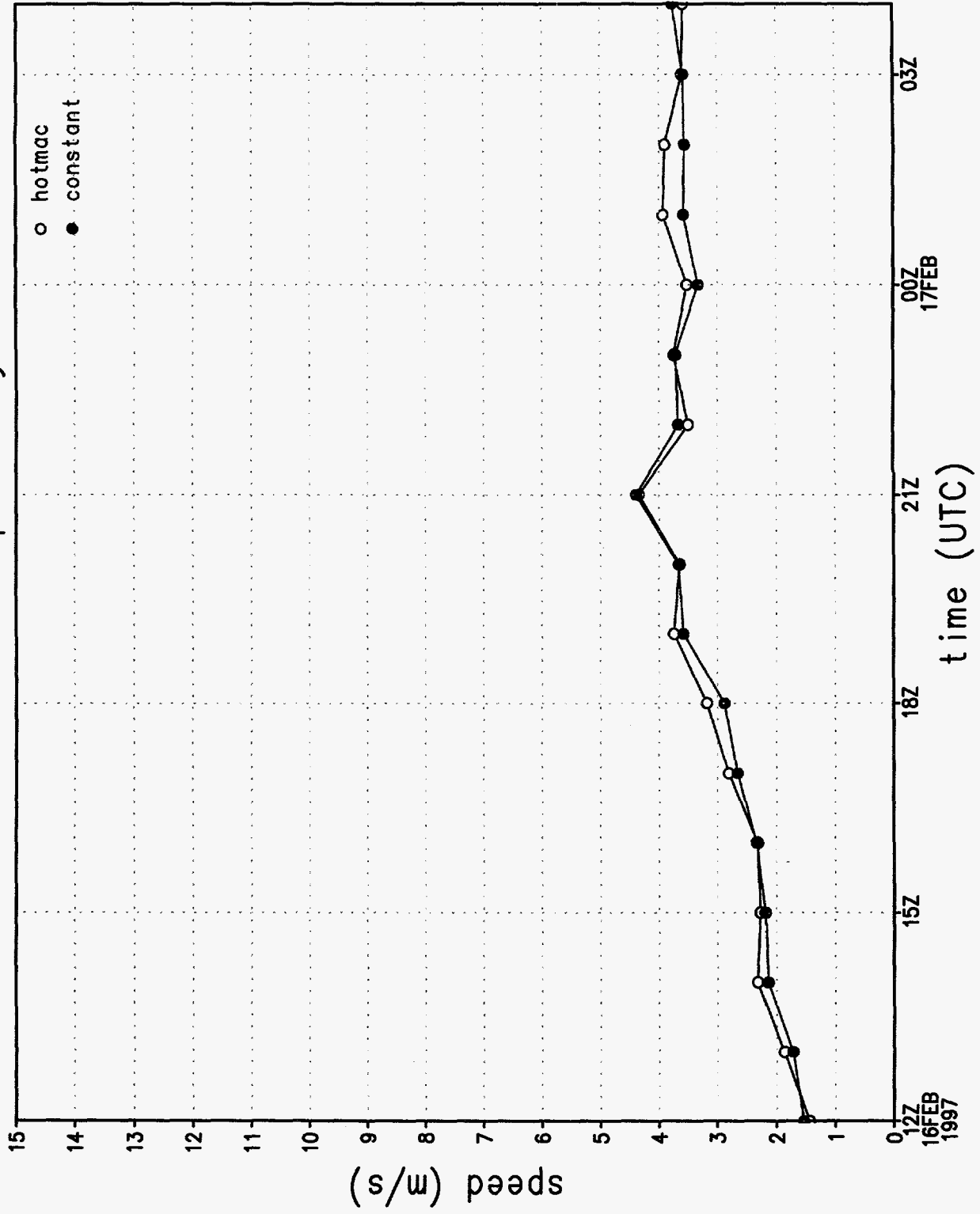


Figure 15h.

# rmse of u wind component by hour

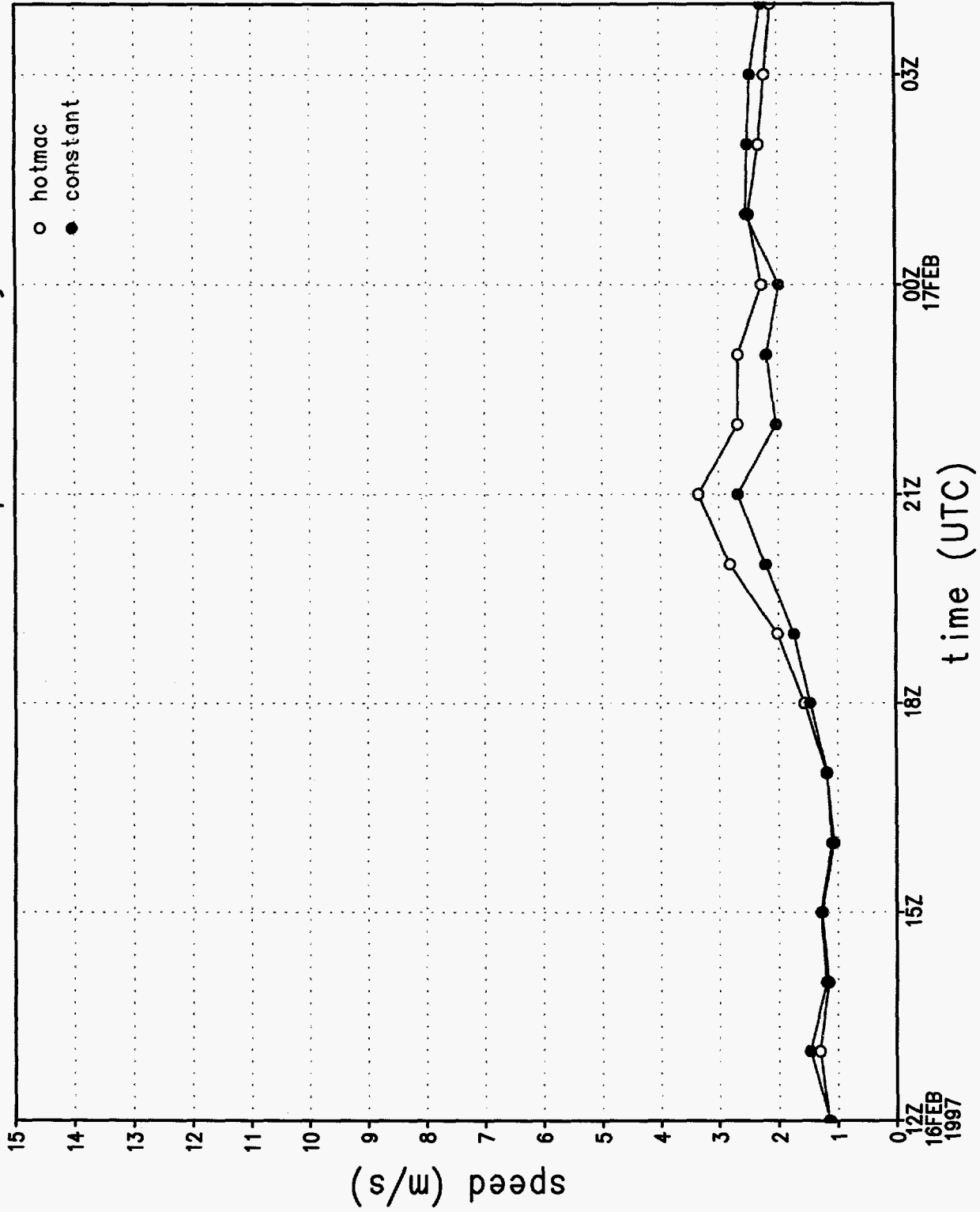


Figure 15i.

rmse of v wind component by hour

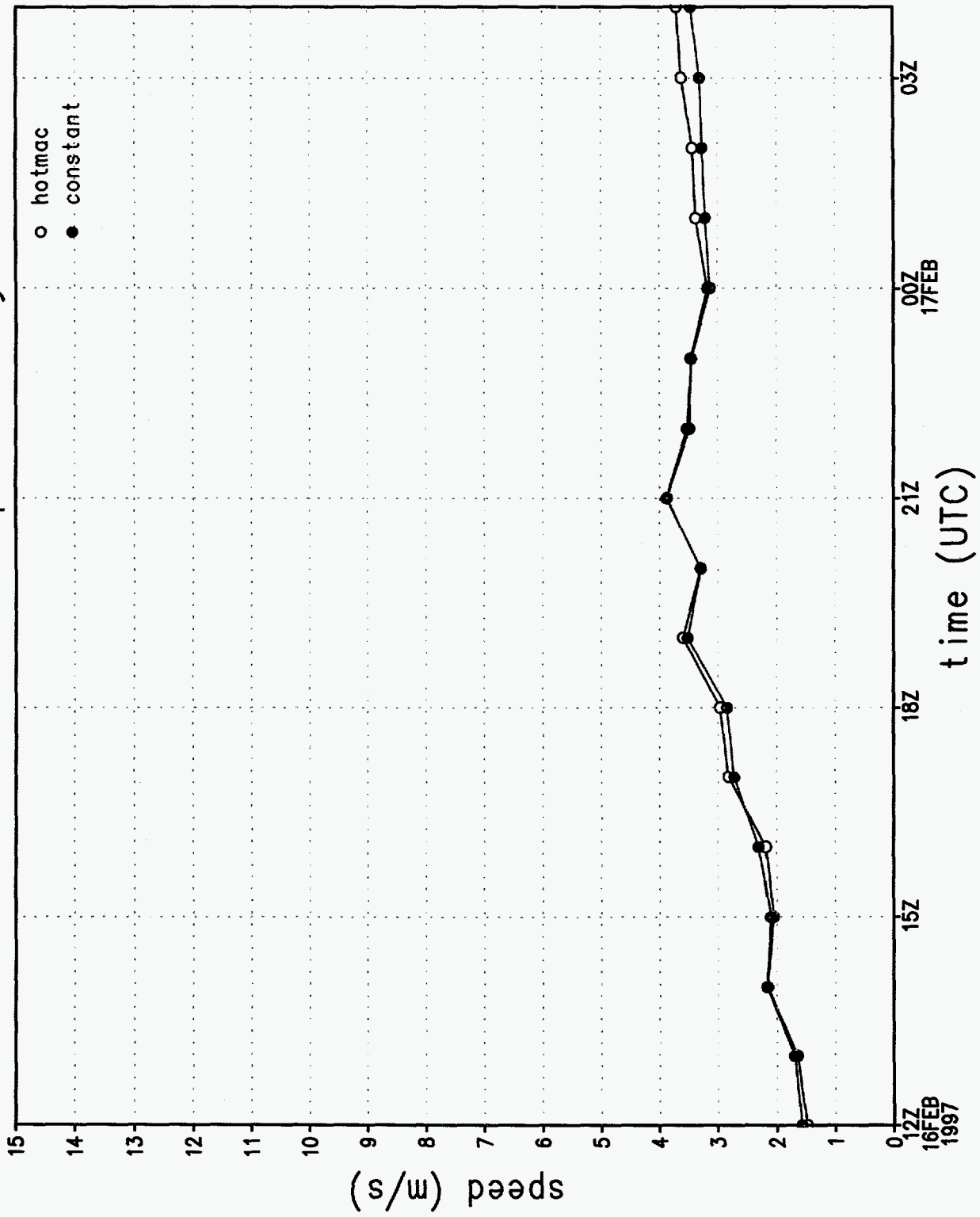


Figure 15j.

# wind direction sounding 1, 1072 m

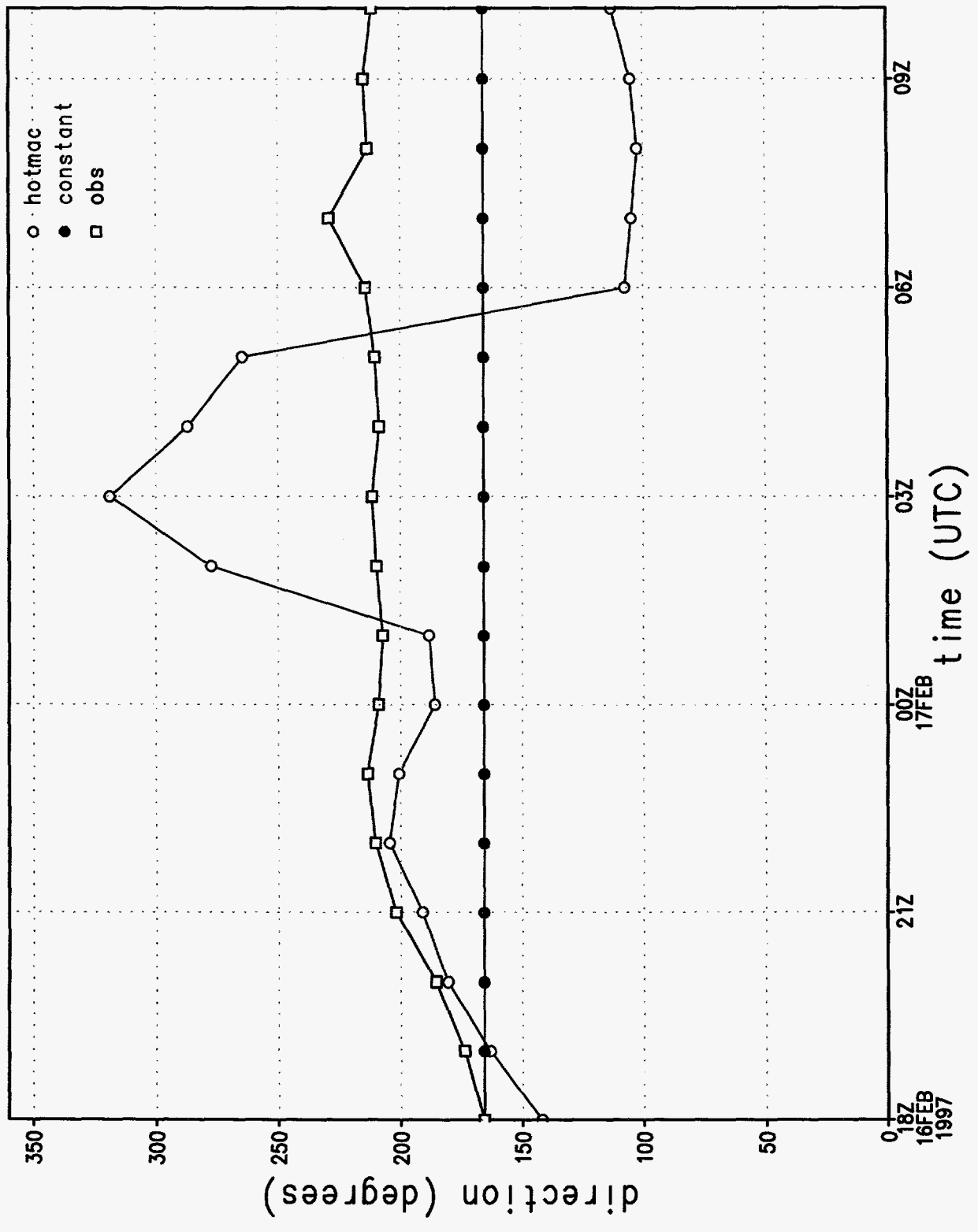


Figure 16a.

# wind speed sounding 1, 1072 m

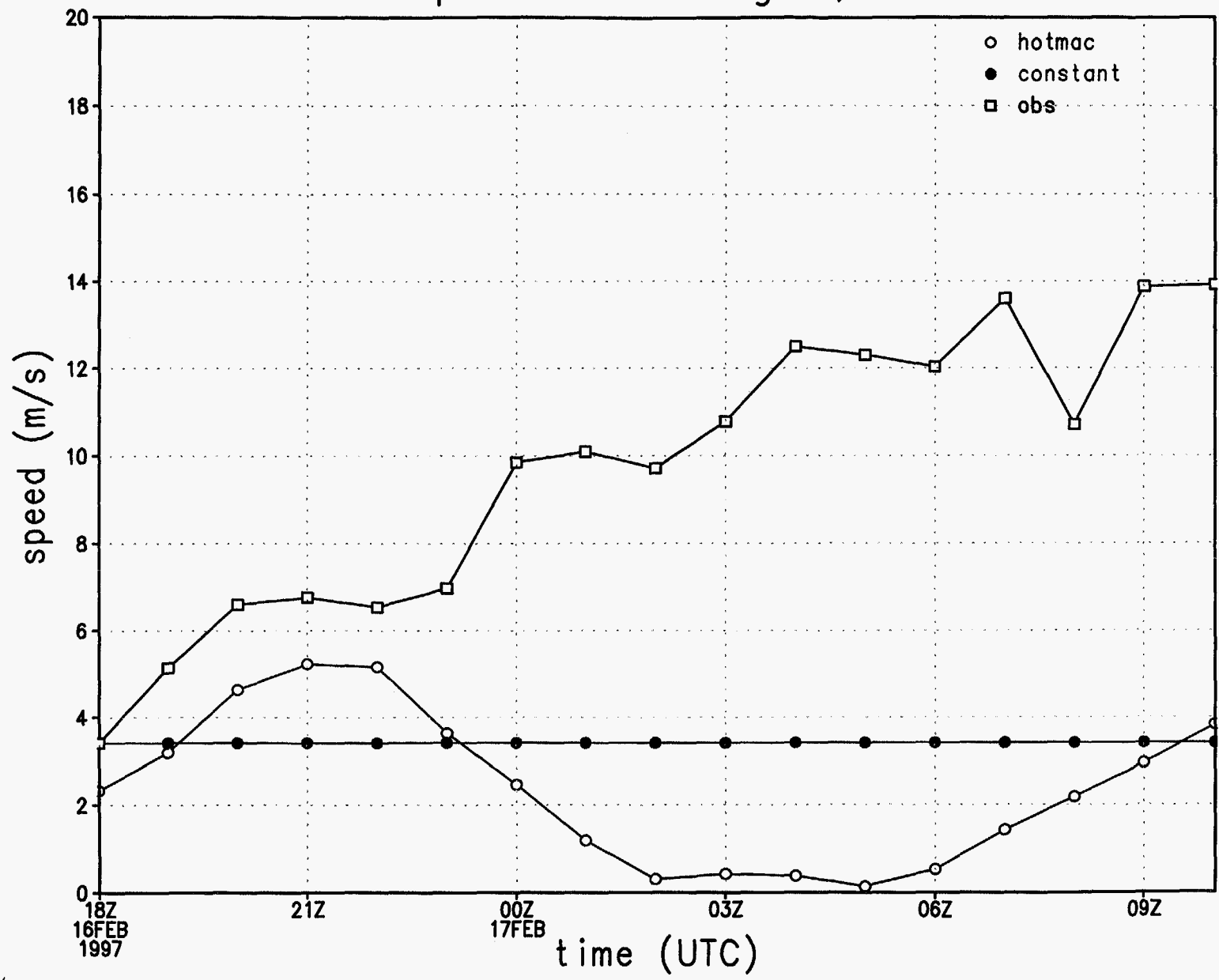


Figure 16b.

# wind direction at station 1

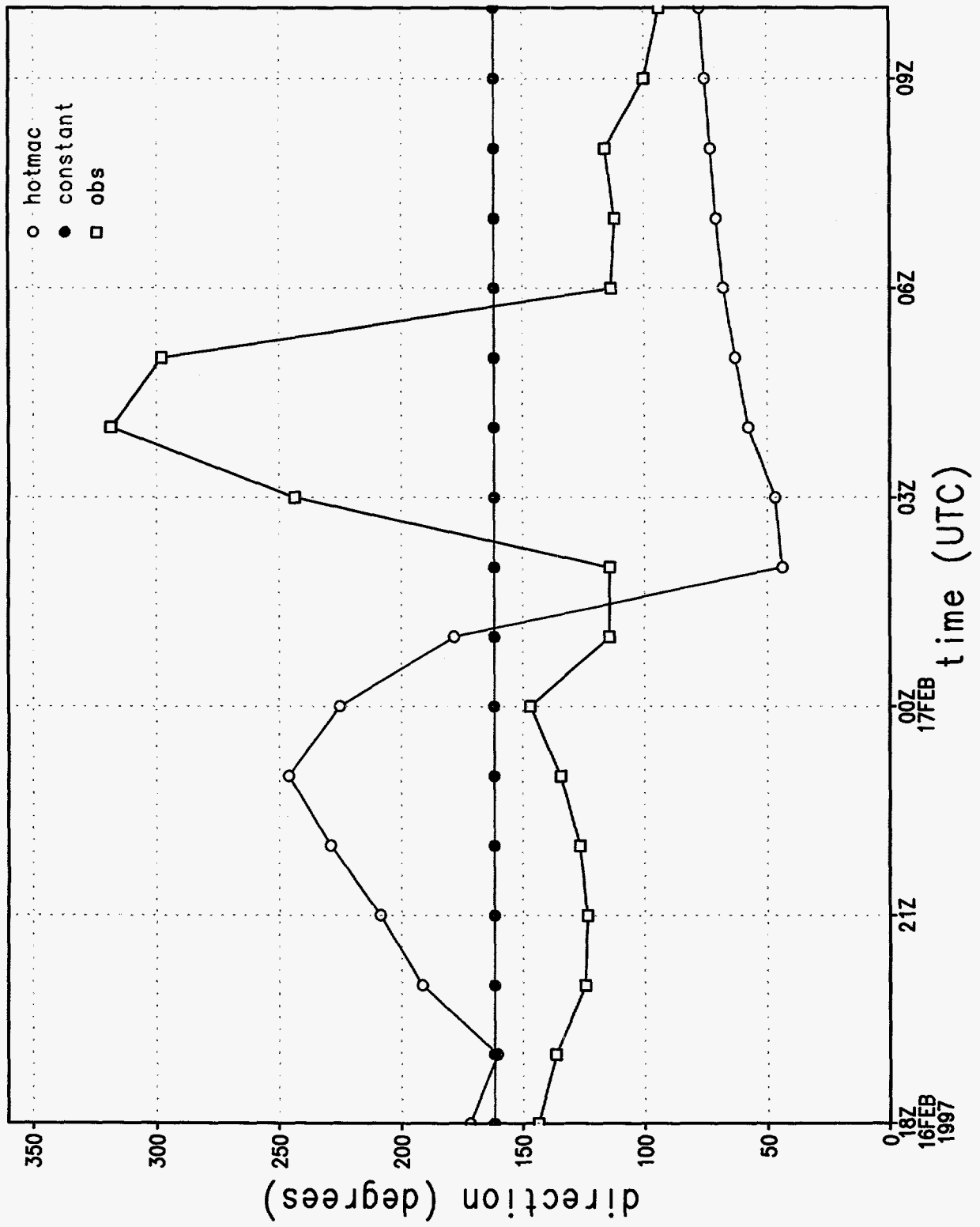


Figure 16c.

# wind speed at station 1

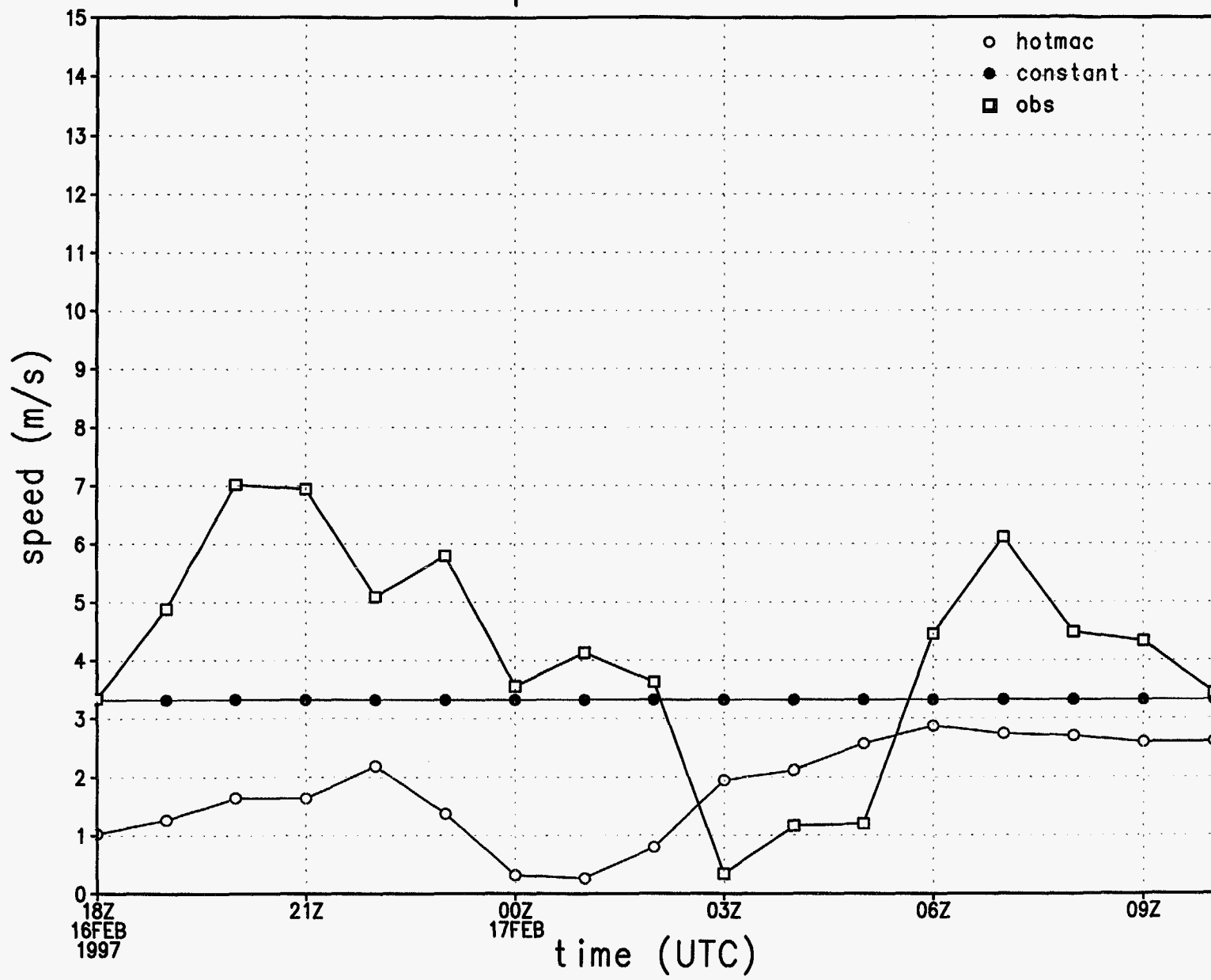


Figure 16d.



# u wind component at station 1

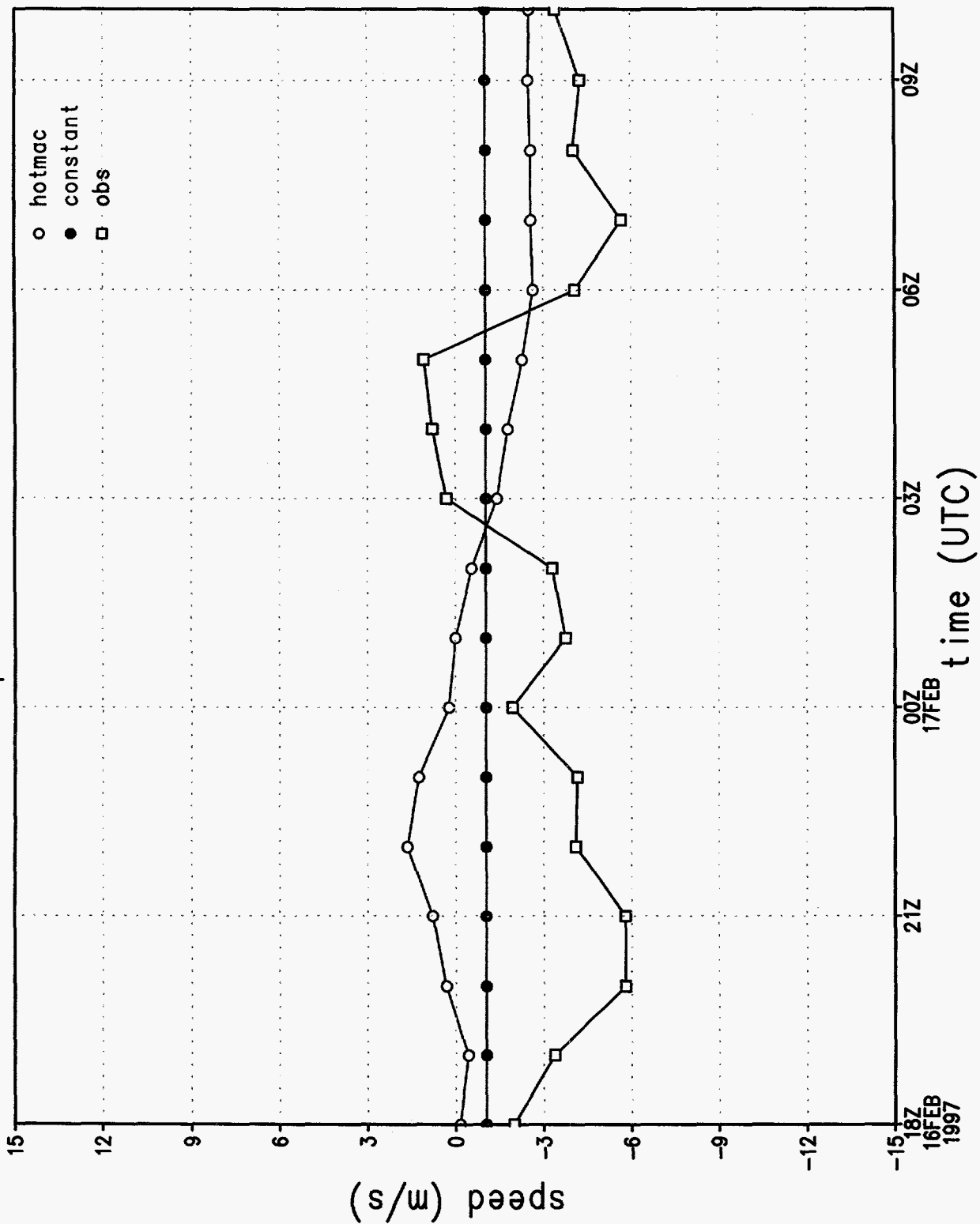


Figure 16e.

# v wind component at station 1

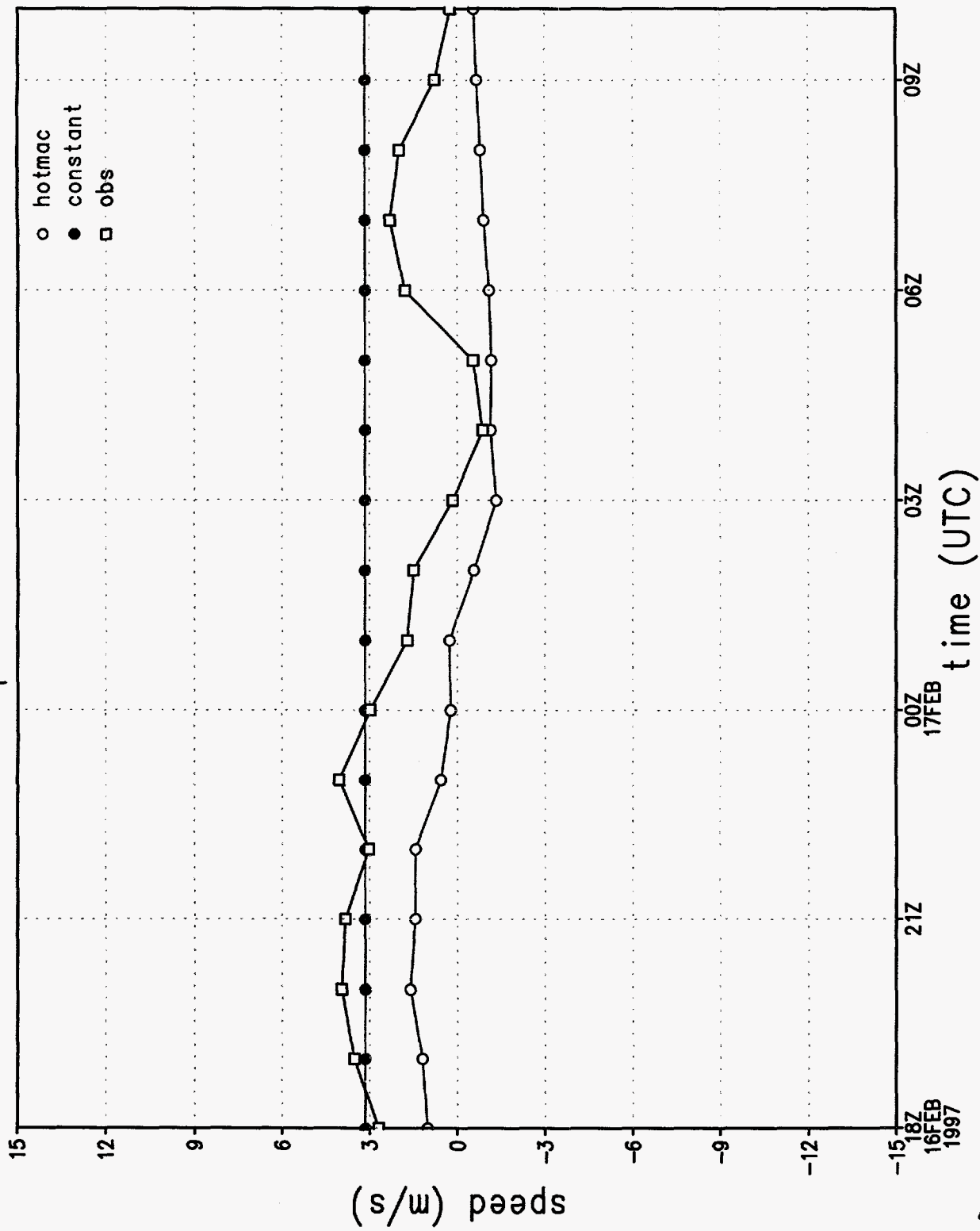


Figure 16 f.

# rmse of wind direction by hour

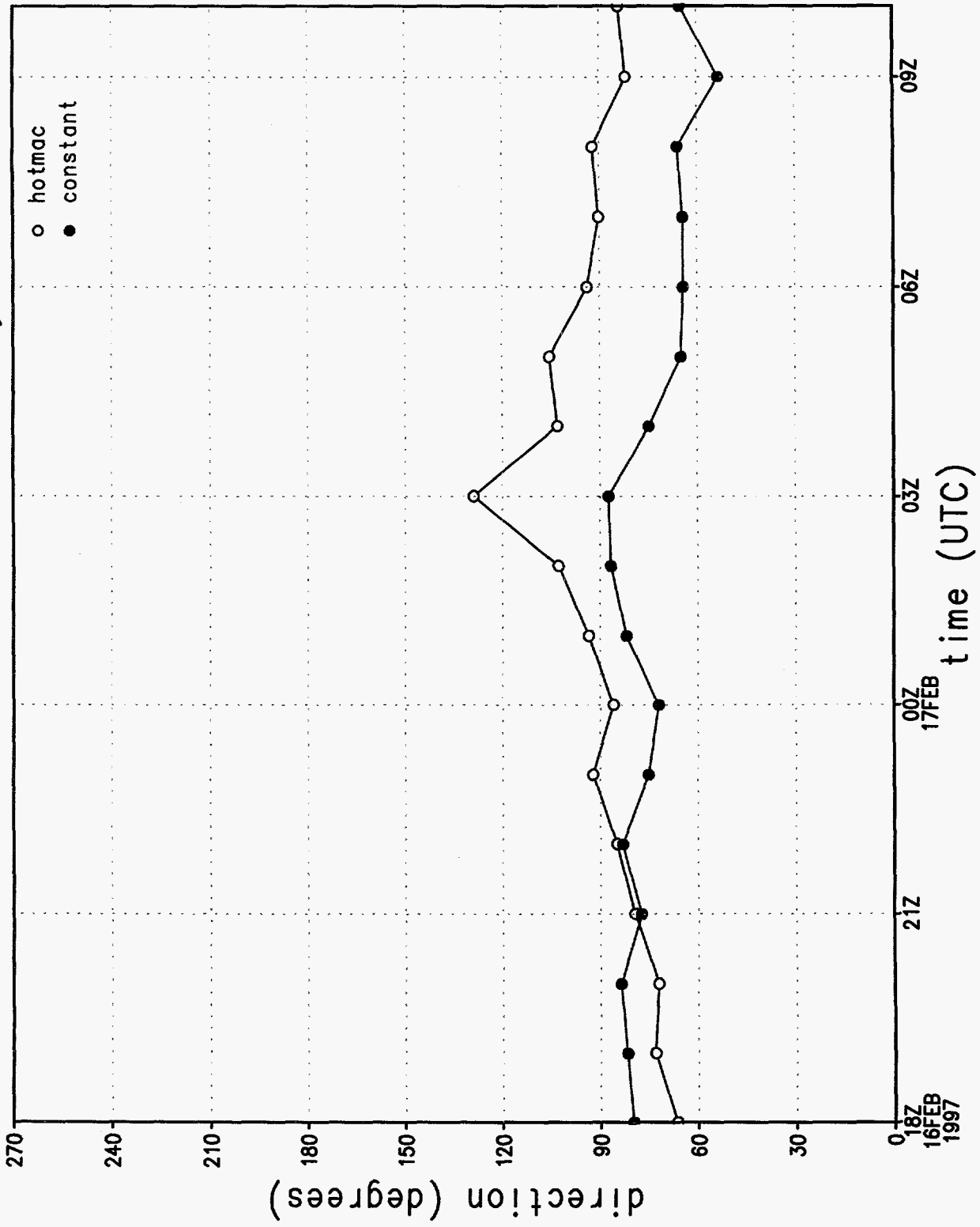


Figure 16g.

# rmse of wind speed by hour

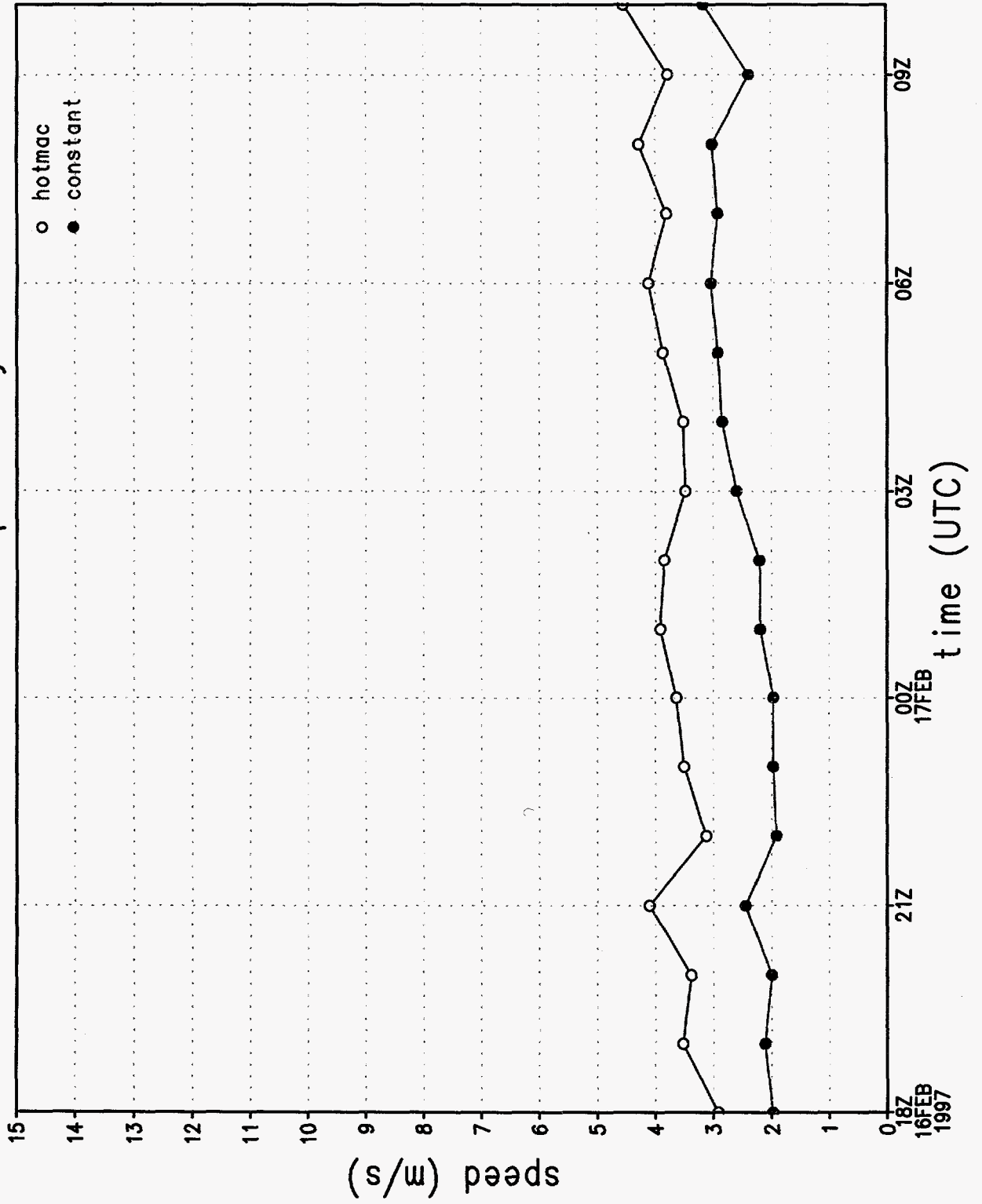


Figure 16h.

rmse of u wind component by hour

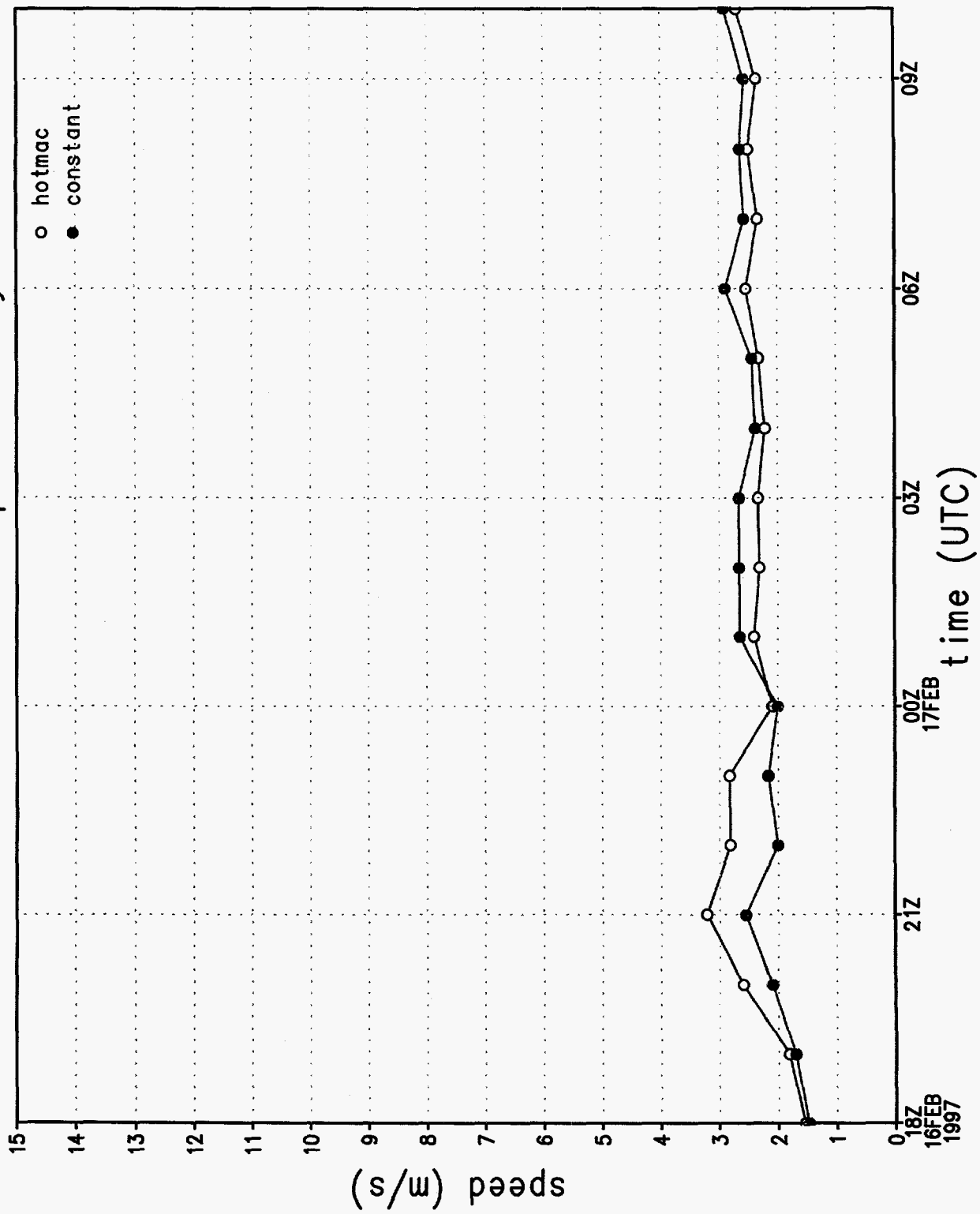


Figure 16i.

# rmse of v wind component by hour

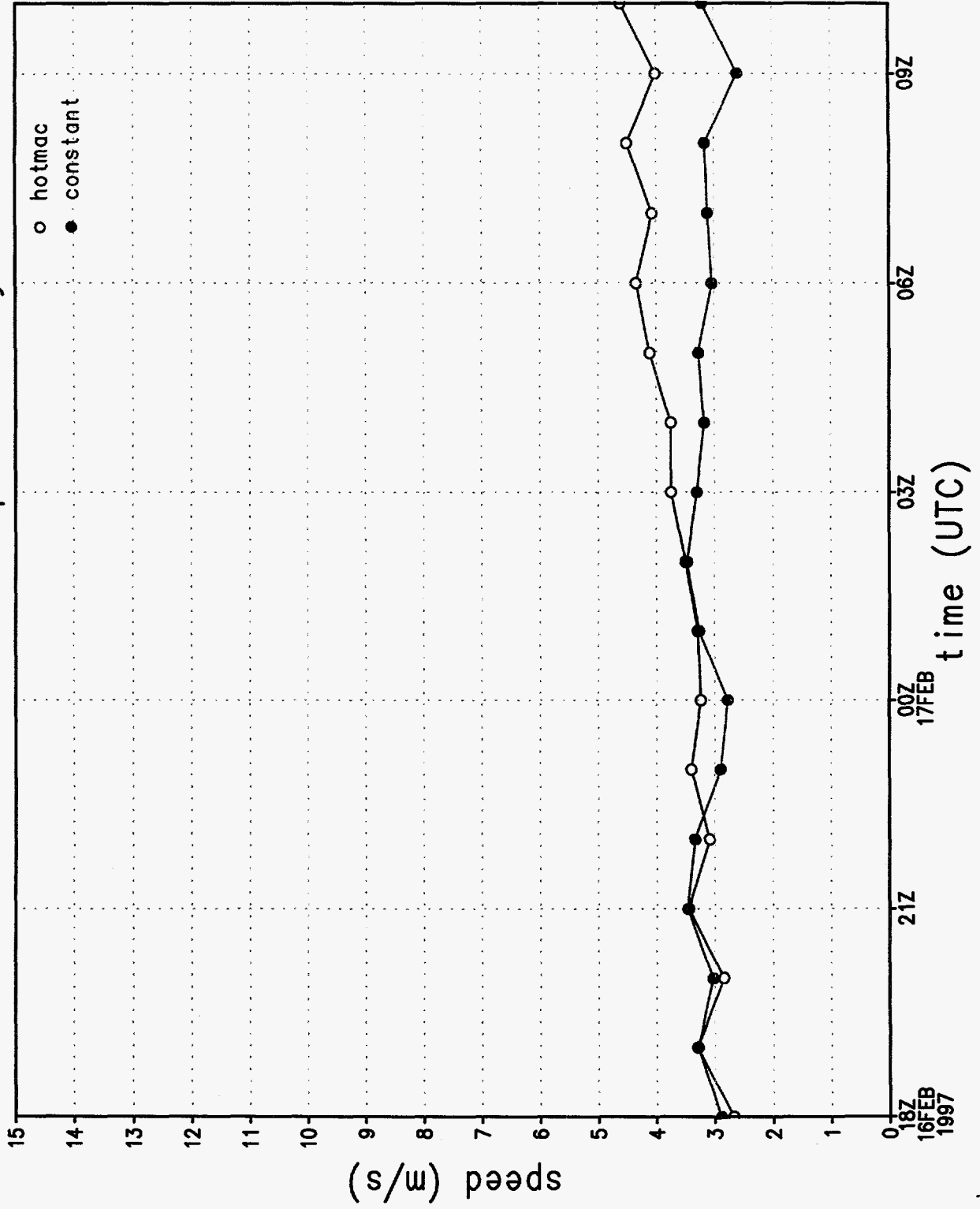


Figure 16j.

# wind direction sounding 1, 1072 m

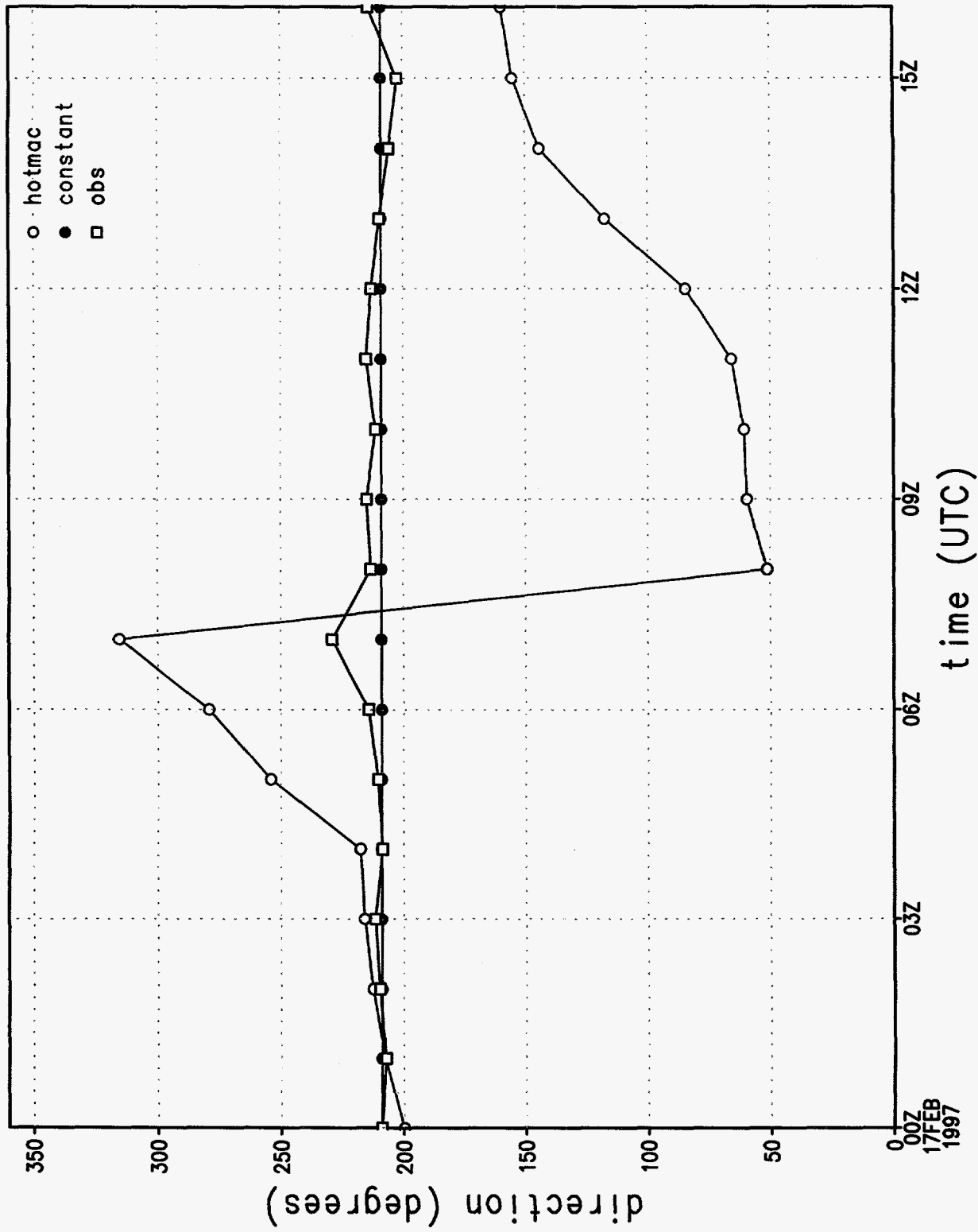


Figure 17a.

# wind speed sounding 1, 1072 m

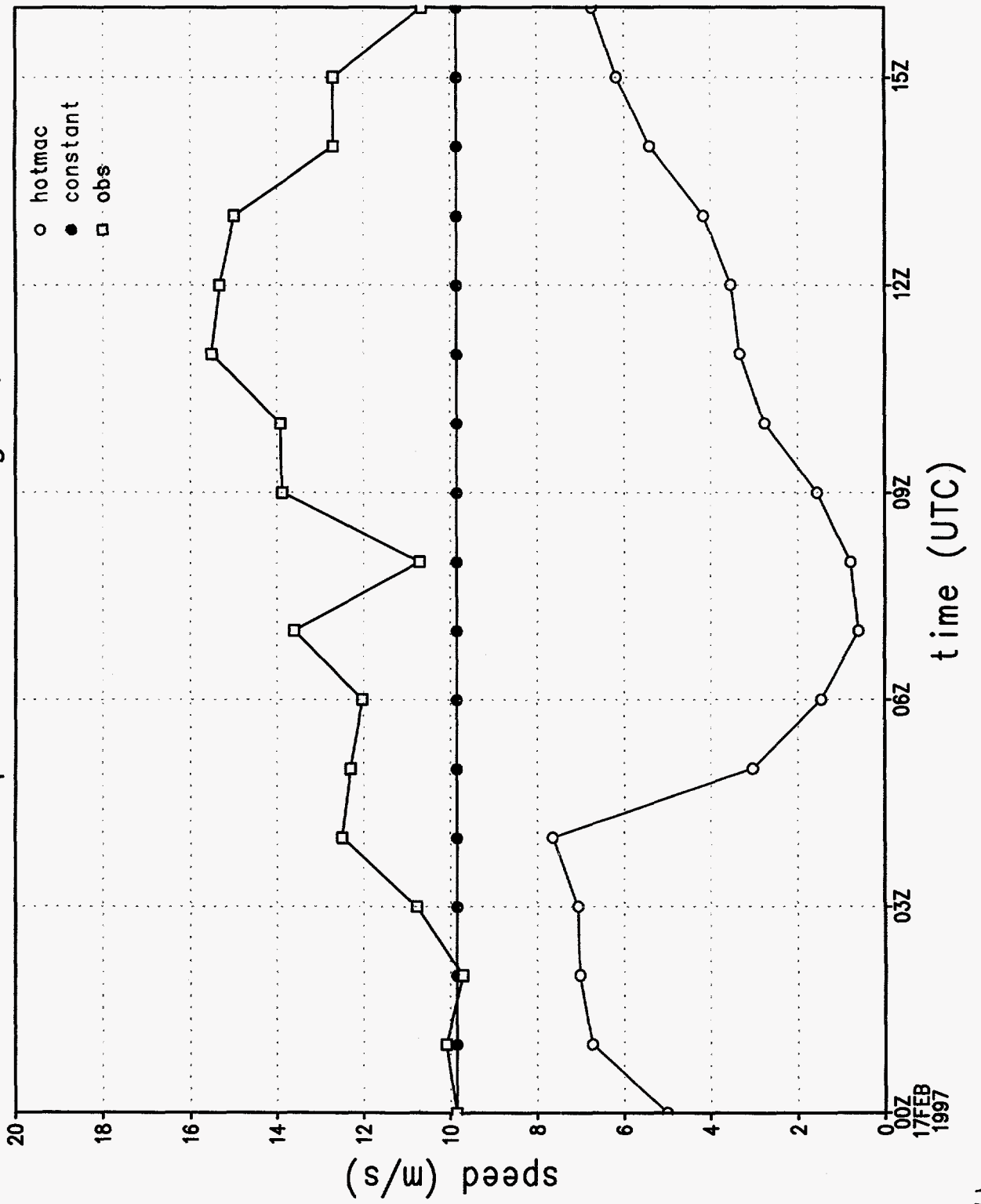


Figure 17b.



# wind direction at station 1

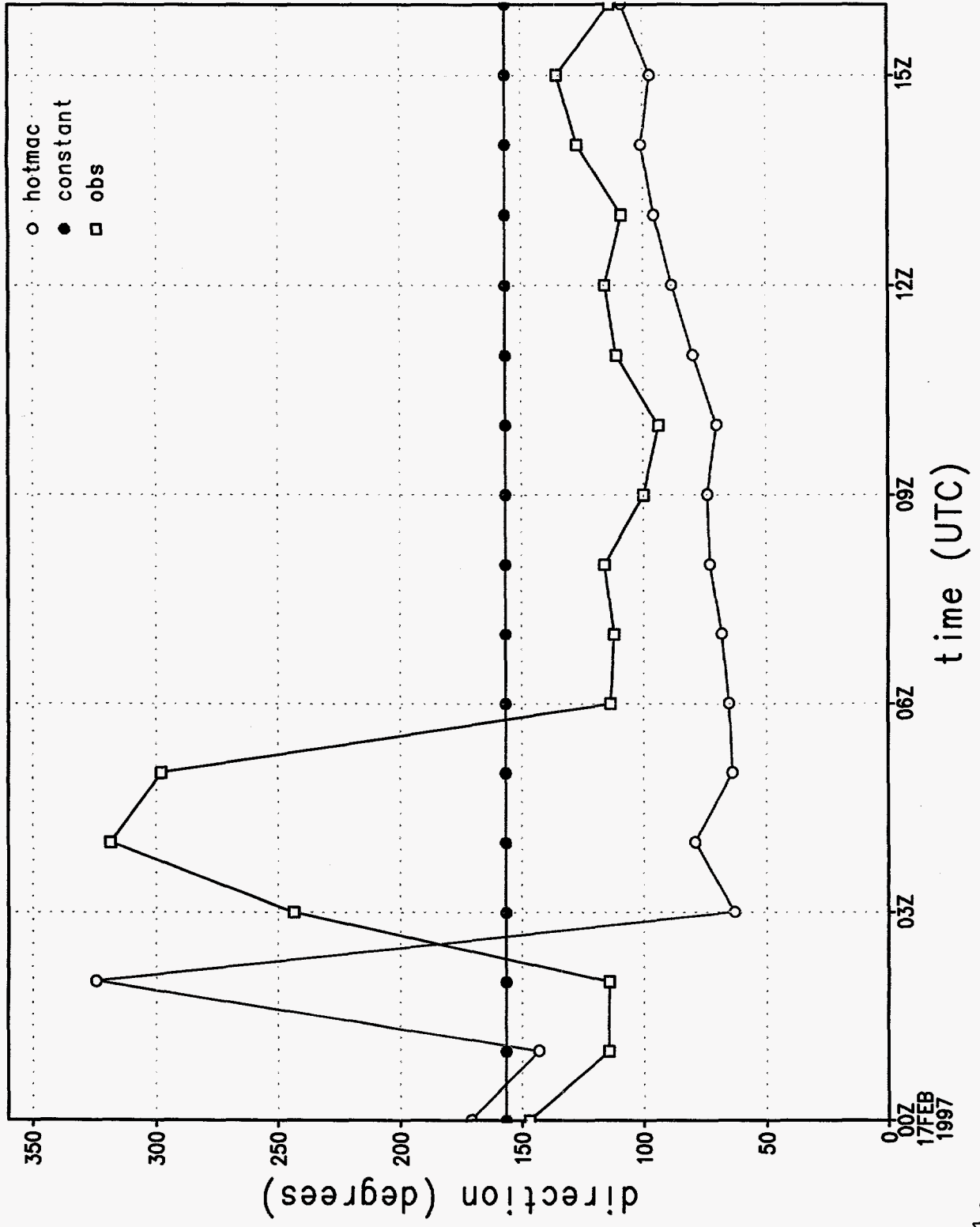


Figure 17c.

# wind speed at station 1

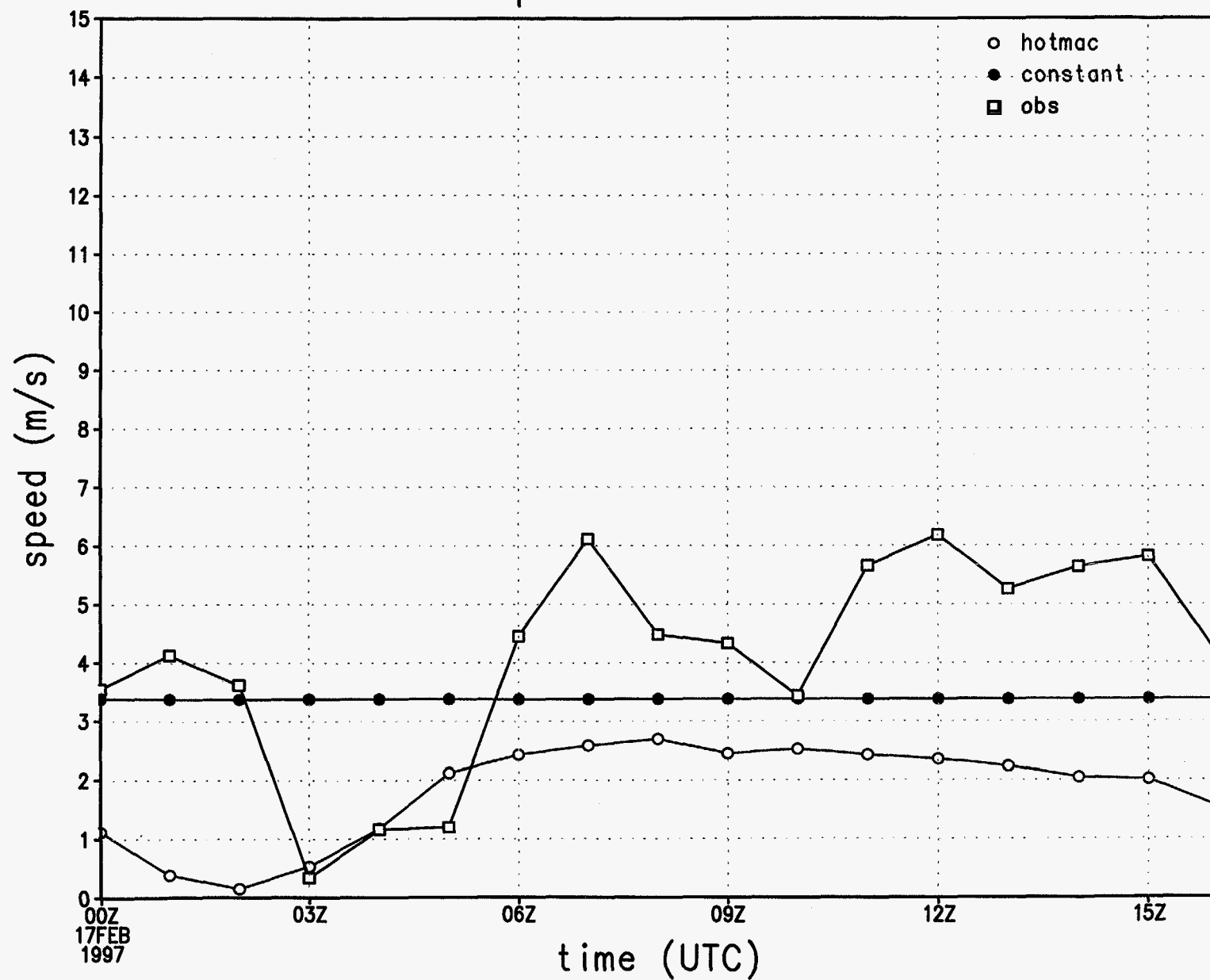


Figure 17d.

# u wind component at station 1

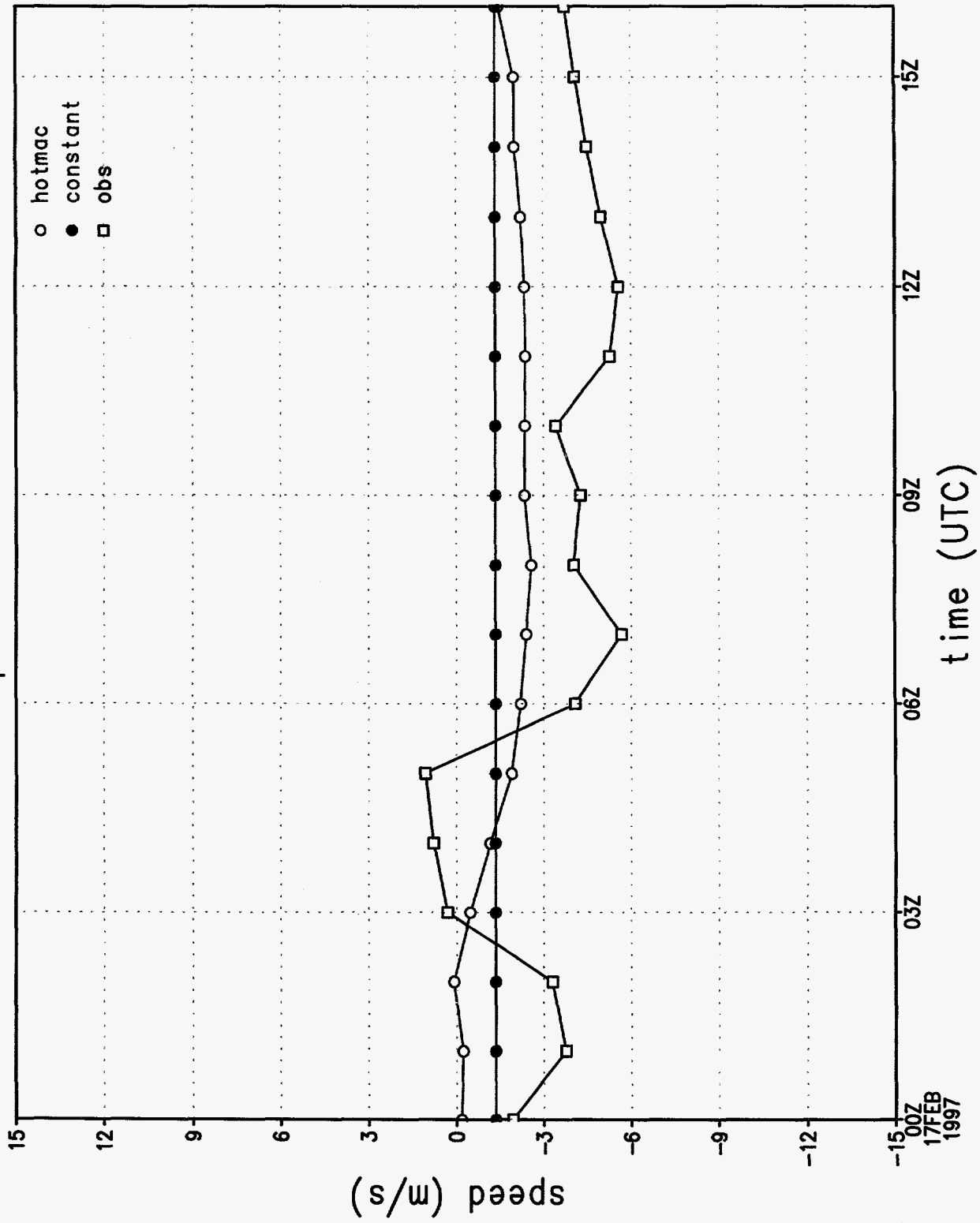


Figure 17e.

v wind component at station 1

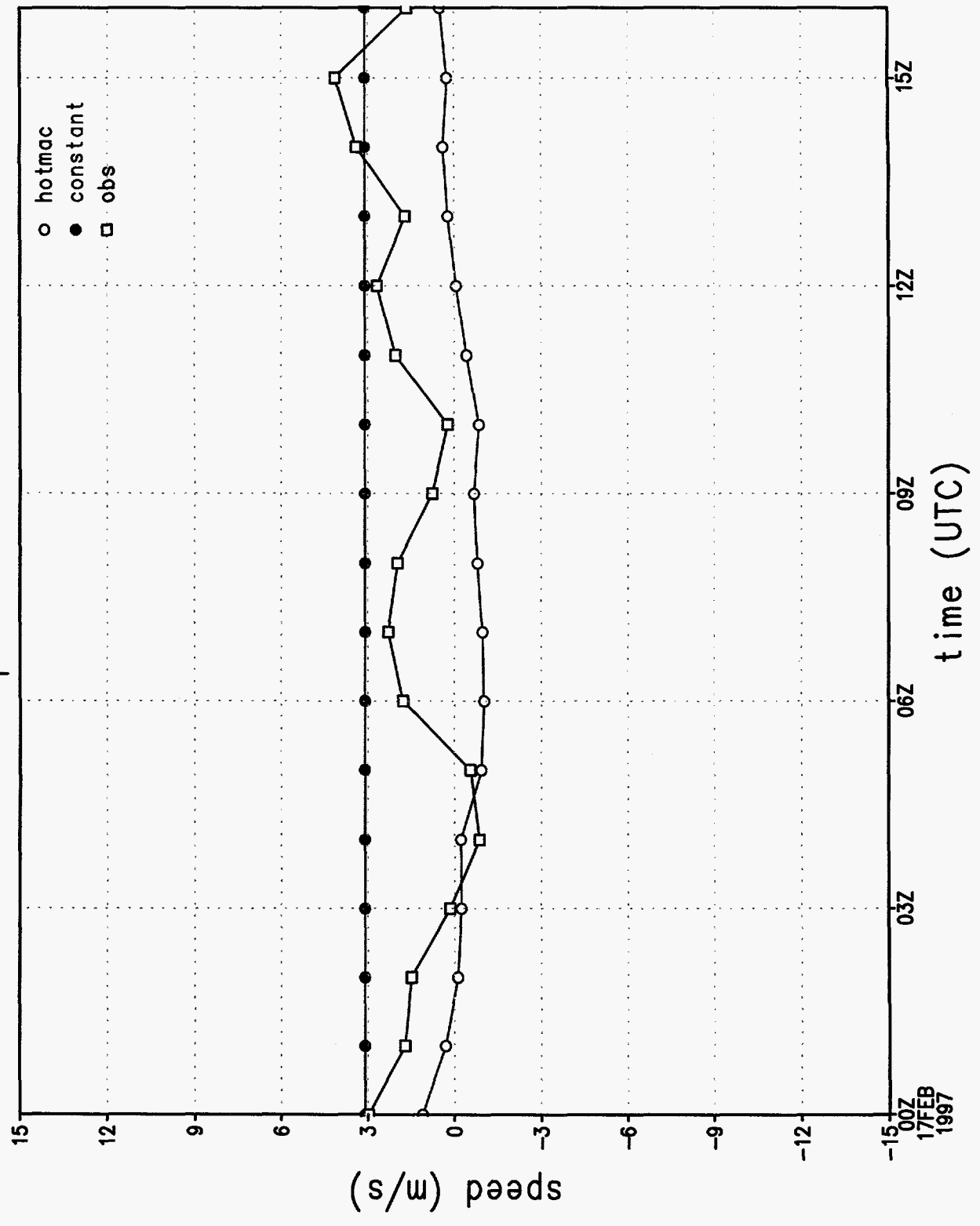


Figure 17f.

rmse of wind direction by hour

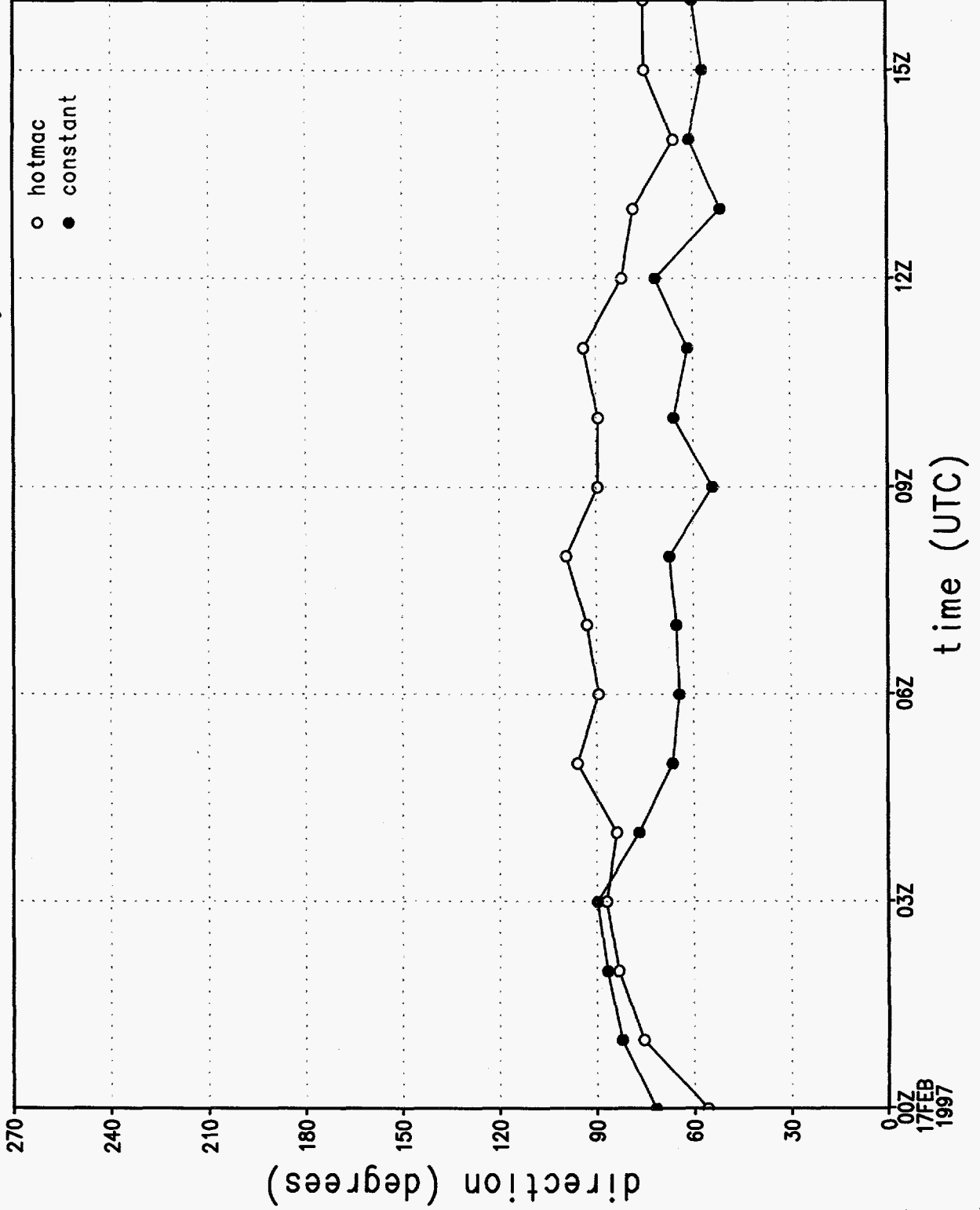


Figure 17g.

# rmse of wind speed by hour

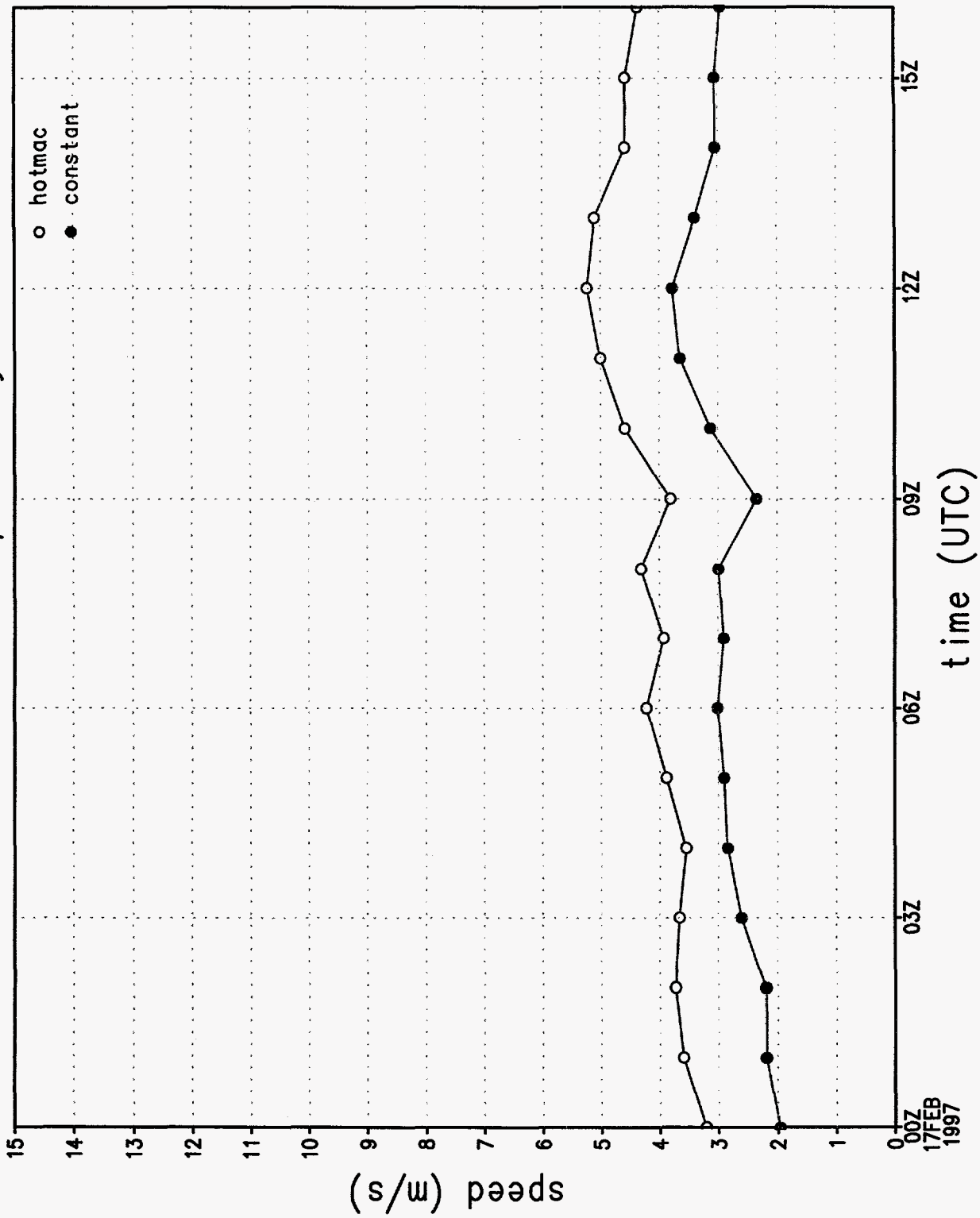


Figure 17h.

rmse of u wind component by hour

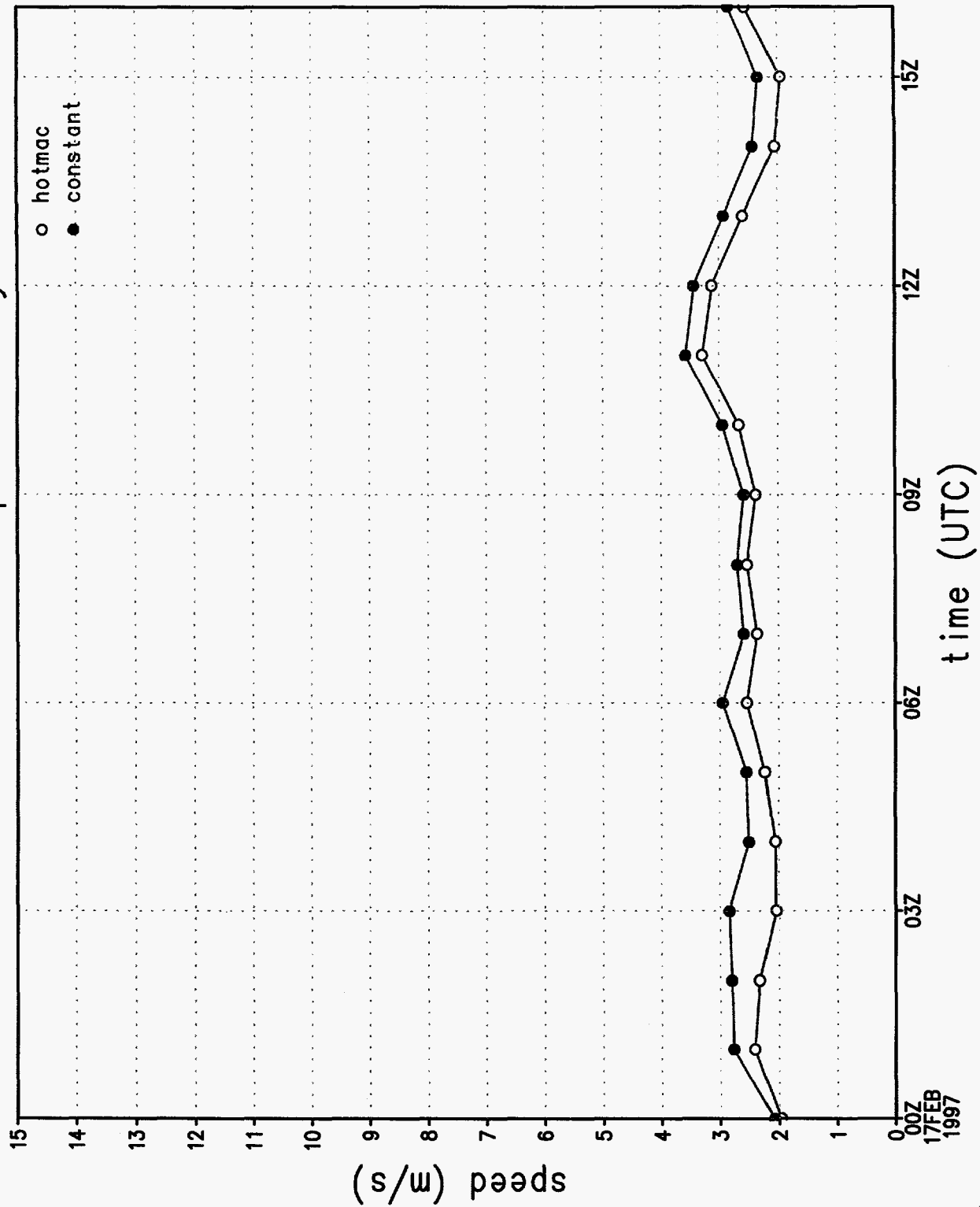


Figure 17i.

# rmse of v wind component by hour

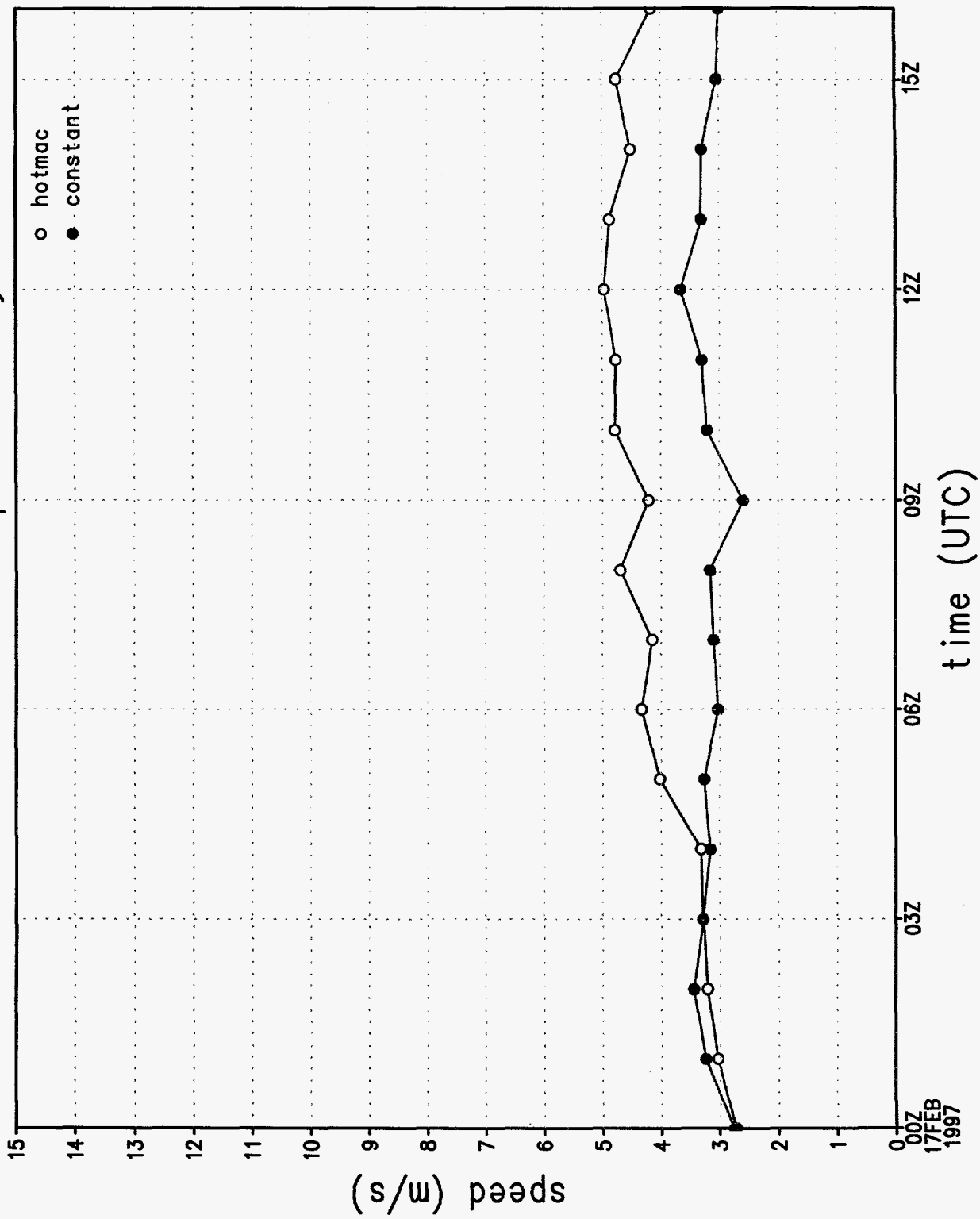


Figure 17j.



# wind direction sounding 1, 1072 m

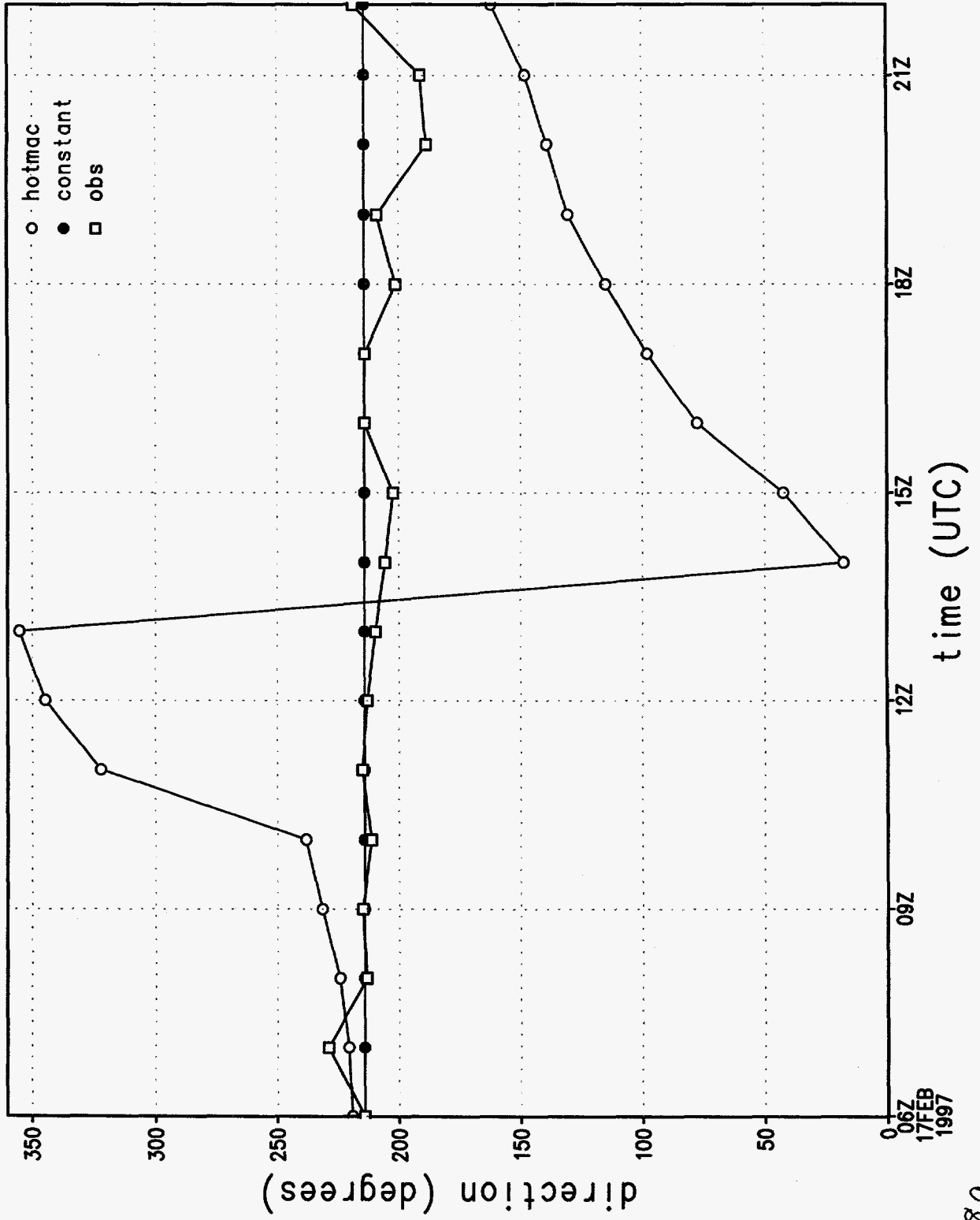


Figure 18a.

# wind speed sounding 1, 1072 m

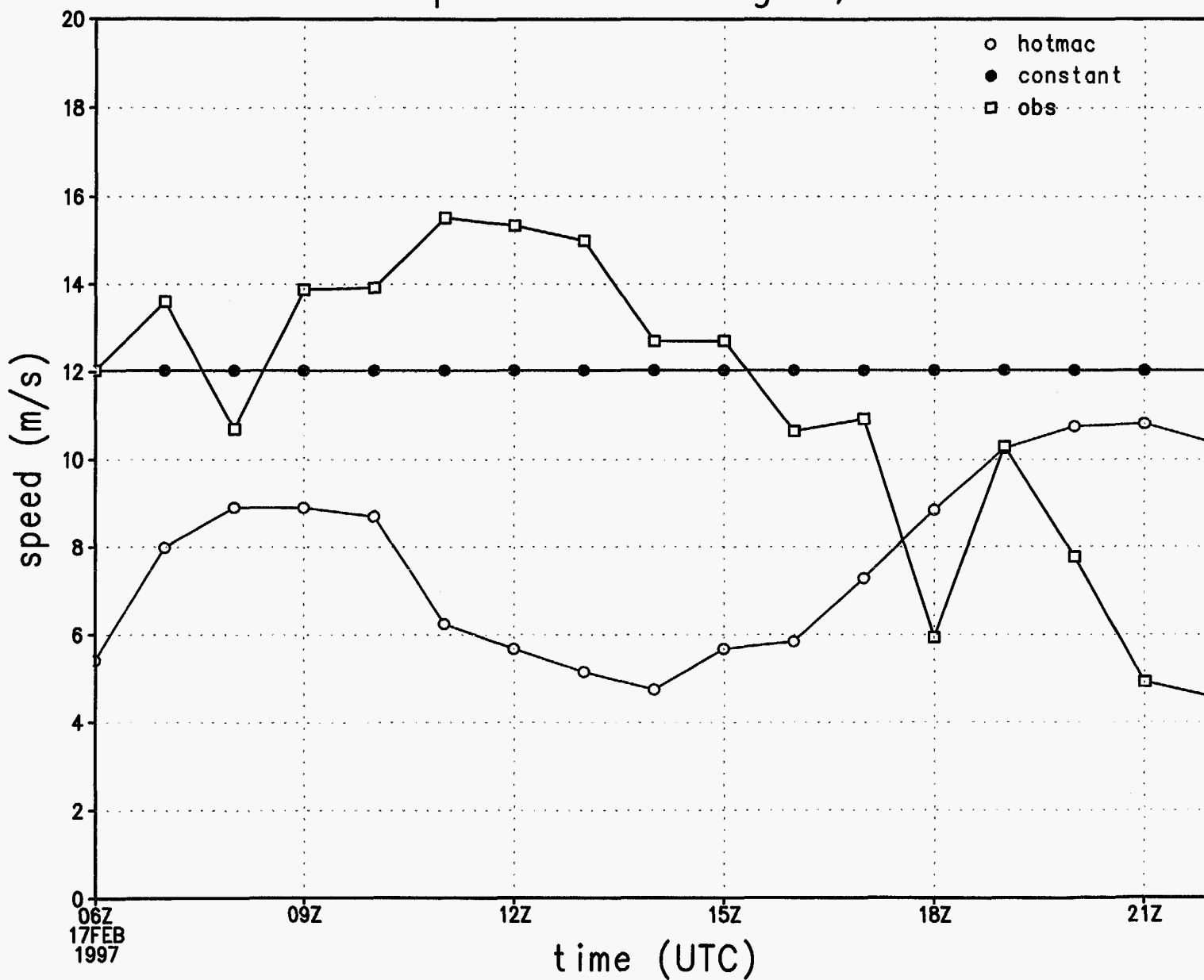


Figure 18b.

# wind direction at station 1

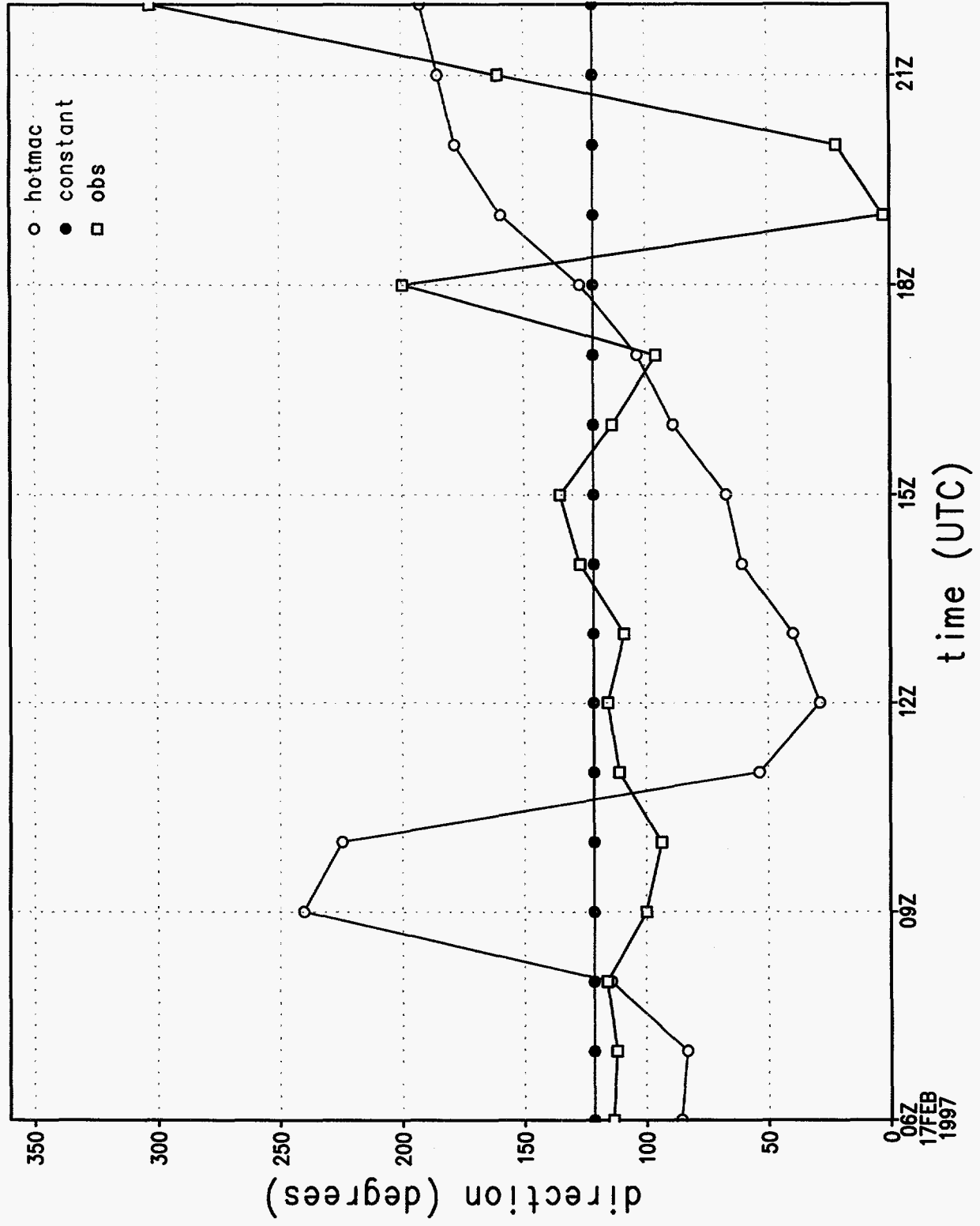


Figure 18c.

wind speed at station 1

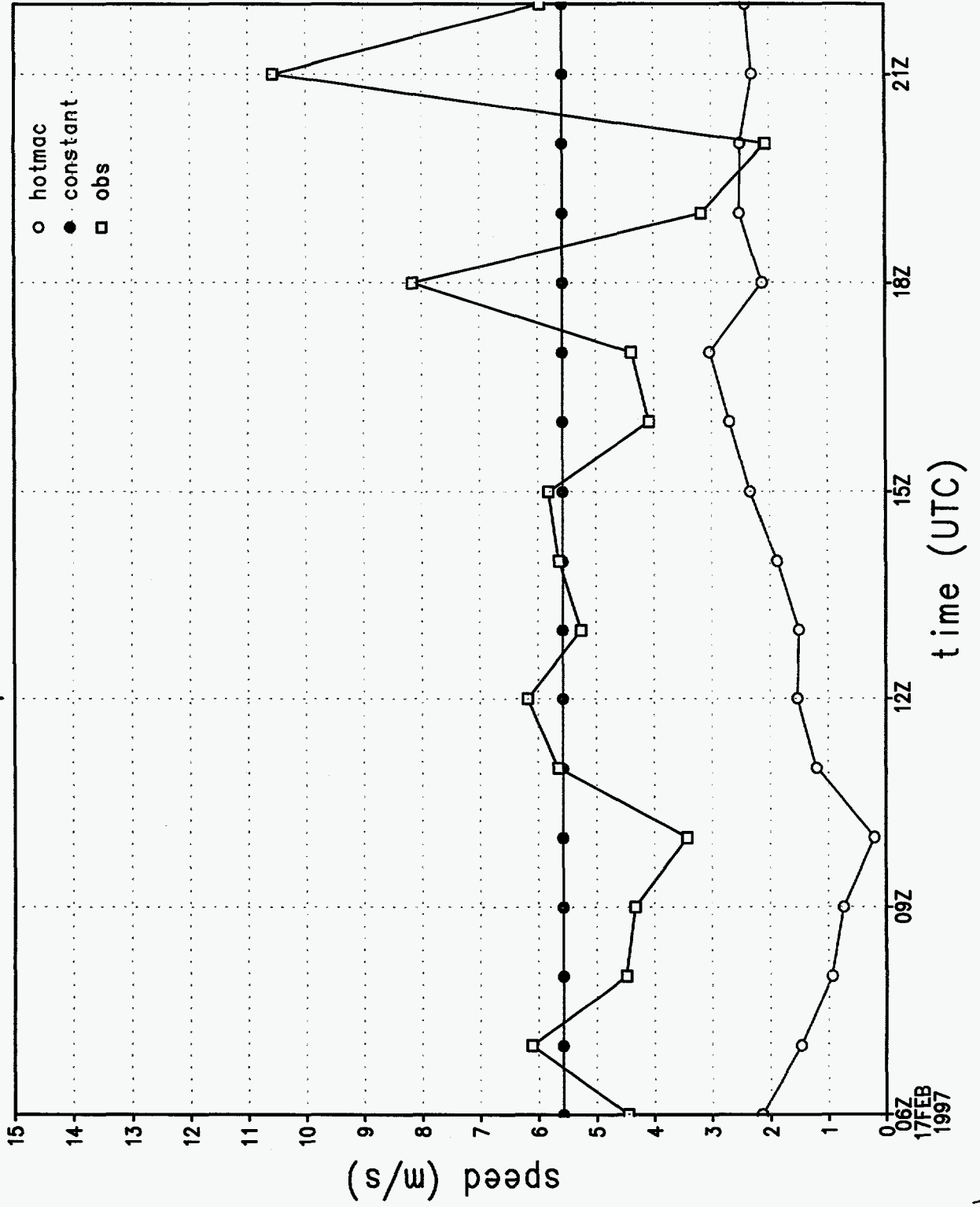


Figure 18d.

v wind component at station 1

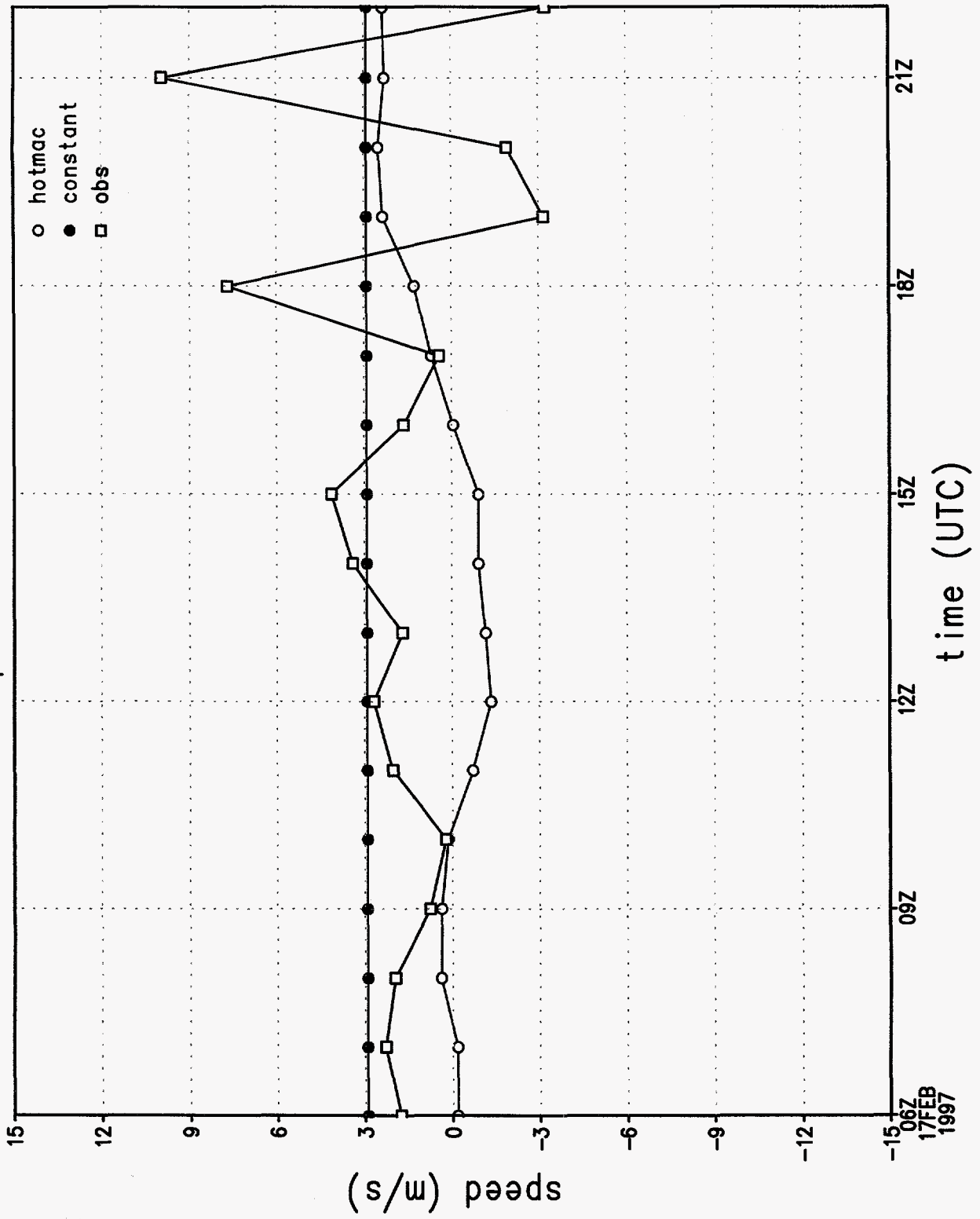


Figure 18e.

u wind component at station 1

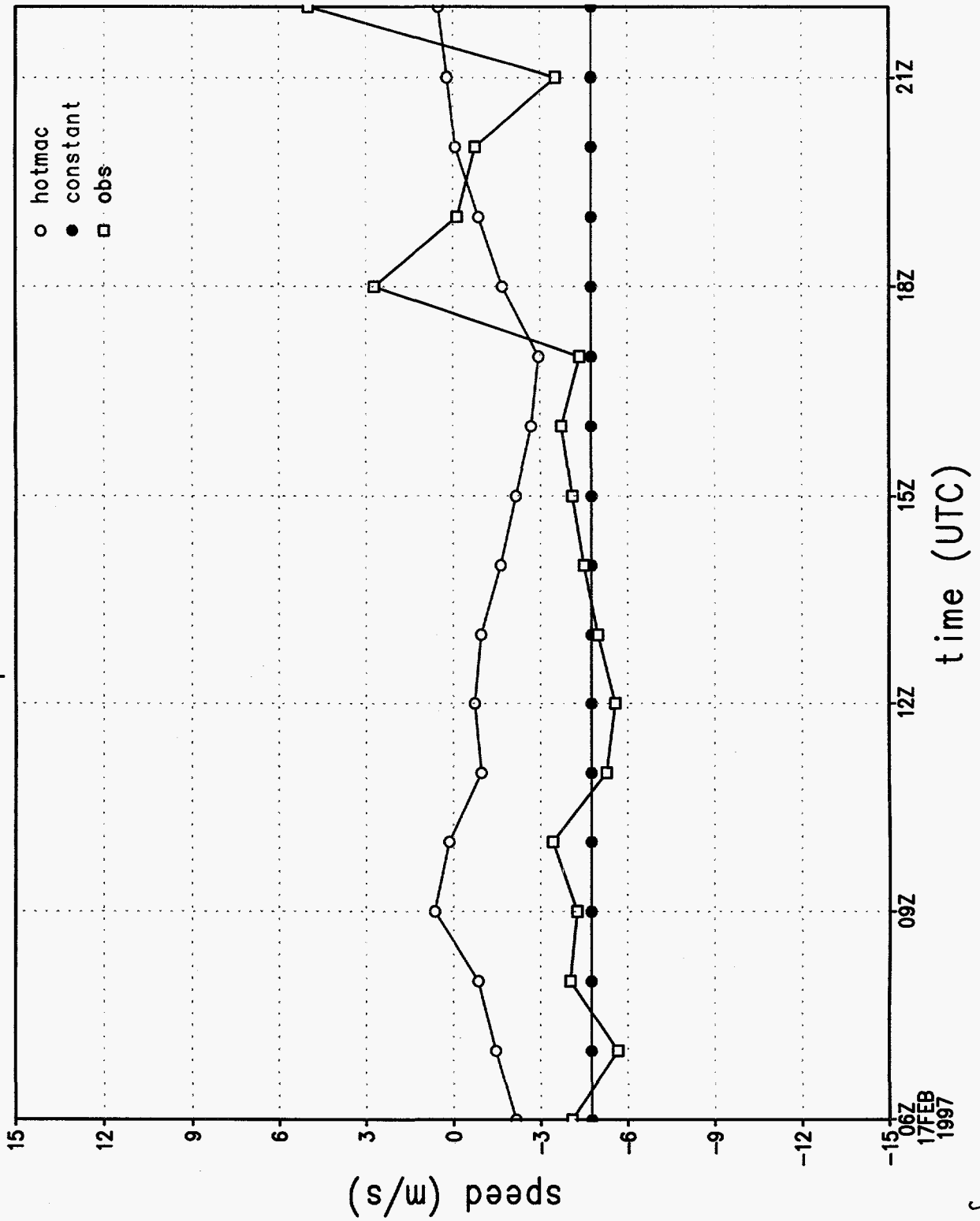


Figure 18f.

# rmse of wind direction by hour

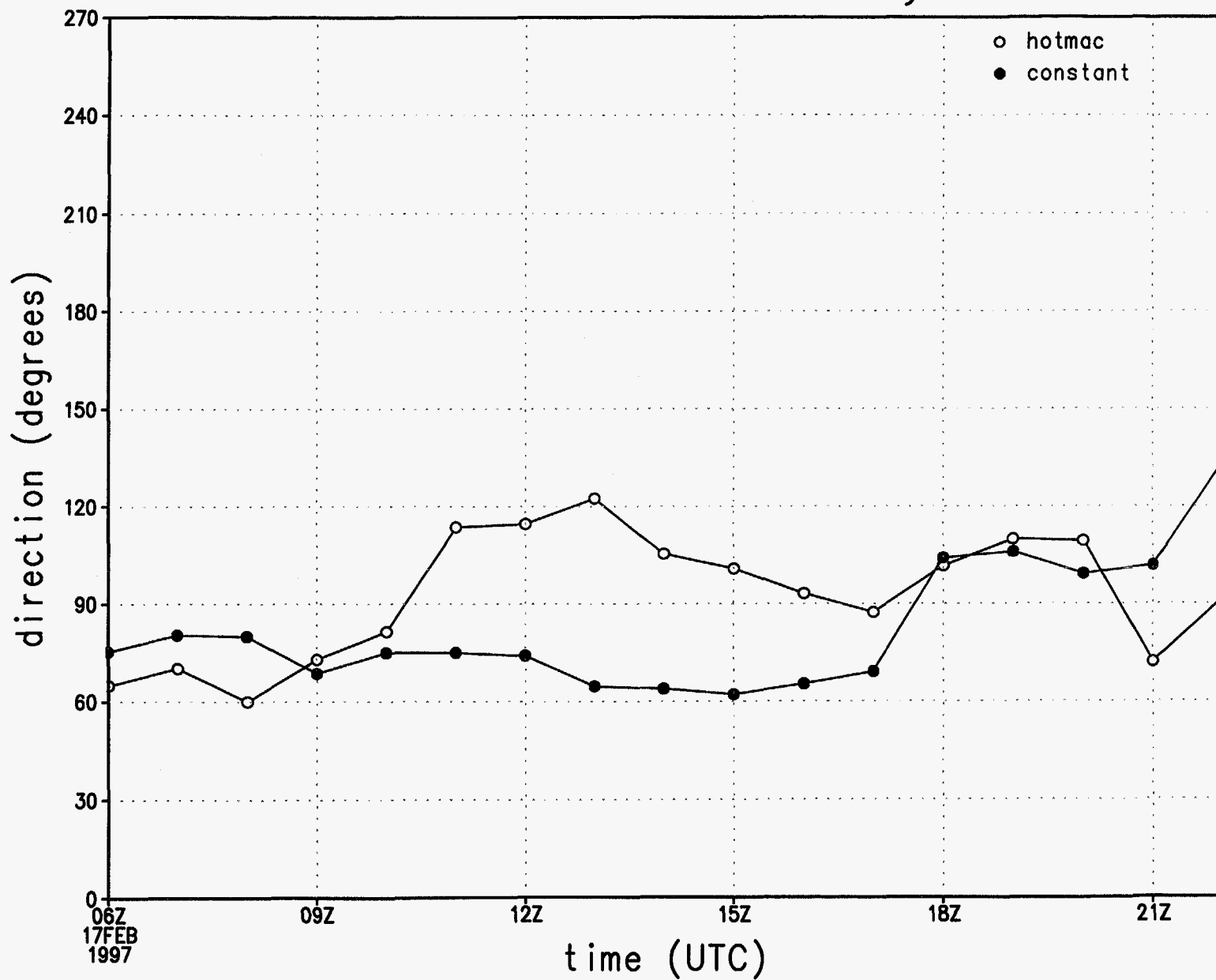


Figure 18g.

# rmse of wind speed by hour

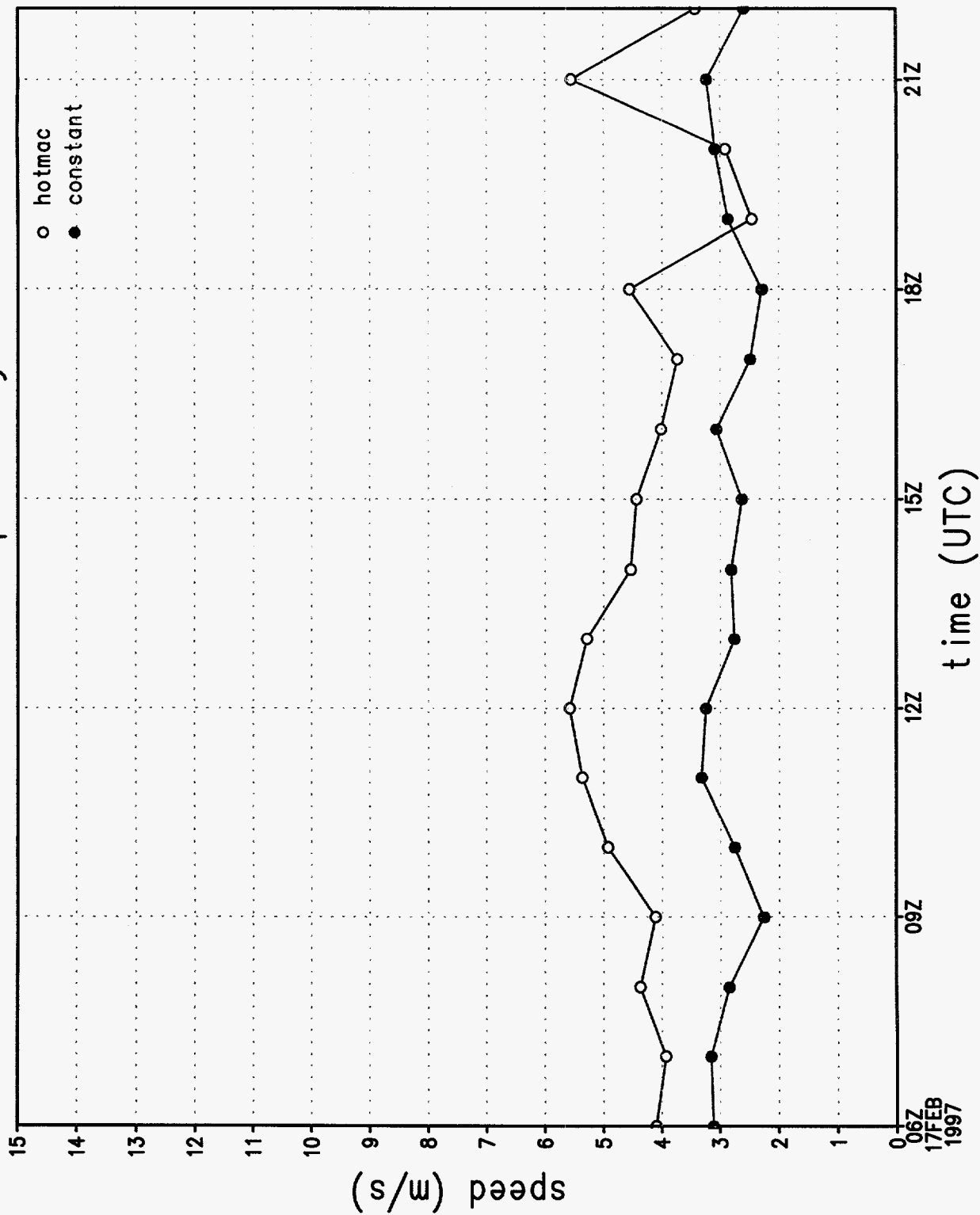


Figure 18h.



# rmse of u wind component by hour

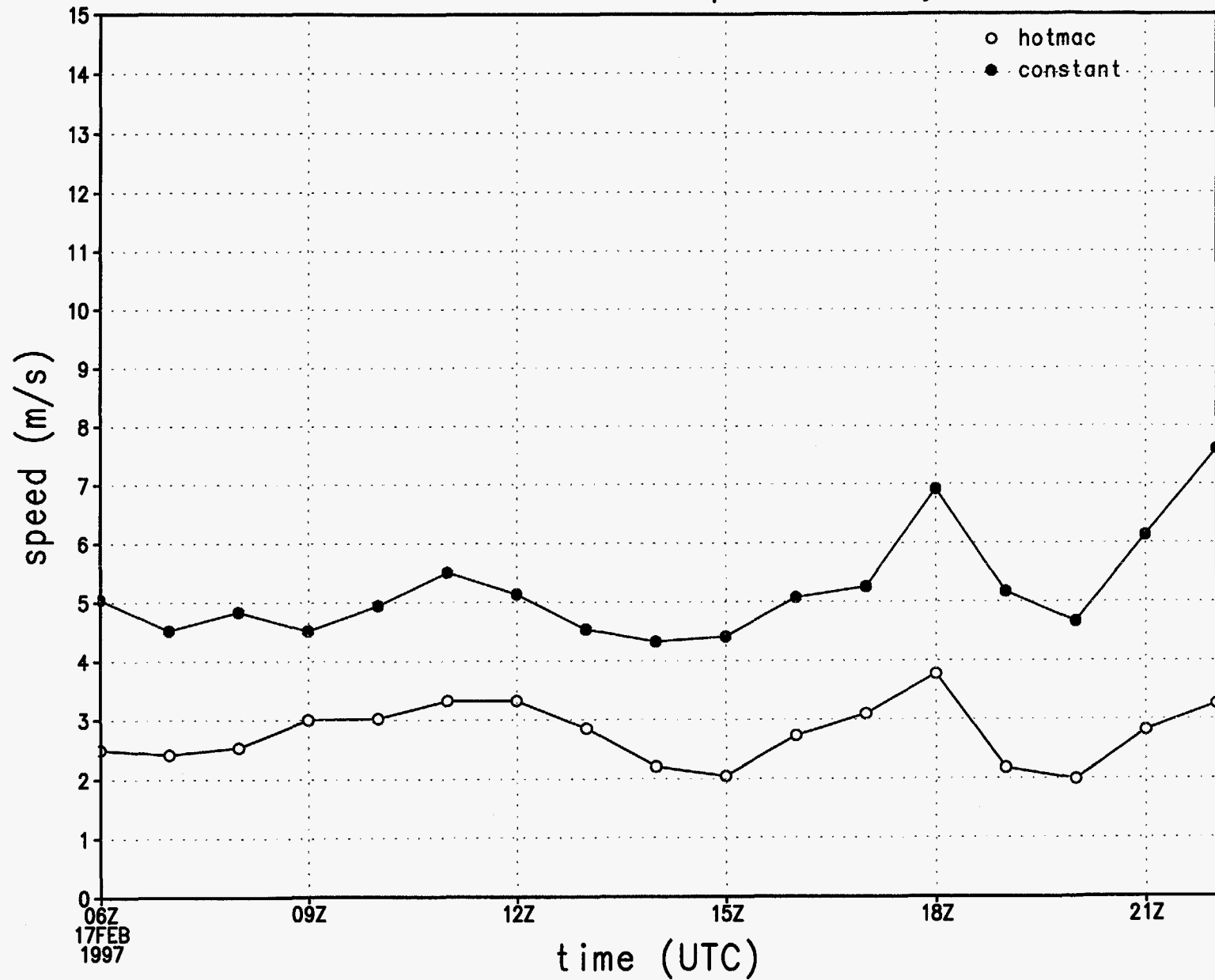


Figure 18i.

rmse of v wind component by hour

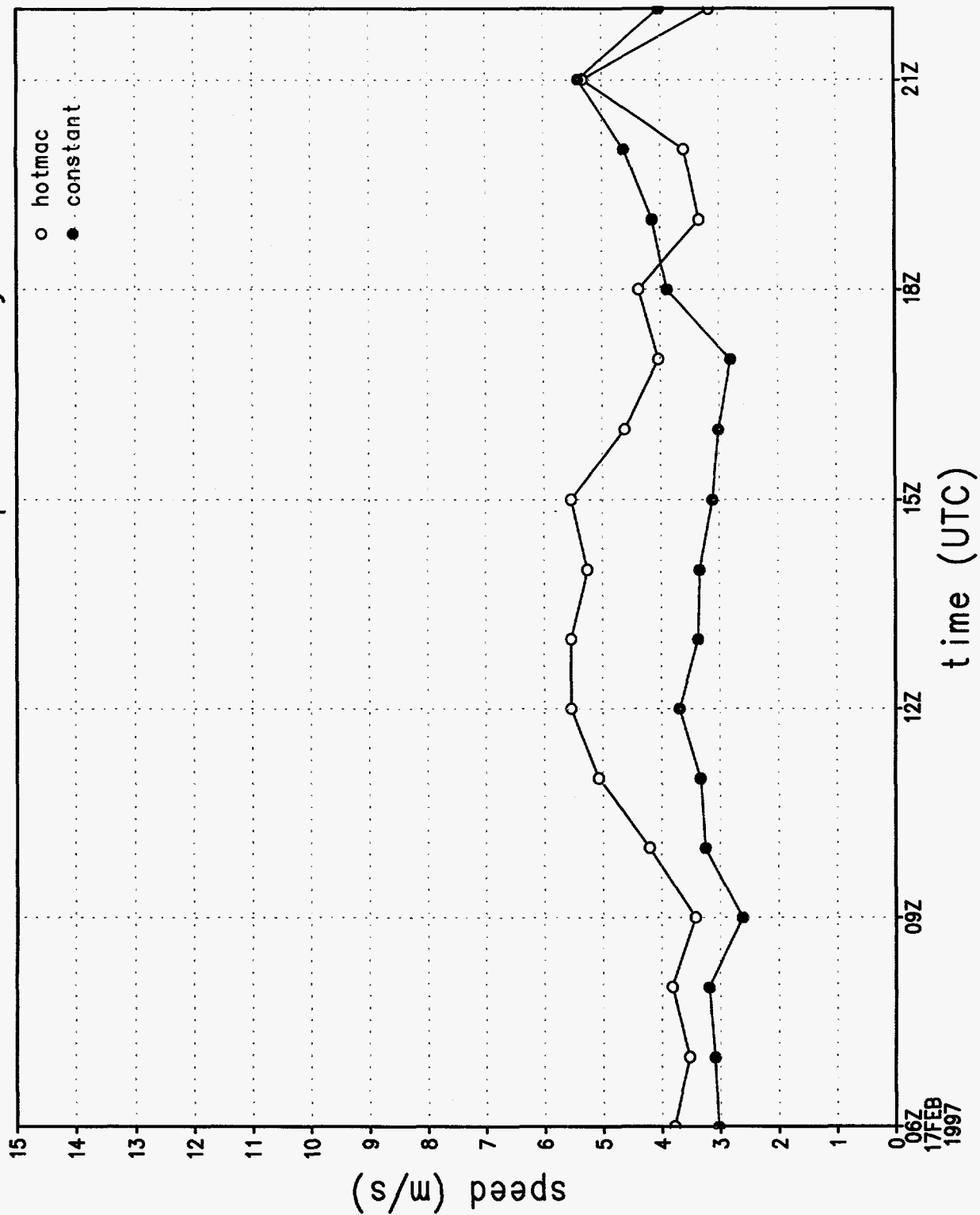


Figure 18j.

# wind direction sounding 1, 1072 m

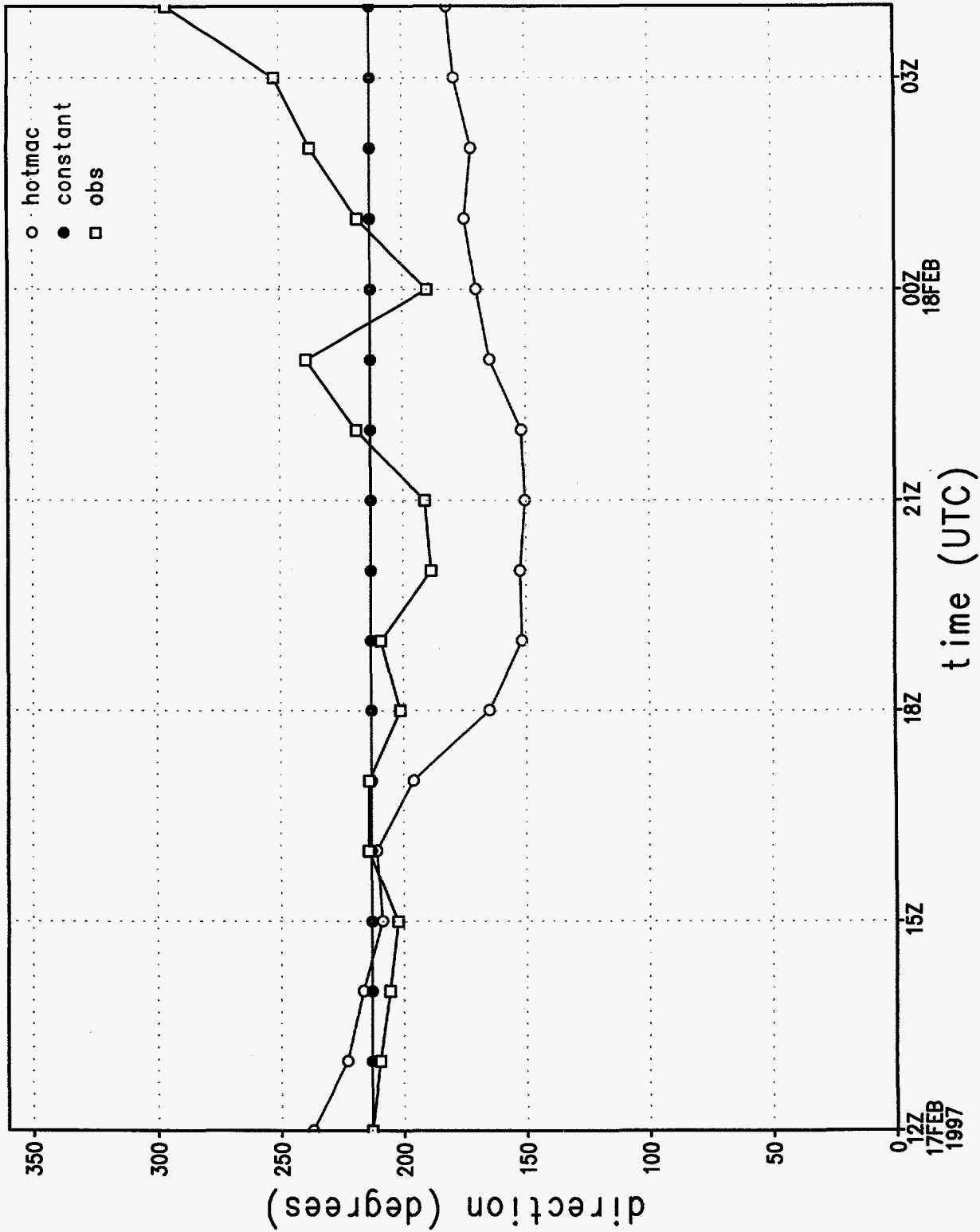


Figure 19a.

# wind speed sounding 1, 1072 m

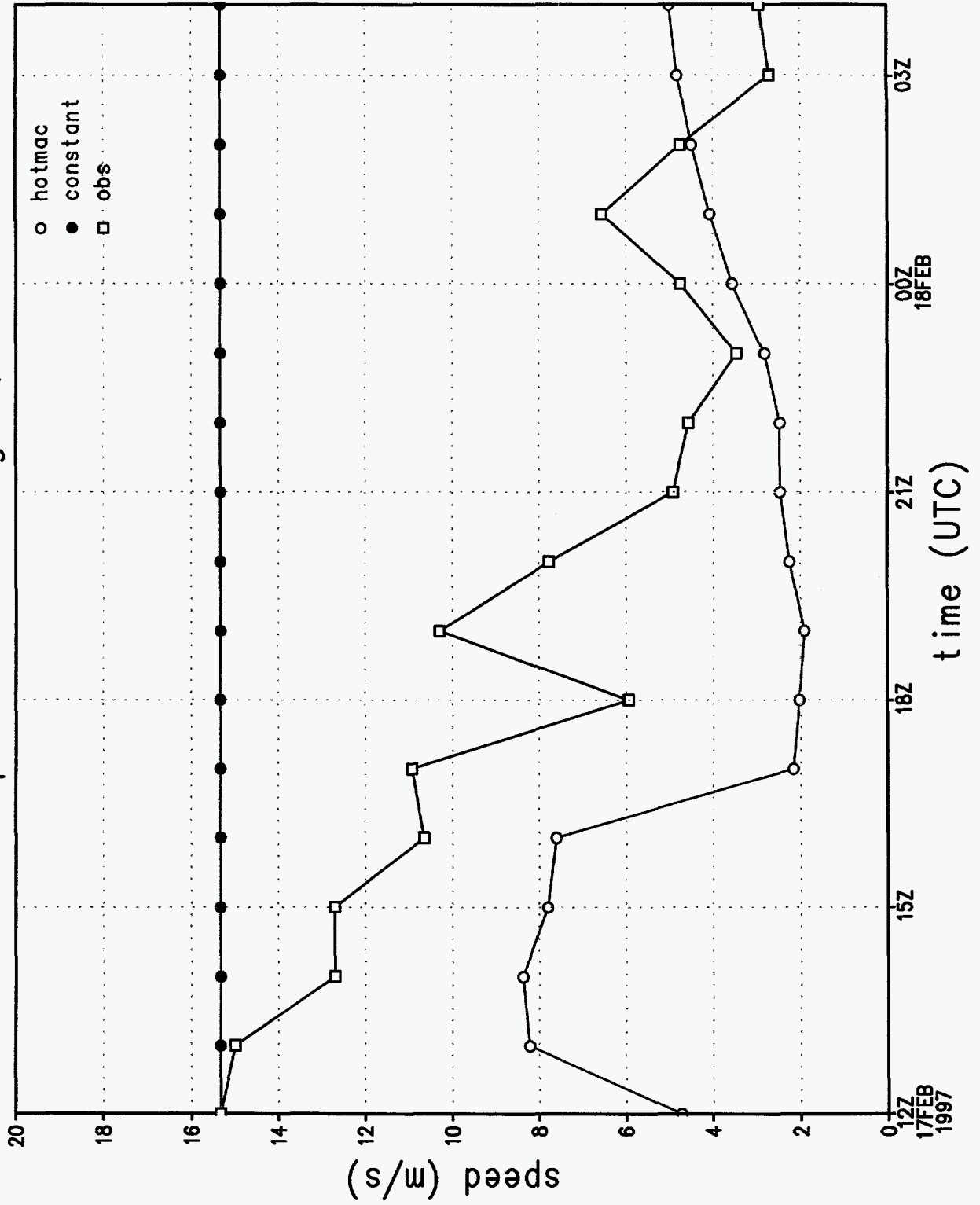


Figure 19 b.

# wind direction at station 1

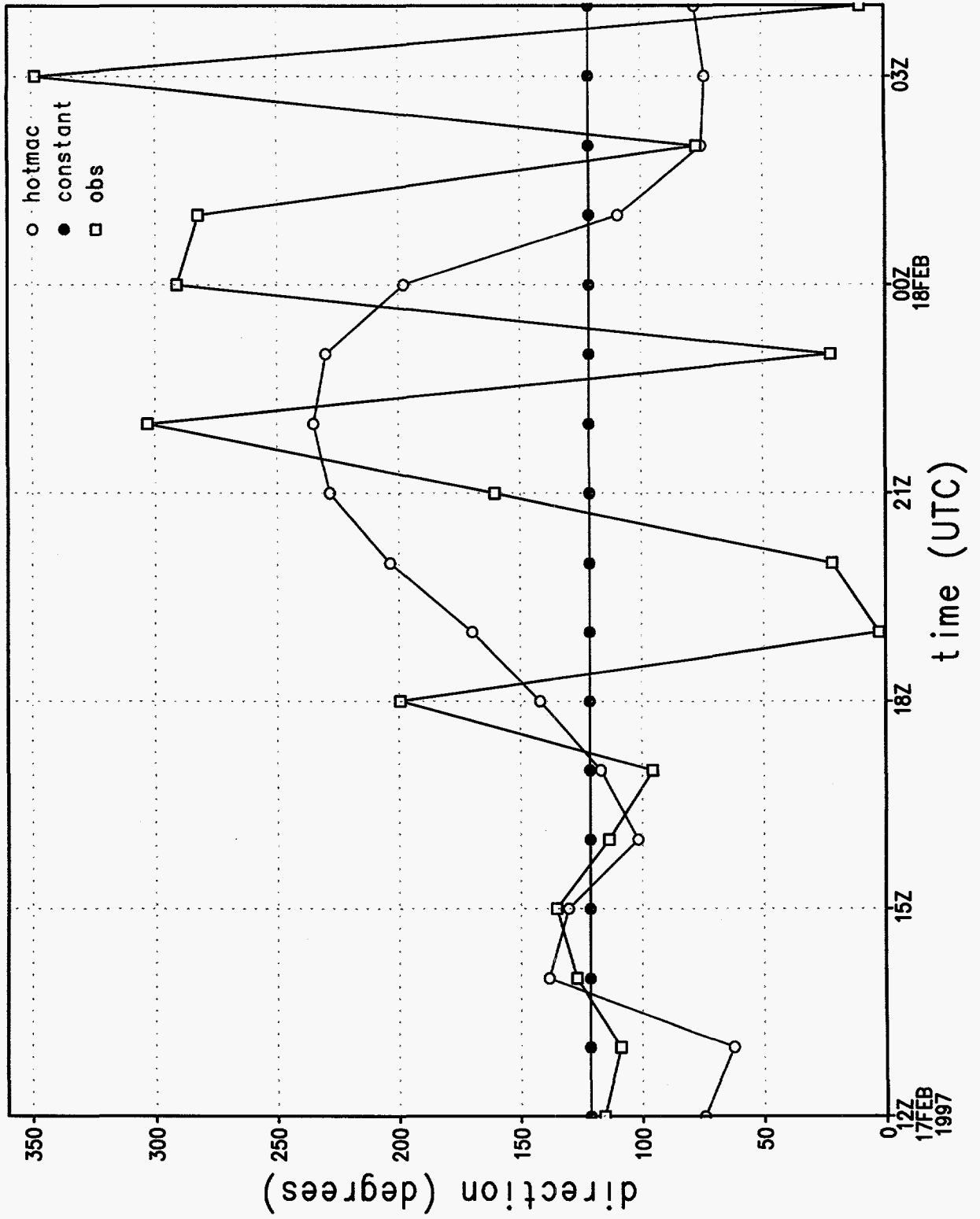


Figure 19c.

# wind speed at station 1

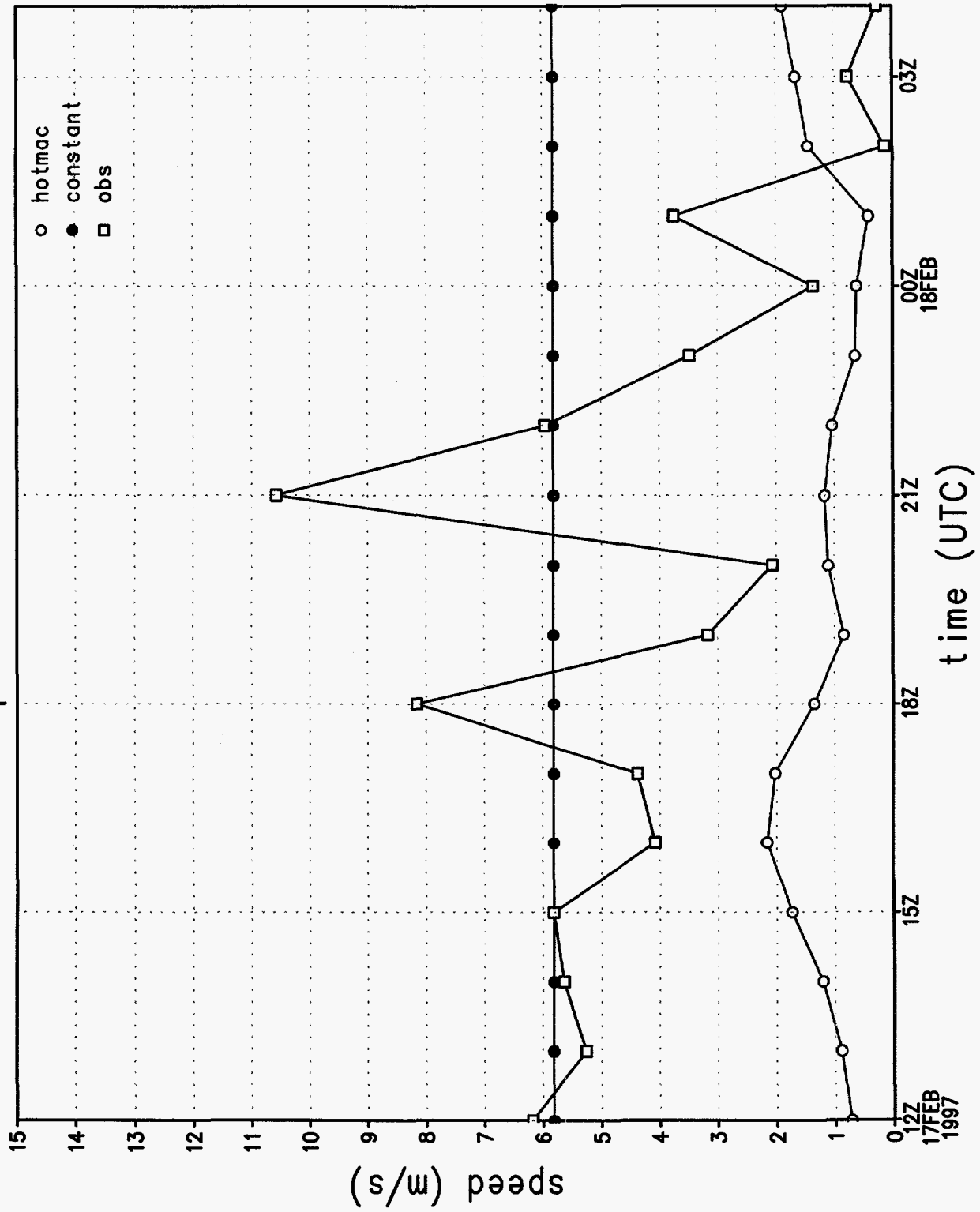


Figure 19d.

# u wind component at station 1

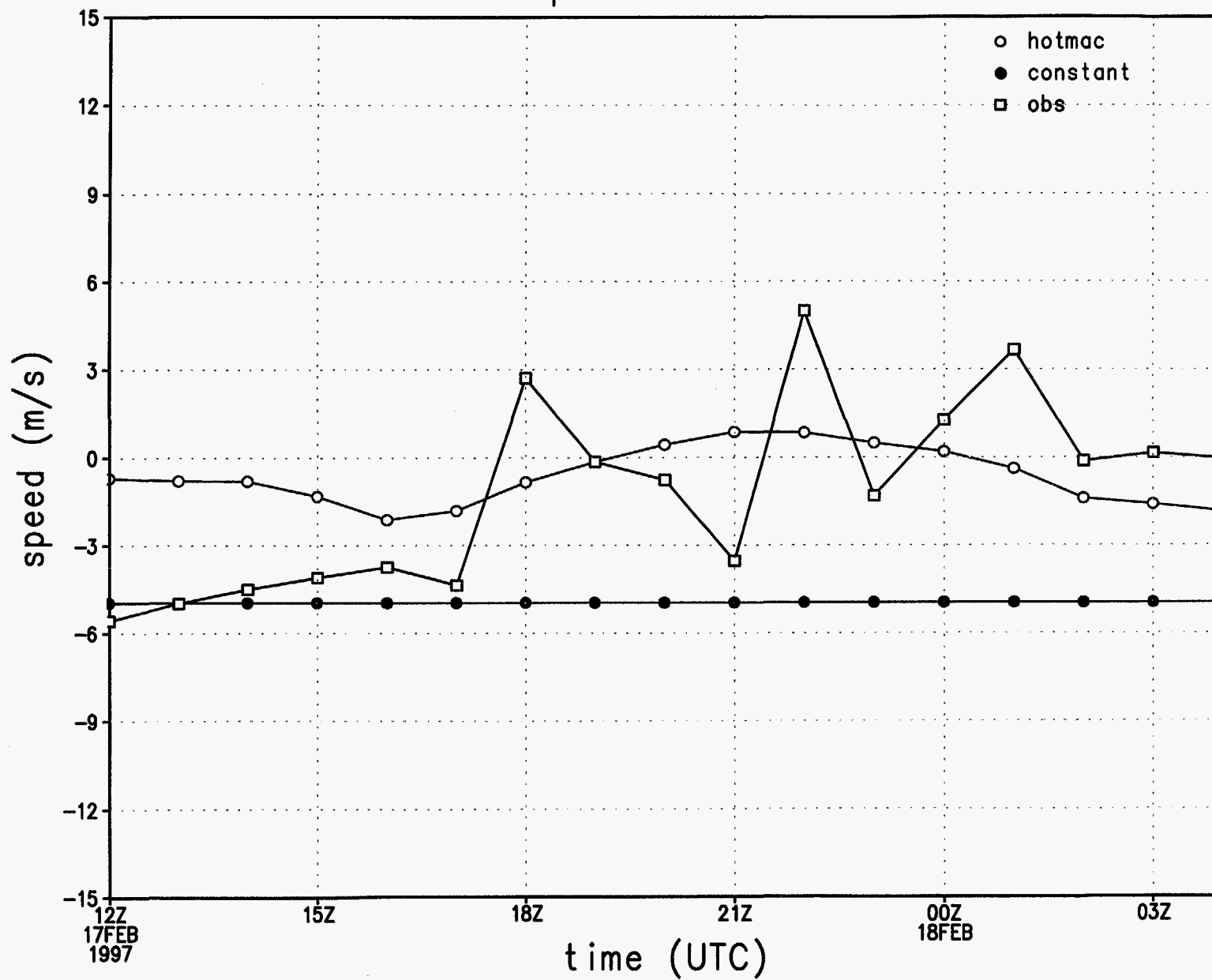


Figure 19e.

# v wind component at station 1

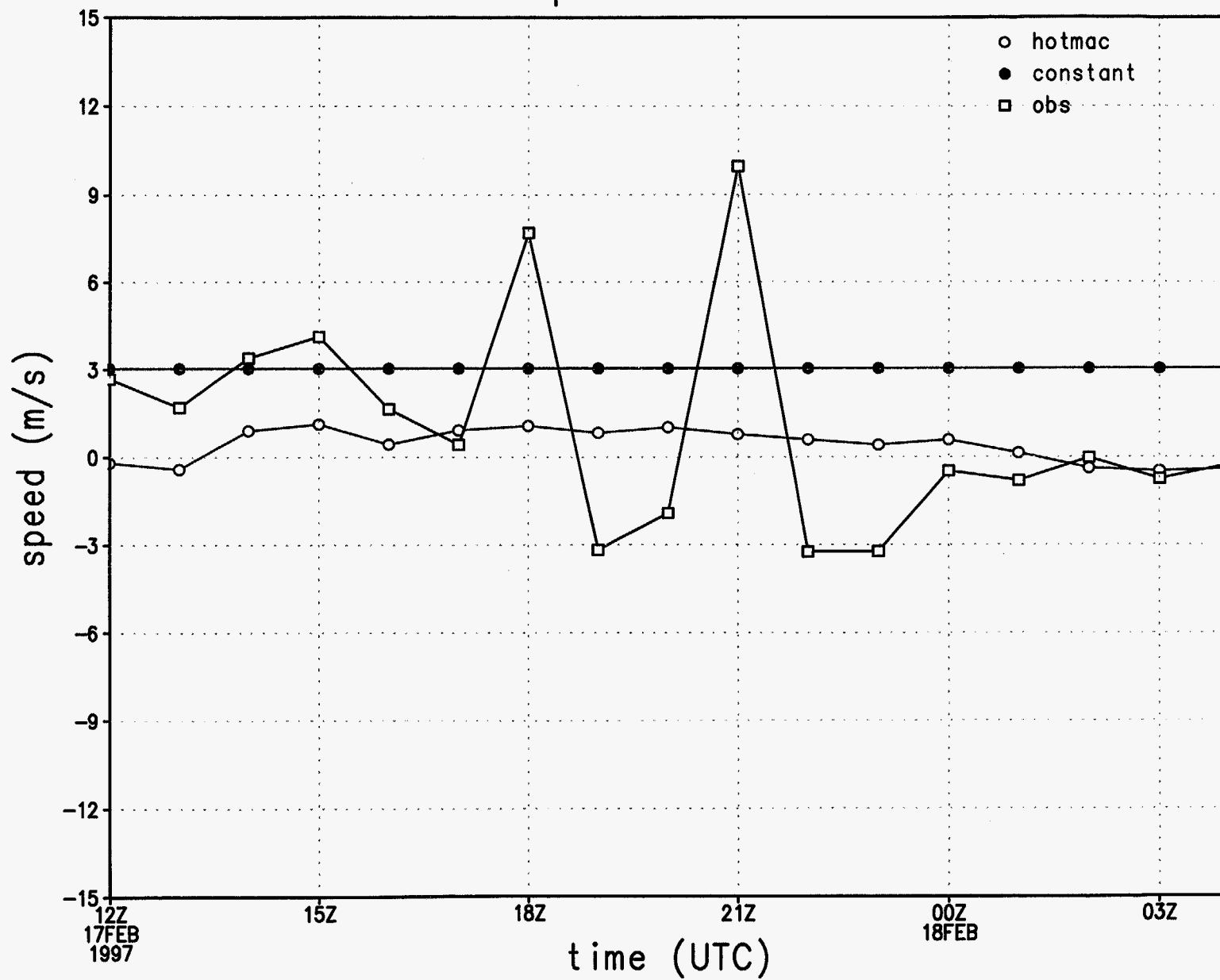


Figure 19f.



rmse of wind direction by hour

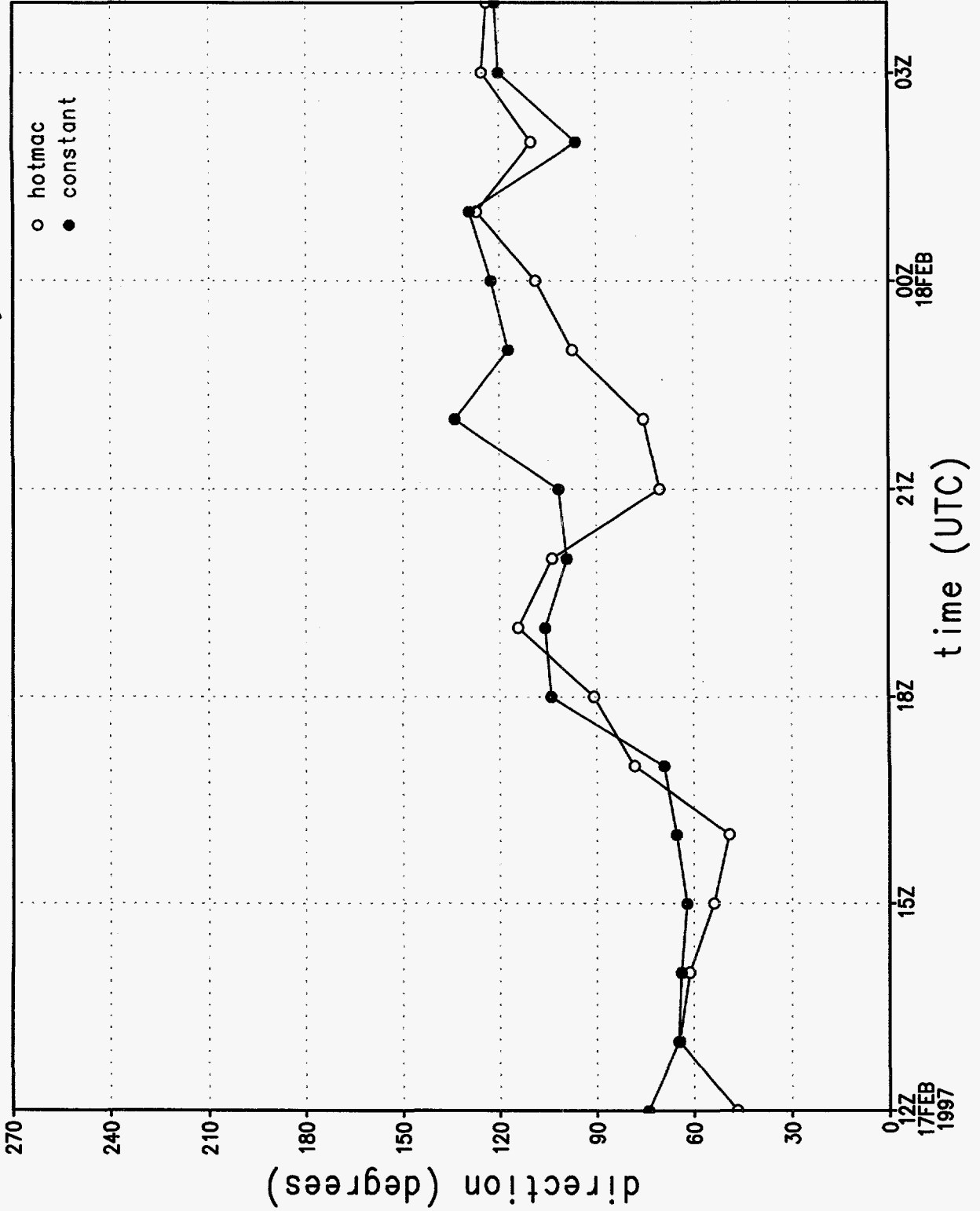


Figure 19g.

# rmse of wind speed by hour

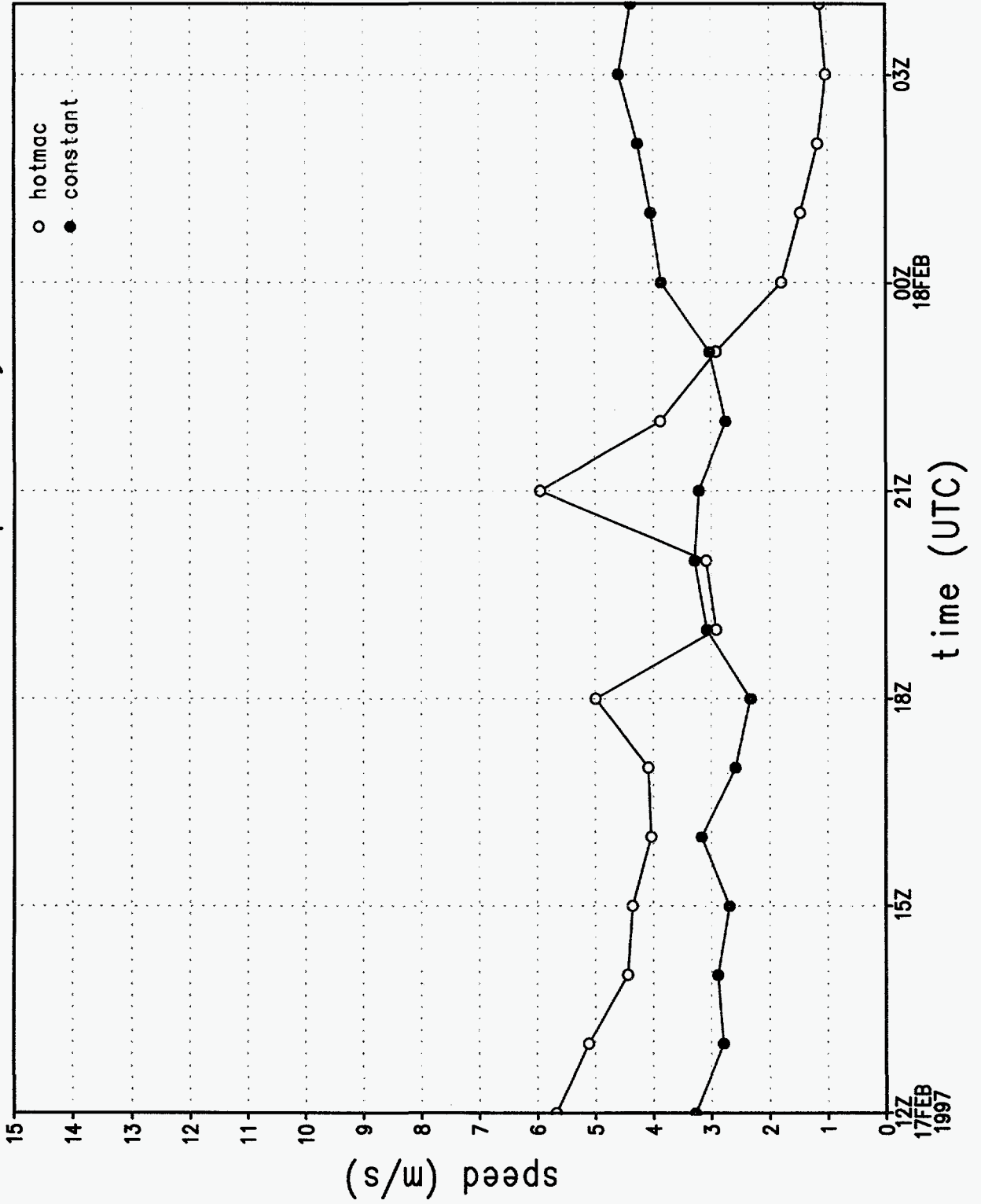


Figure 19 h.

rmse of u wind component by hour

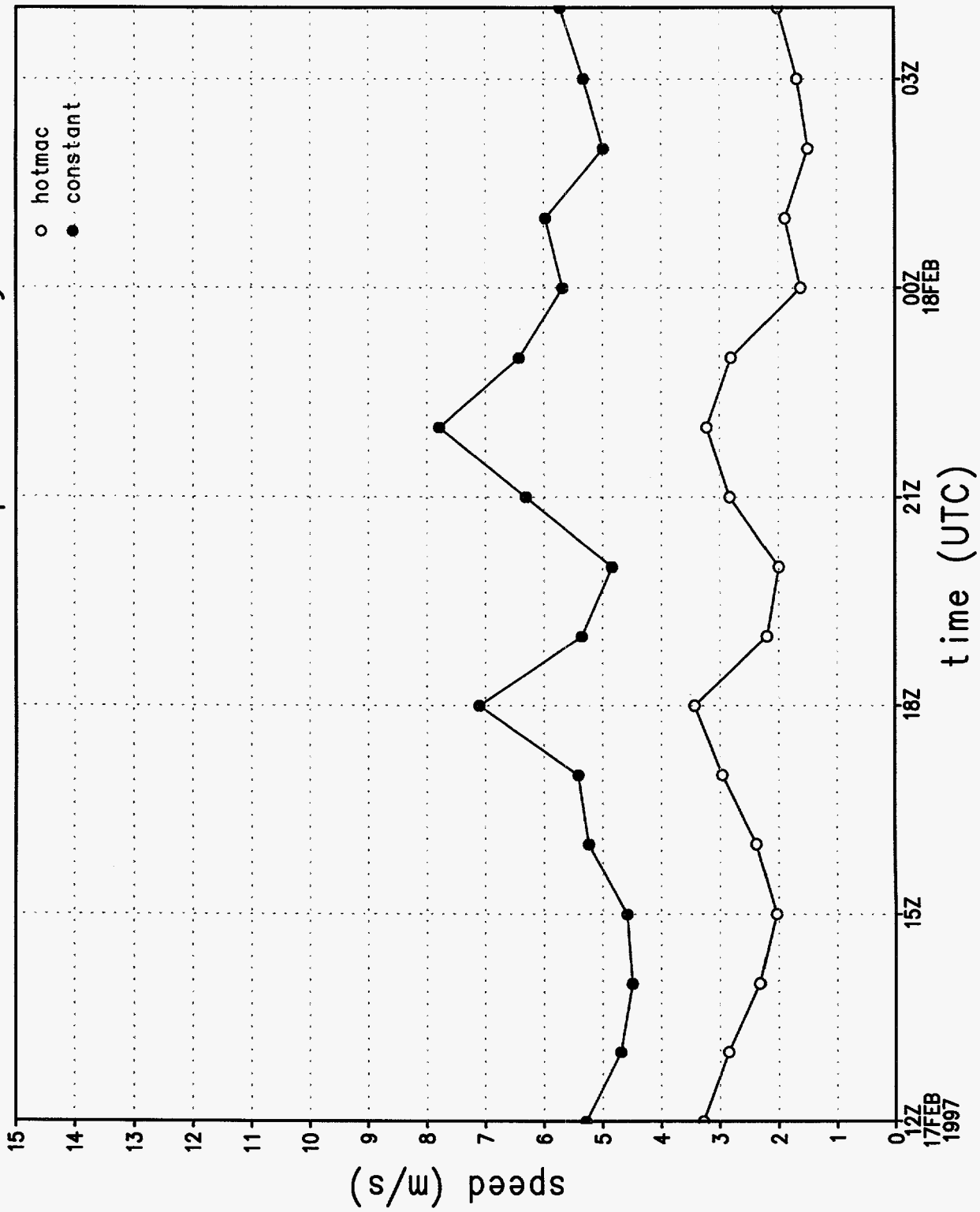


Figure 191.

rmse of v wind component by hour

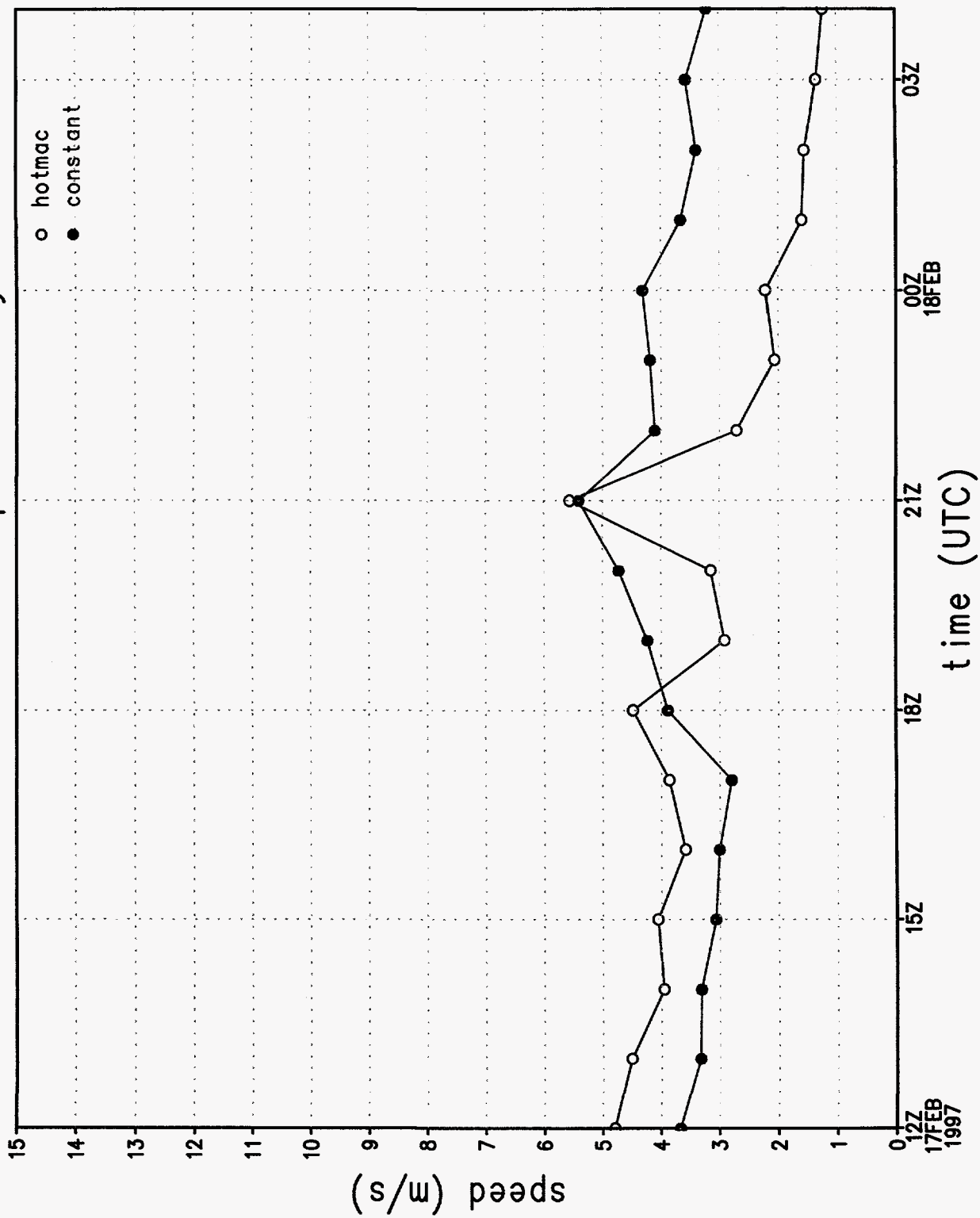


Figure 19j.

# wind direction sounding 1, 1072 m

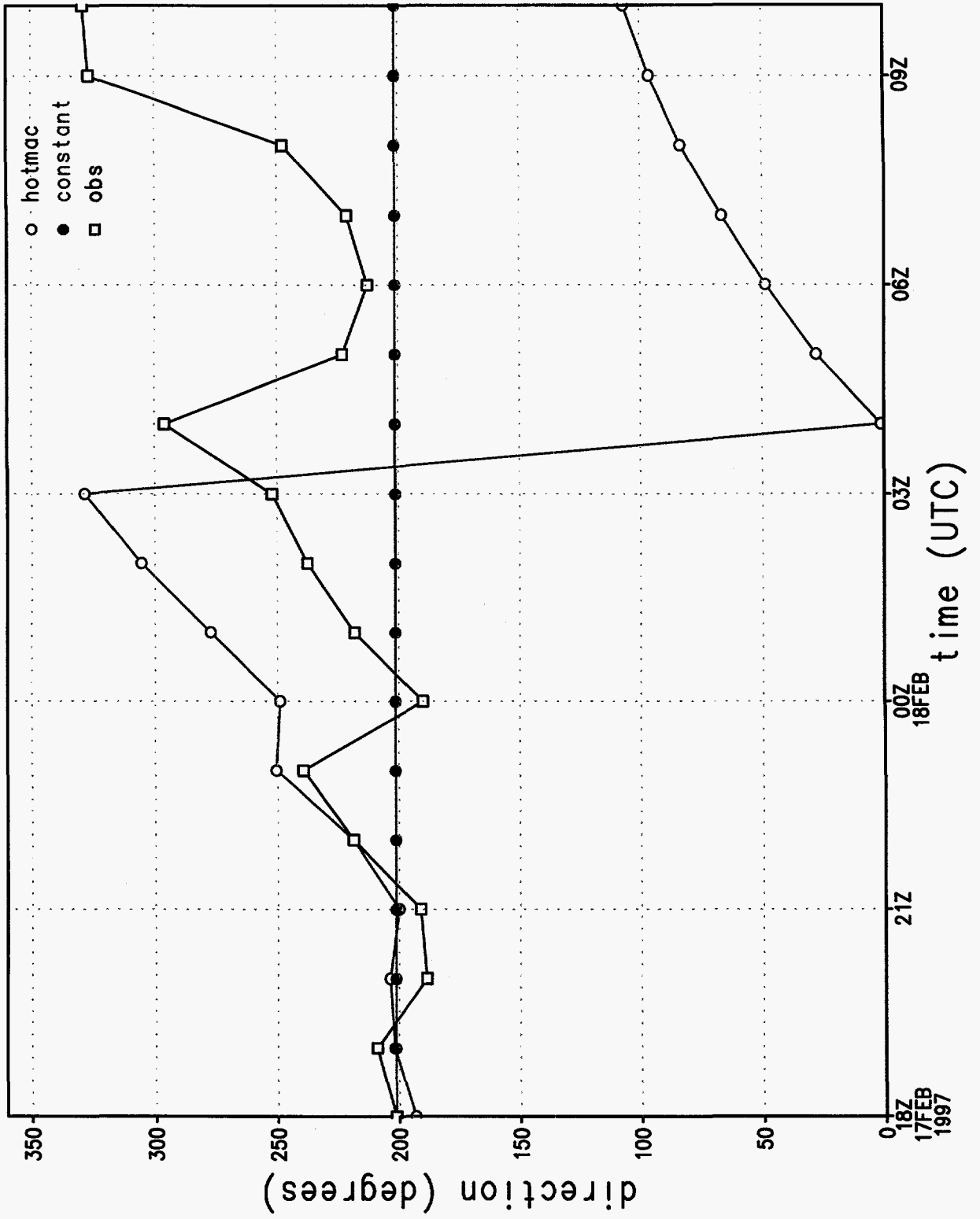


Figure 20a.

# wind speed sounding 1, 1072 m

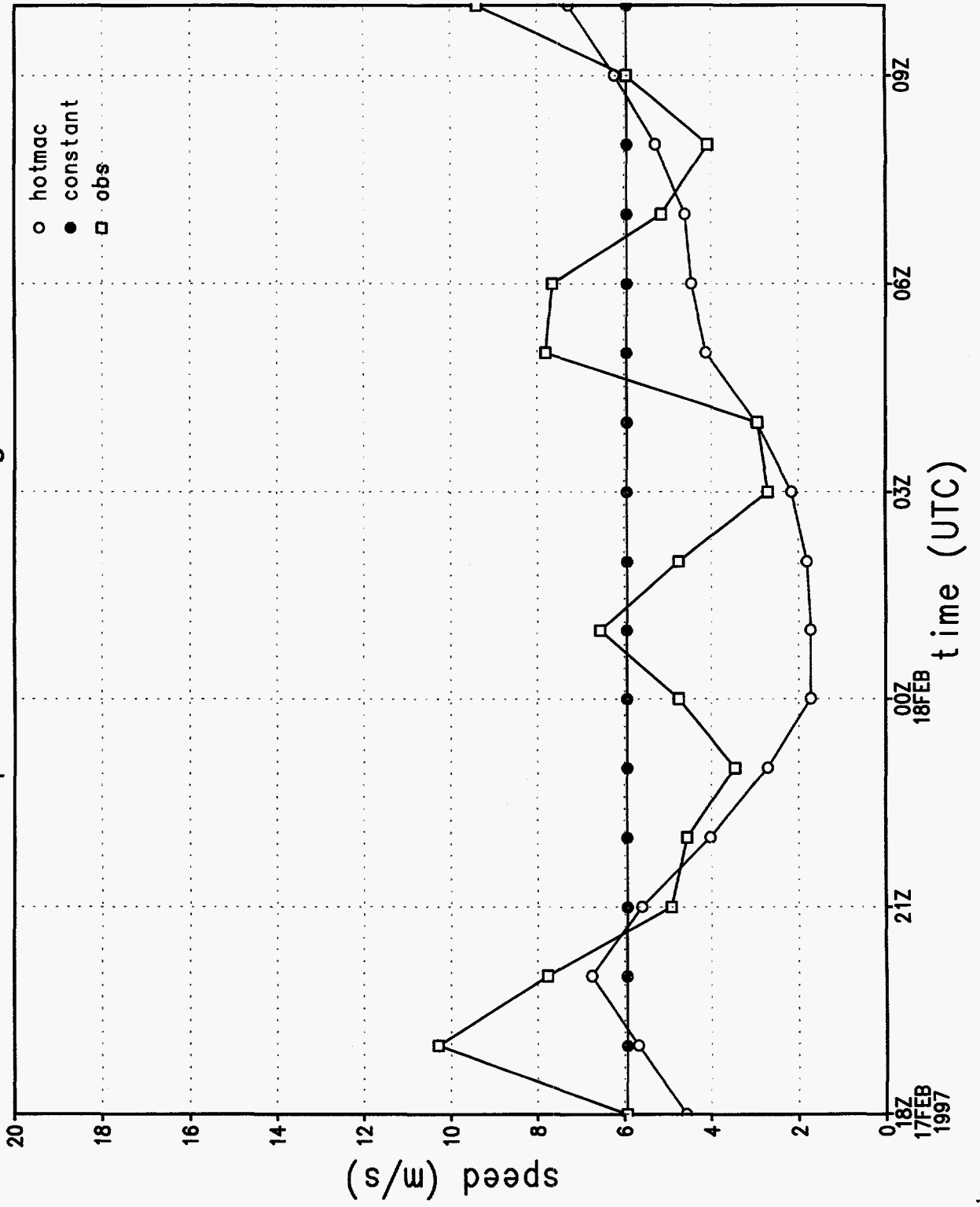


Figure 20b.

# wind direction at station 1

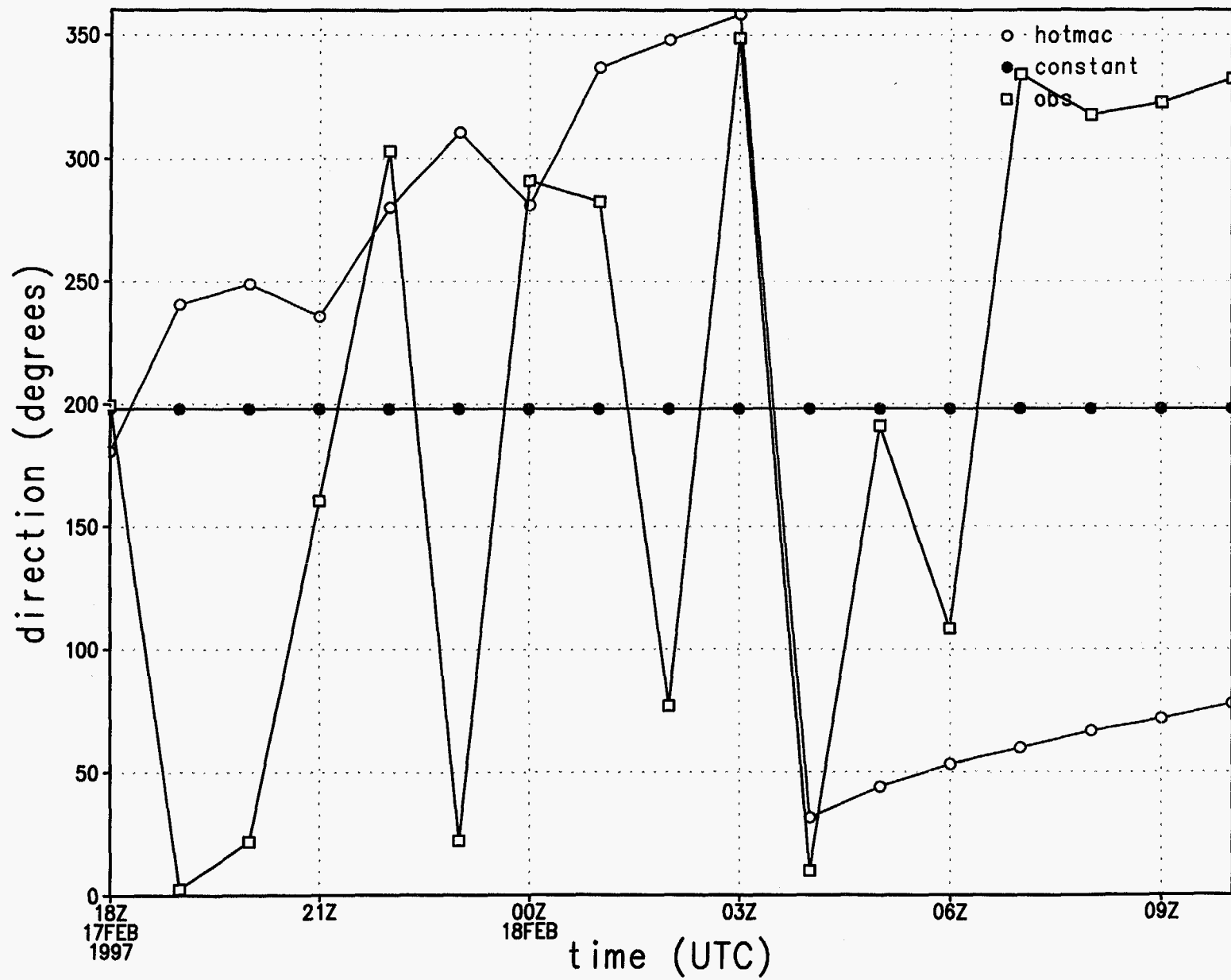


Figure 20c.

# wind speed at station 1

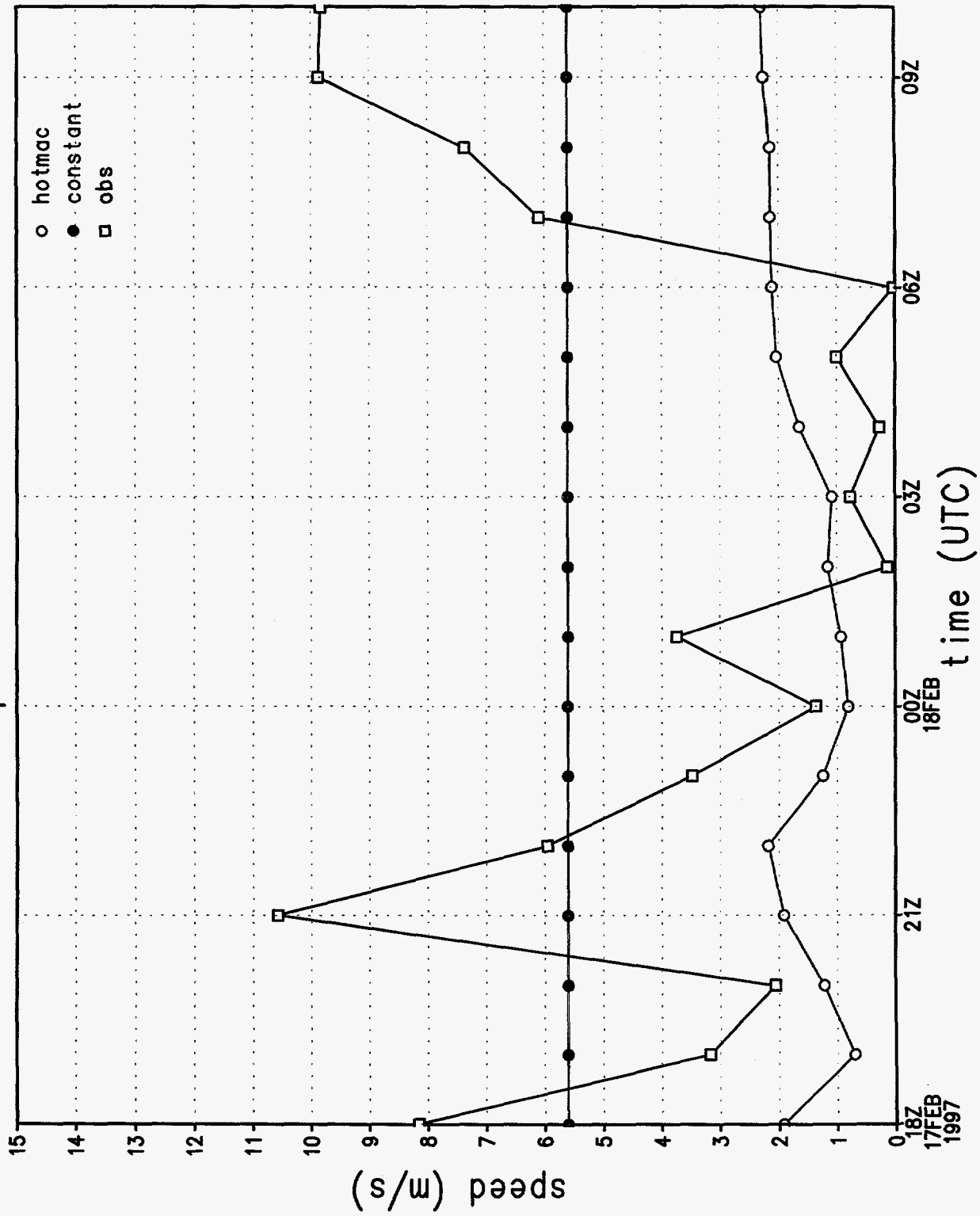


Figure 20d.



# u wind component at station 1

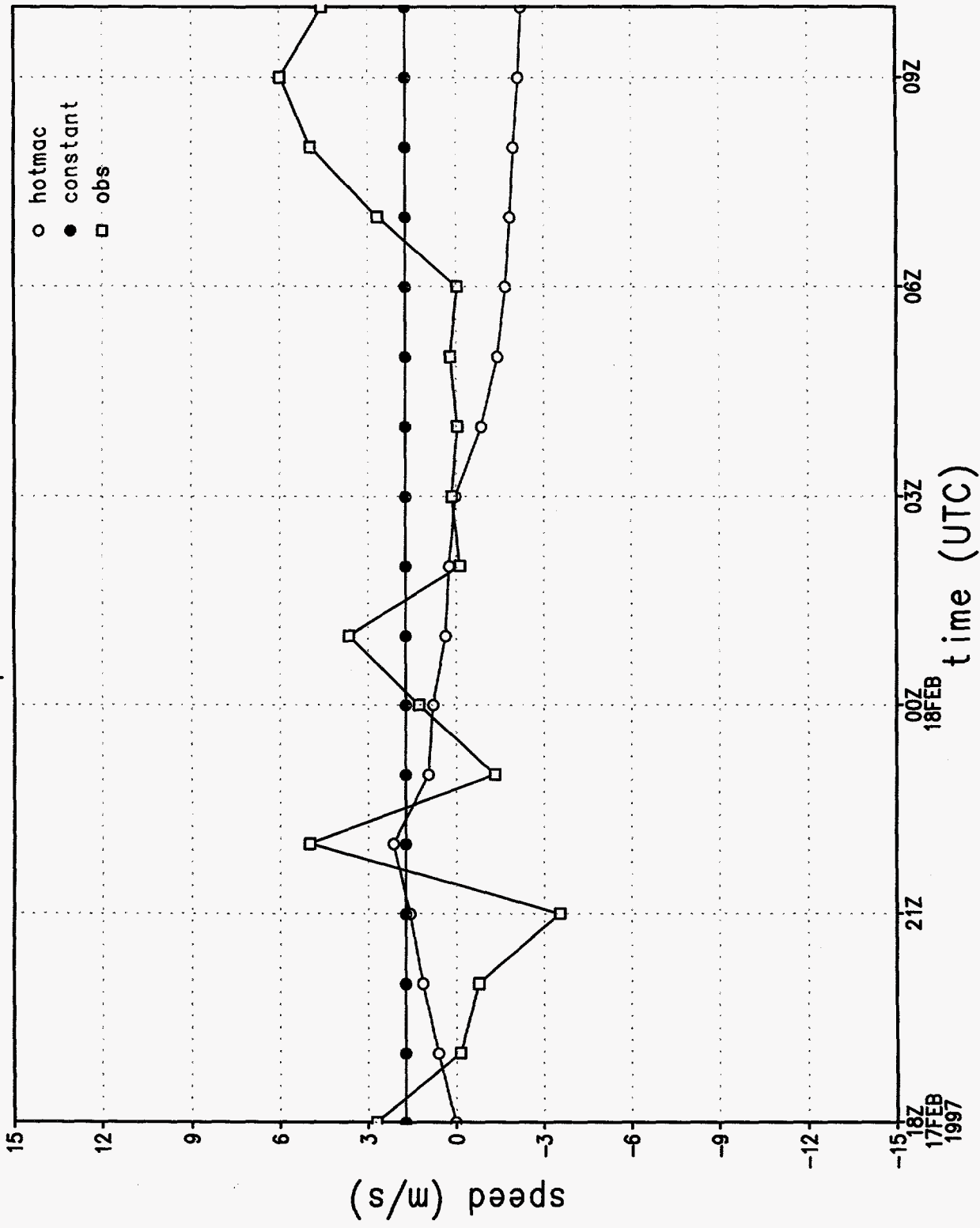


Figure 20e.

# v wind component at station 1

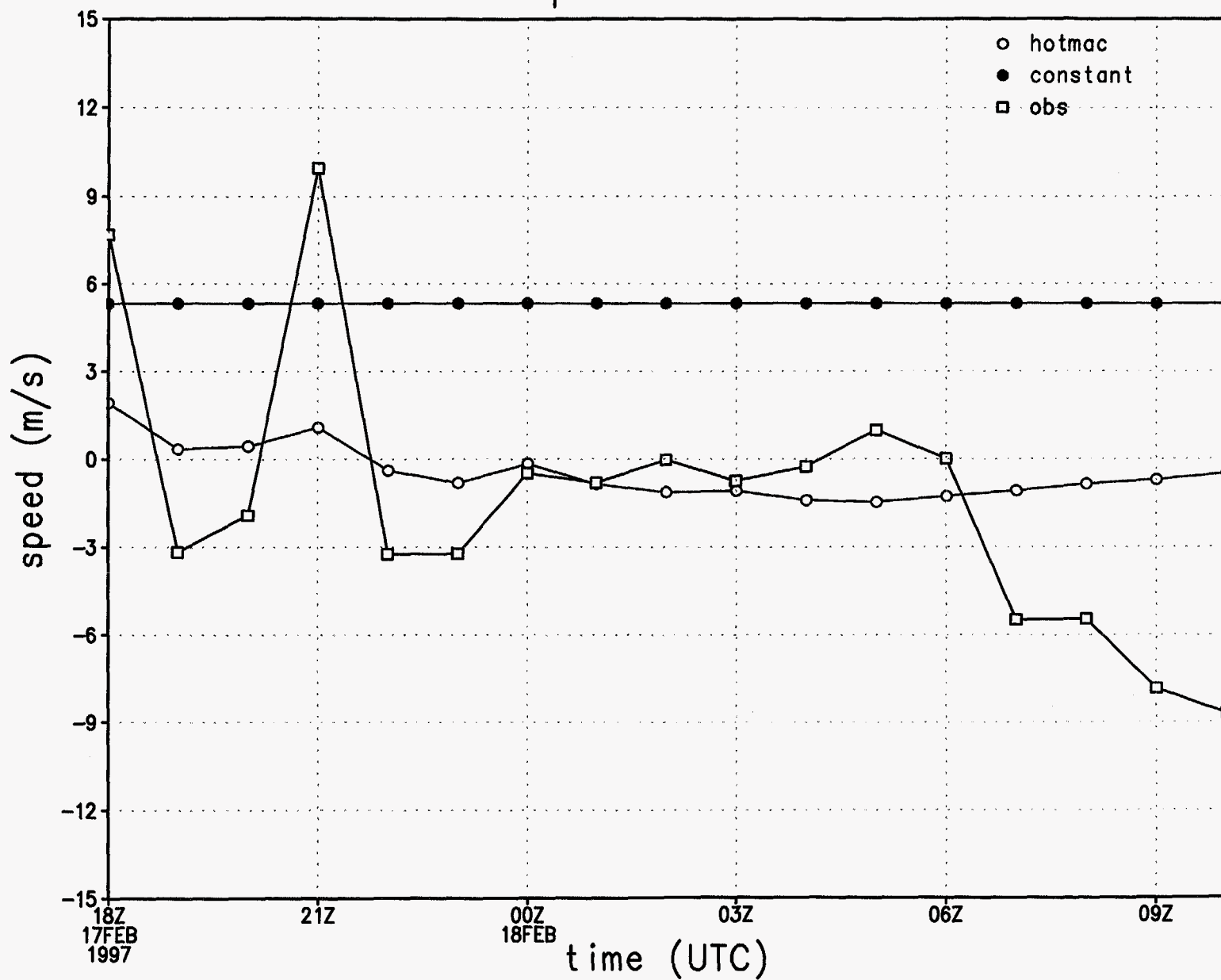


Figure 20f.

# rmse of wind direction by hour

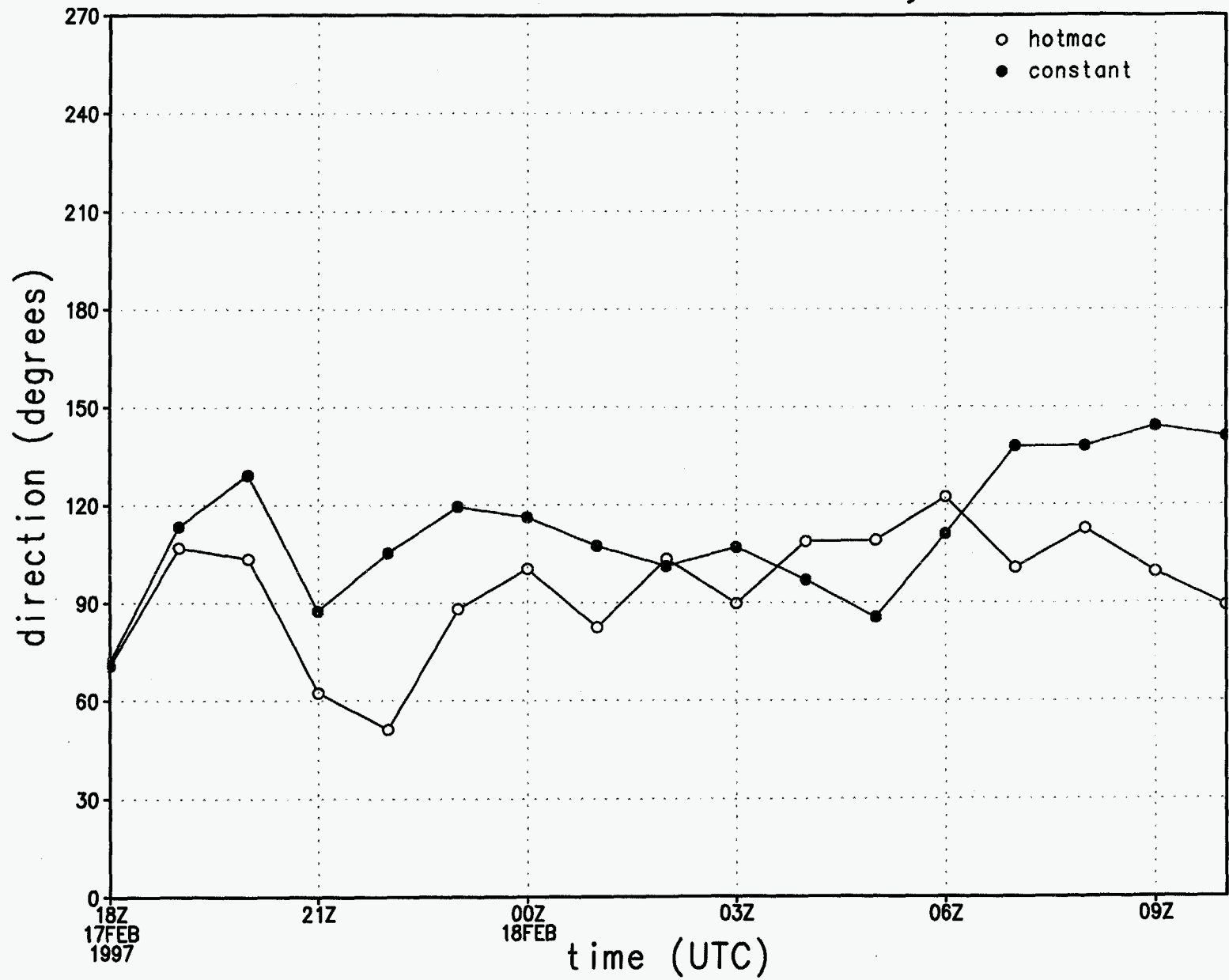


Figure 20g.

# rmse of wind speed by hour

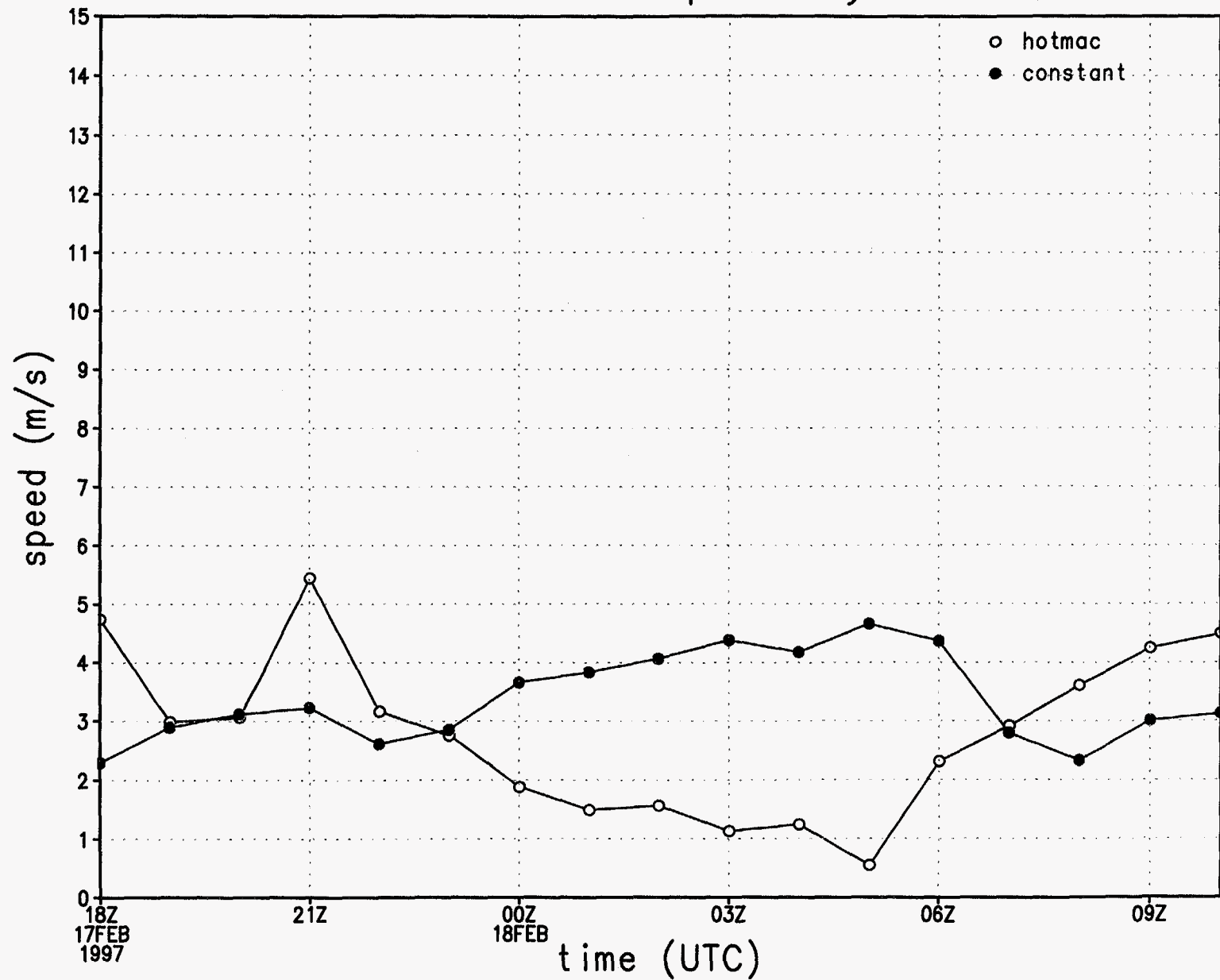


Figure 20h.

# rmse of u wind component by hour

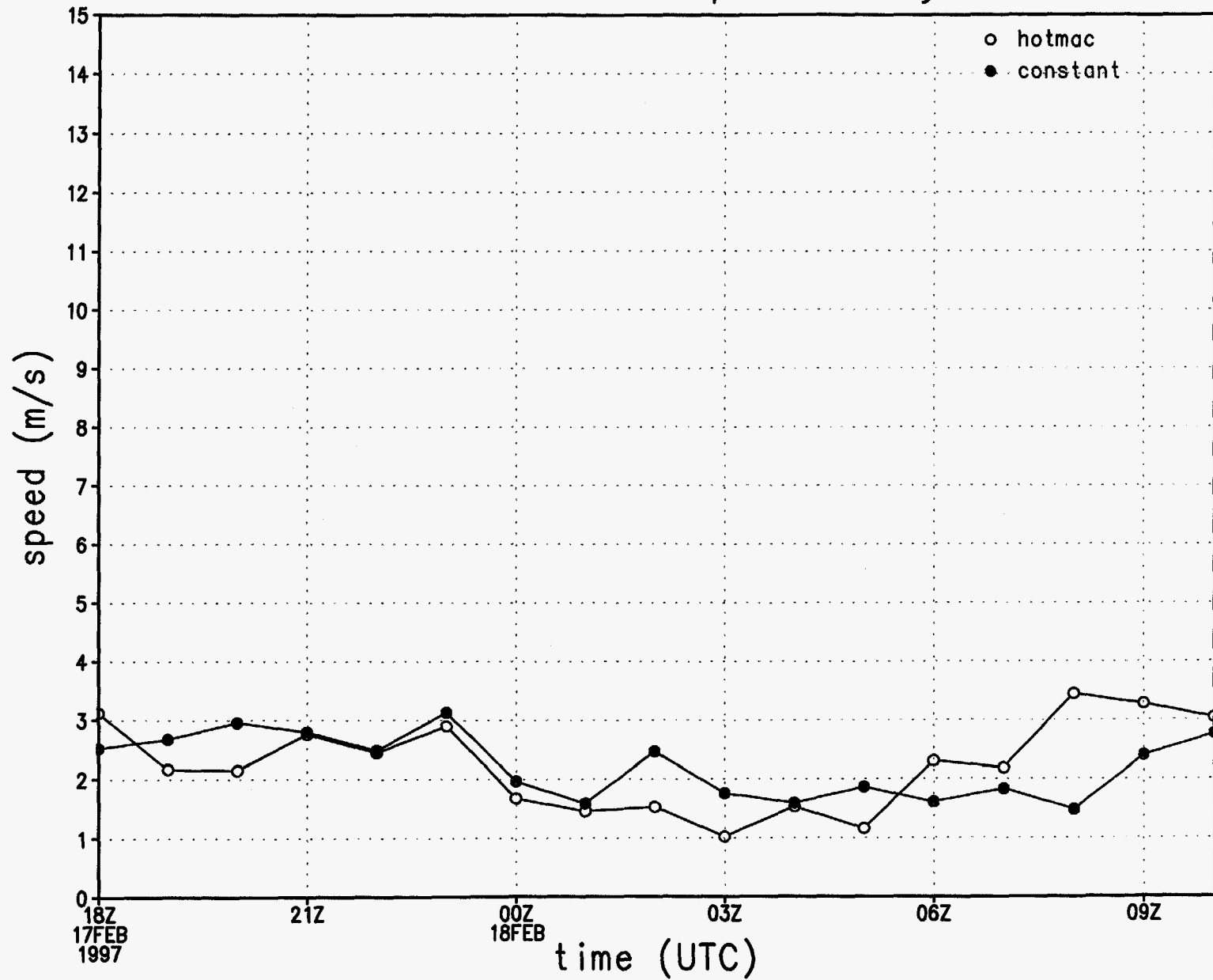


Figure 20i.

rmse of v wind component by hour

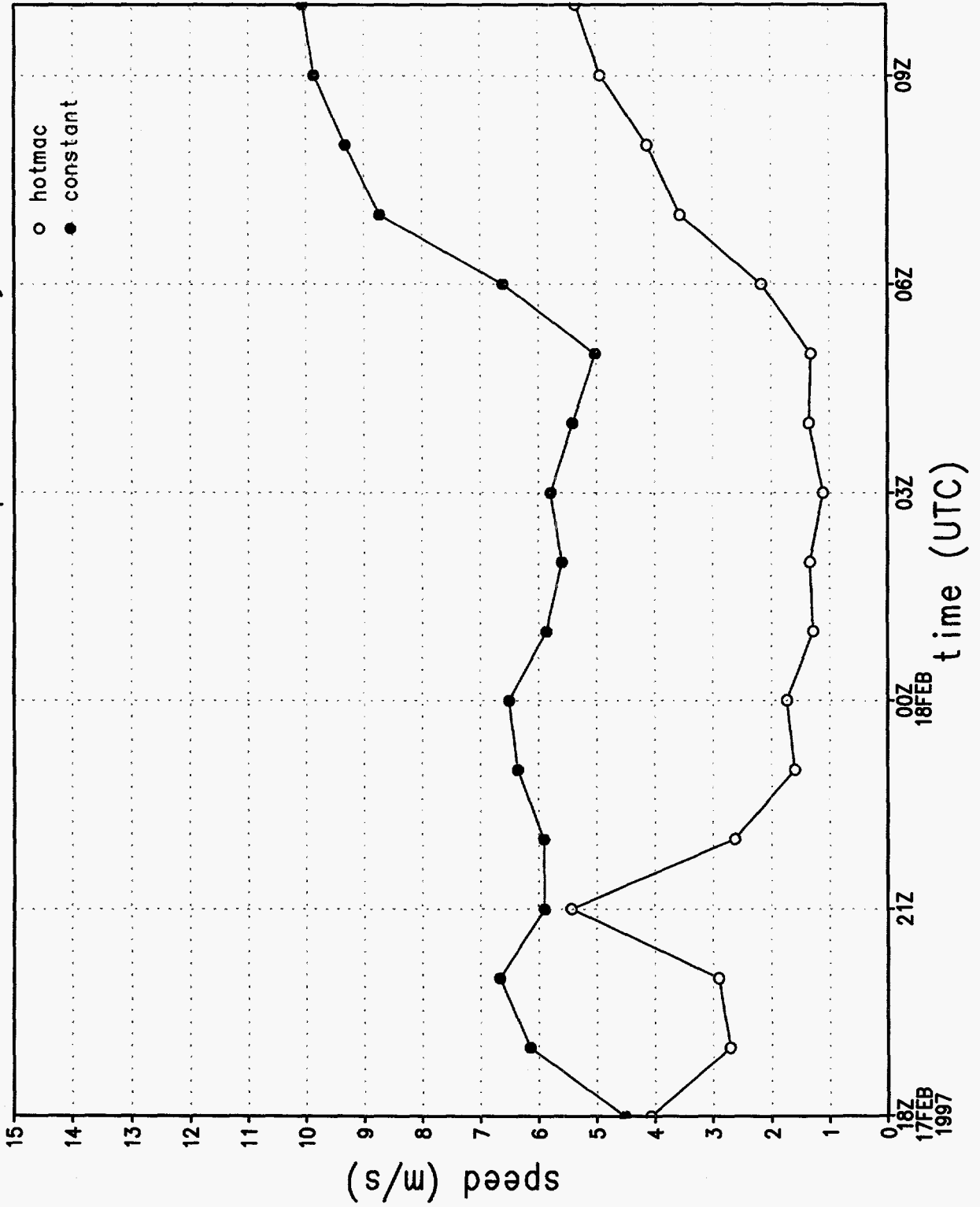


Figure 20i.

# wind direction sounding 1, 1072 m

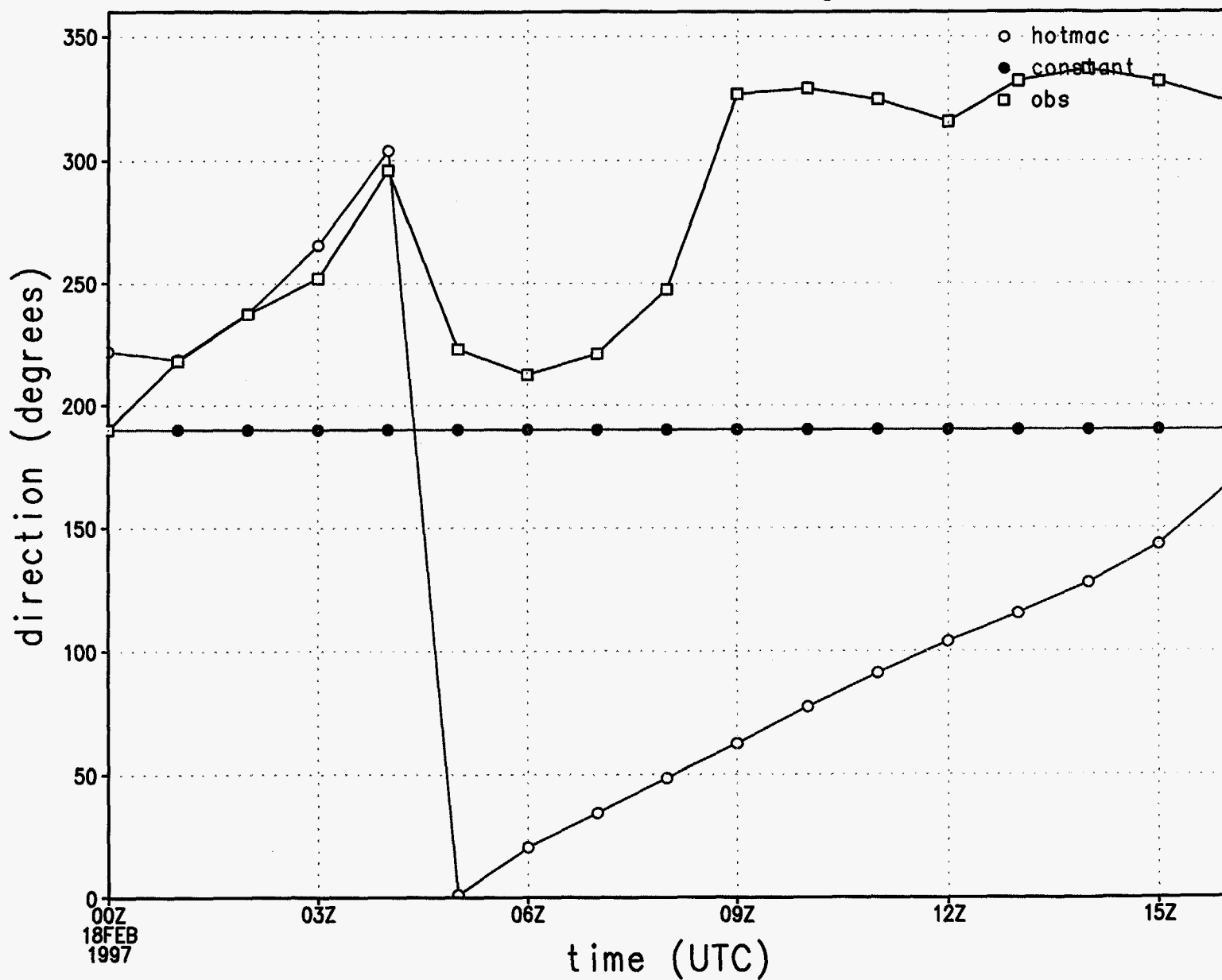


Figure 21a.

# wind speed sounding 1, 1072 m

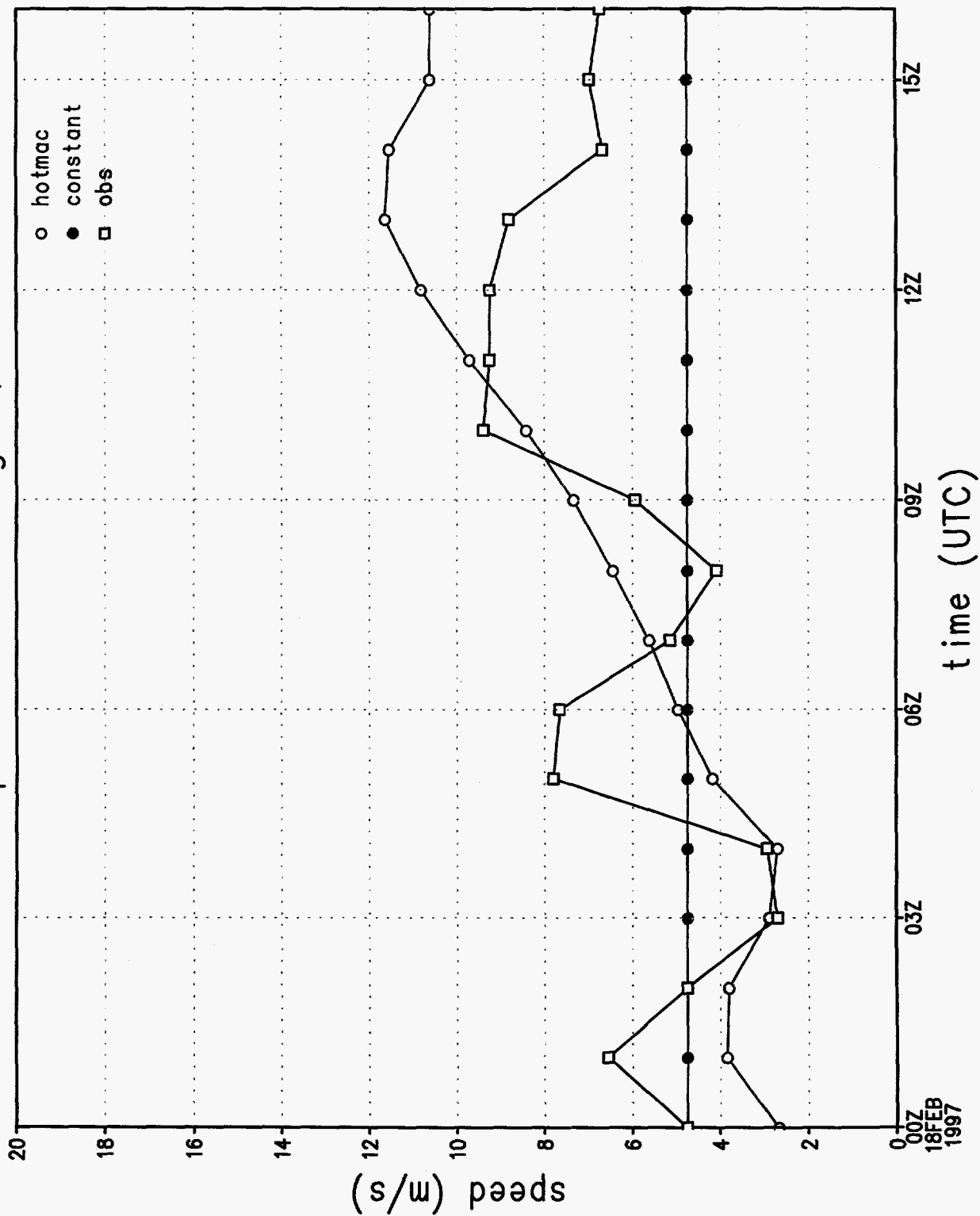


Figure 21b.



# wind direction at station 1

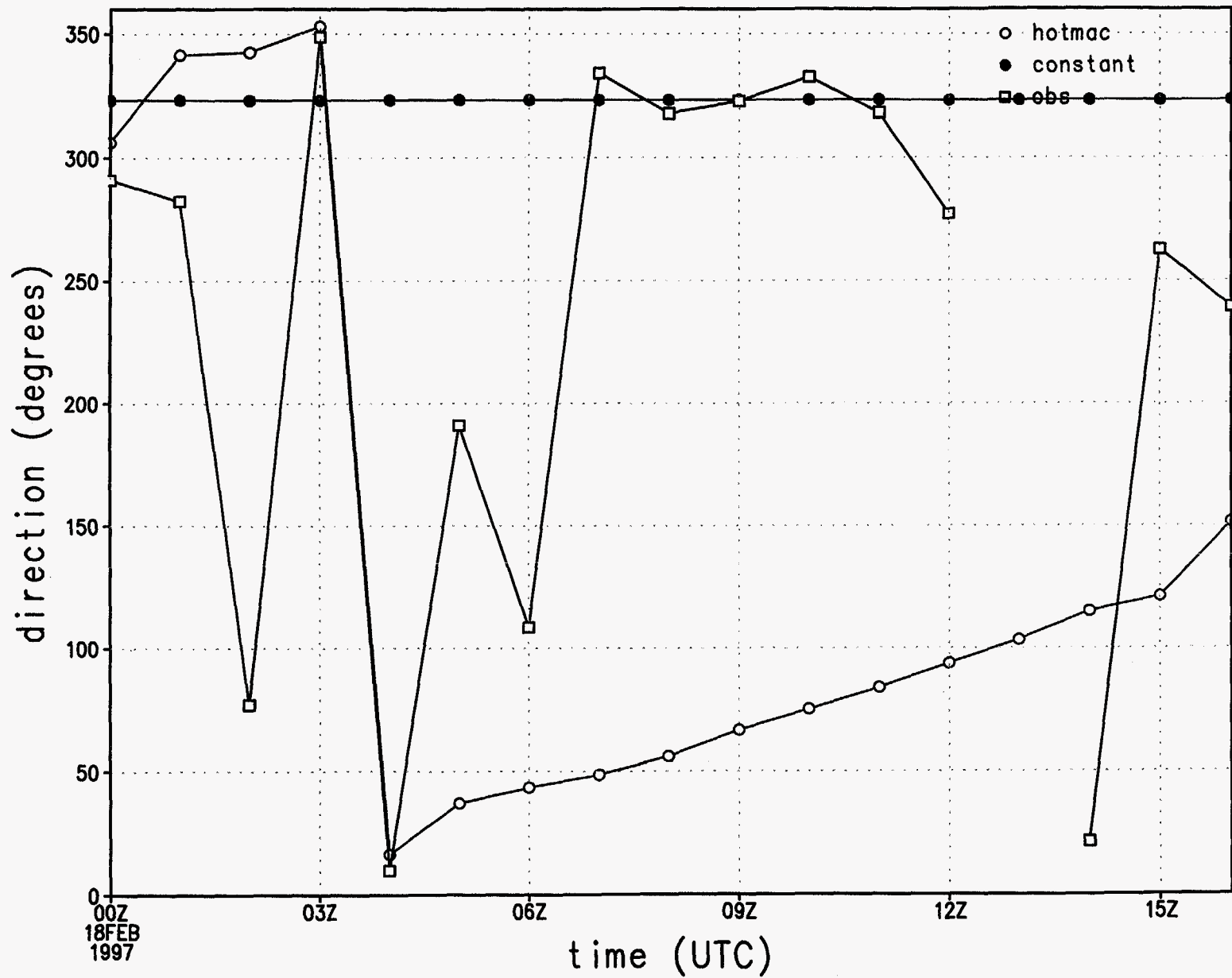


Figure 21c.

# wind speed at station 1

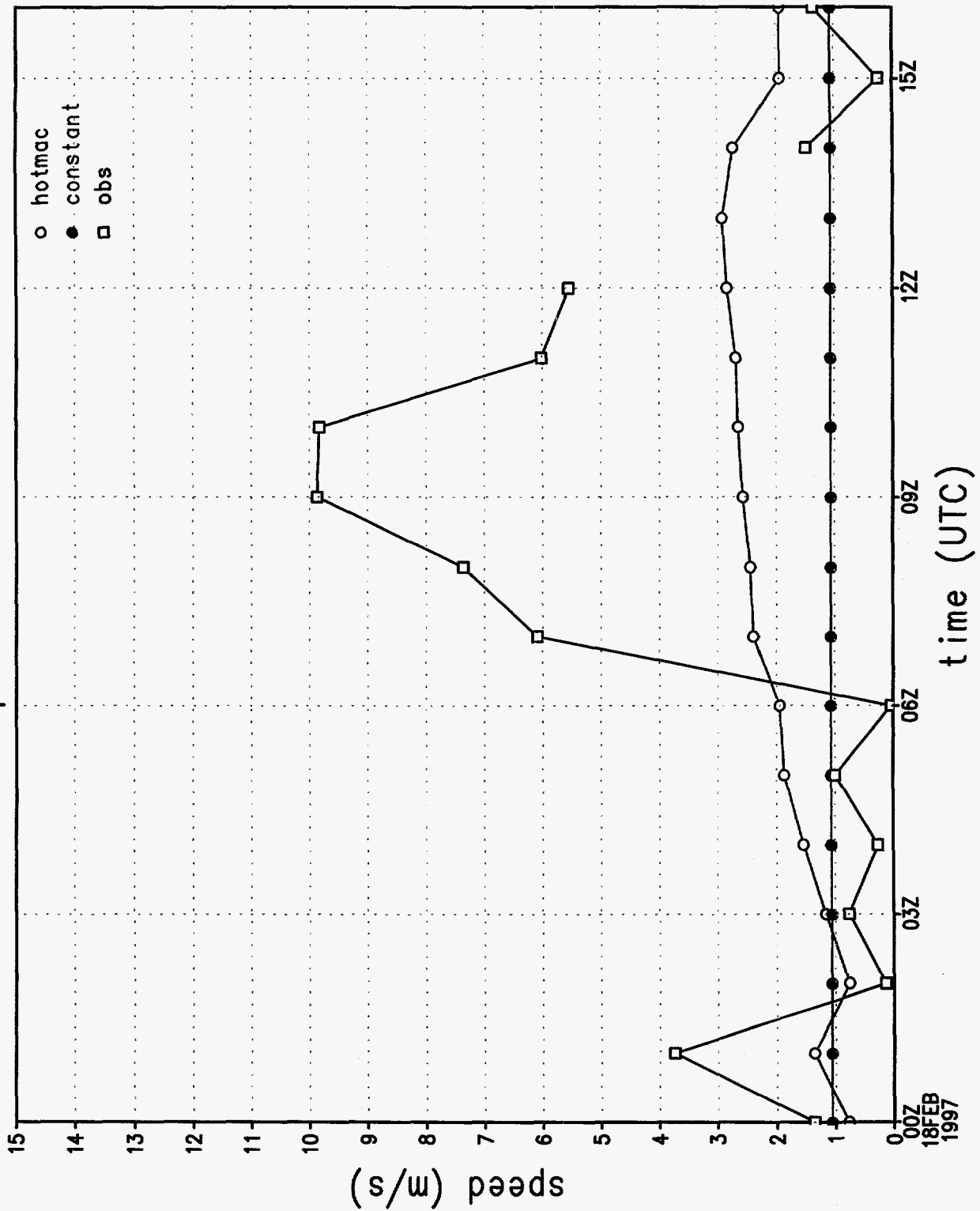


Figure 21d.

# u wind component at station 1

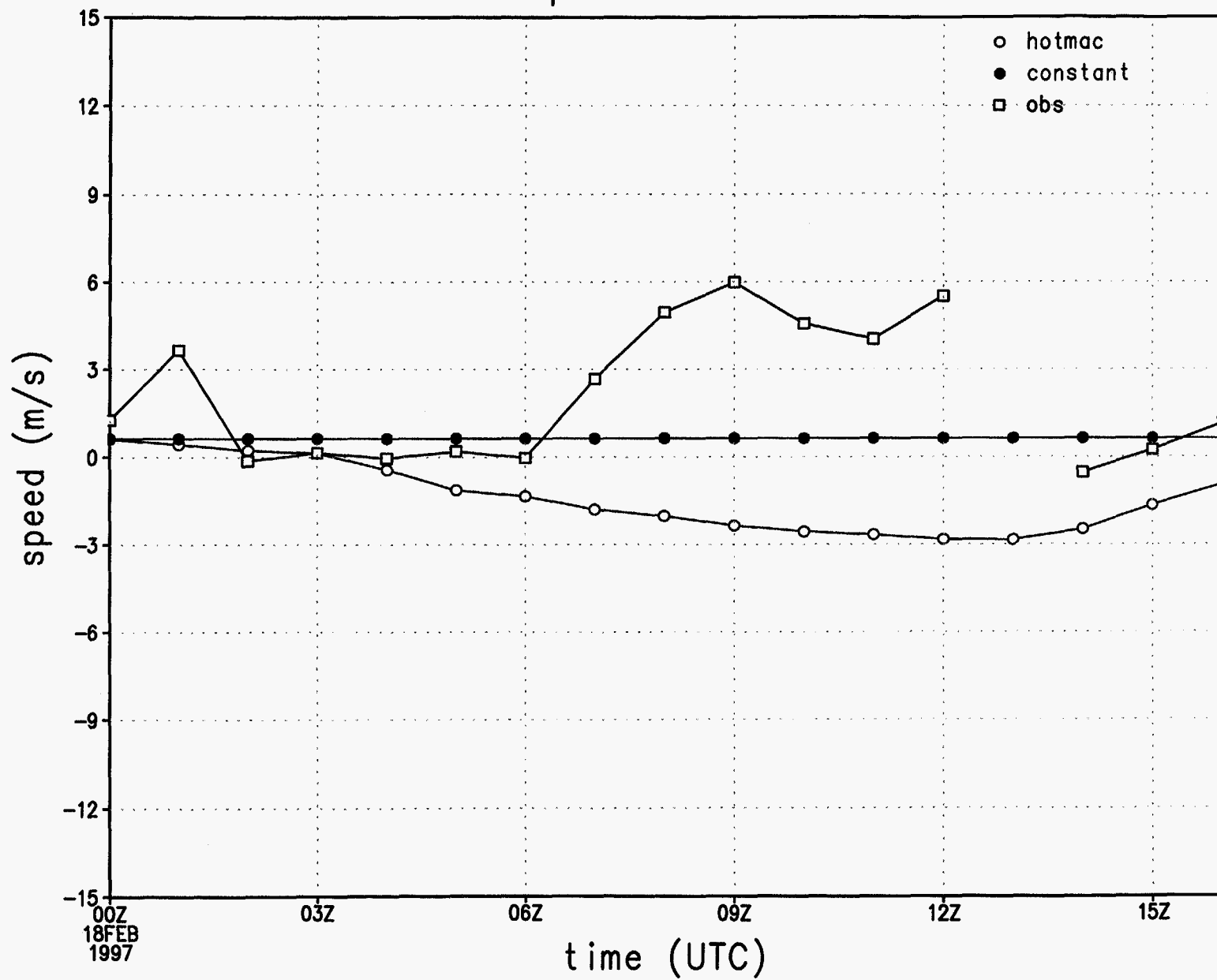


Figure 21e.

v wind component at station 1

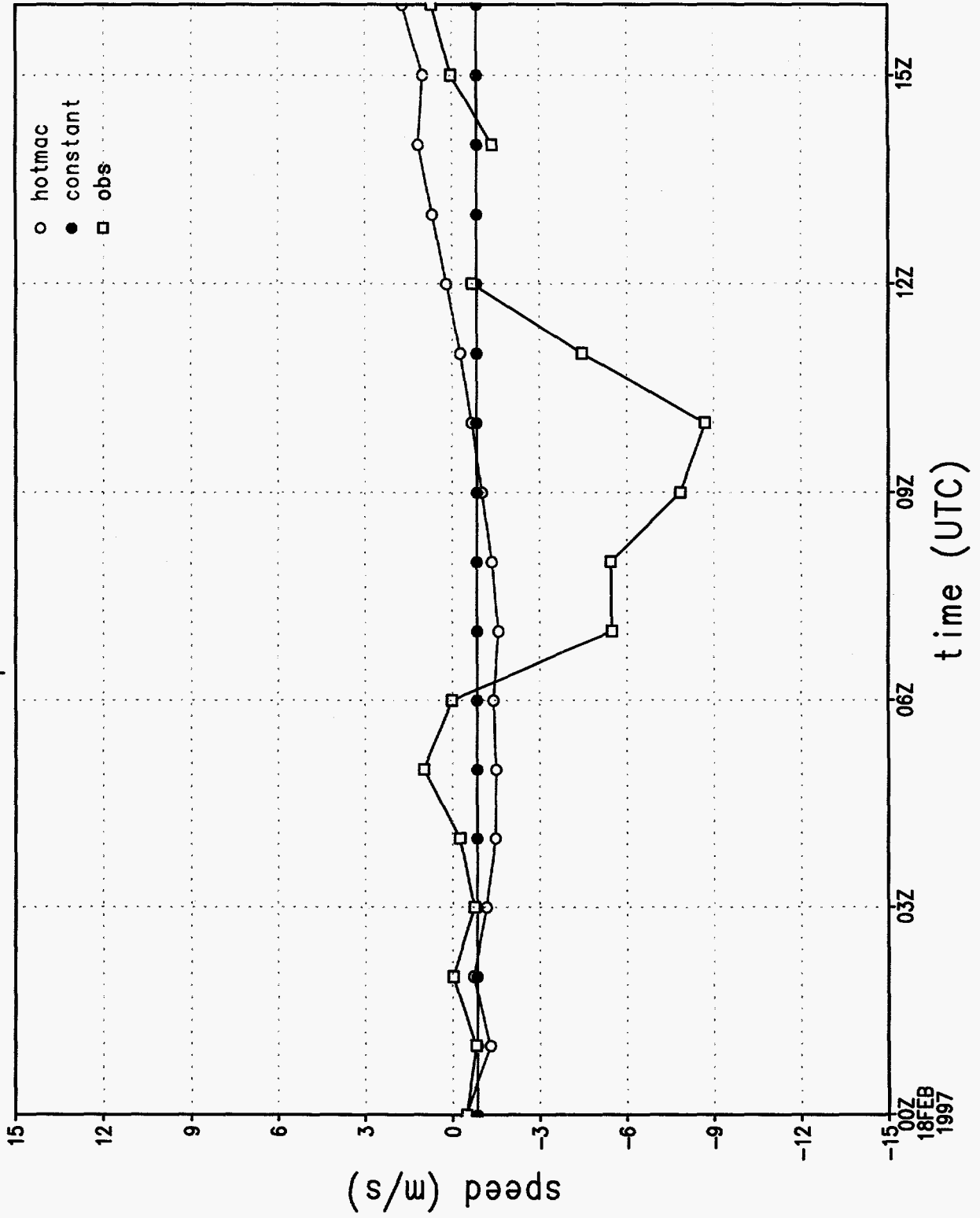


Figure 21f.

# rmse of wind direction by hour

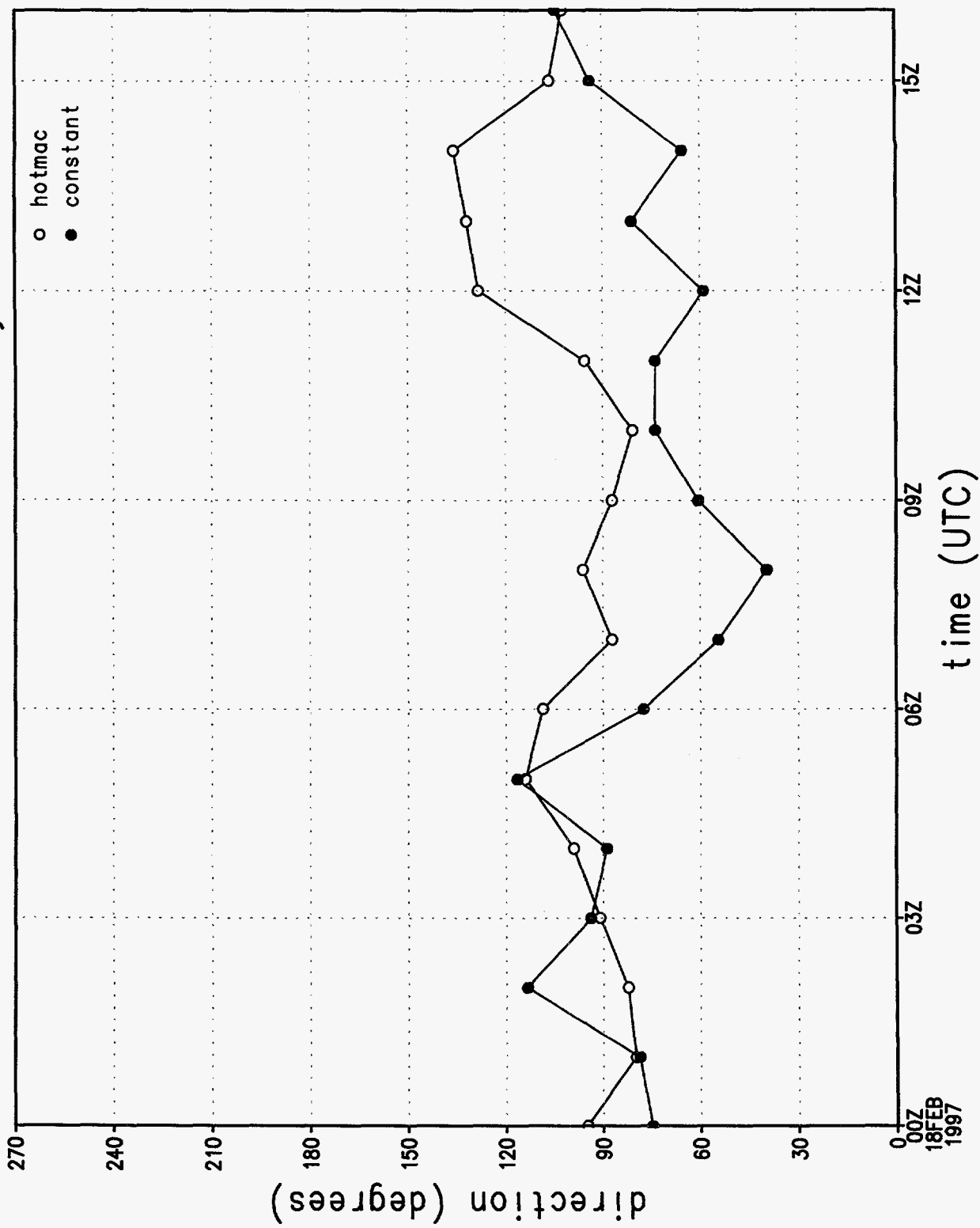


Figure 21g.

# rmse of wind speed by hour

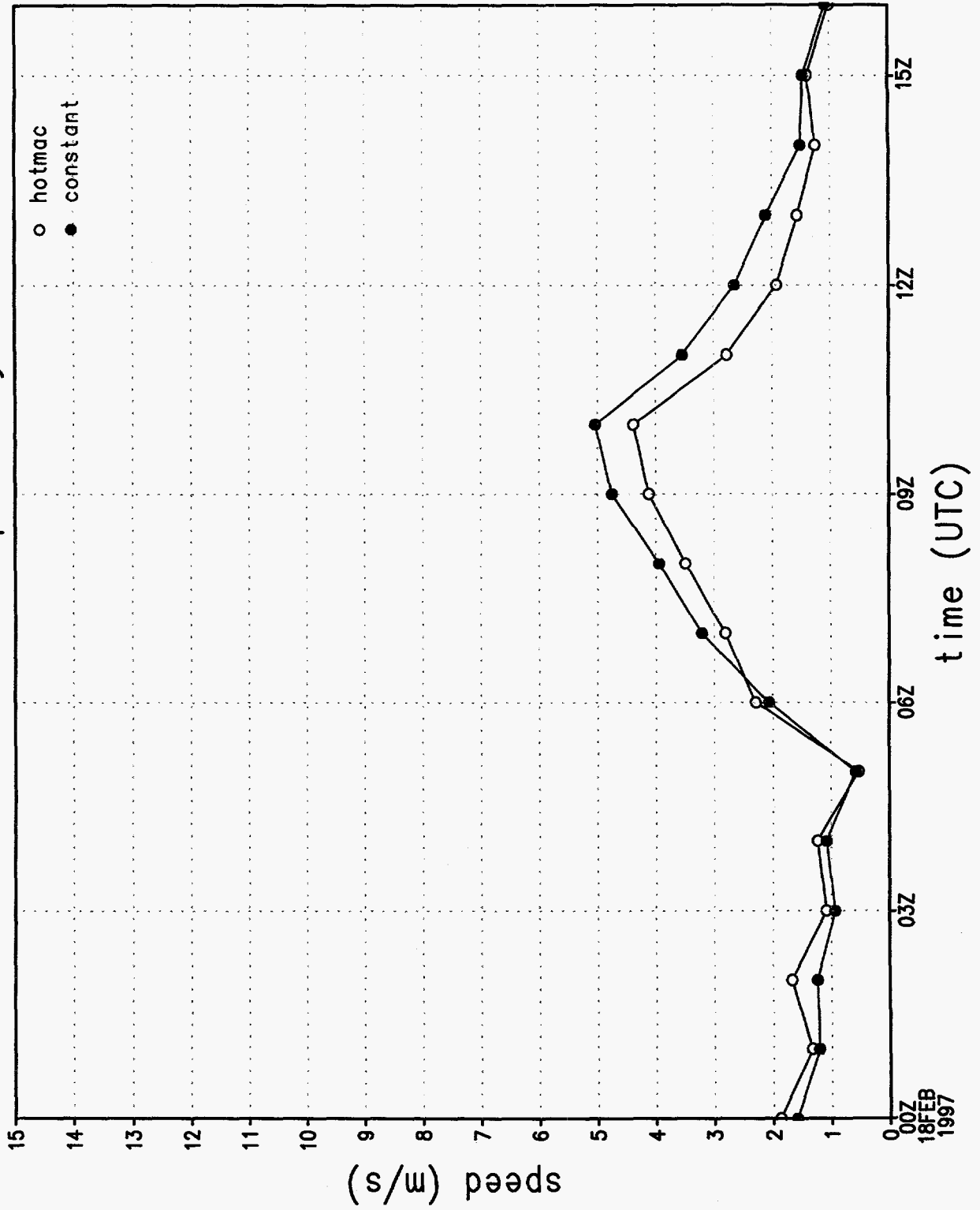


Figure 21h.

rmse of u wind component by hour

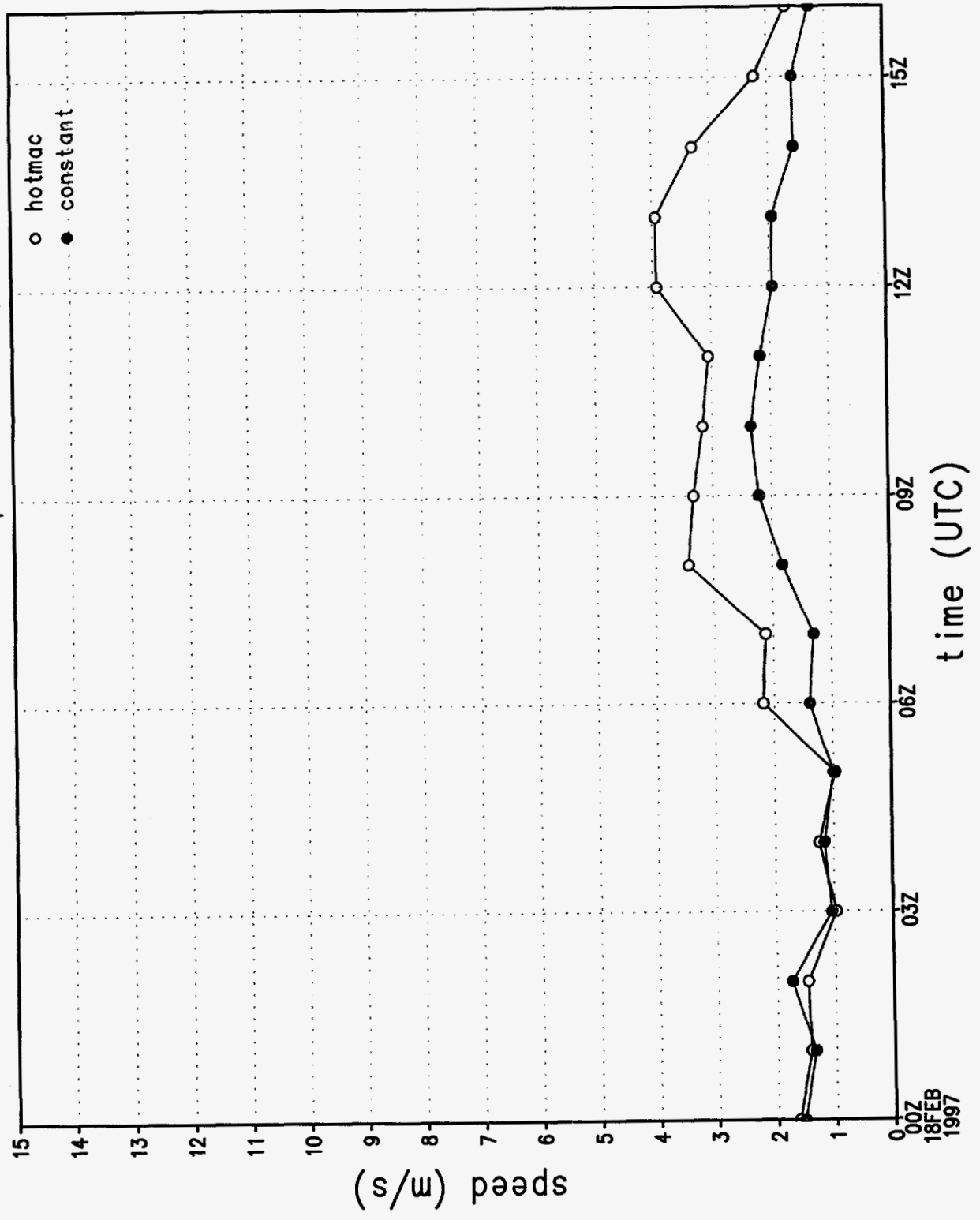


Figure 21 i.

rmse of v wind component by hour

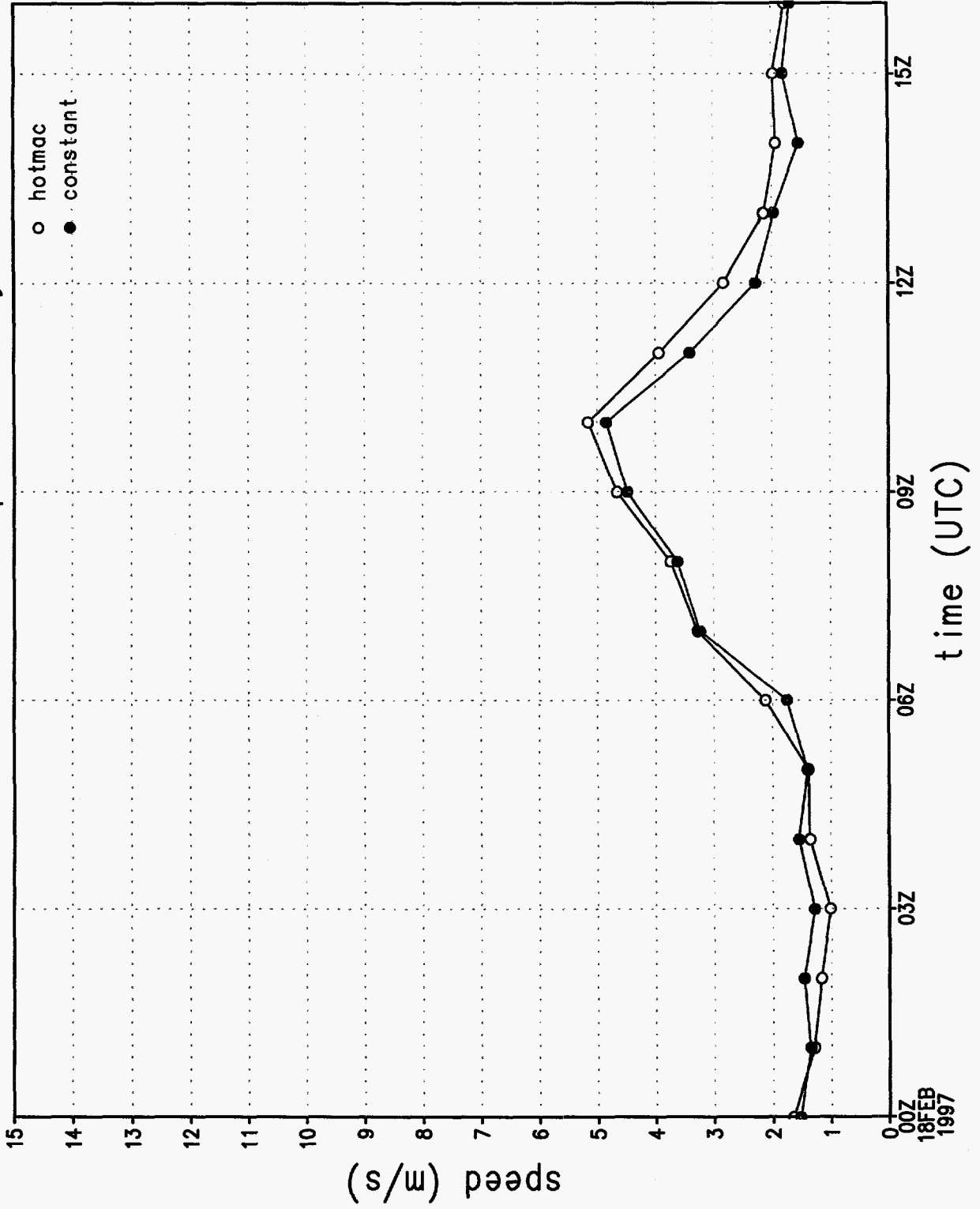


Figure 21j.



# wind direction sounding 1, 1072 m

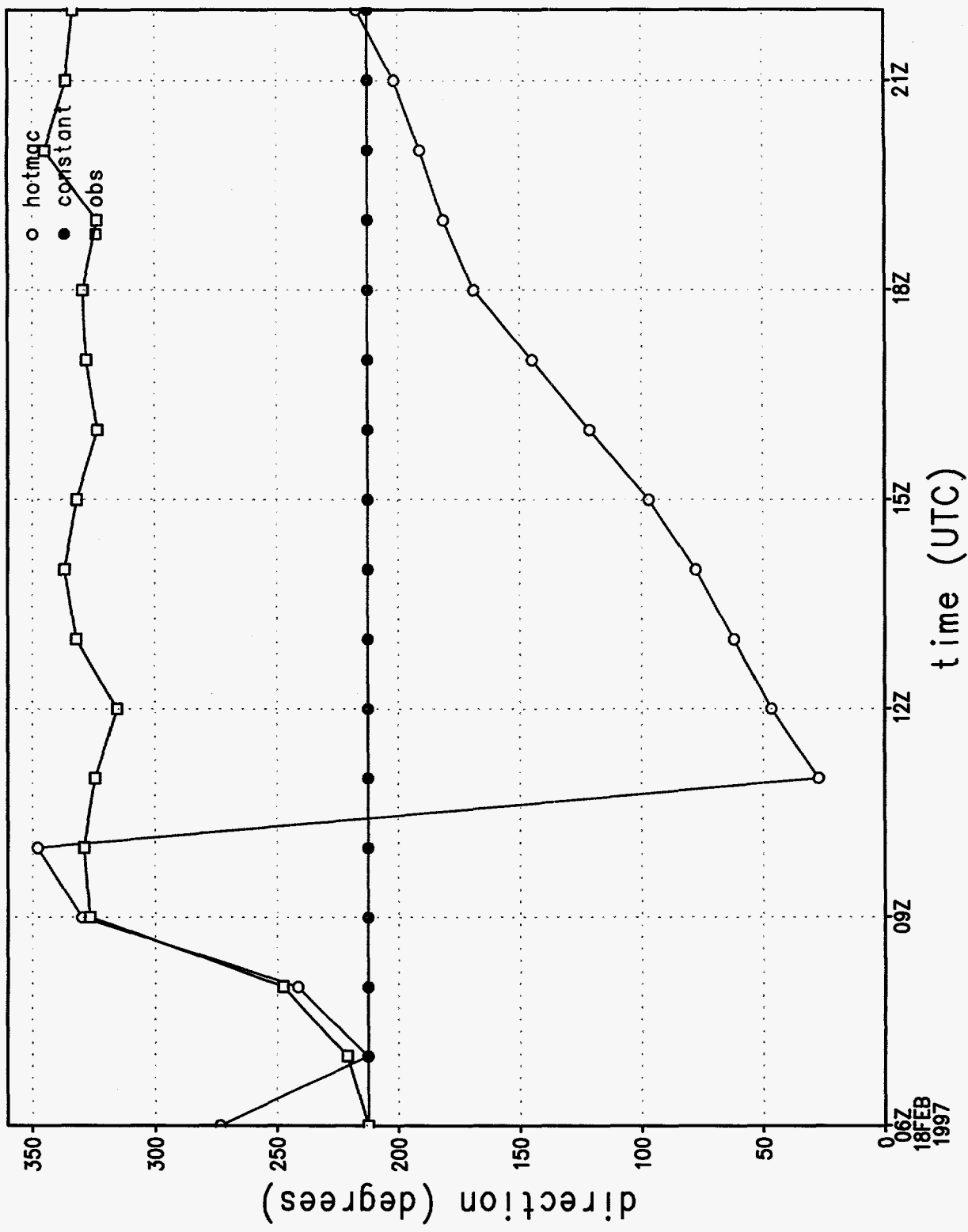


Figure 22a.

# wind speed sounding 1, 1072 m

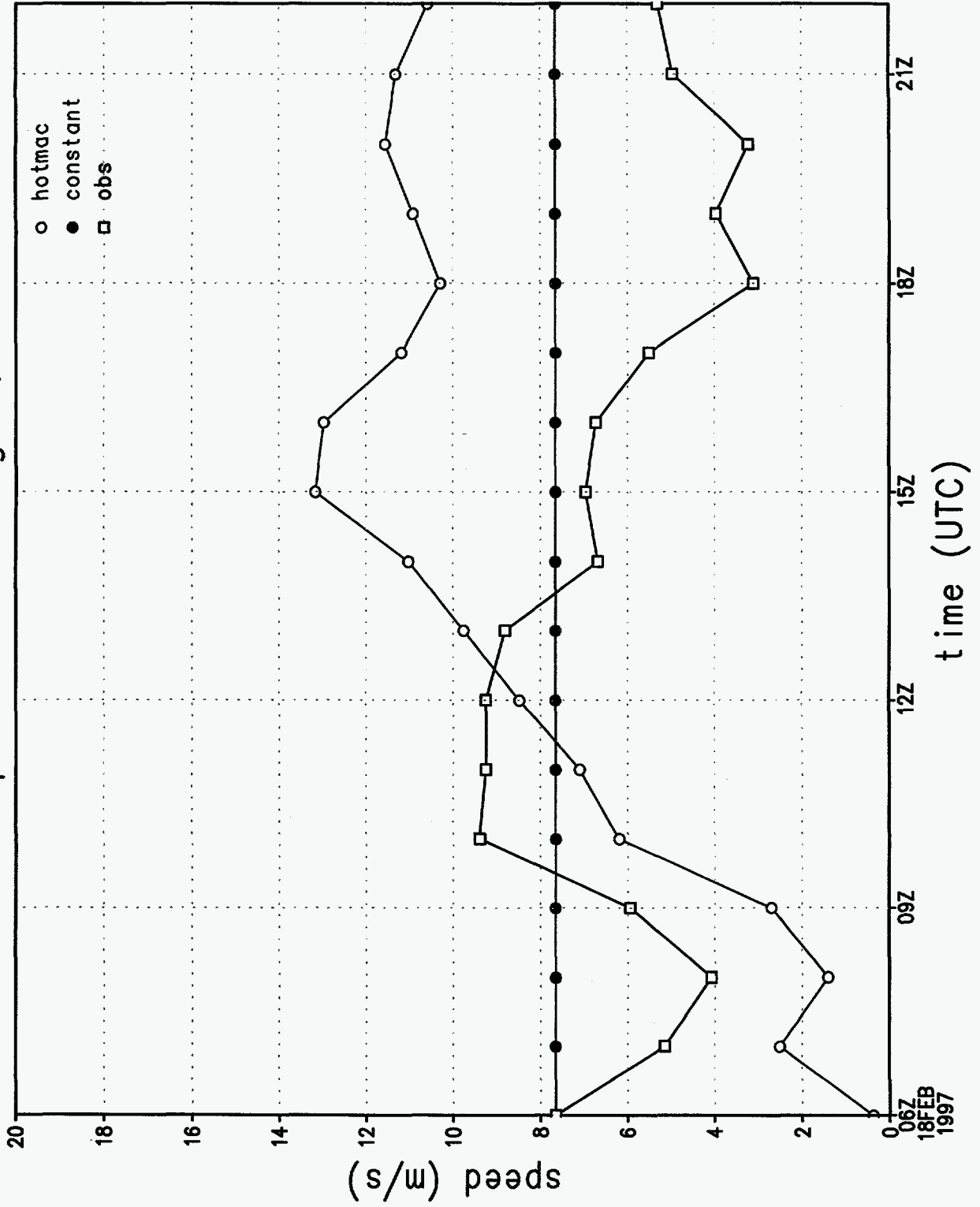


Figure 22b.

# wind direction at station 1

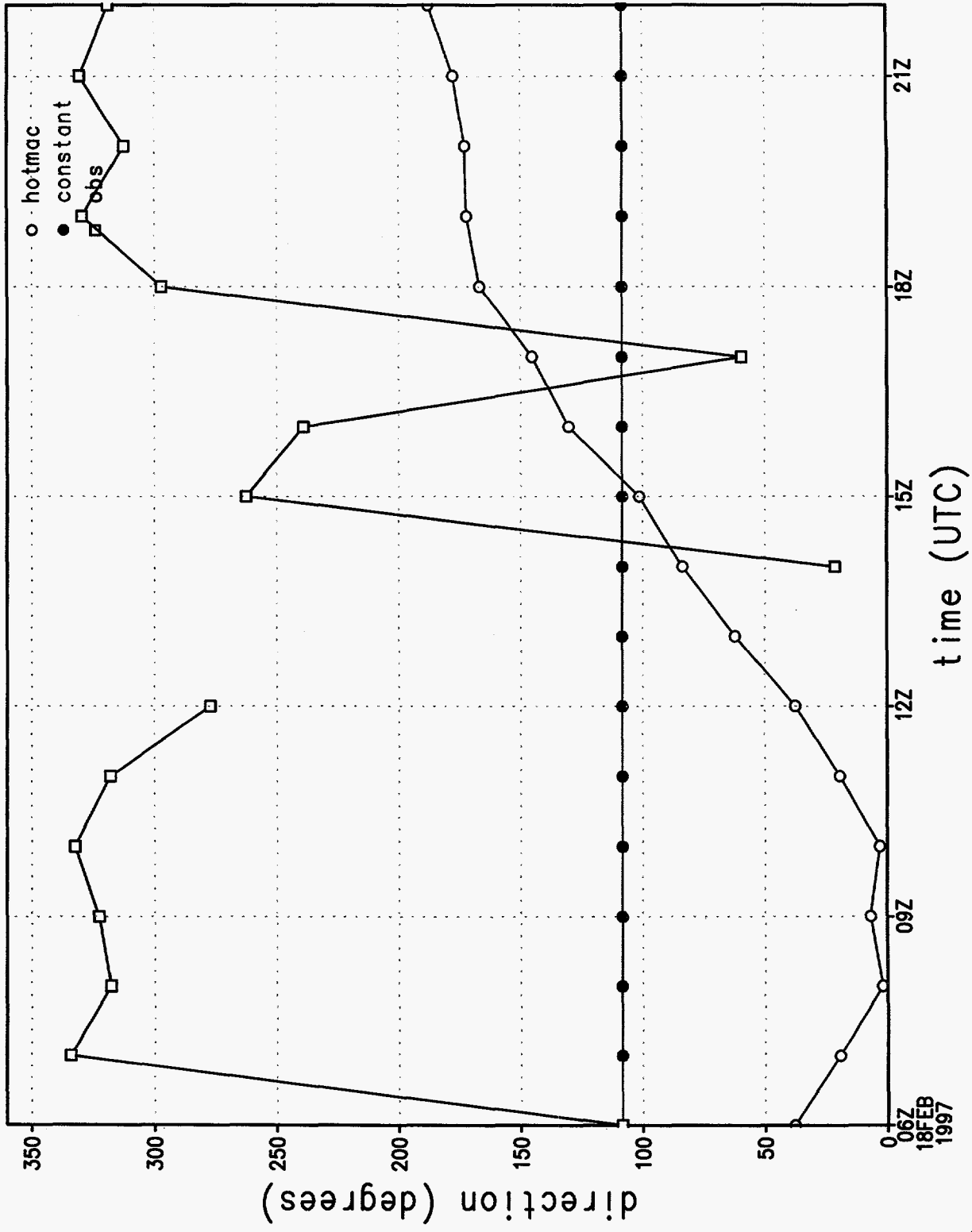


Figure 22c.

# wind speed at station 1

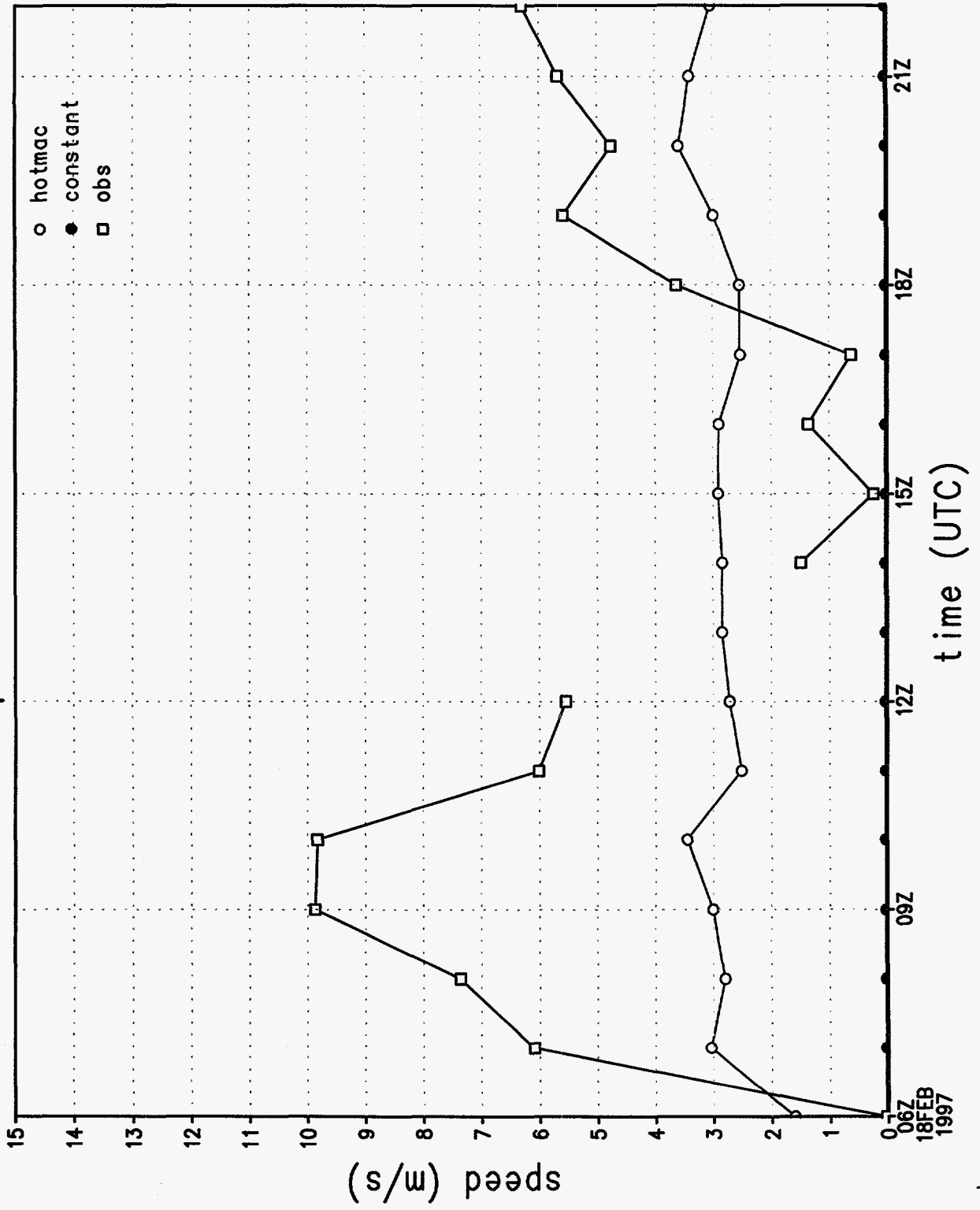


Figure 22d.

# u wind component at station 1

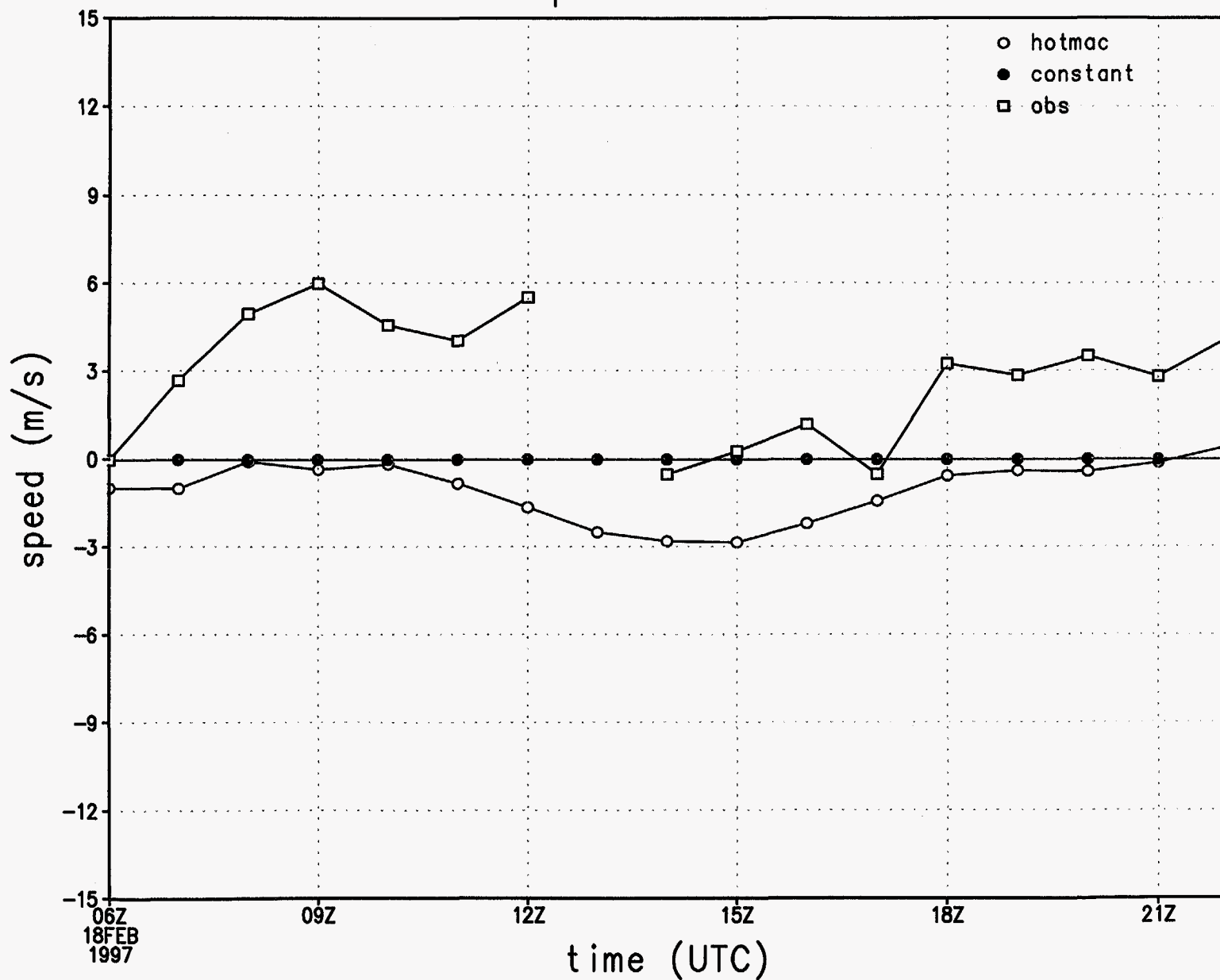


Figure 22e.

# v wind component at station 1

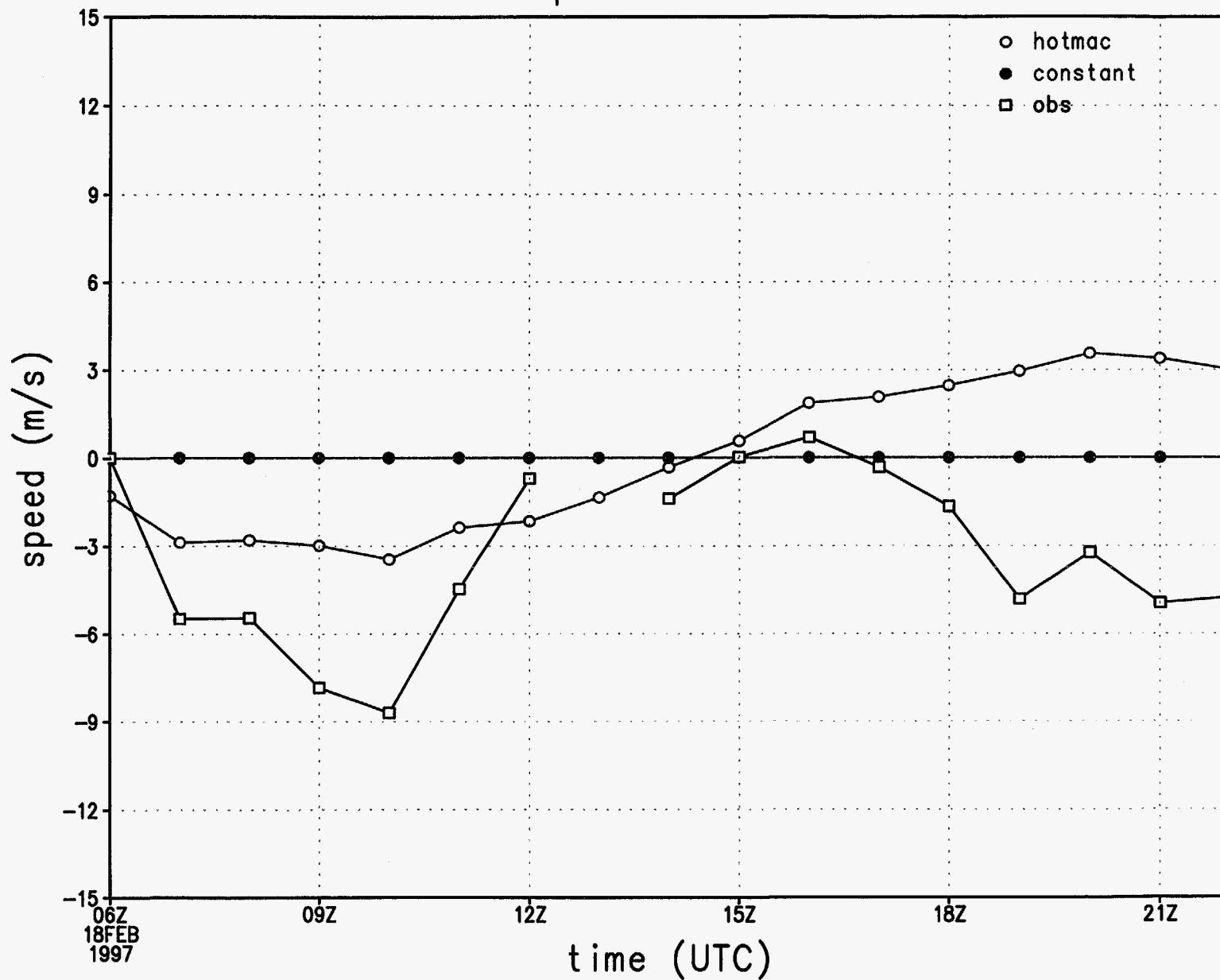


Figure 22 f.

# rmse of wind direction by hour

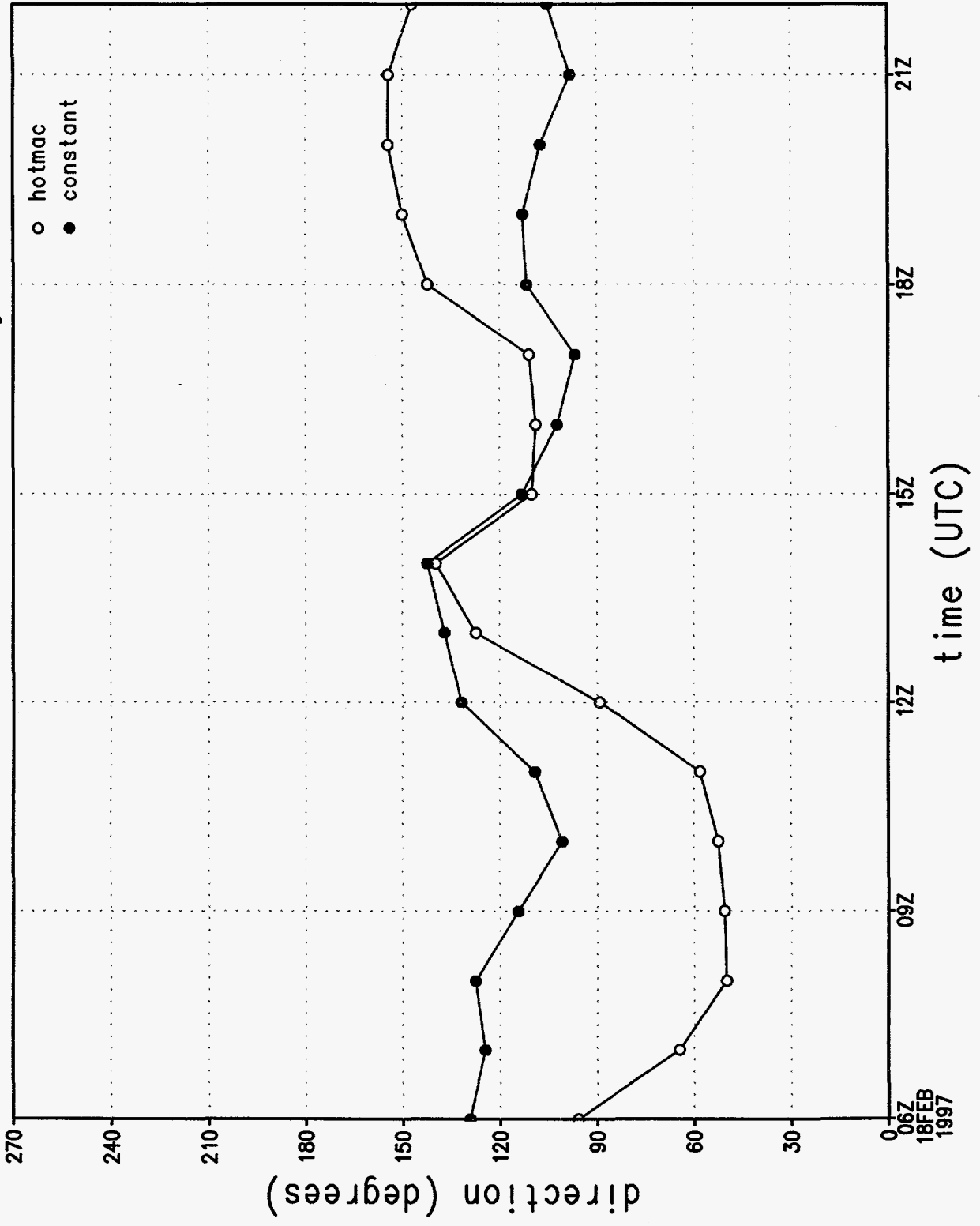


Figure 22g.

# rmse of wind speed by hour

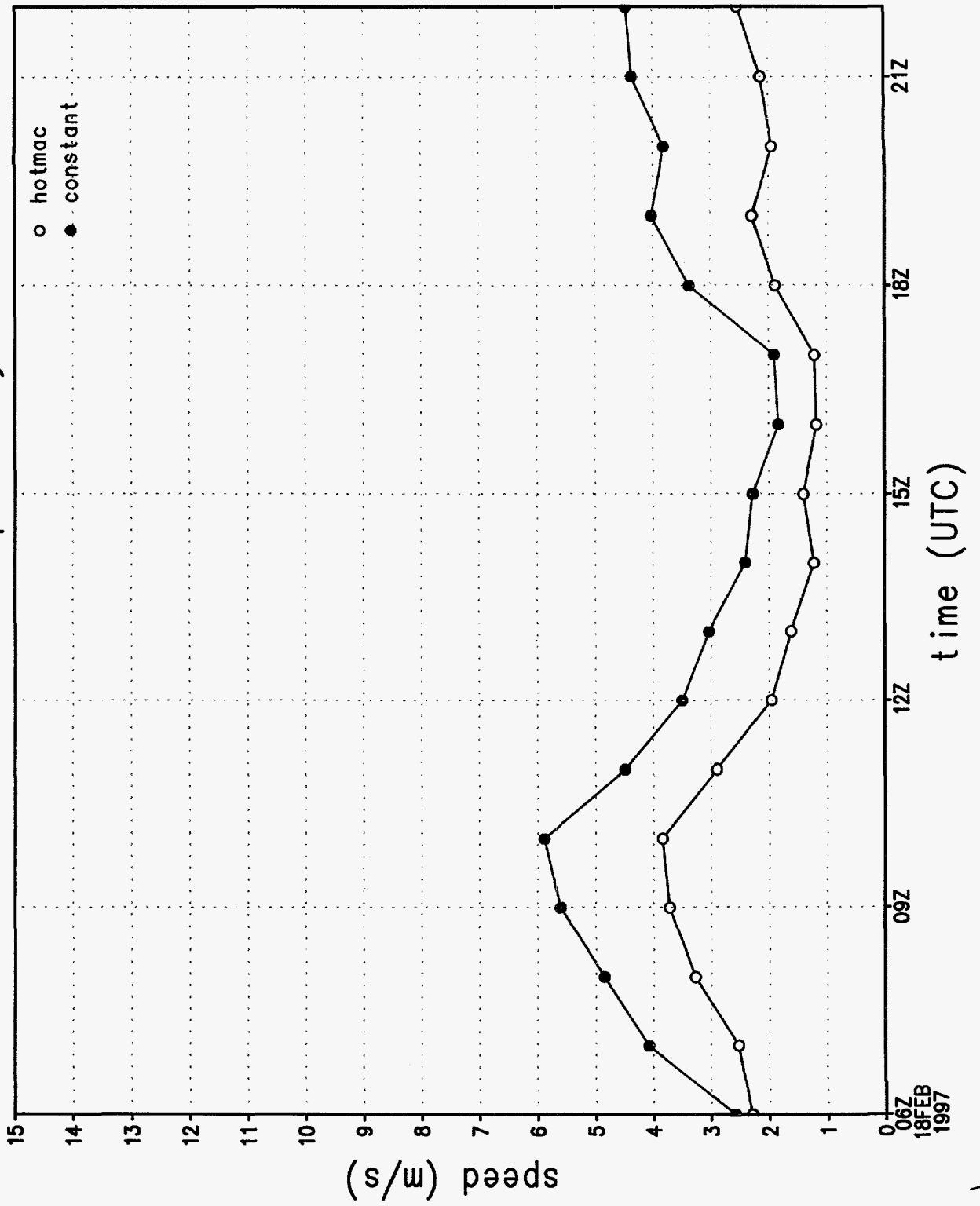


Figure 22 h.



rmse of u wind component by hour

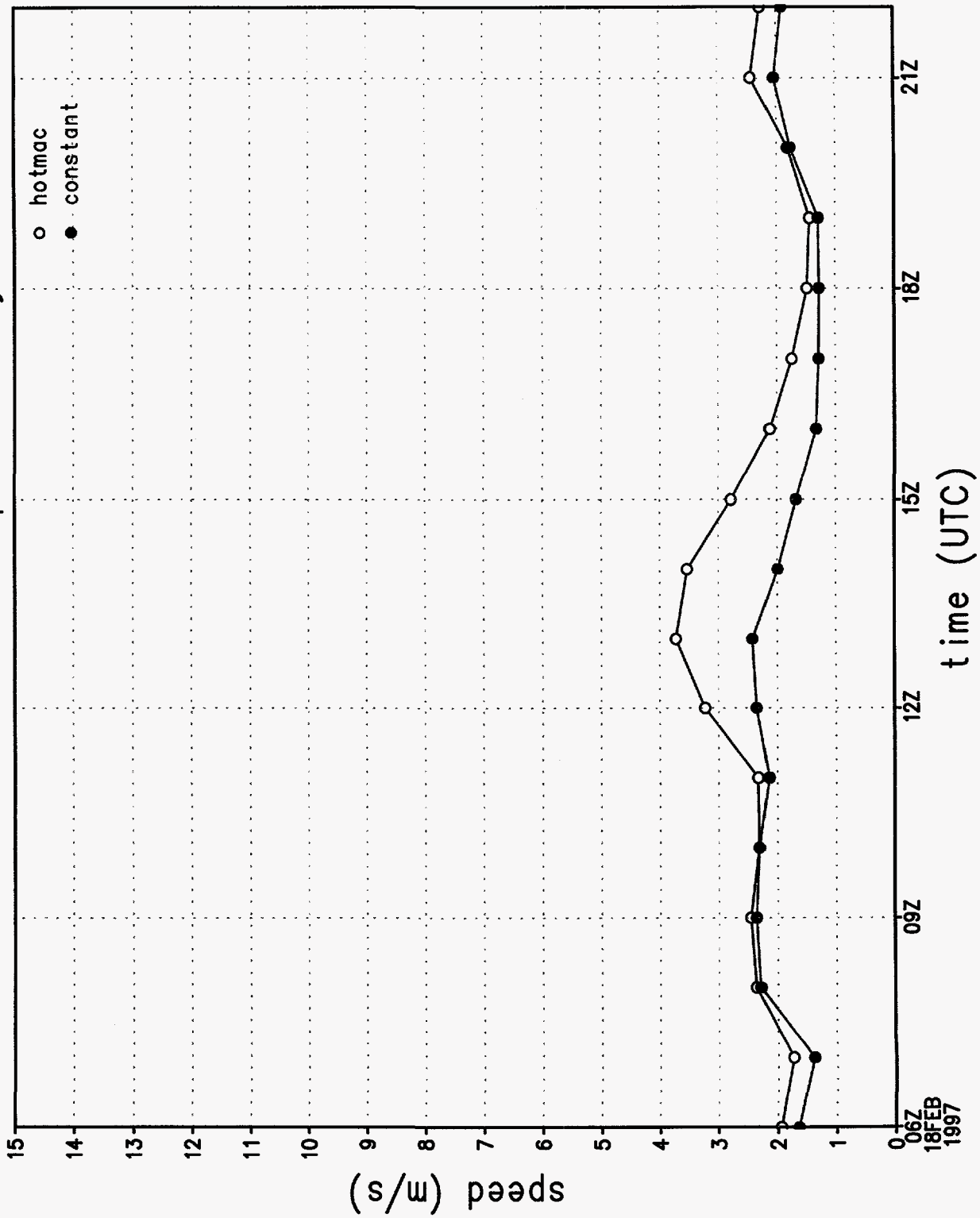


Figure 22i.

rmse of v wind component by hour

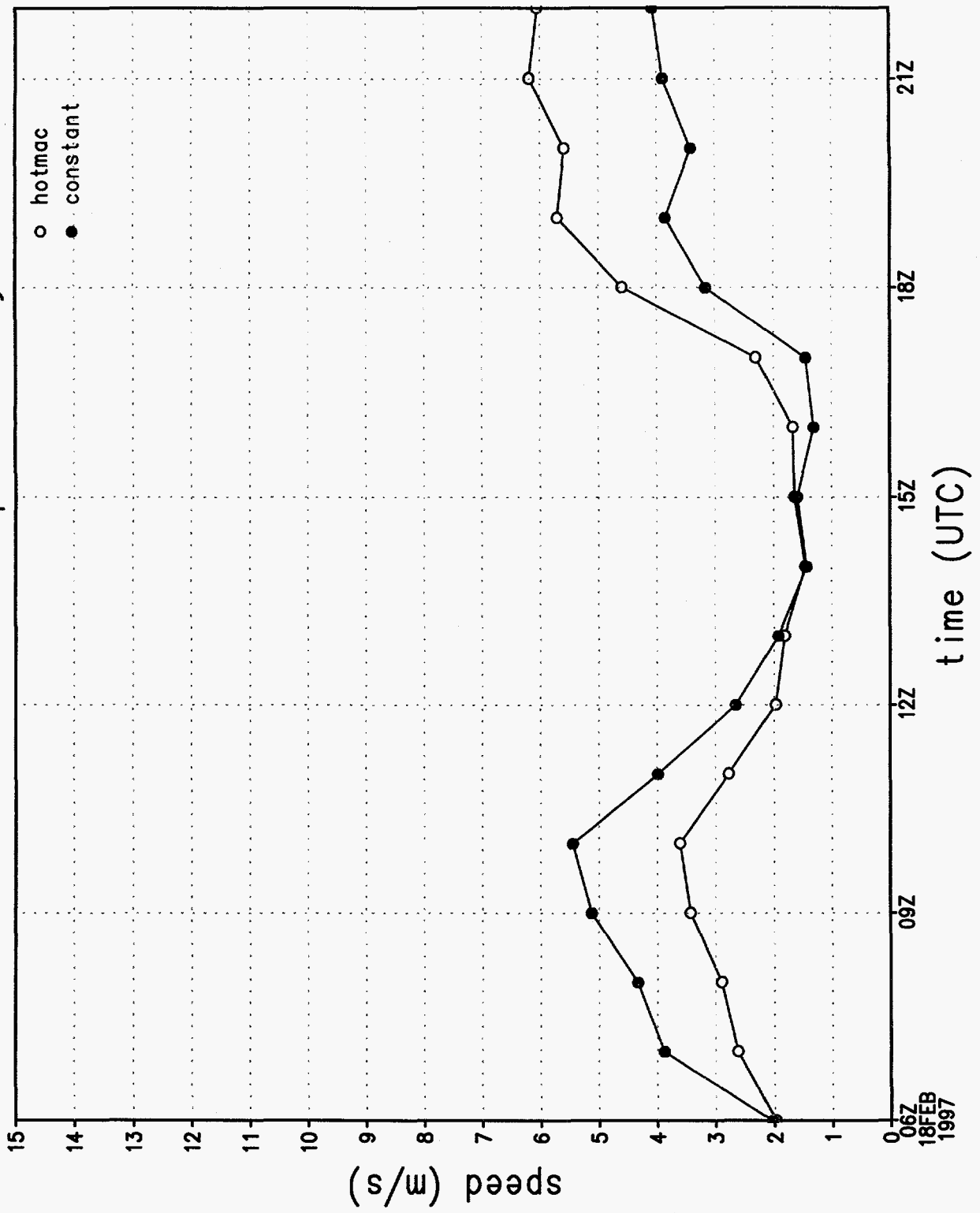


Figure 22j.

wind direction sounding 1, 1072 m

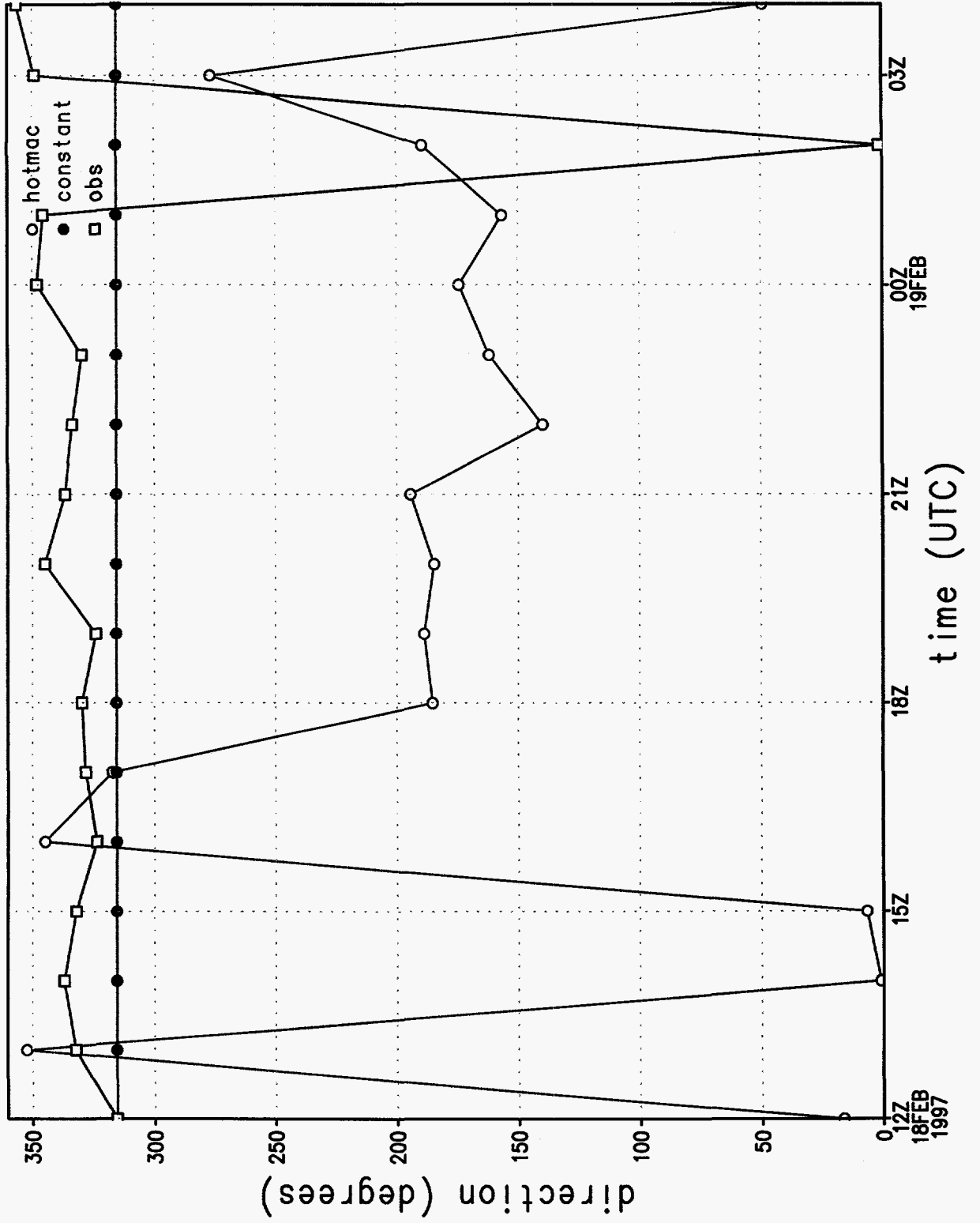


Figure 23a.

# wind speed sounding 1, 1072 m

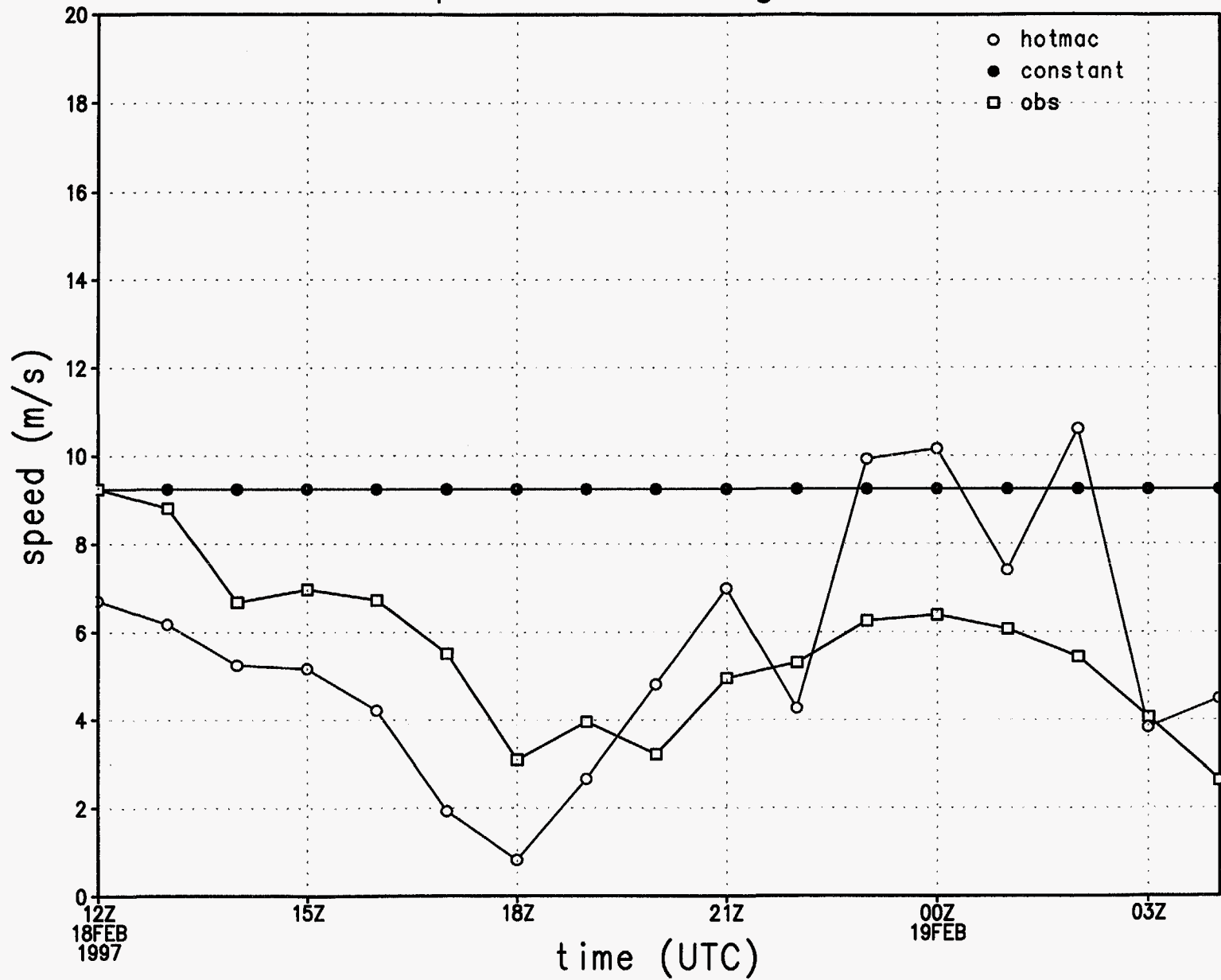


Figure 23 b.

# wind direction at station 1

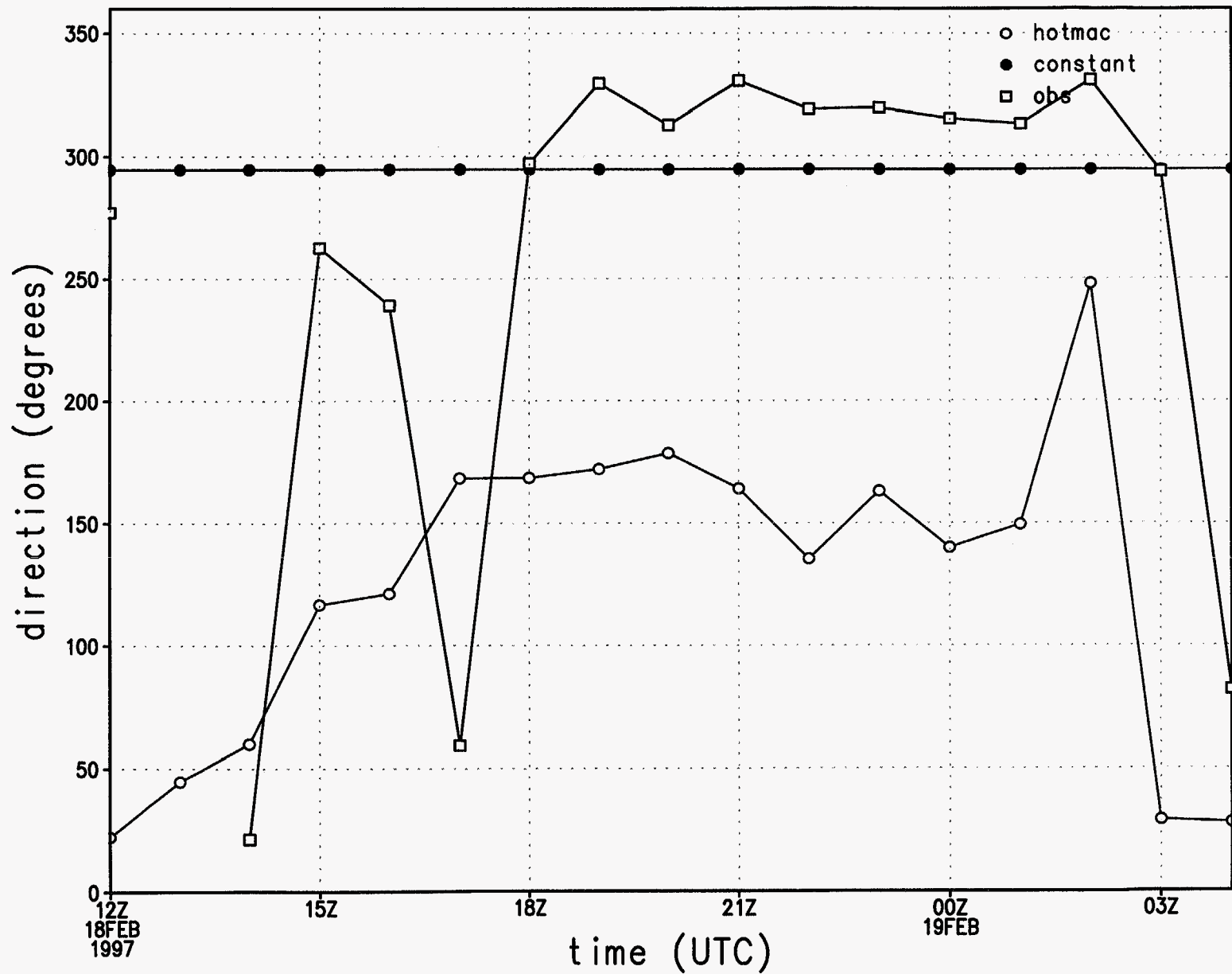


Figure 23c.

# wind speed at station 1

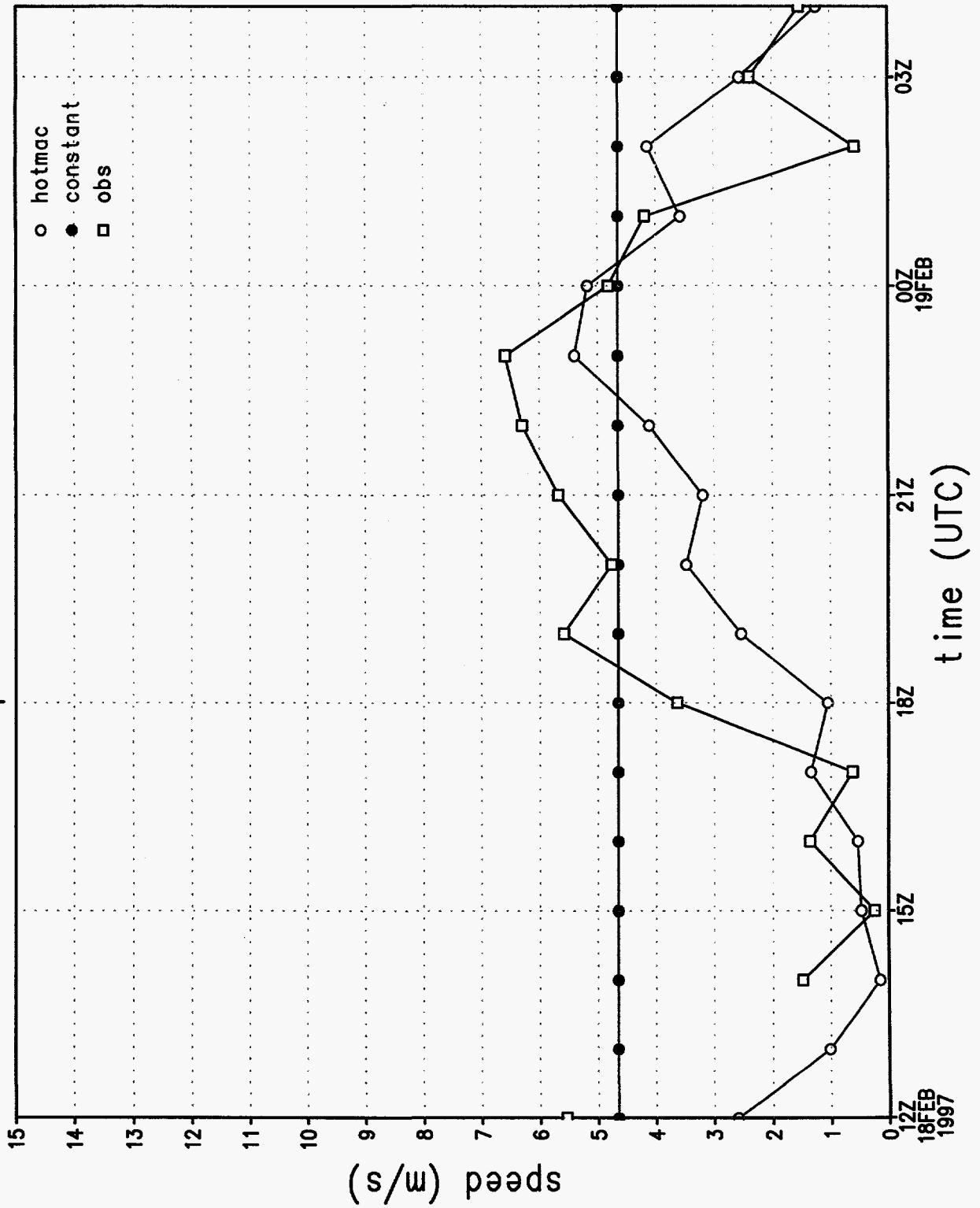


Figure 23d.

u wind component at station 1

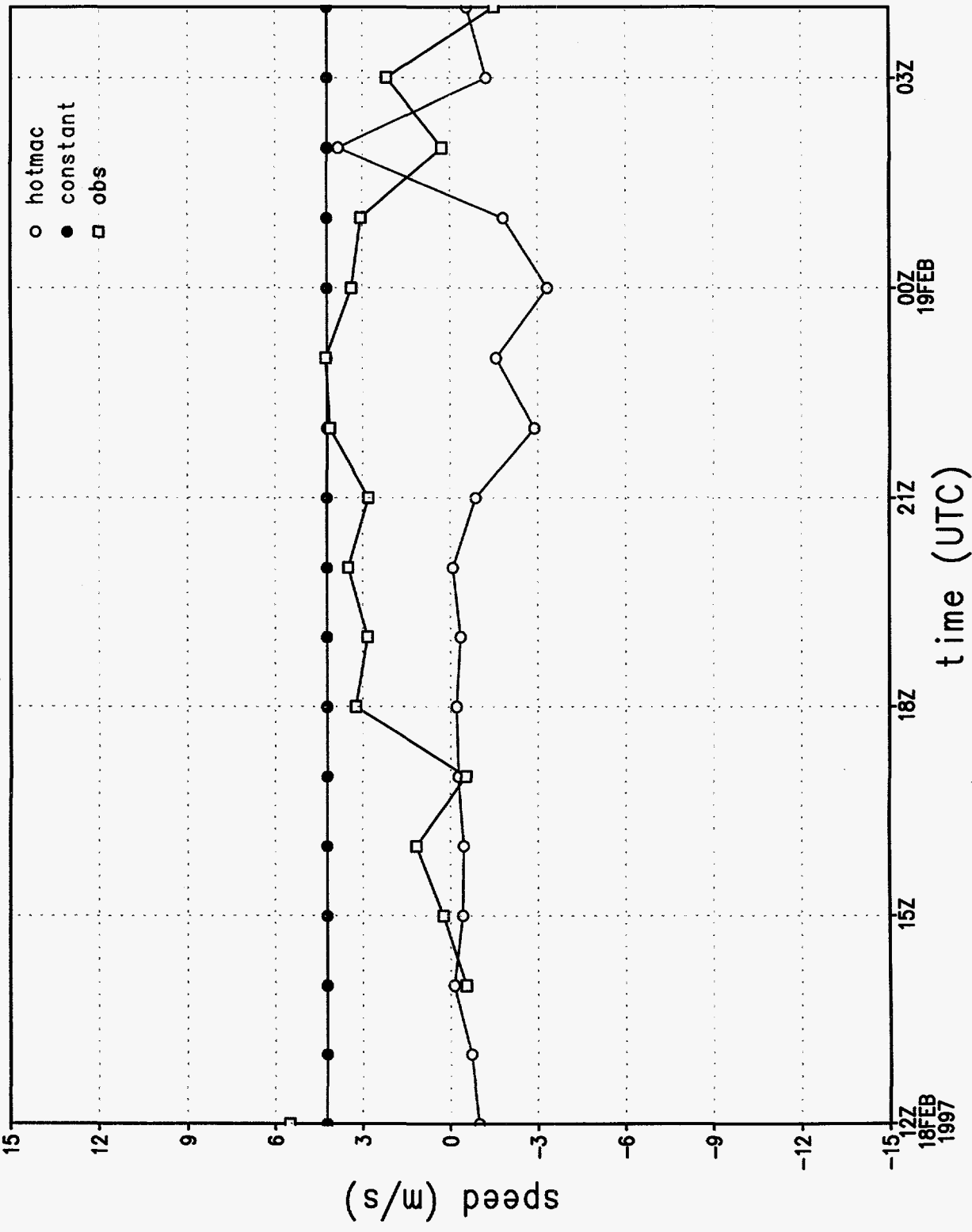


Figure 23c.

# v wind component at station 1

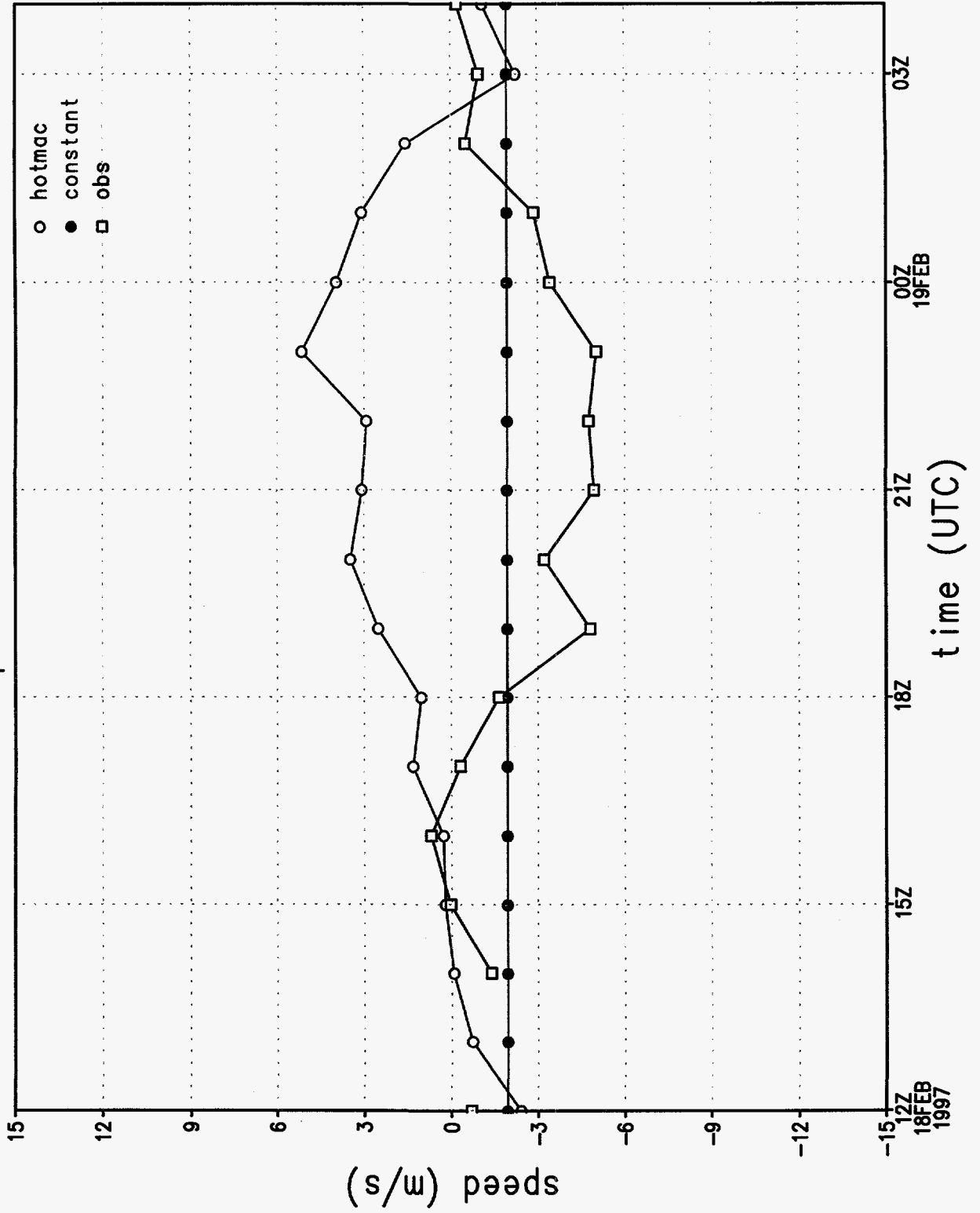


Figure 23f.



# rmse of wind direction by hour

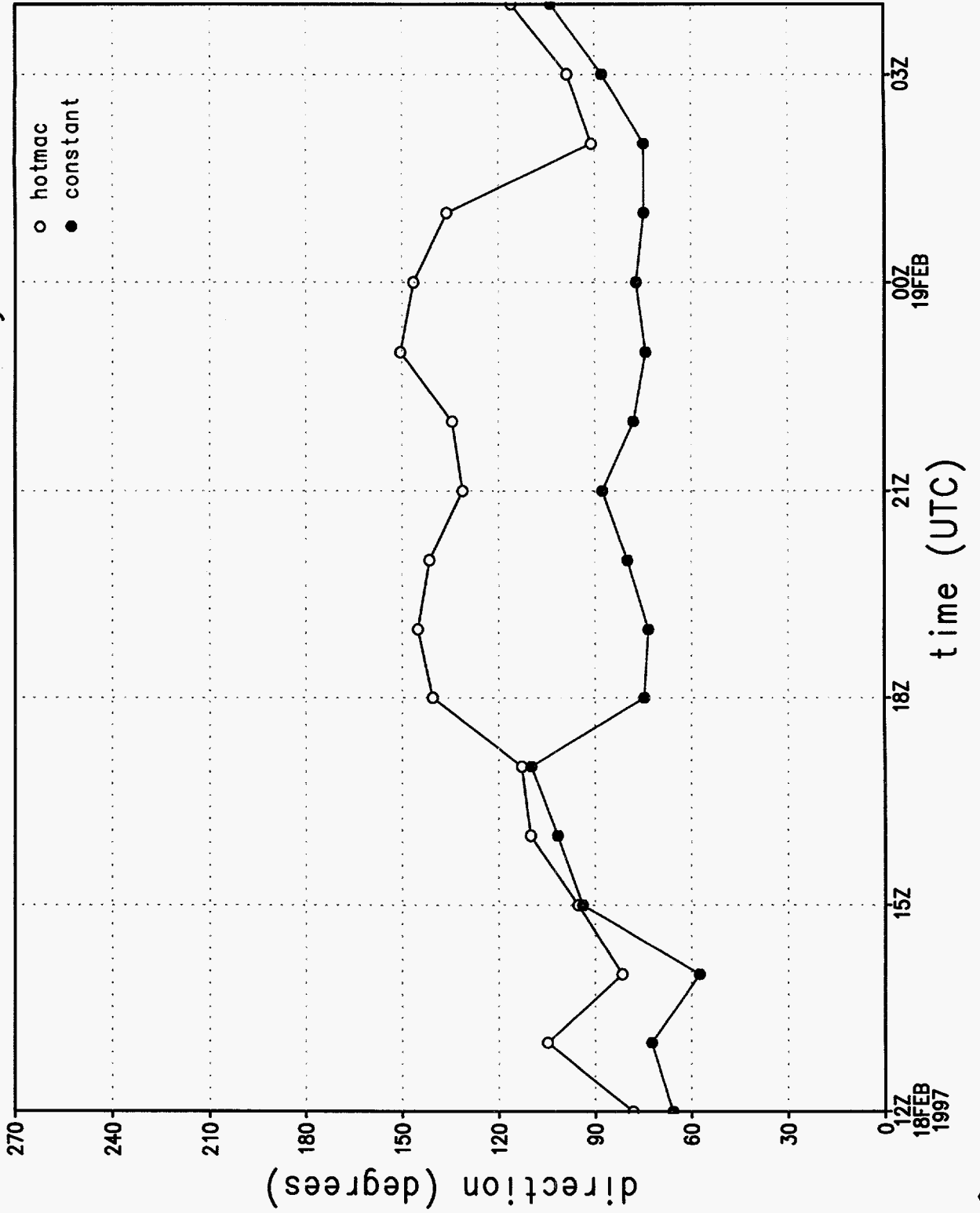


Figure 238.

# rmse of wind speed by hour

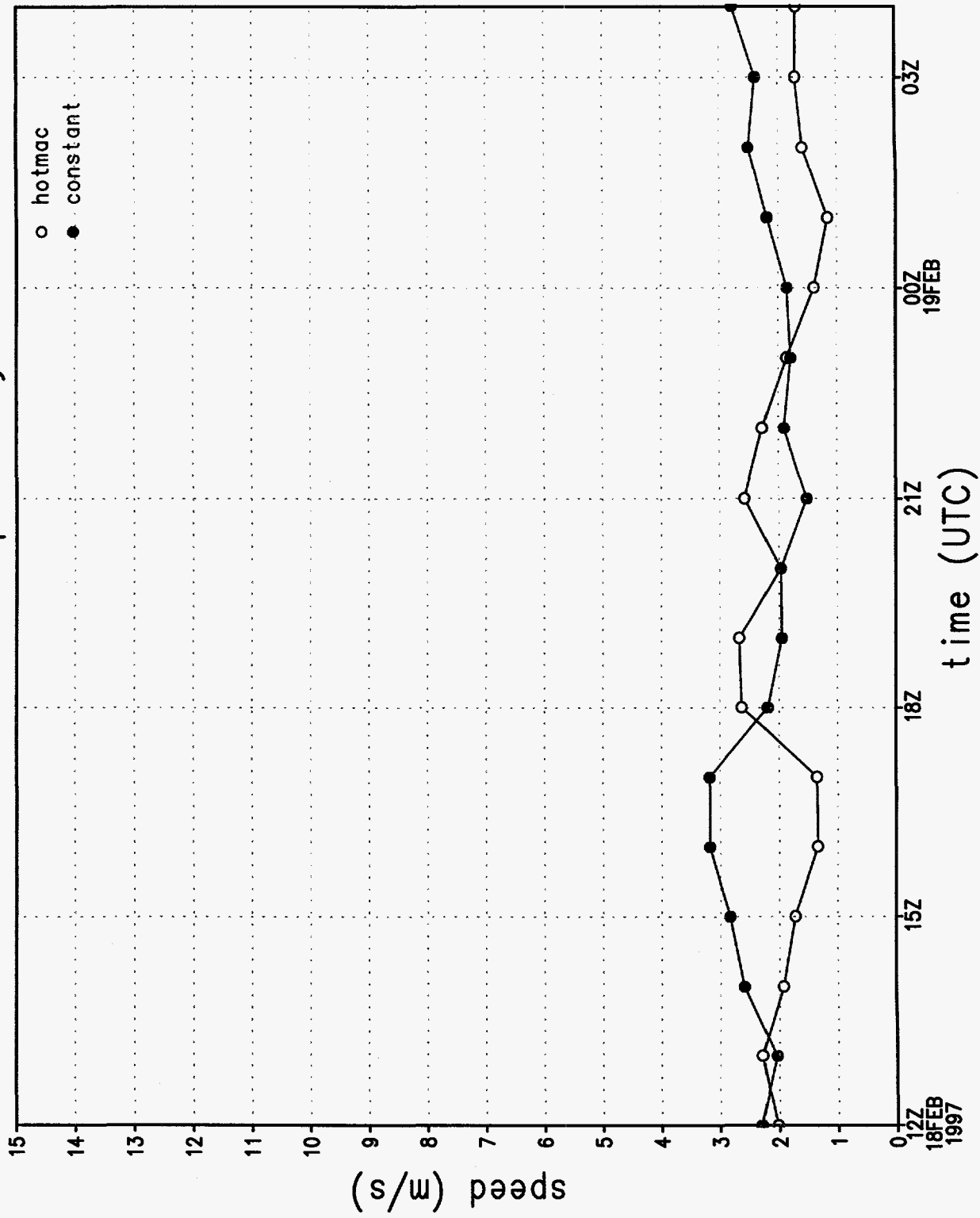


Figure 23h.

# rmse of u wind component by hour

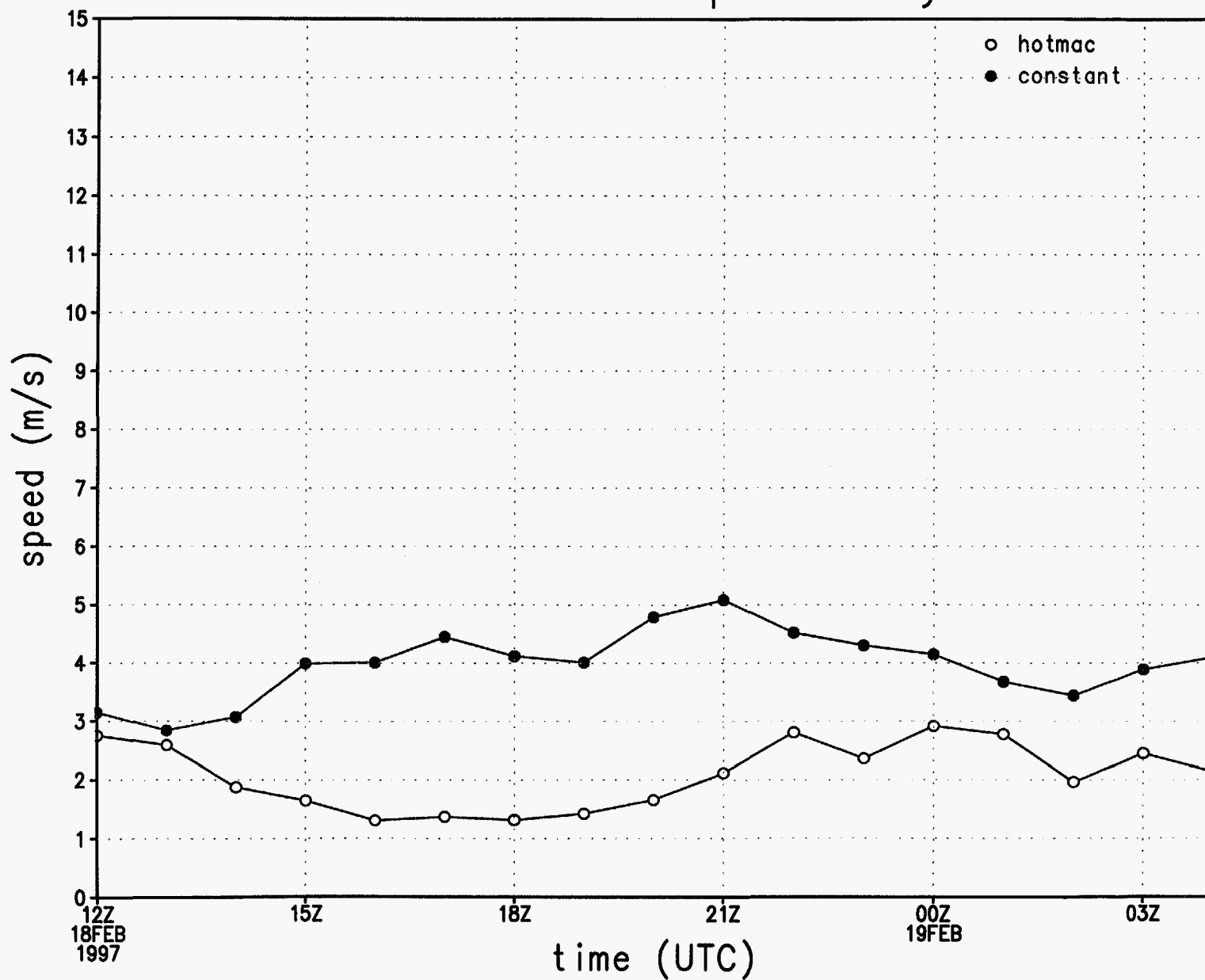


Figure 23i.

rmse of v wind component by hour

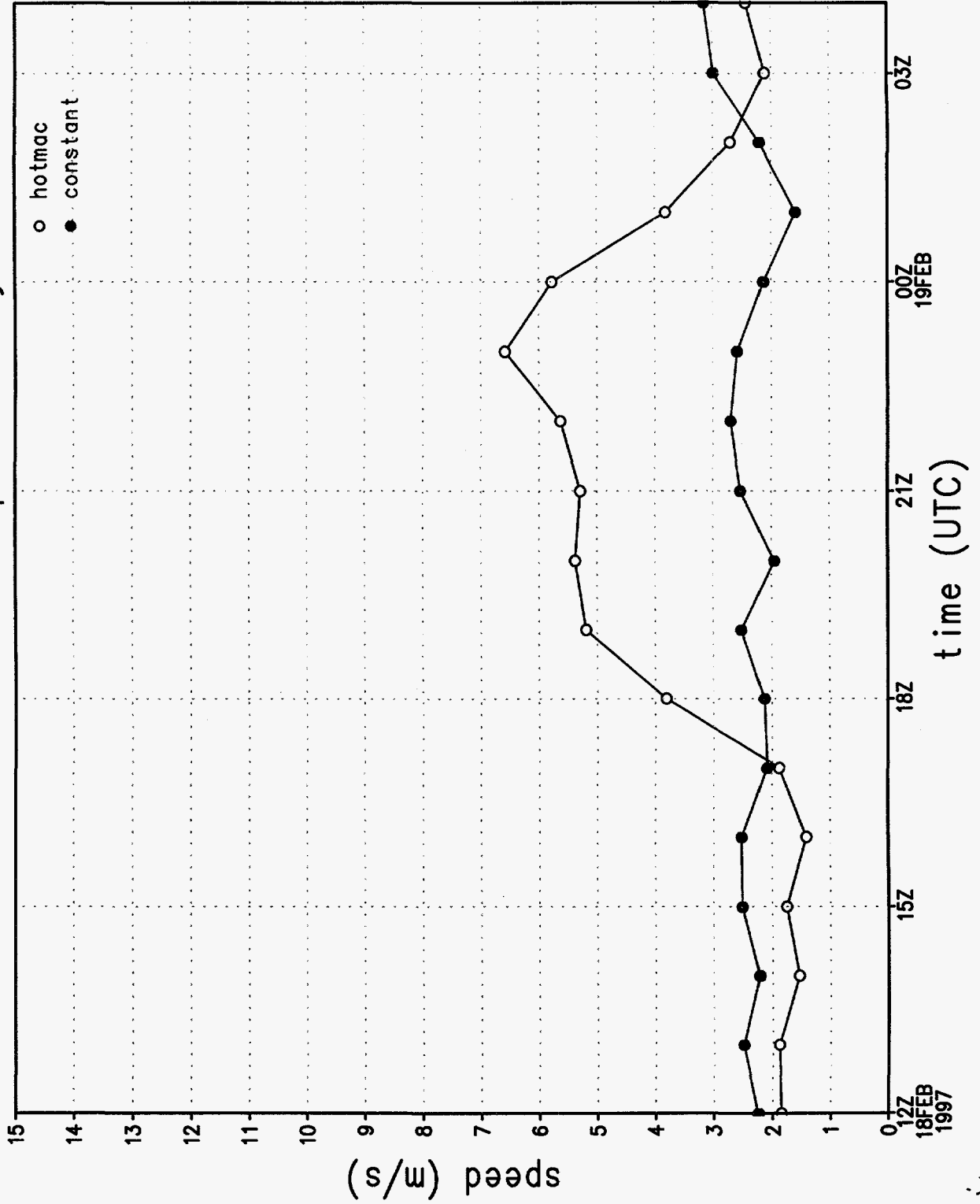


Figure 23j.

wind direction sounding 1, 1072 m

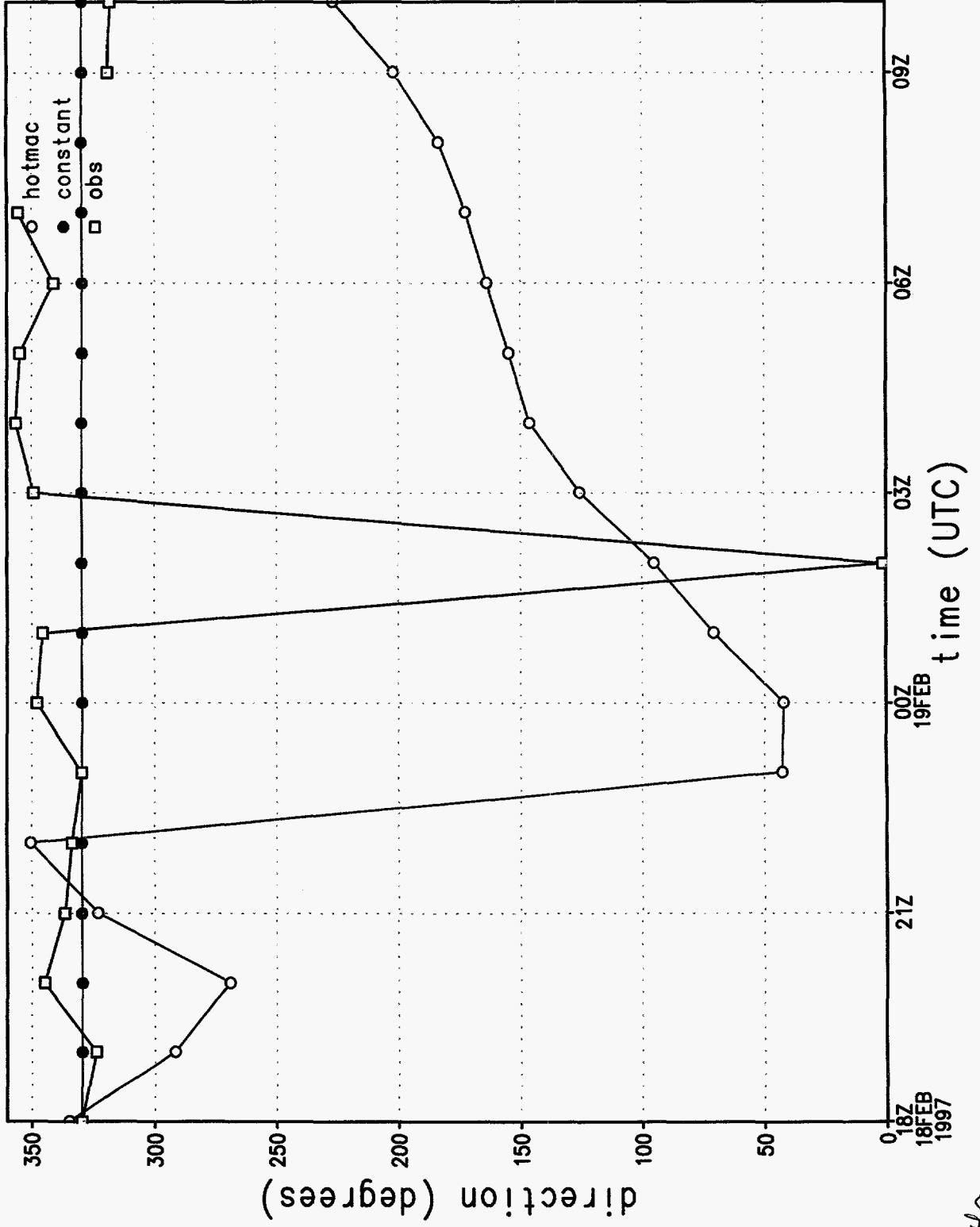


Figure 24a.

wind speed sounding 1, 1072 m

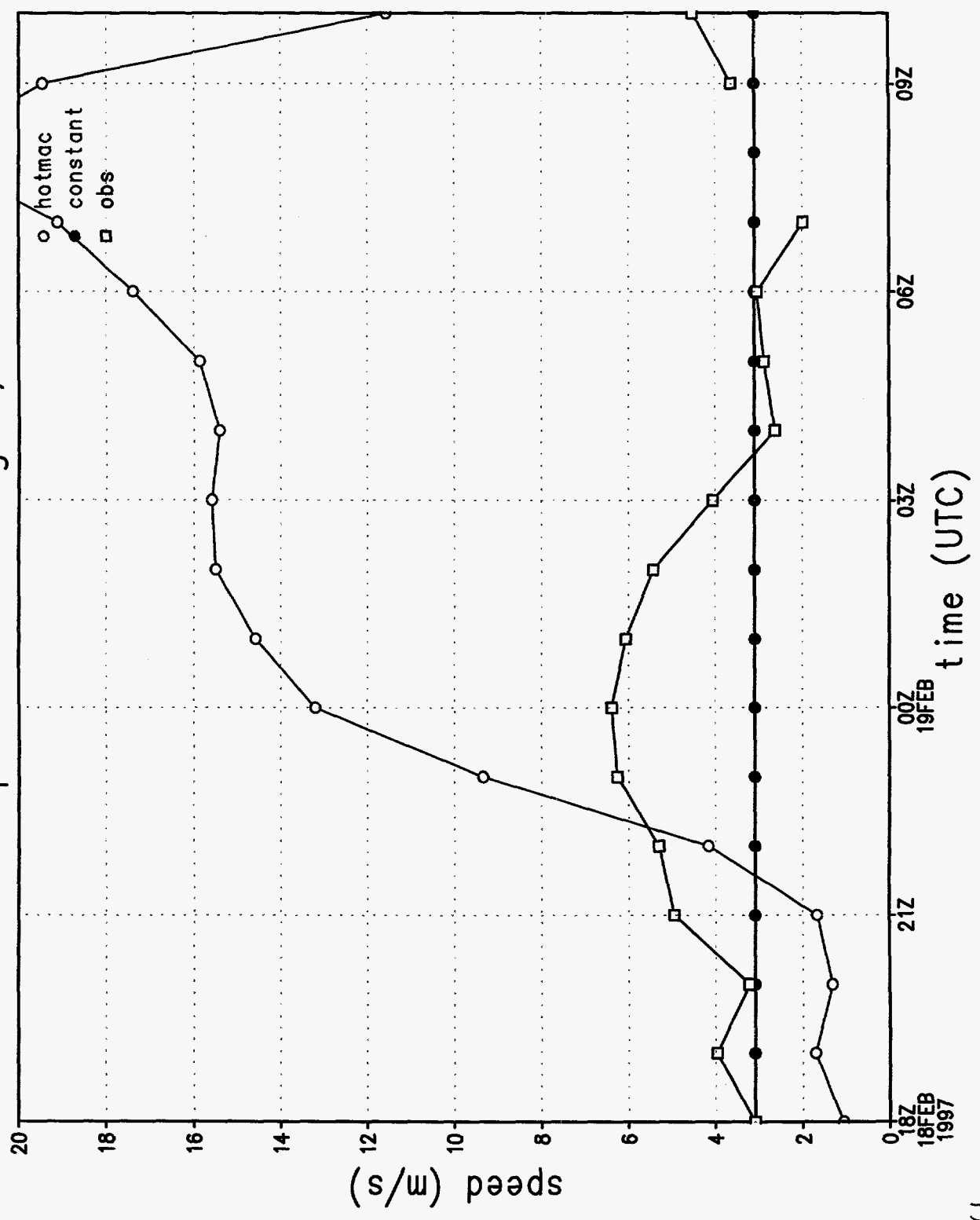


Figure 24b.

# wind direction at station 1

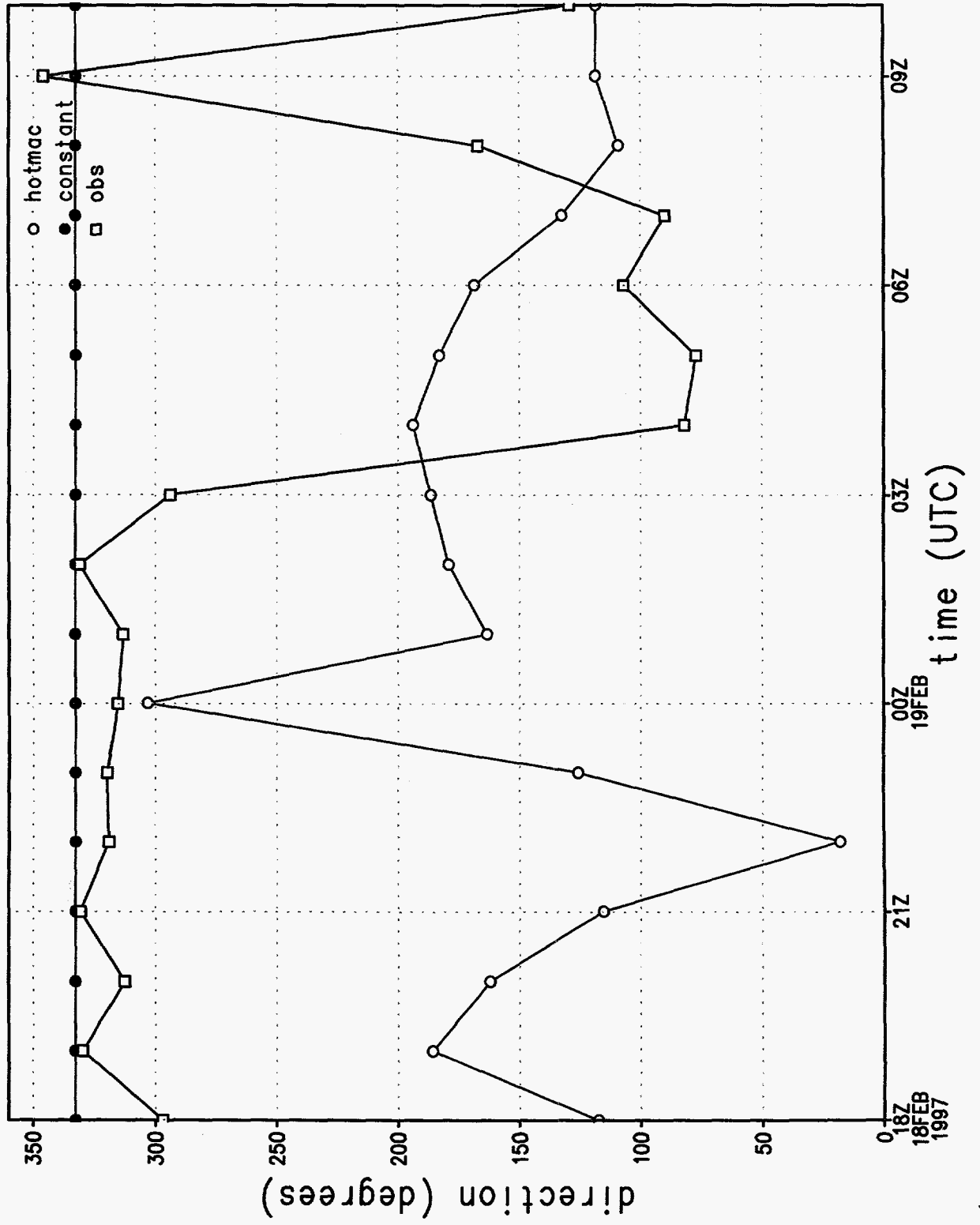


Figure 24c.

# wind speed at station 1

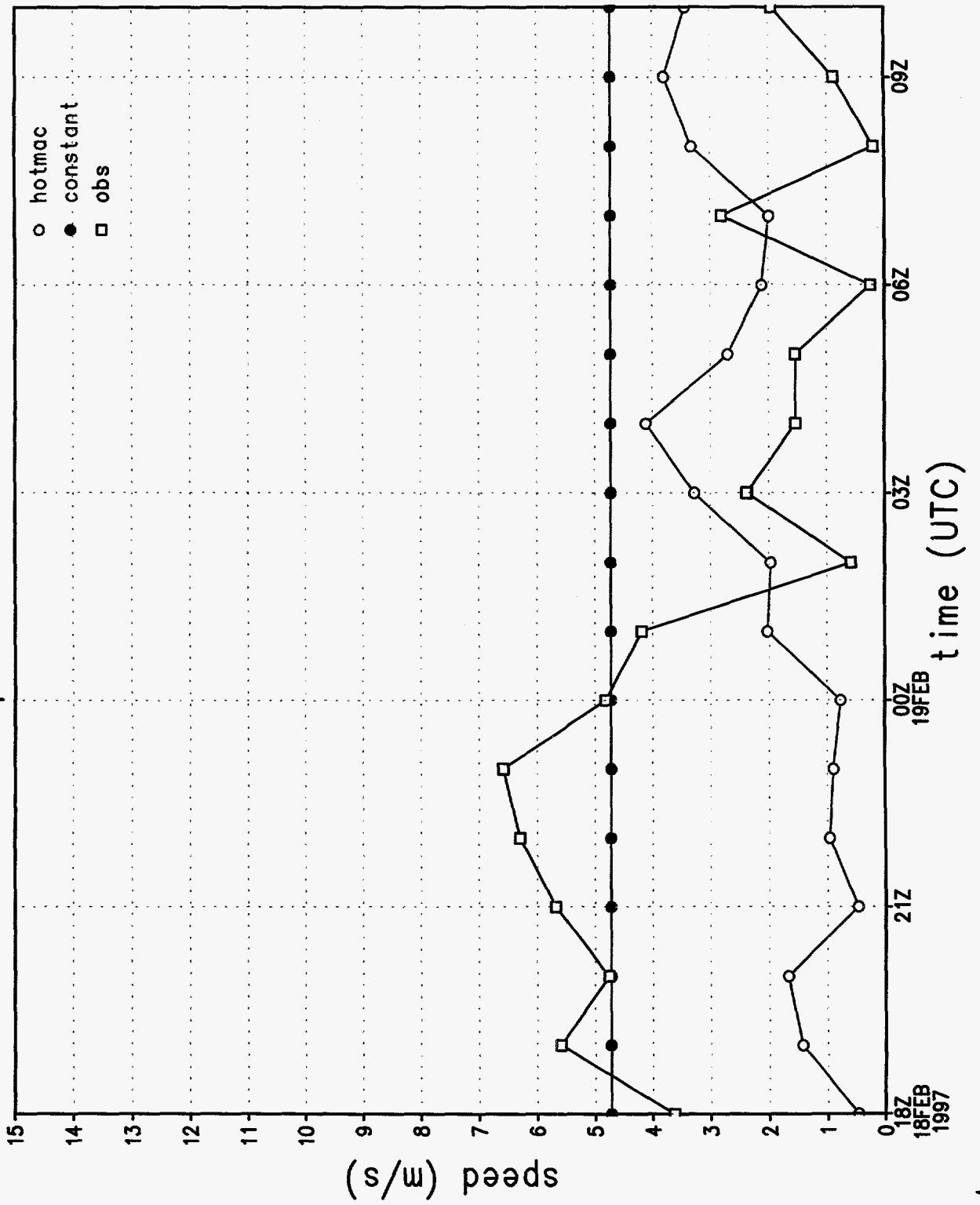


Figure 24d.



u wind component at station 1

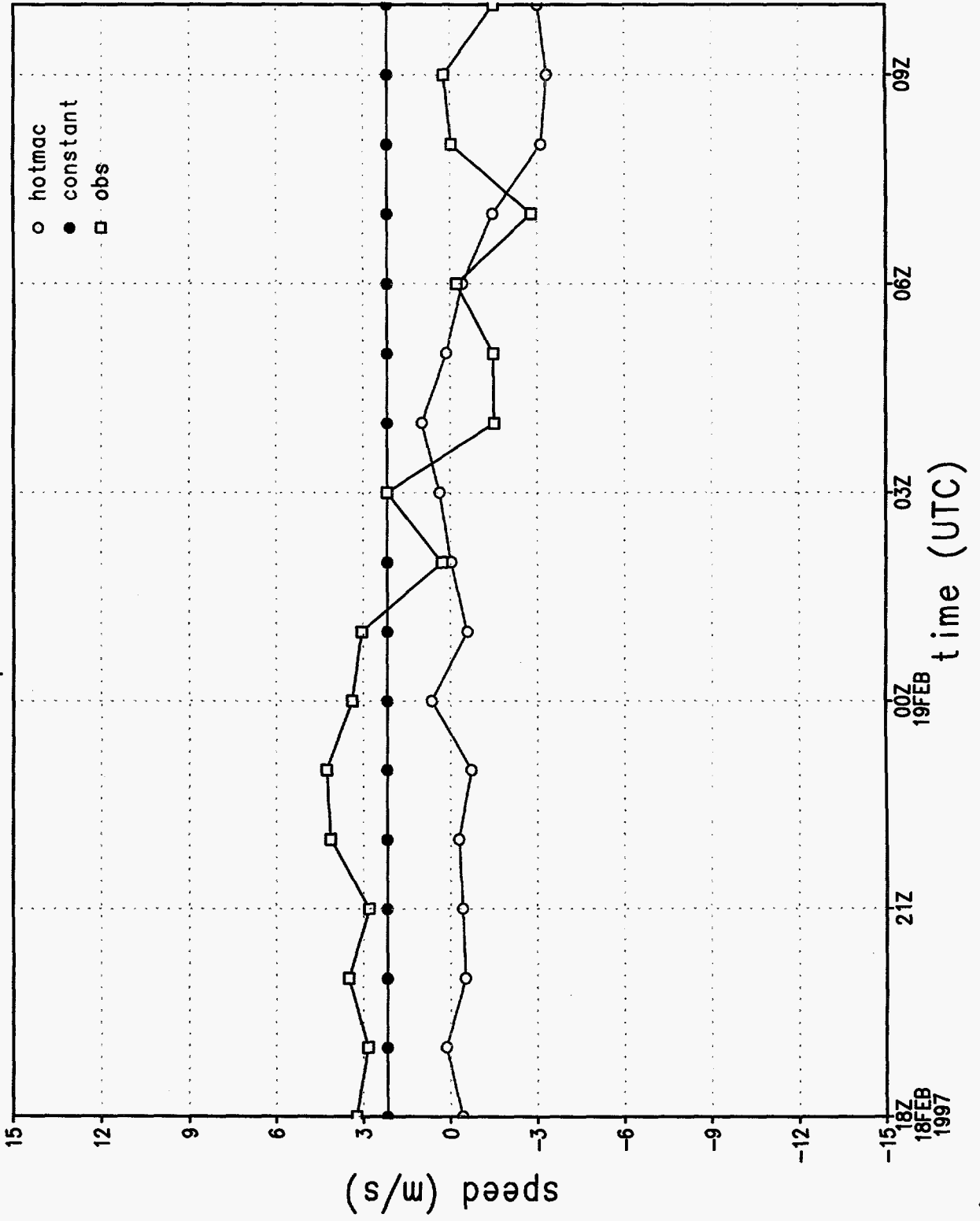


Figure 24e.

# v wind component at station 1

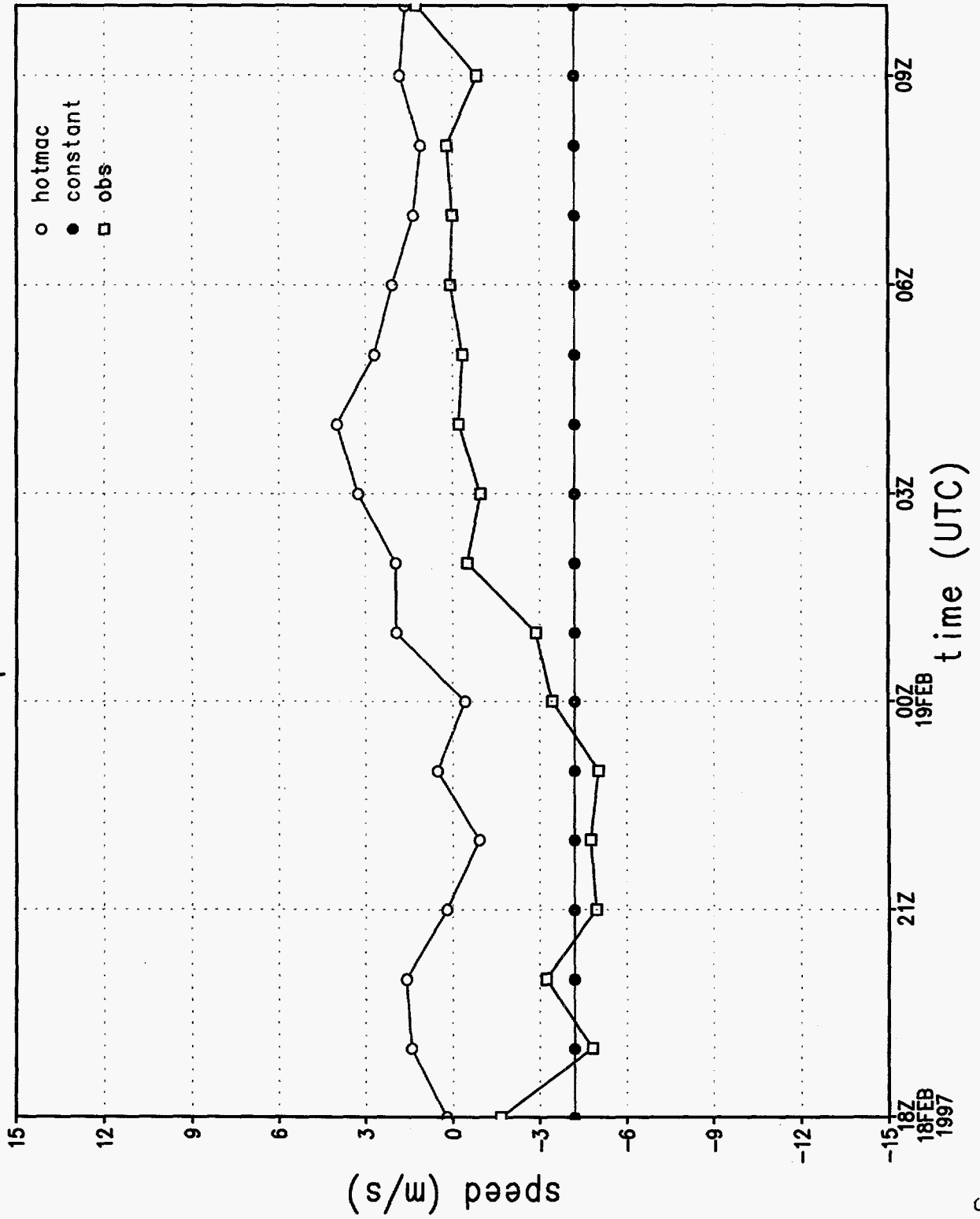


Figure 24f.

# rmse of wind direction by hour

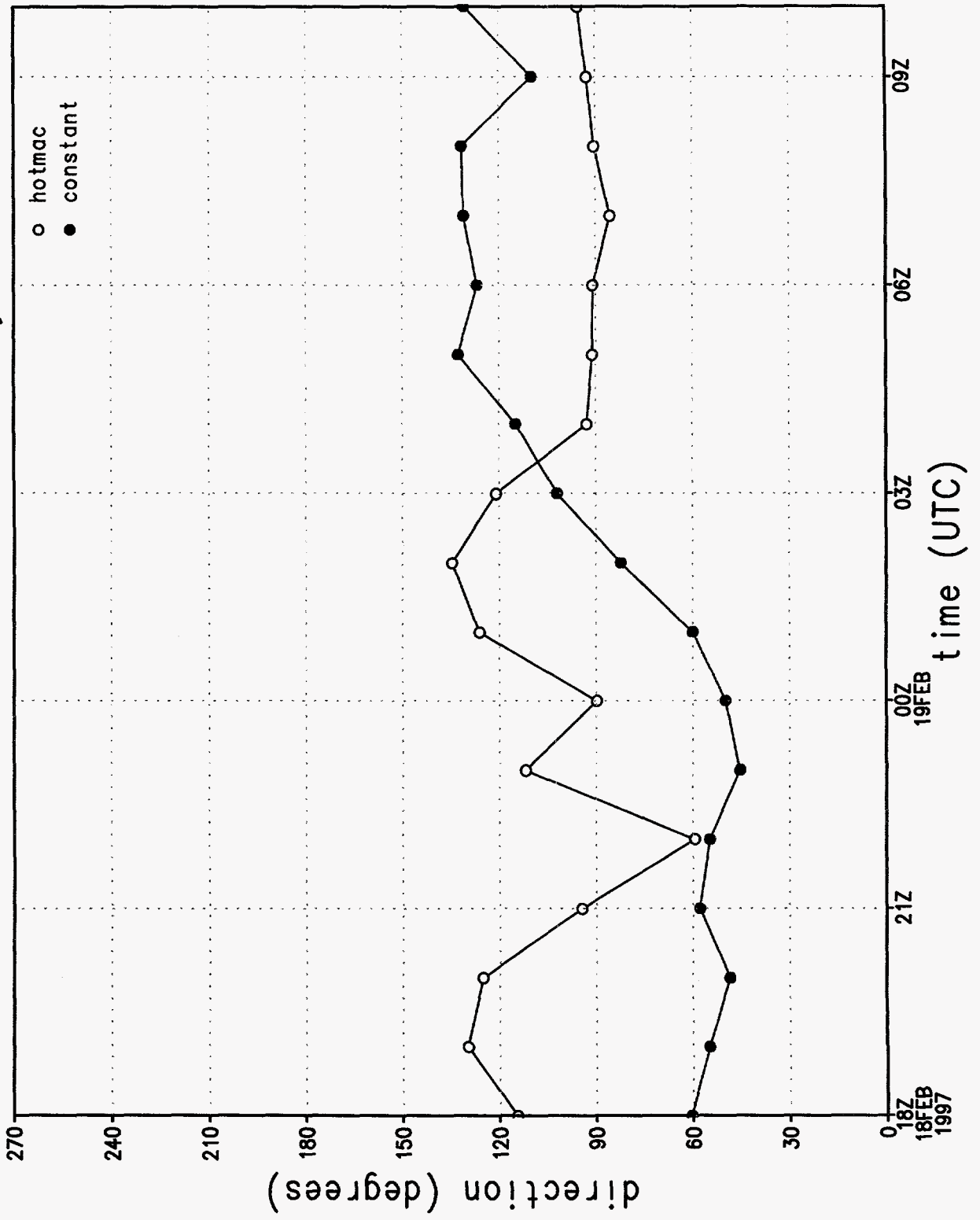


Figure 24g.

# rmse of wind speed by hour

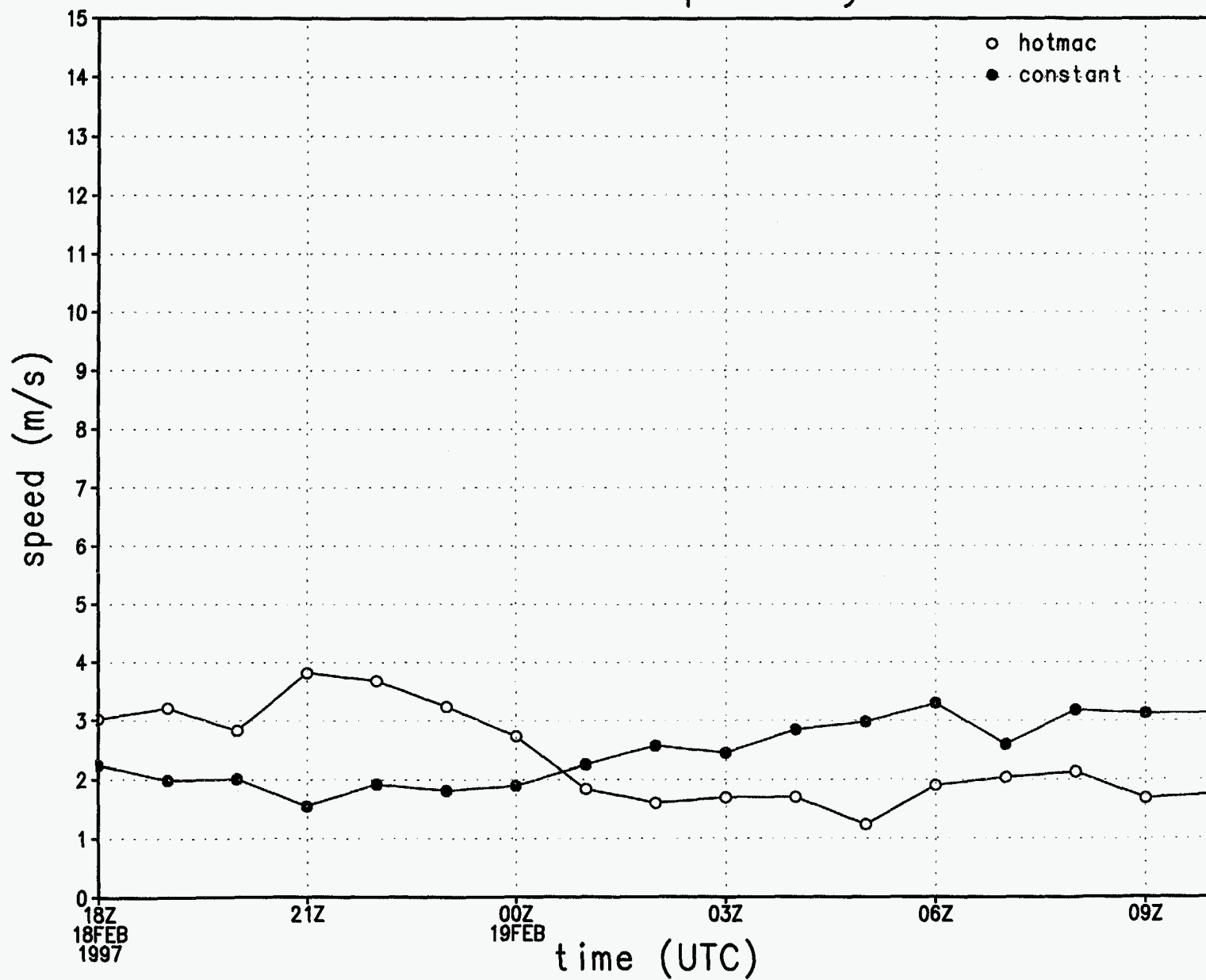


Figure 24h.

rmse of u wind component by hour

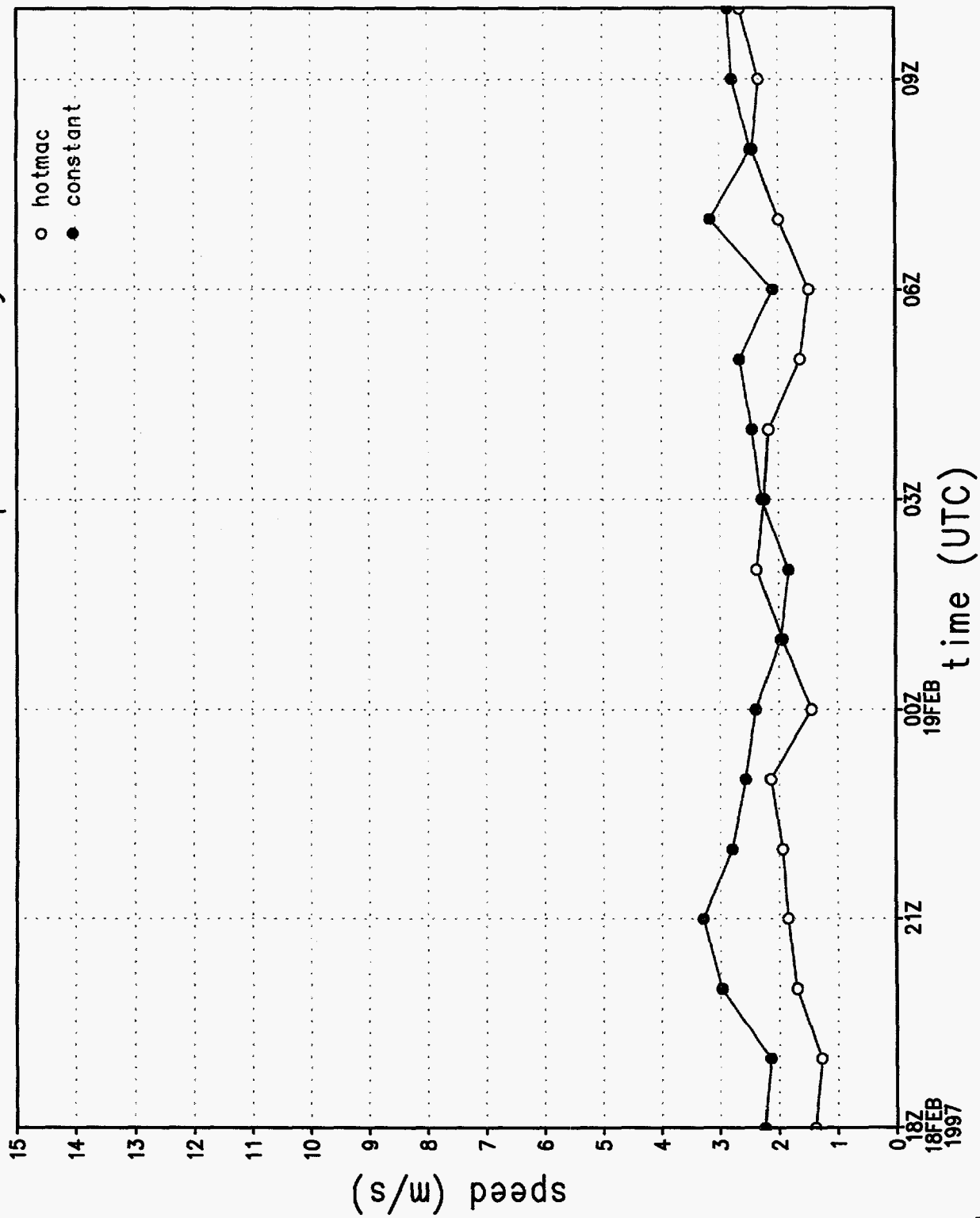


Figure 241.

rmse of v wind component by hour

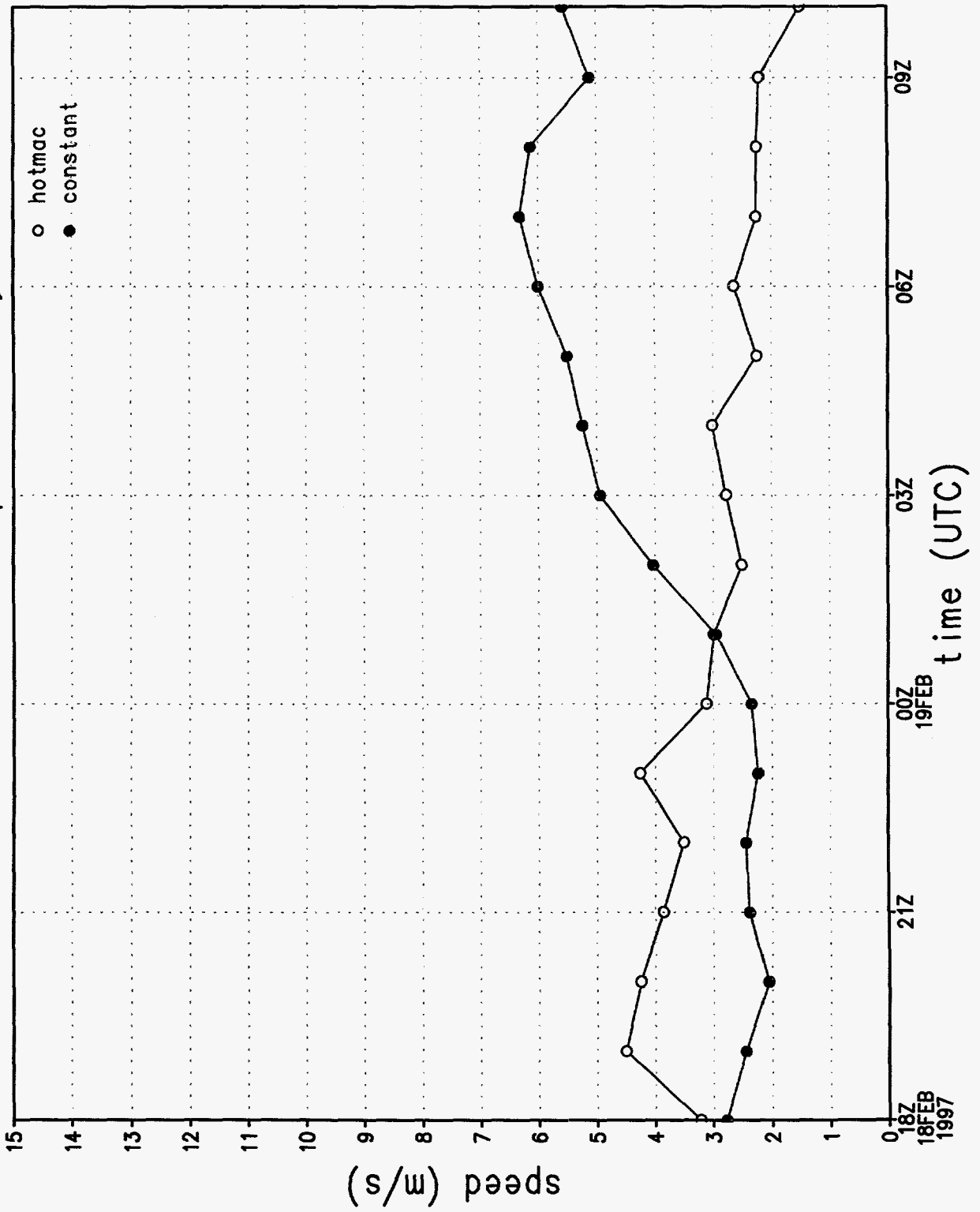


Figure 24j

# wind direction sounding 1, 1072 m

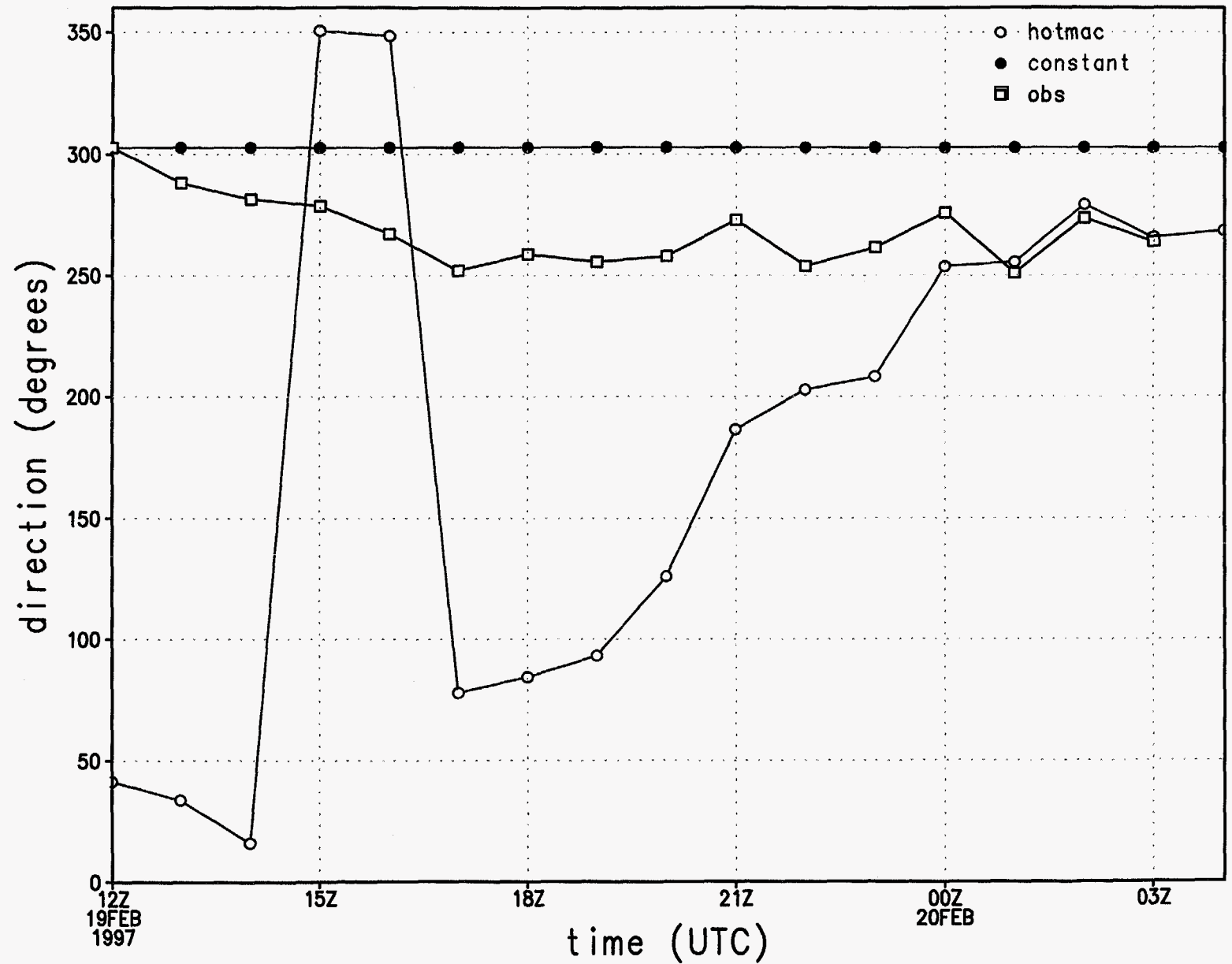


Figure 27a.

# wind speed sounding 1, 1072 m

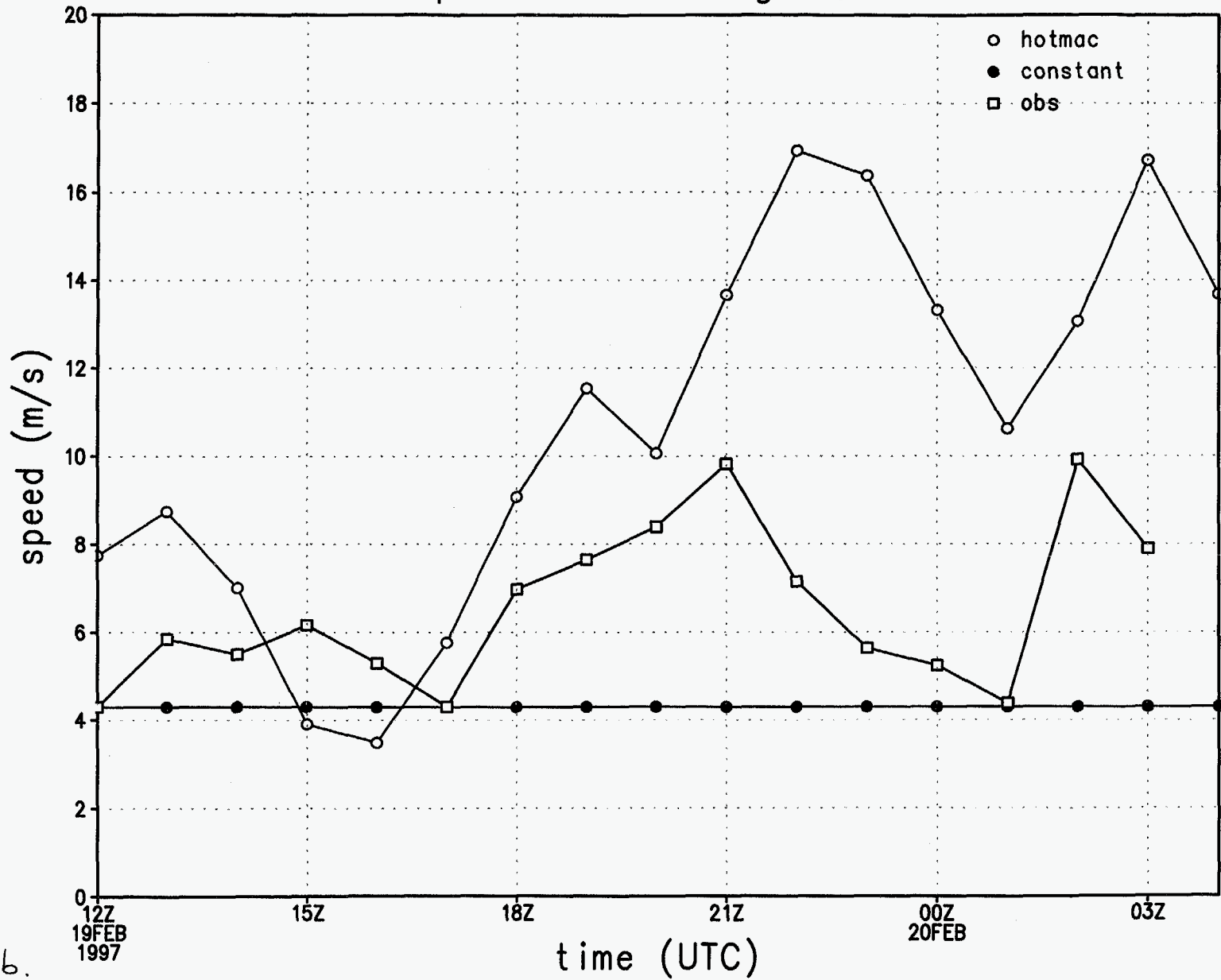


Figure 276.



# wind direction at station 1

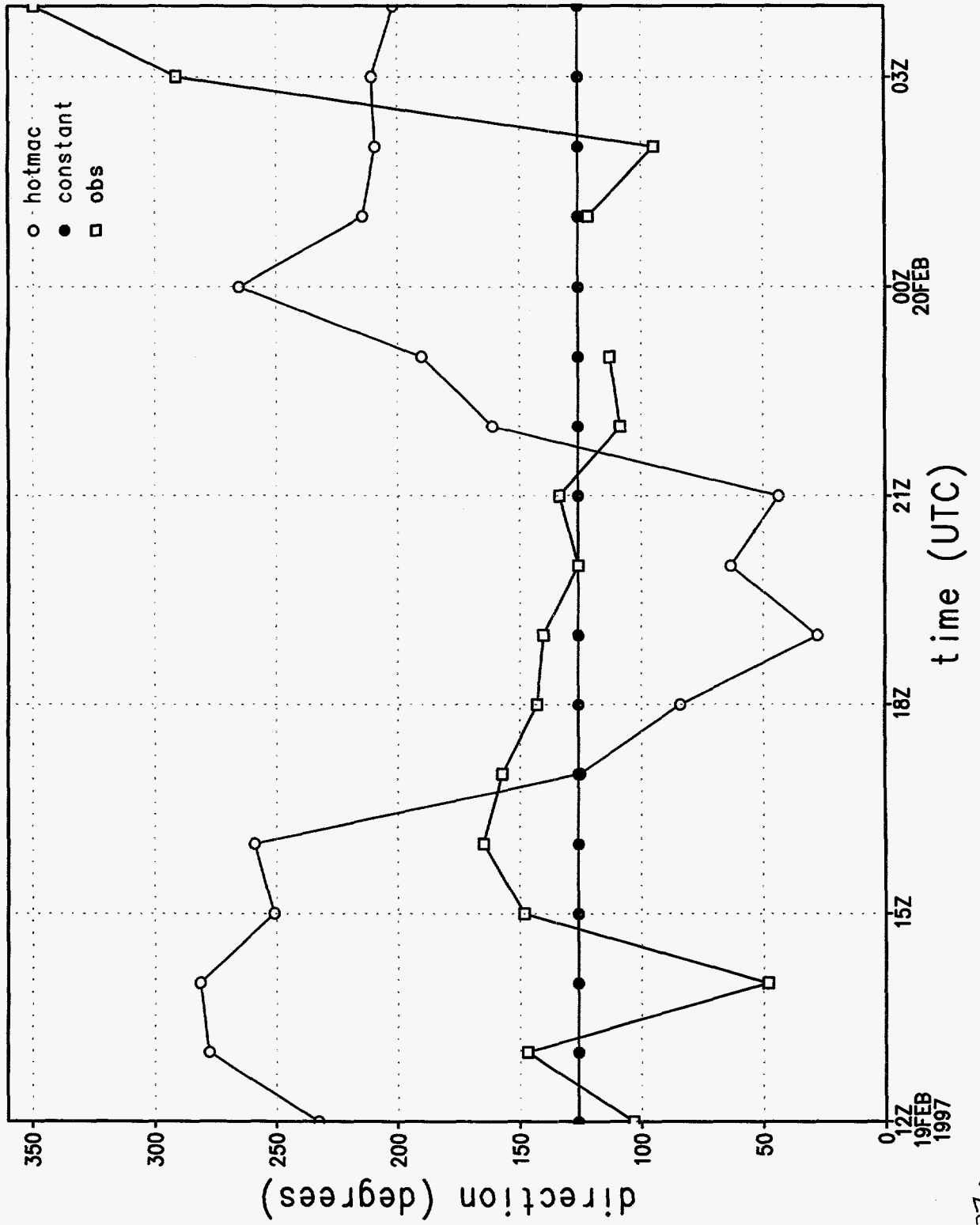


Figure 27c.

# wind speed at station 1

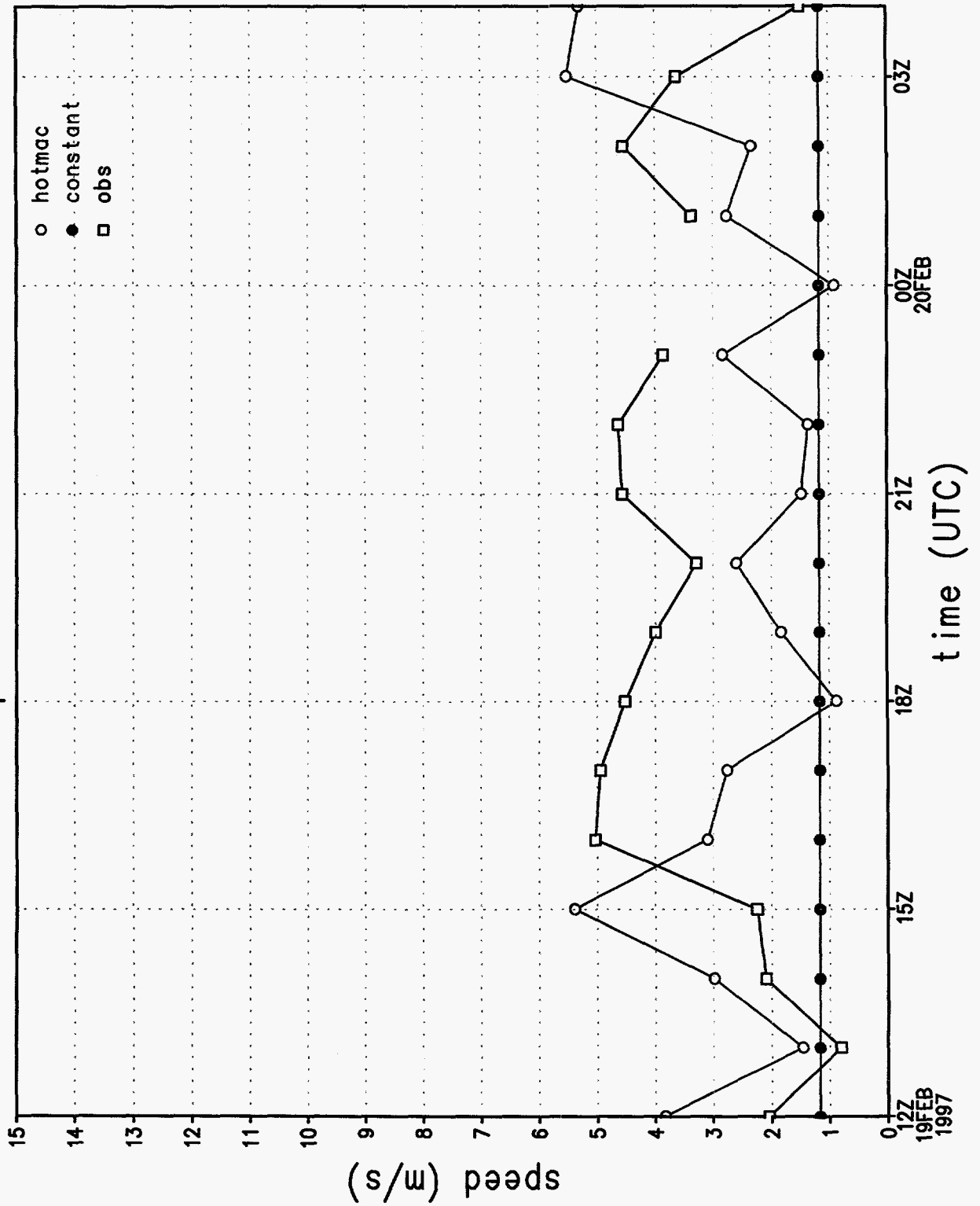


Figure 27d.

# u wind component at station 1

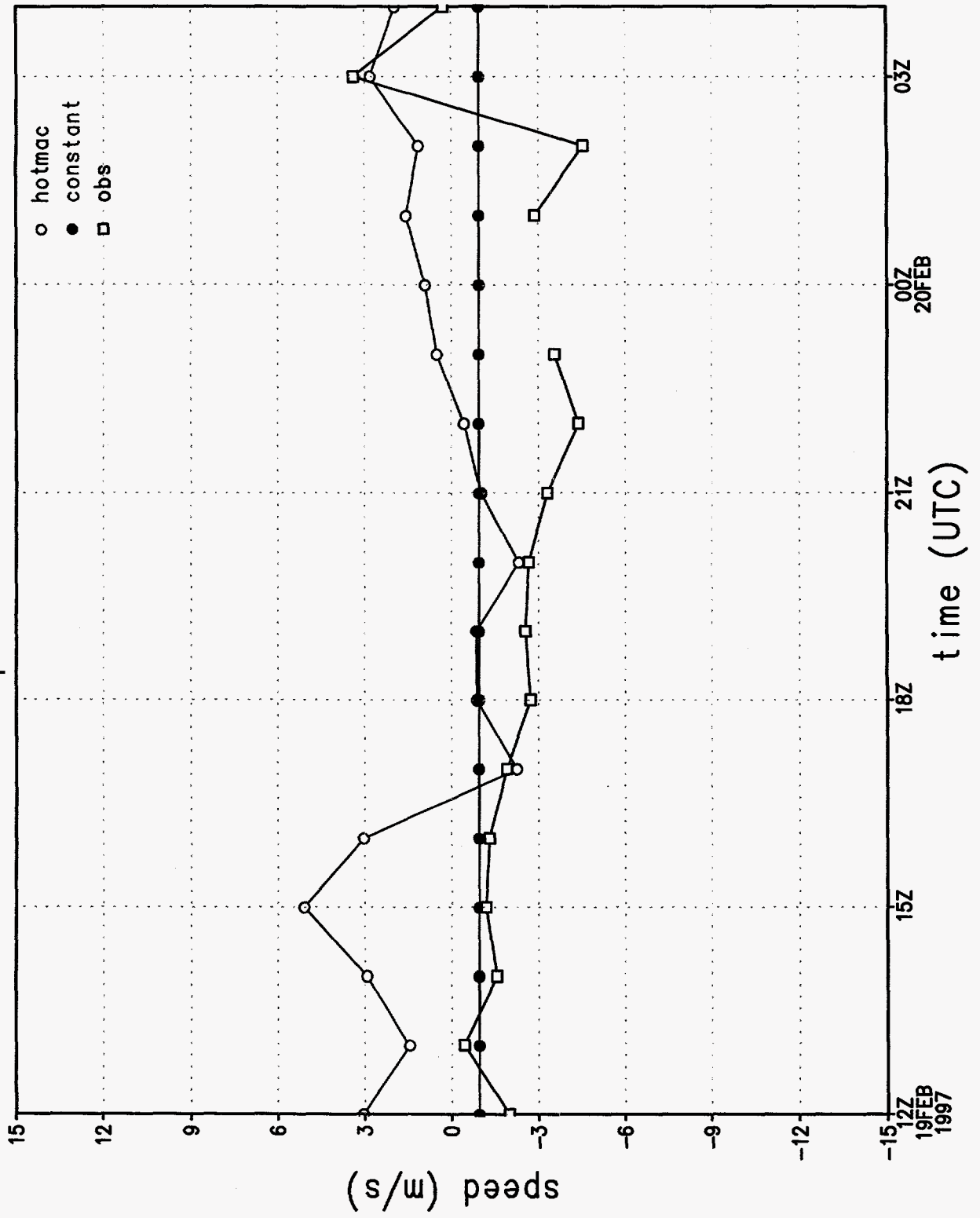


Figure 27e.

# v wind component at station 1

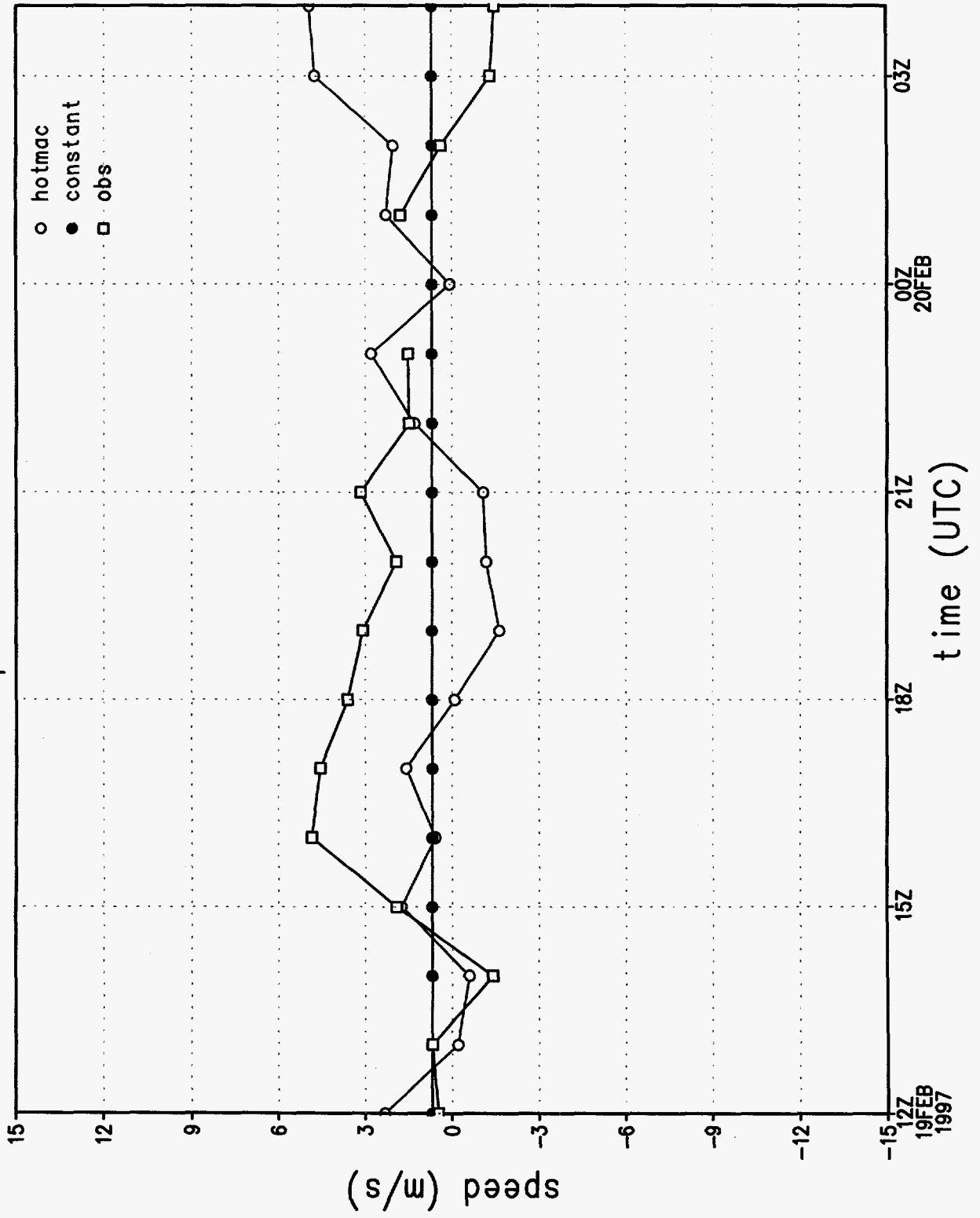


Figure 27f.

# rmse of wind direction by hour

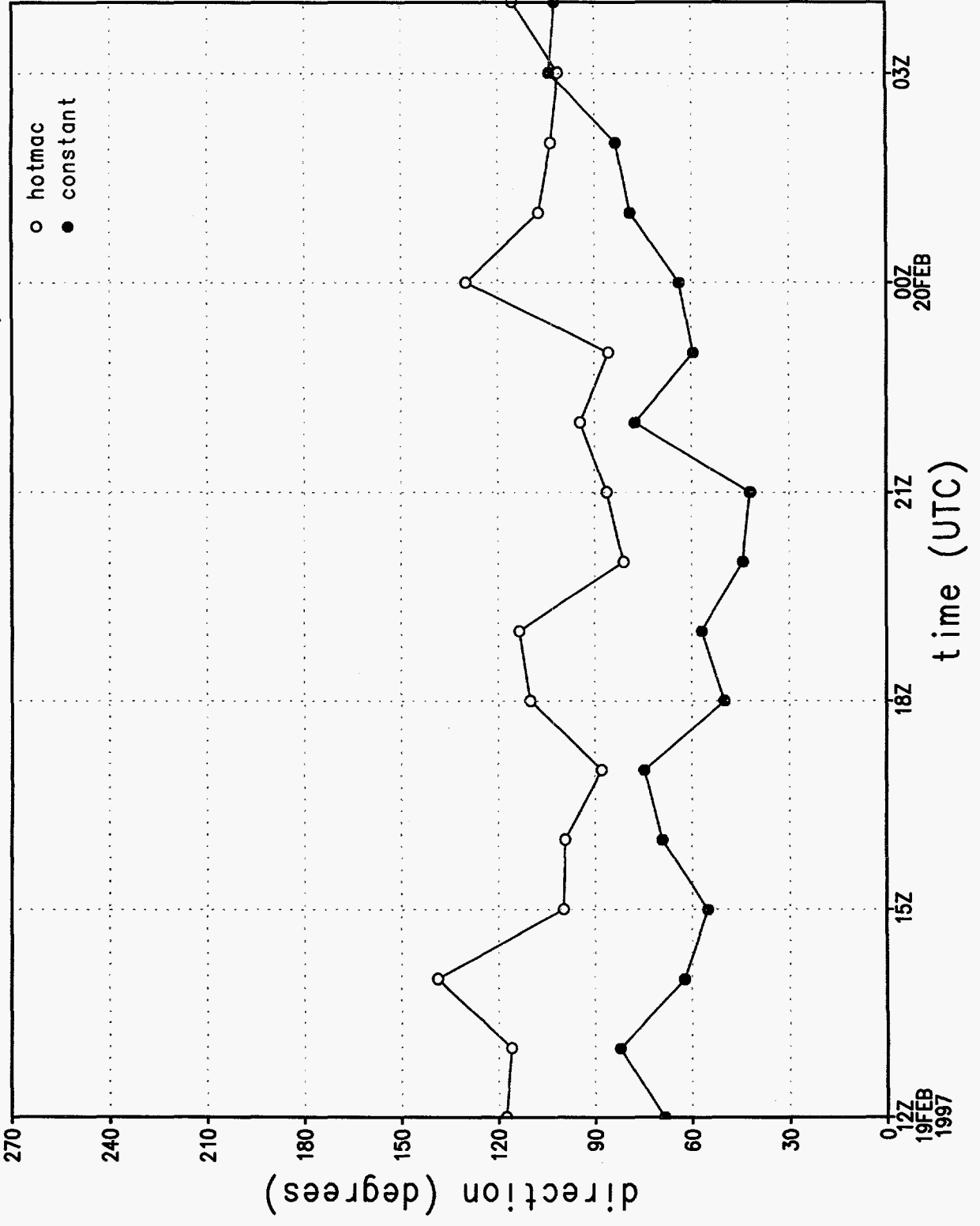


Figure 27g.

# rmse of wind speed by hour

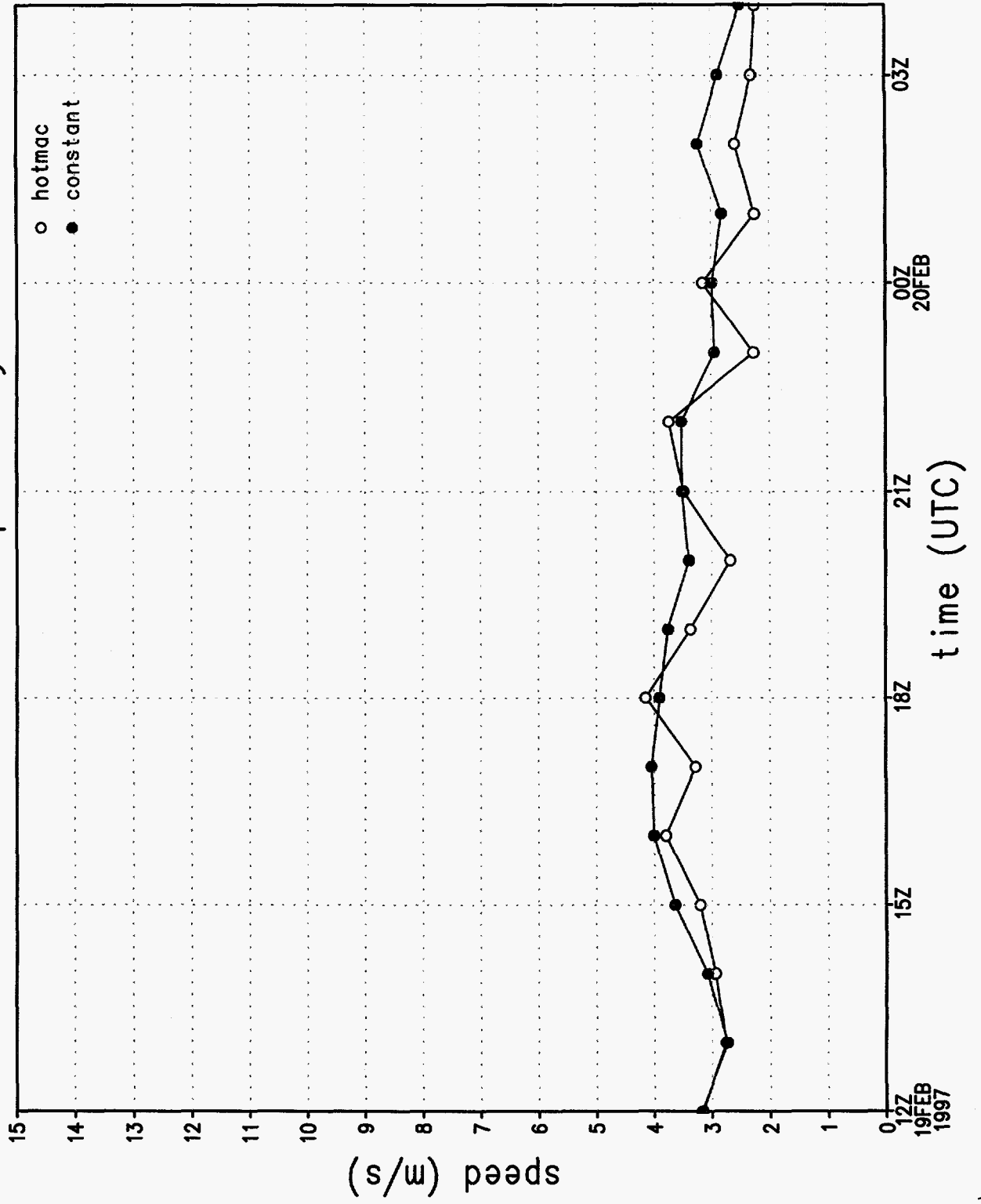


Figure 27h.

# rmse of u wind component by hour

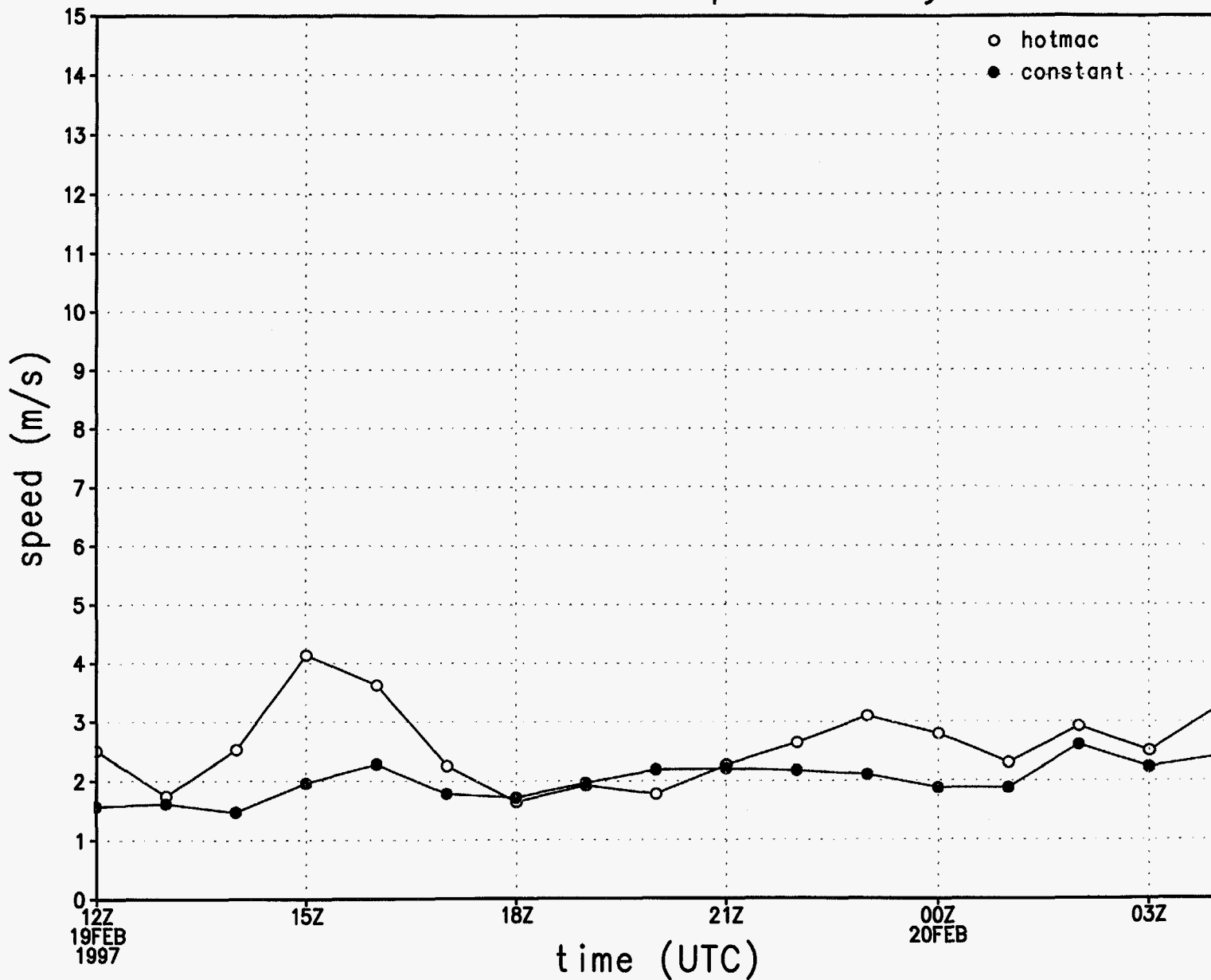


Figure 271.

rmse of v wind component by hour

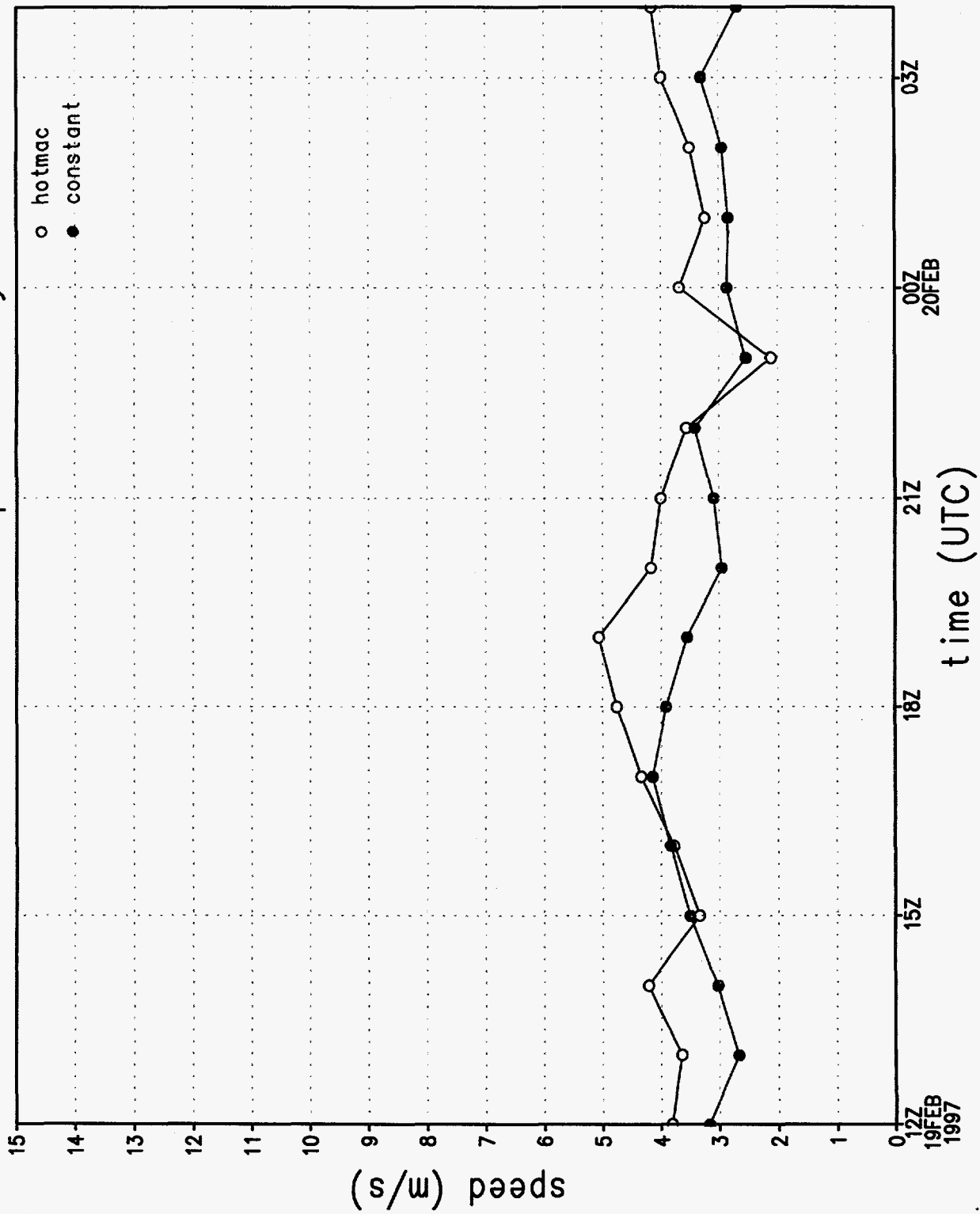


Figure 27j.



# wind direction sounding 1, 1072 m

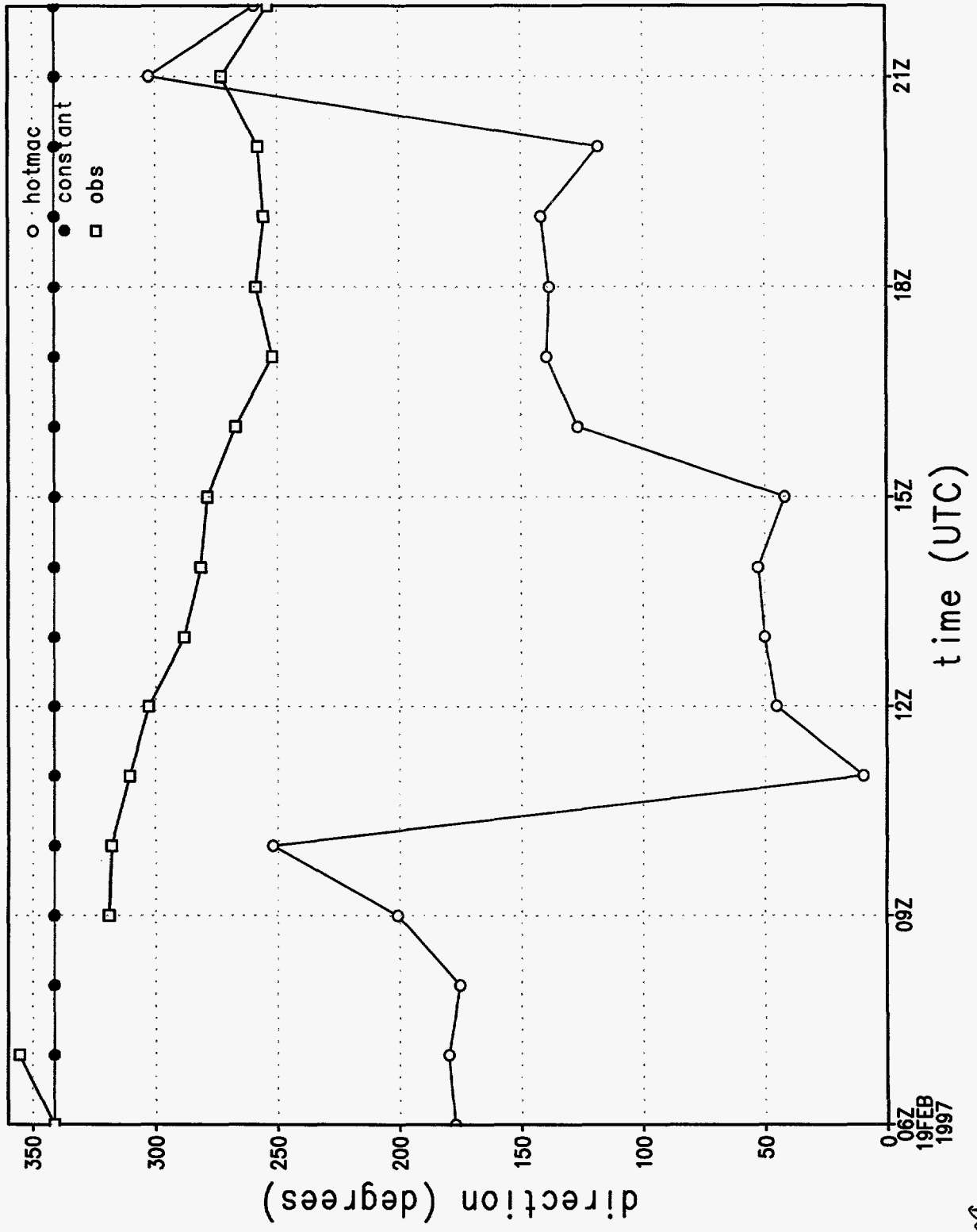


Figure 26a

wind speed sounding 1, 1072 m

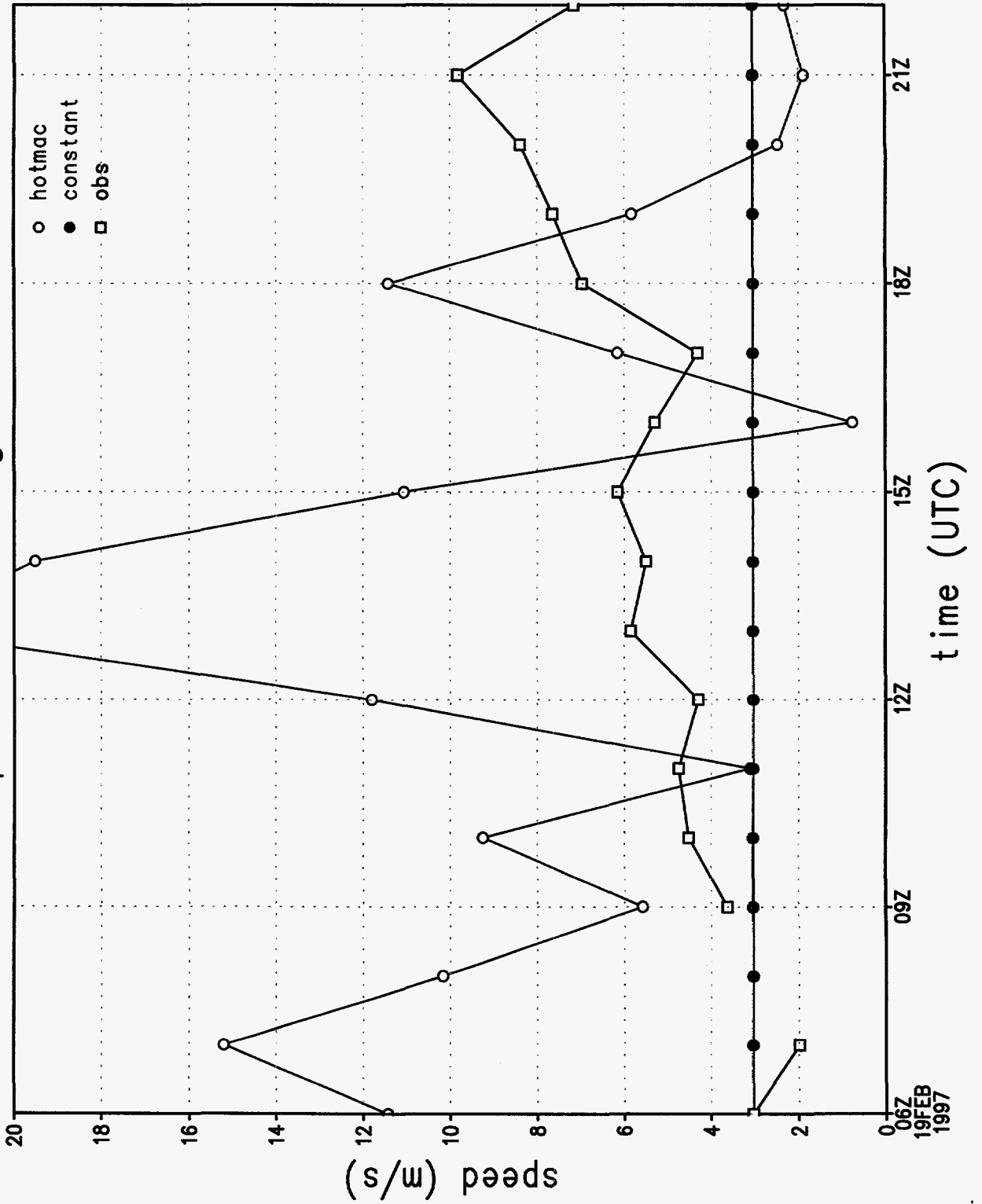


Figure 26b.

wind direction at station 1

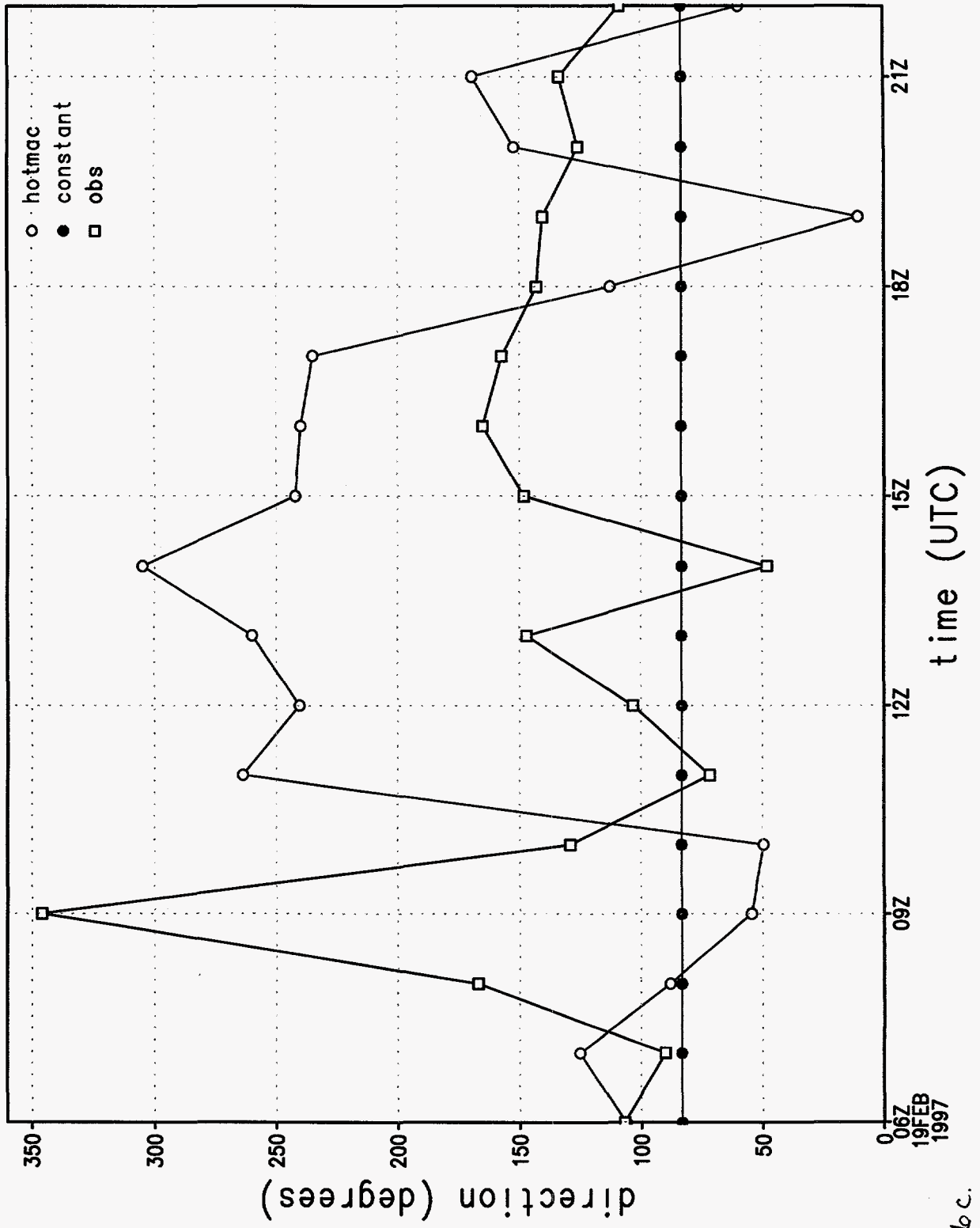


Figure 2bc.

# wind speed at station 1

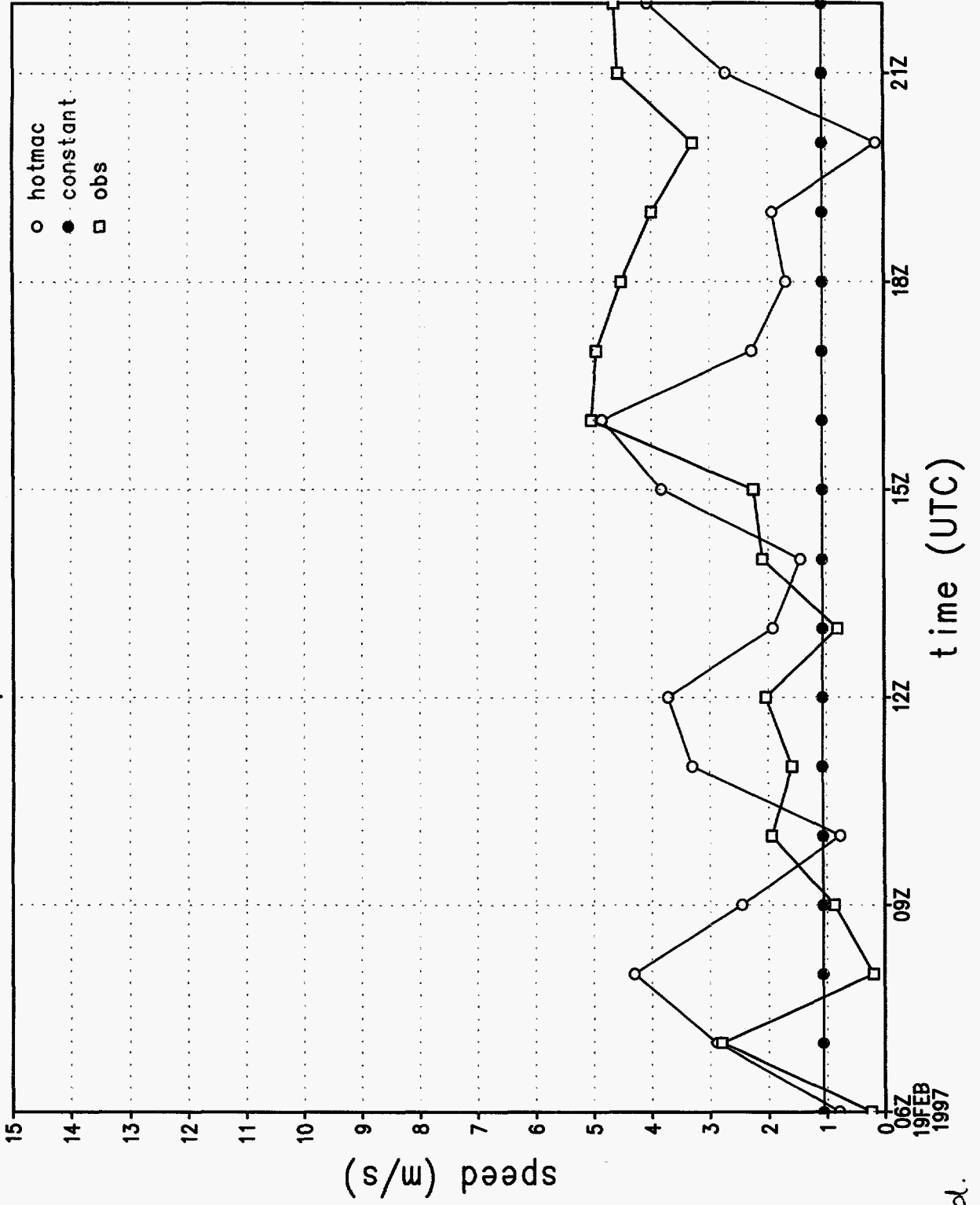


Figure 26d.

u wind component at station 1

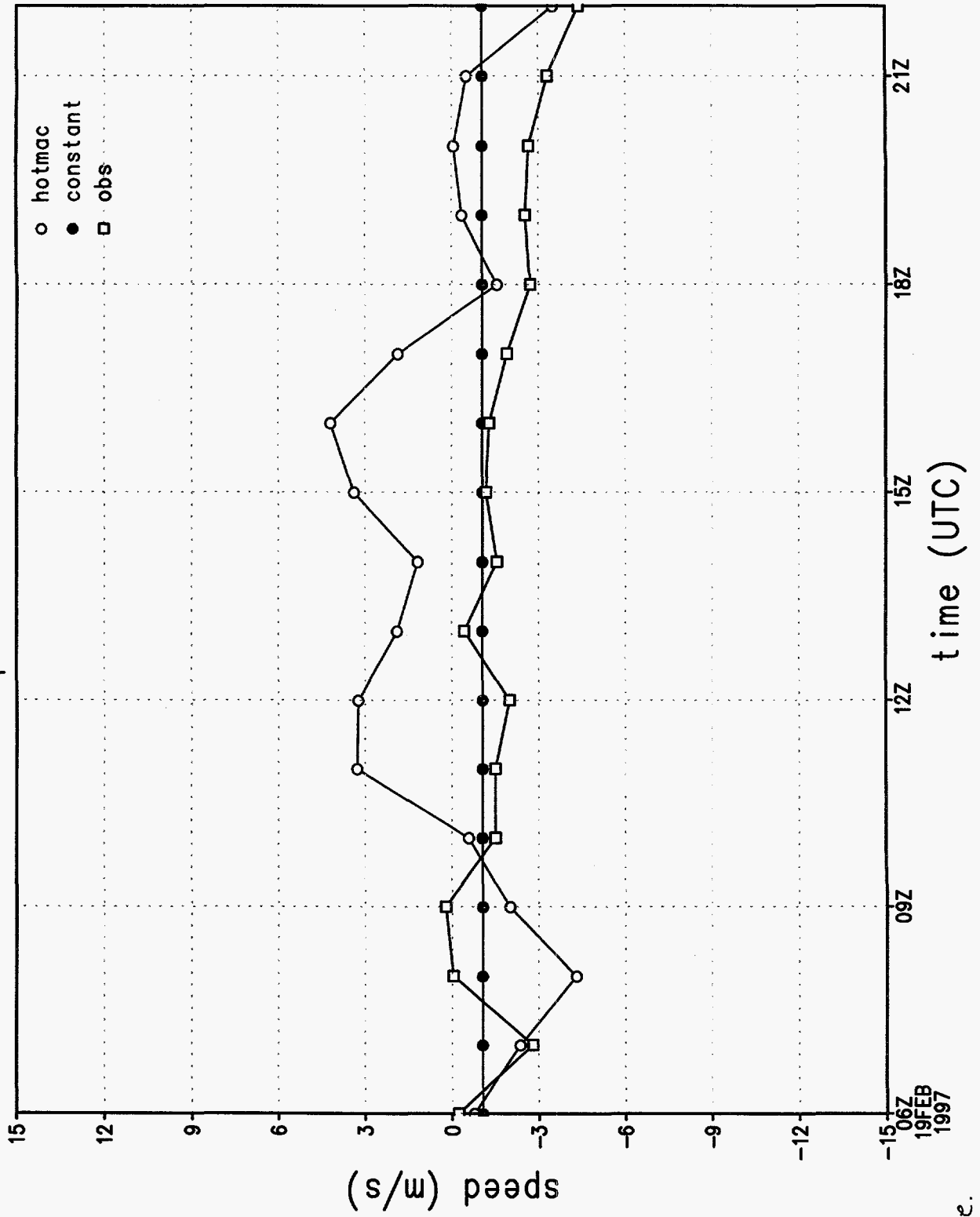


Figure 26e.

# v wind component at station 1

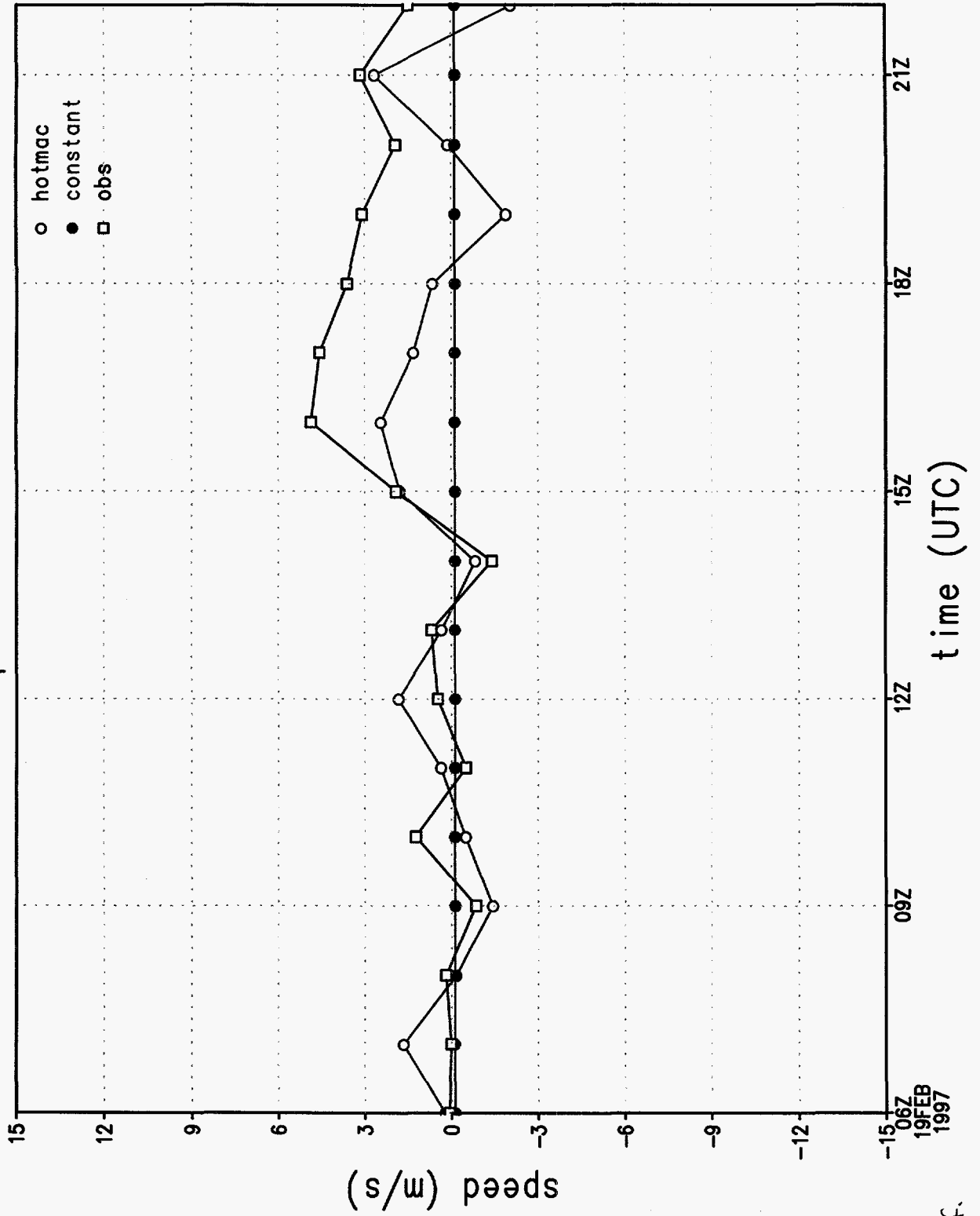


Figure 26f.

# rmse of wind direction by hour

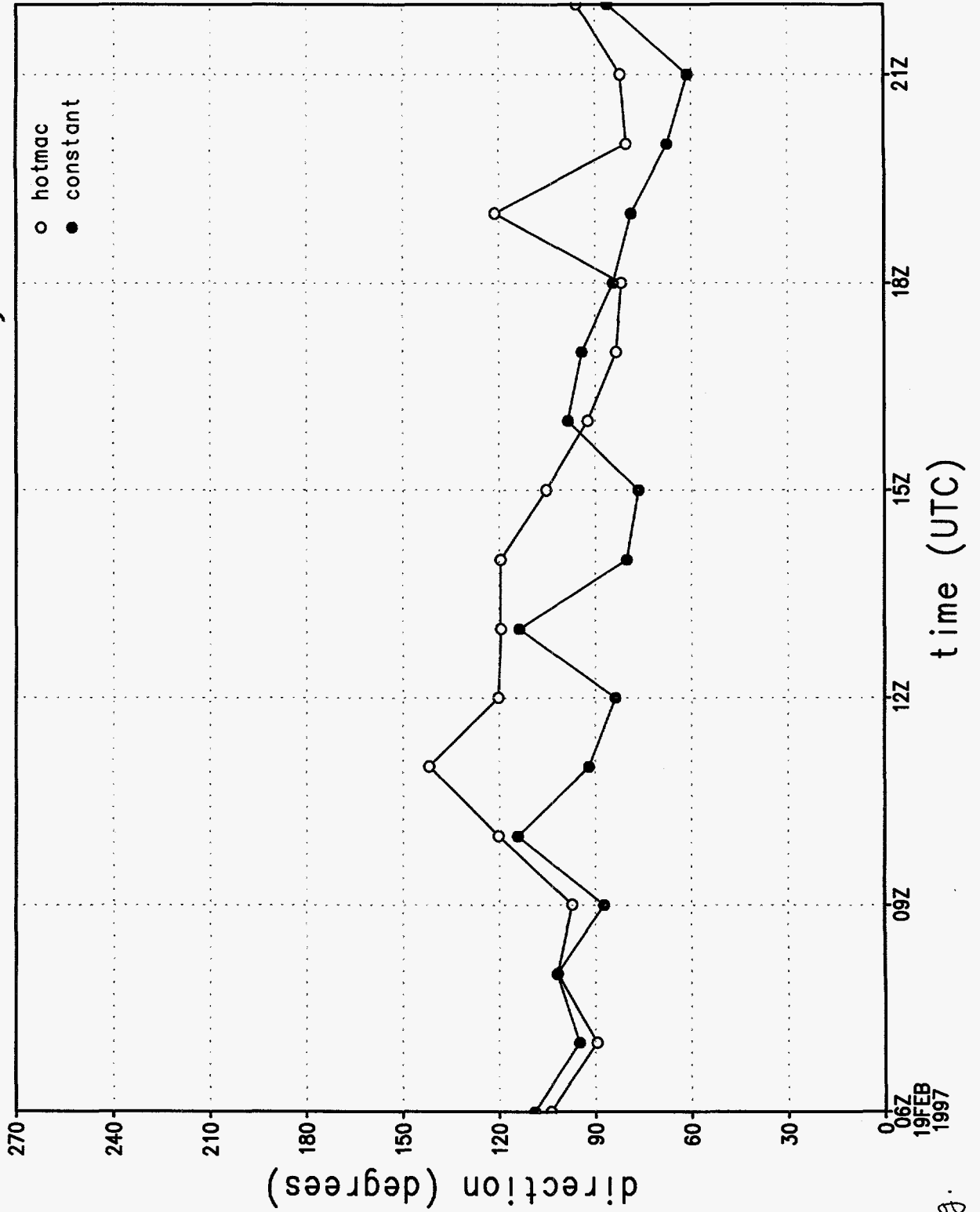


Figure 269.

rmse of wind speed by hour

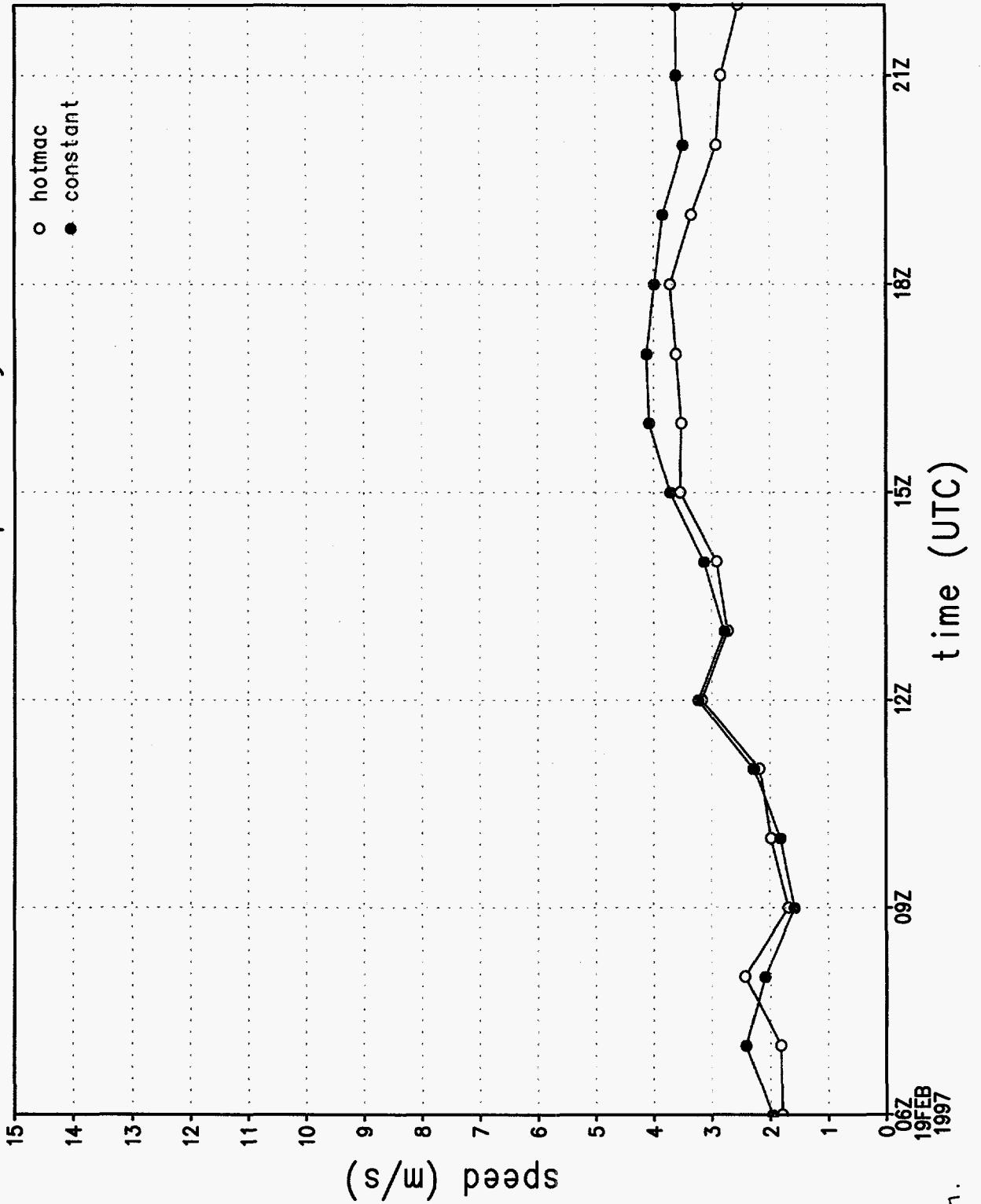


Figure 26h.



rmse of u wind component by hour

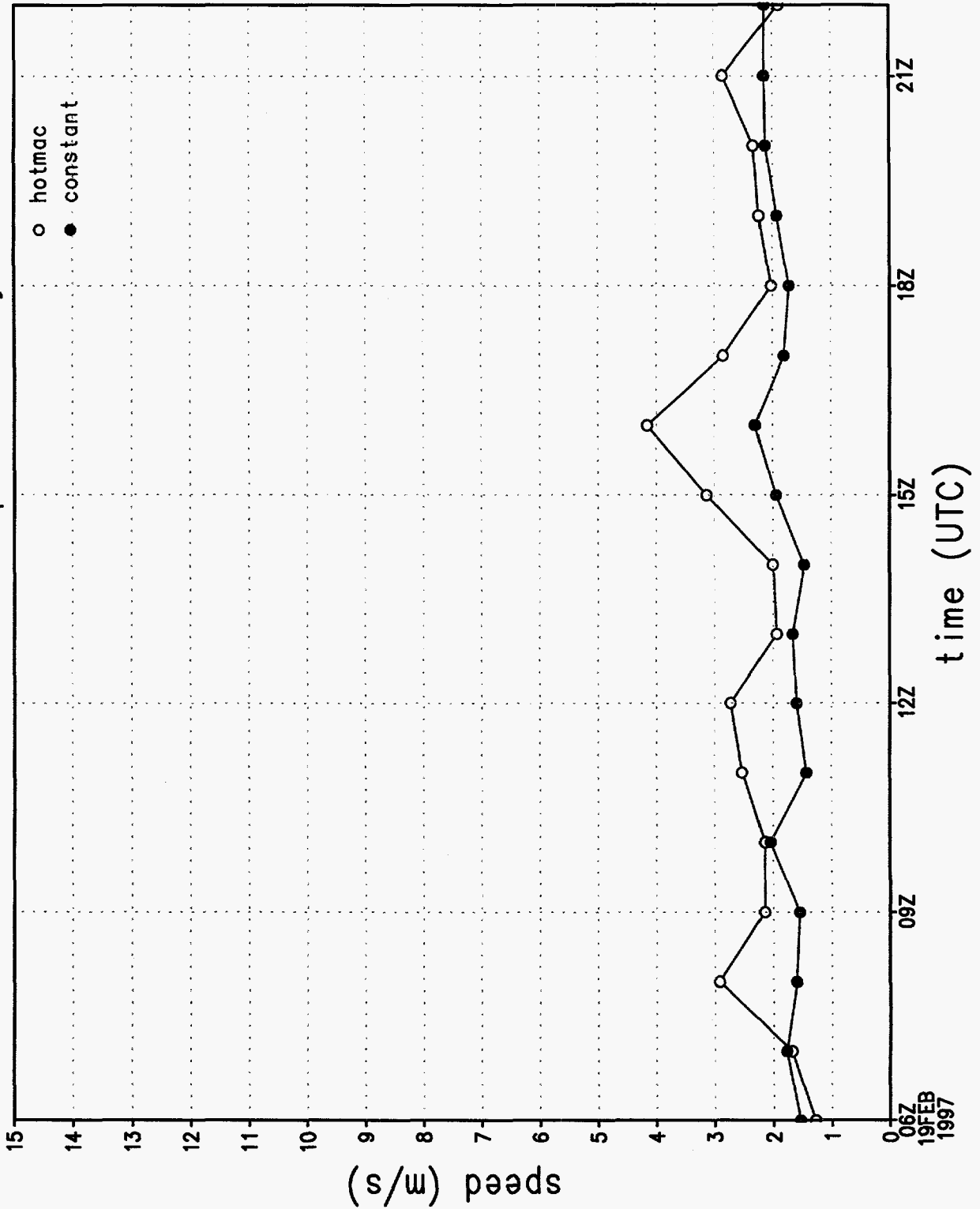


Figure 26i.

# rmse of v wind component by hour

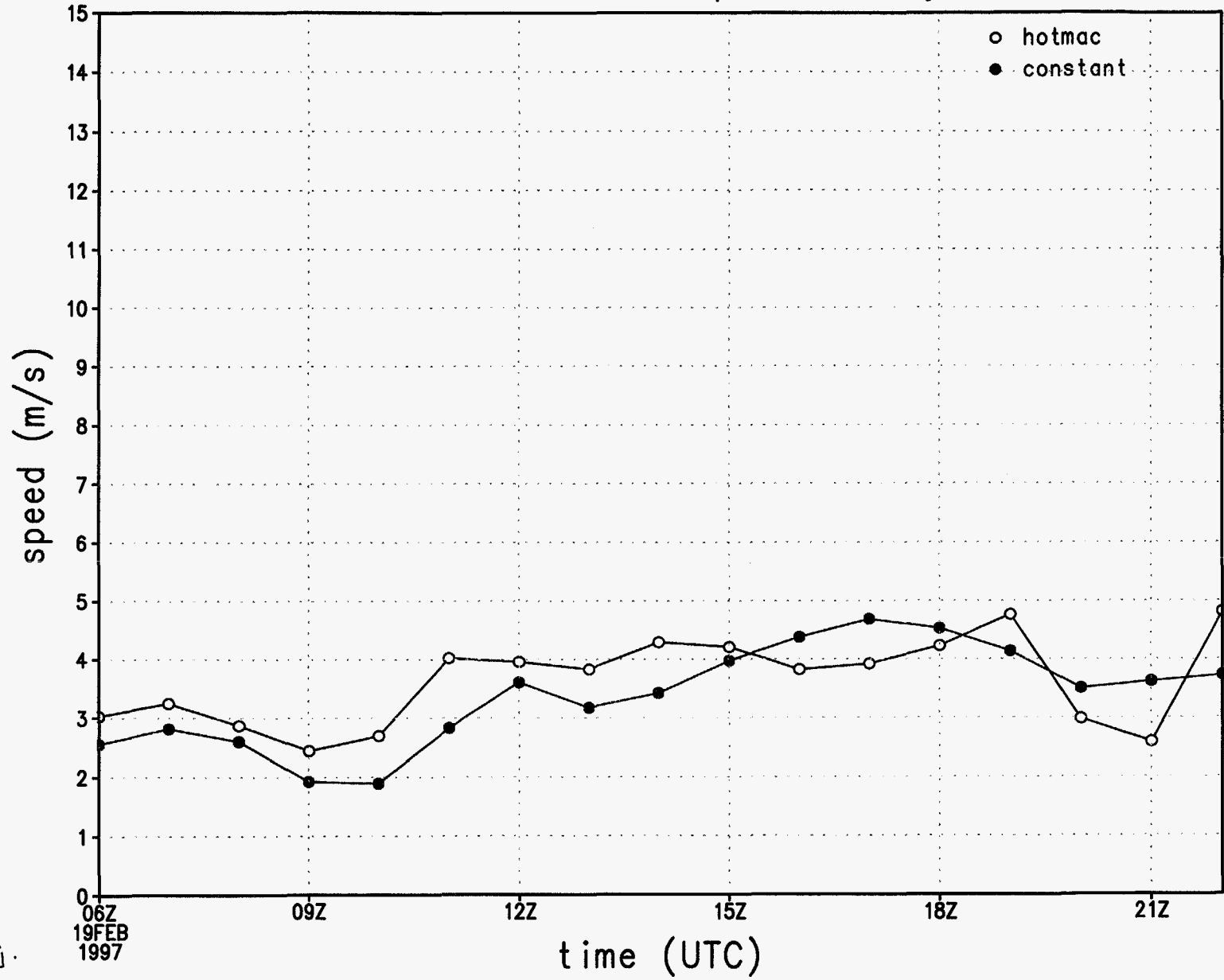


Figure 26j.

# wind direction sounding 1, 1072 m

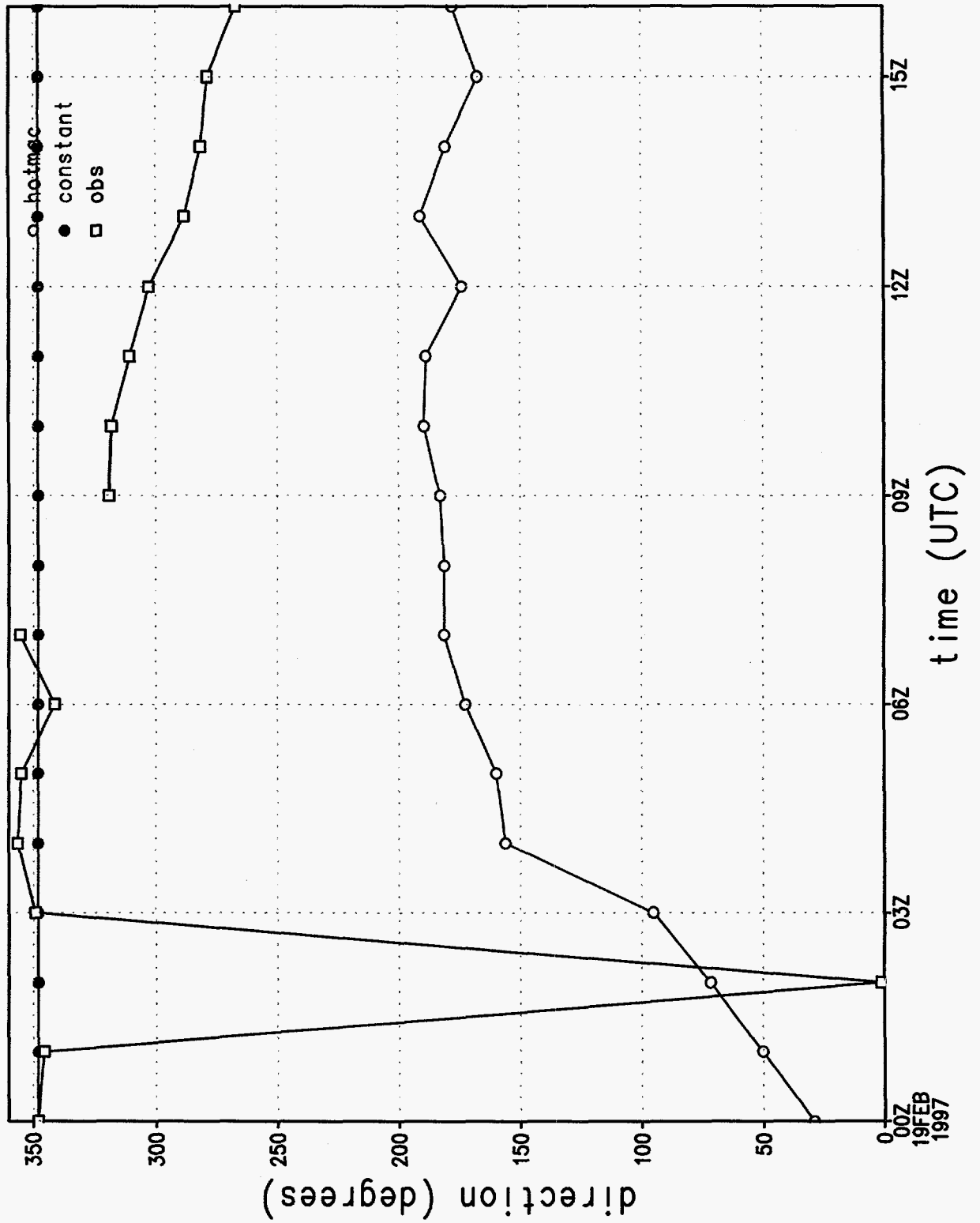


Figure 25a.

# wind speed sounding 1, 1072 m

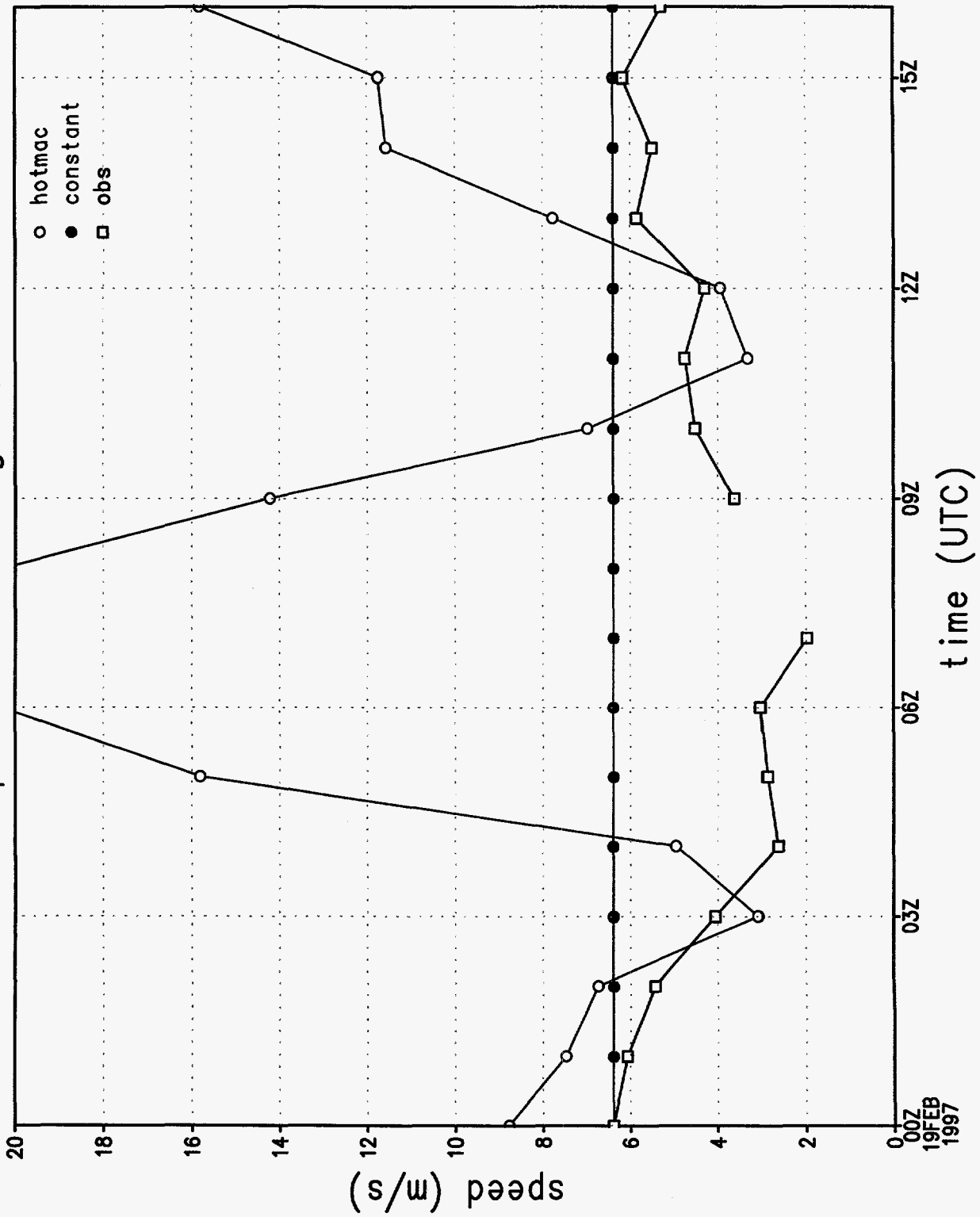


Figure 25b.

# wind direction at station 1

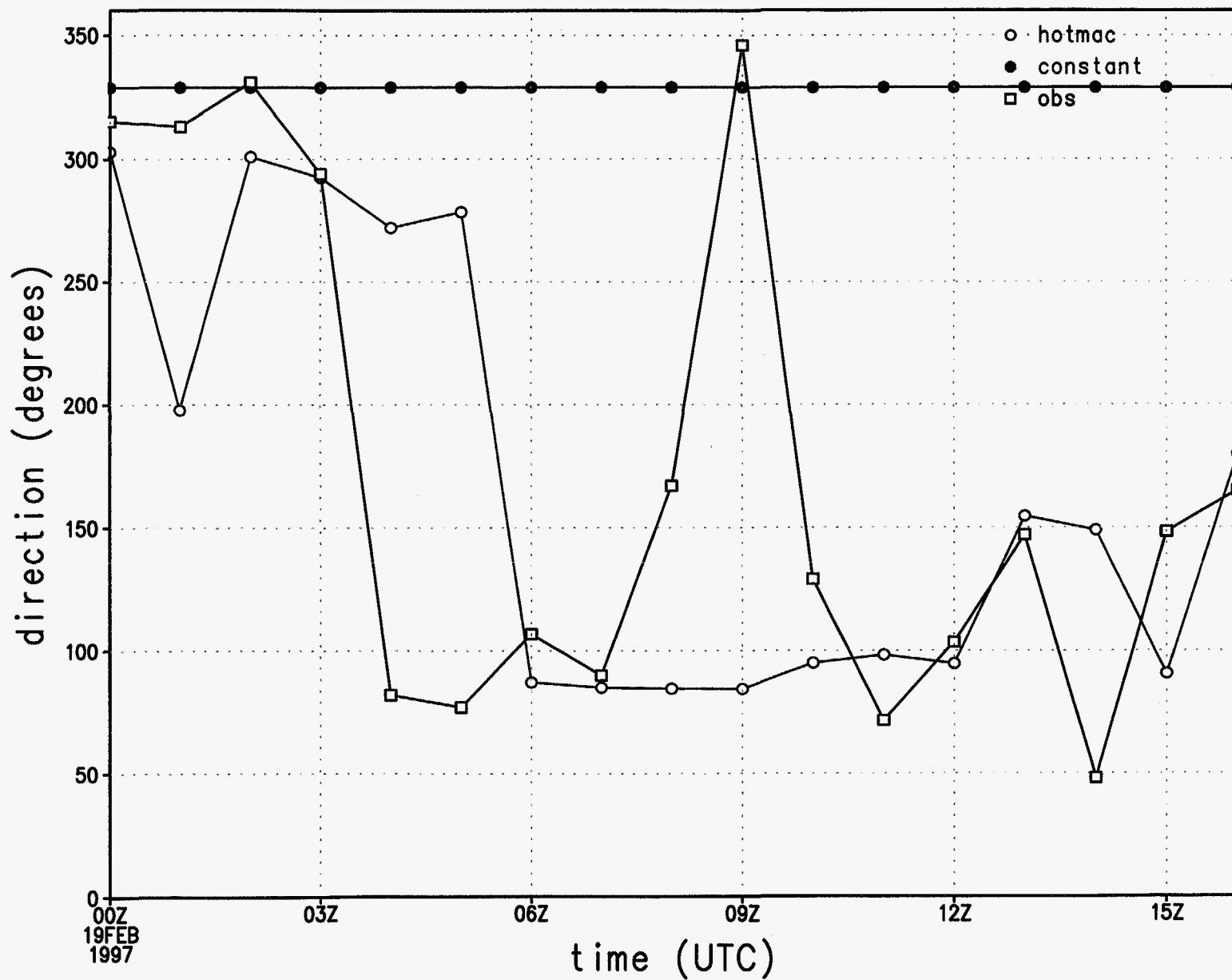


Figure 25c.

# wind speed at station 1

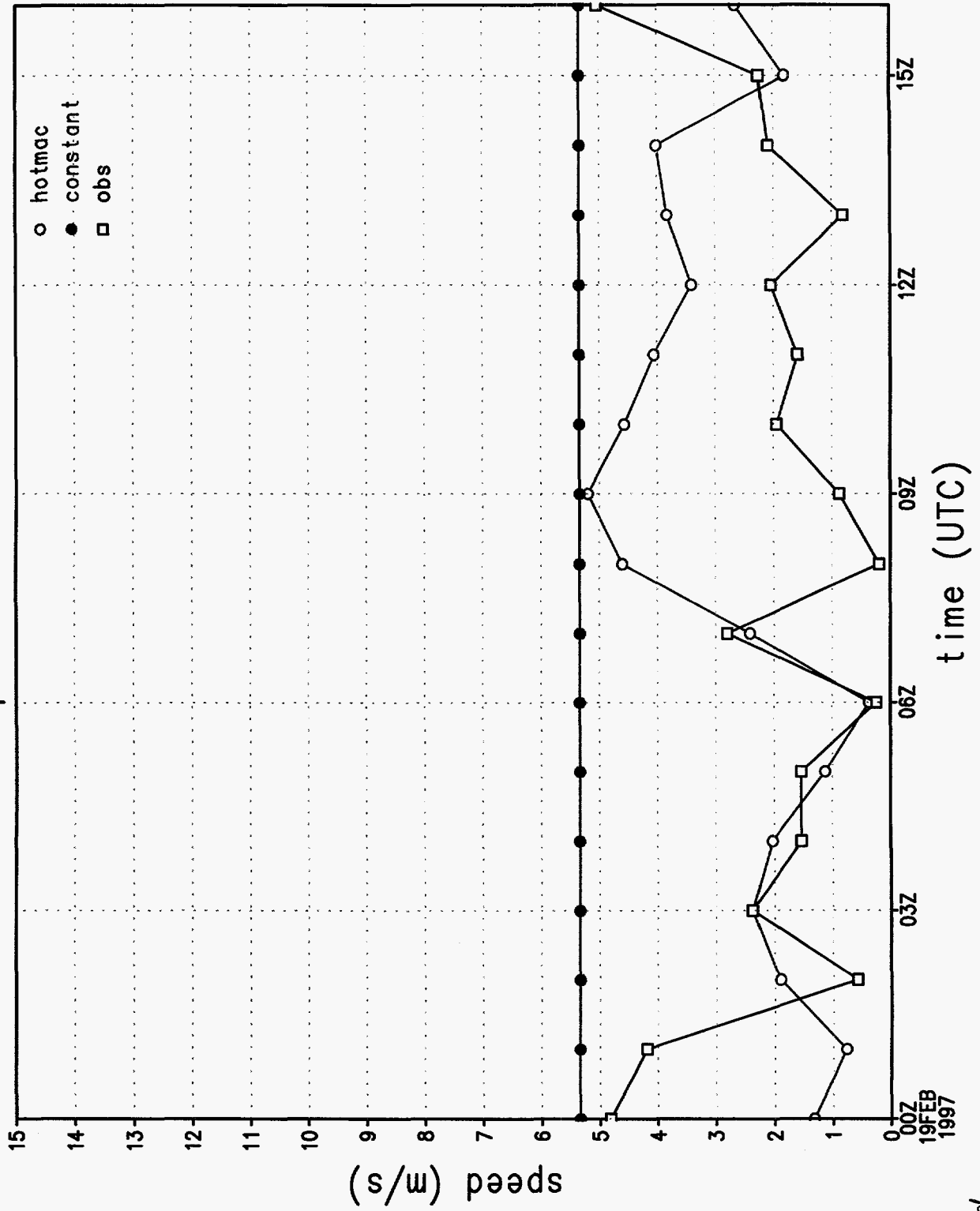


Figure 25d.

# u wind component at station 1

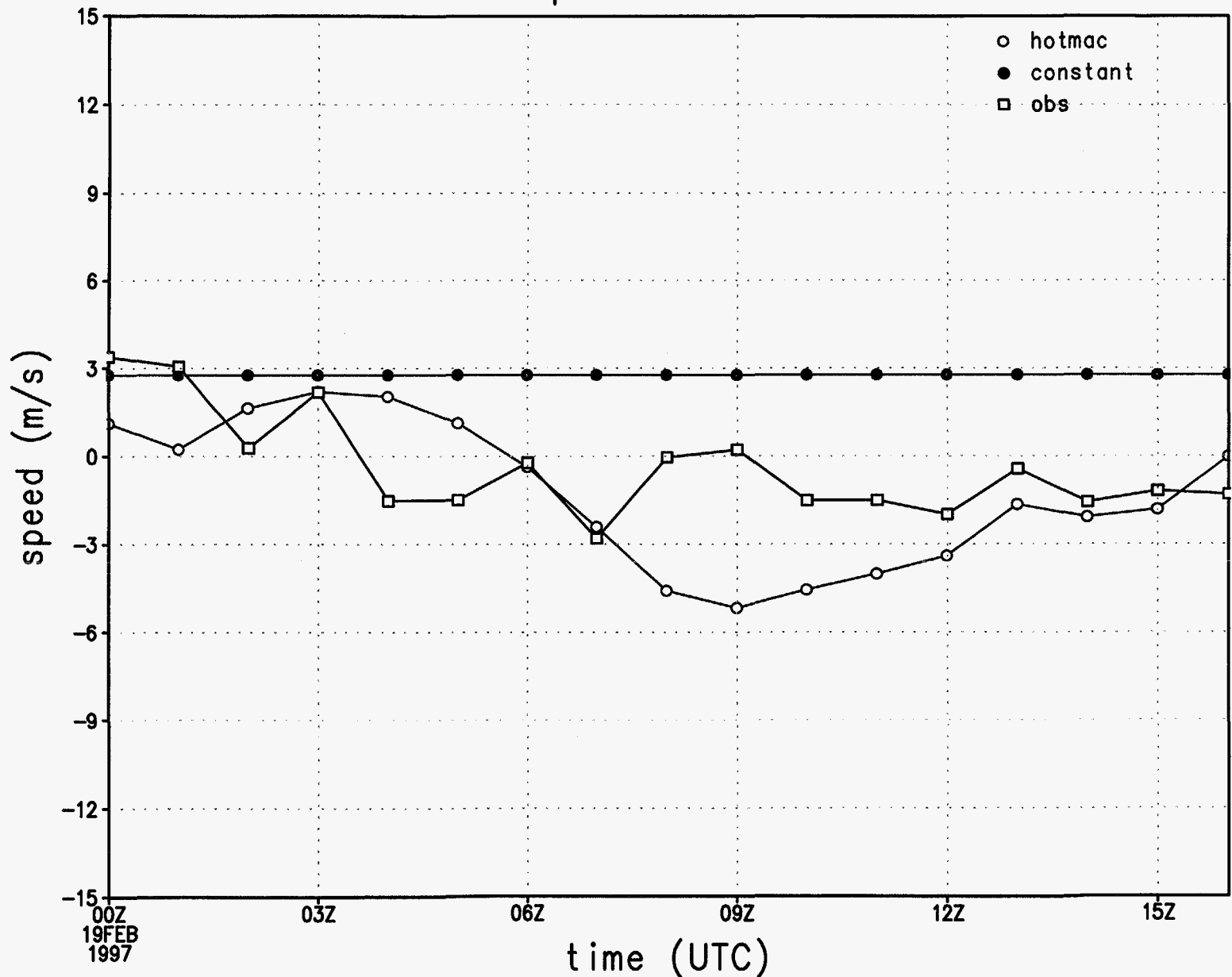


Figure 25e.

# v wind component at station 1

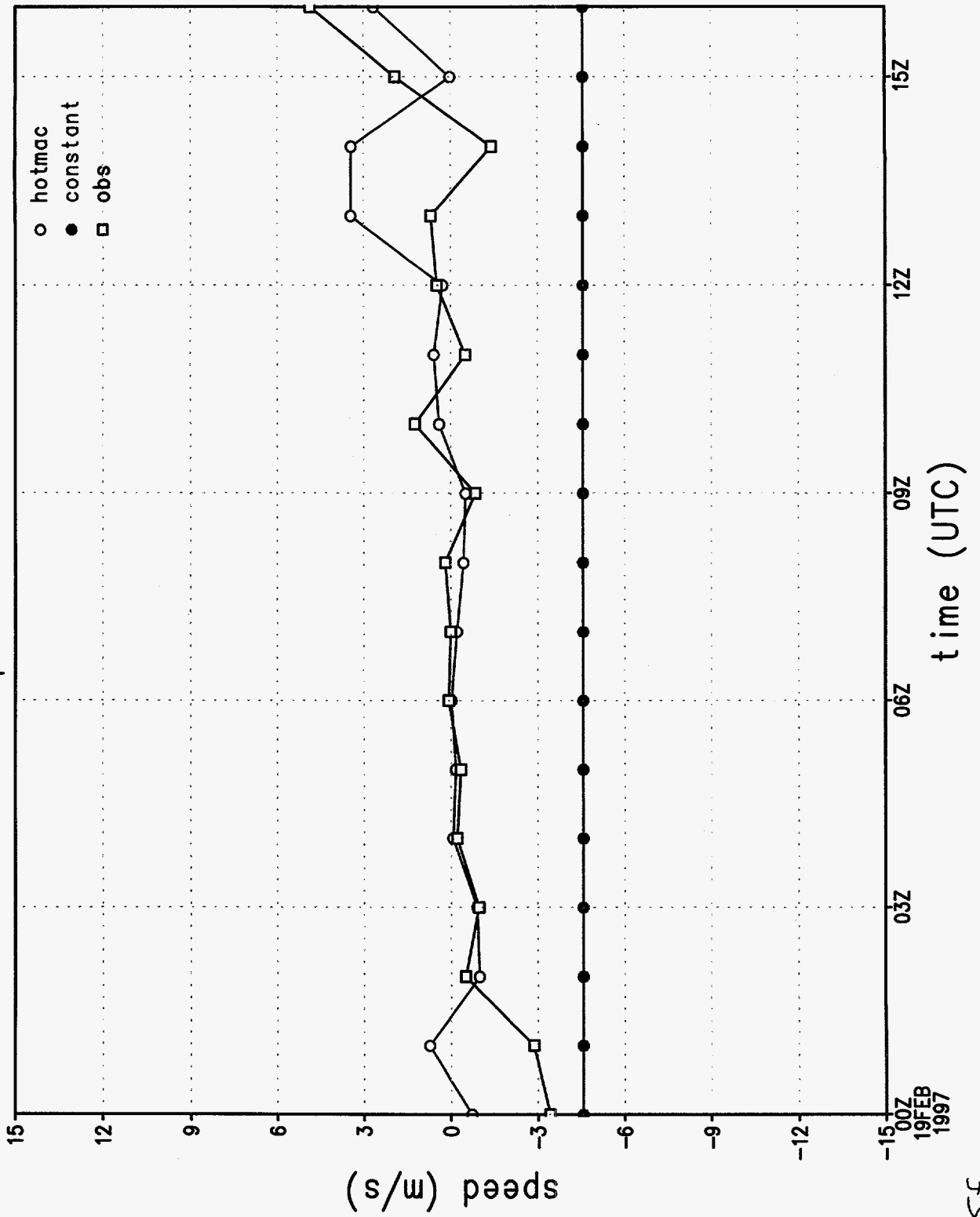


Figure 25f.



# rmse of wind direction by hour

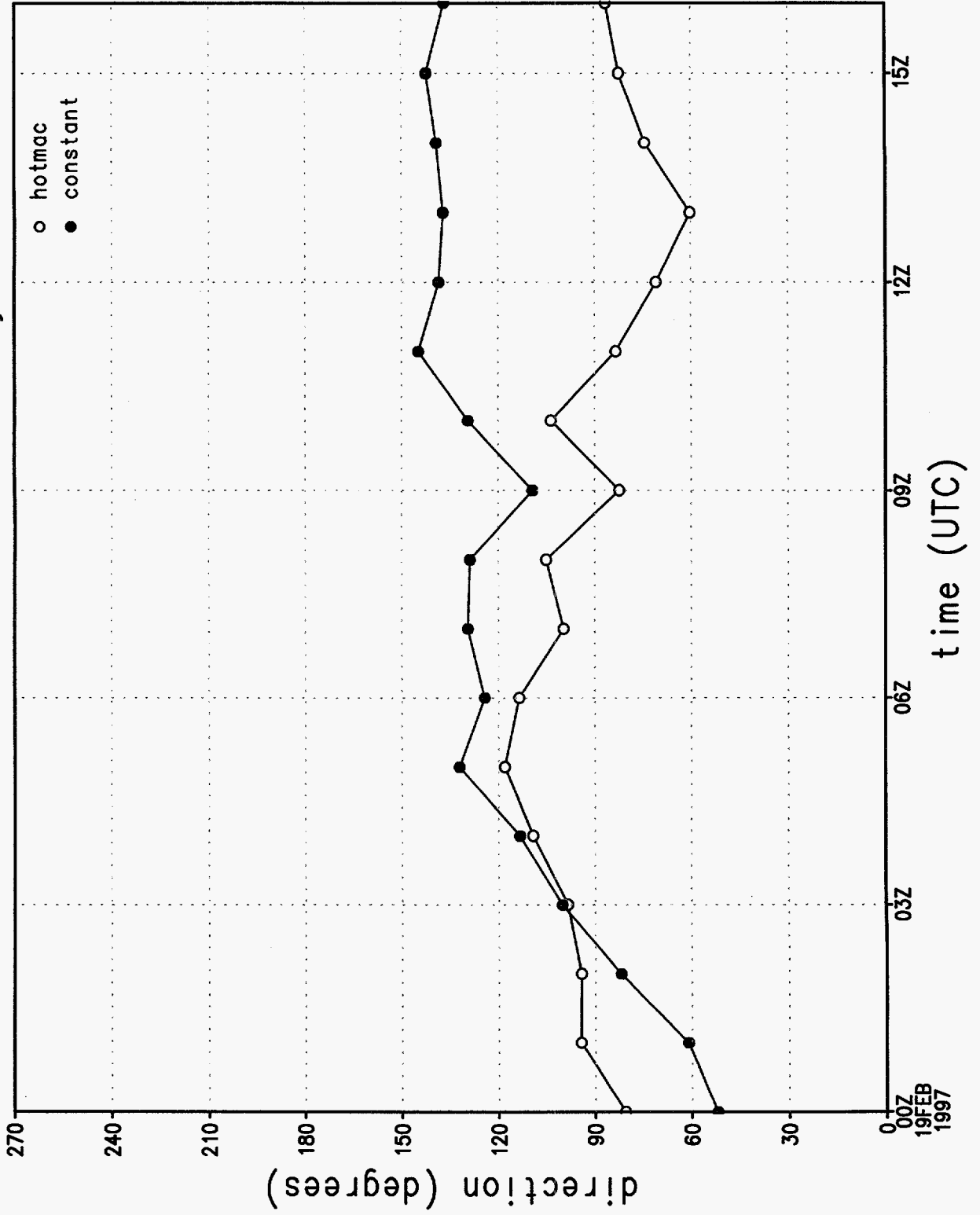


Figure 25g.

# rmse of wind speed by hour

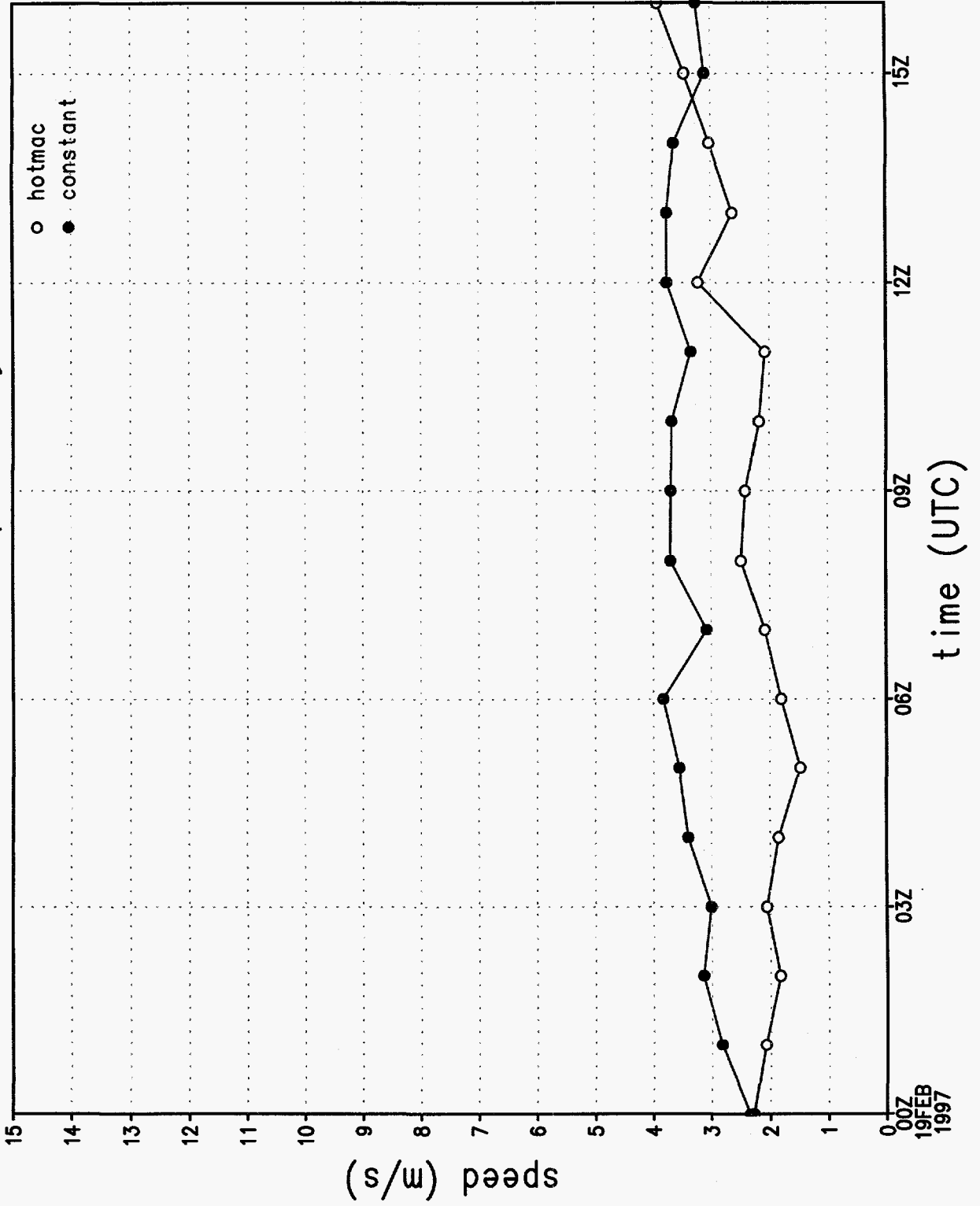


figure 25h

rmse of u wind component by hour

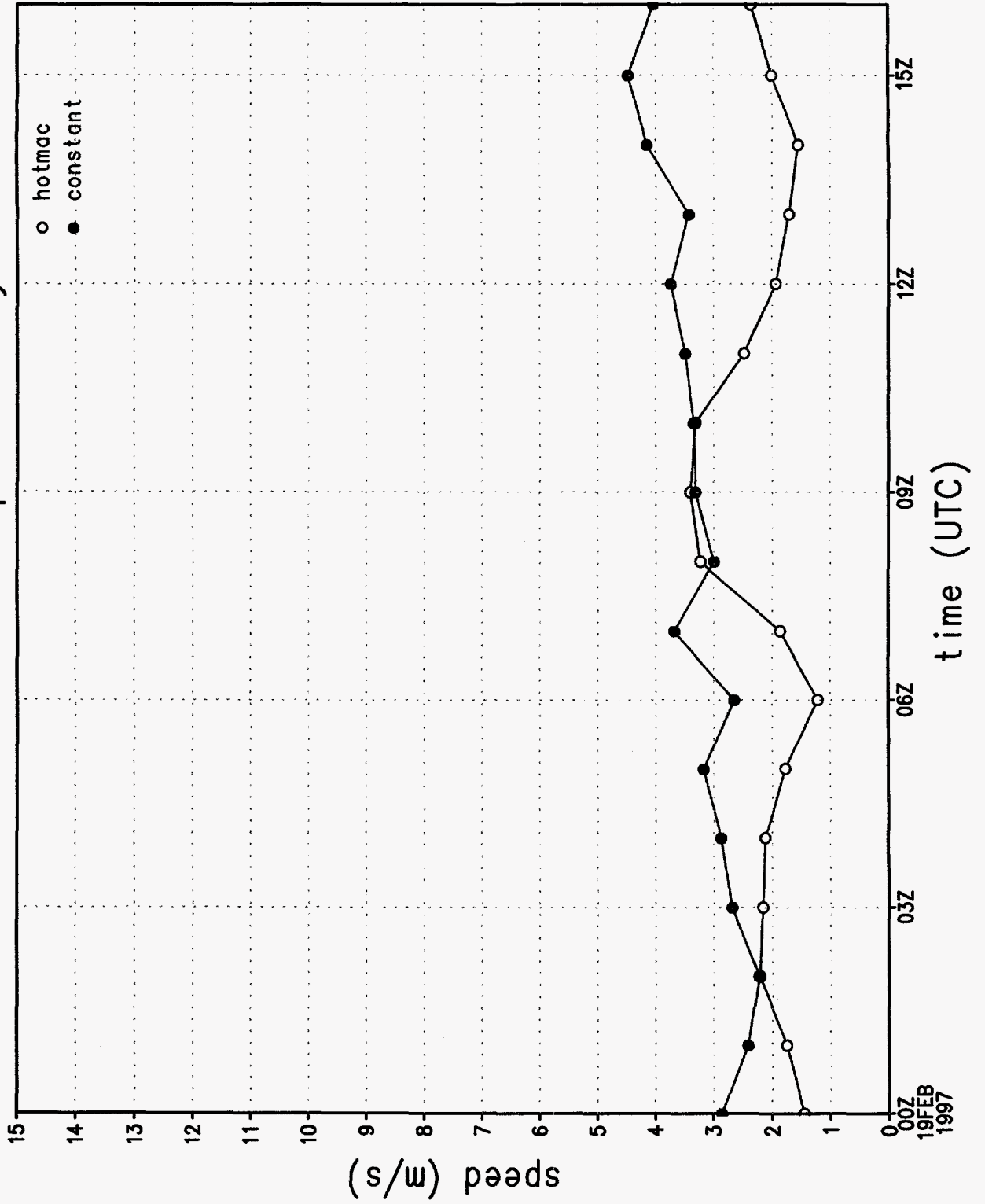


Figure 25i.

rmse of v wind component by hour

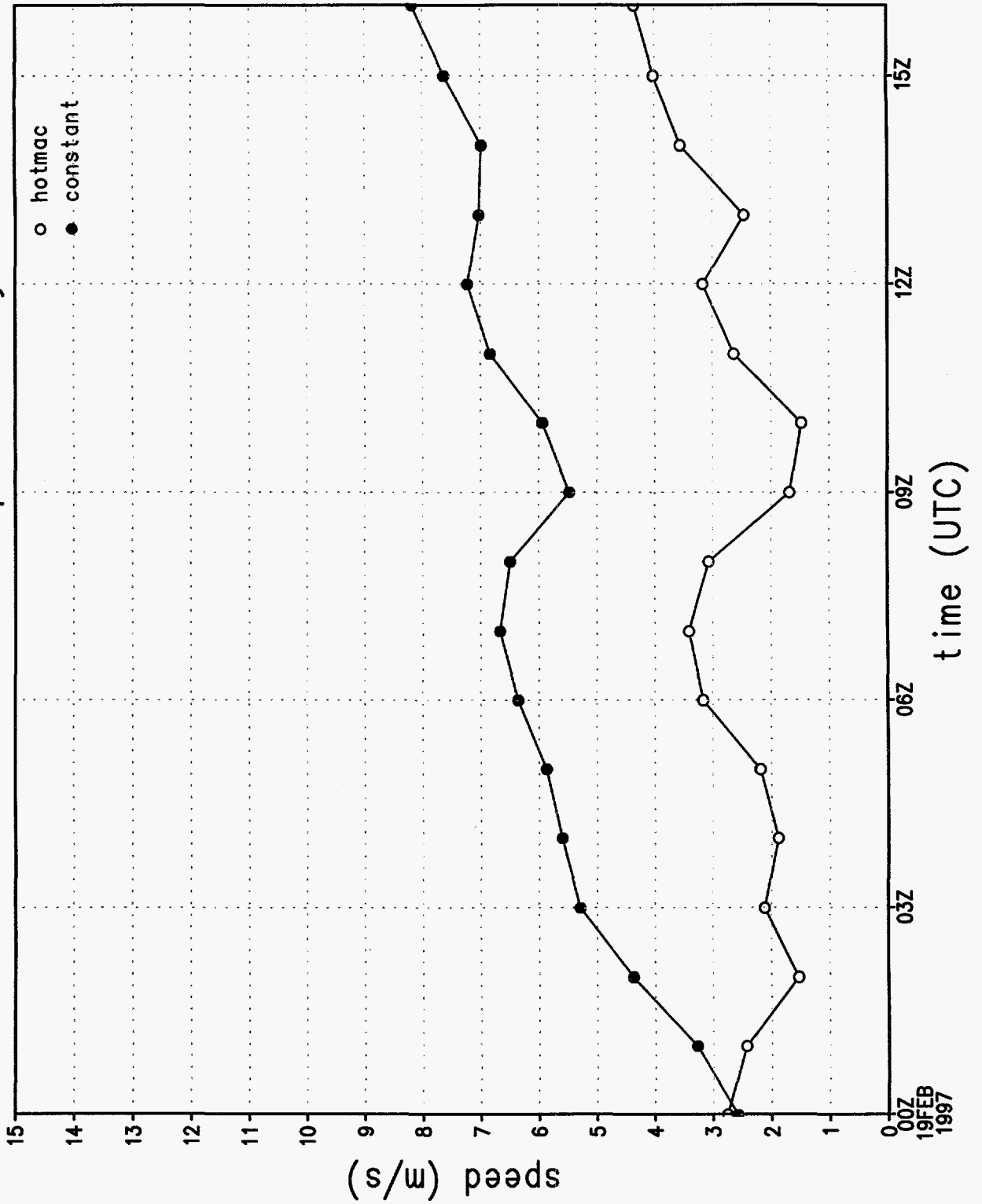


Figure 25j.